

Copyright

by

Emma Leigh McInturff

2014

**The Dissertation Committee for Emma Leigh McInturff Certifies that this is
the approved version of the following dissertation**

**Development of Ruthenium Catalyzed Hydrogenative Carbonyl
Addition Reactions**

Committee:

Michael J. Krische, Supervisor

Eric V. Anslyn

Hung-Wen Liu

Adrian T. Keatinge-Clay

Guangbin Dong

**Development of Ruthenium Catalyzed Hydrogenative Carbonyl
Addition Reactions**

by

Emma Leigh McInturff, B.S.

Dissertation

Presented to the Faculty of the Graduate School of

The University of Texas at Austin

in Partial Fulfillment

of the Requirements

for the Degree of

Doctor of Philosophy

The University of Texas at Austin

May 2014

Dedication

To my parents

Acknowledgements

First and foremost, I must thank Professor Mike Krische for guidance and mentorship during my graduate studies. You have shown me the true meaning of tenacity and the dedication and ambition required to strive for excellence. Thank you for challenging me to continually improve and grow as an individual and as a chemist.

The work described in this document would not exist without the collaboration of many talented Krische group members and chemistry department staff. Acknowledgment is much deserved to Jason Zbieg for his mentorship and instruction when I joined the Krische group, and for his leadership in the projects we worked on together. I am grateful for the opportunity to work with Eiji Yamaguchi and Jeffrey Mowat, and for the knowledge and depth of experience they shared, as it has helped shape me as a chemist. I also must thank Joyce Leung, Andrew Waldeck and Khoa Nguyen for their support and collaboration on projects. It has been a great pleasure to work with you all! Thanks are also due to Steve Sorey, Angela Spangenberg and Vincent Lynch for their assistance with NMR studies and solving x-ray crystal structures, as well as Brette Chapin and Professor Eric Anslyn for their assistance with DFT calculations and insightful discussions.

Finally, I am indebted to my friends and family for their unending encouragement. To my parents and sisters: You are all an inspiration to me. I attribute my successes to you, for you all have set such amazing examples of great achievement through discipline and determination. Above it all, your unconditional love and understanding and occasional silliness has carried me through both good times and bad. To James: Thank you for going on this adventure with me. You've been a source of strength, comfort and balance throughout my time here, and your patience and support means more to me than you will

ever know. Thank you for being my confidant, my counselor and my best friend. To all of the Krische group that I've had the pleasure to work with: You have brightened my days and provided so many unforgettable times! We have truly formed a family, celebrating successes and triumphs and calming frustrations and fears. I will miss these times. To Vanessa and Ryan, Joyce, Jeff, Laina, Dani, Tom, Joe and Jane, Anne Marie and Dan, Ben and Viv, Jason, BoYoung, Angelika: I am so grateful for your friendship and camaraderie both in the lab and outside. I have been so fortunate to be surrounded by such exceptional, encouraging and compassionate people. The bonds we have forged here are so strong! I will look back on great times in Austin with nostalgia, and will look forward to when our paths will cross again.

Development of Ruthenium Catalyzed Hydrogenative Carbonyl Addition Reactions

Emma Leigh McInturff, Ph.D.

The University of Texas at Austin, 2014

Supervisor: Michael J. Krische

Metal-catalyzed, hydrogenative methods for carbon-carbon bond formation are attractive alternatives to traditional carbonyl addition reactions. Through in situ generation of aldehyde and organometallic species, these redox-triggered reactions circumvent the need for preactivation of reactive partners, thereby providing a more atom economic, efficient approach to carbonyl addition products. Efforts have been focused on the development of ruthenium-catalyzed coupling reactions of primary and secondary alcohols to basic feedstock chemicals and easily accessible and stable unsaturated compounds. To perform highly stereoselective reactions, investigation into the factors that control stereoselectivity in ruthenium catalyzed transfer hydrogenative couplings was undertaken. As a critical tool for the construction of organic molecules, modernizing methods for carbonyl addition can contribute to the evolution of synthetic organic methodology.

Table of Contents

List of Tables.....	xii
List of Figures.....	xiv
List of Schemes.....	xx
Chapter 1 Intermolecular Reductive Coupling of Dienes and Carbonyl Compounds	1
1.1 Introduction	1
1.2 Nickel Catalysis.....	1
1.3 Rhodium Catalysis	18
1.4 Iridium Catalysis.....	20
1.5 Ruthenium Catalysis	22
1.6 Platinum Catalysis	32
1.7 Palladium Catalysis.....	33
1.8 Titanium Catalysis.....	35
1.9 Conclusion and Outlook	36
Chapter 2 Diastereoselective Transfer Hydrogenative Allylation	37
2.1 Introduction	37
2.2 Formation of 1,2-Amino alcohols using Allenamides	38
2.2.1 Introduction	38
2.2.2 Reaction Development and Optimization.....	41
2.2.3 Reaction Scope	41
2.2.4 Mechanism and Discussion	43
2.2.5 Conclusion	44
2.3 Formation of All-Carbon Quaternary Centers using 1,1-Disubstituted Allenenes	45
2.3.1 Introduction	45
2.3.2 Reaction Development, Optimization and Scope.....	46

2.3.3 Mechanism and Discussion	50
2.3.4 Conclusion	52
2.4 Summary and Outlook	52
2.5 Experimental Details	53
2.5.1 General Information.....	53
2.5.2 Spectrometry and Spectroscopy.....	53
2.5.3 General Procedures for Formation of 1,2-Amino Alcohols	54
2.5.4 Characterization of 2.3a-2.3l	54
2.5.5 General Procedures for Formation of All-Carbon Quaternary Centers using 1,1-Disubstituted Allenes	79
2.5.6 Characterization of 2.10a, e, f, i, j, h, m	80
Chapter 3 Asymmetric Carbonyl Crotylation Using Butadiene	94
3.1 Introduction	94
3.2 Crotylation Using Butadiene.....	97
3.2.1 Introduction	97
3.2.2 Reaction Development and Optimization.....	99
3.2.3 Reaction Scope	103
3.2.4 Mechanism and Discussion	105
3.2.5 Conclusion	108
3.3 <i>Syn</i> -Crotylation using Butadiene	108
3.3.1 Introduction	108
3.3.2 Reaction Development and Optimization.....	109
3.3.3 Reaction Scope	112
3.3.4 Discussion.....	113
3.3.5 Conclusion	115
3.4 Summary and Outlook	116
3.5 Experimental Details	116
3.5.1 General Information.....	116

3.5.2 Spectrometry and Spectroscopy.....	117
3.5.3 Preparation of BINOL Phosphoric Acid BA ₁₆	118
3.5.4 General Procedures for anti-Crotylation using Butadiene.....	127
3.5.5 Characterization of 3.4a-g	128
3.5.6 Preparation of TADDOL Phosphoric Acid TA ₁₂	149
3.5.7 General Procedures for syn-Crotylation using Butadiene.....	155
3.5.8 Characterization of 3.8a-j	155
3.5.9 Crystal Data and Structure Refinement for 3.10	185
Chapter 4 Reductive Coupling to Ketones.....	208
4.1 Introduction.....	208
4.2 Oxidative Coupling and Spirolactonization using Acrylates.....	211
4.2.1 Introduction.....	211
4.2.2 Reaction Development, Optimization and Scope.....	212
4.2.3 Mechanistic Explanation and Discussion.....	216
4.2.4 Conclusion.....	222
4.3 Vinylation of Ketones via Alkyne Oxidative Coupling.....	223
4.3.1 Introduction.....	223
4.3.2 Reaction Development and Optimization.....	223
4.3.3 Reaction Scope and Product Derivatization.....	224
4.3.4 Discussion and Mechanism.....	227
4.3.5 Conclusion.....	229
4.4 Summary and Outlook.....	229
4.5 Experimental Details.....	230
4.5.1 General Information.....	230
4.5.2 Spectrometry and Spectroscopy.....	231
4.5.3 Computational Analysis.....	231
4.5.4 General Procedures for Spirolactonization.....	231

4.5.5 Characterization of 4.3a-l , 4.6b , 4.8a-b , 4.10a , c-i	232
4.5.6 Crystal Data and Structure Refinement for 4.11	278
4.5.7 General Procedures for Vinylation of Ketones and Furan Formation	294
4.5.8 Characterization of 4.12a-k , 4.12m , 4.13b-h , 4.14c , 4.15a , 4.15e , 4.15l , 4.16c , 4.16e , 4.16h	295
Appendix	347
References.....	349
Vita	357

List of Tables

Table 2.1 Optimization of catalyst and ligand for aminoallylation of 2.6a	41
Table 2.2 Effect of temperature and concentration on diastereoselectivity of 2.10f	47
Table 2.3 Effect of ruthenium counter ion on diastereoselective formation of 2.10a	49
Table 3.1 Optimization of (<i>R</i>)-BINOL phosphoric acid and reaction conditions for <i>anti</i> -crotylation.....	102
Table 3.2 Optimization of TADDOL phosphoric acid structure, ligand and reaction conditions for <i>syn</i> -crotylation.....	110
Table 3.3 Comparison of the effects of BINOL and TADDOL acids used in combination with DPPF and (<i>S</i>)-Segphos on ratio of isomers of product 3.8a	114
Table 3.4 Atomic coordinates ($\times 10^4$) and equivalent isotropic displacement parameters ($\text{\AA}^2 \times 10^3$) for 3.10 . $U(\text{eq})$ is defined as one third of the trace of the orthogonalized U_{ij} tensor.....	186
Table 3.6 Anisotropic displacement parameters ($\text{\AA}^2 \times 10^3$) for 3.10 . The anisotropic displacement factor exponent takes the form: $-2\pi^2 [h^2 a^{*2} U^{11} + \dots + 2$ $h k a^* b^* U^{12}]$	197
Table 3.7 Hydrogen coordinates ($\times 10^4$) and isotropic displacement parameters ($\text{\AA}^2 \times 10^3$) for 3.10	200

Table 3.8 Torsion angles [°] for 3.10	203
Table 4.1 Optimization of catalytic system for spirolactonization of 4.1a	212
Table 4.2 Experimentally observed regioselectivities and LUMO coefficients for diones 4.5i, g, m and m	220
Table 4.3 Optimization of reaction parameters to access α -hydroxy β,γ -unsaturated ketone 4.12a	223
Table 4.3 Atomic coordinates ($\times 10^4$) and equivalent isotropic displacement parameters ($\text{\AA}^2 \times 10^3$) for 4.11 . $U(\text{eq})$ is defined as one third of the trace of the orthogonalized U^{ij} tensor.	279
Table 4.4 Bond lengths [\AA] and angles [°] for 4.11	281
Table 4.5 Anisotropic displacement parameters ($\text{\AA}^2 \times 10^3$) for 4.11 . The anisotropic displacement factor exponent takes the form: $-2\pi^2 [h^2 a^{*2} U^{11} + \dots + 2$ $h k a^* b^* U^{12}]$	287
Table 4.7 Hydrogen coordinates ($\times 10^4$) and isotropic displacement parameters ($\text{\AA}^2 \times 10^3$) for 4.11	289
Table 4.8 Torsion angles [°] for 4.11	291

List of Figures

- Figure 1.1** Ketone insertion into butadiene dimer and trimer Ni complexes **1.2** and **1.4** to access homoallylic tertiary alcohol products **1.3** and **1.5**. 2
- Figure 1.2** Reductive coupling of benzaldehyde and substituted dienes to access products of homoallylation **1.17-1.20** in high levels of diastereoselectivity and regioselectivity. 3
- Figure 1.3** Comparison of Et₃B and Et₂Zn as a reductant for coupling isoprene to aromatic, allylic and aliphatic aldehydes. 4
- Figure 1.4** Plausible mechanism for coupling isoprene and aldehyde, using Et_nM as reductant. The *anti*-selectivity can be explained by chair-like transition state **II**, which avoids 1,3-diaxial interactions between aldehyde and diene substituent. 5
- Figure 1.5** Optimization of catalyst and reductant to afford highly selective three component coupling of benzaldehyde, isoprene and Ph_nM. 8
- Figure 1.6** Four component coupling of aldehyde, diene, alkyne and Me₂Zn reagent to furnish **1.36** in high yield. 9
- Figure 1.7** Proposed mechanism for formation of homoallylic silyl ether (**E**)-**1.40**. 10
- Figure 1.8** Oxidative coupling mechanism to explain (*Z*) olefin selectivity. 12
- Figure 1.9** Asymmetric (*Z*)-selective homoallylation of aldehyde **1.13d** using chiral NHC ligand derived from **1.50**. 13
- Figure 1.10** Ligand controlled (*E*)- or (*Z*)-selective formation of allylsilanes. 14

Figure 1.11 Ligand dependent divergent pathways of coupling aldehyde and diene 1.14 to access both internal and terminal boronates 1.61 and iso-1.61	17
Figure 1.12 Rh catalyzed benzaldehyde coupling with various dienes, exhibiting high levels of regioselectivity.	19
Figure 1.13 Proposed mechanism for Rh catalyzed diene-aldehyde coupling. .	20
Figure 1.14 Cyclometallated iridium complex 1.76 used to access product of crotylation 1.77a by coupling primary alcohol 1.74a and butadiene.	21
Figure 1.15 Hydroacylation under mild conditions using RuHCl(CO)(PPh ₃) ₃	23
Figure 1.16 Redox neutral coupling of dienes and primary alcohols to generate homoallylic alcohol products.	23
Figure 1.17 Proposed mechanism for reductive coupling of isoprene and an aldehyde by ruthenium hydride catalyst.	24
Figure 1.18 Dependence of regiochemical outcome on ruthenium catalyst in coupling 2-substituted dienes 1.68 and paraformaldehyde.....	26
Figure 1.19 Effect of sulfonate counter ion on diastereoselective coupling of butadiene and primary alcohol.	28
Figure 1.20 <i>Anti</i> -Crotylation using butadiene, displaying (<i>R</i>)-BINOL phosphate counter ion controlled selectivity.....	29
Figure 1.21 <i>Syn</i> -Crotylation using butadiene, displaying L-TADDOL-phosphate counter ion controlled selectivity.....	29

Figure 1.22 Proposed mechanism for <i>n</i> -prenylation of ethyl mandelate 1.90	30
Figure 1.23 Proposed mechanism of diastereoselective silaborative coupling of 1,3-diene and aldehyde by way of a platinum-allyl intermediate.	33
Figure 1.24 Effect of ligand to metal ratio for palladium catalyzed telomerization to form 1.103 or 1.104	34
Figure 1.25 Palladium catalyzed reductive coupling of dienes and aldehyde to generate dienyl homoallylic alcohol 1.105	35
Figure 1.26 Titanium catalyzed reductive coupling of aldehyde 1.13e and isoprene.	35
Figure 2.1 Comparison of asymmetric carbonyl allylation methods, including organoboron reagents, Lewis acid catalyzed organostannane additions, Lewis-base catalyzed allylsilane additions, and hydrogenative allylation.	37
Figure 2.2 Hydrogenative carbon-carbon bond formation using hydrogen gas or transfer hydrogenation.	38
Figure 2.3 Ruthenium catalyzed hydrohydroxyalkylation of allenamide 2.2 using primary alcohols.....	42
Figure 2.4 Proposed catalytic mechanism for hydrohydroxyalkylation of allenamide 2.2 using primary alcohol 2.6a	43
Figure 2.5 Chiral ferrocene based ligands for asymmetric aminoallylation.	44

Figure 2.6 Allenes selected for development of allylation to form all-carbon quaternary centers.	45
Figure 2.7 Ruthenium catalyzed hydrohydroxyalkylation of 1-methyl-1-phenylallene 2.7a	49
Figure 2.8 Interconversion of (Z)-I and (E)-I lead to syn-III and anti-III	51
Figure 3.1 Pharmaceutically active polyketides that contain fragments accessible through crotylation.	94
Figure 3.2 Chirally modified allyl-boron reagents used for asymmetric crotylation.	95
Figure 3.3 Organotitanium and organosilicon reagents used for asymmetric crotylation.	95
Figure 3.4 Chiral Lewis acid and Lewis base catalysts used for asymmetric crotylation.	96
Figure 3.5 Chromium and iridium catalysts developed for asymmetric crotylation.	97
Figure 3.6 Influence of size of sulfate counter ion on diastereoselectivity of crotylation using butadiene.....	100
Figure 3.7 Ruthenium catalyzed coupling of butadiene and primary alcohols or aldehydes to generate products of <i>anti</i> -crotylation 3.4a-g	104
Figure 3.8 Proposed mechanism for the hydrohydroxyalkylation of butadiene.	105
Figure 3.9 Stereochemical model of the transition state for carbonyl addition for <i>anti</i> -crotylation.	107

Figure 3.10 Ruthenium catalyzed coupling of butadiene and primary alcohols to generate products of <i>syn</i> -crotylation 3.8a-j	112
Figure 3.11 Stereochemical model of the transition state for carbonyl addition for <i>syn</i> -crotylation.....	113
Figure 3.12 ORTEP representation of crystal structure of Ru(CO)(OAc)[(S)-Segphos][TADDOL-Phosphate] 3.10	115
Figure 3.13 Synthetic Route to BINOL Phosphoric Acid BA₁₆	118
Figure 3.14 Synthetic Route to TADDOL Phosphoric Acid TA₁₂	149
Figure 4.1 Pharmaceutically active natural products containing spiro lactones.	211
Figure 4.2 Spiro lactones 4.3a-l generated upon coupling diols 4.1a-l to methyl acrylate 4.2a	213
Figure 4.3 Spirooxindole products 4.10a, c-i generated by coupling 3-hydroxyoxindole 4.9 and substituted acrylic esters 4.2a, c-i	216
Figure 4.4 Proposed mechanism for oxidative coupling of dione 4.5a and methyl acrylate 4.2a to generate products of spiro lactonization 4.3a	217
Figure 4.5 ORTEP representation of crystal structure of Ru(CO)(DPPP)[(H ₁₅ C ₁₀ CO ₂ ⁻) ₂] 4.11	217
Figure 4.6 Comparison of conformational flexibility of diones 4.5i and 4.5g	221
Figure 4.7 Stereochemical model of ruthenacycle generated upon oxidative coupling to explain diastereocontrol in spirooxindole formation.	221

Figure 4.8 α -hydroxy, β,γ -unsaturated ketones 4.12a-k, m generated upon coupling 1,2-diols 4.1a-k, m and alkyne 4.11a	224
Figure 4.9 α -hydroxy, β,γ -unsaturated ketones 4.12a and 4.13b-h generated upon coupling diol 4.1a and alkynes 4.11a-h	225
Figure 4.10 Cyclodehydration of α -hydroxy β,γ -unsaturated ketones to form tetrasubstituted furans 4.15a, e, i , and 4.16c, e, h	227
Figure 4.11 Proposed mechanism for the generation of dione 4.5a from diol 4.1a and subsequent oxidative coupling.	228
Figure 4.12 Stereochemical models of the ruthenacycle intermediate to explain regiochemical outcome of products 4.12a-k, m	229

List of Schemes

- Scheme 1.1** Product distribution of nickel catalyzed reaction of isoprene and acetaldehyde, showing *mono*- and *bis*-coupled products **1.7-1.12**.
..... 2
- Scheme 1.2** Three component coupling of benzaldehyde, butadiene and Me₂Zn.5
- Scheme 1.3** Three component coupling of ketone leads to 1:2:1 acetone:butadiene:Me₂Zn product..... 6
- Scheme 1.4** Regio- and stereoselective three component coupling of isoprene and benzaldehyde using Me₃B as reductant. 6
- Scheme 1.5** Three component coupling of Ph₂Zn or *t*Bu₂Zn, benzaldehyde and butadiene. 7
- Scheme 1.6** Homoallylation using isoprene with aqueous dialdehyde solution and cyclic hemiacetal. 8
- Scheme 1.7** Nickel catalyzed homoallylation of aldehyde **1.13a** using 1-substituted dienes **1.39**. 9
- Scheme 1.8** Selective formation of (**Z**)-**1.40** using Ni-NHC catalyst 11
- Scheme 1.9** Ligand controlled (*E*)- or (*Z*)-selective formation of allylsilanes **1.44** and **1.45**..... 11
- Scheme 1.10** Three component coupling using PhB(OH)₂..... 13
- Scheme 1.11** Application of chiral spiro phosphoramidite ligand for diastereo- and enantioselective homoallylation of aldehyde. 15

Scheme 1.12 Enantioselective three component coupling of 1,3-diene 1.39 , aldehyde 1.13e and silylborane to generate α -chiral allylsilane.	15
Scheme 1.13 1,3-cyclohexadiene 1.59 engages in reductive coupling with aldehydes under Ni catalysis.	16
Scheme 1.14 Application of $B_2(\text{pin})_2$ to cleave nickelacycle intermediate.	16
Scheme 1.15 Three component coupling of aldehyde, diene, and $B_2(\text{pin})_2$ to access homoallylic diols.	16
Scheme 1.16 α -chiral allylboronate formation using $P(\text{SiMe}_3)_3$ as ligand and subsequent stereotriad formation after workup.	17
Scheme 1.17 Ligand controlled (<i>E</i> - or <i>Z</i> -)selective formation of allylsilanes....	18
Scheme 1.18 Coupling of dienes and paraformaldehyde, where paraformaldehyde serves dual role as aldehyde and reductant.	18
Scheme 1.19 Reductive coupling of cyclohexadiene 1.59 and glyoxal 1.70 via hydrometallation of I and aldehyde insertion to form II	19
Scheme 1.20 Reductive coupling of cyclohexadiene 1.59 and aldehyde 1.13 and redox neutral process using a primary alcohol 1.74 as aldehyde precursor.	21
Scheme 1.21 Hydroacylation of aromatic aldehydes with isoprene.	22
Scheme 1.22 Transfer hydrogenative allylation and hydroacylation of primary alcohols or aldehydes under ruthenium catalysis.	25

Scheme 1.23 Coupling of ethanol and acetaldehyde to 2-substituted dienes 1.68 to form homoallylic alcohols 1.81 containing all-carbon quaternary centers.	26
Scheme 1.24 Silyl group of 1.82 effects diastereoselectivity based on stability of (Z)- and (E)- σ -allyl isomer.	27
Scheme 1.25 Enantioselective <i>syn</i> -crotylation products from coupling primary alcohol or aldehyde and 2-silylbutadiene.	27
Scheme 1.26 <i>N</i> -Prenylation of ethyl mandelate 1.90 using isoprene.	30
Scheme 1.27 Coupling of 3-hydroxyoxindole 1.93 and phenyl-(2-pyridyl)-methanol 1.95 and isoprene to generate <i>n</i> -prenylated products 1.94 and 1.97	31
Scheme 1.28 Formal [4+2] cycloaddition by coupling 1,2-diol 1.98 with isoprene.	31
Scheme 1.29 Formation of 1.101 by silaborative coupling of 1,3-diene 1.72 and benzaldehyde.	32
Scheme 1.30 Divinyltetrahydropyran 1.102 and <i>iso</i> - 1.102 formed upon coupling of butadiene and formaldehyde.	33
Scheme 2.1 Reductive coupling of aldehyde and allenamide to form vinyl substituted 1,2-amino alcohols.	39
Scheme 2.2 Reductive coupling of aldehyde 2.1a and allenamide 2.2 to form 1,2-amino alcohol 2.3a	40
Scheme 2.3 Effects of allene substituent on diastereoselectivity.	40

Scheme 2.4 Reductive coupling of 1,1-disubstituted allenes to aldehydes or paraformaldehyde.	45
Scheme 2.5 Formation of an all-carbon quaternary center via addition of allyltrichlorosilane 2.8 to aldehyde 2.1f in the presence of a chiral Lewis base catalysis.....	46
Scheme 2.6 Initial results of coupling allene 2.7a with alcohols 2.6a and 2.6h , exhibiting a great difference in diastereoselectivity.	46
Scheme 2.7 Counter ion introduction by treating $\text{RuH}_2(\text{CO})(\text{PPh}_3)_3$ with acid. ..	48
Scheme 2.8 Product 2.12f from aldehyde 2.1f exhibits much lower diastereoselectivity than alcohol 2.6f , supporting Curtin-Hammett interpretation of trends in diastereoselectivity.	51
Scheme 3.1 Brown crotylation, including procedure required to generate 3.1b from 2-butene (3.1a), compared to crotylation using butadiene.	98
Scheme 3.2 Hydrohydroxyalkylation of butadiene using transfer hydrogenative ruthenium catalysis.....	99
Scheme 3.3 Allylic (3.5a) and aliphatic (3.7a) substrates for crotylation.....	105
Scheme 3.4 Transfer hydrogenation using 1,4-butanediol to regenerate complex I.	106
Scheme 4.1 Transfer hydrogenative amination of α -hydroxy amide.....	208
Scheme 4.2 Oxidative coupling of an α -keto ester with ethylene and CO using $\text{Ru}_3(\text{CO})_{12}$	209

Scheme 4.3 Oxidative coupling of ethyl mandelate and isoprene under transfer hydrogenative conditions.....	209
Scheme 4.4 Oxidative coupling of 3-hydroxyoxindole or <i>trans</i> -1,2-cyclohexanediol with isoprene under transfer hydrogenative conditions.	210
Scheme 4.5 Oxidative coupling of propene and 3-hydroxyoxindole.	210
Scheme 4.6 Coupling of diol 4.1f , α -hydroxy ketone 4.4f or dione 4.5f with methyl acrylate 4.2a to generate spiro lactone 4.3f	214
Scheme 4.7 Coupling of 4.1a and 2-hydroxymethyl acrylate 4.2b to access α -exocyclic- γ -butyrolactone 4.6b	214
Scheme 4.8 Spirolactonization of α -hydroxy esters 4.7a-b to access spiro lactones 4.8a-b	215
Scheme 4.9 Regeneration of Ru ⁰ catalyst from 4.11	218
Scheme 4.10 Control experiments to probe Lewis acid catalyzed Michael addition.	218
Scheme 4.11 Control experiment to test for Michael addition products.	219
Scheme 4.12 Role of basic additives in diastereoselective spirooxindole formation.	222
Scheme 4.13 Vinylation of α -hydroxy ester 4.7c	226
Scheme 4.14 Vinylation of α -hydroxy ketone 4.4f	226

Chapter 1 Intermolecular Reductive Coupling of Dienes and Carbonyl Compounds

1.1 Introduction

Carbonyl addition chemistry is a cornerstone in synthetic organic chemistry, utilizing the electrophilic character of a C=O double bond to enable formation of carbon-carbon or carbon-heteroatom bonds. For carbon-carbon bond formation, a diverse set of organometallic reagents used as carbon-nucleophiles has been developed.

Catalytic carbonyl addition is possible by reductive coupling with π -unsaturated molecules. Dienes are suitable substrates for reductive coupling and are an attractive precursor to organometallic nucleophiles for carbonyl addition. In contrast to organometallic reagents, many dienes are readily available or naturally occurring compounds. For example, 1,3-butadiene is a byproduct of petroleum cracking, and isoprene is a naturally occurring terpene produced by trees. The direct employment of a diene avoids the need for pre-activation to generate discrete organometallic intermediates and may avoid the moisture sensitivity or functional group incompatibility that limits the use of some organometallic reagents.

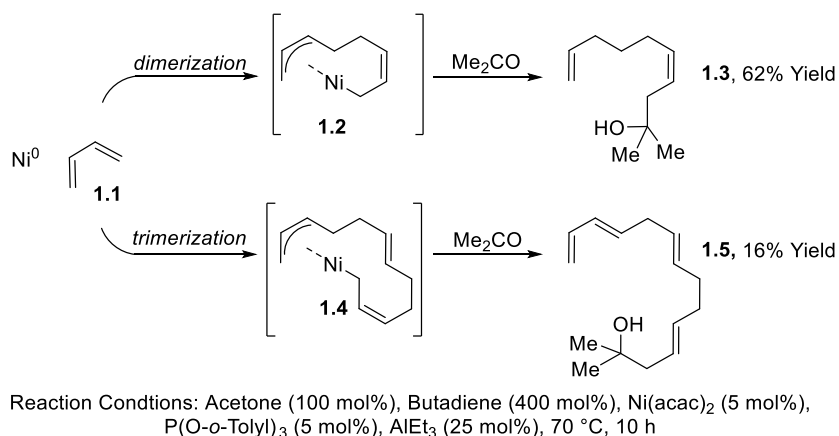
This review will encompass developments in metal-catalyzed intermolecular reductive coupling of carbonyl compounds and 1,3-dienes. Metal-mediated reactions will not be included. While many examples of intramolecular reductive couplings of dienes and aldehydes exist to quickly access complex cyclic structures,¹ this topic will not be included, nor will multi-component couplings that feature an intramolecular process.

1.2 Nickel Catalysis

Early reports of nickel catalyzed reductive coupling of aldehydes and ketones to 1,3-dienes were made in the 1970's. A seminal report by Akutagawa disclosed that using a Ni^0 catalyst, excess 1,3-butadiene or isoprene was found to add to acetone and other methyl-ketones.² The major product (**1.3**) obtained was a 2:1 ratio of diene to ketone, suggesting that a nickel catalyzed diene dimerization precedes carbonyl addition (Figure 1.1). This was supported by the detection of butadiene dimers and higher oligomers, including product **1.5**, a 3:1 diene to

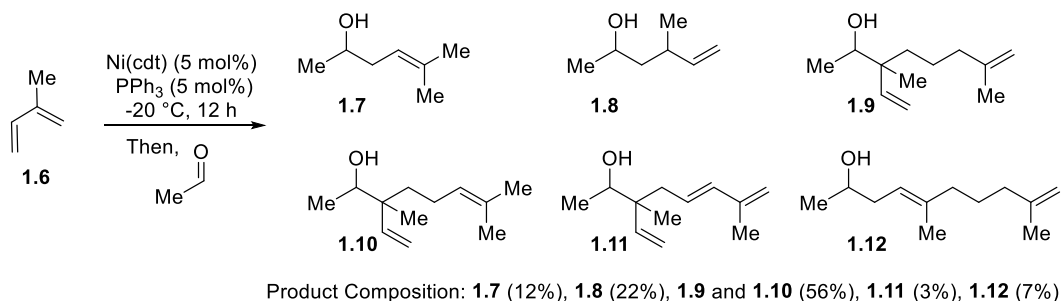
ketone coupling. Electron poor phosphite ligand P(OPh)₃ was found to be uniquely effective, as triphenyl-, trialkylphosphine, and aminophosphine ligands resulted in only diene dimerization. Further mechanistic insight could be inferred from the *cis*-geometry of the product, suggesting that cyclic Ni- π -allyl species **1.2** or **1.4** may undergo insertion by the aldehyde.

Figure 1.1 Ketone insertion into butadiene dimer and trimer Ni complexes **1.2** and **1.4** to access homoallylic tertiary alcohol products **1.3** and **1.5**.



In 1978, Baker and Crimmin reported coupling aldehydes to butadiene and isoprene,³ resulting in a product with a 2:1 ratio of aldehyde to diene. Stirring of nickel catalyst and diene **1.6** at -20 °C overnight followed by addition of aldehyde led to a complex mixture of *mono*-coupled products **1.7** and **1.8** and *bis*-coupled products **1.9**, **1.10**, **1.11** and **1.12** (Scheme 1.1).

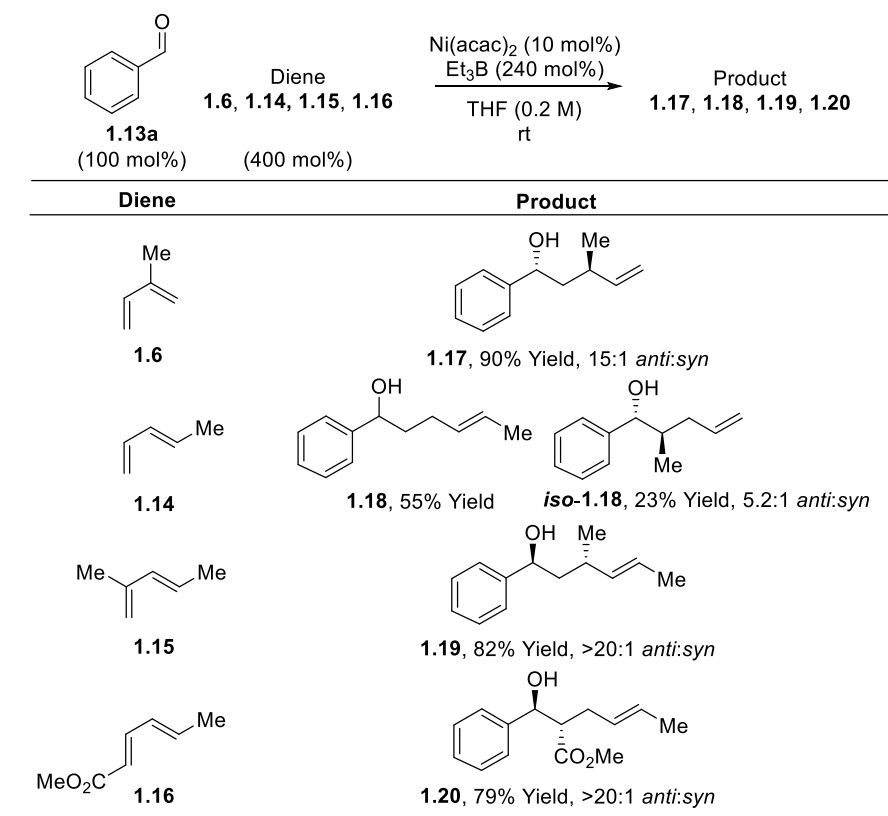
Scheme 1.1 Product distribution of nickel catalyzed reaction of isoprene and acetaldehyde, showing *mono*- and *bis*-coupled products **1.7-1.12**.



The identity of phosphine ligand was found to be crucial in determining product outcome, as variation of electron and steric properties drastically altered the product isomer ratios. Triphenylphosphine, as compared to other trialkyl phosphines was found to provide the most product, while electron-deficient phosphite ligands were ineffective at catalyzing the reaction.

Over the next 20 years, broad development of these initial observations led to highly selective intramolecular reductive coupling reactions. Tamaru, a key contributor to this area, revisited the intermolecular reductive coupling of carbonyl compounds and dienes in 1998. It was found that Ni(acac)₂ in the presence of triethylborane would catalyze the homoallylation of benzaldehyde (**1.13a**) using isoprene (**1.6**) as diene to generate 1-phenyl-4-pentenols **1.17-1.20** (Figure 1.2).⁴

Figure 1.2 Reductive coupling of benzaldehyde and substituted dienes to access products of homoallylation **1.17-1.20** in high levels of diastereoselectivity and regioselectivity.



Notably, this product is formed as a single regioisomer, exhibiting coupling at the C1 position of the diene, with high levels of *anti*-diastereoselectivity. Regioselectivity was found to be highly dependent on diene substitution, where diene **1.14**, with substitution at the C1 position, resulted in a mixture of C1- and C4-coupled products **1.18** and *iso*-**1.18**, but for dienes **1.6** and **1.15**, C2 substitution strongly favored coupling at the C1 position to form products **1.17** and **1.19**, respectively. Diene **1.16**, substituted with an electron withdrawing group, exhibited coupling at the diene position with the highest electron density to form **1.20**. Only 1:1 diene to aldehyde adducts were formed, in contrast to previous reports of 2:1 and 3:1 adduct formation.²⁻³ It was proposed that Et₃B serves dual roles in this process, both in activating the aldehyde toward addition and serving as a reductant for catalyst turnover.

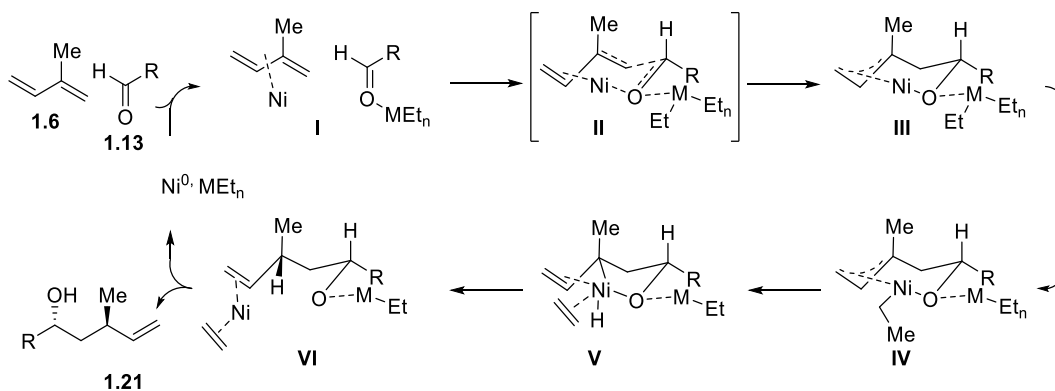
Extension of the scope of this catalytic system was met with marginal success. While aromatic and allylic aldehydes (**1.13a** and **1.13b**) performed well, aliphatic aldehydes (**1.13c**) suffered from low yield, and ketones were unreactive. For these problematic substrates, Et₂Zn was found to be an effective reductant, leading to high levels of homoallylation in very short reaction time (Figure 1.3). For aromatic and allylic substrates, the employment of Et₂Zn resulted in lower yield of **1.21** due to aldehyde ethylation to form side product **1.22**.⁵

Figure 1.3 Comparison of Et₃B and Et₂Zn as a reductant for coupling isoprene to aromatic, allylic and aliphatic aldehydes.

	Et ₃ B ^a			Et ₂ Zn		
	Time h	1.21 Yield (%), <i>anti:syn</i>		Time h	1.21 Yield (%), <i>anti:syn</i>	1.22 Yield (%)
1.13a R = Ph	35	90%, 15:1		4	63%, 15:1	16
1.13b R = (CH ₂) ₂ Ph	70	81%, 20:1		1	0%	28 ^b
1.13c R = <i>t</i> Bu	48	16%		0.5	66%, 15:1	0

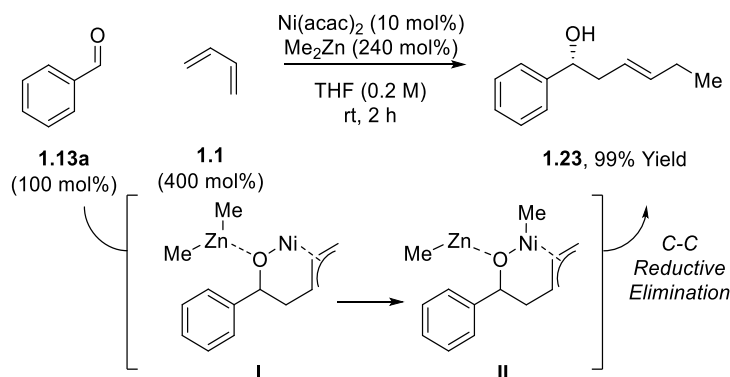
^aNo ethylation product **1.22a-c** was observed. ^bA complex mixture of products was isolated, including the product of conjugate ethyl addition.

Figure 1.4 Plausible mechanism for coupling isoprene and aldehyde, using Et_nM as reductant. The *anti*-selectivity can be explained by chair-like transition state **II**, which avoids 1,3-diaxial interactions between aldehyde and diene substituent.



A possible mechanism for the transformation is shown in Figure 1.4, where coordination of the aldehyde **1.13** and diene **1.6** by Ni^0 and either Et_2Zn or Et_3B (**I**) precedes carbonyl addition through transition state **II** to form complex **III**. The reversible Ni-catalyzed reaction of dienes and carbonyl compounds has been studied by Ogoshi, et al., and structural evidence has suggested that Ni-promoted reductive coupling occurs by way of cyclometallation.⁶ Ethyl migration from zinc or boron to the Ni catalyst generates σ -allyl-ethylnickel^{II} complex (**IV**) that can undergo β -hydride elimination to form a Ni hydride (**V**) and ethylene. Reductive elimination delivers the hydride to the allylic position and the resulting Ni^0 complex can dissociate from product **1.21** to reenter the catalytic cycle.

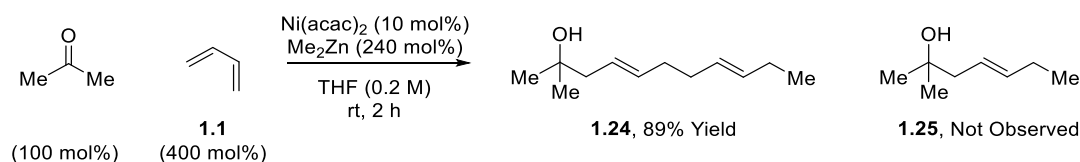
Scheme 1.2 Three component coupling of benzaldehyde, butadiene and Me_2Zn .



It was reasoned that the employment Me_2Zn in place of Et_2Zn would inhibit the β -hydrodenickelation and C-H reductive elimination to form **1.21** (via **IV** to **VI**, Figure 1.4), and instead could undergo C-C reductive elimination (via **I** and **II**, Scheme 1.2) to transfer the methyl group to product **1.23** and regenerate Ni^0 (Scheme 1.2). This formal three component coupling reaction was effective for various aromatic and aliphatic aldehydes.⁷

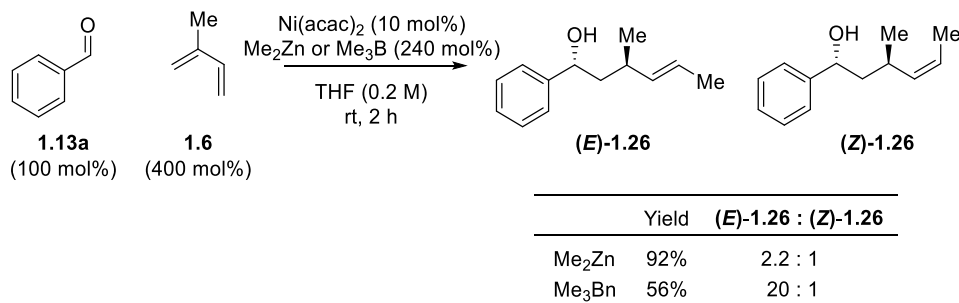
Application of this concept to coupling of butadiene and acetone, a 1:2:1 ratio of ketone:diene:dimethyl zinc was observed in product **1.24**, suggesting that the steric bulk of the *gem*-dimethyl groups may inhibit reductive elimination of the 1:1:1 adduct leading to product **1.25** (Scheme 1.3).

Scheme 1.3 Three component coupling of ketone leads to 1:2:1 acetone:butadiene: Me_2Zn product.



The three component coupling of benzaldehyde, isoprene and organozinc reagent was successful to yield 3-methyl-3-hexenol **1.26**, though the transformation suffered from low olefin (*E*):(*Z*) selectivity (Scheme 1.4)

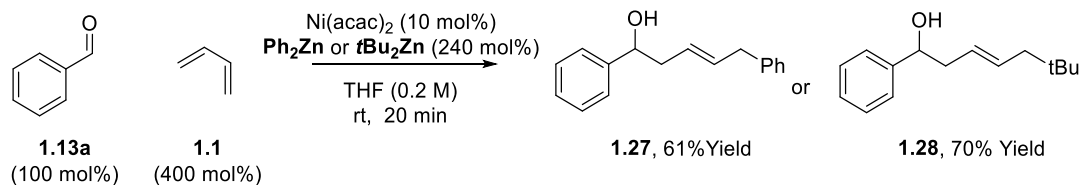
Scheme 1.4 Regio- and stereoselective three component coupling of isoprene and benzaldehyde using Me_3B as reductant.



To circumvent this problem, it was found that Me_3B could be used in place of Me_2Zn to effect the transformation with high levels of (*E*):(*Z*) selectivity. Proposed to proceed through a similar mechanism to the reaction employing Me_2Zn , this reaction represents the first example of Me_3B as a methyl transfer reagent.⁸

By varying the organozinc reagent used in the three component coupling, various structural features could be accessed. Despite concern of side reactivity between aldehyde **1.13a** and more reactive organozinc reagents, Ph_2Zn and $t\text{Bu}_2\text{Zn}$, the three component coupling proceeded smoothly, accessing product **1.27** and **1.28** in good yield and with complete (*E*) olefin selectivity (Scheme 1.5).^{7, 9}

Scheme 1.5 Three component coupling of Ph_2Zn or $t\text{Bu}_2\text{Zn}$, benzaldehyde and butadiene.

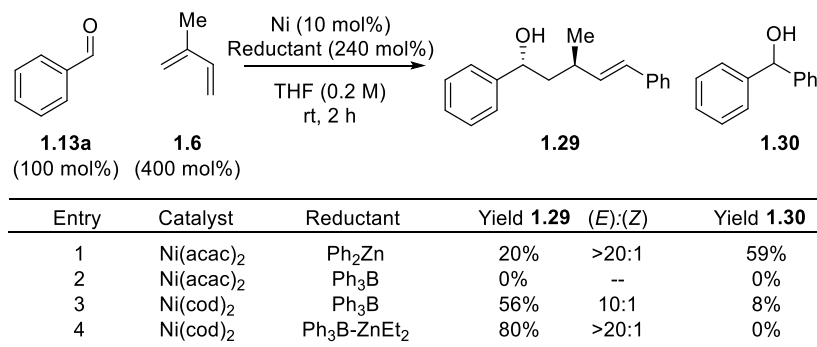


Employing isoprene as diene, however, resulted in only phenyl addition to aldehyde. Previous observations suggested that employing organoboron reagents as reductant may avoid this undesired product. Using Ph_3B in place of Ph_2Zn , no coupling product (**1.29**) was isolated using $\text{Ni}(\text{acac})_2$ as catalyst, but formation of **1.30** was also suppressed (Figure 1.5). The Ni^0 precatalyst $\text{Ni}(\text{cod})_2$ restored reactivity, furnishing product from aromatic, allylic, and aliphatic aldehydes in moderate yield and high (*E*):(*Z*) selectivity. Upon evaluation of other organometallic reagents, organoborate complex $\text{Ph}_3\text{B}-\text{ZnEt}_2$ was found to improve reactivity and olefin selectivity.

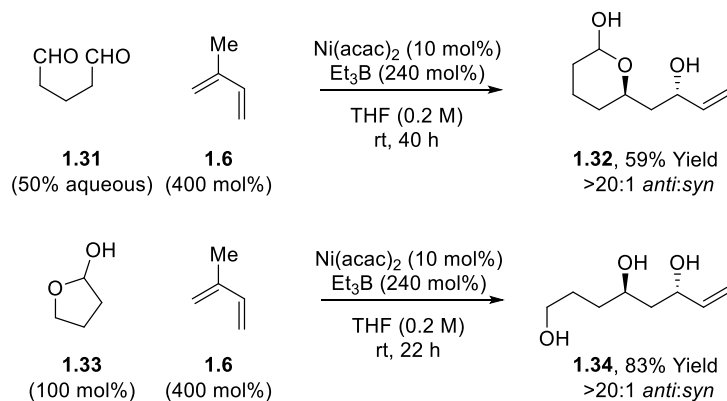
Further extension of this methodology revealed that homoallylation of a 50% aqueous solution of glutaraldehyde (**1.31**) was highly effective using isoprene, $\text{Ni}(\text{acac})_2$ and Et_3B at room temperature. Upon homoallylation, cyclization of the resulting secondary alcohol on the pendant aldehyde resulted in the formation of lactol **1.32** in good yield and complete diastereoselectivity.

This reaction was also effective for cyclic hemiacetal **1.33**, resulting in a homoallylic 1,4-diol **1.34** in good yield and complete diastereoselectivity (Scheme 1.6).¹⁰

Figure 1.5 Optimization of catalyst and reductant to afford highly selective three component coupling of benzaldehyde, isoprene and Ph_nM.



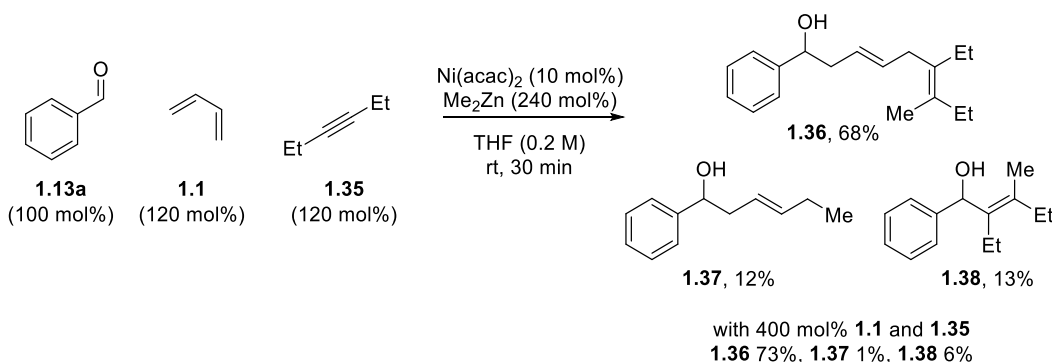
Scheme 1.6 Homoallylation using isoprene with aqueous dialdehyde solution and cyclic hemiacetal.



Inspired by the nickel catalyzed three component couplings of aldehydes, alkynes, and organozinc reagents,¹¹ Tamaru et al. proposed that a four component coupling could be possible to rapidly construct four carbon-carbon bonds in poly-unsaturated secondary alcohols. The four-component coupling product **1.36** was accessed using Me₂Zn, diethylalkyne **1.35**, butadiene **1.1** and aldehyde **1.13a**, using 10 mol% Ni(acac)₂ in 68% yield, accompanied by 12% of three component coupling product **1.37** of Me₂Zn, butadiene **1.1**, and aldehyde **1.13a**, and 13% of the three component coupling product **1.38** of Me₂Zn, alkyne **1.35** and aldehyde **1.13a**. This product

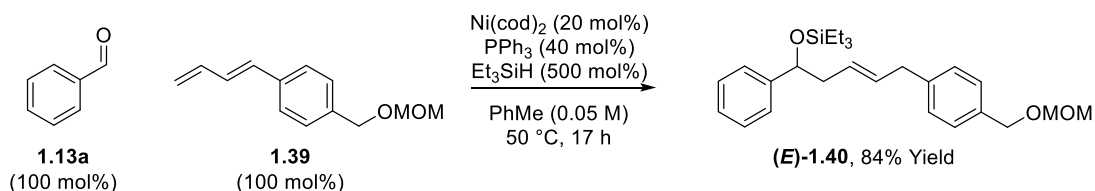
ratio suggests that, remarkably, the four-component coupling reaction is most efficient, and the alkyne and diene three component coupling reactions each occur at a slower rate. Simply increasing the equivalents of alkyne and diene resulted in favored formation of the four component coupling product **1.36** (Figure 1.6).¹²

Figure 1.6 Four component coupling of aldehyde, diene, alkyne and Me₂Zn reagent to furnish **1.36** in high yield.



As a lead contributor to the field of Ni catalyzed reductive couplings of dienes and carbonyl compounds, Tamaru et al. have developed a suite of Ni⁰ catalyzed diene-aldehyde reductive coupling reactions, employing organozinc or organoboron reagents as reductants to supply a hydride (by way of β-hydrodenickelation and C-H reductive elimination) or alkyl group (by C-C reductive elimination). The large structural variety of accessible products, high degree of (*E*):(*Z*) selectivity and mild conditions, give these reductive couplings broad appeal for carbon-carbon bond forming methodologies.¹³

Scheme 1.7 Nickel catalyzed homoallylation of aldehyde **1.13a** using 1-substituted dienes **1.39**.

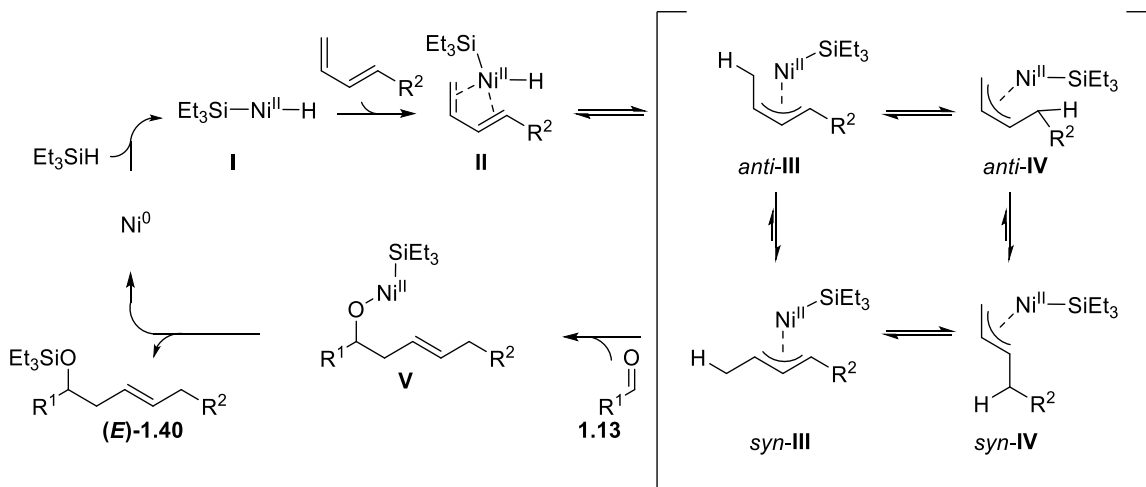


The Mori research group was also pursuing intra- and intermolecular reductive couplings of dienes and aldehydes. In 1998, they reported coupling 1-substituted dienes to aldehydes using

Ni^0 catalyst and Et_3SiH as a reductant. Exposure of **1.13a** and **1.39** to the reaction conditions produced homoallylic silyl ether (**E**)-**1.40** in high yield as a single regioisomer, with complete (*E*) olefin selectivity (Scheme 1.7).¹⁴

A proposed mechanism for this transformation is shown in Figure 1.7. Oxidative addition into the Si-H bond by the Ni^0 precatalyst generates Ni hydride **I**, which can hydrometallate the diene to generate an equilibrating mixture of *syn*- and *anti*- π -allyl isomers **III** and **IV**. Steric interactions between the metal center and allylic substituent likely favor the *syn* isomers. Insertion of aldehyde **1.13** into the Ni-carbon bond of the isomer with the most accessible termini (*syn*-**IV**) forms nickel alkoxide **V**, which generates **1.40** and the Ni^0 catalyst upon O-Si reductive elimination.

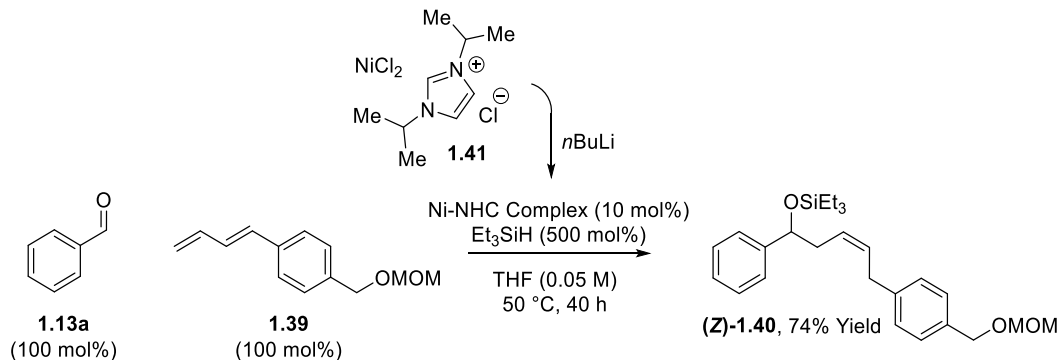
Figure 1.7 Proposed mechanism for formation of homoallylic silyl ether (**E**)-**1.40**.



In 2001, the Mori group reported a new advancement, in which an *N*-heterocyclic carbene (NHC) ligand conveyed a complete switch in the olefin selectivity, affording only the (*Z*)-homoallylic silyl ether.¹⁵ The nickel-NHC complex could be conveniently formed in situ by treating NiCl_2 and imidazolium salt **1.41** with *n*BuLi. Addition of aldehyde **1.13a** and diene **1.39**, and Et_3SiH to the catalyst resulted in product (**Z**)-**1.40**, exhibiting complete olefin stereochemistry (Scheme

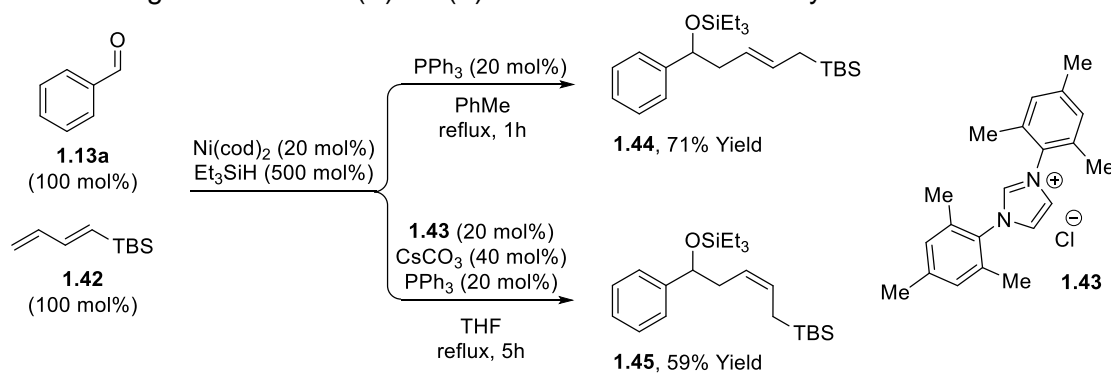
1.8). While the origins of the (*Z*) selectivity are not completely understood, this work suggests the NHC conveys different character to the catalyst than the phosphine ligands.

Scheme 1.8 Selective formation of (*Z*)-**1.40** using Ni-NHC catalyst



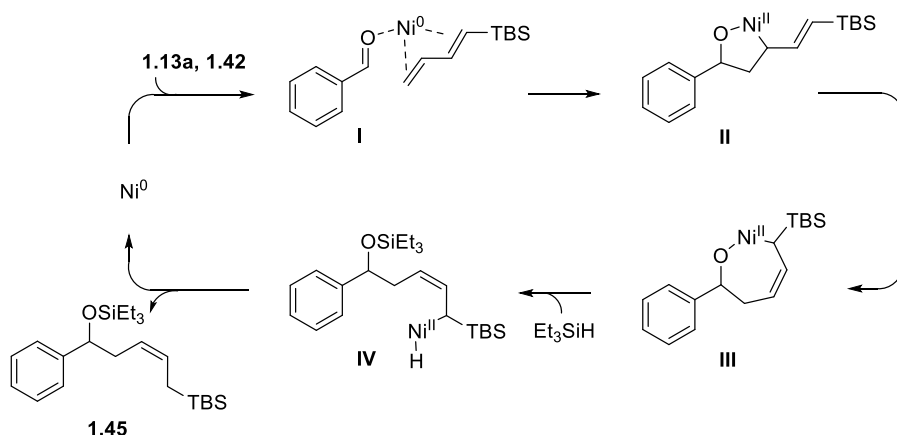
The ligand controlled (*E*)- and (*Z*)- selectivity was used for the formation of (*E*)- and (*Z*)-allyl silanes by coupling to 1-silyldiene **1.42**. For this system, the Ni-NHC complex displayed complete (*Z*)-selectivity, but diminished yield. Optimization of NHC (**1.43** was found to be superior to **1.41**) and reaction parameters improved yield slightly, but change in the color of the reaction from dark red to light red indicated that the nickel NHC complex suffered decomposition. The addition of PPh₃ was proposed to stabilize the Ni-NHC complex, while being labile enough to dissociate and allow reactivity to proceed through the Ni-NHC catalyst. This was found to be effective, maintaining a dark red color throughout the reaction and resulting in an improved yield. Due to the high (*Z*)-selectivity observed, it is proposed that the Ni-NHC complex is the active catalyst that forms upon dissociation of PPh₃ (Scheme 1.9).¹⁶

Scheme 1.9 Ligand controlled (*E*)- or (*Z*)-selective formation of allylsilanes **1.44** and **1.45**.



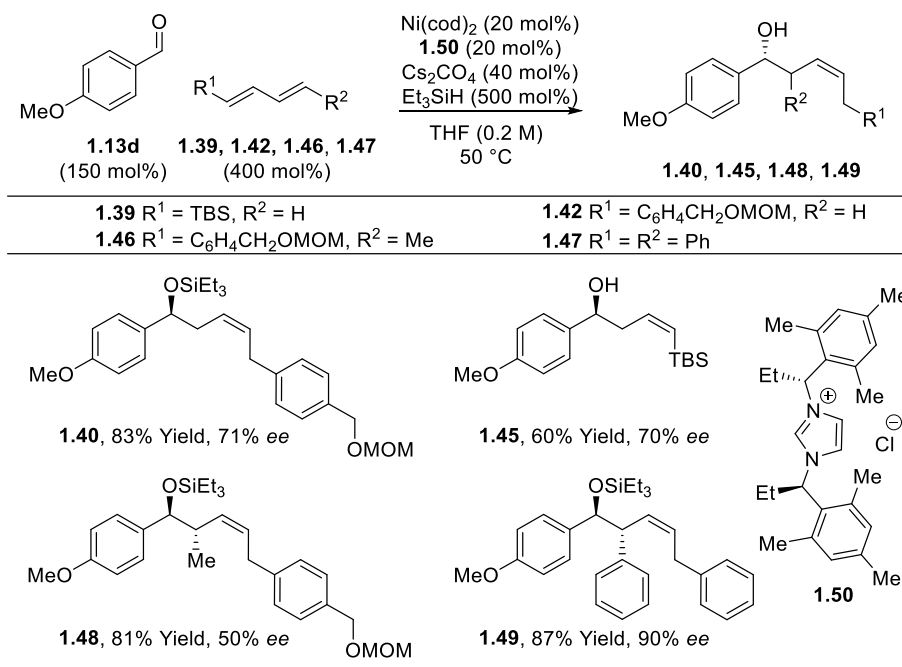
It was proposed that the inversion in selectivity to form the (*Z*)-isomer could be explained by an oxidative coupling mechanism catalyzed by the nickel NHC complex, in contrast to the hydrometallative pathway proposed to form the (*E*)-isomer. A potential route to access **1.45** is shown in Figure 1.8. Oxidative coupling of aldehyde **1.13a** and diene **1.42** via **I** leads to oxanickelacycle **II**, which can undergo a ring expansion to form **III**. Sigma bond metathesis of oxanickelacycle **III** with Et₃SiH would generate **IV**, and reductive elimination would furnish (*Z*)-silyl ether **1.45** and reform Ni⁰.

Figure 1.8 Oxidative coupling mechanism to explain (*Z*) olefin selectivity.



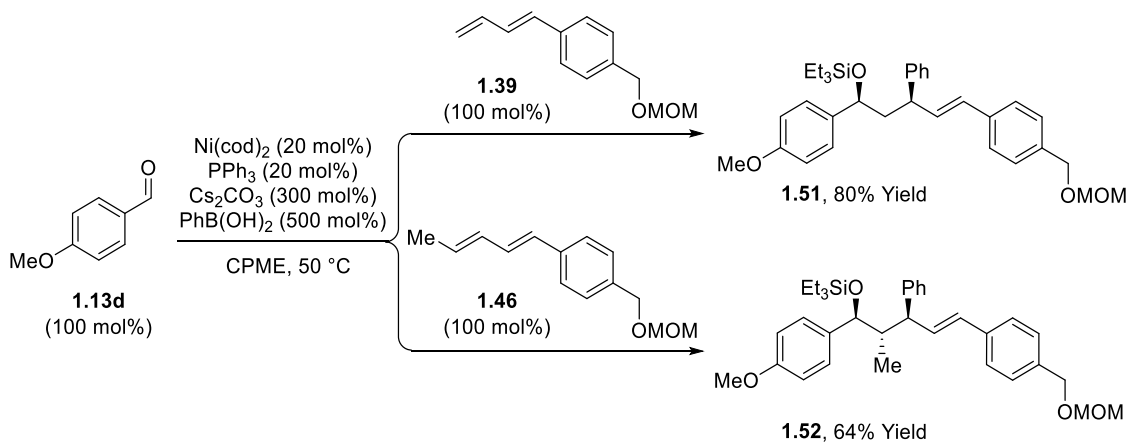
An enantioselective (*Z*)-selective homoallylation was reported by the Sato group, employing chiral NHC precursors. Coupling of aldehydes with 1-substituted and 1,4-substituted symmetric dienes was achieved, with good to excellent levels of enantiomeric induction.¹⁷ Dienes with aryl, silyl and alkyl substitution all performed well in the reaction. Notably, using nonsymmetric 1,4-substituted diene **1.46**, only one regio- and diastereoisomer was formed, although the enantiomeric excess was only moderate. The complete *anti*-diastereoselectivity is thought to be due to on all *trans* configuration of the nickelacycle formed upon oxidative coupling of aldehyde and diene (Figure 1.9).

Figure 1.9 Asymmetric (*Z*)-selective homoallylation of aldehyde **1.13d** using chiral NHC ligand derived from **1.50**.



Sato also proposed that using an organometallic reagent in place of Et₃SiH could facilitate a three component coupling reaction for functionalization at the allylic position. Adapting previously developed conditions to employ **1.43** as NHC precursor and PhB(OH)₂ in place of Et₃SiH, the three component coupling product was obtained in 43% yield and 6:1 *syn:anti* diastereoselectivity. It was found that by changing solvent from THF to cyclopentyl methyl ether

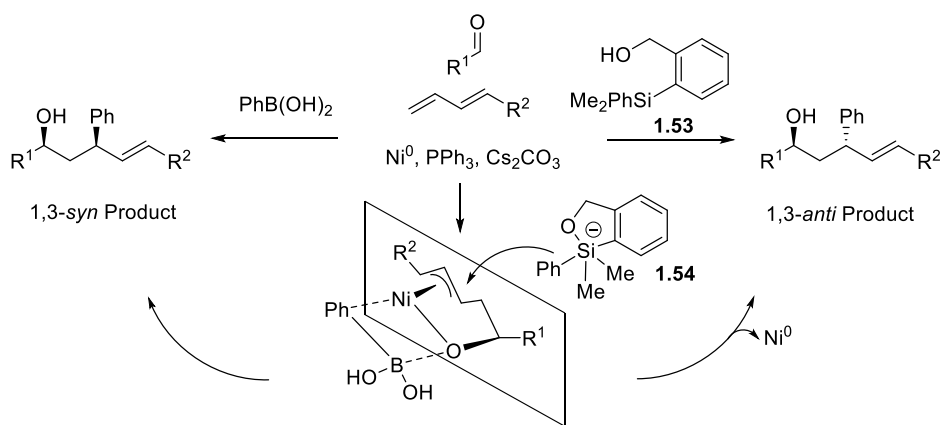
Scheme 1.10 Three component coupling using PhB(OH)₂.



and using PPh_3 as ligand in place of NHC generated from **1.50** improved yield and selectivity, forming only the 1,3-*syn*-diastereomer **1.51**. This reaction could also be used with nonsymmetric 1,4-disubstituted diene **1.46** to access an all *anti*-stereotriad **1.52** (Scheme 1.10).

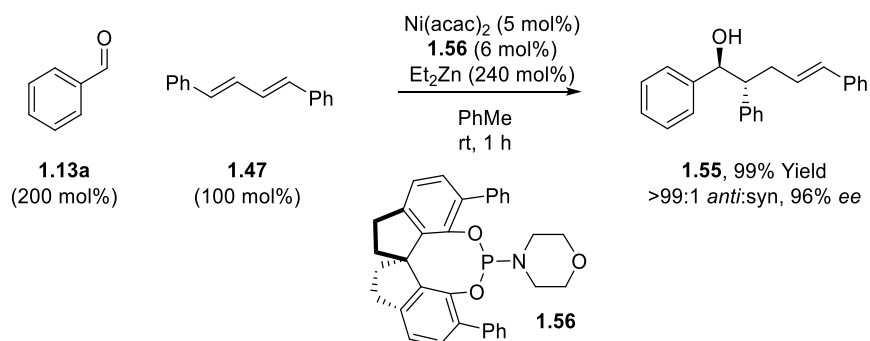
Remarkably, in evaluating other organometallic reagents for three component coupling, it was found that tetraorganosilicon reagent **1.53** was effective in the reaction, but changed selectivity to only form the 1,3-*anti*-diastereomer. The rationale for the complementary diastereoselectivity when using organoboron and organosilicon reagents is shown in Figure 1.10. On left, transmetalation from PhB(OH)_2 delivers the phenyl group to nickel, which can undergo reductive elimination to generate the 1,3-*syn* product. In contrast, silane **1.53** can generate silicate complex **1.54** under the reaction conditions. The phenyl group now adds to the Ni- π -allyl as a nucleophile and displaces Ni, resulting in inversion of the stereocenter to generate the 1,3-*anti* product.

Figure 1.10 Ligand controlled (*E*)- or (*Z*)-selective formation of allylsilanes.



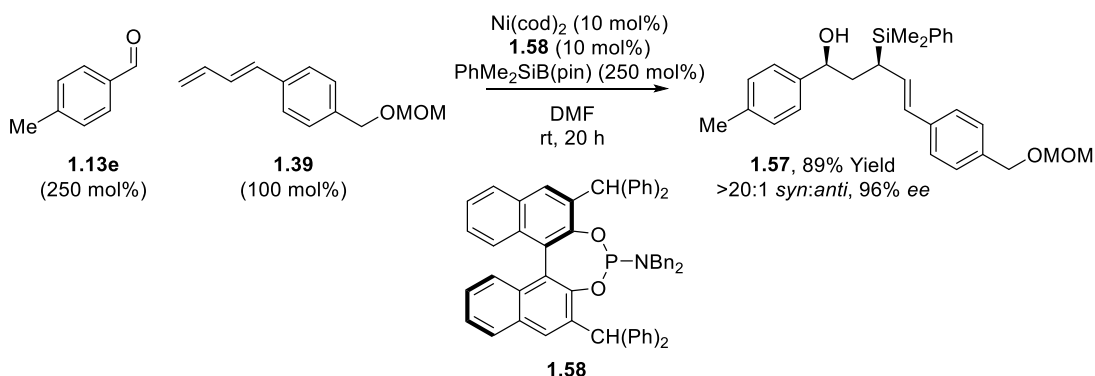
In 2007, Zhou et al. developed a class of chiral spiro phosphoramidite ligands for asymmetric catalysis. Application to nickel catalyzed reductive coupling yielded an asymmetric homoallylic alcohol synthesis by coupling 1,4-diphenyldiene **1.47** and aldehydes using **1.56** as ligand (Scheme 1.11).¹⁸

Scheme 1.11 Application of chiral spiro phosphoramidite ligand for diastereo- and enantioselective homoallylation of aldehyde.



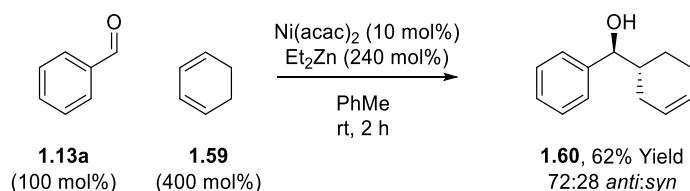
Also using a chiral phosphoramidite ligand, Sato et al. accessed enantiopure α -chiral silanes by three component coupling of dienes, aldehydes and $\text{PhMe}_2\text{SiB}(\text{pin})$. It was found that (*R*)-BINOL derived **1.58** produced a single regioisomeric product **1.57** in complete diastereoselectivity and very high enantioselectivity (Scheme 1.12). In this reaction, transfer of the silyl group from boron to nickel followed by reductive elimination installs the α -silyl group.¹⁹

Scheme 1.12 Enantioselective three component coupling of 1,3-diene **1.39**, aldehyde **1.13e** and silylborane to generate α -chiral allylsilane.



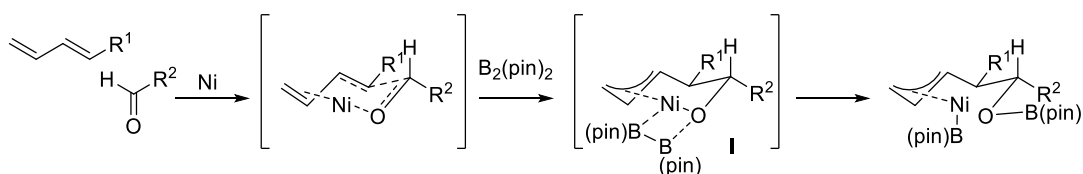
In the development of diene-carbonyl coupling by Tamaru, Mori and Sato, only linear dienes had been studied. Inspired by the need for enantiopure allylic alcohol for indium catalyzed tetrahydropyran cyclizations,²⁰ the Loh group investigated coupling cyclic dienes to aldehydes under nickel catalysis. Using $\text{Ni}(\text{acac})_2$ and Et_2Zn the γ,δ -alkenyl alcohol was formed in good yield, albeit with moderate *anti:syn* selectivity (Scheme 1.13).

Scheme 1.13 1,3-cyclohexadiene **1.59** engages in reductive coupling with aldehydes under Ni catalysis.



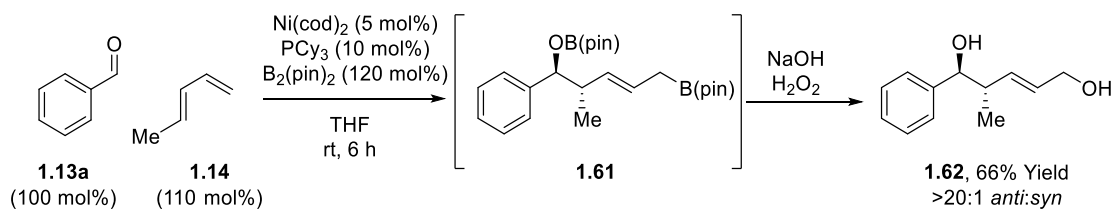
Further development of three component coupling reactions has been contributed by the Morken group. They disclosed that a diboron reagent, $\text{B}_2(\text{pin})_2$, could be used to cleave nickelacycle **I** formed upon diene-aldehyde coupling (Scheme 1.14).

Scheme 1.14 Application of $\text{B}_2(\text{pin})_2$ to cleave nickelacycle intermediate.



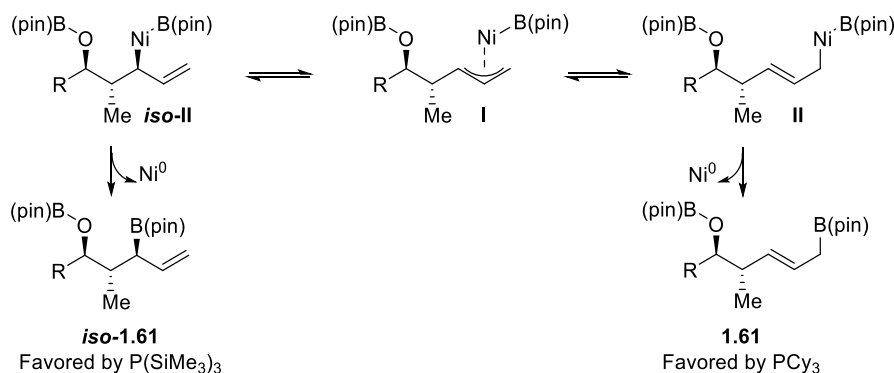
This delivers an organoboronic ester product **1.61**, which yields functionalized homoallylic alcohol **1.62** in good yield and excellent diastereoselectivity after oxidative workup (Scheme 1.15).²¹

Scheme 1.15 Three component coupling of aldehyde, diene, and $\text{B}_2(\text{pin})_2$ to access homoallylic diols.



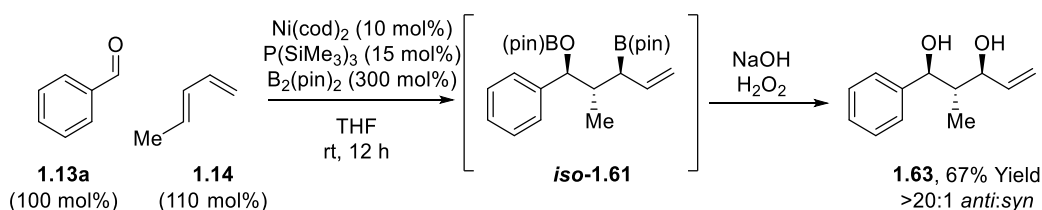
Ligand optimization identified PCy_3 to be highly effective, producing **1.62** as a single regioisomer. The observed selectivity is due to C-B(pin) reductive elimination to the more accessible terminal position of the nickel allyl intermediate. In 2010, the Morken group reported that a different ligand, $\text{P}(\text{SiMe}_3)_3$, drastically reversed this regioselectivity (Figure 1.11).

Figure 1.11 Ligand dependent divergent pathways of coupling aldehyde and diene **1.14** to access both internal and terminal boronates **1.61** and *iso*-**1.61**.



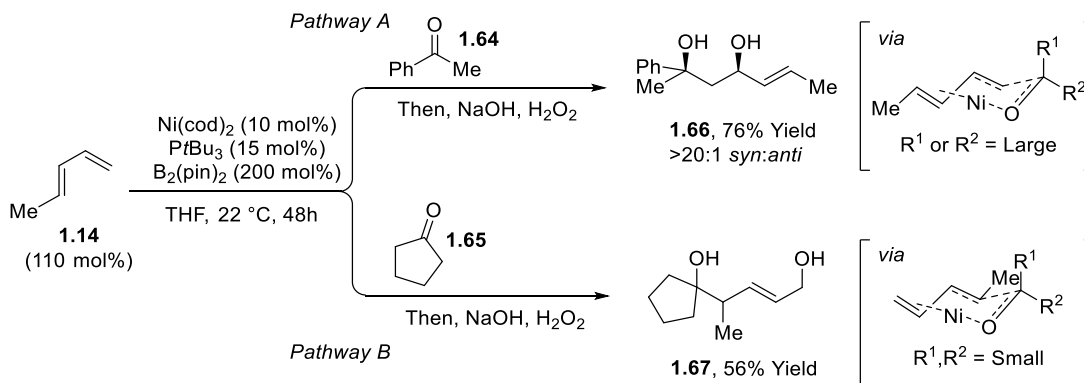
While the effects are not completely understood, it is proposed that the large size of $P(\text{SiMe}_3)_3$ and its electron accepting character may promote reductive elimination via *iso-II* (Figure 1.11), by restricting isomerization back to *I*. Optimization of reaction conditions allowed for complete partitioning of reaction pathways to generate product *iso*-**1.61** in good yield and complete regio- and diastereoselectivity (Scheme 1.16).²²

Scheme 1.16 α -chiral allylboronate formation using $P(\text{SiMe}_3)_3$ as ligand and subsequent stereotriad formation after workup.



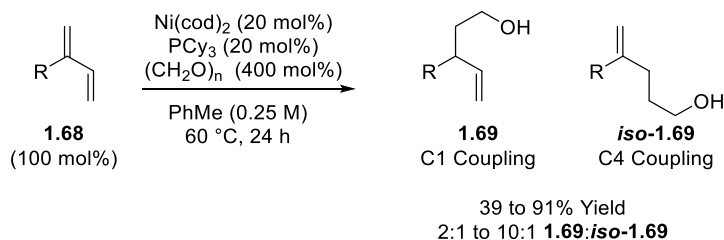
This borylative aldehyde-diene coupling was applied to aryl and alkyl ketones. Under identical conditions, substrate dependent regioselectivity was observed. This difference was proposed to be related to the steric demand of the ketone, where non-hindered carbonyls (aldehydes and dialkyl ketones) react through pathway B to form **1.67**, and carbonyls with larger substituents (aryl ketones) react through pathway A with inversion of the diene to form **1.66** (Scheme 1.17).²³

Scheme 1.17 Ligand controlled (*E*)- or (*Z*)-selective formation of allylsilanes.



Finally, a collaboration between the Breit and Krische groups reported Ni^0 catalyzed coupling of paraformaldehyde and 2-substituted butadienes (**1.68**) in 2013.²⁴ In contrast to previously discussed methods that require an organometallic reductant, paraformaldehyde can act as both electrophile and reductant in this reaction. Using $\text{Ni}(\text{cod})_2$, PCy_3 and Cs_2CO_3 , the product of C1 coupling was obtained in high yield (Scheme 1.18).

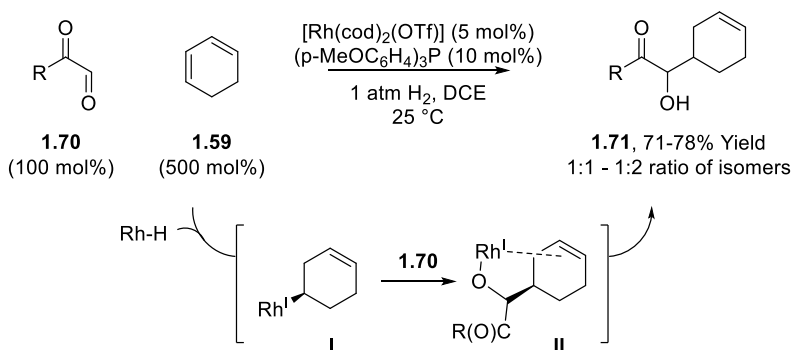
Scheme 1.18 Coupling of dienes and paraformaldehyde, where paraformaldehyde serves dual role as aldehyde and reductant.



1.3 Rhodium Catalysis

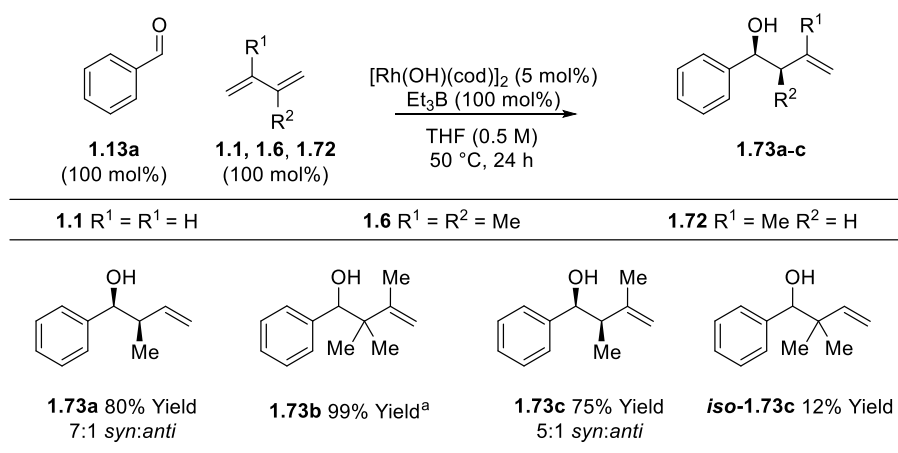
Inspired by the rhodium catalyzed reductive coupling of α -olefins, carbon monoxide, and hydrogen gas for hydroformylation, the Krische group began exploring the extension of coupling π -unsaturates to higher aldehydes under hydrogenative conditions.²⁵ The Rh hydride species formed by exposure of precatalyst $\text{Rh}(\text{cod})_2\text{OTf}$ to H_2 gas can hydrometallate a π -unsaturate. Interception of the resulting organorhodium species by an aldehyde enabled the reductive coupling of 1,3-cyclohexadiene **1.59** and glyoxal derivatives **1.70**.²⁶ (Scheme 1.19)

Scheme 1.19 Reductive coupling of cyclohexadiene **1.59** and glyoxal **1.70** via hydrometallation of **I** and aldehyde insertion to form **II**.



After studying nickel catalyzed reductive coupling of dienes and aldehydes, Kimura et al. reported a rhodium catalyzed variant, exhibiting an interesting change in regioselectivity. Exposure of a 1:1 ratio of aldehyde and diene to $[\text{Rh}(\text{OH})(\text{cod})]_2$ and Et_3B furnished product of C-C coupling at the C2 diene position, favoring the *syn*-isomer. For nonsymmetric 2-substituted dienes, coupling at the less substituted 3 position was favored. 2,3-dimethylbutadiene and cyclic dienes were also suitable substrates, as well as cyclic hemiacetals as aldehyde precursor (Figure 1.12).²⁷

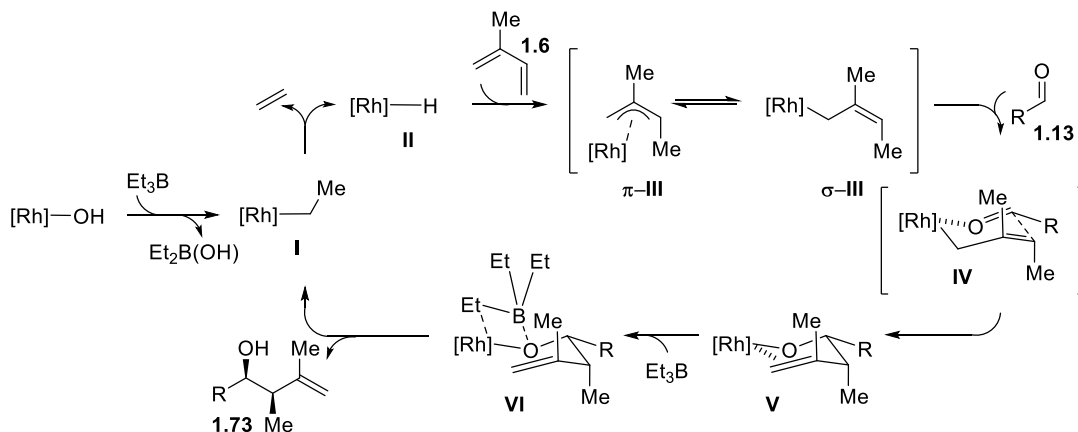
Figure 1.12 Rh catalyzed benzaldehyde coupling with various dienes, exhibiting high levels of regioselectivity.



A plausible mechanism for the transformation is shown in Figure 1.13. Transmetalation of $\text{Rh}(\text{OH})$ with Et_3B generates Rh ethyl complex **I**, and β -hydride elimination forms Rh hydride **II**.

Hydrometallation of diene **1.6** forms rhodium allyl complexes π -III and σ -III, and coordination of aldehyde **1.13** generates a six-membered, chair-like transition state **IV**, which forms Rh alkoxide **V** upon carbonyl addition. The diastereoselectivity is likely due to participation of the more stable (*Z*)- σ -allyl isomer in the C-C bond forming step. σ -Bond metathesis of the ruthenium alkoxide **V** and Et₃B reforms the Ru-ethyl complex **I** and releases product **1.73**.

Figure 1.13 Proposed mechanism for Rh catalyzed diene-aldehyde coupling.



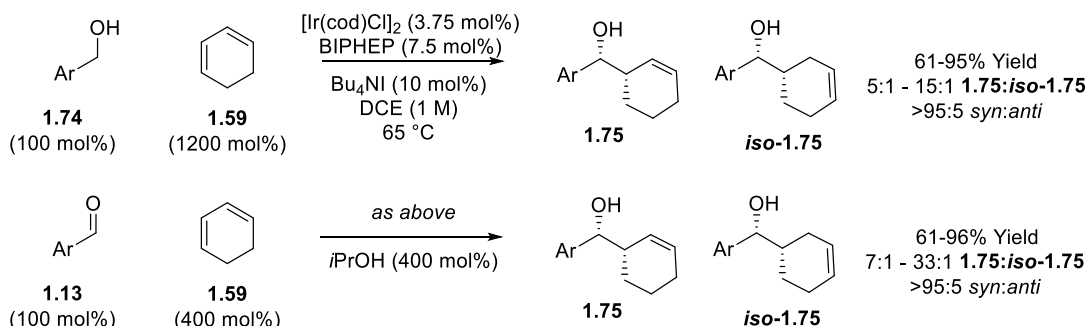
The observed C2 coupling for the rhodium catalyzed reaction is likely due to a hydrometallative mechanism, in contrast to the nickel catalyzed oxidative coupling described previously for C1 coupling.

1.4 Iridium Catalysis

Encouraged by the carbonyl-unsaturate reductive couplings using rhodium, the Krische group began investigating similar processes under conditions of hydrogenative iridium catalysis.²⁵ Using $[\text{Ir}(\text{cod})\text{Cl}]_2$, BIPHEP and Bu_4NI , the coupling of cyclohexadiene **1.59** and aromatic aldehydes was achieved (Scheme 1.20). In this reaction, elemental hydrogen was replaced by isopropanol, a terminal reductant containing an embedded molecule of hydrogen. This transfer hydrogenative protocol allows for better control of the amount of hydrogen present in the reaction, preventing side products of over-reduction. A “hydrogen auto-transfer” protocol was also developed, in which a primary alcohol serves both as hydrogen source and carbonyl precursor.

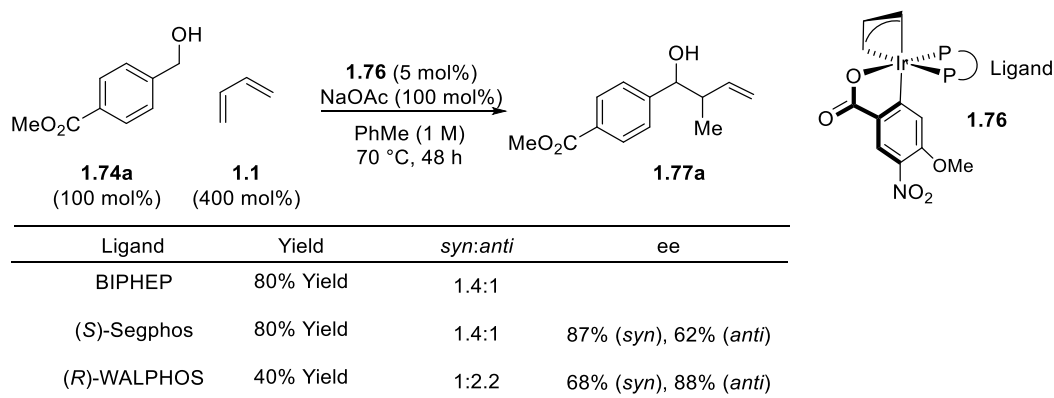
This reaction constitutes a formal carbinol C-H functionalization and is redox neutral, in which oxidation of the primary alcohol to aldehyde is accompanied by reductive coupling to furnish the product of homoallylation.

Scheme 1.20 Reductive coupling of cyclohexadiene **1.59** and aldehyde **1.13** and redox neutral process using a primary alcohol **1.74** as aldehyde precursor.



It was found that addition of NBu_4I improved diastereoselectivity and limited formation of *iso-1.75*. While the effect is not fully understood, the formation of *iso-1.75* appeared to be the result of hydrometallative olefin migration.

Figure 1.14 Cyclometallated iridium complex **1.76** used to access product of crotylation **1.77a** by coupling primary alcohol **1.74a** and butadiene.



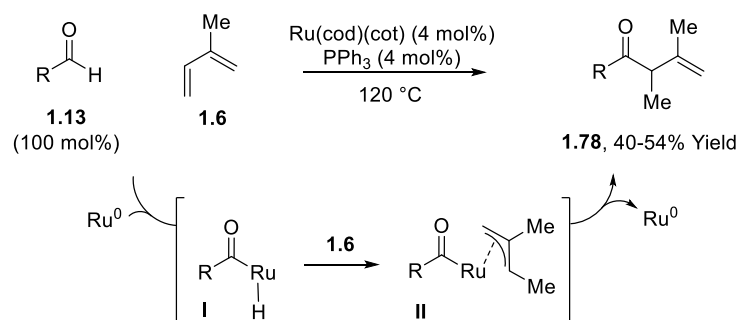
The concept of performing redox neutral C-H functionalization by way of a merged oxidation and reductive coupling manifold became a central focus of research in the Krische group. Another example of this is the iridium-catalyzed hydrohydroxyalkylation of butadiene to

access products of carbonyl crotylation. Despite poor diastereoselectivity, the cyclometallated iridium complex **1.76** resulted in high enantioselectivity (Figure 1.14).²⁸

1.5 Ruthenium Catalysis

Ruthenium catalysts were also found to be effective at reductive coupling of aldehydes and dienes. The first report, in 1998 by Kondo and Mitsudo, was the hydroacylation of aromatic aldehydes using isoprene or 1,3-pentadiene. Using Ru(cod)(cot) precatalyst and PPh₃, the product of hydroacylation was obtained in moderate yield.

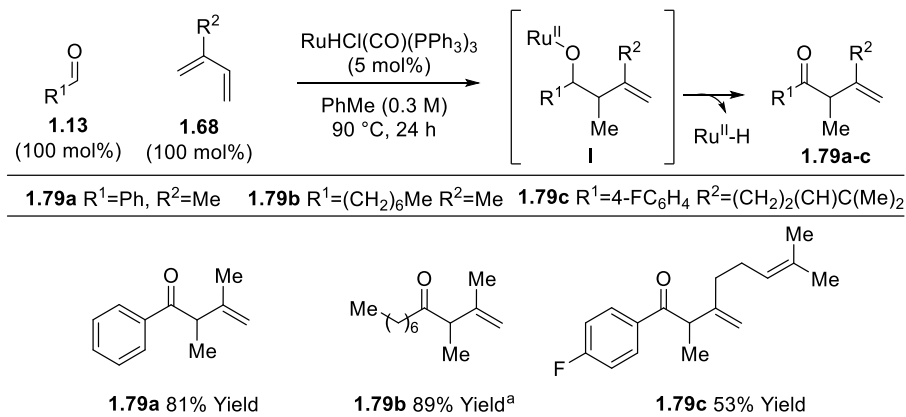
Scheme 1.21 Hydroacylation of aromatic aldehydes with isoprene.



The reaction is proposed to proceed by way of oxidative addition into the aldehyde C-H bond by Ru^0 (Scheme 1.21). The resulting acyl ruthenium hydride **I** can hydrometallate diene **1.6**, and regioselective reduction of the ruthenium-acyl complex **II** generates the β,γ -unsaturated ketone **1.78**.

A decade later, another ruthenium catalyzed hydroacylation of dienes was reported by Ryu et al. A similar product was obtained using $\text{RuHCl}(\text{CO})(\text{PPh}_3)_3$ under much more mild conditions with better yield and greater substrate scope tolerance. The reaction is proposed to occur by generation of a nucleophilic ruthenium allyl upon diene hydrometallation. After aldehyde addition, β -hydride elimination of the ruthenium alkoxide **I** (Figure 1.15) reforms the C-O double bond, releasing product **1.79** and regenerating the Ru hydride catalyst.²⁹

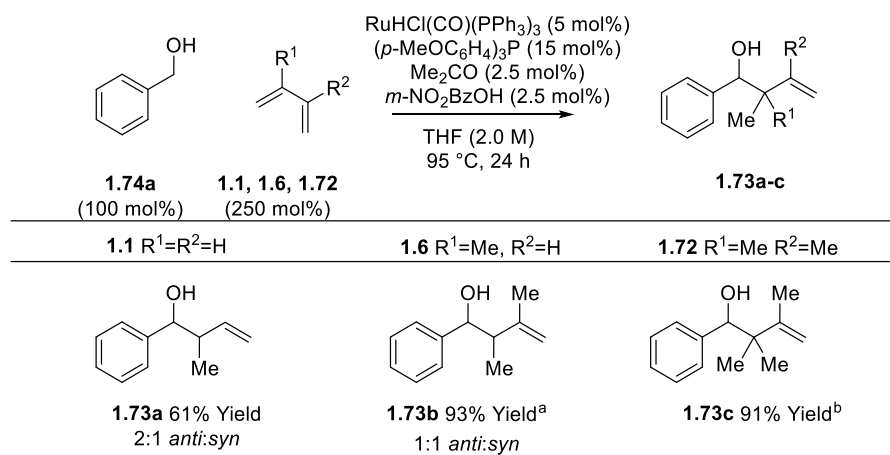
Figure 1.15 Hydroacylation under mild conditions using $\text{RuHCl}(\text{CO})(\text{PPh}_3)_3$.



^a20 mol% catalyst

Using a similar catalytic system, the Krische group also began investigating ruthenium catalyzed reductive coupling of dienes and aldehydes and the redox neutral coupling of dienes and primary alcohols under transfer hydrogenative conditions. Using $\text{RuHCl}(\text{CO})(\text{PPh}_3)_3$ and various phosphine ligands, it was found that primary aromatic alcohols would couple to butadiene, isoprene, and 2,3-dimethylbutadiene to furnish homoallylic alcohols in high yield.³⁰ The addition

Figure 1.16 Redox neutral coupling of dienes and primary alcohols to generate homoallylic alcohol products.



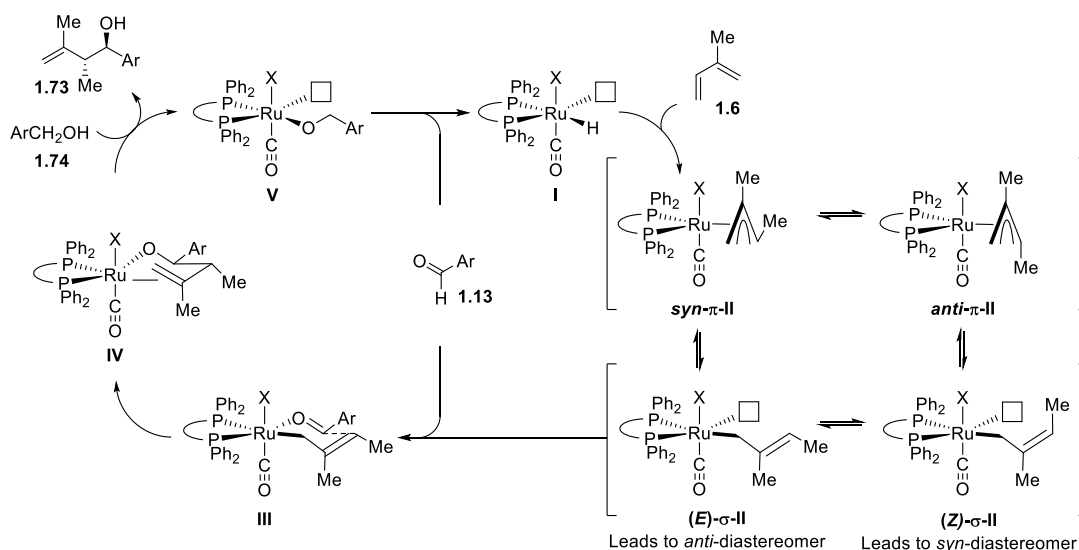
^a*rac*-BINAP (5 mol%) used in place of *(p*-OMePh)₃P ^b110 °C

of phosphine ligand was an important difference between the homoallylation and hydroacylation reported by Ryu.²⁹ It was postulated that the added phosphine ligand can coordinate the catalyst,

blocking an open coordination site required for β -hydride elimination to generate the ketone (Figure 1.16).

A plausible catalytic mechanism is shown in Figure 1.17 (where X=Cl). Hydrometallation of diene **1.6** by Ru hydride **I** generates (*E*)- and (*Z*)- σ -allyl isomers ((*E*)- σ -II and (*Z*)- σ -II), which can equilibrate by way of the pi-allyl intermediates *syn*- π -II and *anti*- π -II. Coordination of the aldehyde substrate generates transition state III to furnish ruthenium alkoxide IV. Protonation of IV with an equivalent of the primary alcohol **1.74** releases the product of aldehyde-diene coupling **1.73** and generates Ru alkoxide V, which can undergo β -hydride elimination to produce the aldehyde coupling partner **1.13** and Ru hydride catalyst **I**. Diastereoselectivity in this process was proposed to be dependent on the σ -allyl isomer that participates in carbonyl addition, in which the (*E*)-isomer leads to the *anti*-product and the (*Z*)-isomer leads to the *syn*-product. Diene substrates butadiene and isoprene exhibited poor diastereoselectivity, suggesting that both σ -allyl isomers are active in carbonyl addition.

Figure 1.17 Proposed mechanism for reductive coupling of isoprene and an aldehyde by ruthenium hydride catalyst.

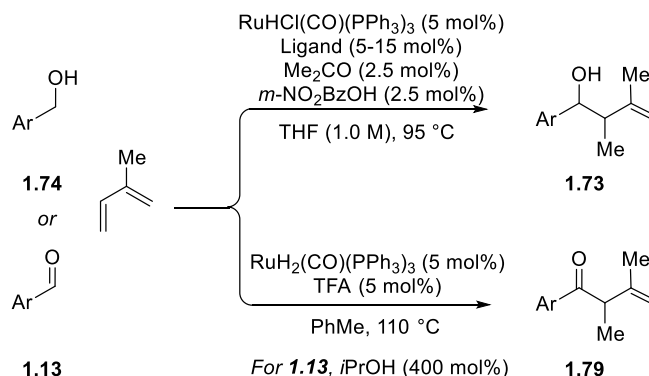


As the reaction conditions for homoallylation were not drastically different from those reported by Ryu et al.²⁹ for hydroacylation of dienes, it was reasoned that similar products of

hydroacylation could be accessed by ruthenium catalyzed coupling of dienes and primary alcohols. It was proposed that the coordinative saturation of Ru intermediate **IV** (Figure 1.12) prevents β -hydride elimination from occurring.

Employment of $\text{RuH}_2(\text{CO})(\text{PPh}_3)_3$ in combination with TFA in PhMe at higher temperature led to the products of hydroacylation in good yield (Scheme 1.23).³¹ It is proposed that the basic Ru hydride can participate in an acid-base reaction with the acid additive, releasing H_2 gas and producing a cationic Ru-center coordinated by the conjugate base of the acid. A loosely associated counter ion would provide an open coordination site for β -hydride elimination to occur at **IV** (Figure 1.17, where X is a non-coordinating counter ion), enabling a hydroacylation pathway. This work demonstrated that either primary alcohol or aldehyde can be used as substrate to generate either homoallylation or hydroacylation product. (Scheme 1.22)

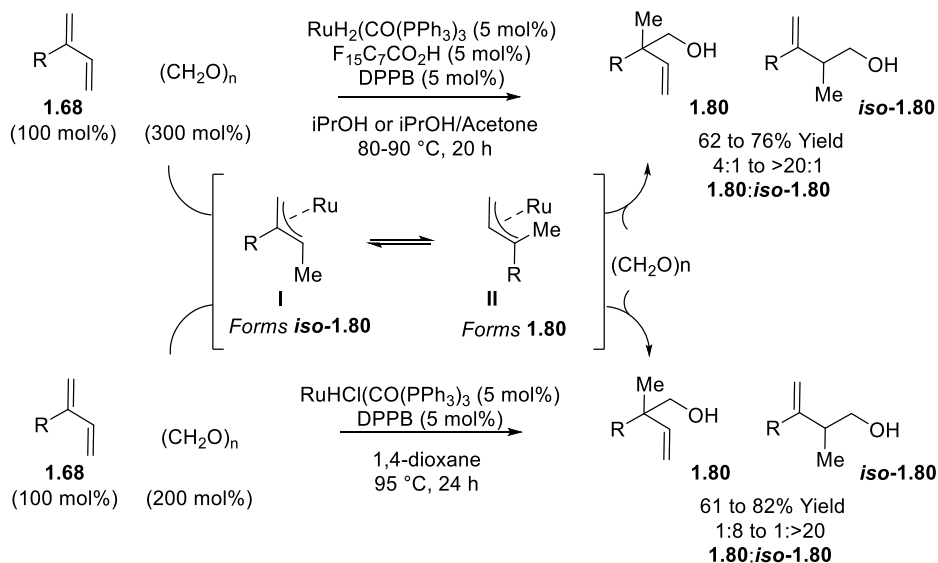
Scheme 1.22 Transfer hydrogenative allylation and hydroacylation of primary alcohols or aldehydes under ruthenium catalysis.



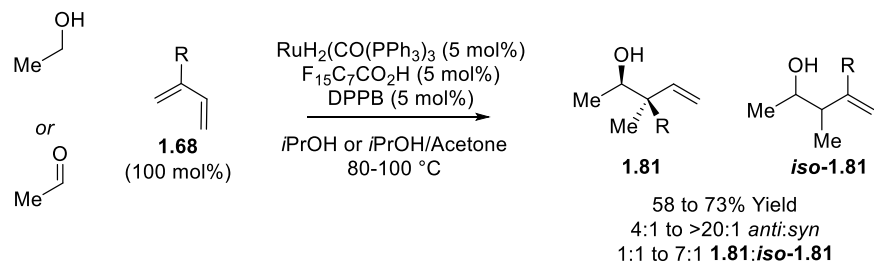
In evaluating the difference in reactivity of the cationic and neutral Ru complexes, an interesting effect was observed when coupling 2-substituted diene **1.68** with paraformaldehyde. Using $\text{RuHCl}(\text{CO})(\text{PPh}_3)_3$ and DPPB as ligand, coupling at the C3 position was favored (Figure 1.19, bottom).²⁴ Using the catalyst formed in situ from $\text{RuH}_2(\text{CO})(\text{PPh}_3)_3$, $\text{F}_{15}\text{C}_7\text{CO}_2\text{H}$ and DPPB, coupling at the C2 position was favored, generating an all-carbon quaternary center upon addition to paraformaldehyde. The inversion in regioselectivity is proposed to be founded in the open coordination site at Ru when using a cationic catalyst. This could facilitate Ru- π -allyl

interconversion, generating σ -allyl isomer **II** that will result in formation of an all-carbon quaternary center (**1.80**) instead of isomer **I**, which leads to the branched regioselectivity seen in **iso-1.80** (Figure 1.18).³²

Figure 1.18 Dependence of regiochemical outcome on ruthenium catalyst in coupling 2-substituted dienes **1.68** and paraformaldehyde.



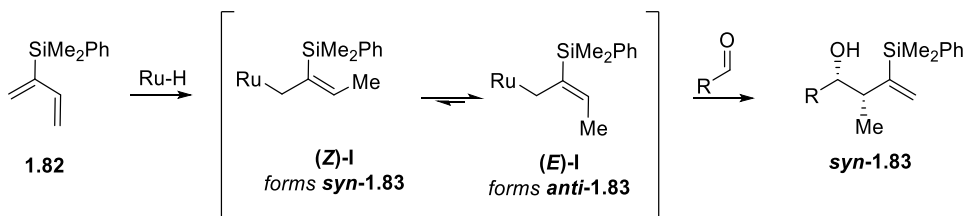
Scheme 1.23 Coupling of ethanol and acetaldehyde to 2-substituted dienes **1.68** to form homoallylic alcohols **1.81** containing all-carbon quaternary centers.



Another example of C2 and C3 diene regioselectivity was observed in the coupling of 2-substituted dienes and ethanol. Using the cationic ruthenium complex generated from $\text{RuH}_2(\text{CO})(\text{PPh}_3)_3$, DPPB and $\text{F}_{15}\text{C}_7\text{CO}_2\text{H}$, the isomer containing an all-carbon quaternary center

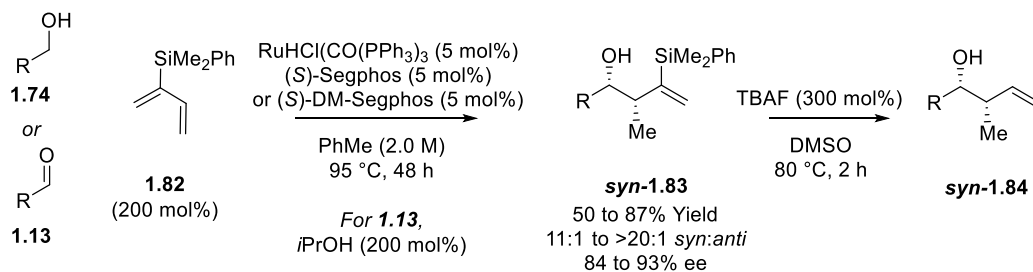
was generally formed, in good to high levels of diastereoselectivity. Analogous results were obtained from the corresponding reaction with acetaldehyde (Scheme 1.23).³³

Scheme 1.24 Silyl group of **1.82** effects diastereoselectivity based on stability of (*Z*)- and (*E*)- σ -allyl isomer.



With the development of catalytic systems to couple alcohols and dienes to access products of aldehyde addition, attention was focused to develop a method to generate the product of carbonyl crotylation. In previous work with butadiene, it was postulated that aldehyde addition by both (*E*)- and (*Z*)- σ -allyl isomers, formed upon hydrometallation of the diene, was responsible for the poor diastereoselectivity (Figure 1.18). In an effort to bias the energetic stability of the (*E*)- and (*Z*)-isomers to preferentially react through one pathway, 2-silylbutadiene **1.82** was prepared and evaluated in the coupling reaction (Scheme 1.24).

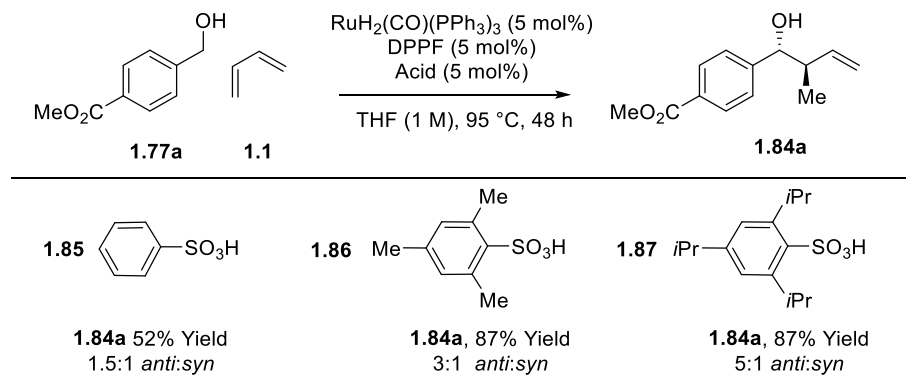
Scheme 1.25 Enantioselective *syn*-crotylation products from coupling primary alcohol or aldehyde and 2-silylbutadiene.



Using diene **1.52**, high levels of *syn*-diastereoselectivity were obtained due to the steric interactions that destabilize (*E*)-I (Scheme 1.25). In the presence of (*S*)-Segphos or (*S*)-DM-Segphos, high levels of enantioselectivity were obtained.³⁴ Upon obtaining **1.83**, in situ protodesilylation could reveal the crotylation product **syn-1.84** (Scheme 1.25).

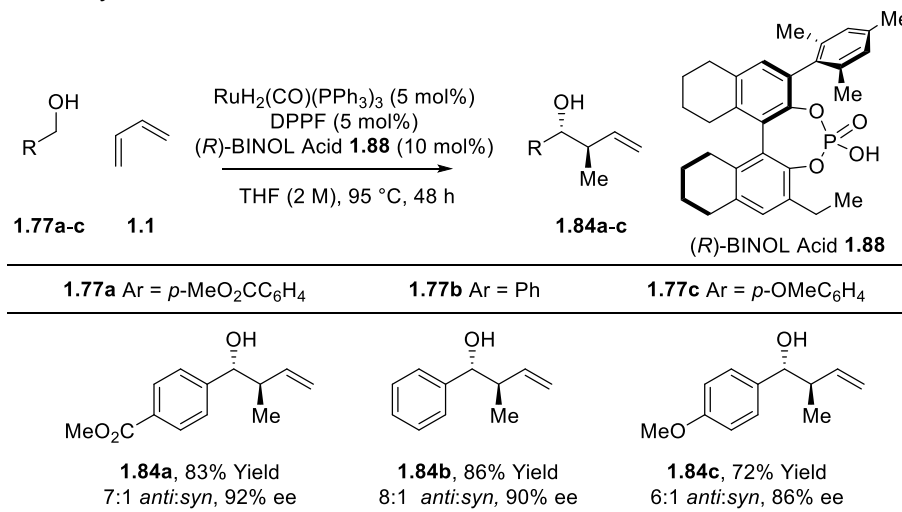
While employment of 2-silylbutadiene **1.82** resulted in a highly selective *syn*-crotylation methodology, the direct hydrogenative coupling of butadiene to an aldehyde would be an attractive alternative. As an inexpensive, abundant feedstock chemical, butadiene is an ideal crotyl donor. Previous iridium and ruthenium catalyzed coupling to butadiene resulted in a diastereomeric mixture of products, but it was found that careful selection of a ruthenium counter ion could enable a diastereoselective process. By treating $\text{RuH}_2(\text{CO})(\text{PPh}_3)_3$ with various sulfonic acids to introduce a sulfonate counter ion, it was found that *anti*-diastereoselectivity increased as the size of the counter ion increased (Figure 1.19). This suggested that the counter ion can partition the (*E*)- and (*Z*)- σ -allyl isomers formed upon hydrometallation of butadiene, shifting reactivity through a single pathway to favor formation of a single diastereomer.

Figure 1.19 Effect of sulfonate counter ion on diastereoselective coupling of butadiene and primary alcohol.



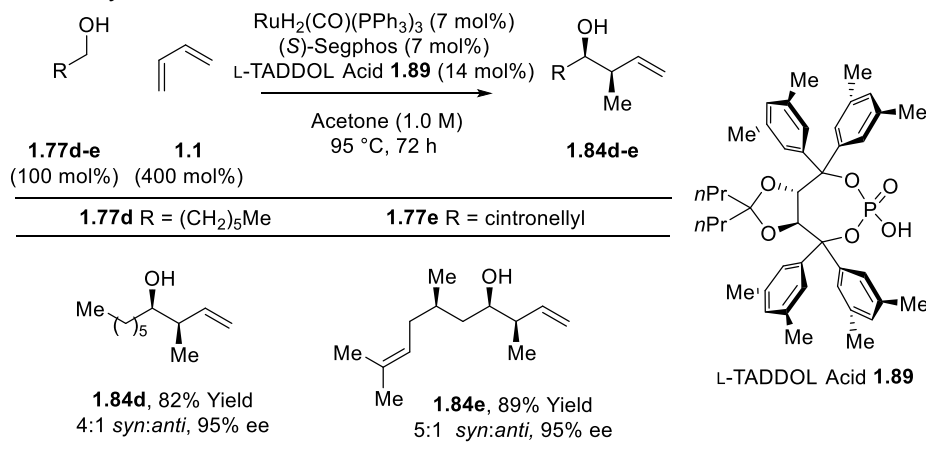
It was proposed that a chiral acid could influence both diastereoselectivity and enantioselectivity in the same way. To probe this hypothesis, phosphoric acids derived from (*R*)-BINOL were prepared and evaluated. C_1 -symmetric, H_8 -BINOL phosphoric acid **1.88** with mesityl and ethyl substitutes at the 3 and 3' positions resulted in high levels of *anti*-diastereoselectivity and enantioselectivity for aromatic alcohols and aldehydes (Figure 1.20).³⁵

Figure 1.20 *Anti*-Crotylation using butadiene, displaying (*R*)-BINOL phosphate counter ion controlled selectivity.



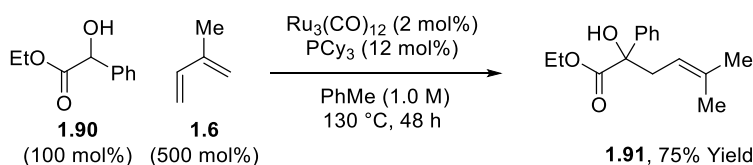
To improve the scope of the reaction, TADDOL derived phosphoric acids were also prepared and evaluated. Remarkably, it was found that for aliphatic alcohols, TADDOL-derived phosphoric acid **1.89** exhibited match/mismatch effects with (*S*) and (*R*) chiral ligands to access the product of *syn*-crotylation in good diastereoselectivity and excellent enantioselectivity (Figure 1.21). In comparing the BINOL and TADDOL phosphoric acids, it was found that both absolute and relative stereochemistry were inverted, independent of the ligand used.³⁶ These methods demonstrate the utility and versatility of chiral phosphoric acids for asymmetric catalysis.

Figure 1.21 *Syn*-Crotylation using butadiene, displaying L-TADDOL-phosphate counter ion controlled selectivity.



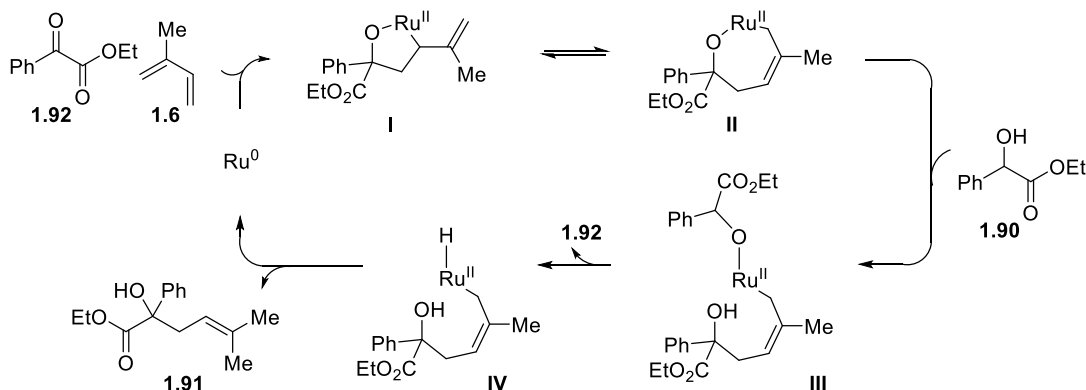
Extension of the ruthenium catalyzed diene coupling to ketones was accomplished by the development of a new catalytic system using $\text{Ru}_3(\text{CO})_{12}$ as precatalyst. Encouraged by literature precedence showing this catalyst was capable of transfer hydrogenations of α -keto amides and oxidative coupling of α -keto esters,³⁷ similar conditions, employing $\text{Ru}_3(\text{CO})_{12}$ and PCy_3 as ligand, were attempted for the hydrogenative carbon-carbon bond formation between ethyl mandelate **1.90** and isoprene. Remarkably, product of ketone addition **1.91** was obtained, exhibiting complete regioselectivity at the C4 position (Scheme 1.26).³⁸

Scheme 1.26 *n*-Prenylation of ethyl mandelate **1.90** using isoprene.



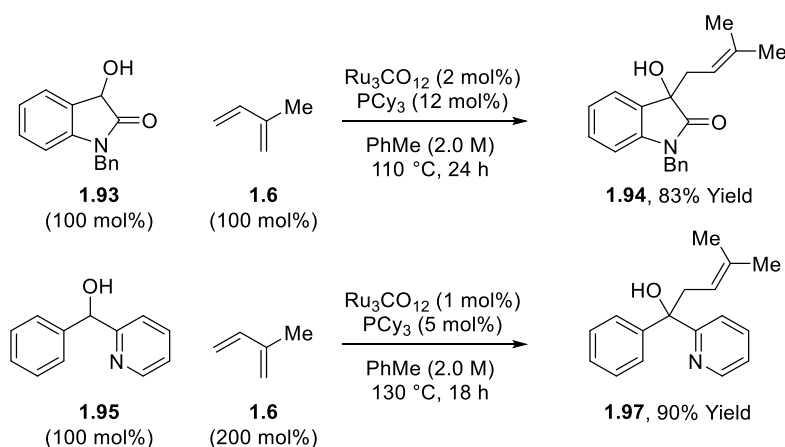
The product regioselectivity suggested that an oxidative coupling mechanism was occurring, in which coupling of α -keto ester **1.92** (formed upon ruthenium catalyzed oxidation of **1.90**) and isoprene would form oxaruthenacycle **I** (Figure 1.22). Isomerization to ruthenacycle **II** may be favored by formation of a primary, rather than secondary, σ -allyl ruthenium isomer. Protonation of the ruthenacycle by the α -hydroxy ester **1.90** would result in **III**, which, upon β -hydride elimination, forms **1.92** and **IV**. Reductive elimination would release product **1.91** of *n*-prenylation and reform Ru^0 catalyst.

Figure 1.22 Proposed mechanism for *n*-prenylation of ethyl mandelate **1.90**.



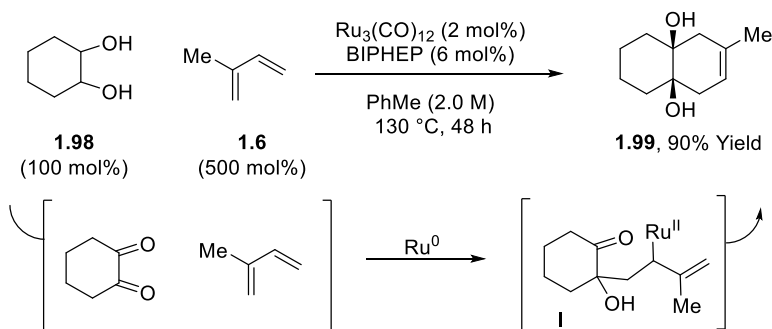
In further development of this reaction, it was identified that a 1,2-dicarbonyl derivative was required for oxidative cyclization. Related systems were also effective coupling partners, including 3-hydroxyoxindole **1.93**³⁹ and phenyl-(2-pyridyl)-methanol **1.95** and other phenyl-(2-heterocyclic)-methanols.⁴⁰ All exhibited C4 coupling to access *n*-prenylated products **1.94** and **1.97** in high yield (Scheme 1.27).

Scheme 1.27 Coupling of 3-hydroxyoxindole **1.93** and phenyl-(2-pyridyl)-methanol **1.95** and isoprene to generate *n*-prenylated products **1.94** and **1.97**.



It was reasoned that 1,2-diols could form 1,2-dicarbonyl compounds upon oxidation by the ruthenium catalyst. The conditions for *n*-prenylation of α -hydroxy esters was applied to this class of substrates, and remarkably, a formal [4+2] cycloaddition product **1.99** was obtained.⁴¹ This was proposed to occur by first *n*-prenylation of one of the ketones to form **I** (Scheme 1.28), followed by intermolecular ruthenium catalyzed allylation.

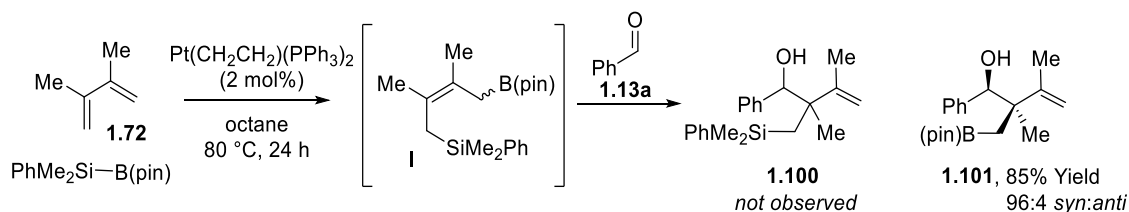
Scheme 1.28 Formal [4+2] cycloaddition by coupling 1,2-diol **1.98** with isoprene.



1.6 Platinum Catalysis

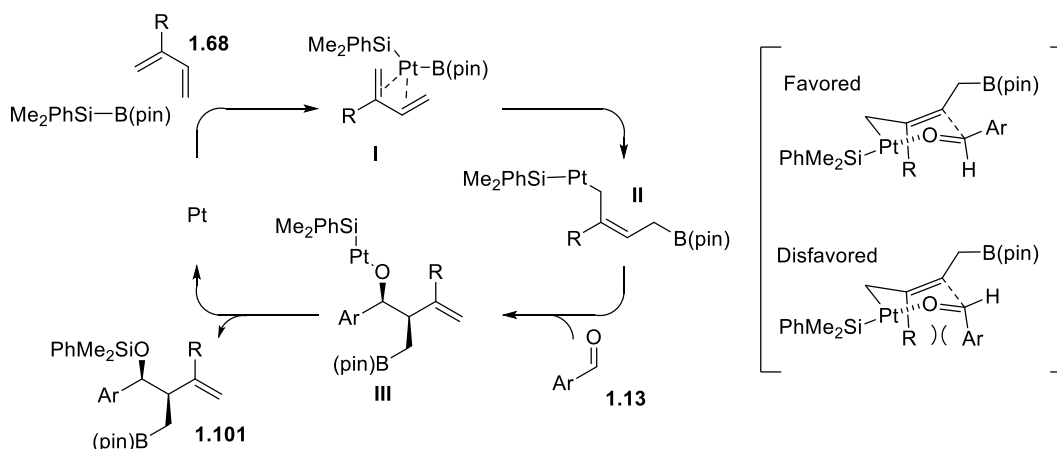
In 1998, the Ito group disclosed a three component silylborative coupling of dienes to aldehydes to access homoallylic borane derivatives in high regio- and stereoselectivity. Previous studies had indicated that Si-B σ -bonds can be activated by palladium or platinum catalysts, and subsequently add to unsaturates to access silylbored products.⁴² Application of this principle to dienes would form silylborene **I** (Scheme 1.29), which was expected to react with an aldehyde to form **1.100** via boron mediated allylation reaction. Surprisingly, **1.101** was the only product isolated, in high yield and excellent diastereoselectivity.⁴³

Scheme 1.29 Formation of **1.101** by silaborative coupling of 1,3-diene **1.72** and benzaldehyde.



The unexpected, highly selective formation of **1.101** suggested that a platinum intermediate must mediate the aldehyde coupling. A possible mechanism for the reaction is shown in Figure 1.23. The platinum catalyst can oxidatively insert into the B-Si bond and coordinate diene **1.68** to generate **I**. Insertion of the less hindered olefin into the Pt-B bond generates organoboron intermediate **II**. This can coordinate the aldehyde, and carbonyl addition can occur by way of the six-membered, chair like transition states shown at right. The favored model avoids the 1,3-diaxial interactions between aldehyde substituent (Ar) and diene substituent (R). The resulting platinum alkoxide **III** can undergo reductive elimination to form product **1.101** and regenerate the catalyst.

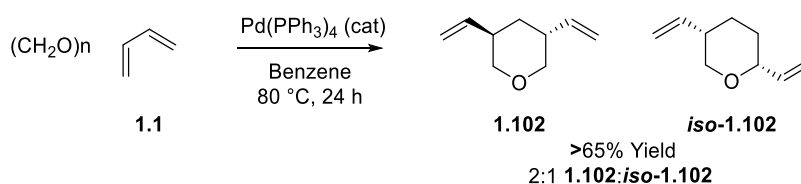
Figure 1.23 Proposed mechanism of diastereoselective silaborative coupling of 1,3-diene and aldehyde by way of a platinum-allyl intermediate.



1.7 Palladium Catalysis

Early work involving diene polymerization revealed that nickel, palladium, rhodium, cobalt and iron were all suitable catalysts,⁴⁴ but the first reports of diene-carbonyl reductive coupling of any transition metals involved palladium catalyzed telomerization of butadiene with paraformaldehyde (Scheme 1.30). In 1970, the Shell Development Company reported an unexpected product, believed to be a divinyltetrahydropyran **1.102**, from a reaction of butadiene and formaldehyde in the presence of catalytic $\text{Pd}(\text{PPh}_3)_4$. While the mechanism was not described, it was suggested that palladium complexation of paraformaldehyde occurs before diene insertion.⁴⁵

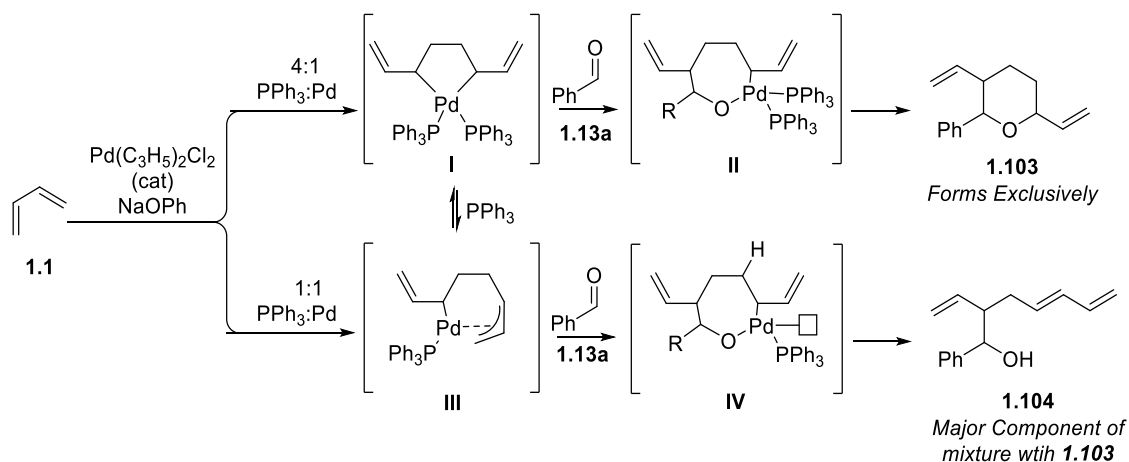
Scheme 1.30 Divinyltetrahydropyran **1.102** and *iso*-**1.102** formed upon coupling of butadiene and formaldehyde.



In the same year, Union Carbide Corporation published the telomerization of butadiene with formaldehyde and higher aldehydes to afford substituted tetrahydropyrans **1.103** and

secondary alcohols **1.104** using Pd(OAc)₂ and PPh₃ (Figure 1.24). Both products incorporate a 2:1 ratio of butadiene to aldehyde. Product formation was effected by altering the metal to ligand ratio, where a 4:1 ratio of Pd to PPh₃ exclusively formed tetrahydropyran **1.103**, and a 1:1 ratio of Pd to PPh₃ formed a mixture of **1.103** and **1.104**, favoring open chain form **1.104**.⁴⁶ In 1971, Tsuji et al. from Toray Industries reported the same transformation, suggesting that butadiene dimerization to form **I** and **III** occurs before insertion of the resultant Pd-allyl into the aldehyde. The formation of product **1.103** or **1.104** is dependent on the presence of an open coordination site at Pd. With excess PPh₃, the formation of **II** can only proceed by reductive elimination to form **1.103**, while the unsaturated complex **III** can instead abstract a hydrogen (**IV**) to generate diene containing **1.103**.⁴⁷

Figure 1.24 Effect of ligand to metal ratio for palladium catalyzed telomerization to form **1.103** or **1.104**.

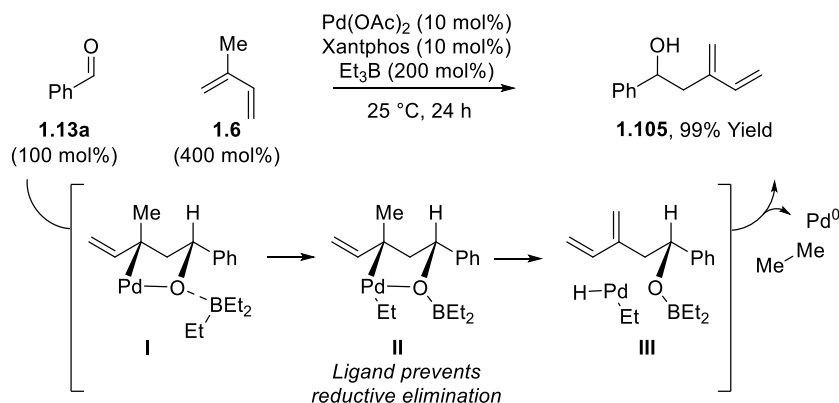


Despite these early reports, the next report of reductive coupling of dienes and aldehydes under palladium catalysis did not appear until 2010. While other metal catalyzed reductive coupling commonly formed functionalized homoallylic alcohol products, this reaction uniquely resulted in a dienyl homoallylic alcohol **1.105**.⁴⁸

Upon oxidative cyclization of aldehyde and isoprene, ethyl transfer from boron to palladium generates **I**. It is proposed that β -hydride elimination from **II** to form the C-C double

bond in **III** occurs because of the wide bite angle of Xantphos ligand, whose *trans* coordination prevents isomerization to the requisite orientation for reductive elimination to occur.

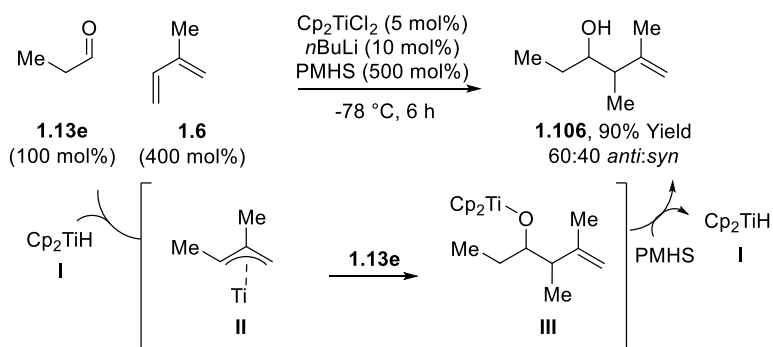
Figure 1.25 Palladium catalyzed reductive coupling of dienes and aldehyde to generate dienylyl homoallylic alcohol **1.105**.



1.8 Titanium Catalysis

While allyl metal complexes of titanium and other early transition metals have been well studied and applied to carbonyl addition chemistry,⁴⁹ only one catalytic variant of diene aldehyde coupling has been reported by a titanium hydride catalyzed mechanism.⁵⁰

Figure 1.26 Titanium catalyzed reductive coupling of aldehyde **1.13e** and isoprene.



Based on precedence of titanium catalyzed hydrosilylation of carbonyl compounds,⁵¹ generation of a highly sensitive titanium hydride catalyst **I** was proposed to form by treating Cp₂TiCl₂ with *n*BuLi in the presence of poly(methylhydrosiloxane) (PMHS). This can rapidly hydrometallate isoprene to generate allyltitanium **II**. It was found that slow addition of aldehyde

prevents undesirable reactivity between the titanium catalyst and aldehyde, instead generating
III. After aldehyde addition, PMHS was used to regenerate the titanium hydride catalyst and release product **1.106**.

1.9 Conclusion and Outlook

In summary, the intermolecular reductive coupling of dienes and carbonyl partners has seen great development, from the initial reports of diene-ketone coupling in the 1970s to many highly regio- and stereoselective methods utilizing nickel, rhodium, iridium, ruthenium, platinum palladium and titanium catalysis. Further advancement of this methodology, including the ability to employ readily available dienes in a stereoselective, catalytic transformations, could have significant impact on the strategies for synthetic chemistry, enabling the rapid construction of complex molecules.

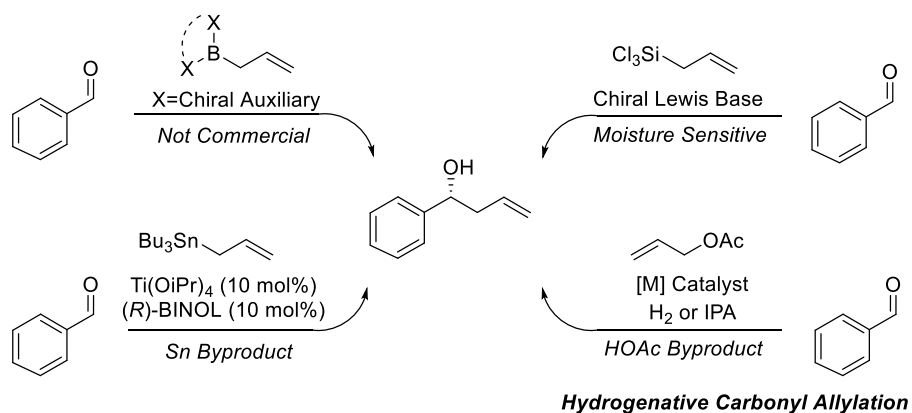
Chapter 2 Diastereoselective Transfer Hydrogenative Allylation

2.1 Introduction

Inspired by the elegant application of hydrogenation for the Fisher-Tropsch reaction and hydroformylation, the Krische group began investigating hydrogenative reductive coupling of π -unsaturated and higher aldehydes to access products of carbonyl addition. Intercepting the organometallic intermediate formed upon hydrogenation with an electrophilic carbonyl moiety would enable carbon-carbon bond formation.

Using rhodium, iridium and ruthenium complexes, the strategy was successful, accessing products of allylation, vinylation, dienylation and propargylation of aldehydes. One distinct advantage of a hydrogenative process is the direct employment of unsaturated as coupling partner. This avoids the use of preformed organometallic reagents, eliminating the generation of stoichiometric metallic waste and handling of potentially air or moisture sensitive organometallic compounds (See Figure 2.1 for a comparison of methods for carbonyl allylation).⁵²

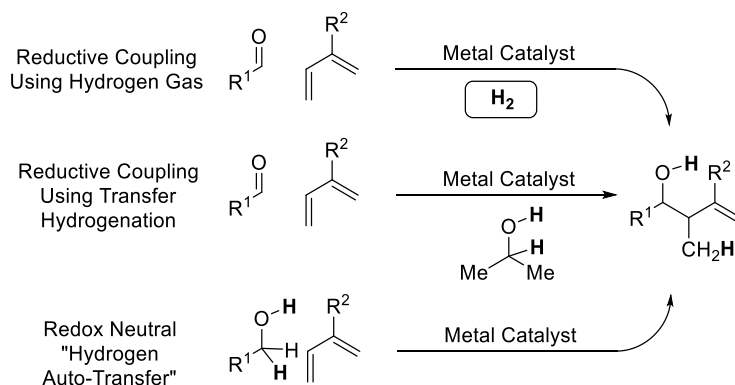
Figure 2.1 Comparison of asymmetric carbonyl allylation methods, including organoboron reagents, Lewis acid catalyzed organostannane additions, Lewis-base catalyzed allylsilane additions, and hydrogenative allylation.



Further development led to reductive coupling conducted under a transfer hydrogenative protocol, in which hydrogen is supplied by a terminal reductant. By embedding hydrogen into an organic molecule, the quantity of hydrogen present in the reaction could be carefully controlled,

thus preventing over reduction of unsaturates due to traditional hydrogenation pathways. Even a primary alcohol could be employed as reductant, enabling a “hydrogen auto-transfer pathway,” where a primary alcohol serves both as hydrogen source and aldehyde precursor. This reaction, a formal C-H functionalization of a primary alcohol, accesses an identical product to that of carbonyl addition but is conducted using the more tractable alcohol substrate. By merging the oxidation and aldehyde addition events into a single catalytic cycle, the process is redox neutral and avoids the requirement for discrete oxidation prior to the reductive C-C bond formation (Figure 2.2). As oxidative processes are severely limited on scale, this strategy represents a more attractive method for performing carbonyl addition reaction.⁵³ In the following chapters, further advancement of transfer hydrogenative C-C bond forming methodologies will be described, with focus on the development of stereoselective ruthenium catalysis and discovery of new modes of reactivity.

Figure 2.2 Hydrogenative carbon-carbon bond formation using hydrogen gas or transfer hydrogenation.



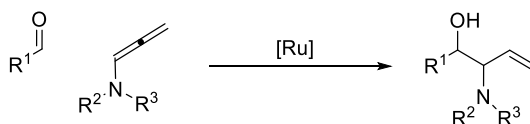
2.2 Formation of 1,2-Amino alcohols using Allenamides

2.2.1 Introduction

In the development of ruthenium catalyzed carbonyl addition reactions using transfer hydrogenation, attention was directed toward accessing functionalized products of carbonyl allylation by reductive coupling of substituted allenamides and aldehydes. One structural feature, a

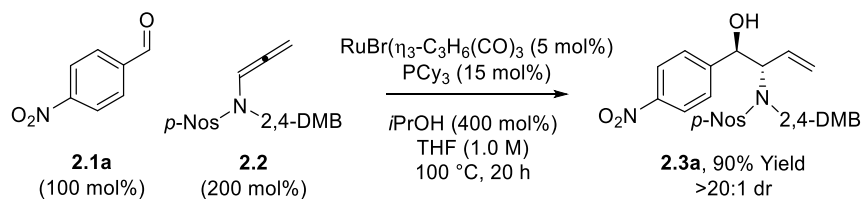
1,2-amino alcohol, could be accessed by ruthenium catalyzed coupling using allenamides as π -unsaturate (Scheme 2.1).

Scheme 2.1 Reductive coupling of aldehyde and allenamide to form vinyl substituted 1,2-amino alcohols.



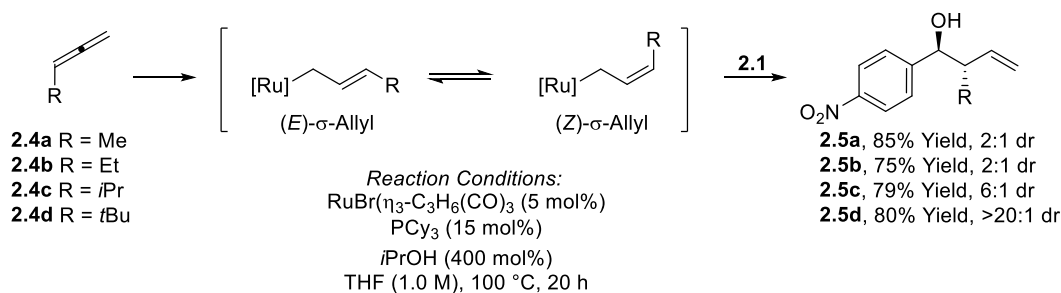
Amino alcohols are ubiquitous in natural products and are commonly found in bioactive compounds and pharmaceutical candidates. As such, numerous methods exist for the formation of 1,2-amino alcohols, usually by way of alkene functionalization.⁵⁴ However, far fewer methods exist for the direct formation of 1,2-amino alcohols by carbon-carbon bond forming reaction. Generally, these reactions involve addition of an organometallic reagent to an imine or an aldehyde. Some examples include zirconium-mediated reactions of chiral aldimines and aldehydes via an aziridinozirconium intermediate,⁵⁵ three-component coupling of alkyl halides, aldehyde and aryl isocyanide mediated by samarium diiodide,⁵⁶ addition of acyloxymethyl radical to imines,⁵⁷ addition of lithiated *N*-benzyl-diphenylphosphinamides to aldehydes,⁵⁸ diphenylamino-substituted allylborane reagents for aldehyde addition,⁵⁹ and cross coupling of chiral *N*-*tert*-butanesulfinylimines and aldehydes.⁶⁰ While some of these methods access 1,2-amino alcohols in an efficient and selective manner, the necessity for stoichiometric metals and the employment of temperature and moisture sensitive organometallic reagents are factors that may limit application and functional group compatibility of these methods on scale. More recently, these limitations have been addressed in the development of Mannich-type reactions of hydroxyl ketones for the diastereo- and enantioselective synthesis of 1,2-amino alcohols.⁶¹ The catalytic, hydrogenative coupling of aldehydes and allenamides could provide another alternative enabling the direct, carbon-carbon bond formation of 1,2-amino alcohols.

Scheme 2.2 Reductive coupling of aldehyde **2.1a** and allenamide **2.2** to form 1,2-amino alcohol **2.3a**.



Beginning with *p*-nitrobenzaldehyde **2.1a**, isopropanol as reductant and a diprotected allenamides **2.2**, optimization of reaction conditions revealed that $\text{Ru}(\text{Br})(\eta^3\text{-C}_3\text{H}_5)(\text{CO})_3$ in combination with PCy_3 was uniquely effective at catalyzing the reaction. By tuning nitrogen protecting groups, it was found that the combination of *p*-nitrosulfonyl and 2,4-dimethoxybenzyl substitution enabled high levels of diastereocontrol, forming only the *anti*-1,2-amino alcohol, as confirmed by ^1H NMR and x-ray crystal diffraction analysis (Scheme 2.2). It was proposed that the observed stereocontrol was due to the preferential formation of a single geometrical isomer upon allene hydrometallation. To examine this hypothesis, 1-methylallene **2.4a**, ethylallene **2.4b**, isopropylallene **2.4c** and tertbutylallene **2.4d** were synthesized and exposed to the previously developed reaction conditions (Scheme 2.3). In each case, the product of allylation **2.5a-d** was formed in high yield and *anti*-diastereoselectivity increased as the size of the allene substituent increased, suggesting reactivity proceeds through the (*E*)- σ -allyl isomer due to steric destabilization of the (*Z*)- σ -allyl isomer.⁶²

Scheme 2.3 Effects of allene substituent on diastereoselectivity.



2.2.2 Reaction Development and Optimization.

To improve hydrogenative aminoallylation, focus was directed to extend reactivity to include alcohol substrates in a redox-neutral reaction pathway.

Table 2.1 Optimization of catalyst and ligand for aminoallylation of **2.6a**.

Reaction scheme showing the aminoallylation of **2.6a** (100 mol%) and allenamide **2.2** (200 mol%) to form product **2.3a**. Conditions: Catalyst (5 mol%), Ligand, THF (1.0 M), 95 °C, 24 h.

Entry	Catalyst	Ligand (mol%)	Yield (%)
1	RuBr(η^3 -C ₃ H ₅)(CO) ₃	PCy ₃ (15)	no reaction
2	RuHCl(CO)(PPh ₃) ₃	none	no reaction
3	RuHCl(CO)(PPh ₃) ₃	PCy ₃ (15)	no reaction
4	RuHCl(CO)(PPh ₃) ₃	PtBuPh ₂ (15)	no reaction
5	RuHCl(CO)(PPh ₃) ₃	Xantphos (5)	no reaction
6	RuHCl(CO)(PPh ₃) ₃	Rac-BINAP (5)	no reaction
7	RuHCl(CO)(PPh ₃) ₃	BIPHEP (5)	29
8	RuHCl(CO)(PPh ₃) ₃	DPPF (5)	58
⇒ 9	RuHCl(CO)(PPh ₃) ₃	DiPPF (5)	86

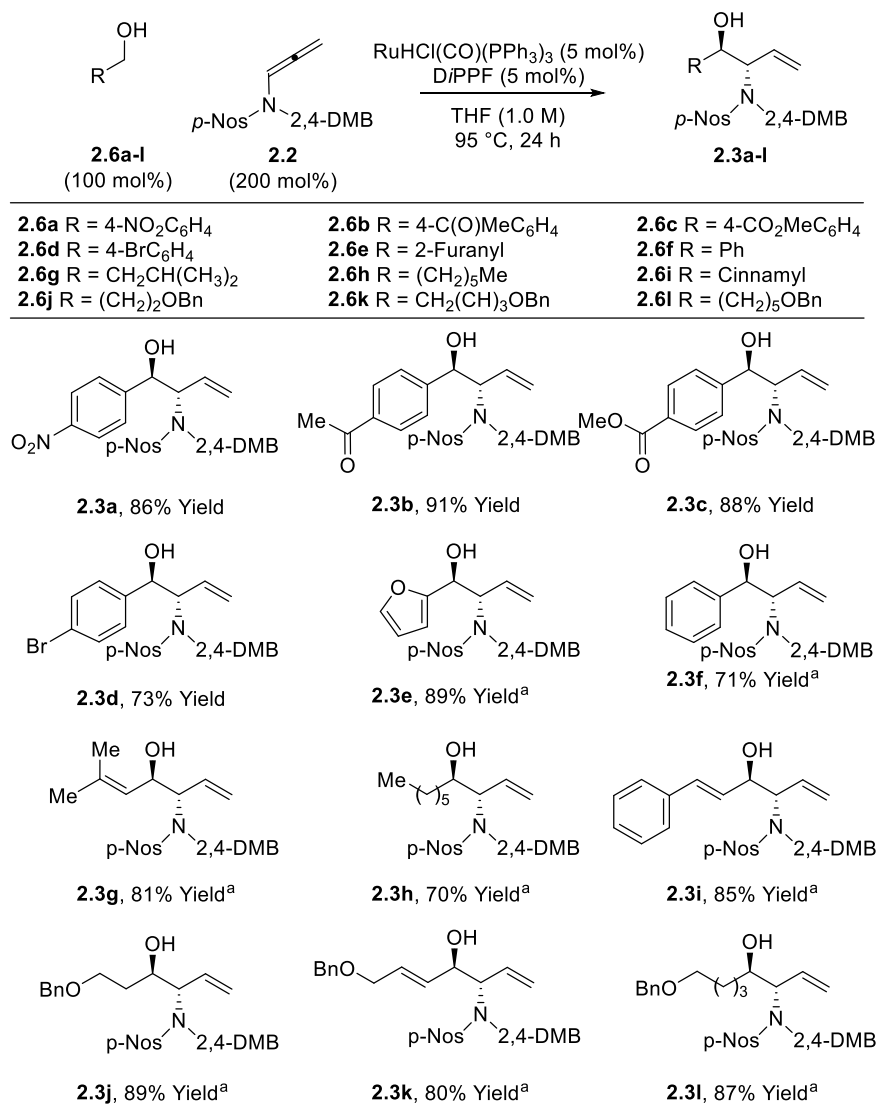
Initial attempts at aminoallylation of *p*-nitrobenzylalcohol **2.6a** under the catalytic system used for aldehyde aminoallylation were unsuccessful (Table 2.1, entry 1). Recently, the Krische group had reported another Ru^{II} catalyst, RuHCl(CO)(PPh₃)₃, capable of transfer hydrogenative reductive couplings of enynes and dienes to primary alcohols.^{30, 63} This catalyst was evaluated in the reaction of alcohol **2.6a** and allenamide **2.2** using a variety of monodentate and bidentate phosphine ligands. Triphenylphosphine (entry 2) was ineffective as ligand, as were more electron rich monodentate phosphine ligands (entries 3-4). Bidentate phosphine ligands Xantphos and *Rac*-BINAP (entry 5-6) were also ineffective, but BIPHEP (entry 7) showed promising reactivity. By screening more rigid, electron rich ferrocene backbone ligand DPPF (entry 8), the yield was improved, and further optimized by using *Di*PPF (entry 9). In all cases, the product was isolated as a >20:1 *anti:syn* mixture of diastereomers.

2.2.3 Reaction Scope

The optimal conditions for aminoallylation were evaluated for a variety of primary alcohol substrates. High isolated yields were obtained for aromatic, allylic and aliphatic alcohols **2.6a-l**.

In some cases, 300 mol% of allenamide **2.2** was required for high yield. This appeared to be due to decomposition of the allenamide (visible by TLC analysis) under the reaction conditions. For substrates that formed less electrophilic aldehydes, decomposition of the allenamide was more significant.⁶⁴

Figure 2.3 Ruthenium catalyzed hydrohydroxyalkylation of allenamide **2.2** using primary alcohols.

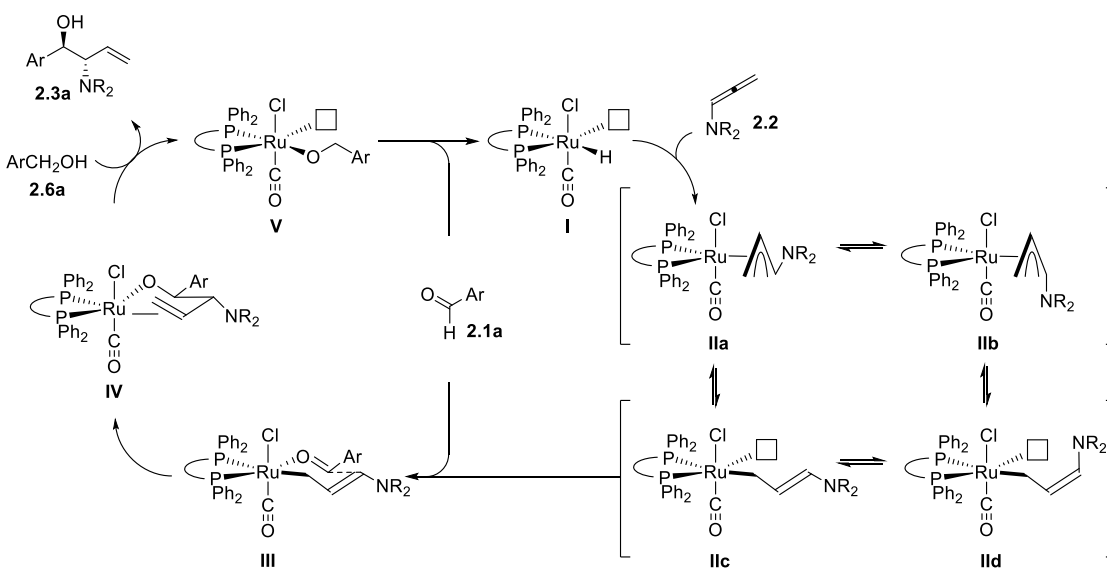


^a300 mol% **2.2**

2.2.4 Mechanism and Discussion

A proposed mechanism for aminoallylation is shown in Figure 2.4. Hydrometallation of allenamide **2.2** by ruthenium hydride **I** leads to ruthenium *syn*- π -allyl **IIa** or *anti*- π -allyl **IIb**.⁶⁵ While equilibration of (*E*)- σ -allyl isomers **IIc** and (*Z*)- σ -allyl isomers **IId** may be possible, isomer **IIc** reacts exclusively, as supported by the observed *anti*-diastereoselectivity. The steric demand of the large protecting groups at nitrogen are likely responsible for the partitioning of **IIc** and **IId**. Coordination of the reactant aldehyde **2.1a**, generated from β -hydride elimination of substrate **2.6a**, to **IIc** forms six-membered, chair-like transition state **III**. After aldehyde addition, coordinatively-saturated ruthenium alkoxide **IV** is formed. 1,2-Amino alcohol **2.3a** is released upon protonation by another equivalent of reactant alcohol **2.6a** and ligand exchange generates ruthenium alkoxide **V**.⁶⁶ This species can undergo β -hydride elimination to form an equivalent of aldehyde **2.1a** and reforms ruthenium hydride **I**, thus closing the catalytic cycle.

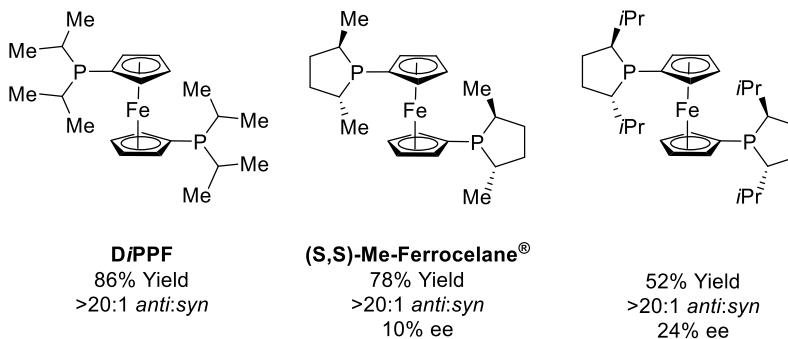
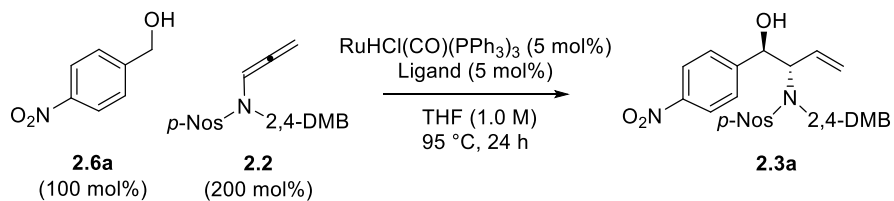
Figure 2.4 Proposed catalytic mechanism for hydrohydroxyalkylation of allenamide **2.2** using primary alcohol **2.6a**.



The aminoallylation of primary alcohols is a highly efficient method for the formation of 1,2-amino alcohols and complements the previously reported aldehyde-allenamide coupling. In both methods, an electron rich ligand was required for good reactivity—the trialkylphosphine PCy_3

for aldehyde coupling and ferrocene based, dialkyl phosphine *D*/PPF for alcohol coupling. The enhanced electron density from the ligands may contribute to the nucleophilicity of the ruthenium-allyl species, creating a more reactive coupling partner. One drawback of the catalytic system is the lack of structurally similar chiral ligands for an asymmetric aminoallylation reaction. Two chiral ligands were screened in this reaction, however only low levels of selectivity were obtained (Figure 2.5).

Figure 2.5 Chiral ferrocene based ligands for asymmetric aminoallylation.



2.2.5 Conclusion

The catalyst formed from $\text{RuHCl(CO)(PPh}_3)_3$ and *D*/PPF was found to catalyze the hydrohydroxyalkylation of allenamides to access 1,2-amino alcohols **2.3a-l**. This method is complementary to the coupling of allenamides and aldehydes, eliminating the need for discrete redox manipulations prior to the ruthenium catalyzed aminoallylation. Optimization of nitrogen protecting groups enabled complete *anti*-diastereoselectivity, providing insight into diastereocontrol for ruthenium catalyzed hydrogenative coupling.

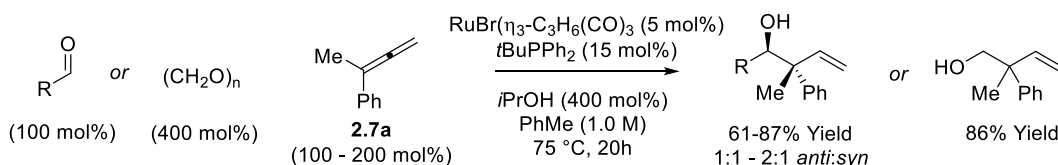
2.3 Formation of All-Carbon Quaternary Centers using 1,1-Disubstituted Allenes

2.3.1 Introduction

Coupling alcohols and 1,1-disubstituted allenes through transfer hydrogenative ruthenium catalysis can access homoallylic alcohols containing an all-carbon quaternary center. The stereospecific formation of all-carbon quaternary centers remains a significant challenge in organic chemistry, as the steric congestion at the chiral center complicates reactivity and selectivity. However, this structural motif is not uncommon in natural products, so the development of efficient, selective methodology in this area has been a focus of research for decades.⁶⁷

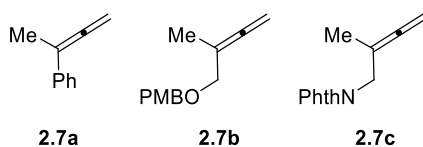
In 2008, the Krische group reported the reductive coupling of 1,1-disubstituted allenes with paraformaldehyde and higher aldehydes using a similar catalyst ($\text{Ru}(\text{Br})(\eta^3\text{-C}_3\text{H}_5)(\text{CO})_3$ and $\text{PtBu}(\text{Ph})_2$) to that developed for the aminoallylation of aldehydes.^{62, 68} This provided homoallylic alcohol products containing an all-carbon quaternary center, in high yield but low diastereoselectivity (1:1 to 2:1 *anti:syn*) (Scheme 2.4).

Scheme 2.4 Reductive coupling of 1,1-disubstituted allenes to aldehydes or paraformaldehyde.



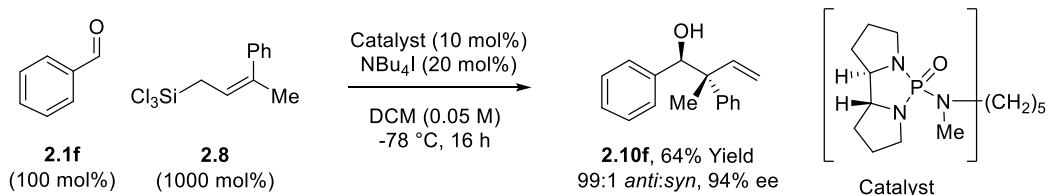
Three allenes from this account were selected and subjected to the conditions optimized for aminoallylation of alcohols (Figure 2.6). The results and optimization of 1-methyl-1-phenylallene **2.7a**, which can easily be prepared by Doering-La Flamme homologation of α -methyl styrene,⁶⁹ will be discussed in the subsequent sections.

Figure 2.6 Allenes selected for development of allylation to form all-carbon quaternary centers.



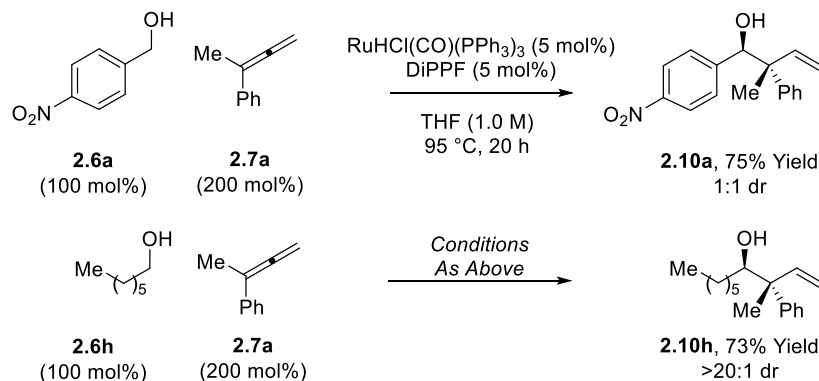
The coupling of 1-methyl-1-phenylallene **2.7a** and an aldehyde or alcohol results in homoallylic alcohol containing an all-carbon quaternary center with aryl, alkyl and vinyl substitution. An identical product, accessed by chiral Lewis base catalyzed allylation of aldehydes using an allyltrichlorosilane **2.8** was reported by Denmark et al. in 2002 (Scheme 2.5).⁷⁰ While this is a highly selective reaction, a reductive coupling method may provide some advantages, as 1-methyl-1-phenylallene **2.7a** is less moisture sensitive than trichlorosilane **2.8**, and cryogenic temperatures are not required for the ruthenium catalyzed process.

Scheme 2.5 Formation of an all-carbon quaternary center via addition of allyltrichlorosilane **2.8** to aldehyde **2.1f** in the presence of a chiral Lewis base catalysis.



2.3.2 Reaction Development, Optimization and Scope

Scheme 2.6 Initial results of coupling allene **2.7a** with alcohols **2.6a** and **2.6h**, exhibiting a great difference in diastereoselectivity.



The catalyst and reaction conditions developed for alcohol-allenamide coupling were applied to coupling primary alcohols with allene **2.7a**. A preliminary screening of alcohol substrates revealed an interesting trend in diastereoselectivity, in which *p*-nitrobenzyl alcohol (**2.6a**) resulted in a 1:1 diastereomeric mixture of homoallylic alcohol product **2.10a**, but heptanol

(**2.6h**) formed only *anti*-diastereomer **2.10h** (Scheme 2.6). Intrigued by the observed trends in diastereoselectivity, attention was focus on further optimization and understanding of stereocontrol in this transformation.

For aliphatic alcohols **2.6h** and **2.6j**, the initial conditions screened produced a single diastereomer. It was found that a more reliable yield could be obtained by lowering reaction temperature and extending reaction time, likely avoiding thermal polymerization of allene **2.7a**.

Aromatic and allylic substrates **2.6a**, **e**, **f**, **i**, **m** displayed high reactivity and varying diastereoselectivity. For benzyl alcohol (**2.6f**), it was found that at constant concentration, diastereoselectivity improved as temperature decreased (Table 2.2, entries 1-3) At constant temperature, dilution of the reaction media improved diastereoselectivity (entries 4-6), though reactivity suffered at low concentration (0.2 M). By carefully balancing temperature and concentration, good levels of *anti*-diastereoselectivity were achieved while maintaining excellent reactivity for aromatic and allylic substrates.

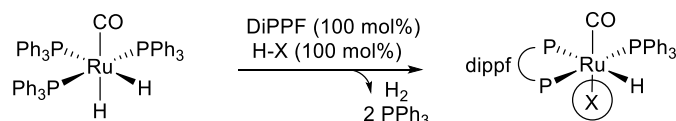
Table 2.2 Effect of temperature and concentration on diastereoselectivity of **2.10f**.

Entry	Concentration (M)	T °C	Yield (%)	<i>anti:syn</i>
<i>Temperature Screen</i>				
1	0.5	70	99	2:1
2	0.5	60	94	5:1
3	0.5	50	86	6:1
<i>Concentration Screen</i>				
4	1.0	60	99	4:1
5	0.5	60	94	5:1
6	0.2	60	26	8:1

p-Nitrobenzyl alcohol (**2.6a**) forms an electron-deficient aldehyde, highly activated for carbonyl addition. Optimization of temperature and concentration proved ineffective for this substrate, as a 1:1 mixture of diastereomers formed at low temperature. Because

diastereoselectivity remained poor after further screening of ligand and other reaction parameters, the ruthenium precatalyst was reexamined. Previously, it was found that $\text{RuH}_2(\text{CO})(\text{PPh}_3)_3$ as precatalyst in combination with an acidic additive had a beneficial effect in the regioselective outcome of coupling 2-substituted dienes with paraformaldehyde.³² The hydride ligands on ruthenium precatalyst $\text{RuH}_2(\text{CO})(\text{PPh}_3)_3$ have basic character, and can participate in an acid-base reaction with the acid additive, liberating H_2 gas and creating a cationic ruthenium center coordinated by the conjugate base of the acid additive (Scheme 2.7).⁷¹ In doing so, both the neutral phosphine ligands and one of the anionic ligands on the Ru^{II} catalyst can be replaced, drastically altering the steric and electronic environment at the metal center.

Scheme 2.7 Counter ion introduction by treating $\text{RuH}_2(\text{CO})(\text{PPh}_3)_3$ with acid.



To examine this effect on the coupling of 1-methyl-1-phenylallene **2.7a** to *p*-nitrobenzyl alcohol **2.6a**, precatalyst $\text{RuH}_2(\text{CO})(\text{PPh}_3)_3$, DiPPF and various acids were combined to generate the cationic ruthenium catalyst in situ. HCl and HBr were surveyed (Table 2.3, entries 1- 2), and reactivity was maintained using these strong acids, but selectivity was poor. Carboxylic acids³² (entry 3-4), and *rac*-BINOL phosphoric acid (entry 5) were similarly ineffective. Fortuitously, selectivity improved with *p*-toluenesulfonic acid (entry 6). Using a more acidic, electron deficient sulfonic acid (entry 7), excellent diastereoselectivity was observed, at the expense of decreased yield. A more sterically hindered aliphatic sulfonic acid (entry 8) did not prove advantageous, but using a more bulky aromatic sulfonic acid provided optimal selectivity and high reactivity (entry 9).

Table 2.3 Effect of ruthenium counter ion on diastereoselective formation of **2.10a**.

Entry	Acid	Yield (%)	<i>anti:syn</i>
1	HCl	99	2:1
2	HBr	99	1:1
3	3,5-Dinitrobenzoic Acid	trace	nd
4	F ₁₅ C ₇ CO ₂ H	31	1:1
5	<i>Rac</i> -BINOL Phosphoric Acid	11	3:1
6	<i>p</i> TsOH	99	8:1
7	F ₉ C ₄ SO ₃ H	22	>20:1
8	Camphor-10-Sulfonic Acid	48	7:1
⇒ 9	2-Mesitylene Sulfonic Acid	79	20:1

Figure 2.7 Ruthenium catalyzed hydrohydroxyalkylation of 1-methyl-1-phenylallene **2.7a**.

Product	Conditions	Product	Conditions	Product	Conditions
2.10a , 86% Yield 20:1 <i>anti:syn</i>	THF (1.0 M) 50 °C, 48 h	2.10h , 77% Yield >20:1 <i>anti:syn</i>	THF (1.0 M) 75 °C, 48 h	2.10j , 67% Yield >20:1 <i>anti:syn</i>	THF (1.0 M) 75 °C, 48 h
2.10e , 99% Yield 10:1 <i>anti:syn</i>	THF (0.5 M) 60 °C, 24 h	2.10i , 99% Yield 5:1 <i>anti:syn</i>	THF (1.0 M) 40 °C, 24 h	2.10m , 85% Yield 4:1 <i>anti:syn</i>	THF (0.5 M) 40 °C, 24 h
2.10f , 99% Yield 6:1 <i>anti:syn</i>	THF (0.5 M) 60 °C, 24 h				

Upon optimization of aliphatic, allylic and aromatic alcohols, a series of substrates representing the scope of reactivity was compiled (Figure 2.7). All alcohols engaged in carbon-

carbon bond formation to generate homoallylic alcohols in high yield (67 to 99%), with good to excellent levels of diastereoselectivity (4:1 to >20:1 *anti:syn*).⁷² The *anti* relationship of the major diastereomer was confirmed by comparison to a product of allene **2.7c** by x-ray diffraction and to known literature compounds.^{70a}

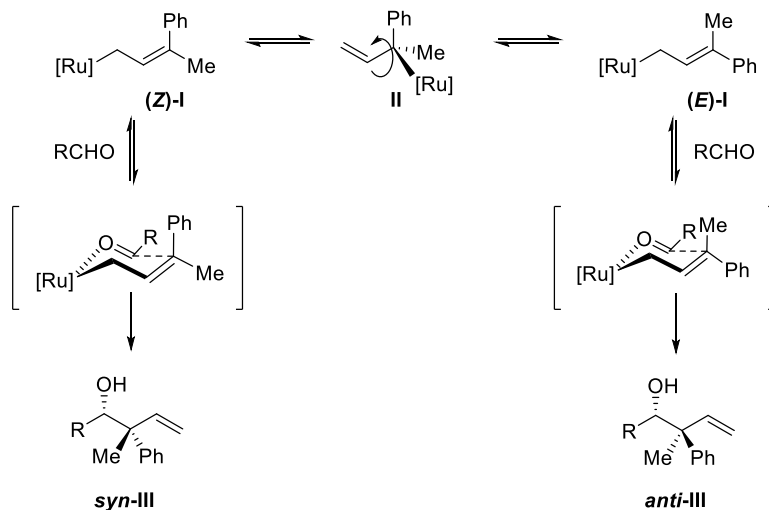
2.3.3 Mechanism and Discussion

The observed trends in diastereoselectivity provide insight into the mechanism and stereo-defining steps. As described by Krische et al.,⁶² diastereoselectivity in similar ruthenium catalyzed hydrometallative processes is determined by the σ -allyl isomer that participates in aldehyde addition. For mono-substituted allenes, there is a distinct energetic difference between the (*E*) and (*Z*) isomers that results in high diastereoselectivity when the allene substituent is large. Using 1-methyl-1-phenylallene **2.7a**, an energetic difference between the (*E*) and (*Z*) isomers may exist, demonstrated by the complete diastereoselectivity observed for aliphatic substrates **2.6h** and **2.6j**, but may not be significant for substrates **2.6a**, **e**, **f**, **i**, **m** that generate aldehydes that are more activated toward carbonyl addition.

The Curtin-Hammett principle can be used to explain the observed effects of temperature and concentration on diastereoselectivity. Hydrometallation of allene **2.7a** forms an equilibrating mixture of (*E*) and (*Z*) isomers (Figure 2.8, (**E-I**) and (**Z-I**)). The energetic barrier of irreversible carbonyl addition is key to selectivity, assuming that addition to unactivated aliphatic substrates (**2.6h**, **j**) will be more energetically demanding than that of aromatic (**2.6a**, **e**, **f**, **m**) or allylic substrates (**2.6i**). The complete diastereoselectivity of aliphatic substrates suggests that reactivity proceeds stereospecifically through the more favored allyl pathway through isomer (**E-I**). As (**E-I**) reacts, equilibration will repopulate the isomer, funneling reactivity through this pathway. For the allylic and aromatic substrates, a lower energetic barrier for addition must exist for both (**E-I**) and (**Z-I**) isomers. This allows both isomers to react, leading to a mixture of products *syn-III* and *anti-III*. By decreasing temperature, less energy is supplied to the reaction, slowing reactivity. If the barrier to aldehyde addition through (**E-I**) is less energetically demanding than through (**Z-I**),

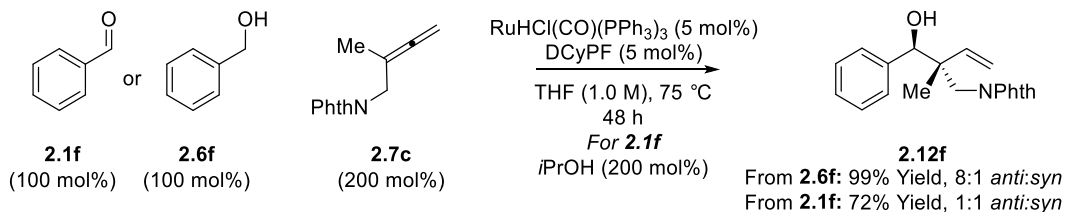
reactivity at low temperature will more likely proceed to form **anti-III**. Also, at lower concentration, carbonyl addition will be slower. This additional time allows for repopulation of the (**E-I**) isomer, funneling reactivity through the pathway to form **anti-III**.

Figure 2.8 Interconversion of (**Z-I**) and (**E-I**) lead to **syn-III** and **anti-III**.



An important parameter to improve stereocontrol was the ability to slow carbonyl addition, either by lowering reaction temperature or by diluting reaction media. Beginning with an alcohol substrate, catalytic formation of aldehyde must precede carbonyl addition. In this way, sub-stoichiometric amounts of aldehyde would be present, lowering the effective concentration of the coupling partners and slowing the reaction. To demonstrate the effect this has on diastereoselectivity, a direct comparison of alcohol and aldehyde reactivity was performed using allene **2.7c** (Scheme 2.8).

Scheme 2.8 Product **2.12f** from aldehyde **2.1f** exhibits much lower diastereoselectivity than alcohol **2.6f**, supporting Curtin-Hammett interpretation of trends in diastereoselectivity.



Two experiments were performed: one using benzyl alcohol **2.6f** as substrate, and one using benzaldehyde **2.1f** as substrate with *i*PrOH as added reductant. Under identical conditions, alcohol substrate **2.6f** resulted in significantly higher diastereoselectivity (8:1 *anti:syn*) than the corresponding aldehyde **2.1f** (1:1 *anti:syn*).⁷²

The counter ion effect on diastereoselectivity that is observed for *p*-nitrobenzylalcohol (**2.6a**) may be explained by a few factors. The cationic ruthenium center that forms upon protonation of the ruthenium hydride has a coordination site that is occupied by the introduced counter ion. If the counter ion is loosely coordinated, this “open” site at the metal center may facilitate equilibration of the (*E*)- and (*Z*)- σ -allyl isomers, which must proceed through sterically hindered tertiary ruthenium σ -allyl isomer **II** (Figure 2.8) to interconvert. Another factor that could influence the selectivity is the increased electronegativity of the cationic ruthenium center. This may shorten the ruthenium-allyl σ -bond length and amplifying the energetic difference between the (*E*)- and (*Z*)- isomers such that a greater energetic preference for the less bulky (*E*) isomer exists.

2.3.4 Conclusion

A method for the formation of homoallylic alcohols containing an all-carbon quaternary center was developed by hydrohydroxyalkylation of 1,1-disubstituted allenes. Trends in diastereoselectivity could be explained by application of the Curtin-Hammett principle for the postulated reaction mechanism. Additionally, the effects of the ruthenium catalyst counter ion were observed and applied to access product in high levels of diastereoselectivity.

2.4 Summary and Outlook

The development of ruthenium catalyzed transfer hydrogenative coupling of alcohols and substituted allenes has added to the repertoire of carbon-carbon bond forming reactions allowing access to products of aldehyde allylation. A significant outcome of this research is a deeper understanding of factors that influence diastereocontrol in these reactions. One shortcoming of these methodologies is the need to employ allenes for allylation, as these require synthetic

investment and may be less stable than other unsaturates (dienes, for example). Further improvement in these methods for allylation could be the development of an asymmetric variant.

2.5 Experimental Details

2.5.1 General Information

All reactions were run under an atmosphere of argon in sealed tubes (13x100 mm²), dried overnight in an oven and cooled under a stream of argon prior to use. Anhydrous solvents were distilled using solvent stills and solvent were transferred by oven-dried syringe. Catalyst RuHCl(CO)(PPh₃)₃ was prepared according to the method of Joseph,⁷³ and catalyst RuH₂(CO)(PPh₃)₃ was prepared according to the method of Williams.⁷⁴ All ligands, substrate alcohols and acidic additives were used without purification. Allenamide **2.2** was synthesized according the method developed by Krische et al.⁶² Allene **2.7a** was prepared by Doering-La Flamme homologation, as described by Krische et al.⁶⁸ Thin-layer chromatography (TLC) was carried out using 0.25 mm commercial silica gel plates (Silicycle Siliaplate F-254). Visualization was accomplished with UV light followed by staining. Purification of product was carried out by flash column chromatography using Silicycle silica gel (40-63 μ m), according to the method described by Still.⁷⁵ The stereochemistry of products **2.3a-i** was confirmed by comparison to data reported by Krische, et al.⁶² The stereochemistry of products **2.10a, e, f, h, i, j, h, m** was confirmed by comparison to data reported by Denmark et al.^{70a}

2.5.2 Spectrometry and Spectroscopy

Infrared spectra were recorded on a Thermo Nicolet 380 spectrometer. Low and high resolution mass spectra (LRMS or HRMS) were obtained on a Karatos MS9 and are reported as m/z (relative intensity). Accurate masses are reported for the molecular ion or a suitable fragment ion. Melting points were obtained on a Stuart SMP3 apparatus and are uncorrected. ¹H NMR spectra were recorded on a Varian Gemini (400 MHz) spectrometer at ambient temperature. Chemical shifts are reported in delta (δ) units, parts per million (ppm), relative to the center of the singlet at 7.26 ppm for deuteriochloroform, or other reference solvents as indicated. Data are

reported as chemical shift, multiplicity (s=singlet, d=doublet, t=triplet, q=quartet, m=multiplet), integration and coupling constant(s) in Hz. ^{13}C NMR spectra were recorded on a Varian Gemini (100 MHz) spectrometer and were routinely run with broadband decoupling. Chemical shifts are reported in ppm, with the center peak of the residual solvent resonance employed as an internal standard (CDCl_3 at 77.0 ppm).

2.5.3 General Procedures for Formation of 1,2-Amino Alcohols

To a re-sealable pressure tube equipped with a magnetic stir bar was added $\text{RuHCl}(\text{CO})(\text{PPh}_3)_3$ (9.5 mg, 0.01 mmol, 5 mol%) and 1,1'-Bis(di-*i*-propylphosphino)ferrocene (4.2 mg, 0.01 mmol, 5 mol%). Alcohol (0.20 mmol, 100 mol%) and allene (1a or 1b) (0.400 mmol, 200 mol%) were added and the tube was sealed with a rubber septum and purged with argon. THF (0.2 mL, 1.0 M concentration with respect to alcohol) was added and the rubber septum was quickly replaced with a screw cap. The mixture was heated at 95 °C (oil bath temperature) for 24 h. The reaction mixture was then concentrated *in vacuo* and subjected to flash column chromatography (SiO_2) under the conditions noted to furnish the corresponding product of *anti*-aminoallylation. All products were isolated as a single, *anti*-diastereomer.

2.5.4 Characterization of 2.3a-2.3l

N-(2,4-dimethoxybenzyl)-*N*-(1-hydroxy-1-(4-nitrophenyl)but-3-en-2-yl)-4-nitrobenzenesulfonamide) (**2.3a**)

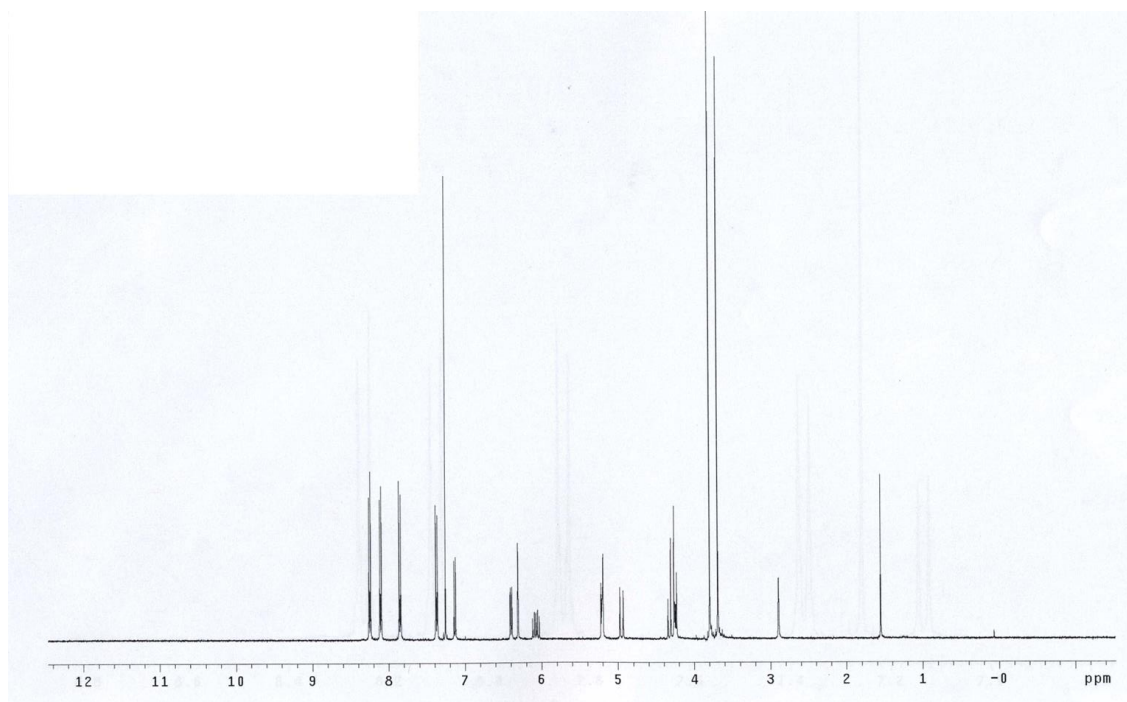
In accordance with the general procedure, the reaction was allowed to stir at 95 °C for 24 h, at which point the mixture was concentrated *in vacuo* and subjected to flash column chromatography (SiO_2 : 25% EtOAc/hexanes) to furnish the title compound (93 mg, 0.17 mmol, 86% yield) as a yellow solid. *The spectroscopic properties of 2.3a were consistent with those reported in the literature.*⁶²

^1H NMR (400 MHz, CDCl_3): δ 8.25 (d, J = 9.0 Hz, 2H), 8.11 (d, J = 8.8 Hz, 2H), 7.85 (d, J = 9.0 Hz, 2H), 7.37 (d, J = 8.8 Hz, 2H), 7.13 (d, J = 8.4 Hz, 1H), 6.39 (dd, J = 8.4, 2.4 Hz, 1H), 6.30 (d,

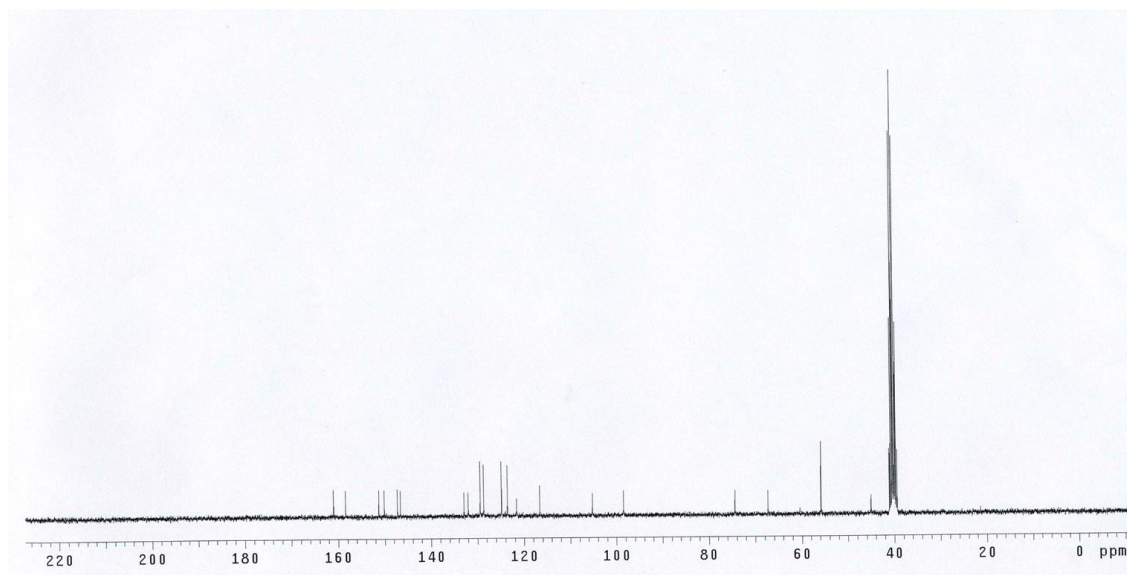
$J = 2.4$ Hz, 1H), 6.07 (ddd, $J = 17.2, 104, 7.2$ Hz, 1H), 5.21 (d, $J = 10.4$ Hz, 1H), 5.20 (d, $J = 5.2$ Hz, 1H), 4.95 (d, $J = 17.2$ Hz, 1H), 4.32 (d, $J = 14.7$ Hz, 1H), 4.25 – 4.24 (m, 1H), 4.25 (d, $J = 14.7$ Hz, 1H), 3.79 (s, 3H), 3.69 (s, 3H), 2.89 ppm (s, 1H).

^{13}C NMR (100 MHz, DMSO): δ 160.9, 158.9, 151.2, 150.0, 147.2, 146.6, 132.8, 131.8, 131.9, 129.4, 128.6, 124.8, 123.5, 121.6, 116.6, 105.2, 98.5, 74.4, 67.3, 55.8, 45.1 ppm.

^1H NMR of **2.3a**



^{13}C NMR of **2.3a**



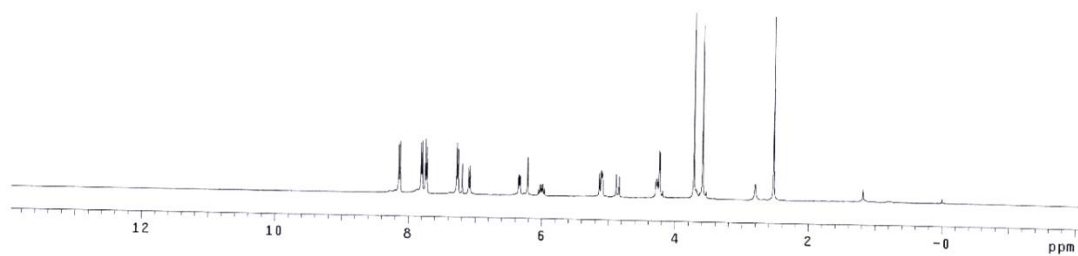
N-(1-(4-acetylphenyl)-1-hydroxybut-3-en-2-yl)-*N*-(2,4-dimethoxybenzyl)-4-nitrobenzenesulfonamide (**2.3b**)

In accordance with the general procedure, the reaction was allowed to stir at 95 °C for 24 h, at which point the reaction mixture was concentrated *in vacuo* to afford the crude product (dr = >20:1 *anti:syn*, as determined by ¹H NMR spectroscopy). The reaction mixture was then subjected to flash column chromatography (SiO₂: 30% EtOAc/hexanes) to furnish **2.3b** (98 mg, 0.18 mmol, 91% yield) as a yellow oil. *The spectroscopic properties of this compound were consistent with the data available in the literature.*⁶²

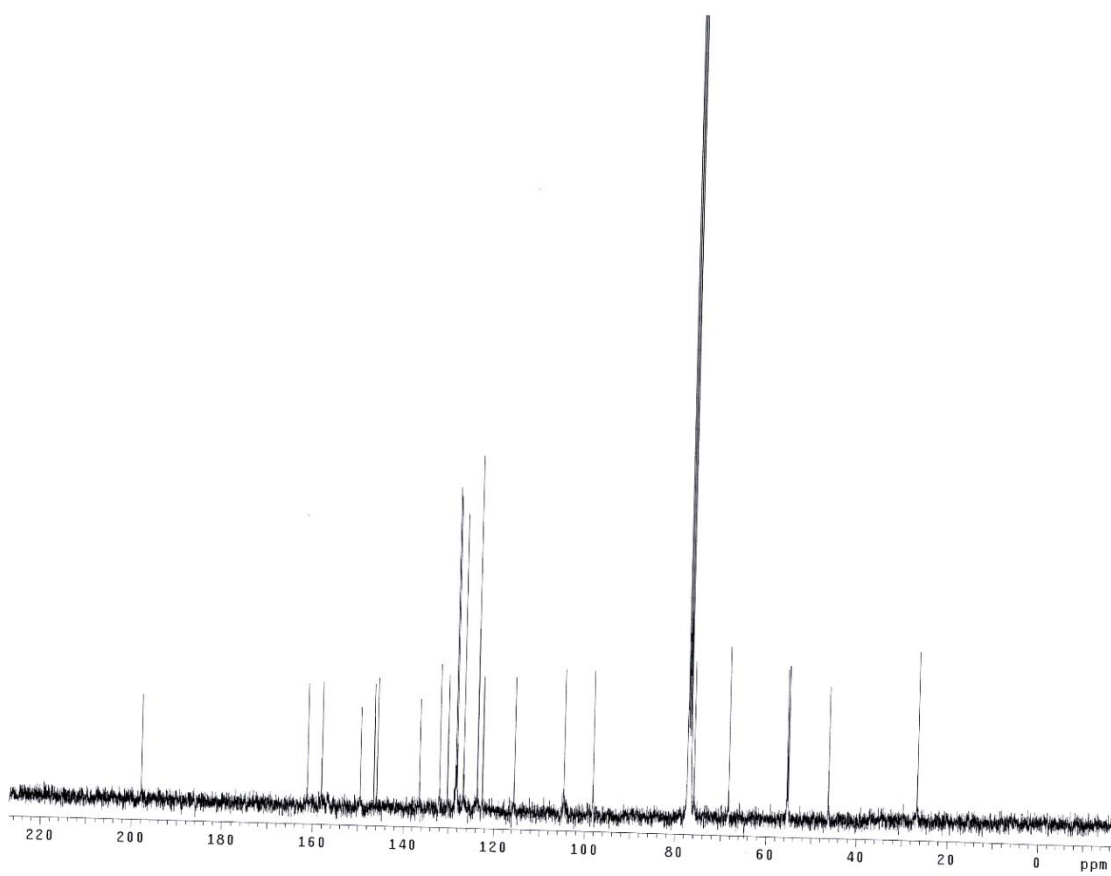
¹H NMR (400 MHz, CDCl₃): δ 8.12 (d, *J* = 9.0 Hz, 2H), 7.86 (d, *J* = 8.4 Hz, 2H), 7.70 (d, *J* = 9.0 Hz, 2H), 7.26 (d, *J* = 8.4 Hz, 2H), 7.08 (d, *J* = 8.4 Hz, 1H), 6.34 (dd, *J* = 8.4, 2.3 Hz, 1H), 6.21 (d, *J* = 2.3 Hz, 1H), 5.99 (ddd, *J* = 17.2, 10.4, 6.8 Hz, 1H), 5.13 (d, *J* = 10.4 Hz, 1H), 5.08 (d, *J* = 4.7 Hz, 1H), 4.87 (d, *J* = 17.2 Hz, 1H), 4.26 (dd, *J* = 6.8, 4.7 Hz, 1H), 4.23 (s, 1H), 4.22 (s, 1H), 3.84 (s, 3H), 3.72 (s, 3H), 3.58 ppm (s, 3H).

¹³C NMR (100 MHz, CDCl₃): δ 166.8, 161.2, 158.1, 149.5, 146.5, 145.7, 132.0, 130.4, 129.5, 129.4, 128.5, 126.6, 123.7, 122.5, 115.6, 104.6, 98.2, 75.8, 68.3, 55.4, 55.2, 52.1, 46.1 ppm.

^1H NMR of **2.3b**



^{13}C NMR of **2.3b**



Methyl 4-(2-(*N*-(2,4-dimethoxybenzyl)-4-nitrophenylsulfonamido)-1-hydroxybut-3

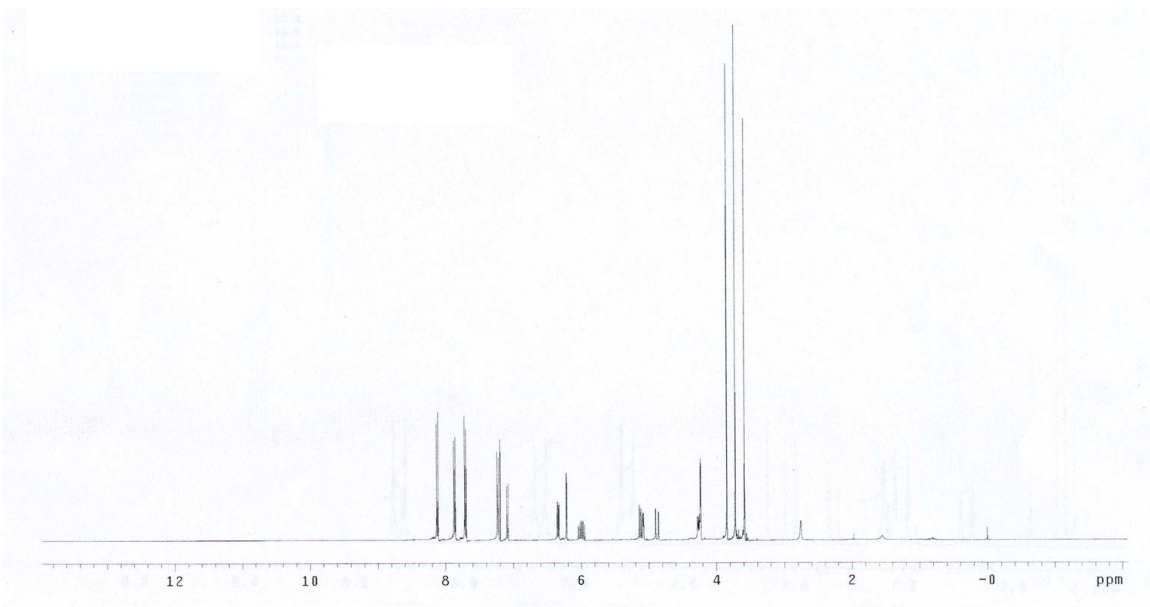
-enyl)benzoate (**2.3c**)

In accordance with the general procedure, the reaction was allowed to stir at 95 °C for 24 h, at which point the reaction mixture was concentrated *in vacuo* the reaction mixture was concentrated *in vacuo* to afford the crude product (dr = >20:1 *anti:syn*, as determined by ¹H NMR spectroscopy). The reaction mixture was then subjected to flash column chromatography (SiO₂: 30% EtOAc/hexanes) to furnish **2.3c** (98 mg, 0.18 mmol, 88% yield) as a yellow oil. *The spectroscopic properties of this compound were consistent with the data available in the literature.*⁶²

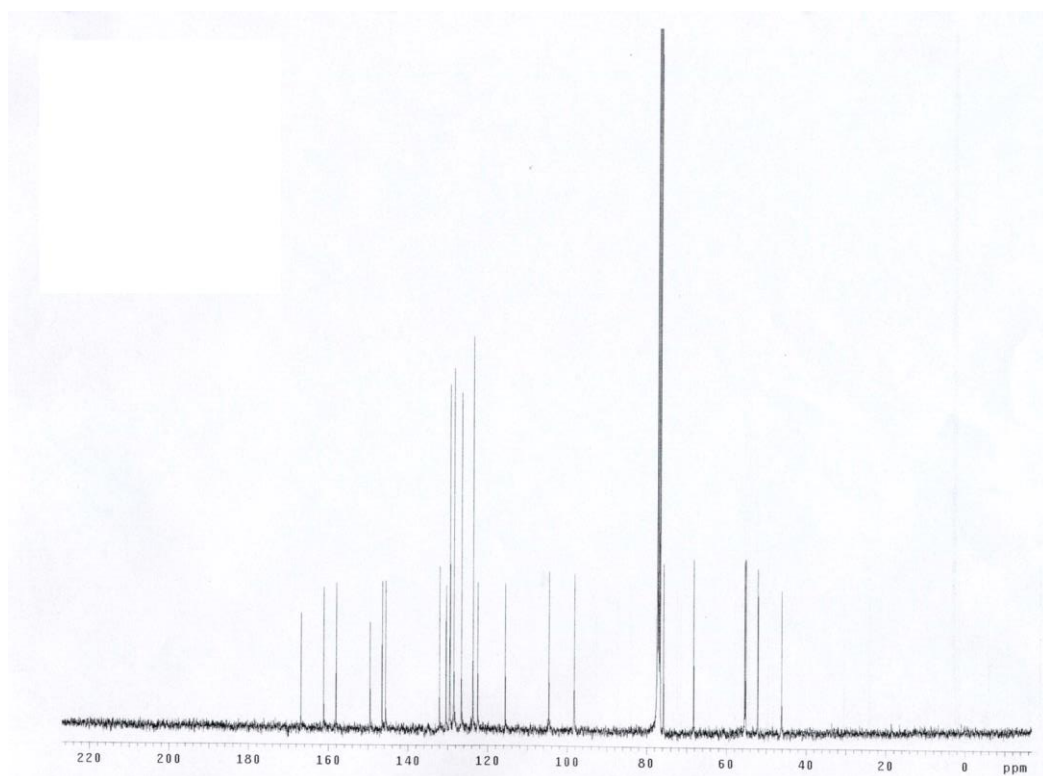
¹H NMR (400 MHz, CDCl₃): δ 8.12 (d, *J* = 9.0 Hz, 2H), 7.86 (d, *J* = 8.4 Hz, 2H), 7.70 (d, *J* = 9.0 Hz, 2H), 7.26 (d, *J* = 8.4 Hz, 2H), 7.08 (d, *J* = 8.4 Hz, 1H), 6.34 (dd, *J* = 8.4, 2.3 Hz, 1H), 6.21 (d, *J* = 2.3 Hz, 1H), 5.99 (ddd, *J* = 17.2, 10.4, 6.8 Hz, 1H), 5.13 (d, *J* = 10.4 Hz, 1H), 5.08 (d, *J* = 4.7 Hz, 1H), 4.87 (d, *J* = 17.2 Hz, 1H), 4.26 (dd, *J* = 6.8, 4.7 Hz, 1H), 4.23 (s, 1H), 4.22 (s, 1H), 3.84 (s, 3H), 3.72 (s, 3H), 3.58 ppm (s, 3H).

¹³C NMR (100 MHz, CDCl₃): δ 166.8, 161.2, 158.1, 149.5, 146.5, 145.7, 132.0, 130.4, 129.5, 129.4, 128.5, 126.6, 123.7, 122.5, 115.6, 104.6, 98.2, 75.8, 68.3, 55.4, 55.2, 52.1, 46.1 ppm.

^1H NMR of **2.3c**



^{13}C NMR of **2.3c**



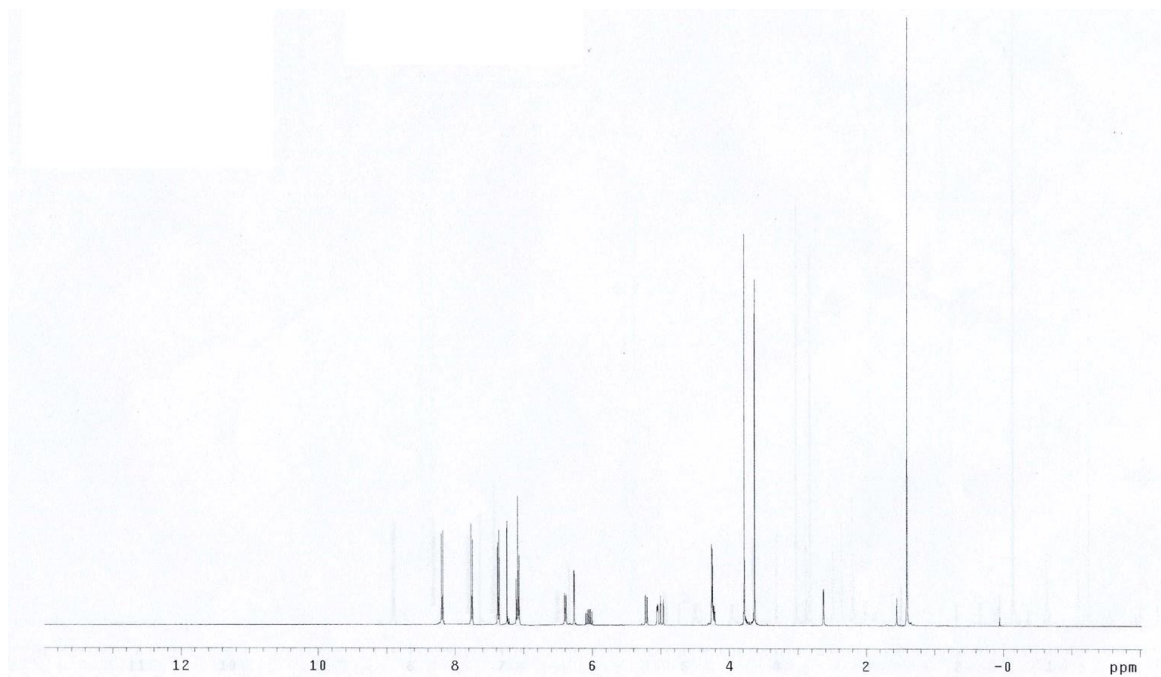
N-(1-(4-bromophenyl)-1-hydroxybut-3-en-2-yl)-*N*-(2,4-dimethoxybenzyl)-4-nitrobenzenesulfonamide (**2.3d**)

In accordance with the general procedure, the reaction was allowed to stir at 95 °C for 24 h, at which point the reaction mixture was concentrated *in vacuo* the reaction mixture was concentrated *in vacuo* to afford the crude product (dr = >20:1 *anti:syn*, as determined by ¹H NMR spectroscopy). The reaction mixture was then subjected to flash column chromatography (SiO₂: 25% EtOAc/hexane) to furnish **2.3d** (84 mg, 0.14 mmol, 73% yield) as a brown foam. *The spectroscopic properties of this compound were consistent with the data available in the literature.*⁶²

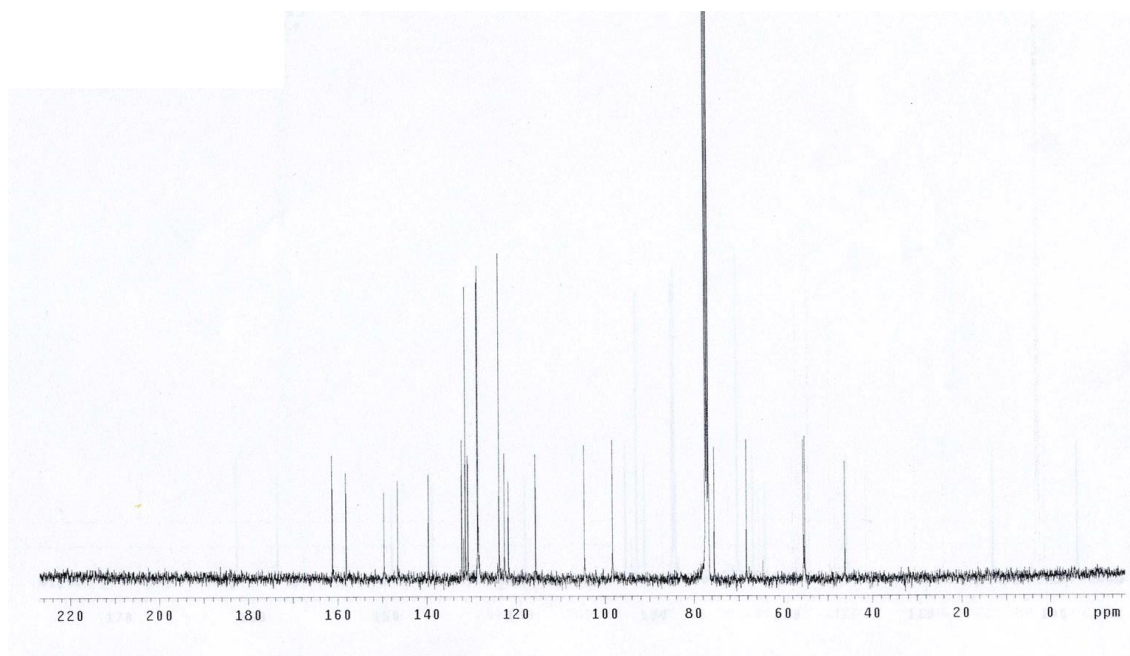
¹H NMR (400 MHz, CDCl₃): δ 8.19 (d, *J* = 8.8 Hz, 2H), 7.75 (d, *J* = 8.8 Hz, 2H), 7.36 (d, *J* = 8.4 Hz, 2H), 7.08 (m, 3H), 6.39 (d, *J* = 8.4 Hz, 1H), 6.26 (d, *J* = 2.3 Hz, 1H), 6.05 (ddd, *J* = 17.2, 10.2, 7.0 Hz, 1H), 5.21 (d, *J* = 10.2 Hz, 1H), 5.04 (dd, *J* = 5.1, 2.6 Hz, 1H), 4.98 (d, *J* = 17.2 Hz, 1H), 4.22 (m, 3H), 3.78 (s, 3H), 3.63 (s, 3H), 2.62 ppm (d, *J* = 2.6 Hz, 1H).

¹³C NMR (100 MHz, CDCl₃): δ 161.2, 158.1, 149.6, 146.5, 139.6, 132.1, 131.2, 130.6, 128.5, 128.4, 123.7, 122.5, 121.6, 115.5, 104.6, 98.2, 75.4, 68.2, 55.4, 55.1, 46.1 ppm.

^1H NMR of **2.3d**



^{13}C NMR of **2.3d**



N-(2,4-dimethoxybenzyl)-*N*-(1-hydroxy-1-phenylbut-3-en-2-yl)-4-nitrobenzenesulfonamide (**2.3e**)

In a modification of the general procedure employing 300 mol% of allene (0.6 mmol), the reaction was allowed to stir at 95 °C for 24 h, at which point the reaction mixture was concentrated *in vacuo* to afford the crude product (dr = >20:1 *anti:syn*, as determined by ¹H NMR spectroscopy). The reaction mixture was then subjected to flash column chromatography (SiO₂: 25% EtOAc/hexanes) to furnish **2.3e** (84 mg, 0.17 mmol, 89% yield) as a yellow oil.

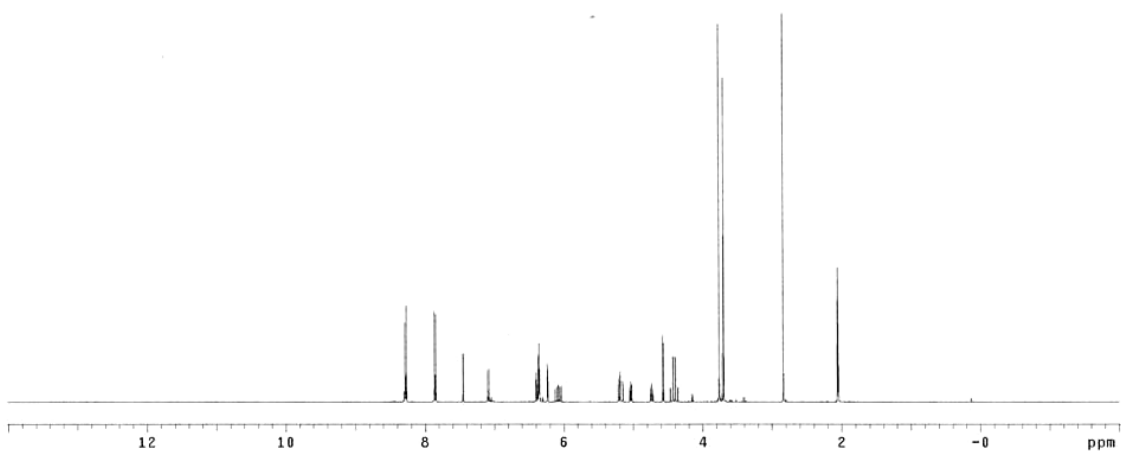
¹H NMR (400 MHz, (CD₃)₂CO): δ 8.28 (d, *J* = 9.2 Hz, 2H), 7.86 (d, *J* = 9.2 Hz, 2H), 7.45 (d, *J* = 2.0 Hz, 1H), 7.08 (d, *J* = 8.4 Hz, 1H), 6.41-6.35 (m, 2H), 6.34 (d, *J* = 2.0 Hz, 1H), 6.23 (d, *J* = 3.2 Hz, 1H), 6.08 (ddd, *J* = 18.0, 10.8, 6.4 Hz, 1H), 5.20-5.18 (m, 1H), 5.16 (m, 2H), 5.03 (dd, *J* = 6.8, 6.0 Hz, 1H), 4.73 (dd, *J* = 8.0, 7.2 Hz, 1H), 4.62 (d, *J* = 6.0 Hz, 1H) 4.44 (d, *J* = 15.0 Hz, 1H), 4.37 (d, *J* = 15.0, 1H), 3.76 (s, 3H), 3.70 ppm (s, 3H).

¹³C NMR (100 MHz, (CD₃)₂CO): δ 161.2, 158.5, 155.3, 149.9, 147.4, 142.1, 133.4, 132.1, 128.9, 124.0, 120.1, 116.6, 112.1, 107.6, 104.8, 97.8, 69.2, 65.0, 55.0, 54.9, 44.9 ppm.

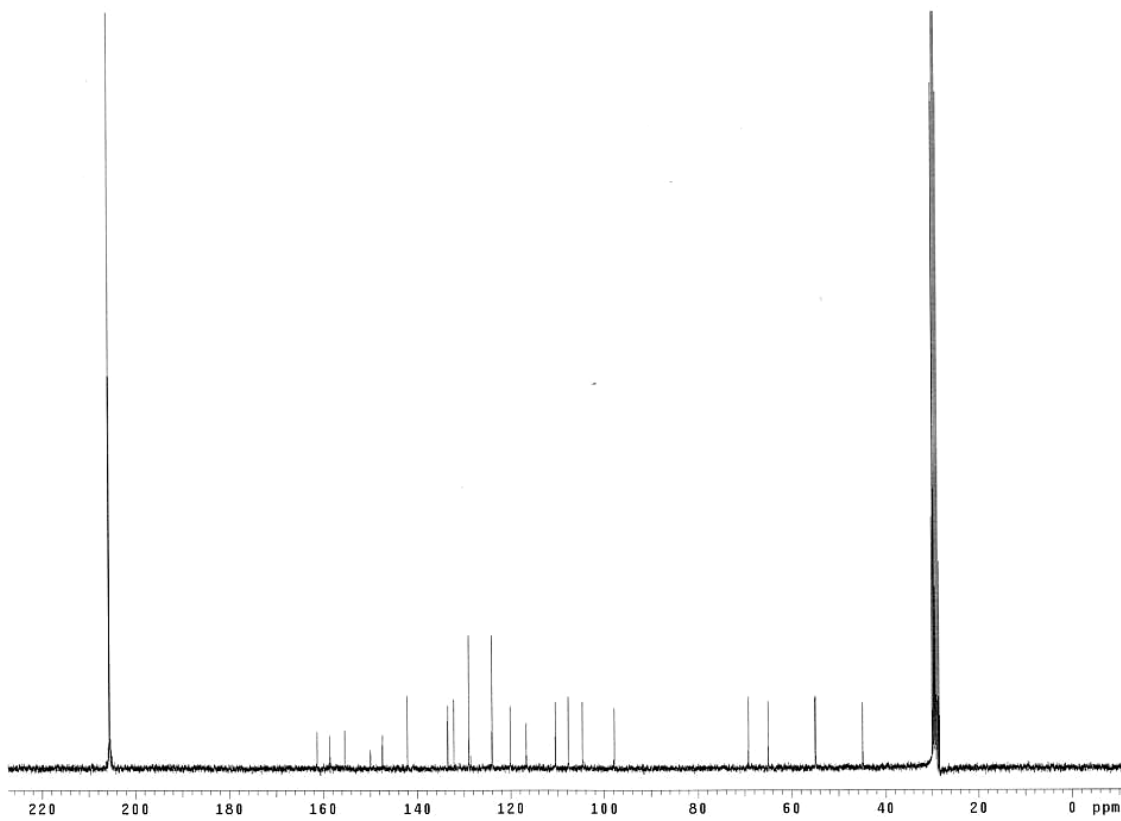
HRMS (CI): Calcd. for C₂₃H₂₈N₂O₇S (M-16): 471.1226, Found: 471.1230.

FTIR (neat): 3505, 2926, 1698, 1611, 1588, 1528, 1508, 1349, 1294, 1257, 1157, 1032, 1010, 935, 735, 686 cm⁻¹.

^1H NMR of **2.3e**



^{13}C NMR of **2.3e**



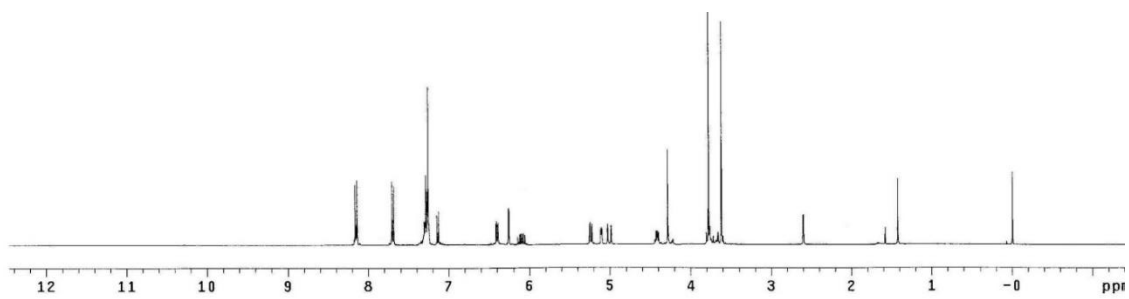
N-(2,4-dimethoxybenzyl)-*N*-(1-hydroxy-1-phenylbut-3-en-2-yl)-4-nitrobenzenesulfonamide (**2.3f**)

In a modification of the general procedure employing 300 mol% of allene (0.6 mmol), the reaction was allowed to stir at 95°C for 24 h, at which point the reaction mixture was concentrated *in vacuo* to afford the crude product (dr = >20:1 *anti:syn*, as determined by ¹H NMR spectroscopy). The reaction mixture was then subjected to flash column chromatography (SiO₂: 25% EtOAc/hexanes) to furnish **2.3f** (71 mg, 0.14 mmol, 71% yield) as a yellow oil. *The spectroscopic properties of this compound were consistent with the data available in the literature.*⁶²

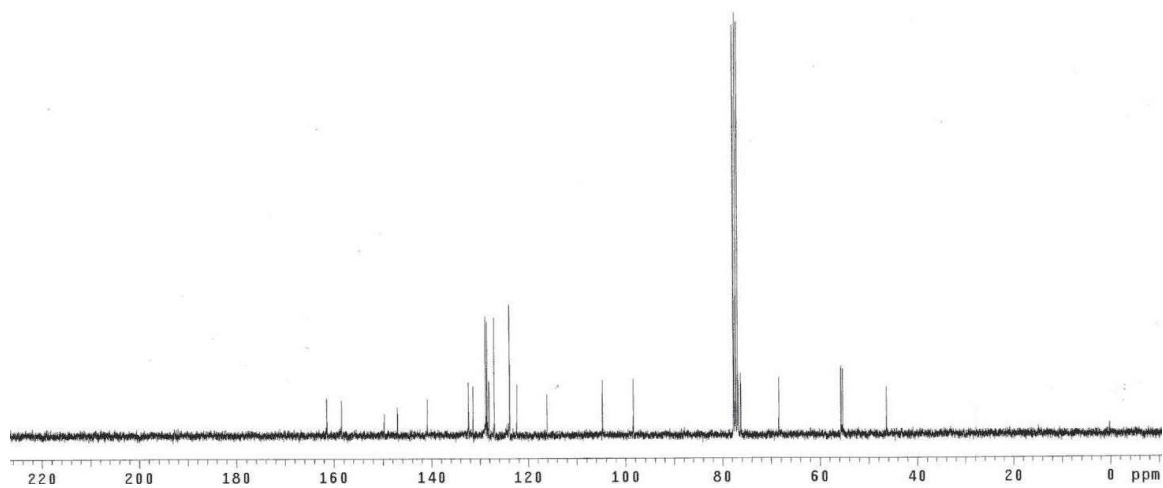
¹H NMR (400 MHz, CDCl₃): δ 8.14 (d, *J* = 8.8 Hz, 2H), 7.80 (d, *J* = 8.8 Hz, 2H), 7.22 – 7.29 (m, 5H), 7.13 (d, *J* = 8.8 Hz, 1H), 6.40 (dd, *J* = 8.8, 2.4 Hz, 1H), 6.26 (d, *J* = 2.4 Hz, 1H), 6.10 (ddd, *J* = 17.2, 10.4, 6.8 Hz, 1H) 5.23 (d, *J* = 10.4 Hz, 1H), 5.10 (dd, *J* = 5.2, 2.4 Hz, 1H), 4.99 (d, *J* = 17.2 Hz, 1H), 4.41 (dd, *J* = 6.8, 5.2 Hz, 1H), 4.28 (s, 2H), 3.78 (s, 3H), 3.62 (s, 3H), 2.60 ppm (d, *J* = 2.4 Hz, 1H).

¹³C NMR (75 MHz, CDCl₃): δ 161.4, 158.4, 149.7, 147.0, 140.9, 132.3, 131.4, 128.8, 128.5, 128.1, 127.0, 123.8, 122.3, 116.1, 104.7, 98.4, 76.2, 68.4, 55.7, 55.3, 46.4 ppm.

^1H NMR of **2.3f**



^{13}C NMR of **2.3f**



N-(2,4-dimethoxybenzyl)-*N*-(4-hydroxy-6-methylhepta-1,5-dien-3-yl)-4-nitrobenzenesulfonamide
(2.3g)

In a modification of the general procedure employing 300 mol% of allene (0.6 mmol), the reaction was allowed to stir at 95 °C for 24 h, at which point the reaction mixture was concentrated *in vacuo* to afford the crude product (dr = >20:1 *anti:syn*, as determined by ¹H NMR spectroscopy). The reaction mixture was then subjected to flash column chromatography (SiO₂: 20% EtOAc/hexanes) to furnish **2.3g** (76 mg, 0.16 mmol, 80% yield) as a yellow oil.

¹H NMR (400 MHz, CDCl₃): δ 8.22 (d, *J* = 9.0 Hz, 2H), 7.83 (d, *J* = 9.0 Hz, 2H), 6.42 (dd, *J* = 8.4, 2.2 Hz, 1H), 6.24 (d, *J* = 2.2 Hz, 1H), 6.00 (ddd, *J* = 17.2, 8.4, 2.0, 1H), 5.28 (dd, *J* = 10.4, 1.6 Hz, 1H), 5.16 (m, 1H), 5.07 (m, 1H), 4.60, (m, 1H), 4.37 (q, *J* = 24.8, 9.6, 2H), 4.21 (dd, *J* = 8.4, 2.8 Hz, 1H), 3.77 (s, 3H), 3.68 (s, 3H), 1.90 (d, *J* = 2.4 Hz, 1H), 1.70 (d, *J* = 1.2 Hz, 3H), 1.65 ppm (d, *J* = 1.2 Hz, 3H)

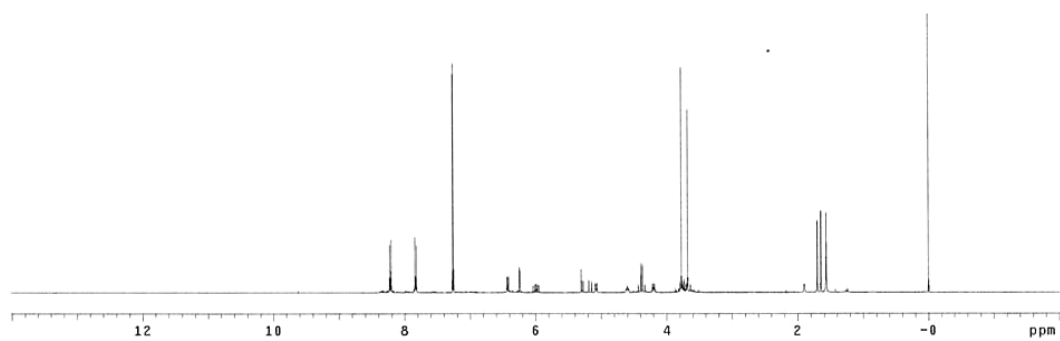
¹³C NMR (100 MHz, CDCl₃): δ 161.0, 158.0, 149.5, 147.0, 138.0, 132.2, 132.0, 128.4, 124.3, 123.7, 121.6, 116.1, 104.4, 98.0, 70.0, 66.7, 55.4, 55.1, 45.2, 25.9, 18.5 ppm.

HRMS (CI): Calcd. for C₂₃H₂₈N₂O₇S (M+1): 477.1695, Found: 477.1695.

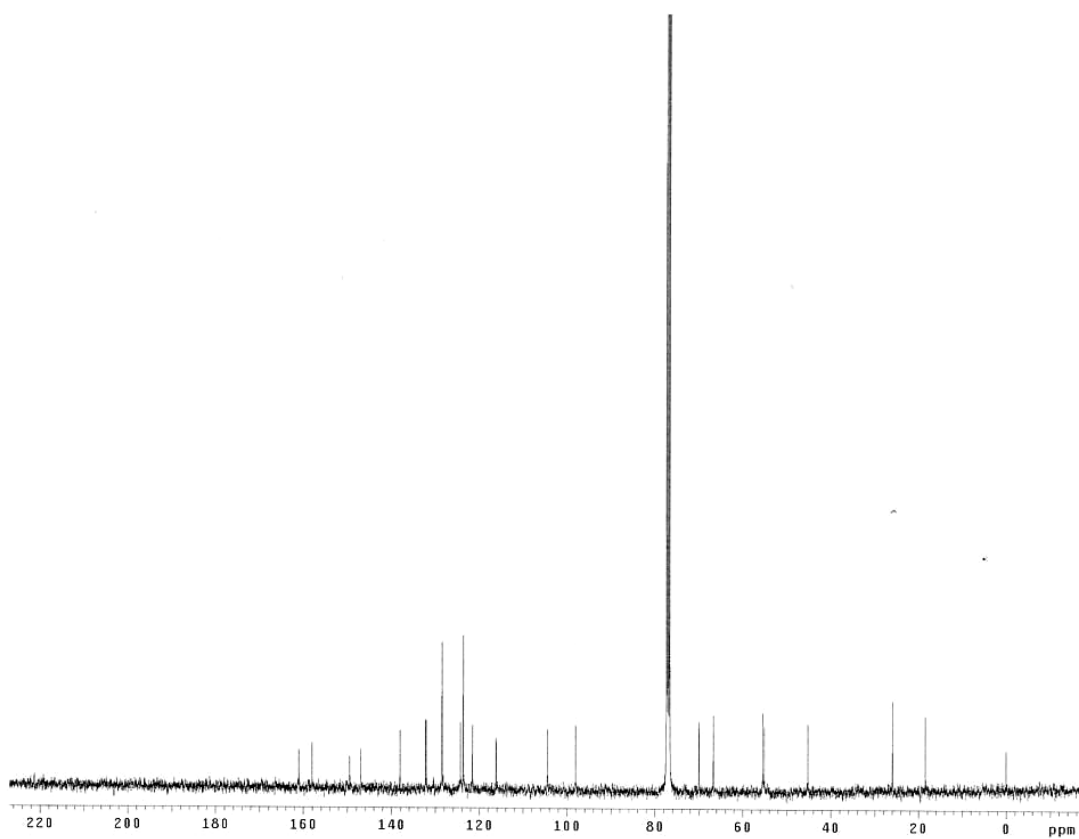
FTIR (neat): 3529, 3104, 2937, 2839, 2361, 2162, 1978, 1528, 1348, 1309, 1293, 1034, 735 cm⁻¹.

1.

^1H NMR of **2.3g**



^{13}C NMR of **2.3g**



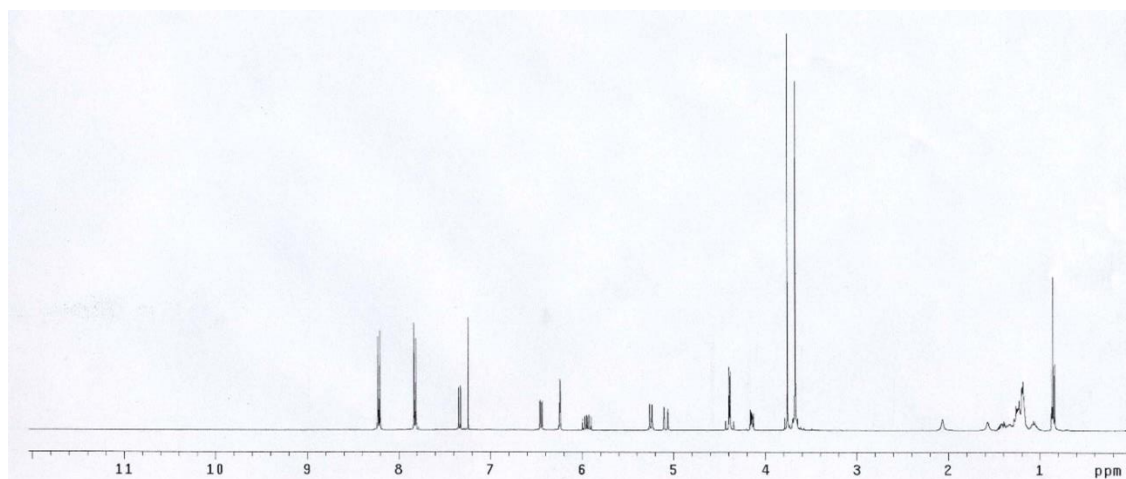
N-(2,4-dimethoxybenzyl)-*N*-(4-hydroxydec-1-en-3-yl)-4-nitrobenzenesulfonamide (**2.3h**)

In a modification of the general procedure employing 300 mol% of allene (0.6 mmol), the reaction was allowed to stir at 95 °C for 24 h, at which point the reaction mixture was concentrated *in vacuo* to afford the crude product (dr = >20:1 *anti:syn*, as determined by ¹H NMR spectroscopy). The reaction mixture was then subjected to flash column chromatography (SiO₂: 20% EtOAc/hexanes) to furnish **2.3h** (67 mg, 0.13 mmol, 68% yield) as a yellow oil. *The spectroscopic properties of this compound were consistent with the data available in the literature.*⁶²

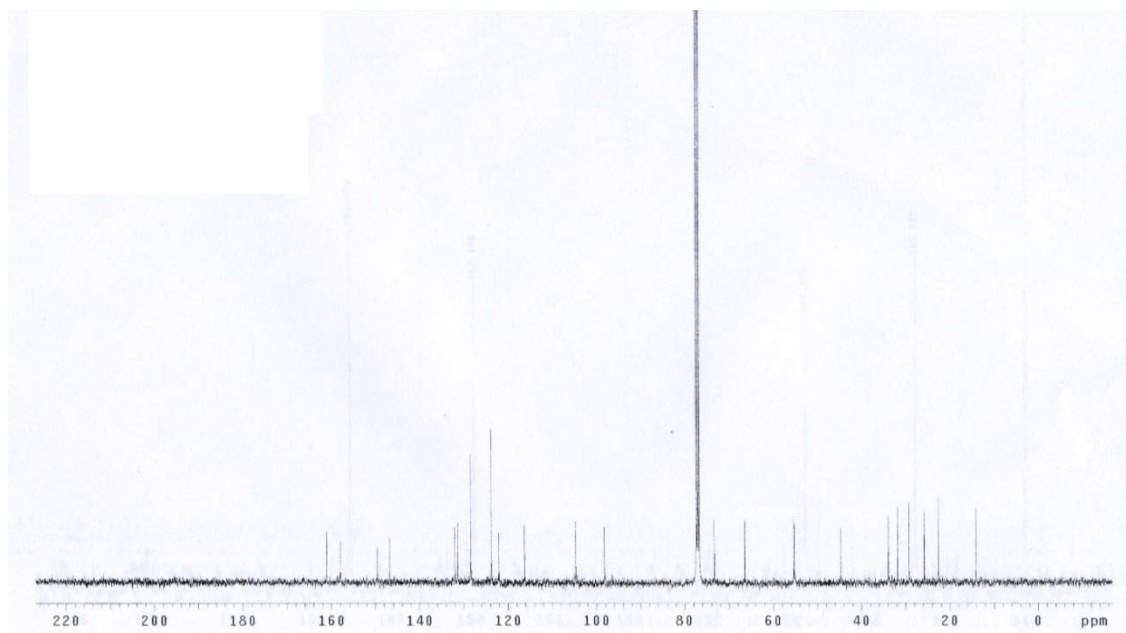
¹H NMR (400 MHz, CDCl₃): δ 8.22 (d, *J* = 9.0 Hz, 2H), 7.82 (d, *J* = 9.0 Hz, 2H), 7.33 (d, *J* = 8.4 Hz, 1H), 6.44 (dd, *J* = 8.4, 2.6 Hz, 1H), 6.23 (d, *J* = 2.6 Hz, 1H), 5.94 (ddd, *J* = 17.2, 10.4, 6.8 Hz, 1H), 5.25 (d, *J* = 10.4 Hz, 1H), 5.08 (d, *J* = 17.2 Hz, 1H), 4.39 (s, 1H), 4.38 (s, 1H), 4.15 (q, *J* = 4.7 Hz, 1H), 3.76 (s, 3H), 3.67 (s, 4H), 2.06 (s, 1H), 1.45 – 1.02 (m, 10H), 0.85 ppm (t, *J* = 6.8 Hz, 3H).

¹³C NMR (100 MHz, CDCl₃): δ 161.0, 157.9, 149.5, 146.8, 131.9, 131.3, 128.4, 123.7, 122.0, 116.2, 104.6, 98.1, 73.3, 66.4, 55.4, 55.2, 44.6, 33.8, 31.8, 29.2, 25.7, 22.6, 14.1 ppm.

^1H NMR of **2.3h**



^{13}C NMR of **2.3h**



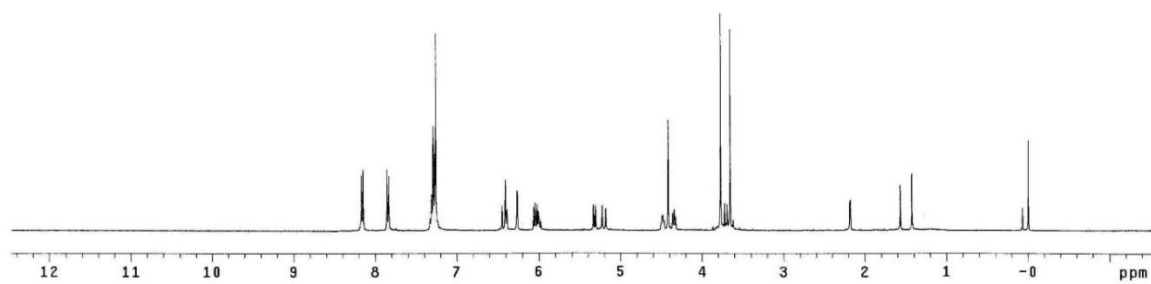
(*E*)-*N*-(2,4-dimethoxybenzyl)-*N*-(4-hydroxy-6-phenylhexa-1,5-dien-3-yl)-4-nitrobenzenesulfonamide (**2.3i**)

In a modification of the general procedure employing 300 mol% of allene (0.6 mmol), the reaction was allowed to stir at 95 °C for 24 h, at which point the reaction mixture was concentrated *in vacuo* to afford the crude product (dr = >20:1 *anti:syn*, as determined by ¹H NMR spectroscopy). The reaction mixture was then subjected to flash column chromatography (SiO₂: 25% EtOAc/hexanes) to furnish **2.3i** (89 mg, 0.17 mmol, 85% yield) as a yellow oil. *The spectroscopic properties of this compound were consistent with the data available in the literature.*⁶²

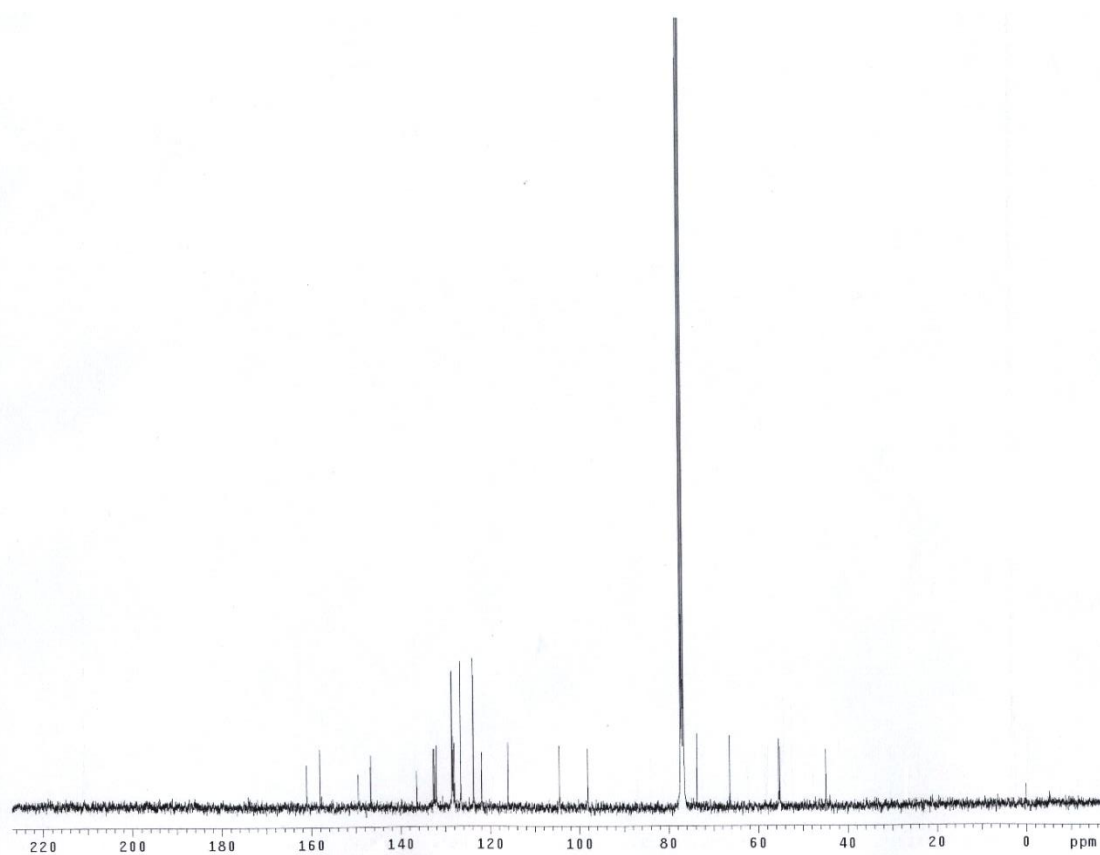
¹H NMR (400 MHz, CDCl₃): δ 8.16 (d, *J* = 8.4 Hz, 2H), 7.84 (d, *J* = 8.4 Hz, 2H), 7.25 – 7.35 (m, 6H), 6.40 (m, 2H), 6.26 (d, *J* = 2.0 Hz, 1H), 6.02 (m, 2H), 5.31 (d, *J* = 10.4 Hz, 1H), 5.20 (d, *J* = 17.2 Hz, 1H), 4.48 (m, 1H), 4.42 (s, 2H), 4.34 (t, *J* = 7.2 Hz, 1H), 3.77 (d, *J* = .8 Hz, 3H), 3.66 (s, 3H), 2.18 ppm (d, *J* = 3.2 Hz, 1H).

¹³C NMR (100 MHz, CDCl₃): δ 161.1, 158.1, 149.5, 146.7, 136.4, 132.7, 132.4, 132.0, 128.6, 128.5, 128.3, 128.0, 126.6, 123.7, 121.9, 116.0, 104.5, 98.1, 73.7, 66.4, 55.4, 55.1, 44.9 ppm.

^1H NMR of **2.3i**



^{13}C NMR of **2.3i**



N-(6-(benzyloxy)-4-hydroxyhex-1-en-3-yl)-*N*-(2,4-dimethoxybenzyl)-4-nitrobenzenesulfonamide
(2.3j)

In a modification of the general procedure employing 300 mol% of allene (0.6 mmol), the reaction was allowed to stir at 95 °C for 24 h, at which point the reaction mixture was concentrated *in vacuo* to afford the crude product (dr = >20:1 *anti:syn*, as determined by ¹H NMR spectroscopy). The reaction mixture was then subjected to flash column chromatography (SiO₂: 20% EtOAc/hexanes) to furnish **2.3j** (99 mg, 0.18 mmol, 89% yield) as a yellow oil..

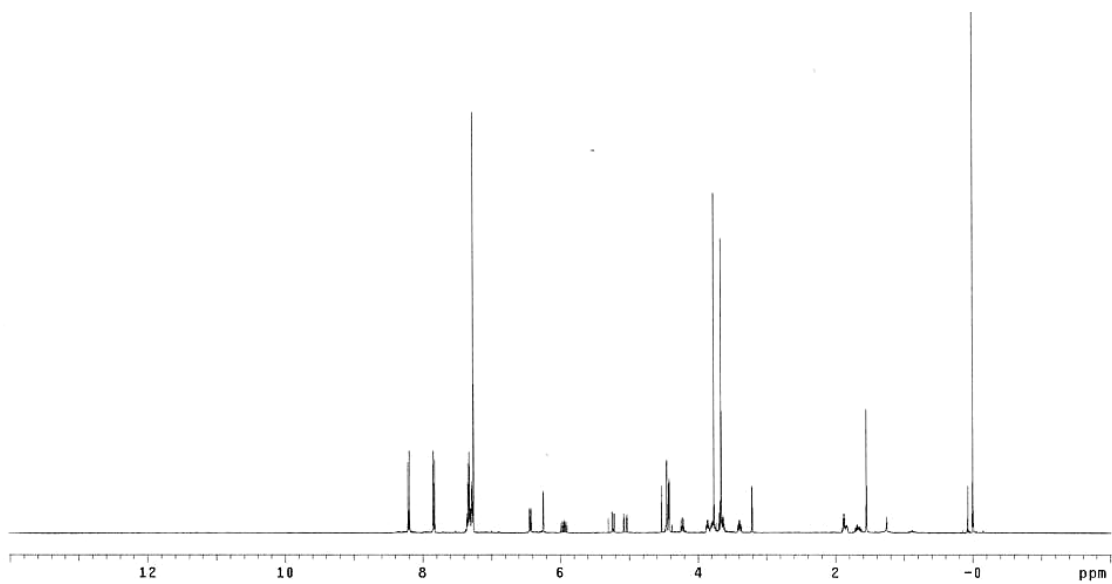
¹H NMR (400 MHz, CDCl₃): δ 8.20 (d, *J* = 9.0 Hz, 2H), 7.83 (d, *J* = 9.0 Hz, 2H), 7.38-7.25 (m, 6H), 6.43 (dd, *J* = 8.4, 2.4 Hz, 1H), 6.24 (d, *J* = 2.4 Hz, 1H), 5.94 (ddd, *J* = 17.2, 10.4, 8.8 Hz, 1H), 5.23 (d, *J* = 17.2 Hz, 1H) 5.05 (d, *J* = 10.4 Hz, 1H), 4.45 (s, 2H), 4.42 (d, *J* = 4.4 Hz, 2H), 4.22 (dd, *J* = 8.8, 7.0 Hz, 1H), 3.89-3.84 (m, 1H), 3.82-3.78 (m, 1H), 3.39 (ddd, *J* = 9.2, 7.0, 3.6 Hz, 1H), 1.90-1.84 (m, 1H), 1.72-1.62 ppm (m, 1H).

¹³C NMR (100 MHz, CDCl₃): δ 161.0, 158.0, 149.5, 146.8, 137.8, 132.1, 132.0, 128.5, 127.8, 127.6, 123.8, 121.4, 116.4, 104.5, 98.0, 73.3, 72.3, 68.9, 65.8, 55.4, 55.1, 44.0, 33.3 ppm.

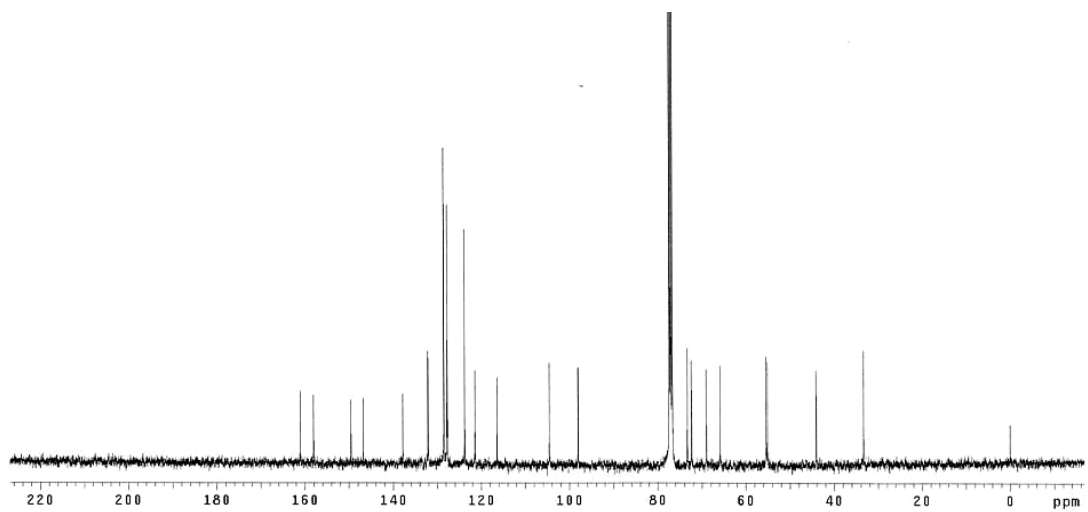
HRMS (CI): Calcd. for C₂₈H₃₂N₂O₈S (M+1):

FTIR (neat) – 3448, 2926, 2857, 2360, 1610, 1400, 1347, 1293, 1263, 1158, 1088, 1032, 880, 735 cm⁻¹.

^1H NMR of **2.3j**



^{13}C NMR of **2.3j**



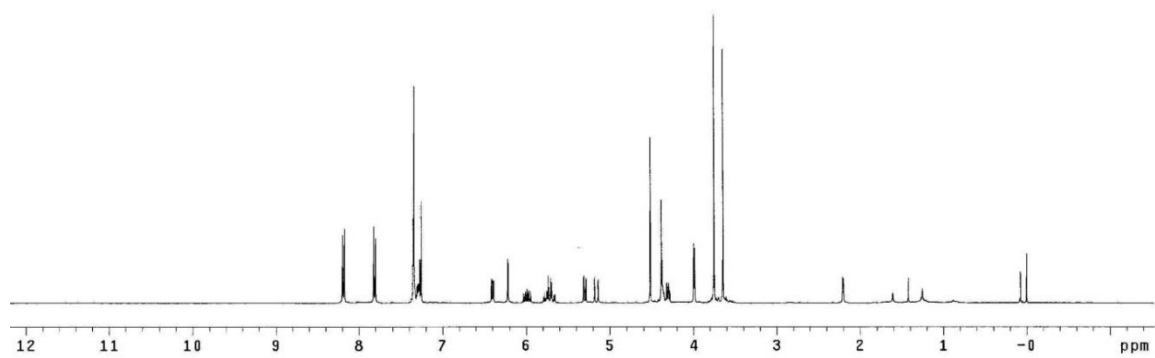
(*E*)-*N*-(7-(benzyloxy)-4-hydroxyhepta-1,5-dien-3-yl)-*N*-(2,4-dimethoxybenzyl)-4-nitrobenzenesulfonamide (**2.3k**)

In a modification of the general procedure employing 300 mol% of allene (0.6 mmol), the reaction was allowed to stir at 95 °C for 24 h, at which point the reaction mixture was concentrated *in vacuo* to afford the crude product (dr = >20:1 *anti:syn*, as determined by ¹H NMR spectroscopy). The reaction mixture was then subjected to flash column chromatography (SiO₂: 30% EtOAc/hexanes) to furnish **2.3k** (92 mg, 0.16 mmol 81% yield) as a yellow oil. *The spectroscopic properties of this compound were consistent with the data available in the literature.*⁶²

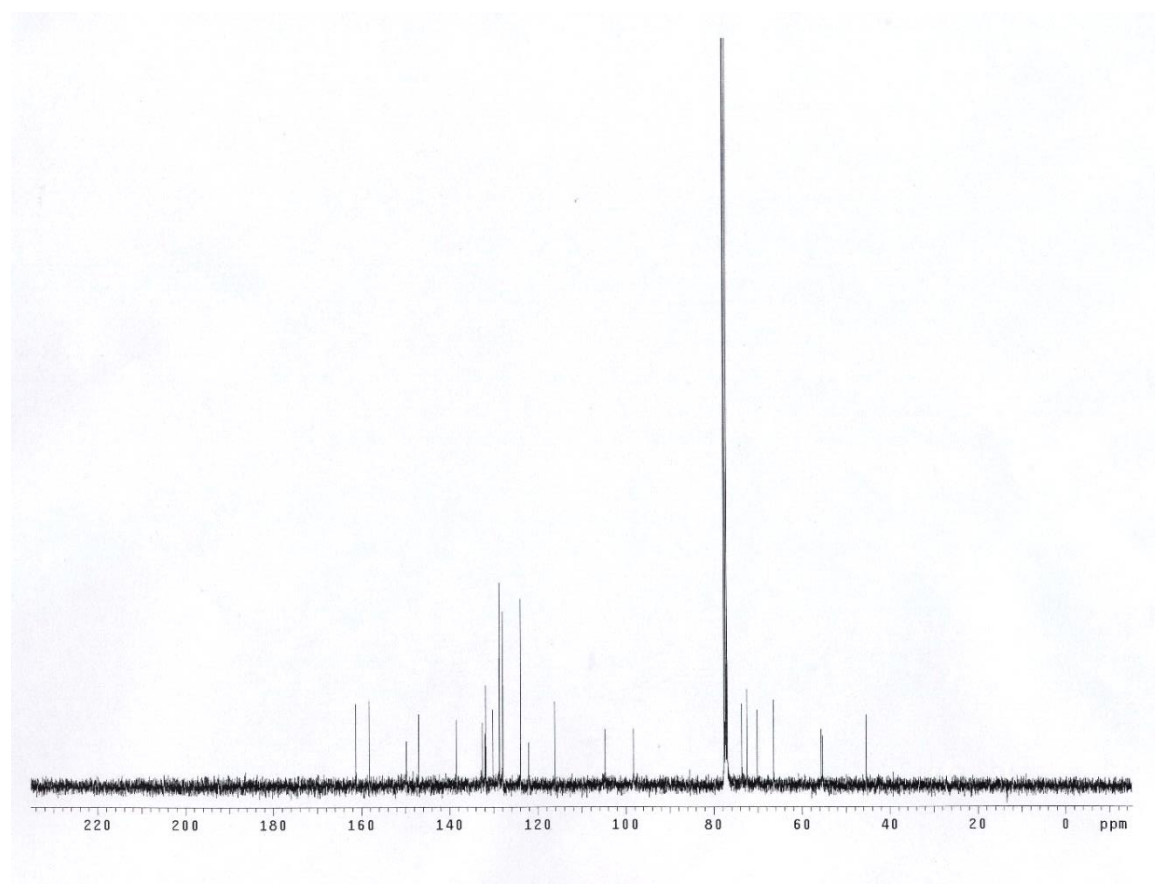
¹H NMR (400 MHz, CDCl₃): δ 8.18 (d, *J* = 8.8 Hz, 2H), 7.80 (d, *J* = 8.8 Hz, 2H), 7.33 – 7.35 (m, 3H), 7.27 – 7.32 (m, 3H), 6.40 (dd, *J* = 8.4, 2.4 Hz, 1H), 6.21 (d, *J* = 2.4 Hz, 1H), 5.99 (ddd, *J* = 17.2, 10.4, 6.8 Hz, 1H), 5.71 (m, 2H), 5.28 (d, *J* = 10.4 Hz, 1H), 5.14 (d, *J* = 17.2 Hz, 1H), 4.52 (s, 2H), 4.39 (s, 2H), 4.37 (m, 1H), 4.30 (m, 1H), 3.99 (d, *J* = 5.2 Hz, 2H), 3.75 (s, 3H), 3.64 (s, 3H), 2.20 ppm (d, *J* = 3.6 Hz, 1H).

¹³C NMR (100 MHz, CDCl₃): δ 162.3, 158.3, 149.7, 147.0, 138.5, 132.5, 131.9, 131.7, 130.2, 128.7, 128.6, 128.0, 127.9, 123.9, 122.1, 116.1, 104.7, 98.2, 73.6, 72.5, 70.1, 66.4, 55.6, 55.3, 45.4 ppm.

^1H NMR of **2.3k**



^{13}C NMR of **2.3k**



N-(8-(benzyloxy)-4-hydroxyoct-1-en-3-yl)-*N*-(2,5-dimethoxybenzyl)-4-nitrobenzenesulfonamide
(2.3I)

In a modification of the general procedure employing 300 mol% of allene (0.6 mmol), the reaction was allowed to stir at 95 °C for 24 h, at which point the reaction mixture was concentrated *in vacuo* to afford the crude product (dr = >20:1 *anti:syn*, as determined by ¹H NMR spectroscopy). The reaction mixture was then subjected to flash column chromatography (SiO₂: 20% EtOAc/hexanes) to furnish **2.3I** (93 mg, 0.16 mmol, 80% yield) as a yellow oil.

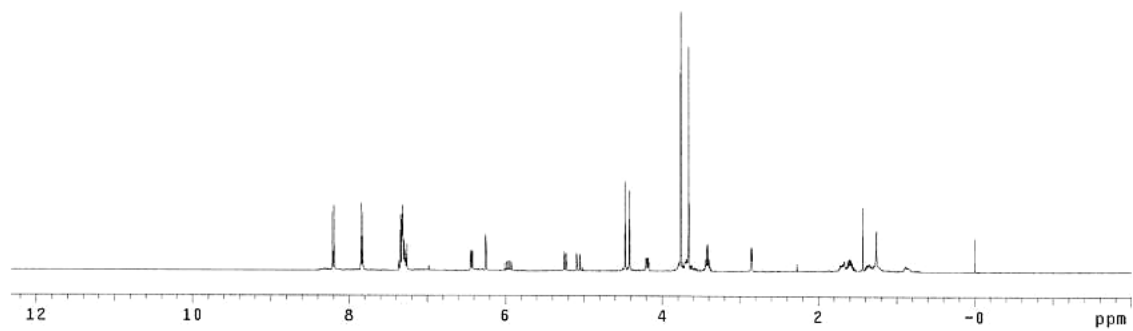
¹H NMR (400 MHz, CDCl₃): δ 8.20 (d, *J* = 9.0 Hz, 2H), 7.83 (d, *J* = 9.0 Hz, 2H), 7.36-7.26 (m, 6H), 6.42 (dd, *J* = 8.4, 2.4 Hz, 1H), 6.24 (d, *J* = 2.4 Hz, 1H), 5.96 (ddd, *J* = 17.2, 10.4, 8.8 Hz, 1H), 5.24 (d, *J* = 17.2 Hz, 1H), 4.47 (s, 2H), 4.41 (s, 2H), 4.19 (dd, *J* = 8.8, 6.0 Hz, 1H), 3.76 (s, 3H), 3.65 (s, 3H), 3.41 (dd, *J* = 12.0, 6.0 Hz, 2H), 2.85 (d, *J* = 3.6 Hz, 1H), 1.74-1.5 (m, 4H), 1.40-1.30 (m, 1H), 0.9-0.8 ppm (m, 1H).

¹³C NMR (100 MHz, CDCl₃): δ 159.9, 156.9, 148.5, 145.7, 137.1, 130.9, 130.9, 127.4, 126.6, 122.7, 120.5, 115.3, 103.5, 97.0, 71.9, 71.6, 69.3, 65.3, 54.4, 54.0, 43.3, 30.3, 25.1 ppm.

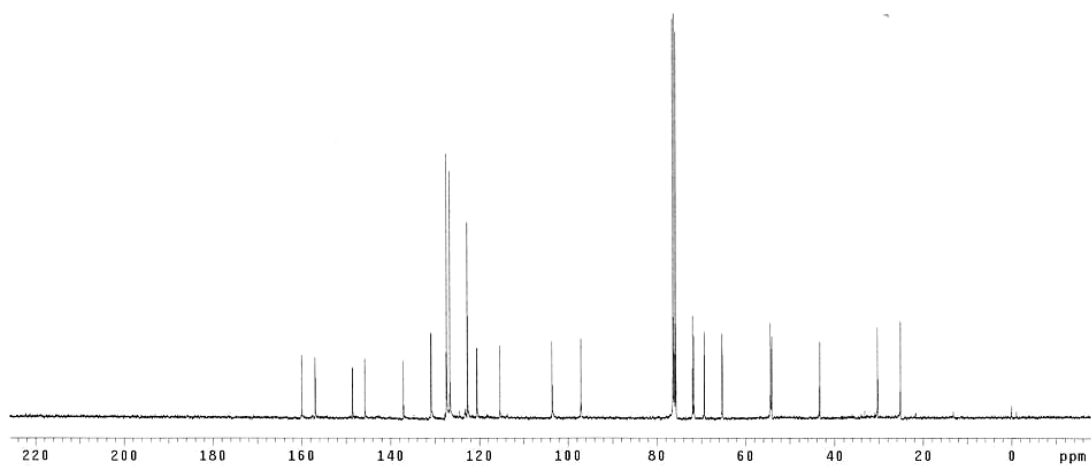
HRMS (CI): Calcd. for C₃₀H₃₇N₂O₈S (M+1): 585.2271, Found: 585.2274

FTIR (neat)- 3525, 3103, 2925, 1610, 1508, 1421, 1401, 1265, 1159, 1131, 1089, 1033, 881, 735 cm⁻¹.

¹H NMR of **2.3I**



¹³C NMR of **2.3I**



2.5.5 General Procedures for Formation of All-Carbon Quaternary Centers using 1,1-Disubstituted Allenes

Procedure A: To a re-sealable pressure tube (13 x 100 mm) equipped with magnetic stir bar, RuHCl(CO)(PPh₃)₃ (9.5 mg, 0.01 mmol, 5 mol%), 1,1'-Bis(di-*i*-propylphosphino)ferrocene (4.2 mg, 0.01 mmol, 5 mol%), and alcohol (0.2 mmol, 100 mol%) were added. The tube was sealed with a rubber septum and purged with argon. Allene **2.7a** (60.1 μ L, 0.4 mmol, 200 mol%) and THF were added and the rubber septum was quickly replaced with a screw cap. The mixture was heated for the indicated time. The reaction mixture was then concentrated *in vacuo* and the ratio of diastereomers was determined by NMR of the crude reaction mixture. The crude reaction mixture was subjected to flash column chromatography under the conditions indicated to furnish the corresponding product of allylation.

Procedure B: To a re-sealable pressure tube (13 x 100 mm) equipped with magnetic stir bar, RuH₂(CO)(PPh₃)₃ (9.2 mg, 0.01 mmol, 5 mol%), 1,1'-Bis(di-*i*-propylphosphino)ferrocene (4.2 mg, 0.01 mmol, 5 mol%), mesitylene sulfonic acid (2.4 mg, 0.01 mmol, 5 mol%) and alcohol starting material (0.2 mmol, 100 mol%) were added. The tube was sealed with a rubber septum and purged with argon. Allene **2.7a** (60.1 μ L, 0.4 mmol, 200 mol%) and THF were added and the rubber septum was quickly replaced with a screw cap. The mixture was heated for the indicated time. The reaction mixture was then concentrated *in vacuo* and the ratio of diastereomers was determined by ¹H NMR of the crude reaction mixture. The reaction mixture was then subjected to flash column chromatography (SiO₂: 5-15% Et₂O/hexanes) to furnish the corresponding product of allylation.

2.5.6 Characterization of 2.10a, e, f, i, j, h, m

2-methyl-1-(4-nitrophenyl)-2-phenylbut-3-en-1 (2.10a)

In accordance with the general procedure B, the reaction was allowed to stir at 50 °C for 48 h, at which point the reaction mixture was then concentrated *in vacuo* to afford the crude product (dr = >20:1 *anti:syn*, as determined by ¹H NMR spectroscopy). The reaction mixture was then subjected to flash column chromatography (SiO₂: 5-15% Et₂O/hexanes) to furnish **2.10a** (47 mg, 0.17 mmol 84% yield) as a clear oil. *The spectroscopic properties of this compound were consistent with the data available in the literature.*⁶⁸

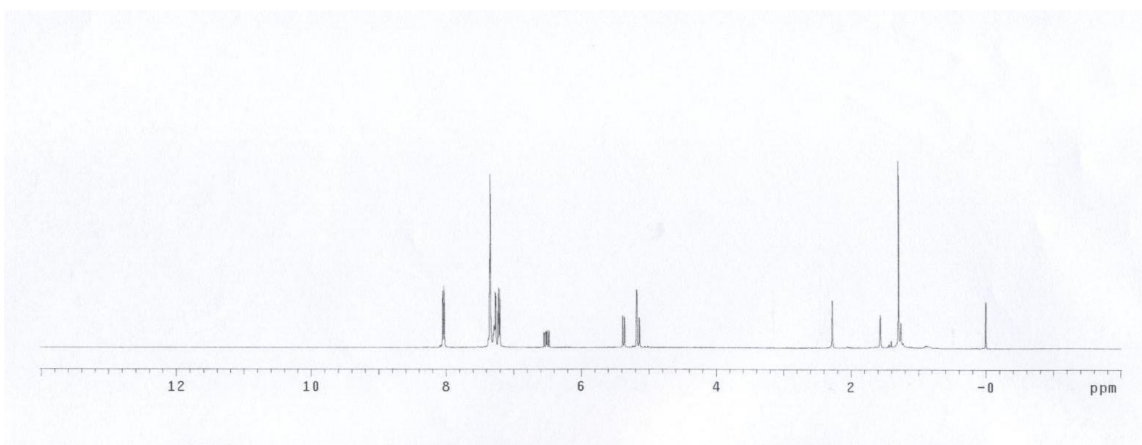
¹H NMR (400 MHz, CDCl₃): δ 8.04 (dd, *J* = 8.8, 2.0 Hz, 2H), 7.56-7.35 (m, 5H), 7.21 (dd, *J* = 8.8, 2.0 Hz, 2H), 6.51 (dd, *J* = 17.6, 11.0 Hz, 1H), 5.37 (dd, *J* = 11.0, 1.4 Hz, 1H), 5.18 (m, 1H), 5.16 (dd, *J* = 17.6, 1.4 Hz, 1H), 2.28 (s, 1H), 1.28 ppm (s, 3H).

¹³C NMR (100 MHz, CDCl₃): δ 147.2, 143.7, 141.5, 128.6, 128.6, 127.1, 122.3, 116.4, 79.3, 77.3, 50.4, 29.7, 19.4 ppm.

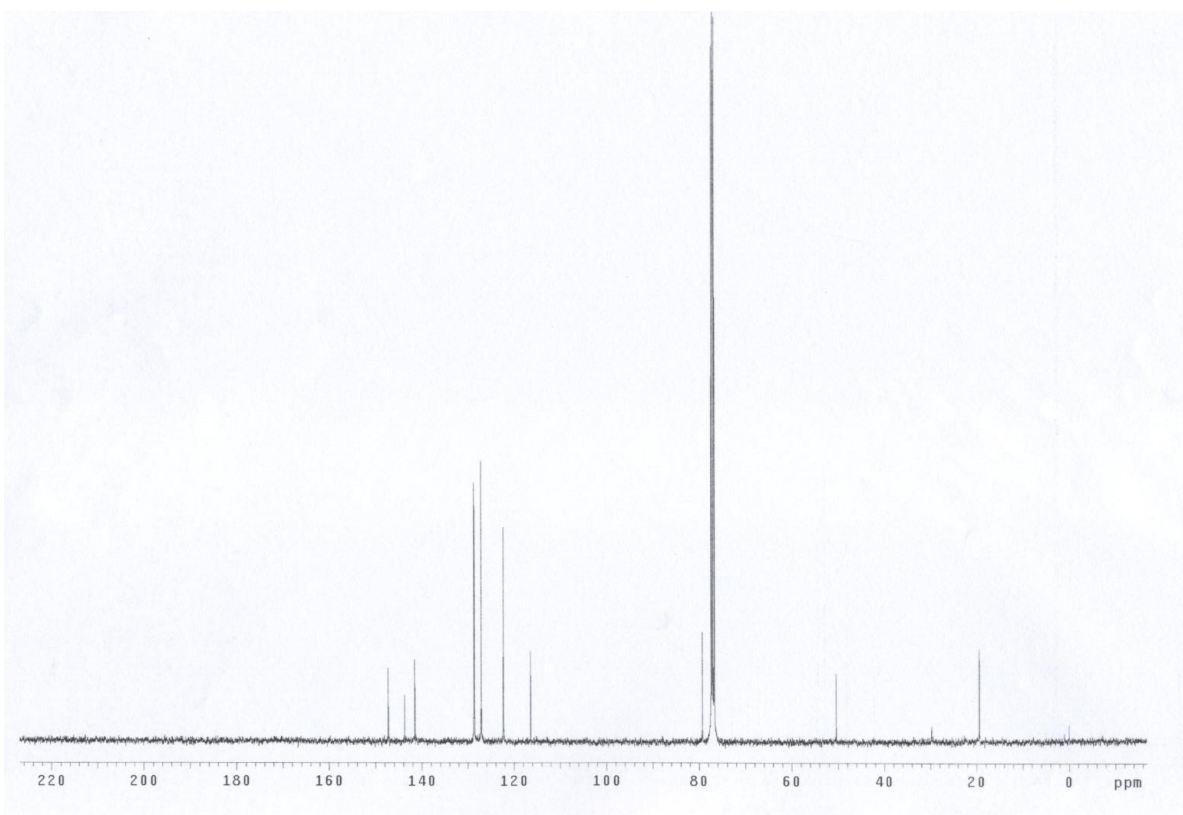
HRMS (CI) Calcd. For C₁₇H₁₇NO₃(M⁺): 284.1287, Found: 284.1286.

FTIR (neat): 3577, 3504, 3480, 3458, 3082, 1637, 1599, 1445, 1413, 1281, 1060, 1030, 919, 764, 700, 667 cm⁻¹.

^1H NMR of **2.10a**



^{13}C NMR of **2.10a**



1-(furan-2-yl)-2-methyl-2-phenylbut-3-en-1-ol (**2.10e**)

In accordance with the general procedure A, THF (0.4 mL, 0.5 M concentration with respect to alcohol) were added and the reaction was heated to 60 °C for 24 h, at which point the reaction mixture was then concentrated *in vacuo* to afford the crude product (dr = 10:1 *anti:syn*, as determined by ¹H NMR spectroscopy). The reaction mixture was then subjected to flash column chromatography (SiO₂: 5-20% Et₂O/hexanes) to furnish **2.10e** (45 mg, 0.20 mmol, 99% yield) as a clear, colorless oil.

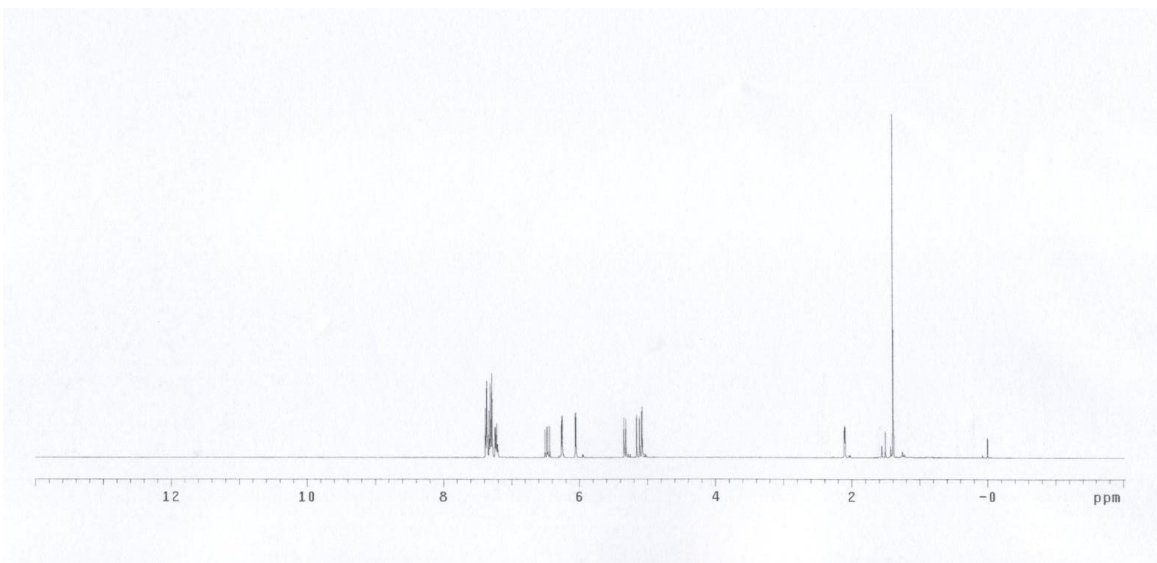
¹H NMR (400 MHz, CDCl₃): δ 7.40-7.22 (m, 6H), 6.49 (dd, *J* = 18.0, 10.8 Hz, 1H), 6.28 (dd, *J* = 3.1, 1.8 Hz, 1H), 6.07 (d, *J* = 3.1, 1H), 5.35 (dd, *J* = 10.8, 1.1 Hz, 1H), 5.16 (dd, *J* = 18.0, 1.1 Hz, 1H), 5.10 (d, *J* = 4.0 Hz, 1H), 2.14 (d, *J* = 4.0 Hz, 1H), 1.42 ppm (s, 3H).

¹³C NMR (100 MHz, CDCl₃): δ 154.2, 144.8, 144.3, 141.6, 128.5, 128.4, 127.7, 127.4, 126.8, 115.7, 110.3, 108.0, 74.8, 50.3, 21.6 ppm.

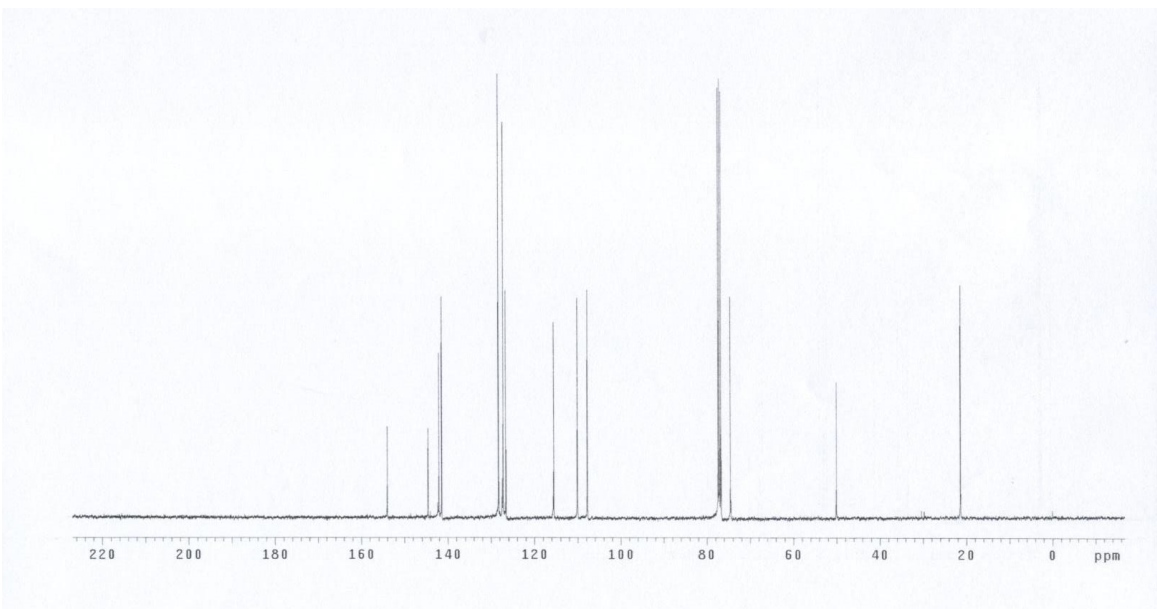
HRMS (CI) Calcd. For C₁₅H₁₇O₂(*M*+1): 229.1229, Found: 229.1222.

FTIR (neat): 2961, 2922, 2852, 1497, 1464, 1445, 1412, 1372, 1261, 1213, 1471, 1076, 1010, 920, 809, 738, 699, 658 cm⁻¹.

^1H NMR of **2.10e**



^{13}C NMR of **2.10e**



2-methyl-1,2-diphenylbut-3-en-1-ol (**2.10f**)

In accordance with the general procedure A, THF (0.4 mL, 0.5 M concentration with respect to alcohol) were added and the reaction was heated to 60 °C for 24 h, at which point the reaction mixture was then concentrated *vacuo* to afford the crude product (dr = 6:1 *anti:syn*, as determined by ¹H NMR spectroscopy). The reaction mixture was then subjected to flash column chromatography (SiO₂: 5-20% Et₂O/hexanes) to furnish **2.10f** (47 mg, 0.20 mol, 99% yield) as a clear, colorless oil. *The spectroscopic properties of this compound were consistent with the data available in the literature.*^{70a}

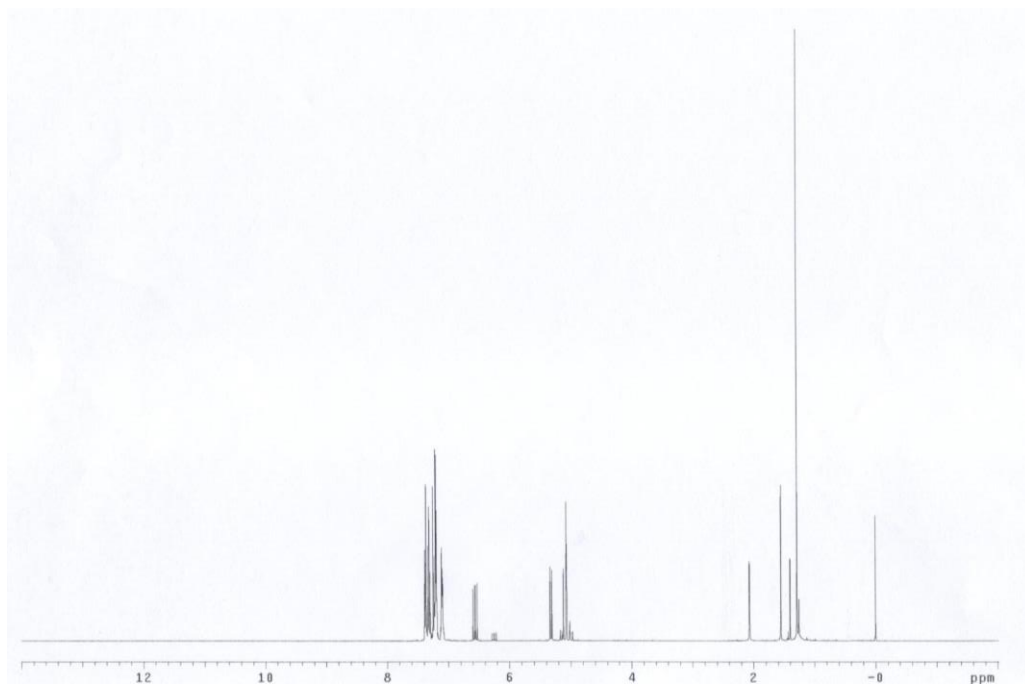
¹H NMR (400 MHz, CDCl₃): δ 7.37-7.35 (m, 2H), 7.33-7.30 (m, 2H), 7.25-7.19 (m, 4H), 7.12-7.09 (m, 2H) 6.56 (dd, *J* = 17.6, 11.0 Hz, 1H), 5.32 (dd, *J* = 11.0, 1.2 Hz, 1H), 5.10 (dd, *J* = 17.6, 1.2 Hz, 1H), 5.07 (d, *J* = 2.0 Hz, 1H), 2.07 (d, *J* = 2.0 Hz, 1H), 1.29 ppm (s, 3H).

¹³C NMR (100 MHz, CDCl₃): δ 145.0, 142.0, 140.0, 128.3, 127.9, 127.4, 127.2, 127.2, 126.5, 115.6, 80.3, 50.3, 20.6 ppm.

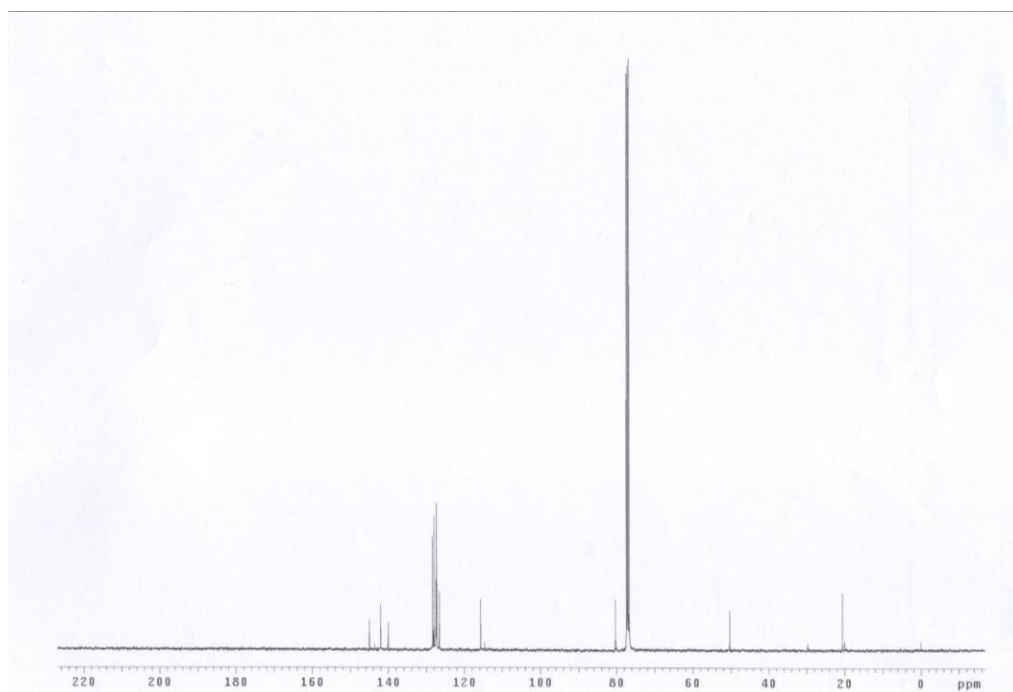
HRMS (CI) Calcd. For C₁₇H₁₈O(M⁺): 238.1358, Found: 238.1355.

FTIR (neat): 3577, 3558, 3479, 3459, 3082, 2954, 2924, 2856, 1636, 1599, 1466, 1445, 1413, 1282, 1061, 1030, 917, 764, 600, 668 cm⁻¹.

^1H NMR of **2.10f**



^{13}C NMR of **2.10f**



3-methyl-3-phenyldec-1-en-4-ol (**2.10h**)

In accordance with the general procedure A, THF (0.2 mL, 1.0 M concentration with respect to alcohol) were added and the reaction was heated to 75 °C for 24 h, at which point the reaction mixture was then concentrated *in vacuo* to afford the crude product (dr = >20:1 *anti:syn*, as determined by ¹H NMR spectroscopy). The reaction mixture was then subjected to flash column chromatography (SiO₂: 0-5% Et₂O/hexanes) to furnish **2.10h** (38 mg, 0.15 mmol, 77% yield) as a clear, colorless oil. *The spectroscopic properties of this compound were consistent with the data available in the literature.*⁶⁴

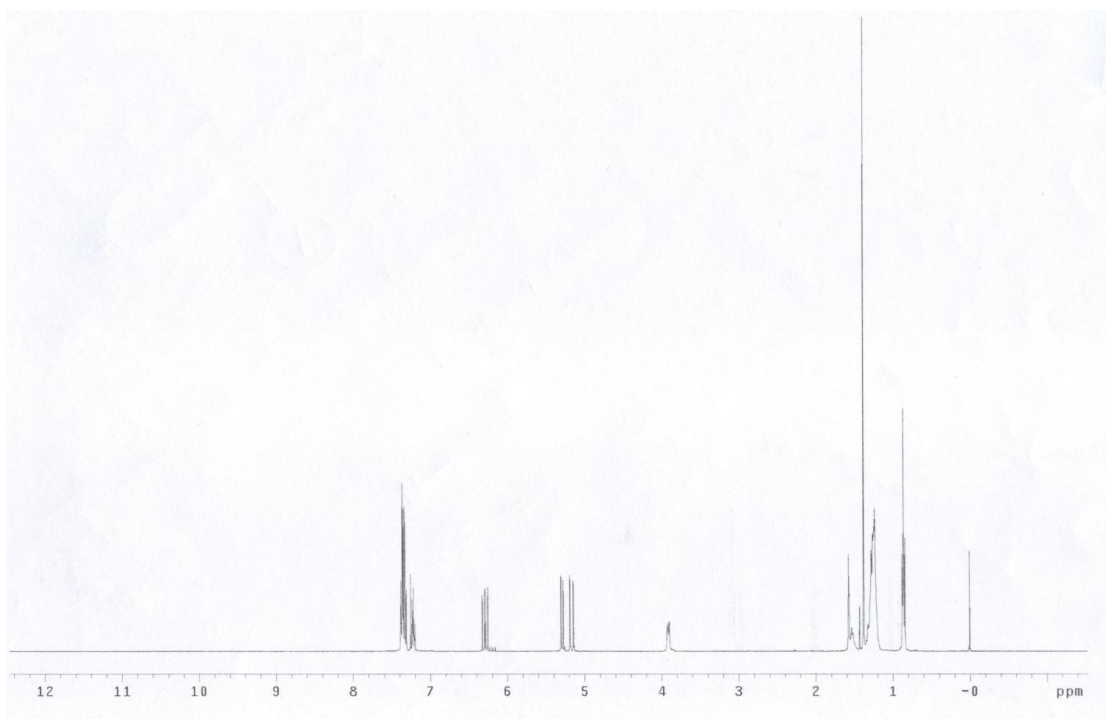
¹H NMR (400 MHz, CDCl₃): δ 7.39-7.31 (m, 4H), 7.24-7.20 (m, 1H), 6.29 (dd, *J* = 18.0, 11.2 Hz, 1H), 5.29 (dd, *J* = 11.2, 1.2 Hz, 1H), 5.17 (dd, *J* = 18, 1.2 Hz, 1H), 3.91 (m, 1H), 1.58 (s, 1H), 1.56-1.51 (m, 2H), 1.38, (s, 3H), 1.29-1.21 (m, 8H), 0.86 ppm (t, *J* = 7.0 Hz, 3H).

¹³C NMR (100 MHz, CDCl₃): δ 145.7, 143.6, 128.7, 127.1, 126.6, 114.8, 49.9, 32.1, 31.7, 31.5, 29.5, 27.3, 22.9, 22.0, 14.3 ppm.

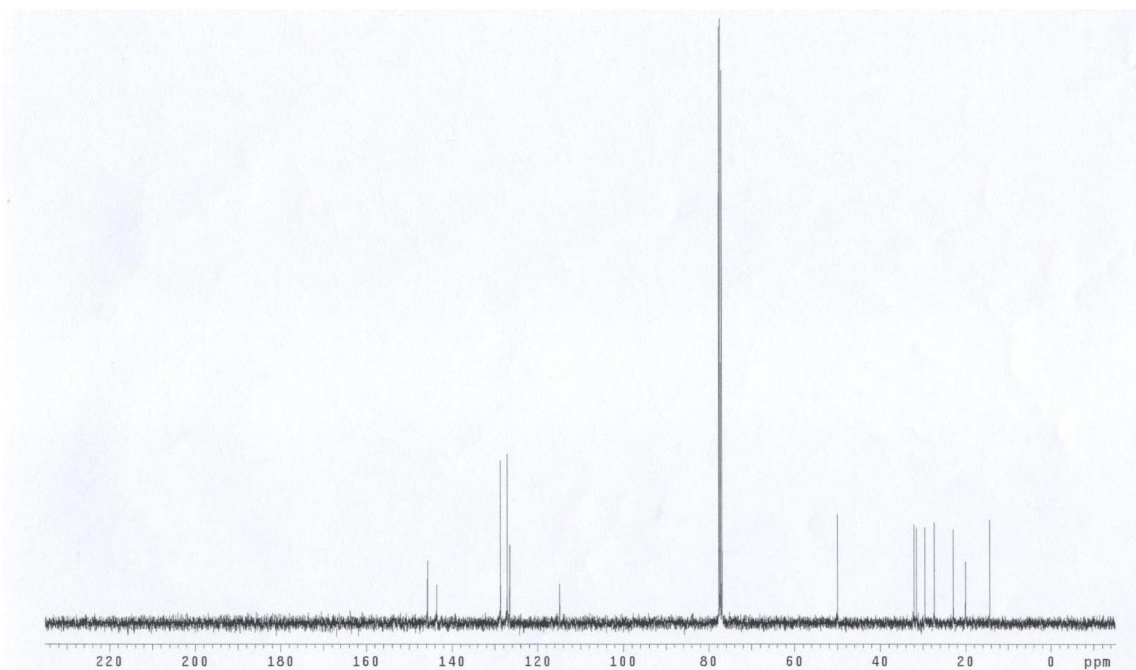
HRMS (CI) Calcd. For C₁₇H₂₅O(M⁺): 246.1984, Found: 246.1987.

FTIR (neat): 3577, 3557, 3505, 3480, 3459, 3083, 2954, 2924, 2856, 1636, 1493, 1466, 1445, 1375, 1114, 1075, 1061, 1030, 917, 764, 747, 700, 668 cm⁻¹.

^1H NMR of **2.10h**



^{13}C NMR of **2.10h**



4-methyl-1,4-diphenylhexa-1,5-dien-3-ol (**2.10i**)

In accordance with the general procedure A, THF (1.0 mL, 0.2 M concentration with respect to alcohol) were added and the reaction was heated to 60 °C for 24 h, at which point the reaction mixture was then concentrated *in vacuo* to afford the crude product (dr = 5:1 *anti:syn*, as determined by ¹H NMR spectroscopy). The reaction mixture was then subjected to flash column chromatography (SiO₂: 5-20% Et₂O/hexanes) to furnish **2.10i** (52 mg, 0.20 mmol, 99% yield) as a clear, colorless oil

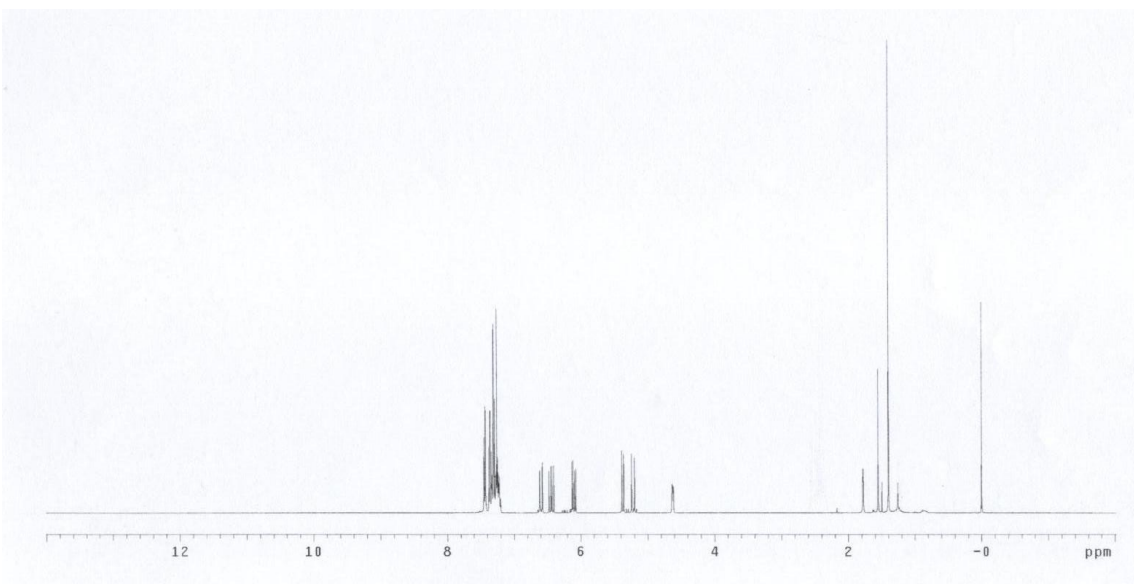
¹H NMR (400 MHz, CDCl₃): δ 7.44 (d, *J* = 7.6, 1.2, 2H), 7.36 (t, *J* = 7.6 Hz, 2H), 7.33-7.27 (m, 6H), 6.59 (d, *J* = 16.0 Hz, 1H), 6.55 (dd, *J* = 18.0, 10.8 Hz, 1H), 6.44 (dd, *J* = 18.0, 10.8 Hz, 1H), 6.10 (dd, *J* = 16.0, 6.6 Hz, 1H), 5.37 (dd, *J* = 10.8, 1.2 Hz, 1H), 5.22 (dd, *J* = 18.0, 1.4 Hz, 1H), 4.63 (dd, *J* = 6.6, 2.8 Hz, 1H), 1.78 (m, 1H), 1.40 ppm (s, 3H).

¹³C NMR (100 MHz, CDCl₃): δ 144.8, 142.2, 136.8, 132.5, 128.5, 128.5, 128.1, 127.6, 127.1, 126.6, 126.5, 115.5, 78.5, 49.7, 21.3 ppm.

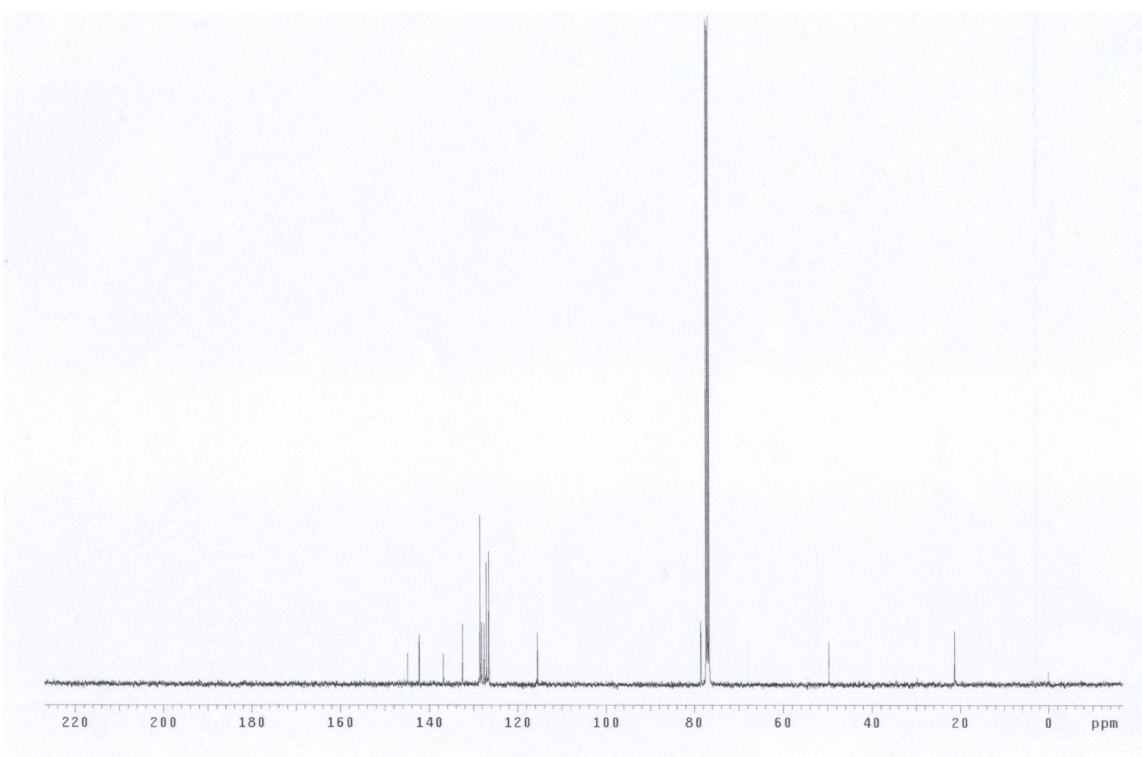
HRMS (CI) Calcd. For C₁₉H₂₁O(M+1): 265.1592, Found: 265.1592.

FTIR (neat): 2958, 2918, 2849, 2365, 2342, 2493, 2446, 1374, 1262, 1097, 1068, 1028, 966, 921, 752, 727, 718, 695, 670 cm⁻¹.

^1H NMR of **2.10i**



^{13}C NMR of **2.10i**



7-(benzyloxy)-3-methyl-3-phenylhept-1-en-4-ol (**2.10j**)

In accordance with the general procedure A, THF (0.2 mL, 1.0 M concentration with respect to alcohol) were added and the reaction was heated to 75 °C for 24 h, at which point the reaction mixture was then concentrated *in vacuo* to afford the crude product (dr = >20:1 *anti:syn*, as determined by ¹H NMR spectroscopy). The reaction mixture was then subjected to flash column chromatography (SiO₂: 0-5% Et₂O/hexanes) to furnish **2.10j** (42 mg, 0.14 mmol, 67% yield) as a clear, colorless oil

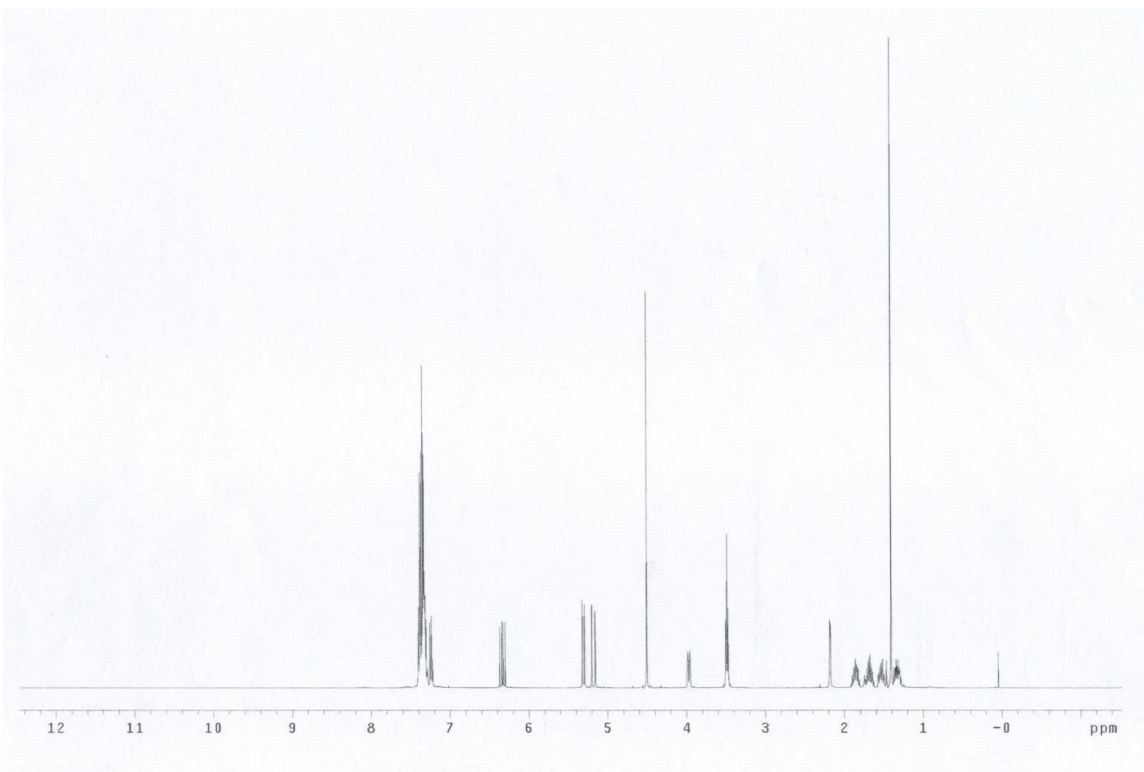
¹H NMR (400 MHz, CDCl₃): δ 7.41-7.28 (m, 9H), 7.26-7.22 (m, 1H), 6.33 (dd, *J* = 17.6, 11.0 Hz), 5.31 (dd, *J* = 11.0, 1.2 Hz, 1H), 5.18 (dd, *J* = 17.6, 1.2 Hz), 4.51 (s, 2H), 3.97 (d, *J* = 10.8 Hz, 1H), 3.49 (t, *J* = 6.2 Hz, 2H), 2.18 (d, *J* = 2.8, 1H), 1.90-1.83 (m, 1H), 1.75-1.64 (m, 1H), 1.57-1.50 (m, 1H), 1.41 (s, 3H), 1.38-1.28 ppm (m, 1H).

¹³C NMR (100 MHz, CDCl₃): δ 145.8, 143.7, 138.7, 128.7, 128.6, 128.0, 127.8, 127.2, 126.5, 114.8, 73.1, 70.6, 49.9, 28.7, 27.4, 20.3 ppm.

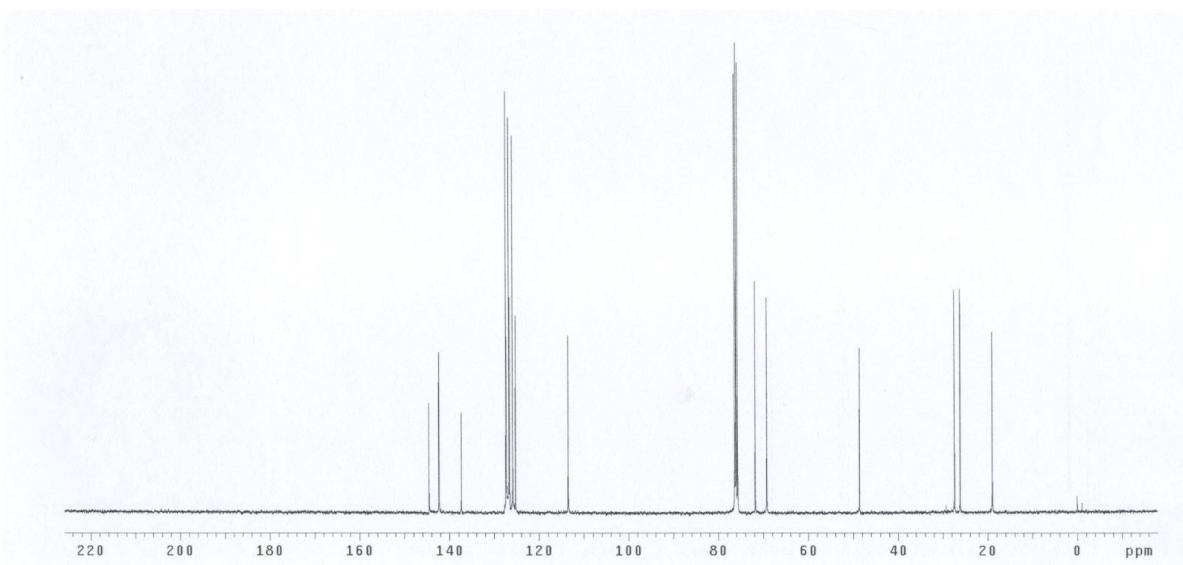
HRMS (CI) Calcd. For C₂₁H₂₇O₂(M+1): 311.2011, Found: 311.2012.

FTIR (neat): 3577, 3558, 3480, 3459, 3083, 2954, 2924, 2856, 1637, 1599, 1493, 1466, 1445, 1413, 1282, 1061, 1030, 917, 764, 700, 668 cm⁻¹.

^1H NMR of **2.10j**



^{13}C NMR of **2.10j**



2-methyl-2-phenyl-1-(4-(trifluoromethyl)phenyl)but-3-en-1-ol (**2.10m**)

In accordance with the general procedure A, THF (0.4 mL, 0.5 M concentration with respect to alcohol) were added and the reaction was heated to 40 °C for 24 h, at which point the reaction mixture was then concentrated *in vacuo* to afford the crude product (dr = 4:1 *anti:syn*, as determined by ¹H NMR spectroscopy). The reaction mixture was then subjected to flash column chromatography (SiO₂: 5-15% Et₂O/hexanes) to furnish **2.10m** (52 mg, 0.17 mmol, 85% yield) as a clear, colorless oil

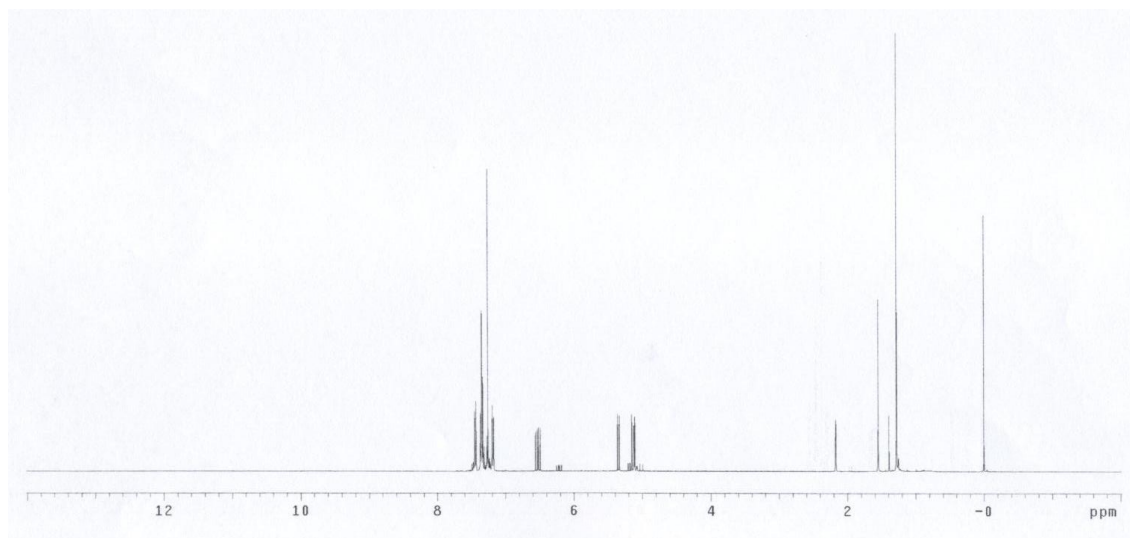
¹H NMR (400 MHz, CDCl₃): δ 7.44 (d, *J* = 8.2, 2H), 7.37-7.27 (m, 5H), 7.19 (d, *J* = 8.2 Hz, 2H), 6.53 (dd, *J* = 17.6, 11.0 Hz, 1H), 5.35 (dd, *J* = 11.0, 1.0 Hz, 1H), 5.13 (dd, *J* = 17.6, 1.0, 1H), 5.12 (d, *J* = 2.0 Hz, 1H), 2.17 (d, *J* = 2.0 Hz, 1H), 1.28 ppm (s, 3H).

¹³C NMR (100 MHz, CDCl₃): δ 144.2, 143.8, 141.6, 129.5 (q, *J* = 32.0 Hz), 128.5, 128.2, 127.2, 126.8, 124.2 (q, *J* = 269 Hz), 124.1 (q, *J* = 3.8 Hz), 116.1, 79.6, 50.3, 19.9 ppm.

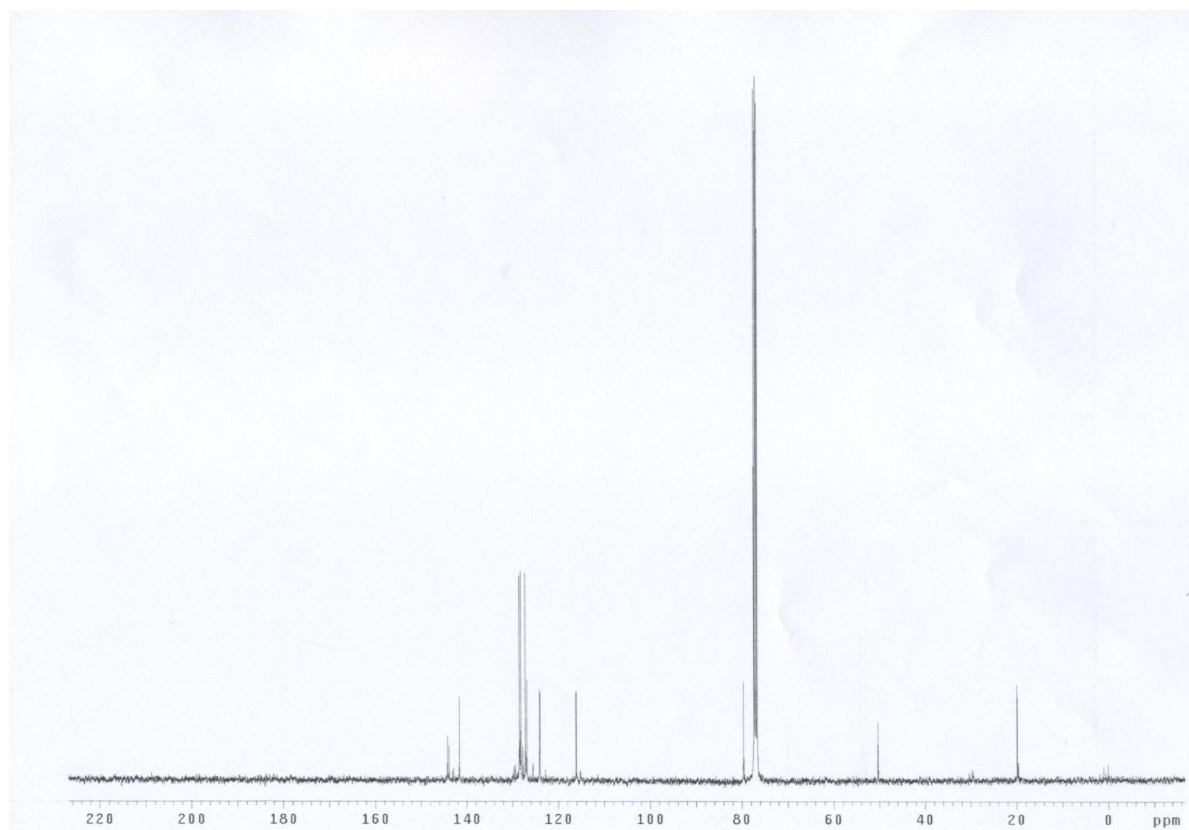
HRMS (CI) Calcd. For C₁₈H₁₈OF₃(M⁺): 307.1310, Found: 307.1305.

FTIR (neat): 3577, 3557, 3479, 3458, 2954, 2924, 2856, 1637, 1559, 1445, 1413, 1281, 1061, 1030, 917, 700 cm⁻¹.

^1H NMR of **2.10m**



^{13}C NMR of **2.10m**

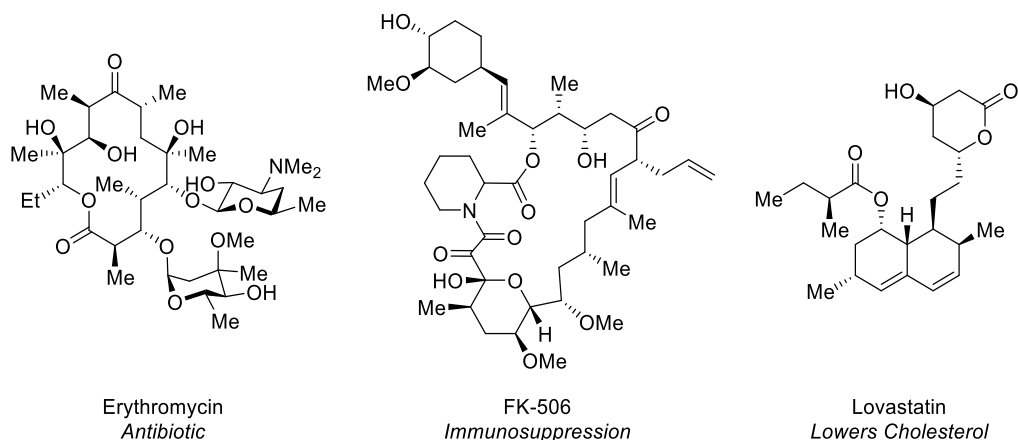


Chapter 3 Asymmetric Carbonyl Crotylation Using Butadiene

3.1 Introduction

Carbonyl crotylation is an effective tool to access polypropionate subunits, a key feature of polyketide natural products characterized by alternating hydroxyl and methyl bearing stereocenters. Total synthesis of polyketide natural products has created a demand for the development of efficient, selective methods to form polypropionate fragments. Many of these natural products have gained interest due to their unique bioactivities and potential as pharmaceutical candidates, but their complex structures and dense arrangement of stereocenters complicate synthetic approaches. Due to this, the production of most therapeutic polyketides, including lovastatin, erythromycin, and FK506 (Figure 3.1), utilize biosynthetic methods to access advanced intermediates through condensation of propionyl fragments followed by asymmetric β -ketoester reduction.

Figure 3.1 Pharmaceutically active polyketides that contain fragments accessible through crotylation.

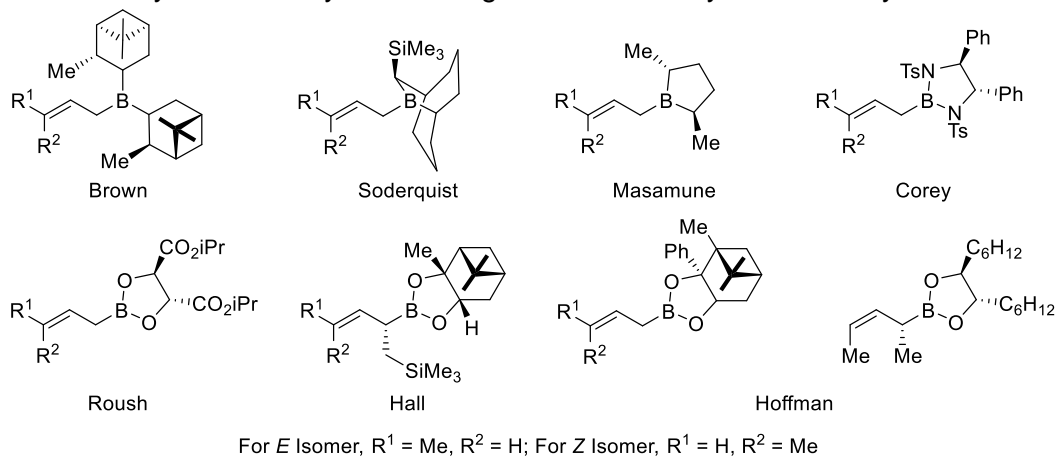


While this strategy for polyketide biosynthesis has proven extremely efficient and cost effective, it does not have universal applicability, as some of the organisms that produce these pharmaceutical targets are bacteria and fungi that are not amenable to culture for large scale production. Furthermore, biosynthesis has limited application in derivatization for medicinal

chemistry as the development of a completely modular polyketide synthase enzyme is still ongoing.⁷⁶

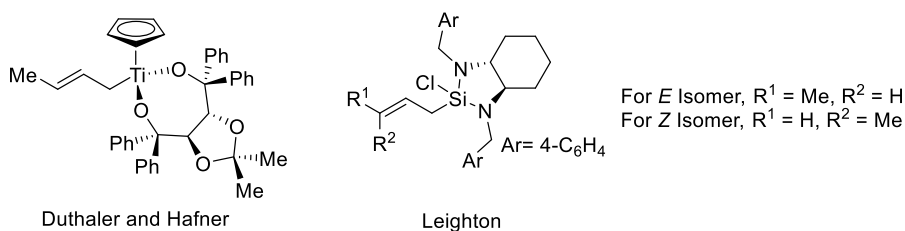
Established methods for crotylation generally feature the addition of an allyl-metal reagent to an aldehyde. Various organometallic reagents have been developed for both stoichiometric and catalytic application.⁷⁷ Stoichiometric organoboron reagents, developed by Hoffman, Brown, Roush, Masamune, Corey, Soderquist and Hall, react by way of a closed, chair-like transition state (Figure 3.2). High levels of selectivity are achieved by control of olefin geometry of the allyl-boron reagent and use of various chirally modified boron sources.⁷⁸

Figure 3.2 Chirally modified allyl-boron reagents used for asymmetric crotylation.



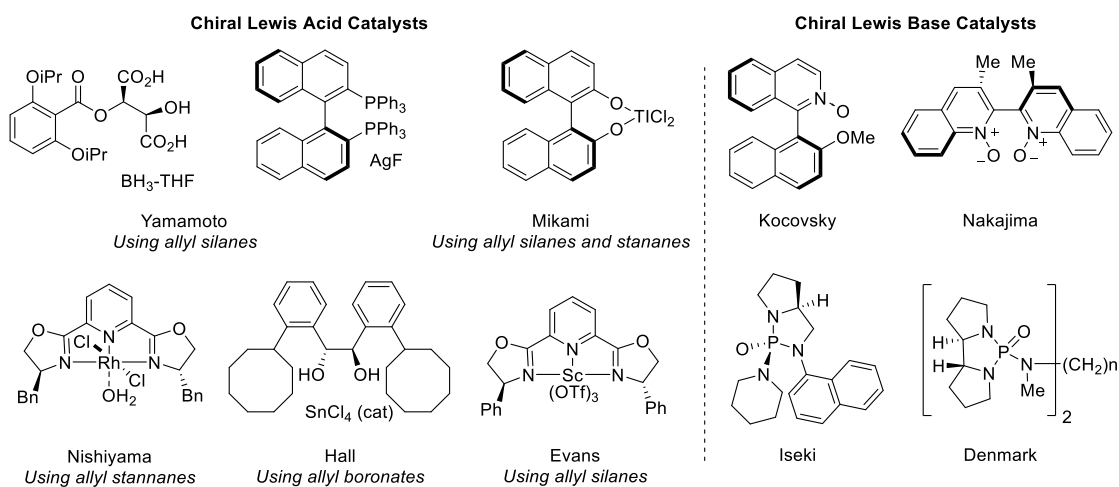
Titanium mediated *anti*-crotylation was developed by Duthaler and Hafner and chiral *cis*- and *trans*-crotyl silane reagents developed by Leighton are highly selective for accessing both *syn* and *anti*-crotylation products.⁷⁹ (Figure 3.3)

Figure 3.3 Organotitanium and organosilicon reagents used for asymmetric crotylation.



Catalytic methods for asymmetric crotylation include chiral Lewis acid and Lewis base catalyzed addition of crotyl organosilicon, organotin, or organoboron reagents, and transition metal catalyzed reductive coupling reactions. Some examples of chiral Lewis acids have been developed by Yamamoto, Mikami, Nishiyama, Evans and Hall to catalyze addition of various allyl metal reagents to aldehydes.⁸⁰ Some chiral Lewis base catalyzed additions of allyl trichlorosilanes have been developed by Denmark, Iseki, Nakajima and Kočovský to access crotylation products.^{52d, 52e, 81} (Figure 3.4)

Figure 3.4 Chiral Lewis acid and Lewis base catalysts used for asymmetric crotylation.

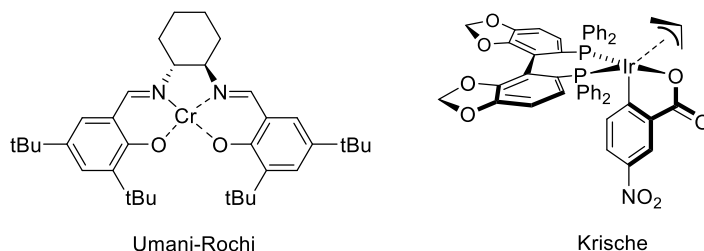


Using transition metal catalysis, catalytic Nozaki-Hiyama coupling of allylic halides has been developed.⁸² Crotylation methodology developed in the Krische group utilizing a chiral cyclometallated iridium complex and α -methyl allyl acetate as crotyl donor has been reported. A transfer hydrogenative protocol has also been developed, enabling employment of primary alcohols as aldehyde precursors. This concept has been extended to the bis-crotylation of 1,3-diols to quickly access fragments containing multiple stereocenters.⁸³ (Figure 3.5)

While only selected methods for carbonyl crotylation have been presented, this list represents some of the breadth and variety of reagents developed for this transformation. The

volume of research in this area attests to the importance of carbonyl crotylation in the context of polyketide total synthesis.⁸⁴

Figure 3.5 Chromium and iridium catalysts developed for asymmetric crotylation.



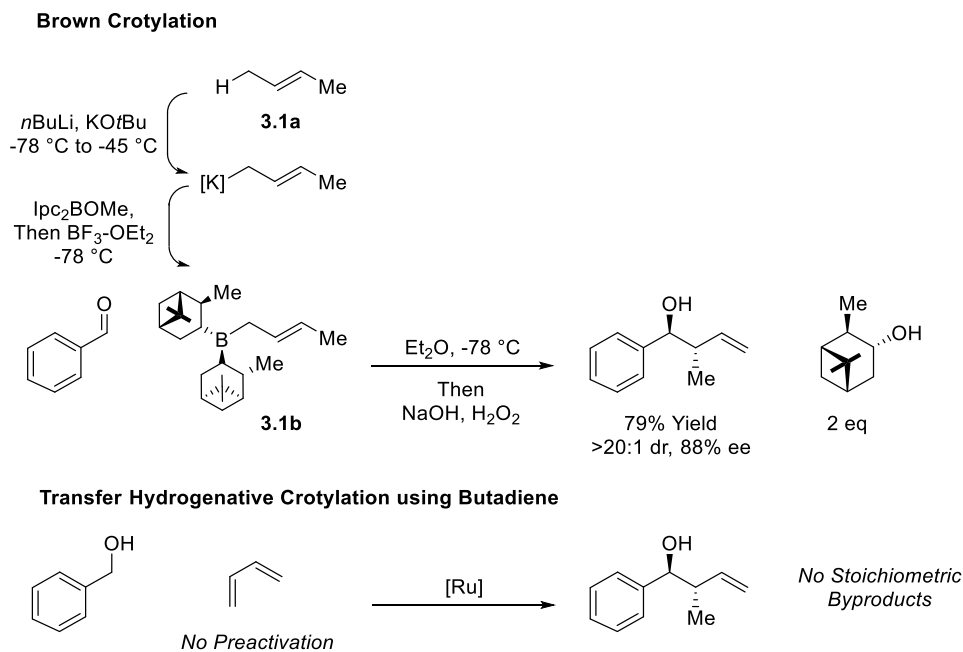
3.2 Crotylation Using Butadiene

3.2.1 Introduction

In developing new methods for ruthenium catalyzed hydrogenative carbonyl addition chemistry, a highly selective method for carbonyl crotylation has been a longstanding challenge. The product of carbonyl crotylation could be accessed by the direct coupling of a primary alcohol and butadiene, a feedstock chemical that is produced on metric ton scale each year as a byproduct of petroleum cracking. Butadiene, commonly used in polymerization processes for plastic and rubber manufacturing, is extremely inexpensive. The direct employment of butadiene as crotyl donor could provide a distinct advantage to traditional methods for carbonyl crotylation that use stoichiometric amounts of organometallic reagents.

Scheme 3.1 provides a comparison to the most common and economical method for carbonyl crotylation is the Brown crotylation.⁸⁵ This protocol also begins with a feedstock chemical 2-butene (**3.1a**). However, prior to carbonyl addition, 2-butene is subjected to potassiation and transmetallation to boron to generate the Brown crotyl donor. Upon exposing an aldehyde to **3.1b**, the product of crotylation is formed in high yield and excellent selectivity.

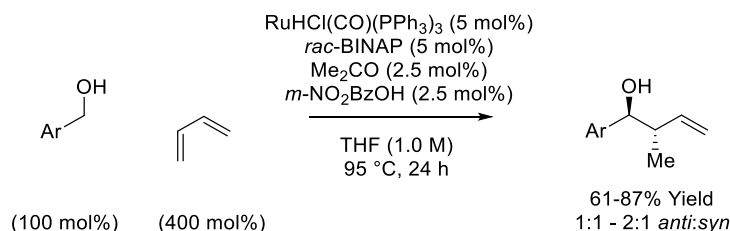
Scheme 3.1 Brown crotylation, including procedure required to generate **3.1b** from 2-butene (**3.1a**), compared to crotylation using butadiene.



While the Brown crotylation is highly effective, a more robust, atom-economic approach could provide some advantages. Formation of the organoboron crotyl donor requires two steps of “preactivation”, which represent the degree of separation between feedstock chemical and reagent, and increases the molecular weight of the crotyl donor from 56 g/mol to 340 g/mol. The additional mass is recovered as a byproduct of the reaction in the form of two equivalents of isopinocampheol, a secondary alcohol which can sometimes complicate isolation of the secondary, homoallylic alcohol product. Eliminating the need for a mass-intensive, moisture sensitive organometallic crotyl donor could reduce the waste generated by this reaction. Additionally, careful control of cryogenic temperature is required for the Brown crotylation to ensure high selectivity, and this can be problematic when considering large scale reactors and long reaction times.

While the employment of butadiene as crotyl donor presents an advantage to previously developed methods for carbonyl crotylation, it brings a significant challenge. In 2009, the Krische group reported the first direct coupling of dienes and alcohols using $\text{RuHCl}(\text{CO})(\text{PPh}_3)_3$ (Scheme 3.2).³⁰ Despite rigorous optimization, this reaction was only effective for aromatic substrates and resulted in very low diastereoselectivities (1:1 to 2:1 *anti:syn*). For application in the synthesis of complex natural products, high levels of diastereo- and enantioselectivity are required, leaving this method insufficient for these purposes.

Scheme 3.2 Hydrohydroxyalkylation of butadiene using transfer hydrogenative ruthenium catalysis.

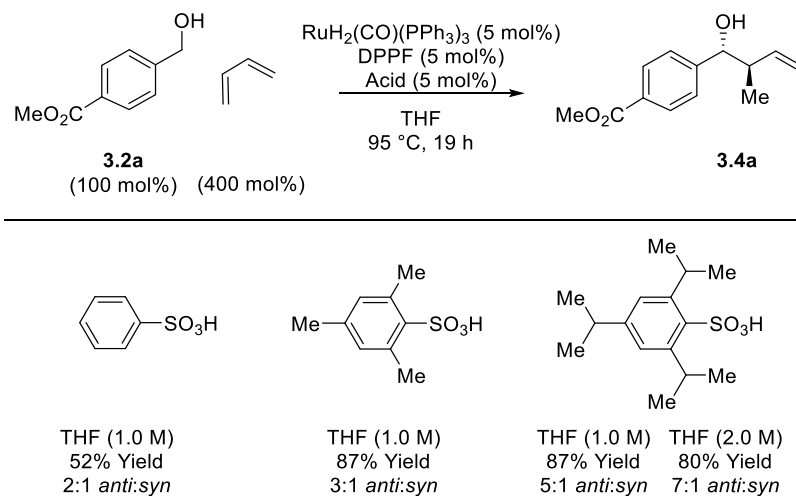


3.2.2 Reaction Development and Optimization

To address the problem of stereoselectivity in this reaction, a new strategy was required. Though hydrometallation of butadiene could potentially occur through a single conformational isomer, the previous work suggests that the (*E*)- and (*Z*)- σ -allyl isomers can interconvert under the reaction conditions, and that both participate in a stereospecific reaction to access a diastereomeric mixture of products. Recent work in the coupling of 1,1-disubstituted allenes with primary alcohols to form all-carbon quaternary centers had revealed that variation of the counter ion on a cationic ruthenium center could influence the stability and/or interconversion of the (*E*)- or (*Z*)- σ -allyl isomers, funneling reactivity through one isomer and thereby controlling diastereoselectivity.⁷² A similar effect was observed for crotylation using butadiene. In screening various aryl sulfonic acids, as steric demand of the acid increased, diastereoselectivity also increased (Figure 3.6). To extend this strategy further, it was proposed that a chiral counter ion

could influence both relative and absolute stereochemistry, resulting in a highly diastereoselective and enantioselective crotylation reaction.

Figure 3.6 Influence of size of sulfate counter ion on diastereoselectivity of crotylation using butadiene.



Asymmetric chemistry controlled by chiral counter ions has been effective in a number of fields, including organocatalysis, phase transfer catalysis and Brønsted acid catalysis.⁸⁶ However, far fewer examples of chiral counter ions used for enantiocontrol for cationic transition metal catalysis exist.⁸⁷ With regards to ruthenium chemistry, only one report was found, in which a chiral phosphate modified ruthenium catalyst was used for styrene hydrovinylation, and only moderate levels of enantioselectivity (34-44%) were observed.⁸⁸

To examine the effects of a chiral counter ion modified ruthenium catalyst in asymmetric crotylation, a structural class of chiral acids was selected – BINOL derived phosphoric acids. Since the first application of BINOL phosphoric acids as Brønsted acid catalysts for asymmetric Mannich reactions in 2004,⁸⁹ this structural class of chiral acids has received broad attention.^{86d} Enantiomerically pure BINOL is relatively inexpensive and, as demonstrated by the large number of BINOL derivatives reported in literature, is highly amenable to modification in only a few simple manipulations. Commonly, functionalization at the 3 and 3' positions of the BINOL core structure has been used to access a large variety of structures with diverse steric and electronic properties.

To evaluate the effect of BINOL phosphoric acid on selectivity, (*R*)-BINOL phosphoric acid was used with $\text{RuH}_2(\text{CO})(\text{PPh}_3)_3$ and DPPF, an inexpensive, achiral ligand that had shown good reactivity in previous work. Forming the BINOL-phosphoric acid modified ruthenium complex in situ, reactivity was probed with alcohol **3.2a** and 4 equivalents of butadiene. The reaction was successful, but with only moderate yield and very low levels of relative and absolute stereocontrol. (Table 3.1, entry 1) A variety of phosphoric acids were quickly evaluated in an effort to improve the stereoselectivity. While all 3,3'-substituted acids screened seemed to generate a catalyst that was effective for the reaction, surprisingly, as acids with larger substituents were surveyed, the diastereoselectivity decreased (entries 2-7). It was postulated that this could be due to an undesirable steric interaction between the substituents on the acid and other ligands at the metal center, displacing the phosphate counter ion. To create a less sterically encumbered acid, mono-substituted BINOL-derived phosphoric acids were synthesized and found to effect an increase in diastereo- and enantioselectivity. Now, increasing the size of the single substituent displaced marked increase in selectivity (entries 8-11). Reintroduction of a second, smaller substituent at the 3' position was advantageous, creating a more sterically defined phosphoric acid (entries 15-16).

A final measure was taken to tune the acid catalyst. High pressure hydrogenation of the (*R*)-BINOL can form (*R*)- H_8 -BINOL, which possesses a more electron rich structure and slightly different biaryl angle (rhodium complexes bearing (*R*)-BINAP and (*R*)- H_8 -BINAP show biaryl angles of $71\text{-}75^\circ$ and 80° , respectively.⁹⁰) Screening of H_8 -BINOL based acids with similar substitution as the previous optimized structure improved selectivity slightly (entries 17-19). By enlarging the biaryl angle, the projection of the 3 and 3' substituents would be wider, allowing more space for the phosphate anion to coordinate ruthenium. It was reasoned that increasing the amount of acid used in the reaction may favor formation of a Ru-phosphate ion pair. Fortuitously, doubling the loading of acid did improve selectivity (entries 19-22). This acid, in combination with the $\text{RuH}_2(\text{CO})(\text{PPh}_3)_3$ and DPPF precatalyst, provided the highest selectivity,

but still suffered from low yield. Extension of reaction time furnished product in high yield and selectivity (entries 22-23).

Table 3.1 Optimization of (*R*)-BINOL phosphoric acid and reaction conditions for *anti*-crotylation.

3.2a
(100 mol%)

$\xrightarrow[\text{THF (2.0 M)}]{\text{RuH}_2(\text{CO})(\text{PPh}_3)_3 \text{ (5 mol\%)} \\ \text{DPPF (5 mol\%)} \\ \text{Acid}} \xrightarrow[95\text{ }^\circ\text{C, Time}]{}$

3.4a

Entry	Acid (mol%)	Butadiene	Time (h)	Yield (%)	<i>anti:syn</i>	ee (%)
1	BA ₁ (5)	400 mol%	19	45	1:1	4
2	BA ₂ (5)	400 mol%	19	48	2:1	33
3	BA ₃ (5)	400 mol%	19	83	1:2	15
4	BA ₄ (5)	400 mol%	19	61	1:1	6
5	BA ₅ (5)	400 mol%	19	80	1:1	9
6	BA ₆ (5)	400 mol%	19	60	1:1	0
7	BA ₇ (5)	400 mol%	19	91	5:1	14
8	BA ₈ (5)	400 mol%	19	83	2:1	38
9	BA ₉ (5)	400 mol%	19	38	1:1	21
10	BA ₁₀ (5)	400 mol%	19	84	3:1	74
11	BA ₁₁ (5)	400 mol%	19	41	2:1	62
12	BA ₁₀ (5)	100 mol%	19	72	3:1	74
13	BA ₁₀ (5)	200 mol%	19	80	3:1	74
14	BA ₁₀ (5)	800 mol%	19	50	3:1	74
15	BA ₁₂ (5)	400 mol%	19	15	6:1	70
16	BA ₁₃ (5)	400 mol%	19	21	5:1	70
17	BA ₁₄ (5)	400 mol%	19	45	3:1	78
18	BA ₁₅ (5)	400 mol%	19	15	5:1	72
19	BA ₁₆ (5)	400 mol%	19	29	4:1	72
20	BA ₁₃ (10)	400 mol%	19	33	7:1	84
21	BA ₁₄ (10)	400 mol%	19	48	3:1	80
22	BA ₁₆ (10)	400 mol%	19	50	7:1	88
⇒ 23	BA ₁₆ (10)	400 mol%	48	80	7:1	88

BA₁: R₁,R₂=H
 BA₂: R₁,R₂=Me
 BA₃: R₁,R₂=iPr
 BA₄: R₁,R₂=SiPh₃
 BA₅: R₁,R₂=4-NO₂C₆H₄
 BA₆: R₁,R₂=TRIP
 BA₇: R₁=Ph R₂=Ph
 BA₈: R₁=Ph R₂=H
 BA₉: R₁=3-Tol R₂=H
 BA₁₀: R₁=Mes R₂=H
 BA₁₁: R₁=TRIP R₂=H
 BA₁₂: R₁=Mes R₂=Me
 BA₁₃: R₁=Mes R₂=Et

BA₁₄: R₁=Mes R₂=H
 BA₁₅: R₁=Mes R₂=Me
 BA₁₆: R₁=Mes R₂=Et

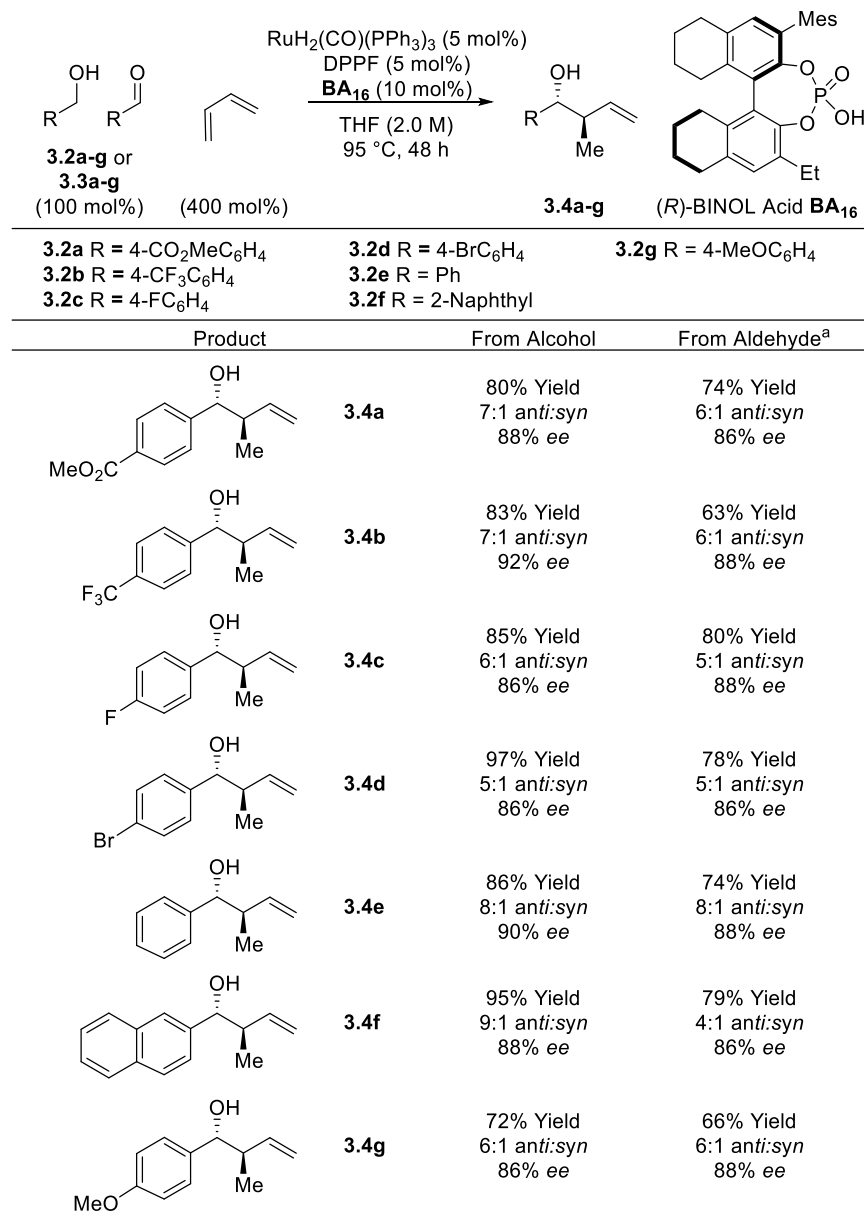
Another feature that was important to control in the optimization of this reaction was the manner and precision in which the reactions were assembled. Butadiene, a gas at room temperature, can be condensed at -78 °C and transferred into the reaction vials quickly by syringe. Initial experiments resulted in highly variable yields. Careful measurement and addition of butadiene revealed that 400 mol% was an optimal amount, with less loading of butadiene resulting in diminished yields. It was important to note that excess butadiene also resulted in lower yields. (entries 12-14) Because dienes can act as ligands for transition metals, it is possible that a large excess of butadiene saturates the ruthenium center, rendering it catalytically inactive.

As the acidic additive is the key feature for stereocontrol in this reaction, the isolation and handling of the phosphoric acids and of the substrates for the reaction was very important. In 2010, List and Ishihara reported that BINOL phosphoric acids readily form calcium phosphate salts, bringing to question whether previous reports employing BINOL phosphoric acids for asymmetric catalysis are actually catalyzed by the acid or the corresponding phosphate salt.⁹¹ To form the desired ruthenium complex, the acid would be required to participate in the acid-base reaction with a ruthenium hydride. Careful measure was taken in developing a method for acid purification, entailing column chromatography using dichloromethane and isopropanol as eluent followed by washing of the acid in DCM solution with 3.0 M HCl. Analysis of phosphoric acids by ¹H and ³¹P NMR confirmed purity. Also, fresh preparation and purification of alcohol and aldehyde substrates was necessary in some cases, due to the racemic background reaction that could occur if carboxylic acid contamination – possible by redox disproportionation of aldehydes - was present.

3.2.3 Reaction Scope

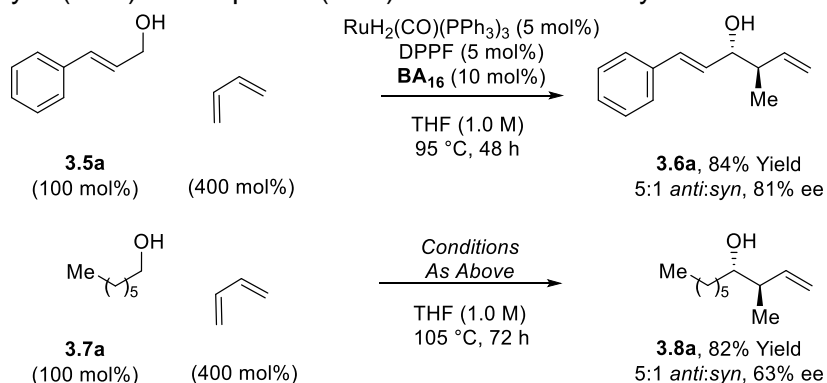
After optimization of chiral acid structure and reaction conditions, the substrate scope was evaluated for other primary alcohols. For aromatic alcohols **3.2a-g** with varying electronic properties, high yields, good diastereoselectivities, and high levels of enantioselectivity were obtained. It was also found that identical products could be accessed from the aldehyde oxidation level using 1,4-butanediol as terminal reductant³⁵ (Figure 3.7). The redox neutral and reductive processes allow for flexibility in designing synthetic routes, as either oxidation level can be used directly in the crotylation reaction.

Figure 3.7 Ruthenium catalyzed coupling of butadiene and primary alcohols or aldehydes to generate products of *anti*-crotylation **3.4a-g**.



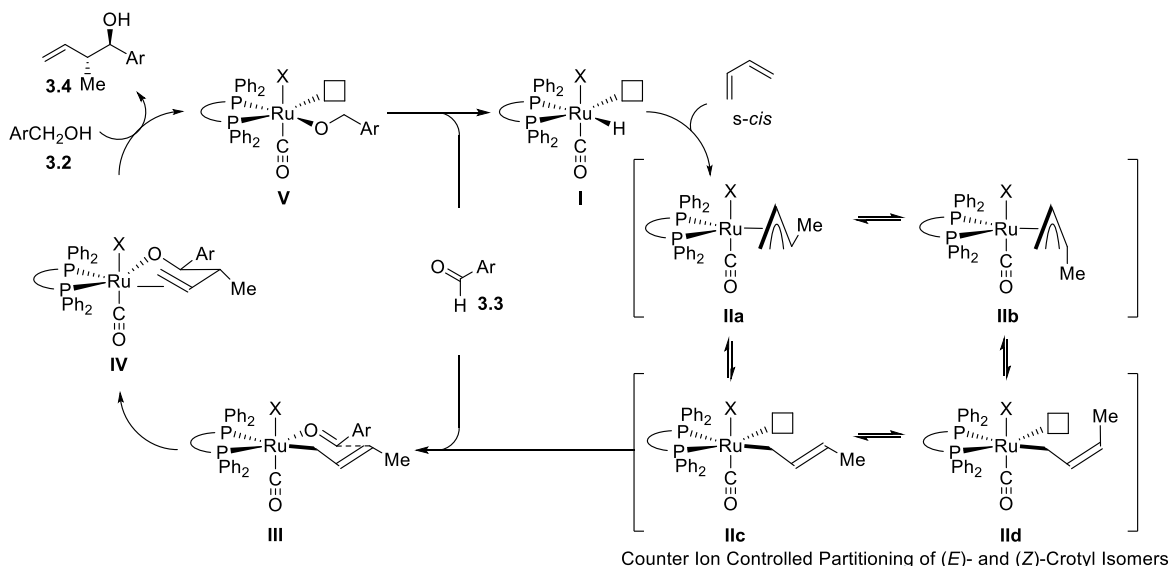
For other classes of alcohols, the diastereo- and enantioselectivity under similar reaction conditions was diminished. Cinnamyl alcohol (**3.5a**) provided product **3.6a** in 84% yield, 5:1 *anti:syn*, and 81% ee, and heptanol (**3.7a**) provided product **3.8a** in 82% yield, 5:1 *anti:syn* and 63% ee. (Scheme 3.3) Heptanol and other aliphatic substrates required higher temperatures for product formation; at 95 °C, trace product was obtained.

Scheme 3.3 Allylic (**3.5a**) and aliphatic (**3.7a**) substrates for crotylation.



3.2.4 Mechanism and Discussion

Figure 3.8 Proposed mechanism for the hydrohydroxyalkylation of butadiene.

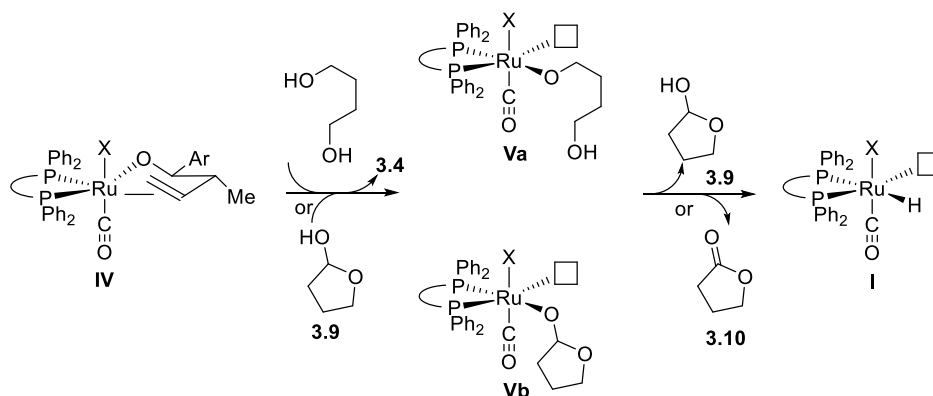


A proposed mechanism for the crotylation of primary alcohols using butadiene is shown in Figure 3.8. Butadiene can exist in a *s-cis* and *s-trans* form, and while hydrometallation may occur preferentially through the *s-cis* form,⁹² the resulting ruthenium species can equilibrate from (*E*)- σ -crotyl species **IIc** to (*Z*)- σ -crotyl species **IId** by way of π -allyl intermediates **IIa** and **IIb**. The observed diastereoselectivity is likely due to counter ion controlled partitioning of the (*E*)- and (*Z*)-crotyl isomers. Coordination of aldehyde **3.3** to the (*E*)-crotyl ruthenium species **IIc** followed by carbon-carbon bond formation through six-membered transition state **III** forms ruthenium alkoxide **IV**, which can undergo protonation by primary alcohol **3.2** to release product **3.4**. β -hydride

elimination of ruthenium alkoxide **V** reforms ruthenium hydride **I** to close the catalytic cycle and reforms reactant aldehyde **3.3**.

An identical catalytic cycle is possible for the transfer hydrogenative coupling of aldehydes and butadiene, except that 1,4-butanediol acts as both proton and hydride source by protonation of ruthenium alkoxide **IV** and subsequent β -hydride elimination to regenerate ruthenium hydride **I**. (Scheme 3.4) Dehydrogenation of 1,4-butanediol generates a monoaldehyde, which can then cyclize to generate lactol **3.9**. This can participate again in protonolysis and β -hydride elimination to generate lactone **3.10** as a side product. In this process, one equivalent of 1,4-butanediol effectively supplies two equivalents of hydrogen and is driven by the formation of **3.10** as a thermodynamic sink.⁹³

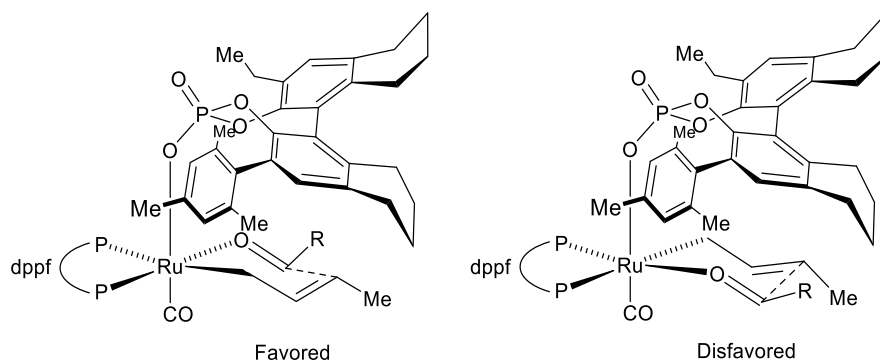
Scheme 3.4 Transfer hydrogenation using 1,4-butanediol to regenerate complex **I**.



Through optimization of (*R*)-BINOL derived phosphoric acid **BA**₁₆, a drastic improvement in yield, relative, and absolute stereocontrol was obtained in the crotylation of aromatic alcohols. While screening of chiral phosphine ligands is a common practice in asymmetric catalysis, this work represents a novel method for introduction of various chiral anionic ligands to a metal center, and the capability of using these ligands for a highly selective process in which traditional ligands were ineffective. Notably, using an inexpensive, achiral ligand, the chiral counter ion controlled the product stereochemistry.

In an attempt to understand the effect the phosphate ion has on reaction selectivity, a stereochemical model for the transformation has been assembled. While the details of the role of the acid additive are not experimentally confirmed, the outcome of the reaction suggests that in the stereodefining step, the counter ion influences which Ru-allyl isomer reacts and determines the facial selectivity of the aldehyde addition. Figure 3.9 shows a postulated transition state to explain these effects. In the favored model, upon comparison of the size of the substituent directly bound to ruthenium in the chair-like transition state, the oxygen of the aldehyde should have less steric demand than the methylene of the crotyl fragment. Placing the more sterically demanding substituent at the same side of the BINOL ring as the mesitylene substituent, which is projected away from the plane of the transition state (left) would lead to the favored enantiomer. The diastereoselectivity of both transition states leads to the *anti*-product, which could be influenced by the projection of the cyclohexyl ring of the H₈-BINOL backbone toward the plane of the transition state.

Figure 3.9 Stereochemical model of the transition state for carbonyl addition for *anti*-crotylation.



While this depiction could support formation of the favored isomer, the model is lacking some key features. Experimental results suggest that an important interaction between ligand counter ion exists, because screening other ferrocene-based ligands (*D*iPPF, DCyPF, and *p*-tolyl-DPPF and 4-CF₃C₆H₄-DPPF derivatives) resulted in decreased selectivity. Although the challenge of developing a clear three-dimensional model of the interaction between the ruthenium crotyl

isomer, aldehyde, phosphoric acid and ligand has not yet been fully addressed, the outcome of this methodology has provided an exciting new direction for developing asymmetric catalytic reactions.

3.2.5 Conclusion

The direct employment of butadiene and primary alcohols or aldehydes to selectively access products of *anti*-crotylation **3.4a-g** represents a significant shift in reaction design from previous crotylation methods, in which an abundant, inexpensive feedstock chemical can replace temperature and moisture sensitive preactivated organometallic reagents. In one step, a value added product can be accessed with relative and absolute stereoselectivity controlled by a uniquely modified ruthenium catalyst. Greater understanding of the elements that are controlling stereoselectivity could help in further improvement and extension of this methodology for crotylation.

3.3 Syn-Crotylation using Butadiene

3.3.1 Introduction

The chiral counter-ion controlled *anti*-selective crotylation reaction using (*R*)-BINOL phosphoric acid **BA₁₆** does suffer from some limitations. While *anti*-crotylation is useful in the context of polyketide synthesis, many times the desired substrates will not have the requisite aromatic functional group needed for high selectivity. The reaction development may have been intrinsically biased, because the aromatic substrate used for optimization resulted in a method that was only highly selective for other aromatic substrates. To expand the scope of ruthenium catalyzed crotylation using butadiene, re-optimization of the reaction was undertaken, using heptanol (**3.7a**) as substrate.

3.3.2 Reaction Development and Optimization

To begin, the BINOL-derived phosphoric acids that had been prepared (Table 3.1) were quickly evaluated. Despite screening of BINOL acid additives and other reaction parameters, no improvement to selectivity was obtained

Another class of phosphoric acids, based on the TADDOL structure, attracted attention as potential acid additives. TADDOL phosphoric acids, first reported in 2001,⁹⁴ are derived from an inexpensive chiral source – L-tartaric acid. Variation of the aryl substituents and ketal moiety allow easy access to a range of diverse acids. TADDOL derived structures have found significance in synthetic organic literature, either by direct employment of the chiral diol, use of the TADDOL derived phosphoric acid for Brønsted acid catalysis, or use of TADDOL phosphonite, phosphite or phosphoramidate ligands asymmetric catalysis.^{86d, 94-95}

Similar conditions to those developed for crotylation of aromatic alcohols were used to evaluate the effects of TADDOL phosphoric acids as chiral counter ion for the ruthenium catalyst (Table 3.2). Initially, the all methyl-substituted acid (entry 1) exhibited very low selectivity. A very slight increase in diastereo- and enantioselectivity was observed with the related tetraphenyl substituted acid (entry 2). Variation of the ketal moiety (entries 2-3) appeared to have little effect on selectivity at this point. Next, steric bulk of the aryl rings was increased by first evaluating the effects of naphthyl and biaryl substituted acids (entries 4-6). Notably, substitution at the 2- and 3-position of the phenyl ring (entries 4-5) appeared to have more impact on enantioselectivity than substitution at the 4-position (entry 6). This pattern of higher selectivity with 3-substituted aromatic substituents was consistent with 3- and 4-tolyl substituted acids, as the 3-tolyl substituted acid exhibited much higher enantioselectivity (63% ee) than the 4-tolyl substituted acid (29% ee) (entry 7-8). This effect could be rationalized by the steric requirement for the aryl substituents, as the 3-substituted aromatic rings must exhibit more steric repulsion toward one another than the 4-substituted aromatic rings, and this may result in more interaction of the counter ion with the substrate in the stereodefining steps.

Table 3.2 Optimization of TADDOL phosphoric acid structure, ligand and reaction conditions for *syn*-crotylation.

Entry	Acid	Ligand	Solvent (M)	T (°C)	Yield (%)	<i>syn:anti</i>	ee (%)
1	TA ₁	DPPF	THF (2.0)	105	64	1.0:1	1
2	TA ₂	DPPF	THF (2.0)	105	82	1.6:1	18
3	TA ₃	DPPF	THF (2.0)	105	63	1.4:1	19
4	TA ₄	DPPF	THF (2.0)	105	45	2.0:1	51
5	TA ₅	DPPF	THF (2.0)	105	50	1.4:1	29
6	TA ₆	DPPF	THF (2.0)	105	84	1.3:1	5
7	TA ₇	DPPF	THF (2.0)	105	58	1.8:1	63
8	TA ₈	DPPF	THF (2.0)	105	78	1.6:1	24
9	TA ₉	DPPF	THF (2.0)	105	85	1.4:1	78
10	TA ₁₀	DPPF	THF (2.0)	105	89	1:1.5	5
11	TA ₁₁	DPPF	THF (2.0)	105	81	1.4:1	56
12	TA ₉	DPPF	THF (1.0)	105	85	1.7:1	69
13	TA ₉	DiPPF	THF (1.0)	105	39	1:1.1	3
14	TA ₉	DPPB	THF (1.0)	105	62	1.8:1	19
15	TA ₉	(<i>R</i>)-Segphos	THF (1.0)	105	48	1.1:1	31
16	TA ₉	(<i>S</i>)-Segphos	THF (1.0)	105	57	1.7:1	89
17	TA ₉	(<i>S</i>)-DM-Segphos	THF (1.0)	105	9	1:1.1	55
18	TA ₉	(<i>S</i>)-Segphos	THF (2.0)	95	57	2.2:1	89
19	TA ₉	(<i>S</i>)-Segphos	PhMe (2.0)	95	62	2.4:1	90
20	TA ₉	(<i>S</i>)-Segphos	<i>t</i> BuOH (2.0)	95	23	2.7:1	94
21	TA ₉	(<i>S</i>)-Segphos	Me ₂ CO (2.0)	95	46	3.0:1	92
22	TA ₁₂	(<i>S</i>)-Segphos	Me ₂ CO (2.0)	95	55	4.1:1	94
23	TA ₁₂	(<i>S</i>)-Segphos	Me ₂ CO (1.0)	95	57	4.6:1	94
⇒ 24	TA ₁₂	(<i>S</i>)-Segphos	Me ₂ CO (1.0)	95	82	4.4:1	95 ^a

TA ₁ : R ¹ , R ² = Me	TA ₇ : R ¹ =Me R ² =3-Tolyl
TA ₂ : R ¹ =Me R ² =Ph	TA ₈ : R ¹ =Me R ² =4-Tolyl
TA ₃ : R ¹ =Et R ² =Ph	TA ₉ : R ¹ =Me R ² = <i>m</i> -Xylyl
TA ₄ : R ¹ =Me R ² =2-Naphthyl	TA ₁₀ : R ¹ =Me R ² =3,5- <i>t</i> BuC ₆ H ₄
TA ₅ : R ¹ =Me R ² =3-PhC ₆ H ₄	TA ₁₁ : R ¹ =Me R ² =3,5-OMeC ₆ H ₄
TA ₆ : R ¹ =Me R ² =4-PhC ₆ H ₄	TA ₁₂ : R ¹ = <i>n</i> Pr R ² = <i>m</i> -Xylyl

^aRuH₂(CO)(PPh₃)₃ (7 mol%), (*S*)-Segphos (7 mol%), TA₁₂ (14 mol%)

Surprisingly, the *syn*-isomer exhibited the increase in enantioselectivity, with the opposite facial selectivity to what was observed for the BINOL phosphoric acid system.³⁵ While unexpected, further acid optimization was undertaken in attempt to improve the diastereoselectivity of the reaction. Increasing the steric environment of the TADDOL aromatic rings led to even higher levels of enantioselectivity. The *m*-xylyl substituted system provided the best selectivity, of 78% ee (entry 9).

Further increase in size or change in electronic character of the aryl substituents did not improve selectivity (entries 10-11). While other racemic ligands were evaluated in the reaction with no increase in selectivity (entries 12-14), it was postulated that a chiral ligand could interact with the phosphate counter ion in a matched or mismatched fashion, to either enhance or diminish selectivity. In screening both enantiomers of chiral Segphos ligand, amplification of enantioselectivity was observed in combination with (*S*)-Segphos, and greatly decreased with (*R*)-Segphos, suggesting that the L-TADDOL acid forms a matched pair with (*S*)-Segphos (entries 15-17).

Taking advantage of the synergistic effects on diastereoselectivity of chiral acid and chiral ligand, the *syn*-isomer was formed with very high enantioselectivity, but the reaction still suffered from a low diastereomeric ratio. Commonly, in contact ion pair interactions, the polarity of the solvent can play an important role. It could be predicted that nonpolar solvents would enhance the selectivity of the reaction, favoring close association of charged ruthenium and phosphate species. Interestingly, it was found that nonpolar solvents (entry 19) actually did not improve the selectivity, but conducting the reaction in polar solvents *t*BuOH and acetone (entries 20-21) did enhance diastereoselectivity. This could be explained by the ability of a polar solvent to coordinate the metal center, blocking sites for coordination of aldehyde necessary for C-C bond formation and effectively slowing down carbonyl addition. Slowing of the reaction may favor reactivity through the more energetically favored pathway. Alternatively, coordination of the catalyst by solvent may inhibit equilibration of the σ -allyl isomers, favoring reactivity through the kinetically-preferred (*E*)- σ -allyl isomer.

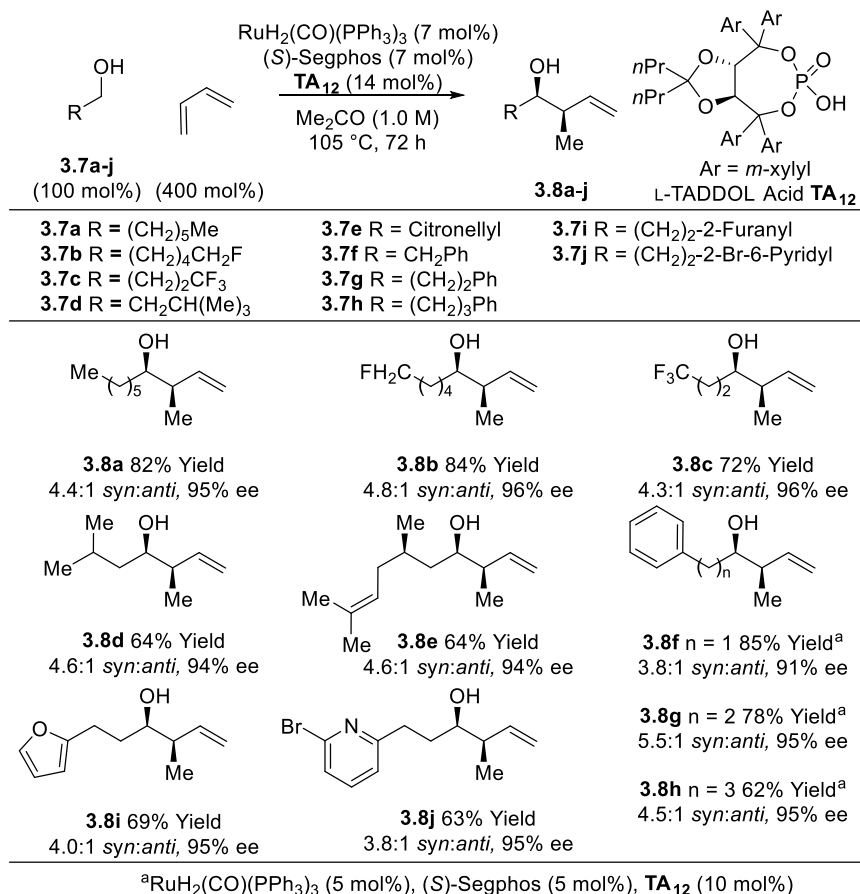
The final parameter that was evaluated for optimization of the TADDOL structure was the ketal moiety. By increasing the size of the substituent from methyl to propyl, an increase in diastereo- and enantioselectivity was observed. Further fine tuning of solvent concentration led to the optimal results for a highly *syn*-selective crotylation method (entries 22-23).

One consequence of enhancing selectivity by retarding the reaction was an impact on overall conversion. Attempts to increase yield by adjusting temperature and reaction time were ineffective. To generate more acceptable yields of product, 7 mol% of catalyst was required (entry 24).

3.3.3 Reaction Scope

The catalytic system for *syn*-crotylation was evaluated for a variety of aliphatic alcohol substrates **3.7a-j** (Figure 3.10). The reaction was efficient with good relative stereocontrol and excellent absolute stereocontrol, including fluorinated alcohols **3.7b-c** and aliphatic alcohols with pendant aromatic functionality **3.7f-j**. Notably, substrates **3.7d-e** with β -branching were also well tolerated in the system.³⁶

Figure 3.10 Ruthenium catalyzed coupling of butadiene and primary alcohols to generate products of *syn*-crotylation **3.8a-j**.

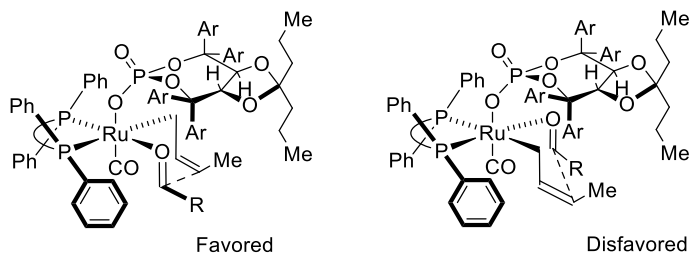


As seen with the *anti*-crotylation of aromatic alcohols, the substrate used for optimization was a strong factor in dictating the substrate scope. In an initial screening, aliphatic alcohols exhibited much higher levels of selectivity than allylic or aromatic substrates. Also, a variety of mono-protected diols were unreactive in this system. While not completely understood, the Lewis basic lone pair electrons on oxygen could play a role in coordination of the metal center to displace the phosphate counter ion or impede catalytic activity.

3.3.4 Discussion

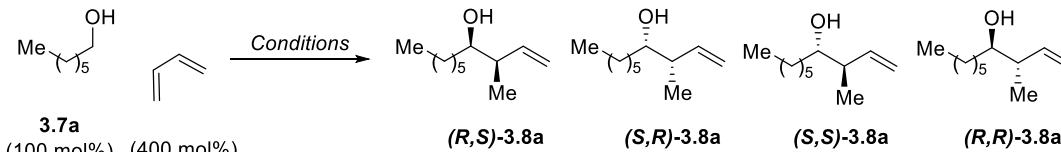
The ruthenium catalyzed crotylation of aliphatic alcohols is likely to proceed through a similar mechanism to that shown for *anti*-crotylation of aromatic alcohols (Figure 3.12). Despite the mechanistic similarities, the stereochemical outcome of the two reactions is quite distinct. While this displays the dramatic effect of introducing a chiral phosphoric acid to the metal center, the intricacies and rationality for selectivity are not completely understood. A stereochemical model for the favored and disfavored transition states are shown in Figure 3.11. If the reaction does indeed proceed through a chair-like transition state, the (*Z*)- σ -allyl isomer must participate in aldehyde addition to form the *syn*-diastereomer. In Figure 3.12, on the left, the less sterically hindered aldehyde is shown at front. The aryl rings of both TADDOL and the phosphine ligand block the front of the aldehyde, favoring allyl addition to the back side. On the right, the larger allyl fragment is shown in front, which may be disfavored due to the steric interactions with the TADDOL and ligand aromatic rings. This model does not account for all of the effects that result in the stereocontrolled process, as neither transition state clearly indicates why the *syn*-isomer is favored.

Figure 3.11 Stereochemical model of the transition state for carbonyl addition for *syn*-crotylation.



To emphasize the difference in selectivity using a BINOL or TADDOL derived phosphoric acid, heptanol was exposed to identical reaction conditions, using DPPF as ligand and the optimized (*R*)-BINOL phosphoric acid for *anti*-crotylation of aromatic alcohols and the TADDOL phosphoric acid for *syn*-crotylation. The same set of experiments were performed using (*S*)-Segphos as ligand (Table 3.3). With either ligand, the reaction with the BINOL acid additive favored formation of *anti* isomer (**(S,S)**-3.8a, and the reaction with the TADDOL acid favored formation of *syn* isomer (**(S,R)**-3.8a, showing that selectivity in the reaction is dictated by phosphate counter ion and not ligand. It is interesting to note that when using DPPF as ligand, the disfavored diastereomer is formed as a racemic mixture, meaning the chiral counter ion only controls the enantiomer ratio in the favored diastereomer. For both BINOL and TADDOL acids, the use of (*S*)-Segphos in place of DPPF increased the enantioselectivity of the favored isomer.

Table 3.3 Comparison of the effects of BINOL and TADDOL acids used in combination with DPPF and (*S*)-Segphos on ratio of isomers of product **3.8a**.



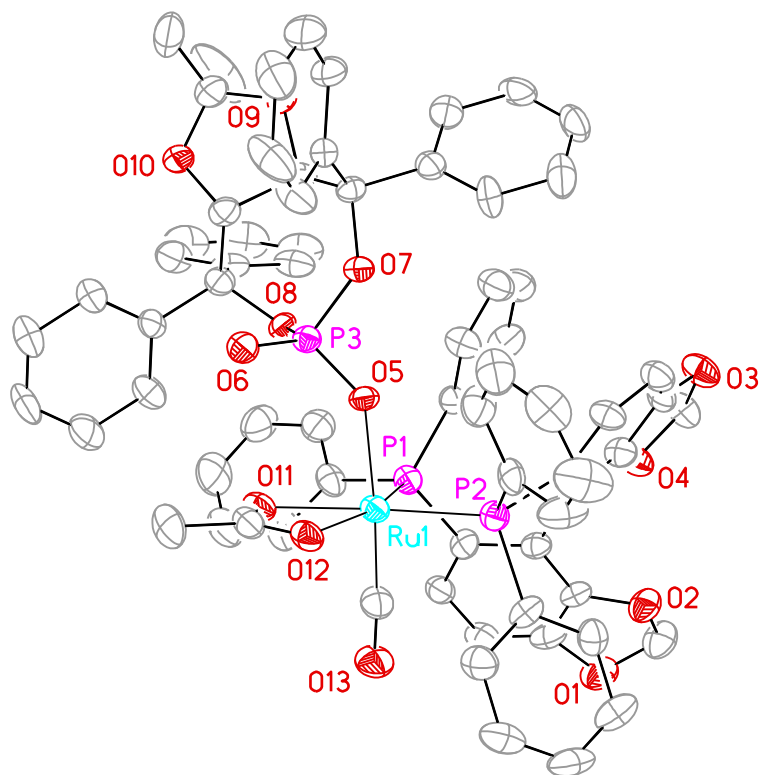
Conditions	Acid	Yield	Ratio of Products (<i>R,S</i>) : (<i>S,R</i>) : (<i>S,S</i>) : (<i>R,R</i>)
RuH ₂ (CO)(PPh ₃) ₃ (5 mol%) DPPF (5 mol%) Acid (10 mol%) THF (1.0 M), 95 °C, 48 h	TA ₁₂	66%	8 : 61 : 16 : 15
RuH ₂ (CO)(PPh ₃) ₃ (7 mol%) (<i>S</i>)-Segphos (7 mol%) Acid (14 mol%) Me ₂ (CO) (1.0 M), 95 °C, 72 h	TA ₁₂	82%	2 : 79 : 7 : 12
	BA ₁₆	10% ^a	15 : 17 : 65 : 3

^aReaction was performed at 115 °C

Other than experimental results for a highly selective *anti*- and *syn*-crotylation, little had been confirmed about the actual role of the phosphate counter ion in the reaction. Obtaining a crystal structure of the catalyst or some catalytic intermediate was a daunting goal, but fortuitously, a model system was formed and recrystallized to yield complex **3.10** (Figure 3.12), in which ruthenium is modified by both (*S*)-Segphos and **TA**₂. As would be anticipated by *trans*-effects, the phosphate anion is positioned opposite the carbonyl ligand.^{65h} An interesting feature

of the structure is that the aryl rings on the TADDOL structure and the phenyl rings on (*S*)-Segphos appear to project between one another, perhaps providing the basis for the match and mismatch effects that were observed experimentally.

Figure 3.12 ORTEP representation of crystal structure of Ru(CO)(OAc)[(*S*)-Segphos][TADDOL-Phosphate] **3.10**



3.10

3.3.5 Conclusion

TADDOL-derived phosphoric acid **TA**₁₂ was identified as a highly effective acid additive in combination with (*S*)-Segphos for enantioselective *syn*-selective crotylation. An x-ray crystal structure of ruthenium complex **3.10** exhibits steric interactions between ligand and acid, suggesting the basis for experimentally observed match and mismatch effects. In a comparison of the BINOL phosphoric acid (**BA**₁₆) developed for *anti*-crotylation of aromatic alcohols under

identical reaction conditions, it was found that the identity of the phosphoric acid dictated both relative and absolute stereocontrol.

3.4 Summary and Outlook

Upon completion of this work, complementary methods for accessing products of *anti*- and *syn*- crotylation were established. Using transfer hydrogenative, reductive coupling, either alcohol or aldehyde could be employed as carbonyl partner and butadiene could be used directly as unsaturate, dramatically simplifying the protocol for crotylation. Notably, the important role of counter ion was displayed in both the *anti*- and *syn*- selective crotylation methods, illustrating the variety, flexibility and amenity to optimization of BINOL and TADDOL derived phosphoric acids for asymmetric transition metal catalysis.

3.5 Experimental Details

3.5.1 General Information

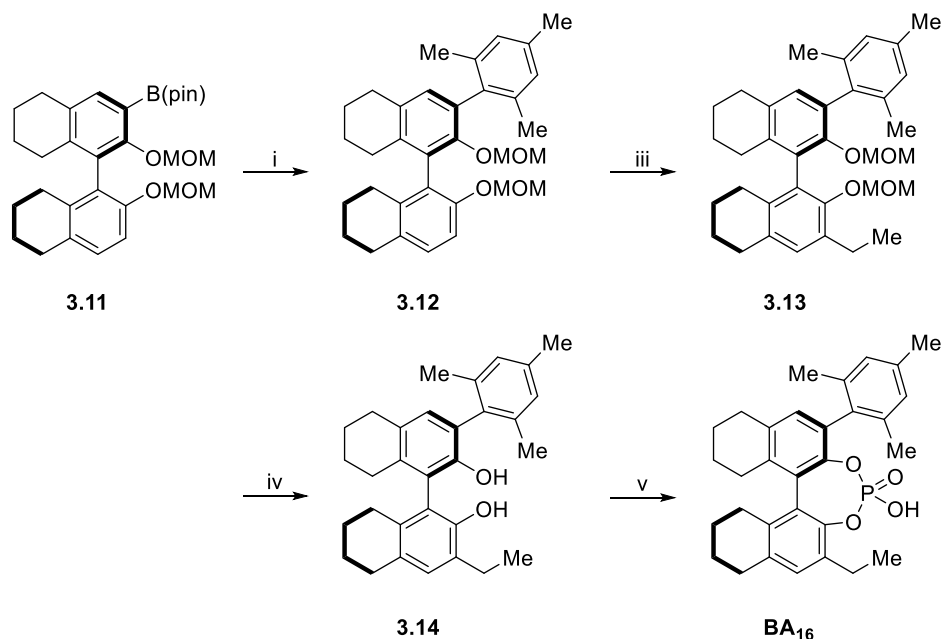
All reactions were run under an atmosphere of argon in sealed tubes (13x100 mm²), dried overnight in an oven and cooled under a stream of argon prior to use. Anhydrous solvents were distilled using solvent stills and solvent were transferred by oven-dried syringe. Catalyst RuH₂(CO)(PPh₃)₃ was prepared according to the method of Williams.⁷⁴ All ligands were used without purification. Alcohol and aldehyde substrates were purified by distillation or recrystallization prior to use. BINOL derived phosphoric acids were prepared in analogy to procedure described by Akiyama,⁹⁶ and TADDOL derived phosphoric acids were prepared in analogy to procedure described by Seebach et al.⁹⁷ and Akiyama et al.^{89b} Thin-layer chromatography (TLC) was carried out using 0.25 mm commercial silica gel plates (Silicycle Siliaplate F-254). Visualization was accomplished with UV light followed by staining. Purification of product was carried out by flash column chromatography using Silicycle silica gel (40-63 μm), according to the method described by Still.⁷⁵

3.5.2 Spectrometry and Spectroscopy

Infrared spectra were recorded on a Thermo Nicolet 380 spectrometer. Low and high resolution mass spectra (LRMS or HRMS) were obtained on a Karatos MS9 and are reported as m/z (relative intensity). Accurate masses are reported for the molecular ion or a suitable fragment ion. Melting points were obtained on a Stuart SMP3 apparatus and are uncorrected. ^1H NMR spectra were recorded on a Varian Gemini (400 MHz) spectrometer at ambient temperature. Chemical shifts are reported in delta (δ) units, parts per million (ppm), relative to the center of the singlet at 7.26 ppm for deuteriochloroform, or other reference solvents as indicated. Data are reported as chemical shift, multiplicity (s=singlet, d=doublet, t=triplet, q=quartet, m=multiplet), integration and coupling constant(s) in Hz. ^{13}C NMR spectra were recorded on a Varian Gemini (100 MHz) spectrometer and were routinely run with broadband decoupling. Chemical shifts are reported in ppm, with the center peak of the residual solvent resonance employed as an internal standard.

3.5.3 Preparation of BINOL Phosphoric Acid BA₁₆

Figure 3.13 Synthetic Route to BINOL Phosphoric Acid BA₁₆



(i) Pd(PPh₃)₄ (5 mol%), 2-bromomesitylene (300 mol%), NaOH (350 mol%), THF, H₂O, 95 °C, 18 h. (ii) *n*BuLi (150 mol%), iodoethane (150 mol%), THF, 18 h (iii) HCl, EtOH, 18 h (iv) POCl₃ (130 mol%), pyridine 115 °C, then H₂O, 3 h.

(*R*)-3-mesityl-2,2'-bis(methoxymethoxy)-5,5',6,6',7,7',8,8'-octahydro-1,1'-binaphthalene (**3.12**)

To a flame dried resealable pressure tube equipped with a magnetic stir bar was added compound **3.11** (prepared by the method of Sasai et al.⁹⁸) (3.72 g, 9.2 mmol, 100 mol%), Pd(PPh₃)₄ (0.53 g, 0.46 mmol, 5 mol%), and NaOH (1.3 g, 32.2 mmol, 350 mol%). The tube was sealed with a rubber septum and purged with argon. THF (46 mL, 0.2 M concentration with respect to compound **3.11**), water (18.4 mL, 0.5 M concentration with respect to compound **3.11**) and bromomesitylene (4.2 mL, 27.6 mmol, 300 mol%) were added. The solution was then vigorously degassed and the rubber septum quickly replaced with a screw cap. The mixture was heated at 95 °C (oil bath temperature) for 18 h, at which point the reaction mixture was allowed to cool to ambient temperature. The reaction mixture was transferred to separatory funnel and extracted with CH₂Cl₂ (3x100 mL). The combined organic extracts were washed with brine, dried (Na₂SO₄), and concentrated *in vacuo*. The residue was purified by flash column chromatography

(SiO₂; EtOAc:hexanes, 1:15) to furnish the title compound (3.50 g, 7.2 mmol, 78% yield) as a white solid.

m.p.: 64-65 °C

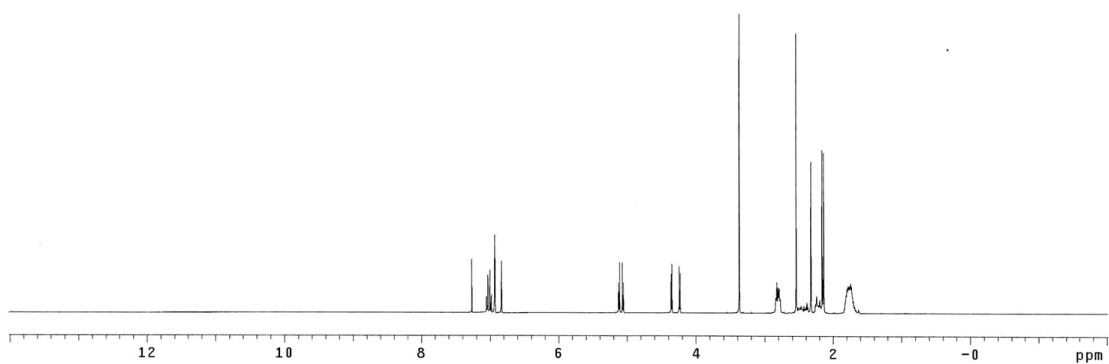
¹H NMR (400 MHz, CDCl₃): δ 7.04 (d, *J* = 8.6 Hz, 1H), 6.99 (d, *J* = 8.6 Hz, 1H), 6.93 (s, 2H), 6.83 (s, 1H), 5.12 (d, *J* = 6.7 Hz, 1H), 5.06 (d, *J* = 6.7 Hz, 1H), 4.36 (d, *J* = 5.5 Hz, 1H), 4.24 (d, *J* = 5.5 Hz, 1H), 3.37 (s, 3H), 2.84-2.78 (m, 4H), 2.54 (s, 3H), 2.47-2.38 (m, 2H), 2.33 (s, 3H), 2.26-2.20 (m, 2H), 2.16 (s, 3H), 2.14 (s, 3H), 1.81-1.63 ppm (m, 8H).

¹³C NMR (100 MHz, CDCl₃): δ 152.5, 149.7, 137.1, 136.8, 136.7, 136.2, 136.0, 135.7, 132.9, 131.5, 131.3, 130.8, 130.7, 128.8, 127.9, 127.8, 127.1, 112.1, 97.7, 94.7, 55.6, 55.6, 29.6, 29.4, 27.5, 27.3, 23.3, 23.2, 23.1, 23.1, 21.1, 20.9, 20.8 ppm.

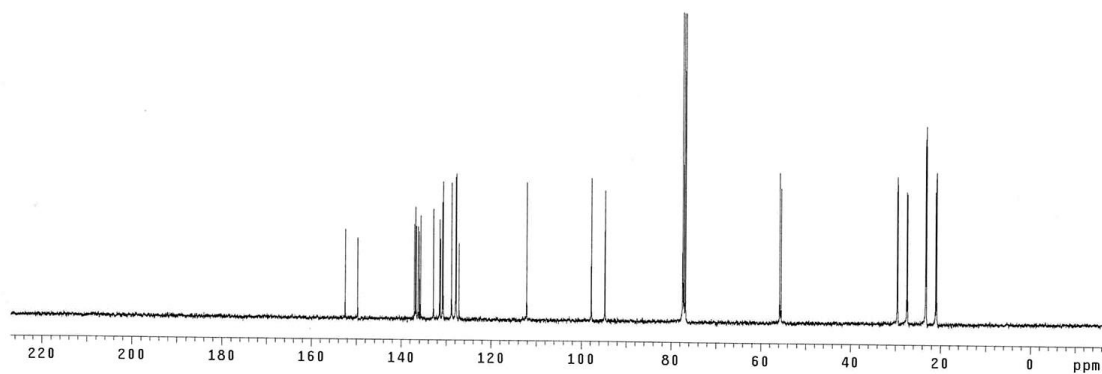
LRMS (Cl⁺): *m/z* 500 [M]⁺.

FTIR (neat): 2922, 1478, 1244, 1206, 1060, 1016, 984, 922, 849, 807 cm⁻¹.

¹H NMR of **3.12**



¹³C NMR of **3.12**



(R)-3-ethyl-3'-mesityl-2,2'-bis(methoxymethoxy)-5,5',6,6',7,7',8,8'-octahydro-1,1'-binaphthalene
(3.13)

To a flame dried, 100 mL round bottom flask compound **3.12** (1.70 g, 3.4 mmol, 100 mol%) was added, and the flask was sealed and purged with argon. THF (11 mL, 0.3 M concentration of **3.12**) is added and the solution is cooled to 0 °C. A solution of 2.5 M *n*BuLi in hexanes (2.0 mL, 5.1 mmol, 150 mol%) was added dropwise and stirred for 10 minutes. The reaction mixture was allowed to warm to RT and stir for 3 h. Iodoethane (0.4 mL, 5.1 mmol, 150 mol%) was added dropwise and the mixture was stirred for 18 h. Upon complete consumption of starting material, ammonium chloride (15 mL, sat. aq. sol.) was added. The organic layer was extracted with CH₂Cl₂ (3x50 mL) and the combined organic extracts were dried (MgSO₄), filtered, and concentrated *in vacuo*. The residue was purified by column chromatography (SiO₂; Et₂O:hexanes, 1:20) to provide **3.13** (1.12 g, 2.1 mmol, 63% yield) as a white solid.

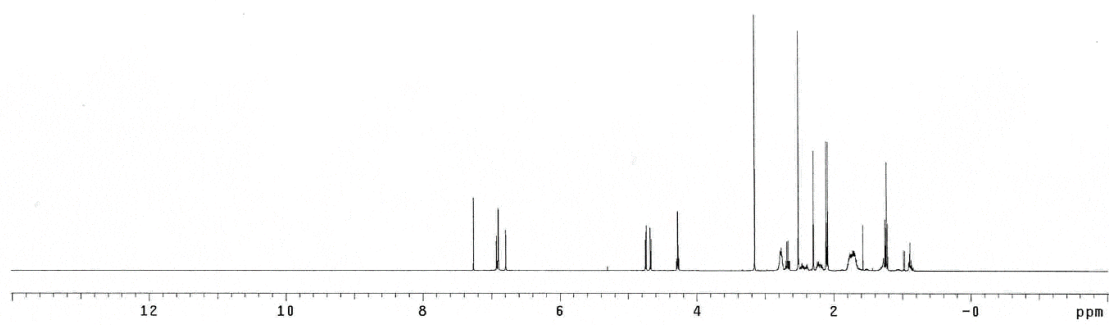
m.p.: 63-66 °C

¹H NMR (400 MHz, CDCl₃): δ 6.93 (s, 3H), 6.90 (s, 3H), 6.79 (s, 3H), 4.75 (d, *J* = 5.5 Hz, 1H), 4.67 (d, *J* = 5.5 Hz, 1H), 4.29 (d, *J* = 5.7 Hz, 1H), 4.27 (d, *J* = 5.7 Hz, 1H), 3.15 (s, 3H), 2.78-2.75 (m, 2H), 2.67 (q, *J* = 7.5 Hz, 2H), 2.52 (s, 3H), 2.48-2.39 (m, 2H), 2.30 (s, 3H), 2.30-2.18 (m, 2H), 2.11 (s, 3H), 2.09 (s, 3H), 1.78-1.69 (m, 8H), 1.23 ppm (t, *J* = 7.5 Hz, 3H).

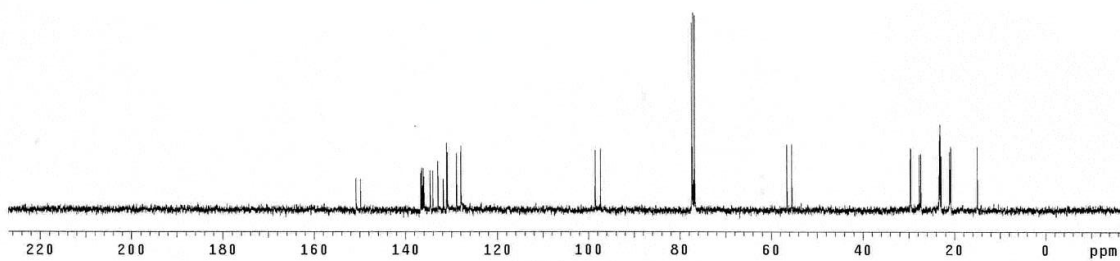
¹³C NMR (100 MHz, CDCl₃): δ 150.8, 149.8, 136.7, 136.5, 136.4, 136.1, 135.9, 134.6, 134.0, 132.9, 131.1, 131.0, 130.9, 128.9, 128.0, 127.9, 98.5, 97.3, 56.5, 55.5, 31.6, 29.6, 29.6, 27.7, 27.4, 23.3, 23.2, 23.1, 22.9, 21.1, 20.9, 20.8, 14.9 ppm.

LRMS (CI⁺): *m/z* 528 [M]⁺.

FTIR (neat): 2926, 1711, 1437, 1359, 1280, 1095, 909 cm⁻¹.



^{13}C NMR of 3.13



(*R*)-3-ethyl-3'-mesityl-5,5',6,6',7,7',8,8'-octahydro-[1,1'-binaphthalene]-2,2'-diol (**3.14**)

To a 250 mL round bottom flask compound **3.13** (1.12 g, 2.1 mmol, 100 mol%) is added. Ethanol (70 mL, 0.03 M concentration with respect to compound **3.13**) and *conc.* hydrochloric acid (7 mL, 0.3 M concentration with respect to compound **3.13**) were added sequentially. The reaction mixture was stirred at room temperature overnight. Upon complete consumption of starting material, as determined by TLC analysis, the reaction mixture was concentrated *in vacuo*. The residue was purified by column chromatography (SiO₂; DCM:hexanes, 1:1) to provide the **3.14** (0.88 g, 2.0 mmol, 95% yield) as a white solid.

m.p.: 89-92 °C

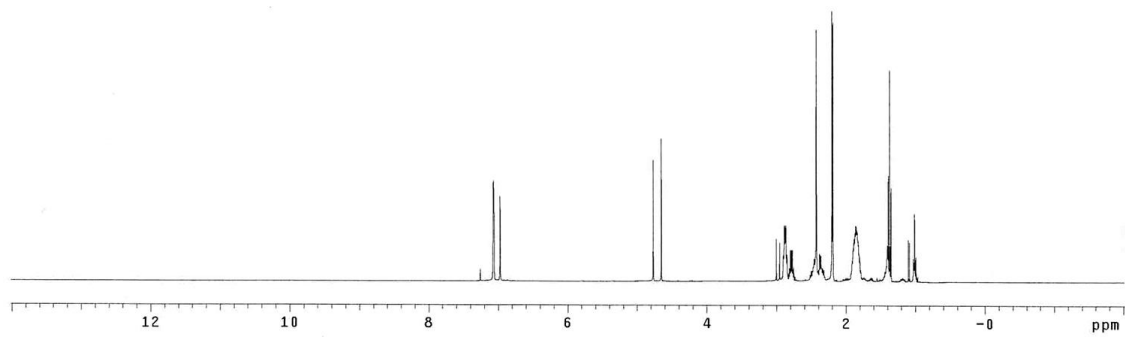
¹H NMR (400 MHz, CDCl₃): δ 7.07 (s, 2H), 7.06 (s, 1H), 6.97 (s, 1H), 4.77 (s, 1H), 4.65 (s, 1H), 2.88 (q, *J* = 7.4 Hz, 2H), 2.81-2.75 (m, 4H), 2.52-2.31 (m, 7H), 2.20 (s, 3H), 2.19 (s, 3H), 1.91-1.73 (m, 8H), 1.37 ppm (t, *J* = 7.4 Hz, 3H).

¹³C NMR (100 MHz, CDCl₃): δ 148.8, 148.6, 137.2, 137.1, 137.0, 136.5, 133.8, 133.5, 131.7, 130.1, 130.0, 129.3, 128.5, 128.4, 127.7, 125.0, 119.9, 119.5, 31.7, 29.4, 27.2, 27.0, 23.4, 23.3, 23.2, 23.2, 22.8, 21.2, 20.7, 20.6, 14.2 ppm.

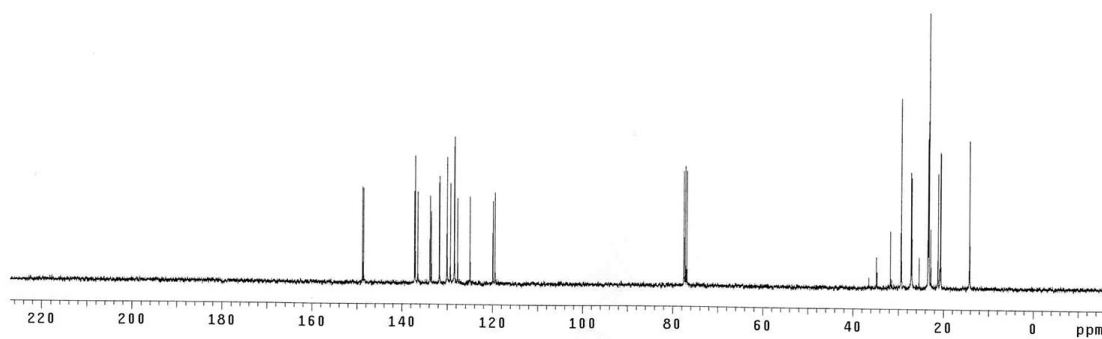
LRMS (Cl⁺): *m/z* 440 [M]⁺.

FTIR (neat): 2926, 1450, 1264, 1154, 982, 736 cm⁻¹.

^1H NMR of **3.14**



^{13}C NMR of **3.14**



(*R*)-2-ethyl-4-hydroxy-6-mesityl-8,9,10,11,12,13,14,15-octahydrodinaphtho[2,1-d:1',2'-f][1,3,2]dioxaphosphepine 4-oxide (**BA₁₆**)

To a 100 mL round bottom flask, was added compound **3.14** (0.44g, 1 mmol, 100 mol%), pyridine (2 mL, 0.5 M concentration with respect to compound **3.14**) and POCl₃ (0.170 mL, 1.8 mmol, 180 mol%). The mixture was refluxed at 115 °C (oil bath temperature) for 18 h, at which point the reaction mixture was allowed to cool to ambient temperature. Water (1 mL, 1.0 M concentration with respect to compound **3.14**) was added dropwise and then heated to 115 °C for an additional 3 h. Upon complete consumption of starting material, as determined by TLC, the reaction mixture was cooled to ambient temperature and a solution of hydrochloric acid (10 mL, 3M aq. sol.) was added. The organic layer was extracted with DCM (3x50 mL) and the combined organic extracts were dried (MgSO₄), filtered, and concentrated *in vacuo*. The residue was purified by column chromatography (SiO₂; 0-20% IPA:DCM) and concentrated *in vacuo*. The residue was diluted with DCM then washed with a solution of hydrochloric acid (10 mL, 3.0 M) and concentrated *in vacuo* to provide **BA₁₆** (0.46 g, 0.92 mmol, 92% yield) as a white solid.

m.p.: 228-230 °C.

¹H NMR (400 MHz, CDCl₃): δ 8.17 (brs, 1H), 6.90 (s, 1H), 6.84 (s, 1H), 6.76 (s, 1H), 2.81-2.69 (m, 4H), 2.66-2.55 (m, 3H), 2.49-2.42 (m, 1H), 2.27-2.12 (m, 2H), 2.10 (s, 3H), 2.05 (s, 3H), 1.88 (s, 3H), 1.79-1.66 (m, 8H), 1.11 ppm (t, *J* = 7.5 Hz, 3H).

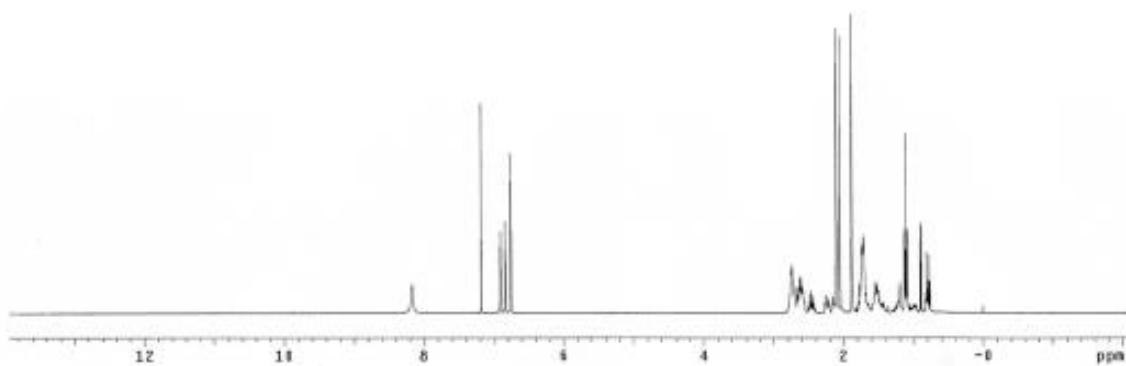
¹³C NMR (100 MHz, CDCl₃): δ 144.1, 144.0, 143.5, 143.4, 136.9, 136.8, 136.5, 135.1, 135.0, 133.3, 132.8, 131.6, 130.2, 129.7, 128.5, 127.6, 126.7, 126.2, 29.3, 29.2, 27.8, 27.7, 22.8, 22.7, 22.7, 22.6, 22.3, 21.0, 20.8, 20.2, 14.0 ppm.

³¹P NMR (162 MHz, CDCl₃): 2.5 ppm.

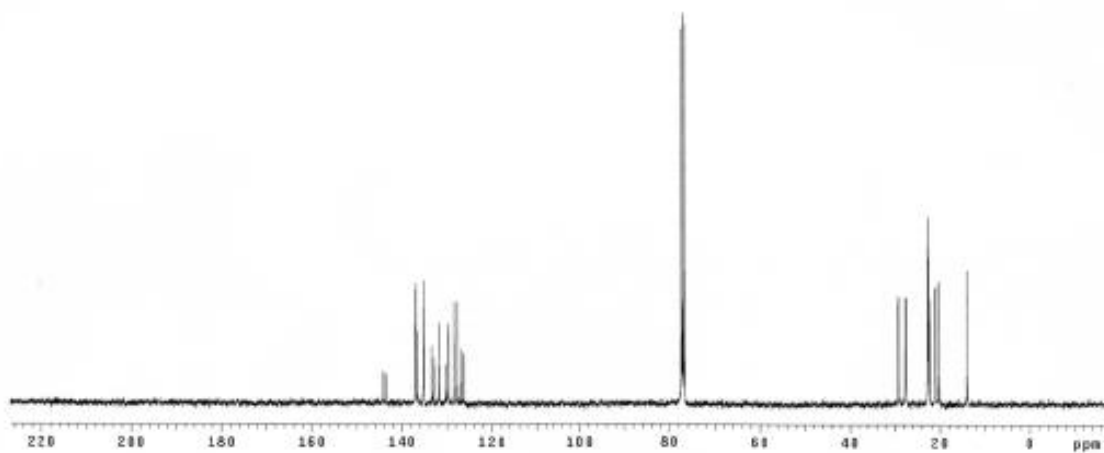
LRMS (Cl⁺): *m/z* 502 [M]⁺.

FTIR (neat): 2931, 1612, 1434, 1245, 1202, 1017, 905, 728 cm⁻¹.

^1H NMR of **BA₁₆**



^{13}C NMR of **BA₁₆**



3.5.4 General Procedures for anti-Crotylation using Butadiene

Procedure A: To a re-sealable pressure tube (13 x 100 mm) equipped with magnetic stir bar, $\text{RuH}_2(\text{CO})(\text{PPh}_3)_3$ (13.8 mg, 0.015 mmol, 5 mol%), 1,1'-Bis(diphenylphosphino)ferrocene (8.3 mg, 0.01 mmol, 5 mol%), and (*R*)-BINOL phosphoric acid **BA**₁₆ (15 mg, 0.03 mmol, 10 mol%) were added. The tube was sealed with a rubber septum and purged with argon. Alcohol (0.3 mmol, 100 mol%) and THF (0.15 mL, 2.0 M with respect to alcohol) were added, and the reaction tube was cooled to -78 °C. Butadiene (0.10 mL, 1.20 mmol, 400 mol%) was quickly added and the rubber septum replaced with a screw cap. The mixture was heated at 95 °C (oil bath temperature) for 48 h, at which point the reaction mixture was allowed to cool to ambient temperature. The reaction mixture was then concentrated in vacuo and the ratio of diastereomers was determined by NMR of the crude reaction mixture. The crude reaction mixture was subjected to flash column chromatography (SiO_2 ; 0-10% EtOAc/hexanes) to furnish the corresponding product of crotylation.

Procedure B for aldehyde substrates 3.3a-g: To a re-sealable pressure tube (13 x 100 mm) equipped with magnetic stir bar, $\text{RuH}_2(\text{CO})(\text{PPh}_3)_3$ (13.8 mg, 0.015 mmol, 5 mol%), 1,1'-Bis(diphenylphosphino)ferrocene (8.3 mg, 0.01 mmol, 5 mol%), and (*R*)-BINOL phosphoric acid **BA**₁₆ (15 mg, 0.03 mmol, 10 mol%) were added. The tube was sealed with a rubber septum and purged with argon. Aldehyde (0.3 mmol, 100 mol%), 1,4-butanediol (53 μL , 0.60 mmol, 200 mol%) and THF (0.15 mL, 2.0 M with respect to alcohol) were added, and the reaction tube was cooled to -78 °C. Butadiene (0.10 mL, 1.20 mmol, 400 mol%) was quickly added and the rubber septum replaced with a screw cap. The mixture was heated at 95 °C (oil bath temperature) for 48 h, at which point the reaction mixture was allowed to cool to ambient temperature. The reaction mixture was then concentrated in vacuo and the ratio of diastereomers was determined by NMR of the crude reaction mixture. The crude reaction mixture was subjected to flash column chromatography (SiO_2 ; 0-10% EtOAc/hexanes) to furnish the corresponding product of crotylation.

3.5.5 Characterization of 3.4a-g

methyl 4-((1R,2R)-1-hydroxy-2-methylbut-3-en-1-yl)benzoate (**3.4a**)

In accordance with procedure A using alcohol **3.2a**, upon stirring at 95 °C for 48 h, the reaction mixture was concentrated *in vacuo* to afford the crude product (dr = 7:1 *anti:syn*, as determined by ¹H NMR spectroscopy). The reaction mixture was then subjected to flash column chromatography (SiO₂: 0-20% EtOAc/hexanes) to furnish **3.4a** (53 mg, 0.24 mmol 80% yield, 88% ee) as a clear oil.

In accordance with procedure B using aldehyde **3.3a**, upon stirring at 95 °C for 48 h, the reaction mixture was concentrated *in vacuo* to afford the crude product (dr = 6:1 *anti:syn*, as determined by ¹H NMR spectroscopy). The reaction mixture was then subjected to flash column chromatography (SiO₂: 0-20% EtOAc/hexanes) to furnish **3.4a** (53 mg, 0.24 mmol, 80% yield, 86% ee) as a clear oil. *The spectroscopic properties of this compound were consistent with the data available in the literature.*⁹⁹

¹H NMR (400 MHz, CDCl₃): δ 7.97 (d, *J* = 8.0 Hz, 2H), 7.36 (d, *J* = 8.0 Hz, 2H), 5.79-5.69 (m, 1H), 5.17-5.12 (m, 2H), 4.40 (d, *J* = 7.2 Hz, 1H), 3.88 (s, 3H), 2.49-2.36 (m, 2H), 0.86 ppm (d, *J* = 6.8 Hz, 3H).

¹³C NMR (100 MHz, CDCl₃): δ 147.9, 140.1, 129.7, 129.6, 127.0, 117.5, 77.3, 52.3, 46.5, 16.6 ppm.

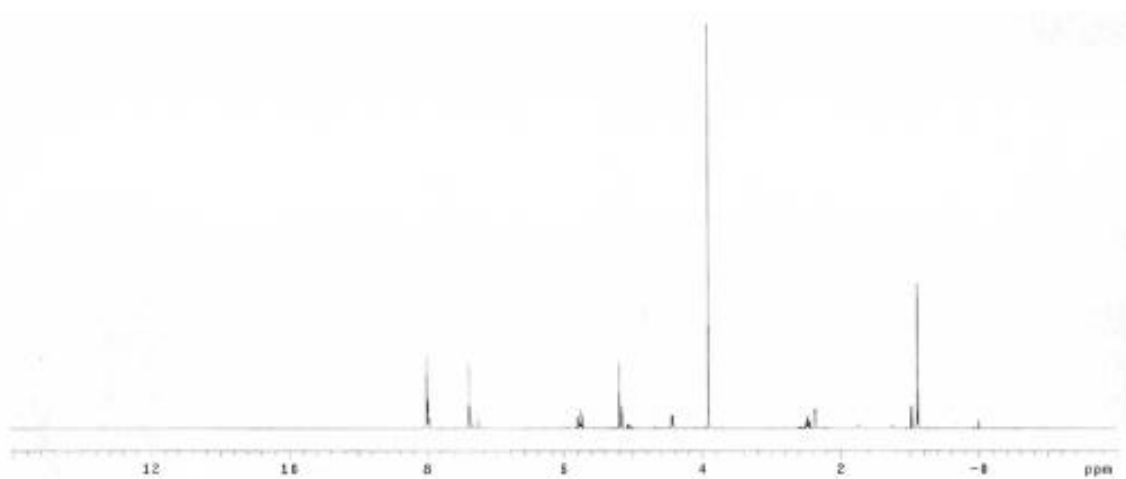
LRMS (CI+): *m/z* 221 [M+H]⁺

[α]_D²⁵ = +41.4 (c = 1.0, CHCl₃).

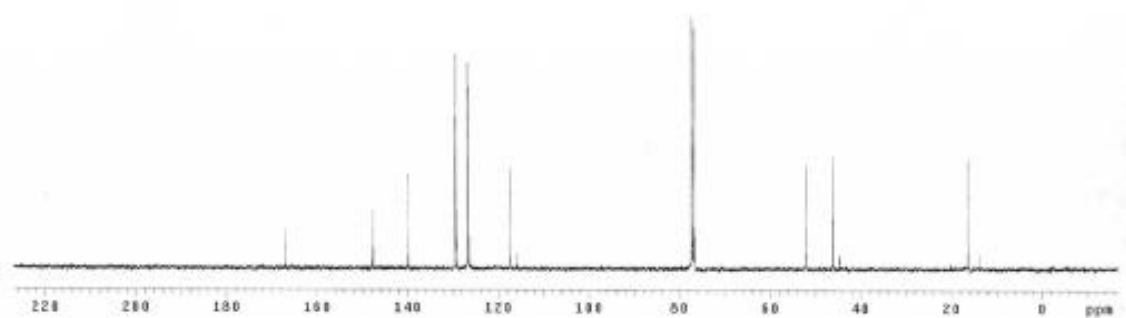
FTIR (neat): 3467, 2953, 1719, 1435, 1276, 1177, 1110, 1017, 915, 810, 709 cm⁻¹.

HPLC (Chiralcel AD-H column, hexanes:*i*-PrOH = 95:5, 0.5 mL/min, 230 nm): *t*_{major}=27.9 min, *t*_{minor}=33.2 min.

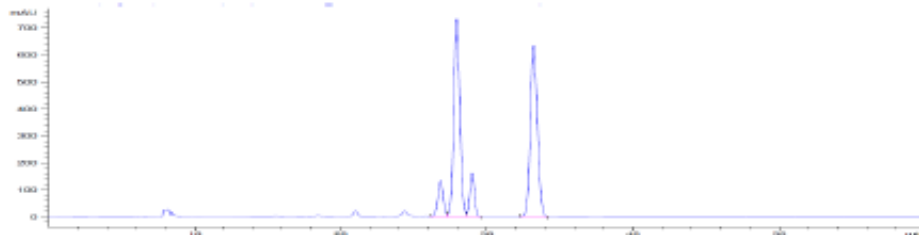
^1H NMR of **3.4a**



^{13}C NMR of **3.4a**



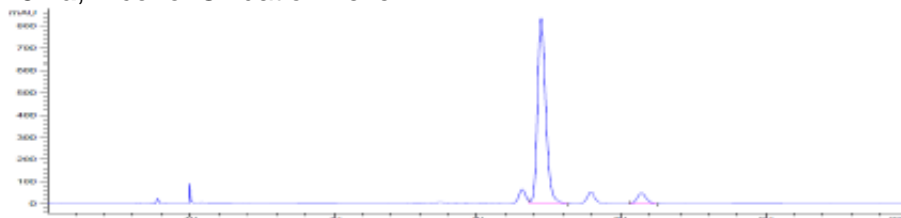
Racemic HPLC **3.4a**



Signal 1: DAD1 D, Sig=230,16 Ref=360,100

Peak #	RetTime [min]	Type	Width [min]	Area [mAU*s]	Height [mAU]	Area %
1	26.829	VV	0.4213	3614.49023	132.89398	7.2899
2	27.934	VV	0.4491	2.11800e4	732.98383	42.7168
3	28.972	VB	0.3489	3641.41187	161.56358	7.3441
4	33.189	BB	0.5157	2.11465e4	633.12537	42.6492

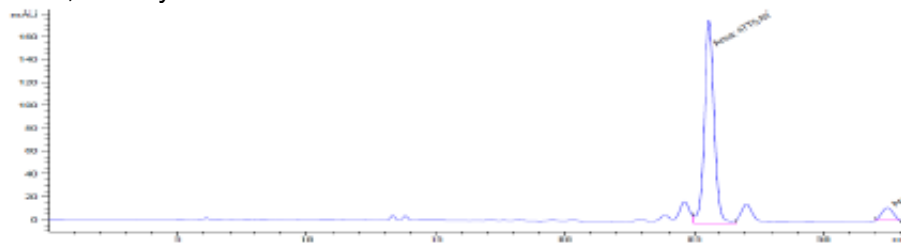
HPLC of **3.4a**, Alcohol Oxidation Level



Signal 1: DAD1 D, Sig=230,16 Ref=360,100

Peak #	RetTime [min]	Type	Width [min]	Area [mAU*s]	Height [mAU]	Area %
1	34.472	VB	0.5980	3.24260e4	833.27014	93.8669
2	41.461	BB	0.6686	2119.67383	49.17524	6.1331

HPLC of **3.4a**, Aldehyde Oxidation Level



Signal 1: DAD1 D, Sig=230,16 Ref=360,100

Peak #	RetTime [min]	Type	Width [min]	Area [mAU*s]	Height [mAU]	Area %
1	25.978	MM	0.4504	4776.66992	176.73450	93.3899
2	32.485	MM	0.4940	338.02231	11.40450	6.6101

(1*R*,2*R*)-2-methyl-1-(4-(trifluoromethyl)phenyl)but-3-en-1-ol (**3.4b**)

In accordance with procedure A using alcohol **3.2b**, upon stirring at 95 °C for 48 h, the reaction mixture was concentrated *in vacuo* to afford the crude product (dr = 7:1 *anti:syn*, as determined by ¹H NMR spectroscopy). The reaction mixture was then subjected to flash column chromatography (SiO₂: 0-10% EtOAc/hexanes) to furnish **3.4b** (57 mg, 0.25 mmol, 83% yield, 92% ee) as a clear oil.

In accordance with procedure B using aldehyde **3.3b**, upon stirring at 95 °C for 48 h, the reaction mixture was concentrated *in vacuo* to afford the crude product (dr = 6:1 *anti:syn*, as determined by ¹H NMR spectroscopy). The reaction mixture was then subjected to flash column chromatography (SiO₂: 0-10% EtOAc/hexanes) to furnish **3.4b** (44 mg, 0.19 mmol, 63% yield, 88% ee) as a clear oil. *The spectroscopic properties of this compound were consistent with the data available in the literature.*^{81d}

¹H NMR (400 MHz, CDCl₃): δ 7.60 (d, *J* = 8.0 Hz, 2H), 7.44 (d, *J* = 8.0 Hz, 2H), 5.81-5.72 (m, 1H), 5.23-5.18 (m, 2H), 4.43 (dd, *J* = 7.2 Hz, 2.6 Hz, 1H), 2.51-2.42 (m, 1H), 2.26 (d, *J* = 2.6 Hz, 1H) 0.89 ppm (d, *J* = 6.8 Hz, 3H).

¹³C NMR (100 MHz, CDCl₃): δ 146.3, 139.8, 129.7 (q, *J* = 32 Hz), 127.1, 125.2 (q, *J* = 3.7 Hz), 124.0 (q, *J* = 271 Hz), 117.6, 77.2, 46.4, 16.4 ppm.

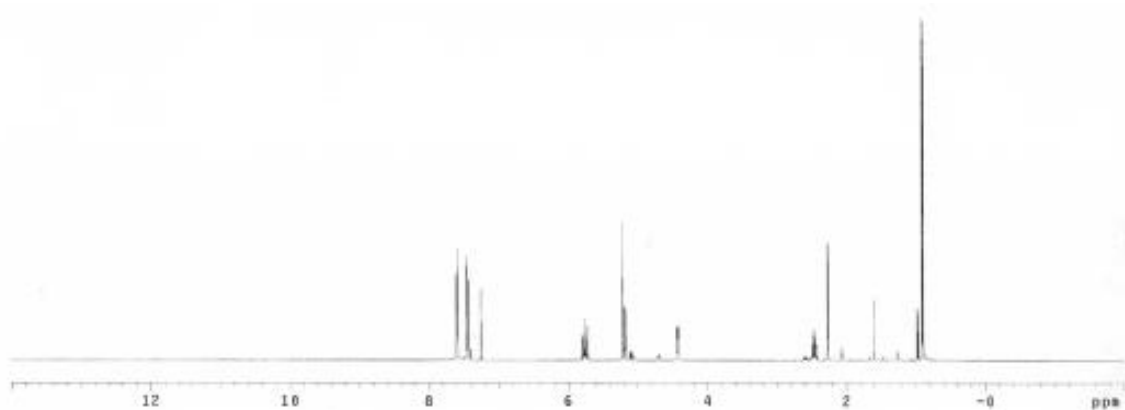
LRMS (Cl⁺): *m/z* 213 [M-OH]⁺

[α]_D²⁵ = +52 (c = 1.0, CHCl₃) reported for 92% ee of the (*R,R*) compound [α]_D²⁵ = +55 (c = 1.0, CHCl₃).

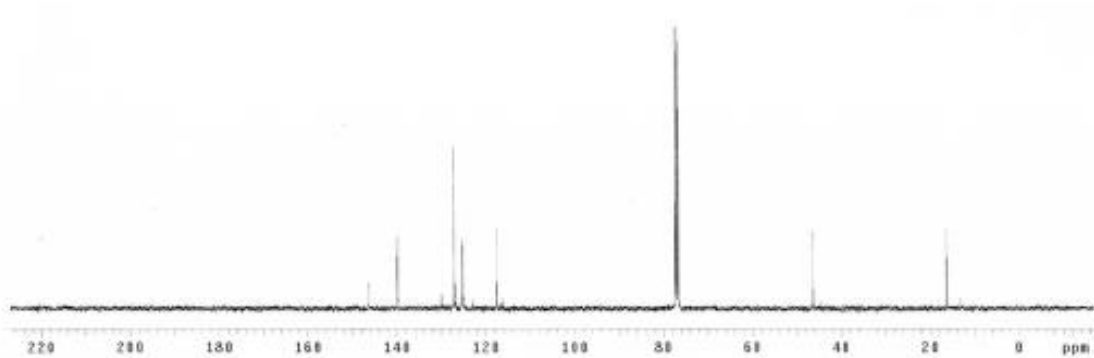
FTIR (neat): 3380, 2976, 1620, 1458, 1418, 1323, 1162, 1120, 1066, 1016, 917, 831, 763, 741, 684 cm⁻¹.

HPLC (Compound **3c** was converted to the 4-nitro-benzoate for analysis, Chiralcel OD-H/OD-H/OD-H column, hexanes:*i*-PrOH = 97:3, 0.3 mL/min, 254 nm): t_{major}=71.5 min, t_{minor}=75.9 min.

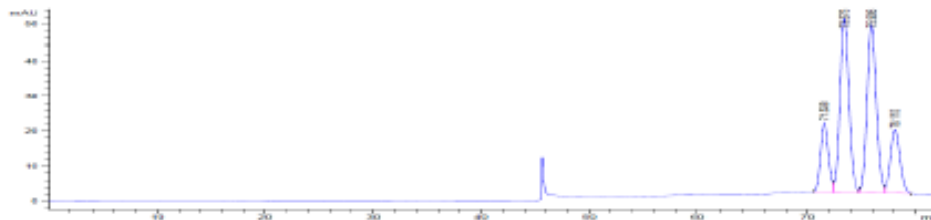
^1H NMR of **3.4b**



^{13}C NMR of **3.4b**



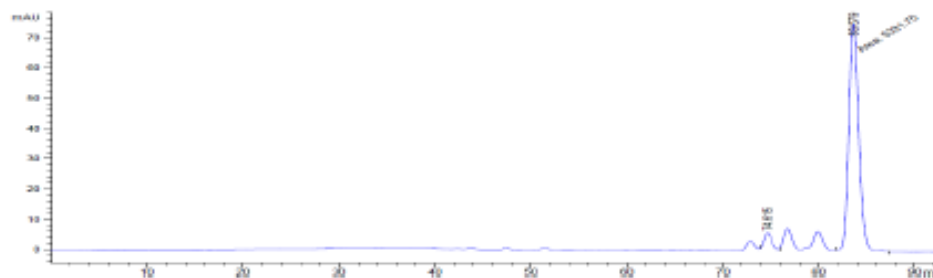
Racemic HPLC 3.4b



Signal 1: DAD1 B, Sig=254,16 Ref=360,100

Peak #	RetTime [min]	Type	Width [min]	Area [mAU*s]	Height [mAU]	Area %
1	71.538	MB	0.8227	1070.34790	19.95071	13.8908
2	73.375	VB	0.8762	2782.27124	49.01735	36.1078
3	75.906	MB	0.9000	2755.28467	47.27272	35.7575
4	78.110	VB	0.9231	1097.55933	18.10957	14.2439

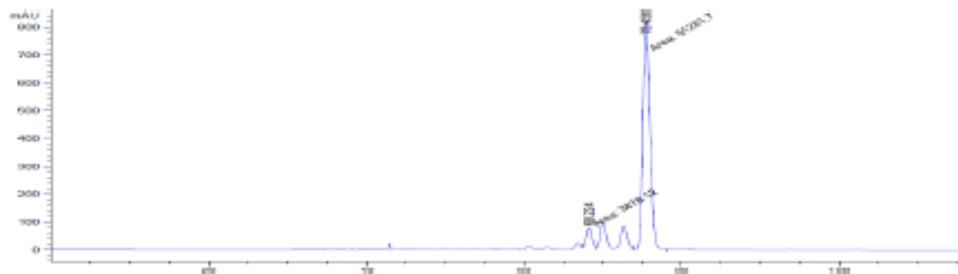
HPLC of 3.4b, Alcohol Oxidation Level



Signal 1: DAD1 B, Sig=254,16 Ref=360,100

Peak #	RetTime [min]	Type	Width [min]	Area [mAU*s]	Height [mAU]	Area %
1	74.615	MB	0.6295	251.10977	5.02046	4.4979
2	83.979	MM	1.1806	5331.75098	75.27206	95.5021

HPLC of 3.4b, Aldehyde Oxidation Level



Signal 1: DAD1 B, sig=254,16 ref=360,100

Peak #	RetTime [min]	Type	Width [min]	Area [mAU*s]	Height [mAU]	Area %
1	68.224	MM	0.8067	3478.12378	71.85876	6.3516
2	75.456	MM	1.0425	5.12817e4	819.85419	93.6484

(1*R*,2*R*)-1-(4-fluorophenyl)-2-methylbut-3-en-1-ol (**3.4c**)

In accordance with procedure A using alcohol **3.2c**, upon stirring at 95 °C for 48 h, the reaction mixture was concentrated *in vacuo* to afford the crude product (dr = 6:1 *anti:syn*, as determined by ¹H NMR spectroscopy). The reaction mixture was then subjected to flash column chromatography (SiO₂: 0-20% EtOAc/hexanes) to furnish **3.4c** (46 mg, 0.26 mmol, 85% yield, 86% ee) as a clear oil.

In accordance with procedure B using aldehyde **3.3c**, upon stirring at 95 °C for 48 h, the reaction mixture was concentrated *in vacuo* to afford the crude product (dr = 5:1 *anti:syn*, as determined by ¹H NMR spectroscopy). The reaction mixture was then subjected to flash column chromatography (SiO₂: 0-20% EtOAc/hexanes) to furnish **3.4c** (43 mg, 0.24 mmol, 80% yield, 88% ee) as a clear oil.

¹H NMR (400 MHz, CDCl₃): δ 7.31-7.26 (m, 2H), 7.05-7.00 (m, 2H), 5.82-5.73 (m, 1H), 5.22-5.17 (m, 2H), 4.33 (dd, *J* = 7.6 Hz, 2.4 Hz, 1H), 2.47-2.38 (m, 1H), 2.24 (d, *J* = 2.4 Hz, 1H), 0.85 ppm (d, *J* = 6.8 Hz, 3H).

¹³C NMR (100 MHz, CDCl₃): δ 162.3 (d, *J*=244.0 Hz), 140.4, 138.1 (d, *J*=3.0 Hz), 128.4 (d, 8.2 Hz), 117.1, 115.0 (d, 21.6 Hz), 77.1, 46.5, 16.5 ppm.

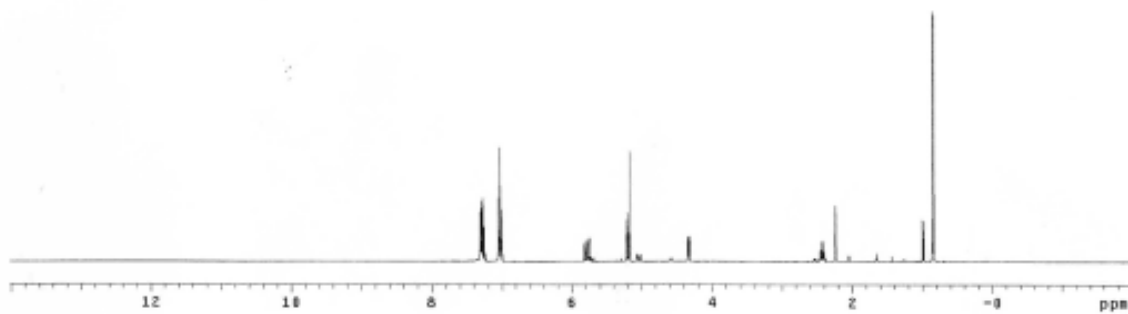
LRMS (CI⁺): *m/z* 181 [M+H]⁺.

[α]_D²⁵ = +56.6 (c =1.0, CHCl₃).

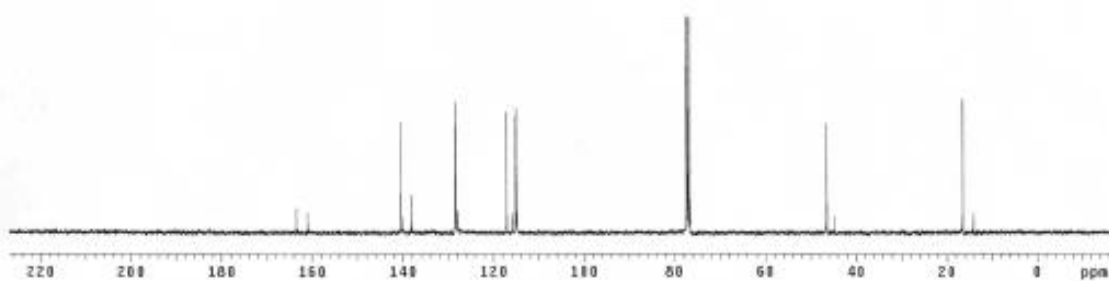
FTIR (neat): 3411 3412, 2975, 1634, 1603, 1509, 1417, 1220, 1157, 1012, 829, 676 cm⁻¹.

GC (Cyclosil-B: Initial temperature: 50 °C (5 min hold); 50-100 °C, rate: 0.4 °C/min (25 min hold); 100-150 °C, rate: 0.4 °C/min): *t*_{major}=153.2 min, *t*_{minor}=159.1 min.

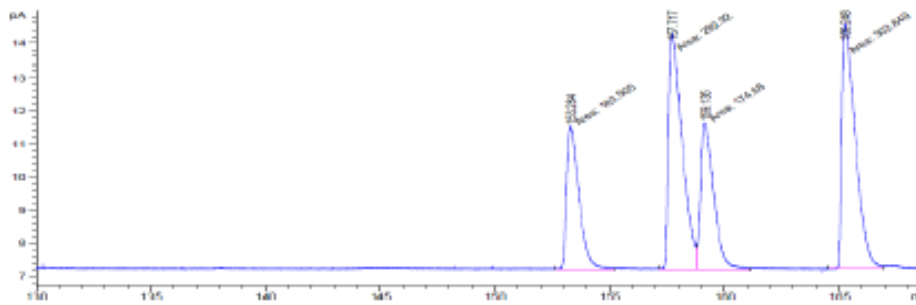
^1H NMR of **3.4c**



^{13}C NMR of **3.4c**

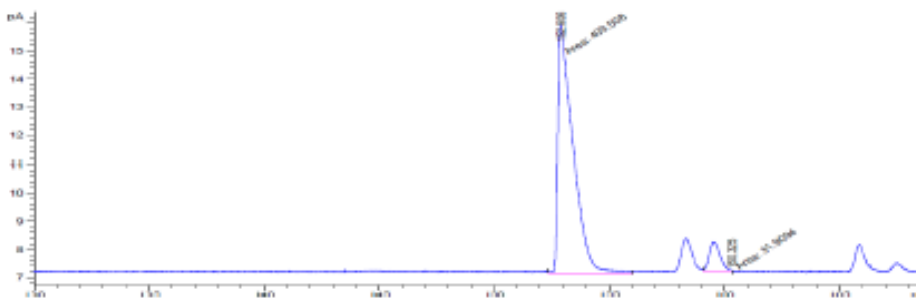


Racemic HPLC 3.4c



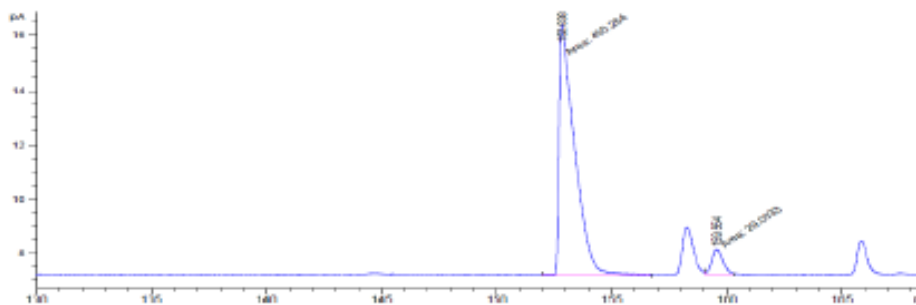
Peak #	RetTime [min]	Type	Width [min]	Area [pA*s]	Height [pA]	Area %
1	153.284	MM	0.6296	163.50467	4.32844	17.50671
2	157.717	MM	0.6507	292.92029	7.06814	31.36345
3	159.135	MM	0.6552	174.67996	4.44339	18.70326
4	165.248	MM	0.6844	302.84937	7.37467	32.42658

HPLC of 3.4c, Alcohol Oxidation Level



Peak #	RetTime [min]	Type	Width [min]	Area [pA*s]	Height [pA]	Area %
1	152.906	MM	0.7791	405.50766	8.75974	92.77114
2	160.325	MM	0.0000	31.90941	5.93895e-3	7.22886

HPLC of 3.4c, Aldehyde Oxidation Level



Peak #	RetTime [min]	Type	Width [min]	Area [pA*s]	Height [pA]	Area %
1	152.838	MM	0.8133	450.26407	9.22715	93.94842
2	158.554	MM	0.5249	29.00325	9.20927e-1	6.05158

(1*R*,2*R*)-1-(4-bromophenyl)-2-methylbut-3-en-1-ol (**3.4d**)

In accordance with procedure A using alcohol **3.2d**, upon stirring at 95 °C for 48 h, the reaction mixture was concentrated *in vacuo* to afford the crude product (dr = 5:1 *anti:syn*, as determined by ¹H NMR spectroscopy). The reaction mixture was then subjected to flash column chromatography (SiO₂: 0-20% EtOAc/hexanes) to furnish **3.4d** (70 mg, 0.29 mmol, 97% yield, 86% ee) as a clear oil.

In accordance with procedure B using aldehyde **3.3d**, upon stirring at 95 °C for 48 h, the reaction mixture was concentrated *in vacuo* to afford the crude product (dr = 5:1 *anti:syn*, as determined by ¹H NMR spectroscopy). The reaction mixture was then subjected to flash column chromatography (SiO₂: 0-20% EtOAc/hexanes) to furnish **3.4d** (59 mg, 0.24 mmol, 78% yield, 86% ee) as a clear oil. *The spectroscopic properties of this compound were consistent with the data available in the literature.*⁹⁹

¹H NMR (400 MHz, CDCl₃): δ 7.46 (d, *J* = 8.0 Hz, 2H), 7.18 (d, *J* = 8.0 Hz, 2H), 5.81-5.71 (m, 1H), 5.22-5.16 (m, 2H), 4.32 (d, *J* = 7.6 Hz, 1H), 2.45-2.37 (m, 1H), 2.20 (s, 1H), 0.87 ppm (d, *J* = 6.8 Hz, 3H).

¹³C NMR (100 MHz, CDCl₃): δ 141.4, 140.1, 131.3, 128.6, 121.4, 117.3, 77.1, 46.4, 16.4 ppm.

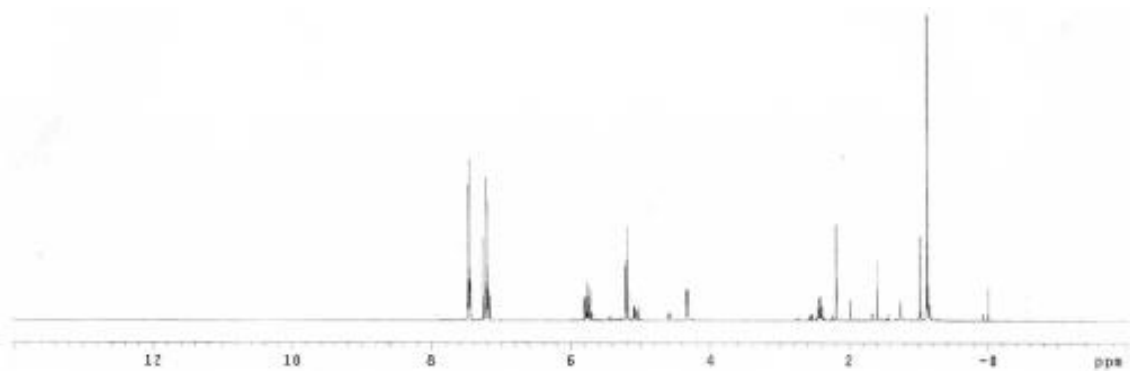
LRMS (CI⁺): *m/z* 223 [M-OH]⁺.

[α]_D²⁵ = +53 (c = 1.0, CHCl₃).

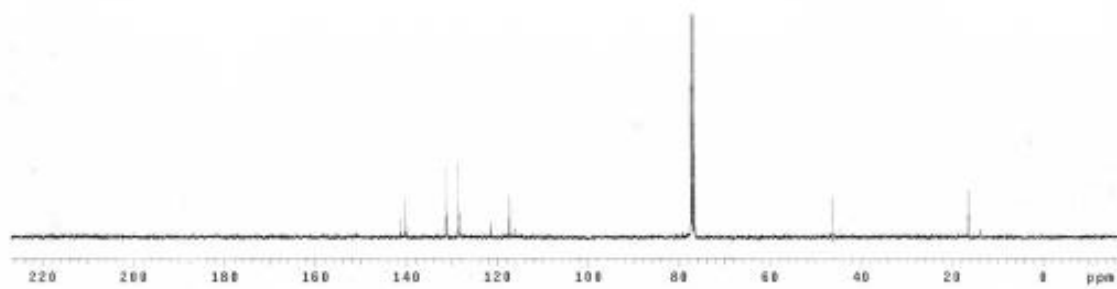
FTIR (neat): 3404, 2972, 2928, 1486, 1070, 1009, 916, 817, 755, 666 cm⁻¹.

HPLC (Chiralcel AS-H/AS-H column, hexanes:*i*-PrOH = 98.5:1.5, 0.5 mL/min, 230 nm): *t*_{major}=36.1 min, *t*_{minor}=42.1 min.

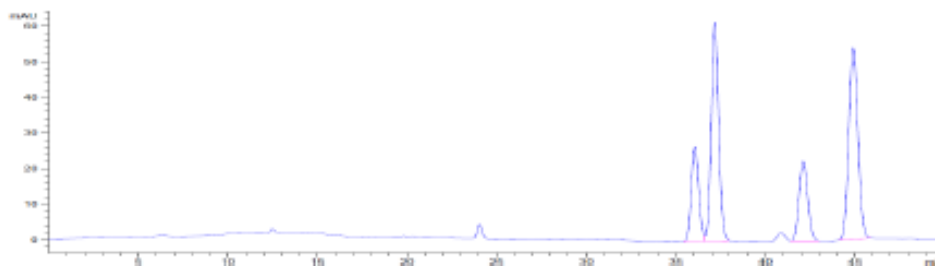
^1H NMR of **3.4d**



^{13}C NMR of **3.4d**



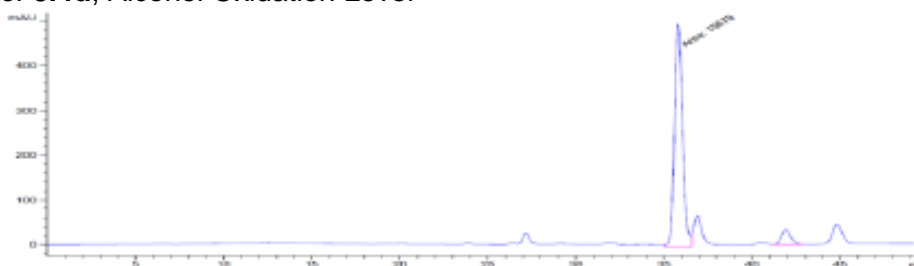
Racemic HPLC 3.4d



Signal 1: DAD1 D, Sig=230,16 Ref=360,100

Peak #	RetTime [min]	Type	Width [min]	Area [mAU*s]	Height [mAU]	Area %
1	36.059	BV	0.4445	755.69861	26.51514	14.4623
2	37.171	VB	0.4590	1816.62524	61.43822	34.7659
3	42.107	VB	0.5178	753.44275	22.43484	14.4191
4	44.890	BB	0.5520	1099.53650	53.78403	36.3527

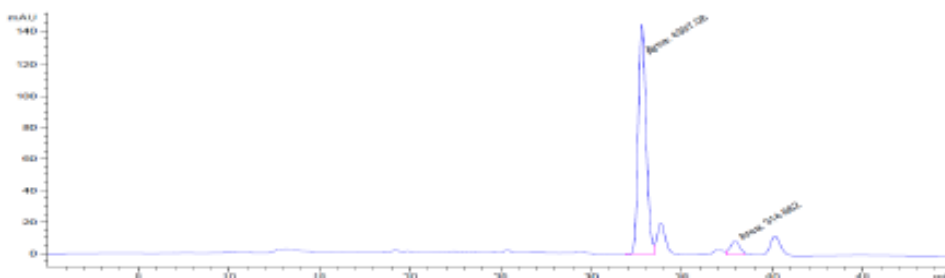
HPLC of 3.4d, Alcohol Oxidation Level



Signal 1: DAD1 D, Sig=230,16 Ref=360,100

Peak #	RetTime [min]	Type	Width [min]	Area [mAU*s]	Height [mAU]	Area %
1	35.784	MM	0.5248	1.56790e4	497.92374	92.9868
2	41.902	VB	0.5521	1182.53137	33.47377	7.0132

HPLC of 3.4d, Aldehyde Oxidation Level



Signal 1: DAD1 D, sig=230,16 Ref=360,100

Peak #	RetTime [min]	Type	Width [min]	Area [mAU*s]	Height [mAU]	Area %
1	32.791	MM	0.5067	4397.08496	144.62340	93.3218
2	37.920	MM	0.6218	314.66193	8.43464	6.6782

(1*R*,2*R*)-2-methyl-1-phenylbut-3-en-1-ol (**3.4e**)

In accordance with procedure A using alcohol **3.2e**, upon stirring at 95 °C for 48 h, the reaction mixture was concentrated *in vacuo* to afford the crude product (dr = 8:1 *anti:syn*, as determined by ¹H NMR spectroscopy). The reaction mixture was then subjected to flash column chromatography (SiO₂: 0-10% EtOAc/hexanes) to furnish **3.4e** (42 mg, 0.26 mmol, 86% yield, 90% ee) as a clear oil.

In accordance with procedure B using aldehyde **3.3e**, upon stirring at 95 °C for 48 h, the reaction mixture was concentrated *in vacuo* to afford the crude product (dr = 8:1 *anti:syn*, as determined by ¹H NMR spectroscopy). The reaction mixture was then subjected to flash column chromatography (SiO₂: 0-20% EtOAc/hexanes) to furnish **3.4e** (36 mg, 0.22 mmol, 74% yield, 88% ee) as a clear oil. *The spectroscopic properties of this compound were consistent with the data available in the literature.*^{83b}

¹H NMR (400 MHz, CDCl₃): δ 7.26-7.38 (m, 5H), 5.86-5.76 (m, 1H), 5.24-5.17 (m, 2H), 4.35 (d, J = 8.0 Hz, 1H), 2.52-2.45 (m, 1H), 2.07 (br s, 1H), 0.87 ppm (d, J = 6.8 Hz, 3H)

¹³C NMR (100 MHz, CDCl₃): δ 142.6, 140.9, 128.5, 127.9, 127.1, 117.1, 78.1, 46.6, 16.8 ppm.

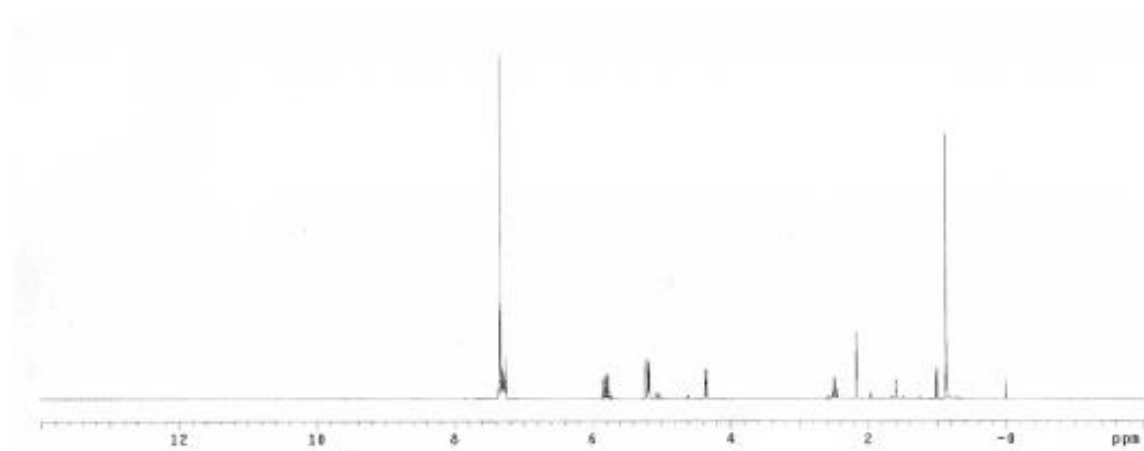
LRMS (CI⁺): *m/z* 145 [M-OH]⁺.

[α]_D²⁵ = +51 (c = 1.0, CH₂Cl₂).

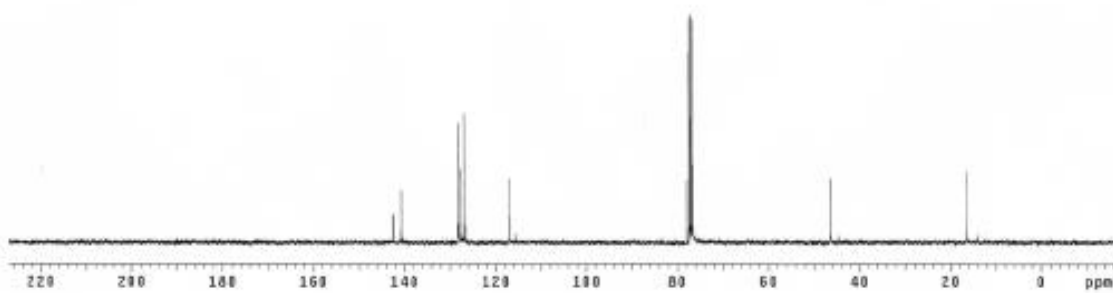
FTIR (neat): 3411, 3064, 3029, 2964, 2927, 2356, 1940, 1638, 1493, 1453, 1416, 1372, 1261, 1195, 1075, 1018, 912, 800, 759, 700, 680 cm⁻¹.

GC (Cyclosil-B: Initial temperature: 50 °C (5 min hold); 50-100 °C, rate: 0.5 °C/min (20 min hold); 100-135 °C, rate: 0.5 °C/min): *t*_{major}=128.5 min, *t*_{minor}=129.5 min.

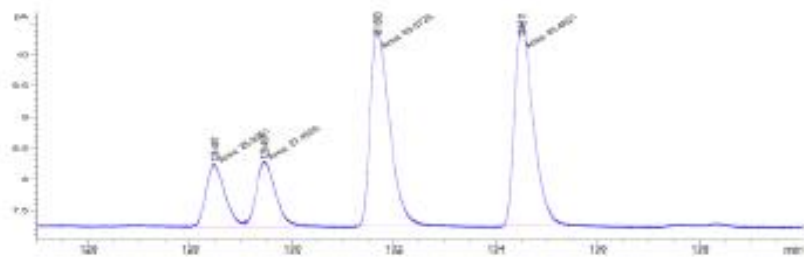
^1H NMR of **3.4e**



^{13}C NMR of **3.4e**



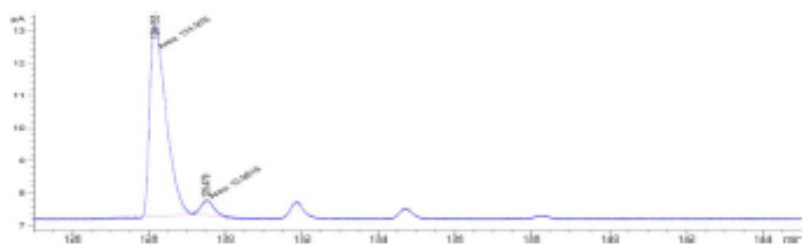
Racemic HPLC 3.4e



Signal 1: FID1 A, Front signal

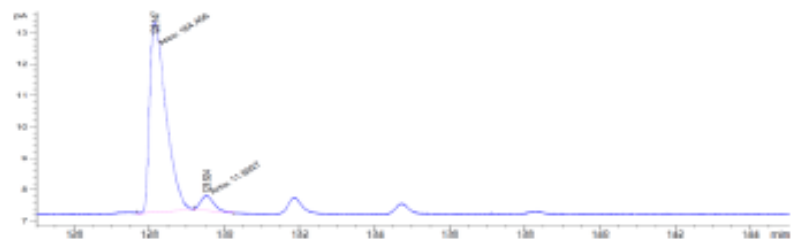
Peak #	RetTime [min]	Type	Width [min]	Area [pA*s]	Height [pA]	Area %
1	129.487	MM	0.4274	25.93510	1.01129	11.79269
2	129.457	MM	0.4346	27.45553	1.05302	12.40403
3	131.683	MM	0.4412	83.07246	3.13815	37.77306
4	134.511	MM	0.4255	83.46207	3.26915	37.95022

HPLC of 3.4e, Alcohol Oxidation Level



Peak #	RetTime [min]	Type	Width [min]	Area [pA*s]	Height [pA]	Area %
1	128.150	MM	0.4959	175.98094	5.51434	94.67967
2	129.534	MM	0.3749	9.88889	4.39651e-1	5.32033

HPLC of 3.4e, Aldehyde Oxidation Level



Signal 1: FID1 A, Front signal

Peak #	RetTime [min]	Type	Width [min]	Area [pA*s]	Height [pA]	Area %
1	128.147	MM	0.5053	184.45619	6.08412	93.94309
2	129.524	MM	0.4021	11.89270	4.92998e-1	6.05692

(1*R*,2*R*)-2-methyl-1-(naphthalen-2-yl)but-3-en-1-ol (**3.4f**)

In accordance with procedure A using alcohol **3.2f**, upon stirring at 95 °C for 48 h, the reaction mixture was concentrated *in vacuo* to afford the crude product (dr = 9:1 *anti:syn*, as determined by ¹H NMR spectroscopy). The reaction mixture was then subjected to flash column chromatography (SiO₂: 0-20% EtOAc/hexanes) to furnish **3.4f** (60 mg, 0.29 mmol, 95% yield, 88% ee) as a clear oil.

In accordance with procedure B using aldehyde **3.3f**, upon stirring at 95 °C for 48 h, the reaction mixture was concentrated *in vacuo* to afford the crude product (dr = 4:1 *anti:syn*, as determined by ¹H NMR spectroscopy). The reaction mixture was then subjected to flash column chromatography (SiO₂: 0-20% EtOAc/hexanes) to furnish **3.4f** (50 mg, 0.24 mmol, 79% yield, 86% ee) as a clear oil. *The spectroscopic properties of this compound were consistent with the data available in the literature.*^{52e}

¹H NMR (400 MHz, CDCl₃): δ 7.85-7.83 (m, 3H), 7.78 (s, 1H), 7.51-7.46 (m, 3H), 5.91-5.82 (m, 1H), 5.27-5.20 (m, 2H), 4.53 (dd, *J* = 8.0 Hz, 2.0 Hz, 1H), 2.65-2.56 (m, 1H), 2.32 (d, *J* = 2.0 Hz, 1H), 0.92 ppm (d, *J* = 6.8 Hz, 3H).

¹³C NMR (100 MHz, CDCl₃): δ 140.6, 139.9, 133.2, 133.1, 128.1, 128.0, 127.7, 126.1, 126.0, 125.8, 124.7, 117.0, 78.0, 46.2, 16.6 ppm.

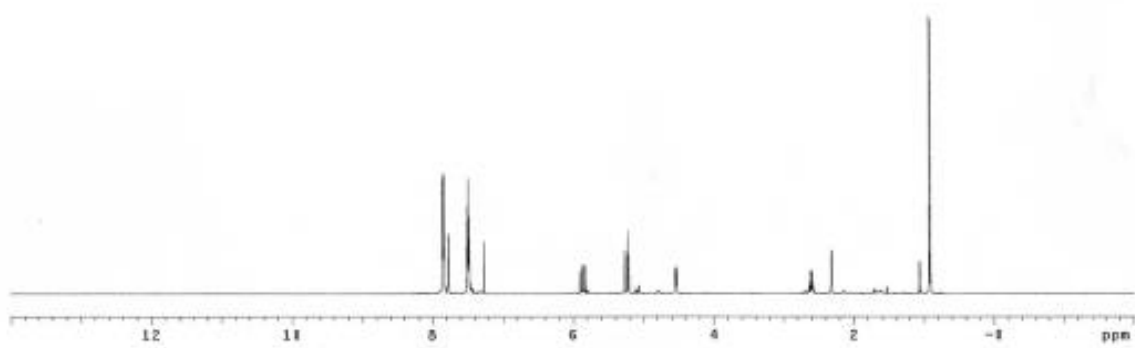
LRMS (CI+): *m/z* 213 [M+H]⁺.

[α]_D²⁵ = +57 (c = 1.0, CHCl₃).

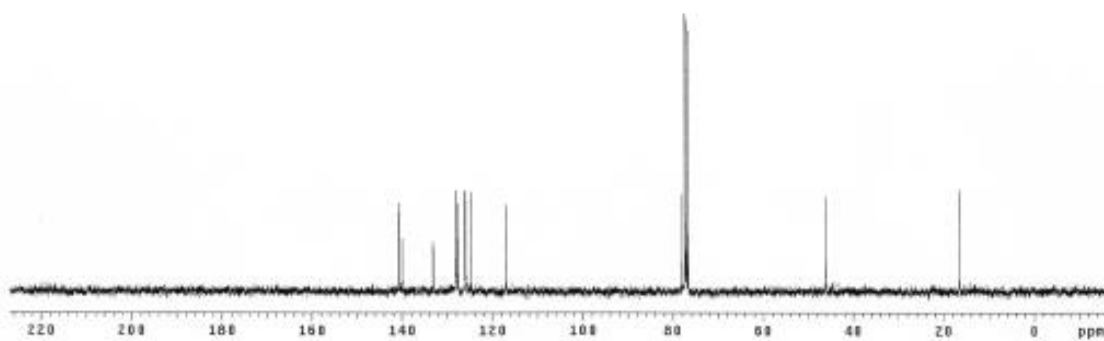
FTIR (neat): 3411, 3056, 2972, 2869, 2359, 1932, 1636, 1507, 1371, 1270, 1159, 1123, 1018, 908, 817, 731 cm⁻¹.

HPLC (Chiralcel AS-H/AS-H column, hexanes:*i*-PrOH = 95:5, 0.5 mL/min, 230 nm): *t*_{major}=74.2 min, *t*_{minor}=92.3 min.

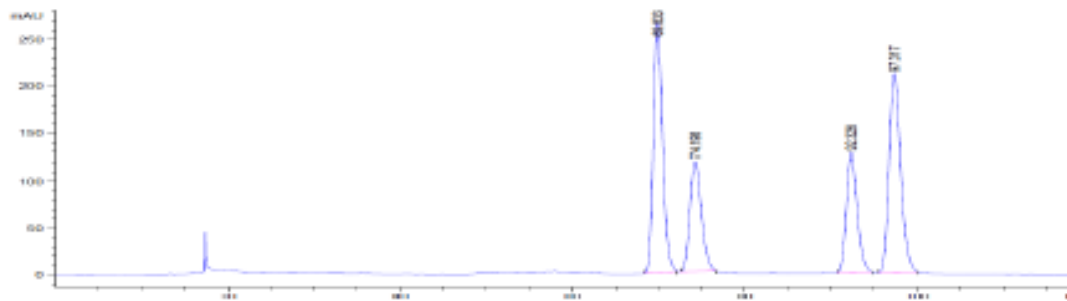
^1H NMR of **3.4f**



^{13}C NMR of **3.4f**

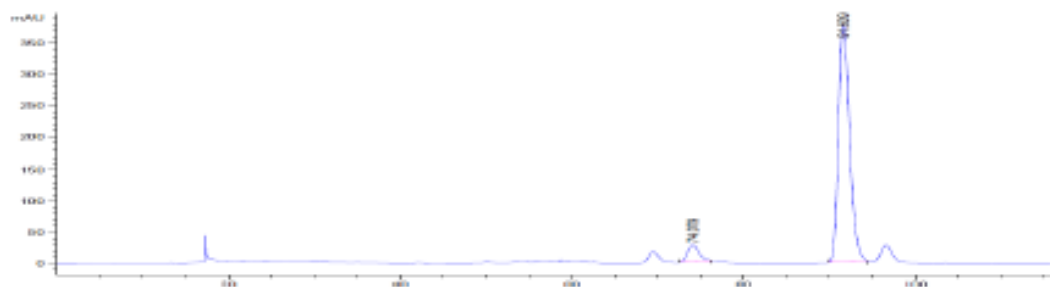


Racemic HPLC 3.4f



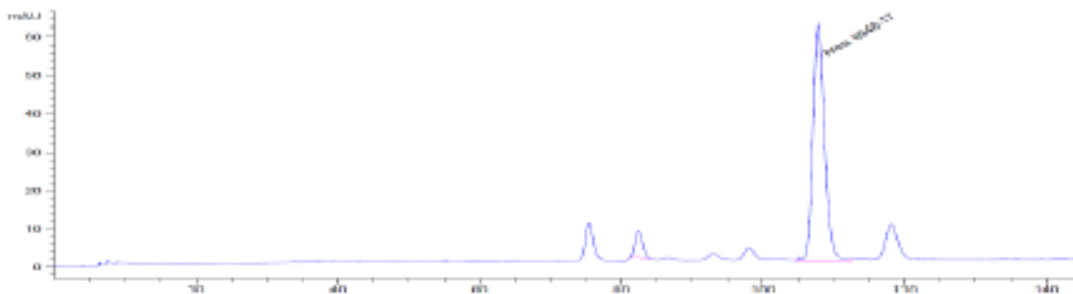
Peak #	RetTime [min]	Type	Width [min]	Area [mAU*s]	Height [mAU]	Area %
1	69.833	BB	1.1523	1.98477e4	265.46753	32.1878
2	74.198	BB	1.4103	1.09874e4	118.00423	17.8187
3	92.326	BB	1.3431	1.10806e4	126.10297	17.9699
4	97.317	BB	1.4340	1.97466e4	210.59084	32.0237

HPLC of 3.4f, Alcohol Oxidation Level



Peak #	RetTime [min]	Type	Width [min]	Area [mAU*s]	Height [mAU]	Area %
1	74.079	BB	1.2793	2362.48633	26.83085	6.5819
2	91.609	BB	1.3594	3.35310e4	377.10840	93.4181

HPLC of 3.4f, Aldehyde Oxidation Level



Peak #	RetTime [min]	Type	Width [min]	Area [mAU*s]	Height [mAU]	Area %
1	82.392	BB	0.9000	515.88889	6.83912	6.9135
2	107.752	BB	1.8871	6946.17285	61.34930	93.0865

(1*R*,2*R*)-1-(4-methoxyphenyl)-2-methylbut-3-en-1-ol (**3.4g**)

In accordance with procedure A using alcohol **3.2g**, upon stirring at 95 °C for 48 h, the reaction mixture was concentrated *in vacuo* to afford the crude product (dr = 6:1 *anti:syn*, as determined by ¹H NMR spectroscopy). The reaction mixture was then subjected to flash column chromatography (SiO₂: 0-20% EtOAc/hexanes) to furnish **3.4g** (42 mg, 0.22 mmol, 72% yield, 86% ee) as a clear oil.

In accordance with procedure B using aldehyde **3.3g**, upon stirring at 95 °C for 48 h, the reaction mixture was concentrated *in vacuo* to afford the crude product (dr = 6:1 *anti:syn*, as determined by ¹H NMR spectroscopy). The reaction mixture was then subjected to flash column chromatography (SiO₂: 0-20% EtOAc/hexanes) to furnish **3.4g** (38 mg, 0.20 mmol, 66% yield, 88% ee) as a clear oil. *The spectroscopic properties of this compound were consistent with the data available in the literature.*¹⁰⁰

¹H NMR (400 MHz, CDCl₃): δ 7.25 (d, J = 7.8 Hz, 2H), 6.88 (d, J = 7.8 Hz, 2H), 5.86-5.77 (m, 1H), 5.29-5.16 (m, 2H), 4.30 (d, J = 8.0 Hz, 1H), 3.80 (s, 3H), 2.50-2.41 (m, 1H), 2.15 (s, 1H), 0.85 ppm (d, J = 6.8 Hz, 3H).

¹³C NMR (100 MHz, CDCl₃): δ 159.1, 141.0, 134.6, 128.0, 116.7, 113.6, 77.5, 55.3, 46.4, 16.6 ppm.

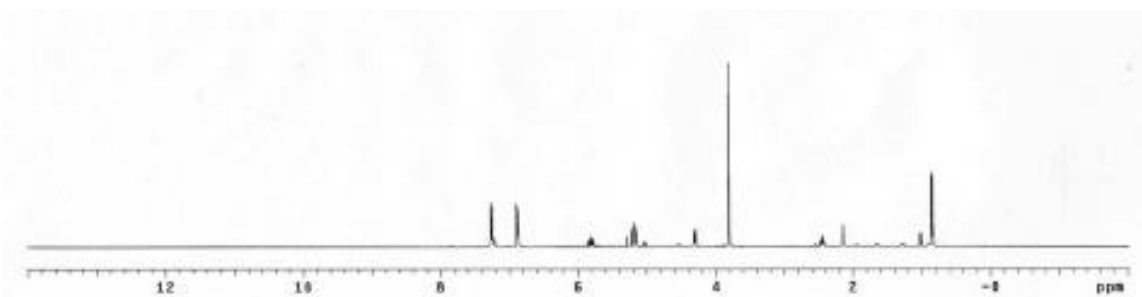
LRMS (CI+): *m/z* 193 [M+H]⁺.

[α]_D²⁵ = +51.8 (c = 1.0, CHCl₃).

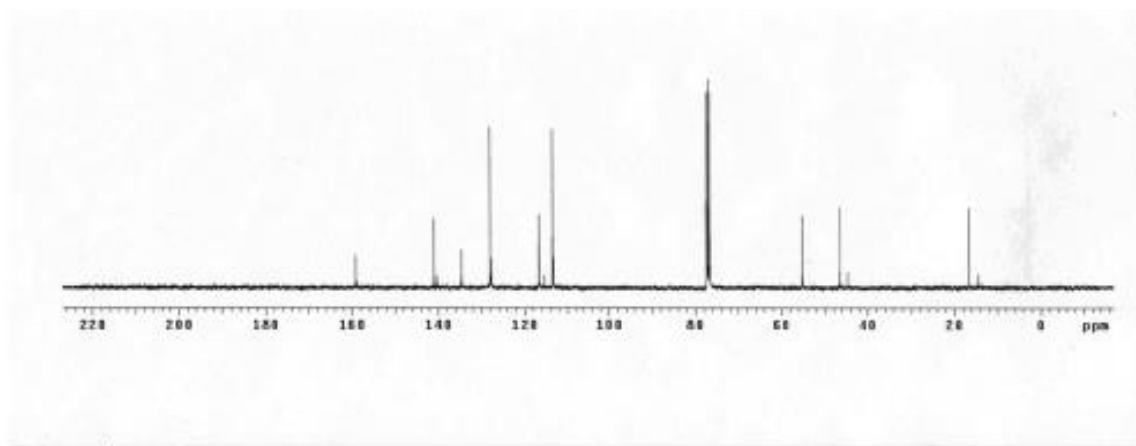
FTIR (neat): 2961, 1611, 1510, 1458, 1302, 1260, 1173, 1032, 911, 731 cm⁻¹.

GC (Cyclosil-B: Initial temperature: 50 °C (5 min hold); 50-115 °C rate: 0.5 C/min (20 min hold); 115-165 °C, rate: 0.475 °C/min) *t*_{major}=184.9 min, *t*_{minor}=187.3 min.

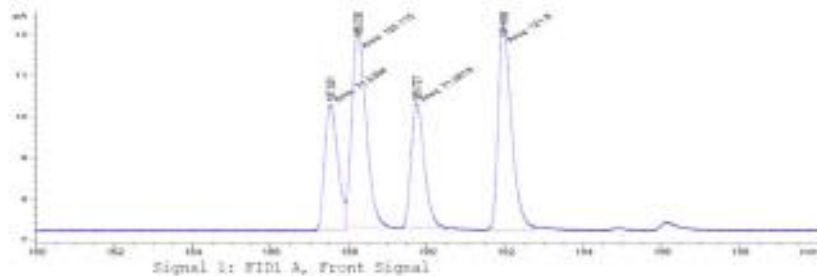
^1H NMR of **3.4g**



^{13}C NMR of **3.4g**

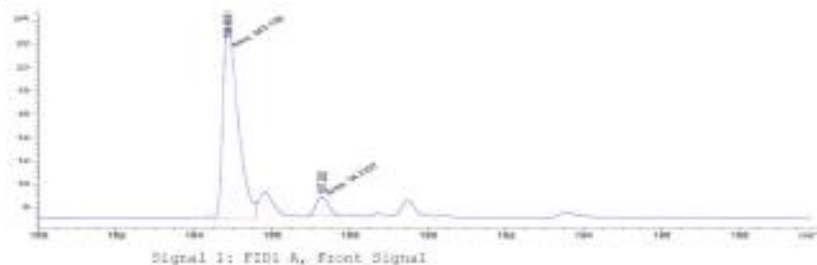


Racemic HPLC **3.4g**



Peak #	RetTime [min]	Type	Width [min]	Area [pA*s]	Height [pA]	Area %
1	147.531	MM	0.3824	71.53925	3.11795	18.57991
2	148.230	MM	0.4194	129.11469	4.78511	31.19569
3	149.127	MM	0.3924	71.58181	3.03949	18.56093
4	151.958	MM	0.4030	121.88029	5.03745	31.63347

HPLC of **3.4g**, Alcohol Oxidation Level



Peak #	RetTime [min]	Type	Width [min]	Area [pA*s]	Height [pA]	Area %
1	144.859	MM	0.4058	443.10431	16.56563	92.82821
2	147.282	MM	0.3435	14.29370	1.66111	7.17173

HPLC of **3.4g**, Aldehyde Oxidation Level

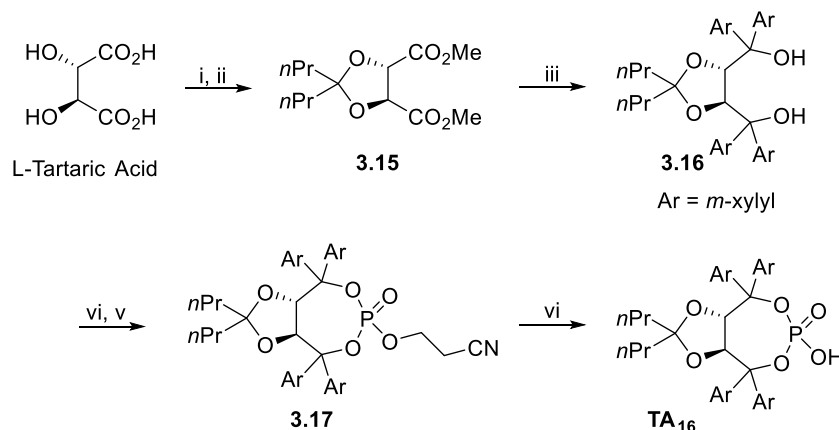


Signal 1: FID1 A, Front Signal

Peak #	RetTime [min]	Type	Width [min]	Area [pA*s]	Height [pA]	Area %
1	144.922	MM	0.4288	379.26254	14.40639	93.42543
2	147.329	MM	0.3610	26.48959	1.23206	6.57457

3.5.6 Preparation of TADDOL Phosphoric Acid TA₁₂

Figure 3.14 Synthetic Route to TADDOL Phosphoric Acid TA₁₂



(i) SOCl₂, MeOH, rt, 18 h (ii) 4-heptanone (100 mol%), HC(OMe)₃ (130 mol%), *p*TsOH (10 mol%), reflux, 8 h (iii) 3,5-dimethylphenylmagnesium bromide (800 mol%), THF, reflux, 18 h (vi) PCl₃ (105 mol%), Et₃N (340 mol%), THF, 0 °C 1 h, then 3-hydroxypropionitrile (110 mol%), rt, 18 h (v) H₂O₂ (620 mol%), DCM, rt, 0.5 h (iv) DBU (105 mol%), THF, rt, 0.5 h

((4*R*,5*R*)-2,2-dipropyl-1,3-dioxolane-4,5-diyl)bis[di(3,5-dimethylphenyl)-3-ylmethanol] (**3.16**)

(*R,R*)-2,2-Dipropyl-[1,3]dioxolane-4,5-dicarboxylic acid dimethylester **3.15** (prepared by method described by Bittman and Thiel¹⁰¹) (1.37 g, 5 mmol) in THF (10 mL) was added dropwise to a solution of 3,5-dimethylphenylmagnesium bromide (40 mmol, prepared from 5.5 mL of 5-bromo-*m*-xylene and 1.10 g of Mg) in THF (40 mL). The reaction mixture was stirred for 18 h and then treated with saturated aqueous NH₄Cl solution. The organic layer was extracted with Et₂O (3 x 50 mL) and the combined organic extracts were washed with brine, dried (MgSO₄), filtered, and concentrated *in vacuo*. The residue was subjected to flash column chromatography (SiO₂; hexanes:Et₂O = 10:1) to furnish **3.16** (2.07 g, 1.3 mmol 65% yield) as a white foam.

TLC (SiO₂): R_f = 0.13 (hexanes:Et₂O = 10:1).

m.p.: 106-108 °C.

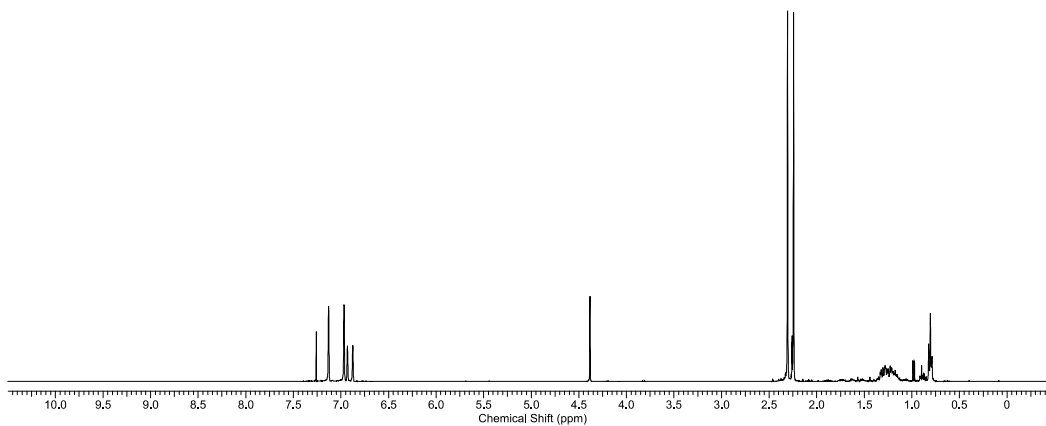
¹H NMR (400 MHz, CDCl₃): δ 7.13 (s, 4H), 6.97 (s, 4H), 6.93 (s, 2H), 6.87 (s, 2H), 4.38 (s, 2H), 4.05 (brs, 2H), 2.31 (s, 12H), 2.24 (s, 12H), 1.35-1.16 (m, 8 H), 0.81 ppm (t, *J* = 7.04 Hz, 6H).

¹³C NMR (100 MHz, CDCl₃): δ 146.2, 142.6, 137.3, 136.3, 129.1, 126.6, 126.3, 125.4, 111.2, 80.5, 78.0, 39.9, 21.6, 17.2, 14.4 ppm.

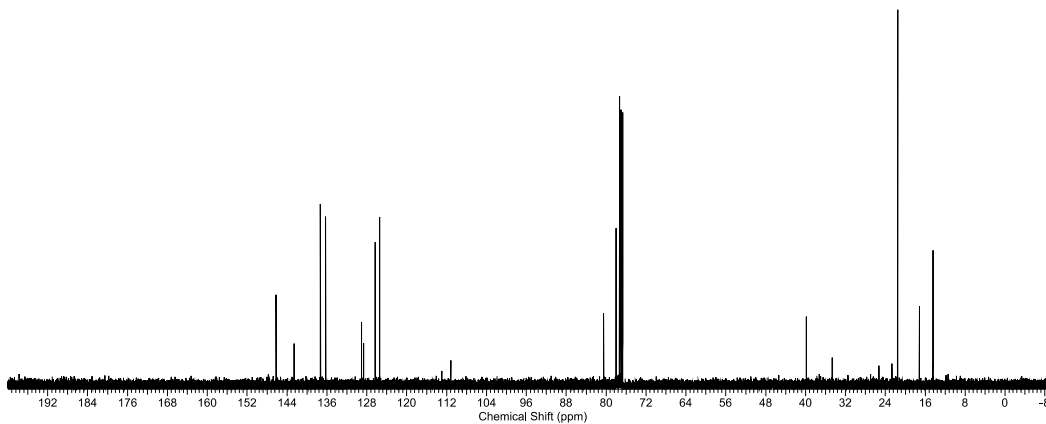
HRMS (ESI): Calcd. for C₄₃H₅₄NaO₄ [M+Na]⁺: 657.3914, Found: 657.3910.

FTIR (neat): 3293, 2958, 2916, 2359, 1601, 1454, 1314, 1167, 1060, 850, 736 cm⁻¹.

¹H NMR of **3.16**



¹³C NMR of **3.16**



3-([(3a*R*,8a*R*)-2,2-dipropyl-4,4,8,8-tetrakis(3,5-dimethylphenyl)-6-oxidotetrahydro-[1,3]dioxolo[4,5-*e*][1,3,2]dioxaphosphepin-6-yl]oxy)propanenitrile (**3.17**)

To a stirred solution of (*R,R*)-(*n*-Pr,*n*-Pr)-TADDOL-(xylyl) **3.16** (1.26 g, 2.0 mmol) and triethylamine (0.94 mL, 6.8 mmol, 340 mol%) in dry THF (10 mL) at 0 °C was added dropwise PCl₃ (184 μL, 2.1 mmol, 105 mol%). The resulting mixture was stirred at 0 °C for 1 h. The 3-hydroxypropionitrile (150 μL, 2.2 mmol, 110 mol%) in dry THF (10 mL) was then added dropwise via cannula. The reaction mixture was allowed to warm to room temperature and stirred for 18 h. The reaction mixture was diluted with Et₂O and the triethylammonium chloride salts were filtered through a celite pad. The solvent was removed *in vacuo*. To the crude phosphine in DCM (20 mL) was added 30% aqueous H₂O₂ (1.40 mL, 12.4 mmol, 6.2 equiv). The biphasic mixture was stirred vigorously for 30 min and then quenched by the addition of 50 mL of saturated aqueous NaHCO₃ solution. The mixture was extracted with DCM and the combined organic extracts were washed with saturated aqueous NaCl, dried (MgSO₄), filtered and concentrated. Purification by flash chromatography (hexane:Et₂O = 80:20 to 0:100) afforded 1.16 g (77% for two steps) of **3.17** as a white solid.

TLC (SiO₂): R_f = 0.35 (hexanes:Et₂O = 1:1)

m.p.: 120-122 °C.

¹H NMR (400 MHz, CDCl₃): δ 7.20n (s, 2H), 7.18 (s, 2H), 7.02 (s, 1H), 6.99 (s, 2H), 6.96 (s, 1H), 6.92 (s, 1H), 6.91 (s, 1H), 6.91 (s, 2H), 5.32 (d, *J* = 8.4 Hz, 1H), 5.11 (d, *J* = 8.4 Hz, 1H), 3.99-3.91 (m, 1H), 3.41-3.34 (m, 1H), 2.36 (s, 6H), 2.34 (s, 6H), 2.30 (s, 6H), 2.25 (s, 6H), 2.23-2.17 (m, 1H), 2.03-1.97 (m, 1H), 1.31-0.86 (m, 8H), 0.68 (t, *J* = Hz, 3H), 0.56 ppm (t, *J* = Hz, 3H).

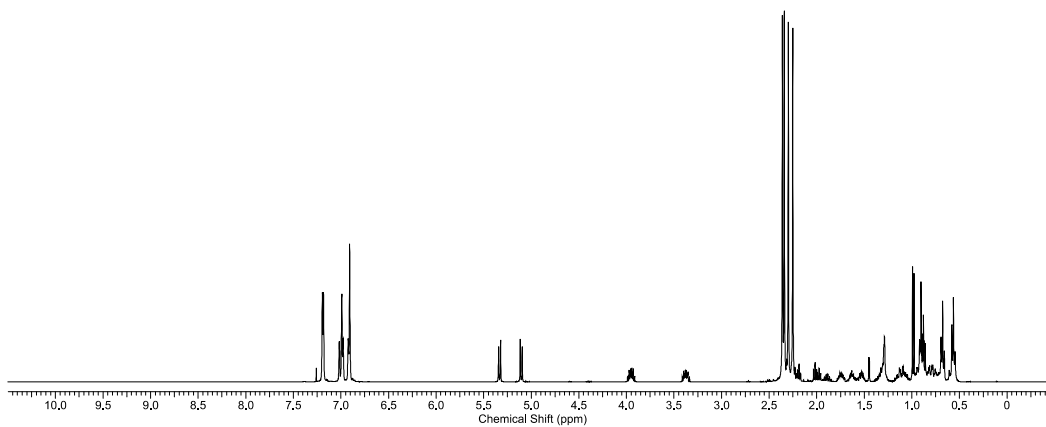
¹³C NMR (100 MHz, CDCl₃): δ 143.9, 143.4 (d, *J*_{P-C} = 3.0 Hz), 140.1 (d, *J*_{P-C} = 7.5 Hz), 139.5 (d, *J*_{P-C} = 6.0 Hz), 137.9, 137.4, 136.7, 136.4, 130.0, 129.9, 129.4, 129.3, 126.8, 126.2, 125.2, 124.7, 116.3, 116.1, 89.5 (d, *J*_{P-C} = 7.5 Hz), 88.5 (d, *J*_{P-C} = 8.3 Hz), 79.5, 61.7 (d, *J*_{P-C} = 4.5 Hz), 39.6, 39.2, 21.6, 21.5, 21.5, 21.4, 18.9 (d, *J*_{P-C} = 8.9 Hz), 16.6, 16.7, 14.2, 14.1 ppm.

³¹P NMR (162 MHz, CDCl₃): δ -13.1 ppm.

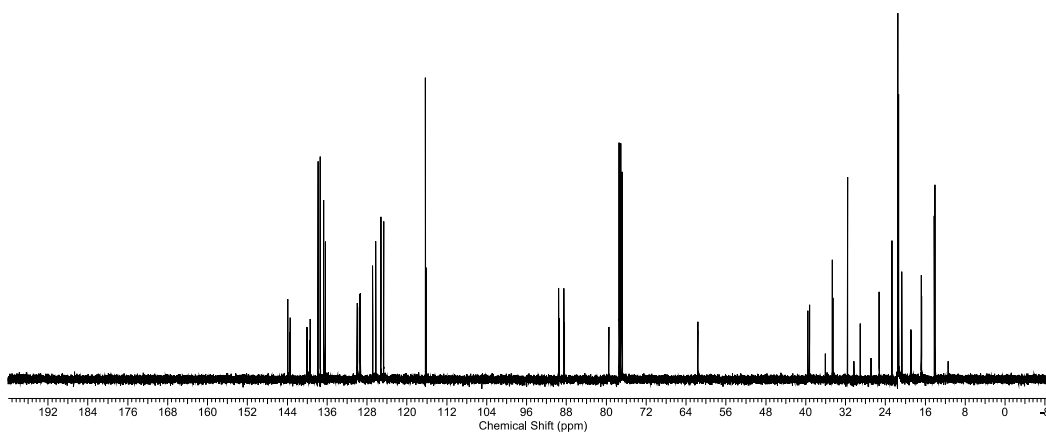
HRMS (ESI): Calcd. for C₄₆H₅₆NNaO₆P [M+Na]⁺: 772.3738, Found: 772.3738.

FTIR (neat): 2953, 2240, 1603, 1456, 1285, 1032, 994, 854, 741 cm⁻¹.

¹H NMR of **3.17**



¹³C NMR of **3.17**



(3aR,8aR)-2,2-dipropyl-4,4,8,8-tetrakis(3,5-dimethylphenyl)tetrahydro[1,3]-dioxolo[4,5-e][1,3,2]dioxaphosphepin-6-ol 6-oxide (**TA₁₆**)

To a stirred solution of ester **3.17** (2.92 g, 3.9 mmol) in dry DCM (40 mL) was added, dropwise at room temperature, DBU (0.61 mL, 4.1 mmol, 1.05 equiv). The solution was stirred 30 min at room temperature and when the reaction was complete by TLC, AcOH (0.3 mL) was added, followed by H₂O (40 mL). The organic layer was then washed two times by a 0.3M HCl solution, saturated aqueous NaCl, and dried (MgSO₄), filtered and concentrated. The residue was purified by column chromatography (SiO₂; 0-10% *i*PrOH:DCM) and concentrated *in vacuo*. The residue was diluted with DCM then washed with a solution of hydrochloric acid (10 mL, 0.3M aq. sol.) and concentrated *in vacuo* to provide **TA₁₆** (2.55 g, 3.7 mmol, 94% yield) as a white solid.

TLC (SiO₂): R_f = 0.43 (DCM:IPA = 100:5).

m.p.: 160-162 °C.

¹H NMR (400 MHz, CDCl₃): δ 9.41 (brs, 1H), 7.20 (s, 4H), 6.94 (s, 2H), 6.88 (s, 4H), 6.80 (s, 2H), 5.18 (s, 2H), 2.28 (s, 12H), 2.16 (s, 12H), 1.01-0.82 (m, 4H), 0.66-0.56 ppm (m, 10 H).

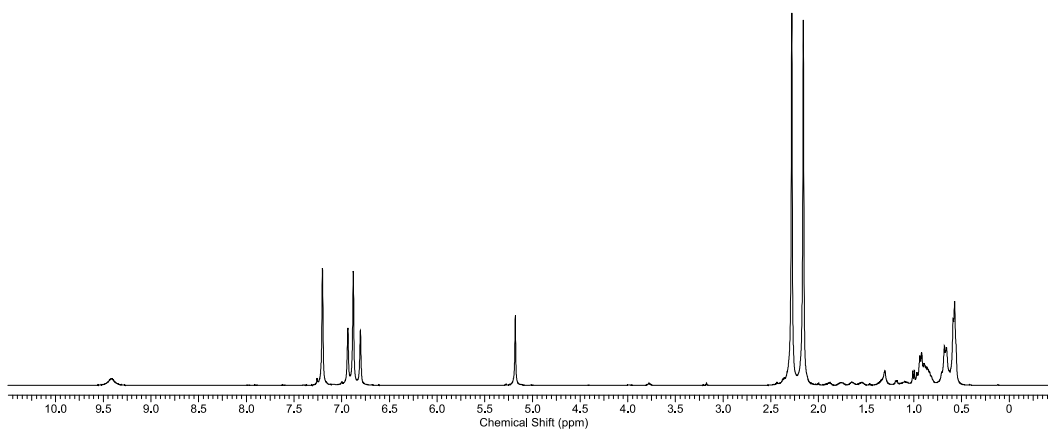
¹³C NMR (100 MHz, CDCl₃): δ 143.0, 140.1 (d, JP-C = 12.0 Hz), 137.3, 136.2, 129.8, 129.0, 126.3, 125.0, 116.6, 88.4, 79.2, 39.7, 21.5, 21.3, 16.6, 14.2 ppm.

³¹P NMR (162 MHz, CDCl₃): δ -7.67.

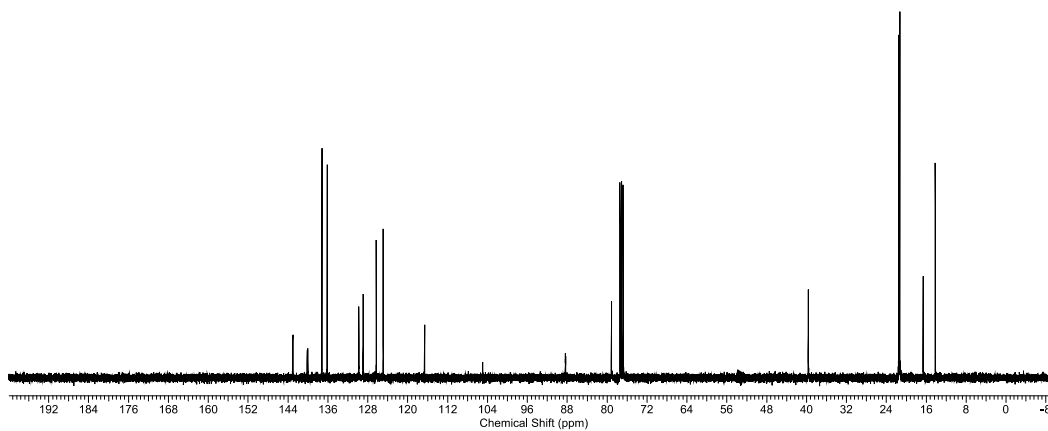
HRMS (ESI): Calcd. for C₄₃H₅₂O₆P [M]⁺: 695.35065, Found: 695.35070.

FTIR (neat): 2958, 2918, 1603, 1455, 1264, 1235, 1013, 737 cm⁻¹.

^1H NMR of **TA₁₆**



^{13}C NMR of **TA₁₆**



3.5.7 General Procedures for *syn*-Crotylation using Butadiene

General procedure: To a re-sealable pressure tube (13 x 100 mm) equipped with magnetic stir bar, RuH₂(CO)(PPh₃)₃ (19 mg, 0.021 mmol, 7 mol%), (*S*)-(-)-5,5'-Bis(diphenylphosphino)-4,4'-bi-1,3-benzodioxole (13 mg, 0.021 mmol, 7 mol%), L-TADDOL phosphoric acid (29 mg, 0.042 mmol, 14 mol%) were added. The tube was sealed with a rubber septum and purged with argon. Alcohol (0.3 mmol, 100 mol%) and acetone (0.30 mL, 1.0 M with respect to alcohol) was added, and the reaction tube was cooled to -78 °C. Butadiene (0.10 mL, 1.20 mmol, 400 mol%) was quickly added and the rubber septum replaced with a screw cap. The mixture was heated at 95 °C (oil bath temperature) for 72 h, at which point the reaction mixture was allowed to cool to ambient temperature. The reaction mixture was then concentrated *in vacuo* and the ratio of diastereomers was determined by NMR of the crude reaction mixture. The crude reaction mixture was subjected to flash column chromatography (SiO₂; 0-10% EtOAc/hexanes) to furnish the corresponding product of crotylation.

3.5.8 Characterization of 3.8a-j

(3*R*,4*R*)-3-methyl-1-decen-4-ol (**3.8a**)

In accordance with the general procedure using alcohol **3.7a**, upon stirring at 95 °C for 72 h, the reaction mixture was concentrated *in vacuo* to afford the crude product (dr = 4.4:1 *syn:anti*, as determined by ¹H NMR spectroscopy). The reaction mixture was then subjected to flash column chromatography (SiO₂; 0-10% EtOAc/hexanes) to furnish **3.8a** (42 mg, 0.25 mmol, 82% yield, 95% ee) as a clear, colorless oil. *The spectroscopic properties of this compound were consistent with the data available in the literature.*¹⁰²

TLC (SiO₂): R_f = 0.4 (hexanes:EtOAc = 5:1).

¹H NMR (400 MHz, CDCl₃): δ 5.77-5.72 (m, 1H), 5.06-4.99 (m, 2H), 3.44-3.39 (m, 1H), 2.25-2.15 (m, 1H), 1.57-1.16 (m, 10 H), 0.96 (d, *J* = 6.9 Hz, 3H), 0.81 ppm (t, *J* = 6.7 Hz, 3H).

¹³C NMR (100 MHz, CDCl₃): δ 114.1, 115.2, 74.7, 43.4, 34.0, 31.8, 29.4, 26.1, 22.6, 14.1, 14.0 ppm.

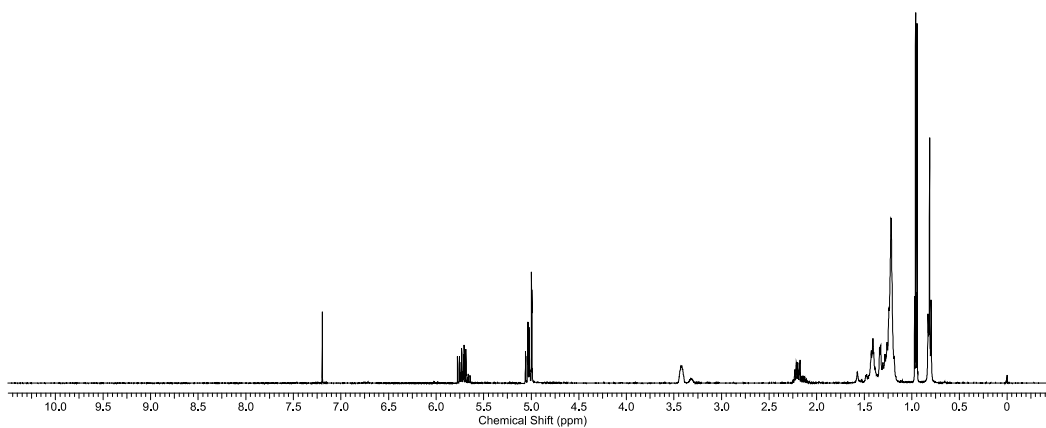
LRMS (CI+) *m/z* 171 [M+H]⁺.

FTIR (neat): 3392, 2957, 2927, 2856, 1458, 1119, 910, 733 cm⁻¹.

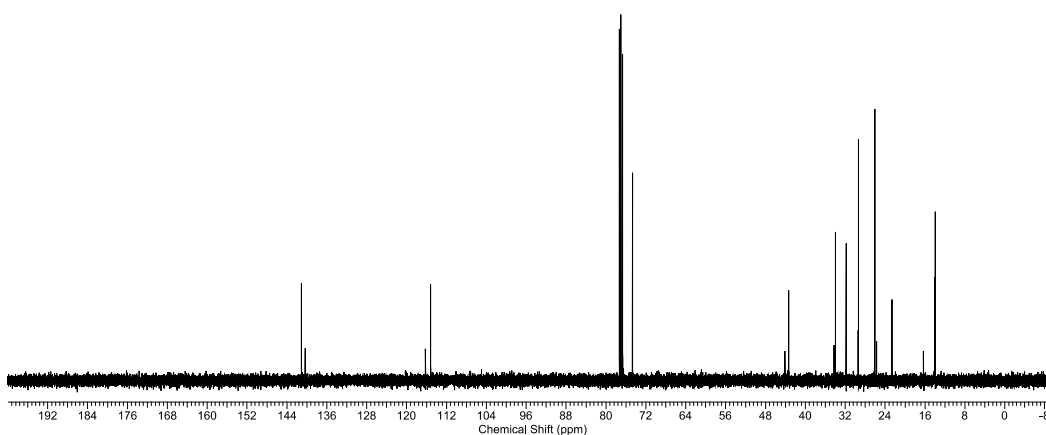
GC (Cyclosil-B: Initial temperature: 50 °C (5 min hold); 130 °C, rate: 3 °C/min): *t*_{minor}=28.7 min, *t*_{major}=28.9 min.

[α]_D²⁵ = 37.5 ° (c = 1.0, CHCl₃).

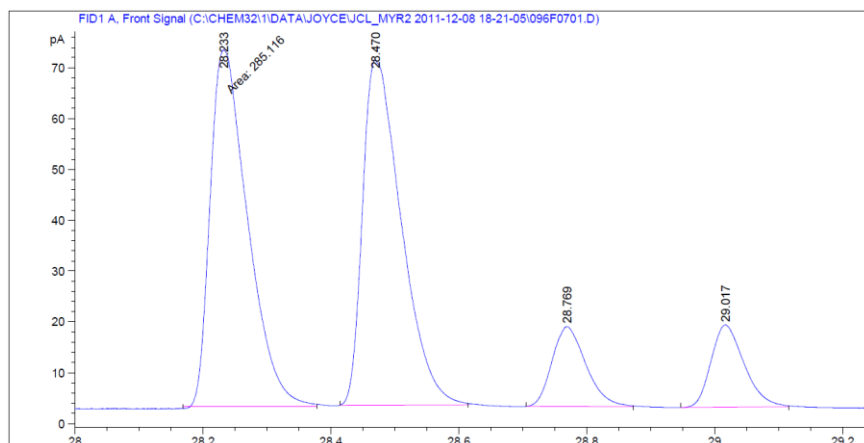
¹H NMR of **3.8a**



¹³C NMR of **3.8a**

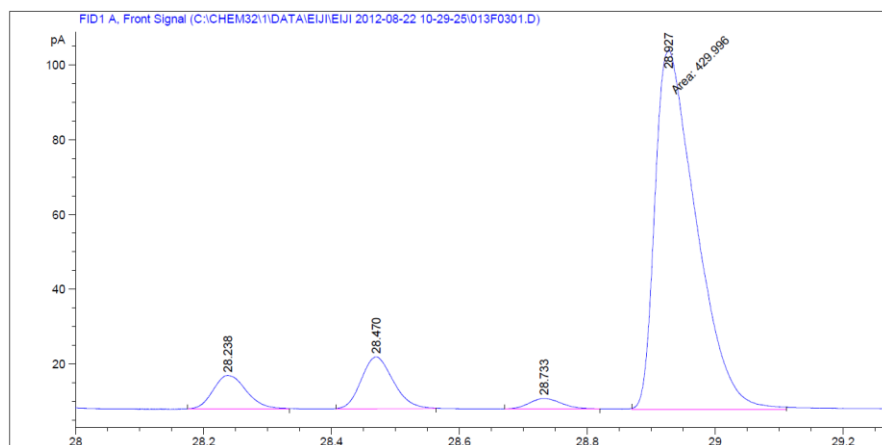


GC of *rac*-3.8a



Peak #	RetTime [min]	Type	Width [min]	Area [pA*s]	Height [pA]	Area %
1	28.233	MM	0.0677	285.11609	70.14124	41.55134
2	28.470	BB	0.0595	285.04620	67.68720	41.54115
3	28.769	BB	0.0573	57.82202	15.73872	8.42668
4	29.017	BB	0.0563	58.19354	16.19599	8.48082

GC of 3.8a



Peak #	RetTime [min]	Type	Width [min]	Area [pA*s]	Height [pA]	Area %
1	28.238	BB	0.0557	32.14819	8.91363	6.18251
2	28.470	BB	0.0533	48.11090	13.85561	9.25235
3	28.733	BB	0.0535	9.73064	2.78858	1.87133
4	28.927	MM	0.0745	429.99585	96.17088	82.69380

(3*R*,4*R*)-9-Fluoro-3-methylnon-1-en-4-ol (**3.8b**)

In accordance with the general procedure using alcohol **3.7b**, upon stirring at 95 °C for 72 h, the reaction mixture was concentrated *in vacuo* to afford the crude product (dr = 4.8:1 *syn:anti*, as determined by ¹H NMR spectroscopy). The reaction mixture was then subjected to flash column chromatography (SiO₂: 0-10% EtOAc/hexanes) to furnish **3.8b** (44 mg, 0.25 mmol, 84% yield, 96% ee) as a clear, colorless oil.

TLC (SiO₂): R_f = 0.45 (hexanes:EtOAc = 10:1).

¹H NMR (400 MHz, CDCl₃): δ 5.83-5.74 (m, 1H), 5.14-5.06 (m, 2H), 4.50 (t, *J* = 6.2 Hz, 1H), 4.36 (t, *J* = 6.2 Hz, 1H), 3.49 (ddd, *J* = 8.6, 5.1, 3.3 Hz, 1H), 2.32-2.23 (m, 1H), 1.77-1.64 (m, 2H), 1.56-1.36 (m, 6H), 1.03 ppm (d, *J* = 7.0 Hz, 1H).

¹³C NMR (100 MHz, CDCl₃): δ 140.9, 115.4, 85.1 (d, *J* = 164.6 Hz), 74.5, 43.5, 33.8, 30.4 (*J* = 19.5 Hz), 25.7, 25.2 (*J* = 5.2 Hz), 14.0 ppm.

¹⁹F NMR (376 MHz, CDCl₃): δ -218.0 to -218.4 (m).

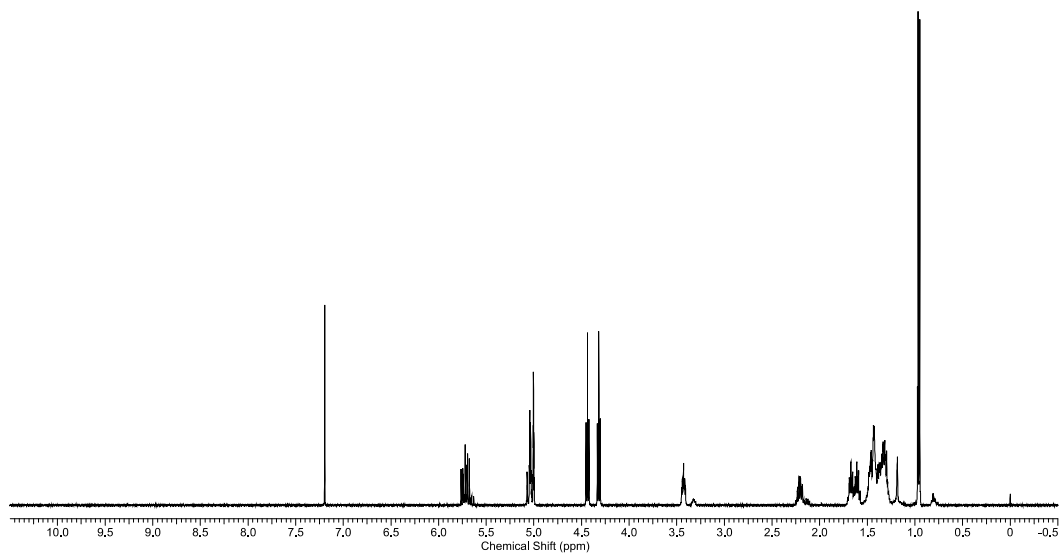
LRMS (CI⁺): *m/z* 175 [M+H]⁺.

FTIR (neat): 3413, 2934, 2860, 1459, 1390, 1243, 997, 912 cm⁻¹.

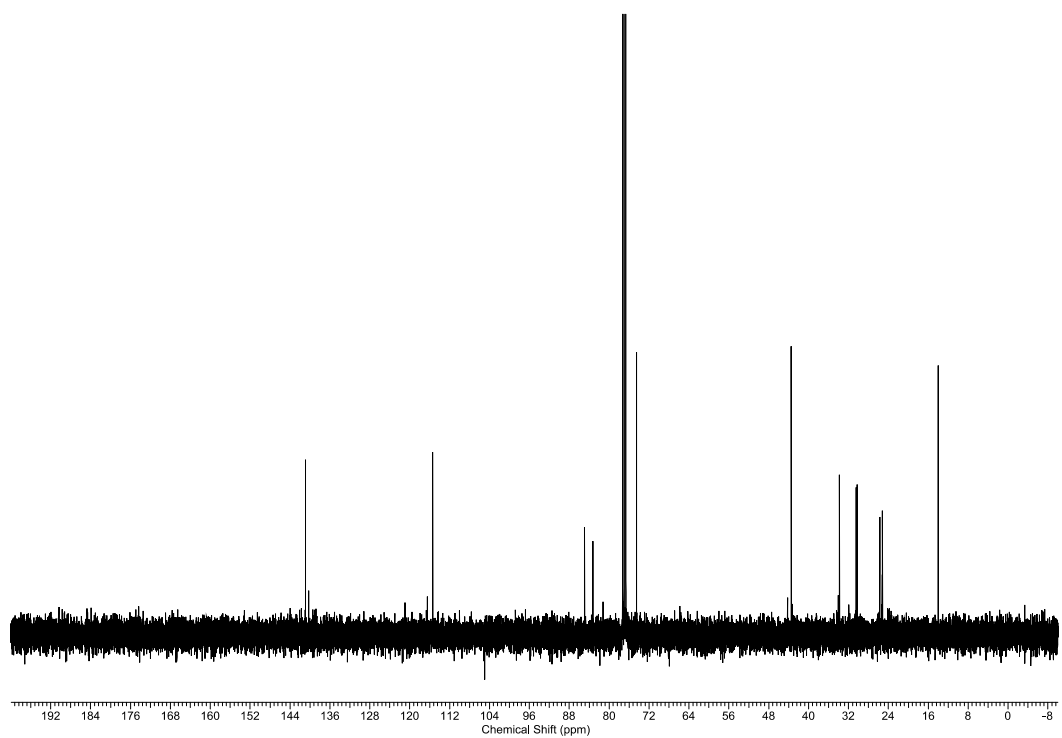
GC (Cyclosil-B: Initial temperature: 50 °C (5 min hold); 80°C (5 min hold), rate: 2 °C/min; 130 °C, rate: 1.5 °C/min): *t*_{minor}=48.3 min, *t*_{major}=48.5 min.

[α]_D²⁵ = 66.6° (c = 1.0, CHCl₃).

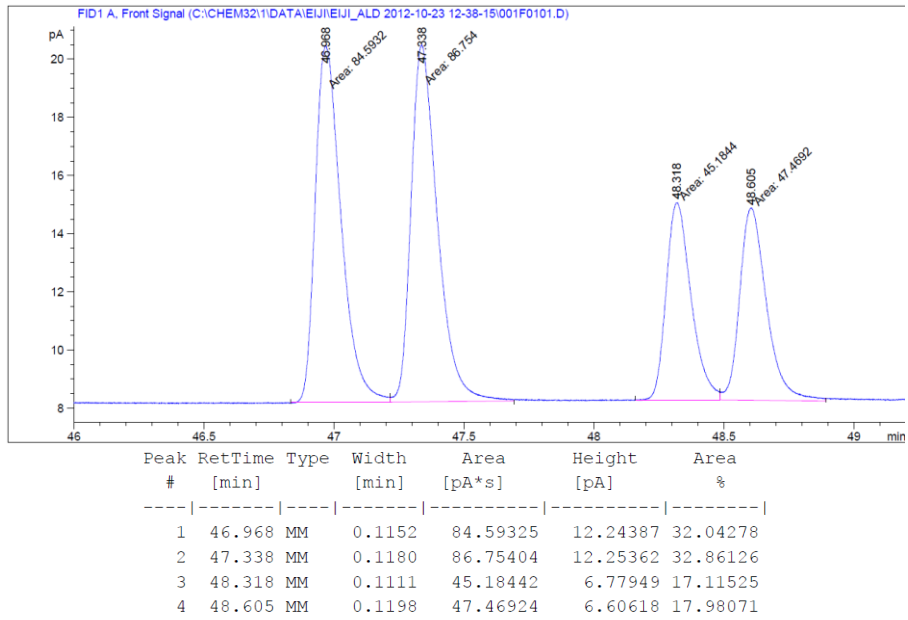
^1H NMR of **3.8b**



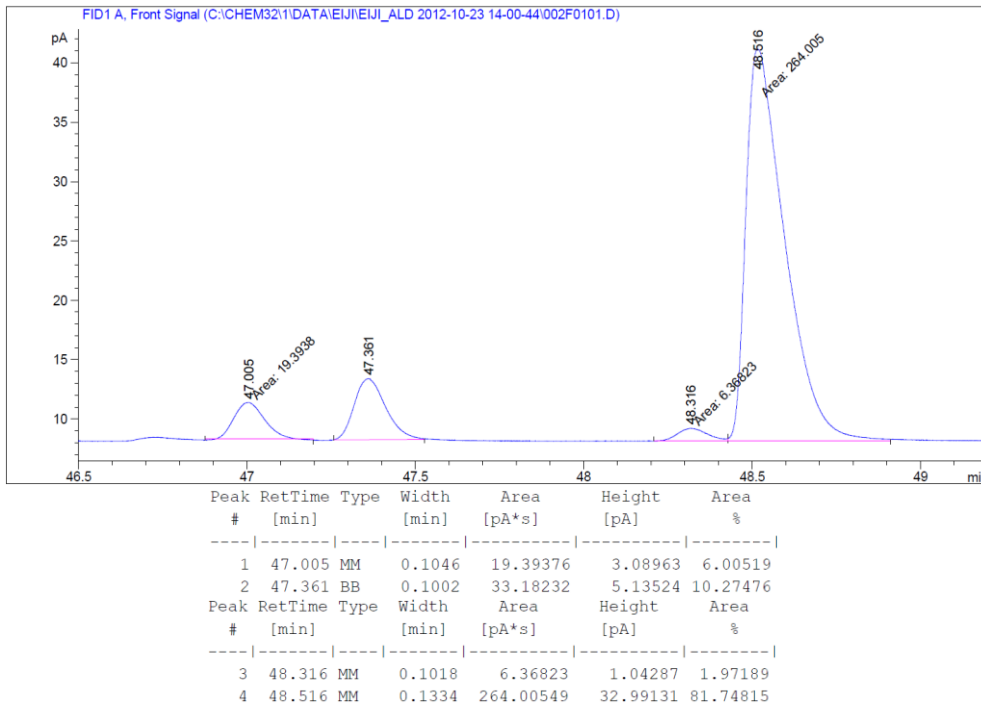
^{13}C NMR of **3.8b**



GC of *rac*-3.8b



GC of 3.8b



(3*R*,4*R*)-7,7,7-Trifluoro-3-methylhept-1-en-4-ol (**3.8c**)

In accordance with the general procedure using alcohol **3.7c**, upon stirring at 95 °C for 72 h, the reaction mixture was concentrated *in vacuo* to afford the crude product (dr = 4.3:1 *syn:anti*, as determined by ¹H NMR spectroscopy). The reaction mixture was then subjected to flash column chromatography (SiO₂: 0-10% EtOAc/hexanes) to furnish **3.8c** (39 mg, 0.21 mmol, 72% yield, 96% ee) as a clear, colorless oil.

TLC (SiO₂): R_f = 0.4 (hexanes:EtOAc = 10:1).

¹H NMR (400 MHz, CDCl₃): δ 5.80-5.68 (m, 1H), 5.20-5.11 (m, 2H), 3.54-3.49 (m, 1H), 2.43-2.26 (m, 2H), 2.22-2.06 (m, 1H), 1.82-1.73 (m, 1H), 1.64-1.53 (m, 2H), 1.06 ppm (d, *J* = 6.9 Hz, 3H).

¹³C NMR (100 MHz, CDCl₃): δ 139.8, 127.4 (q, *J* = 276.0 Hz), 116.3, 73.4, 43.9, 30.7 (q, *J* = 29.2 Hz), 26.3 (q, *J* = 3.0 Hz), 14.5 ppm.

¹⁹F NMR (376 MHz, CDCl₃): δ -66.37 (*J* = 10.9 Hz).

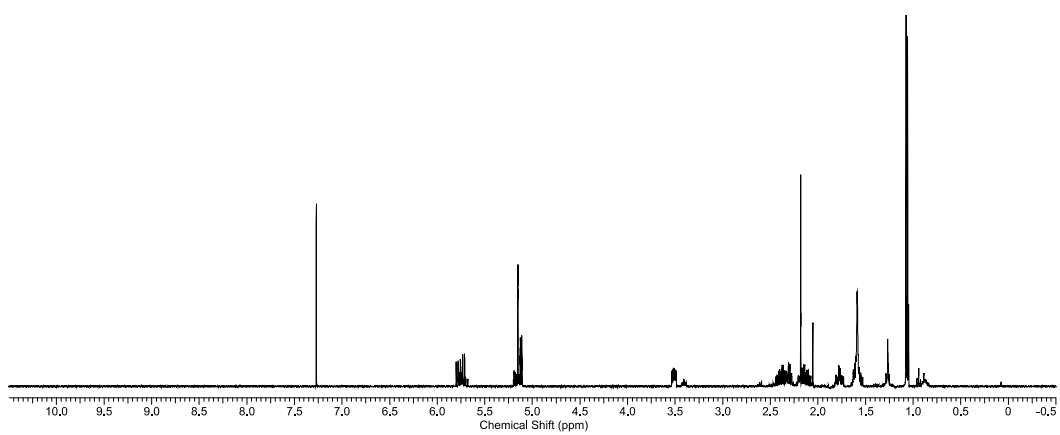
LRMS (Cl⁺): *m/z* 183 [M+H]⁺.

FTIR (neat): 3373, 2964, 2358, 1455, 1383, 1225, 1138, 1032, 1005, 918, 800 cm⁻¹.

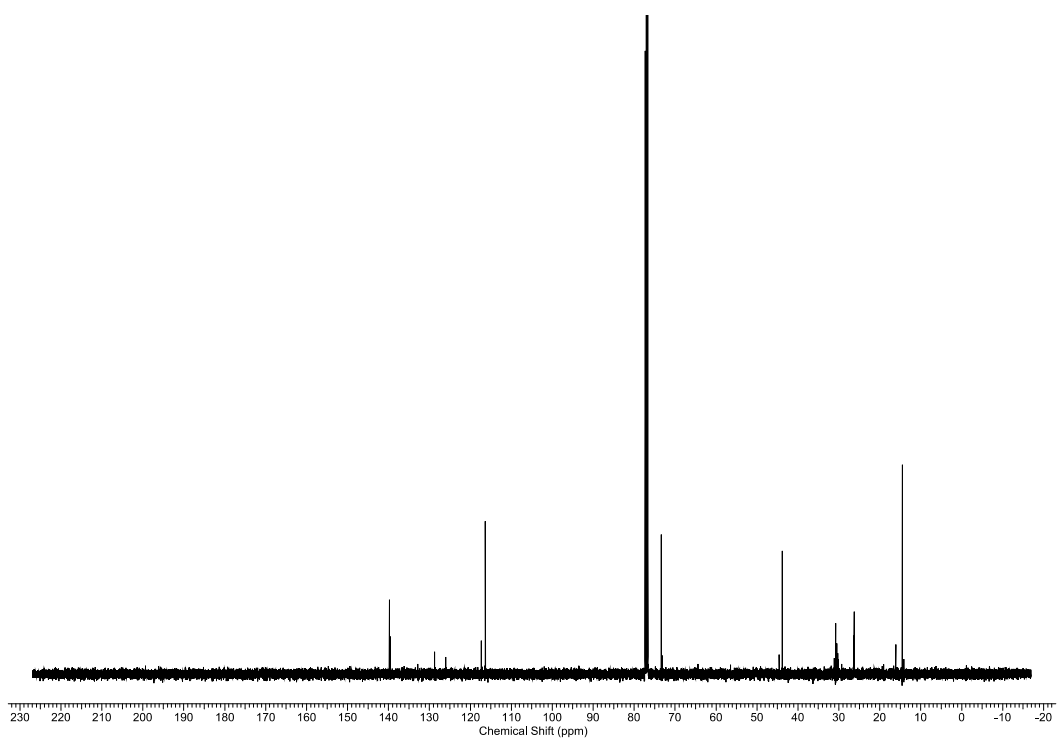
GC (Cyclosil-B: Initial temperature: 50 °C (5 min hold); 130 °C, rate: 3 °C/min): *t*_{minor}=18.1 min, *t*_{major}=18.9 min.

[α]_D²⁵ = 20.1° (c = 1.0, CHCl₃).

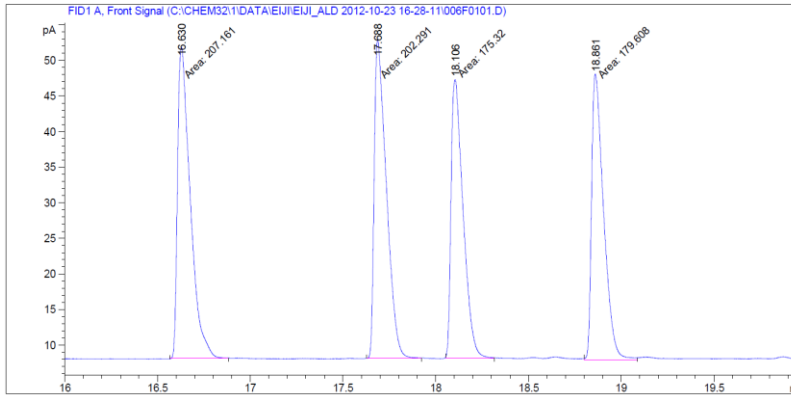
¹H NMR of 3.8c



¹³C NMR of 3.8c

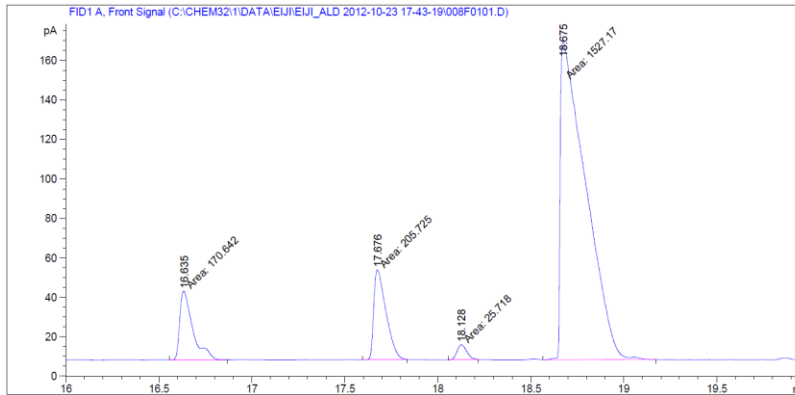


GC of *rac*-3.8c



Peak #	RetTime [min]	Type	Width [min]	Area [pA*s]	Height [pA]	Area %
1	16.630	MM	0.0792	207.16109	43.59585	27.10185
2	17.688	MM	0.0754	202.29076	44.74445	26.46469
3	18.106	MM	0.0747	175.31981	39.09904	22.93621
4	18.861	MM	0.0747	179.60822	40.08700	23.49725

GC of 3.8c



Peak #	RetTime [min]	Type	Width [min]	Area [pA*s]	Height [pA]	Area %
1	16.635	MM	0.0813	170.64178	34.98223	8.84494
2	17.676	MM	0.0757	205.72536	45.31288	10.66344
3	18.128	MM	0.0581	25.71798	7.37326	1.33305
4	18.675	MM	0.1568	1527.17419	162.28458	79.15858

(3*R*,4*R*)-3,6-dimethylhept-1-en-4-ol (**3.8d**)

In accordance with the general procedure using alcohol **3.7d**, upon stirring at 95 °C for 72 h, the reaction mixture was concentrated *in vacuo* to afford the crude product (dr = 4.6:1 *syn:anti*, as determined by ¹H NMR spectroscopy). The reaction mixture was then subjected to flash column chromatography (SiO₂: 0-10% EtOAc/hexanes) to furnish **3.8d** (27 mg, 0.19 mmol, 72% yield, 94% ee) as a clear, colorless oil. *The spectroscopic properties of this compound were consistent with the data available in the literature.*^{79d}

TLC (SiO₂): R_f = 0.4 (hexanes:EtOAc = 8:1).

¹H NMR (400 MHz, CDCl₃): δ 5.73 (ddd, *J* = 17.6, 10.0, 7.4 Hz, 1H), 5.07-4.99 (m, 2H), 3.62-3.57 (m, 1H), 2.28-2.23 (m, 1H), 1.83-1.77 (m, 1H), 1.45 (brs, 1H), 1.38-1.22 (m, 2H), 1.03 (d, *J* = 7.0 Hz, 3H), 0.94 (d, *J* = 6.8 Hz, 3H), 0.91 ppm (d, *J* = 6.8 Hz, 3H).

¹³C NMR (100 MHz, CDCl₃): δ 141.0, 115.3, 72.5, 43.8, 43.1, 24.7, 23.7, 21.7, 14.0 ppm.

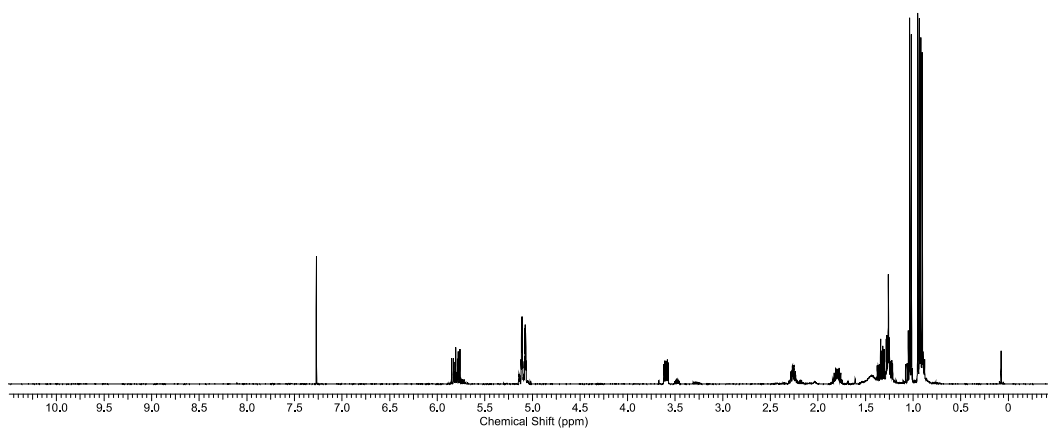
LRMS (CI⁺): *m/z* 143 [M+H]⁺.

FTIR (neat): 3623, 2955, 2924, 1718, 1464, 1367, 966, 910, 694 cm⁻¹.

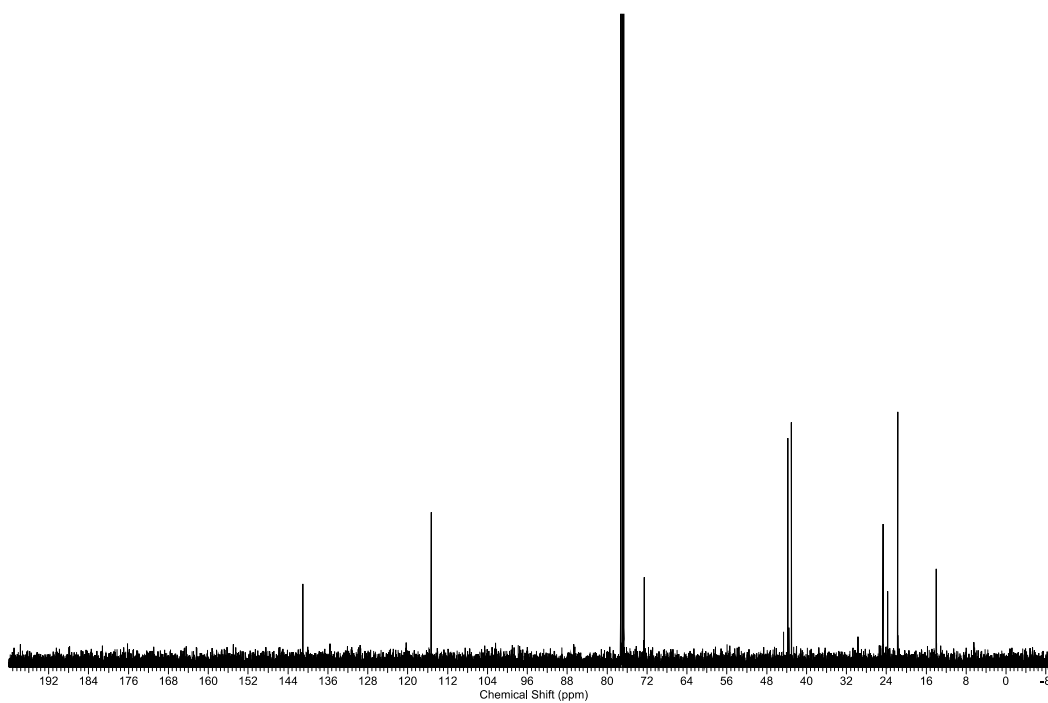
GC (Cyclosil-B: Initial temperature: 50 °C (5 min hold); 130 °C, rate: 3 °C/min): *t*_{minor}=19.1 min, *t*_{major}=19.5 min.

[α]_D²⁵ = 56.2° (c = 1.50, CH₂Cl₂). ([α]_D²⁵ = 45.2° (c = 1.45, CH₂Cl₂) was reported for 96% ee of the (3*R*,4*R*) compound.^{79d})

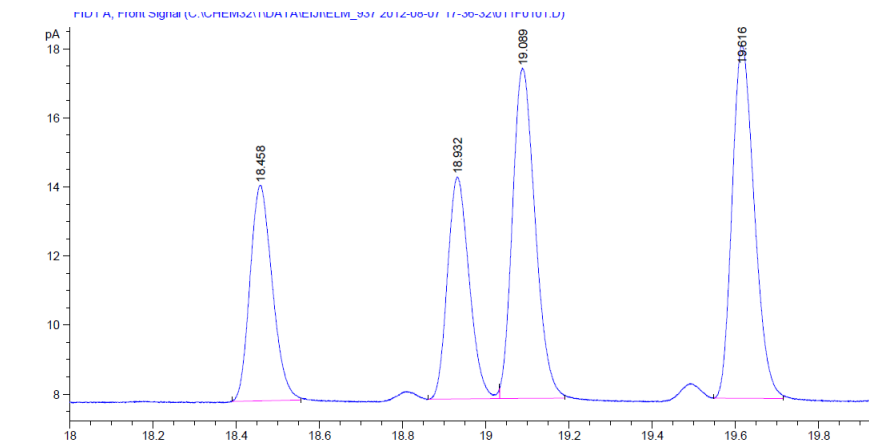
¹H NMR of 3.8d



¹³C NMR of 3.8d

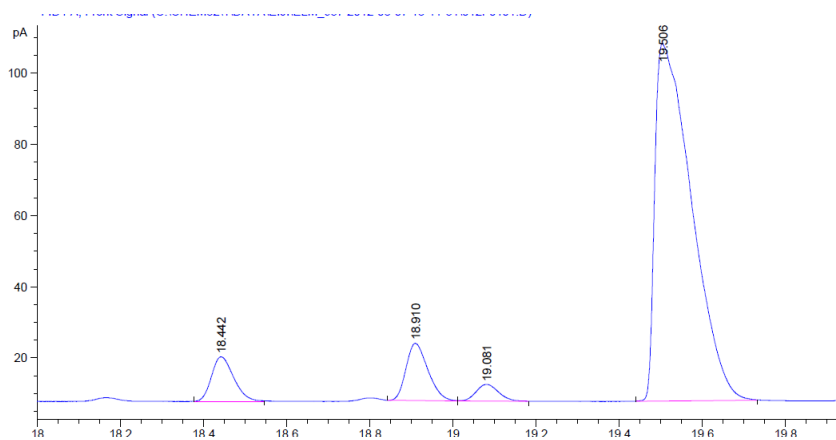


GC of *rac*-3.8d



Peak #	RetTime [min]	Type	Width [min]	Area [pA*s]	Height [pA]	Area %
1	18.458	BB	0.0579	23.27678	6.24192	19.27926
2	18.932	BB	0.0576	23.31637	6.42052	19.31206
3	19.089	BB	0.0594	36.18595	9.55269	29.97143
4	19.616	BB	0.0578	37.95570	10.20461	31.43725

GC of 3.8d



Peak #	RetTime [min]	Type	Width [min]	Area [pA*s]	Height [pA]	Area %
1	18.458	BB	0.0579	23.27678	6.24192	19.27926
2	18.932	BB	0.0576	23.31637	6.42052	19.31206
3	19.089	BB	0.0594	36.18595	9.55269	29.97143
4	19.616	BB	0.0578	37.95570	10.20461	31.43725

(3*R*,4*R*,6*R*)-3,6,10-trimethylundeca-1,9-dien-4-ol (**3.8e**)

In accordance with the general procedure using alcohol **3.7e**, upon stirring at 95 °C for 72 h, the reaction mixture was concentrated *in vacuo* to afford the crude product (dr = 4.6:1 *syn:anti*, as determined by ¹H NMR spectroscopy). The reaction mixture was then subjected to flash column chromatography (SiO₂: 0-10% EtOAc/hexanes) to furnish **3.8e** (52 mg, 0.27 mmol, 89% yield, 95% ee) as a clear, colorless oil. *The spectroscopic properties of this compound were consistent with the data available in the literature.*¹⁰³

TLC (SiO₂): R_f = 0.45 (hexanes:EtOAc = 8:1).

¹H NMR (400 MHz, CDCl₃): δ 5.81 (ddd, *J* = 17.6, 9.8, 7.2 Hz, 1H), 5.13-5.06 (m, 3H), 3.65-3.59 (m, 1H), 2.30-2.21 (m, 1H), 2.07-1.88 (m, 2H), 1.68 (s, 3H), 1.60 (s, 3H), 1.59 (brs, 1H), 1.49-1.38 (m, 2H), 1.35-1.05 (m, 3H), 1.01 (d, *J* = 6.9 Hz, 3H), 0.93 ppm (d, *J* = 6.7 Hz, 3H).

¹³C NMR (100 MHz, CDCl₃): δ 141.13, 131.24, 124.8, 115.3, 72.5, 43.4, 41.4, 36.3, 29.4, 25.7, 25.3, 20.5, 17.6, 13.6 ppm.

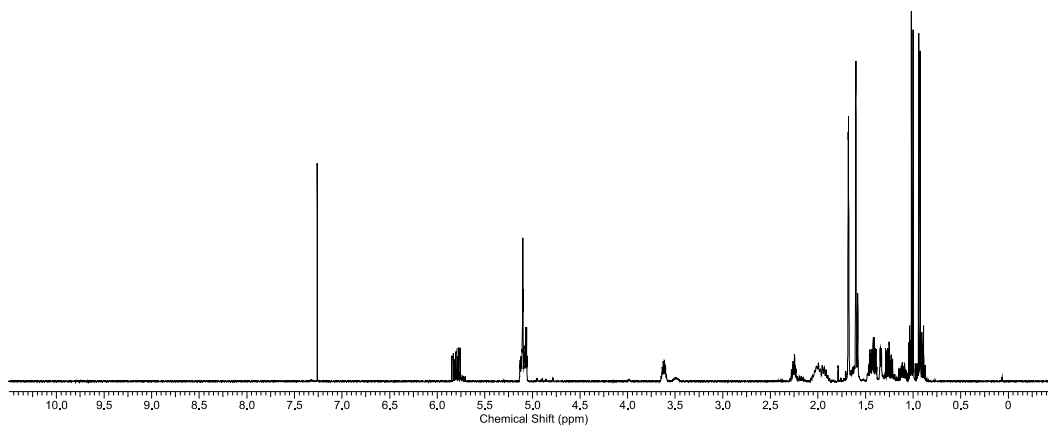
LRMS (CI⁺): *m/z* 211 [M+H]⁺.

FTIR (neat): 3358, 2963, 2924, 1639, 1455, 1376, 1091, 996, 910, 734 cm⁻¹.

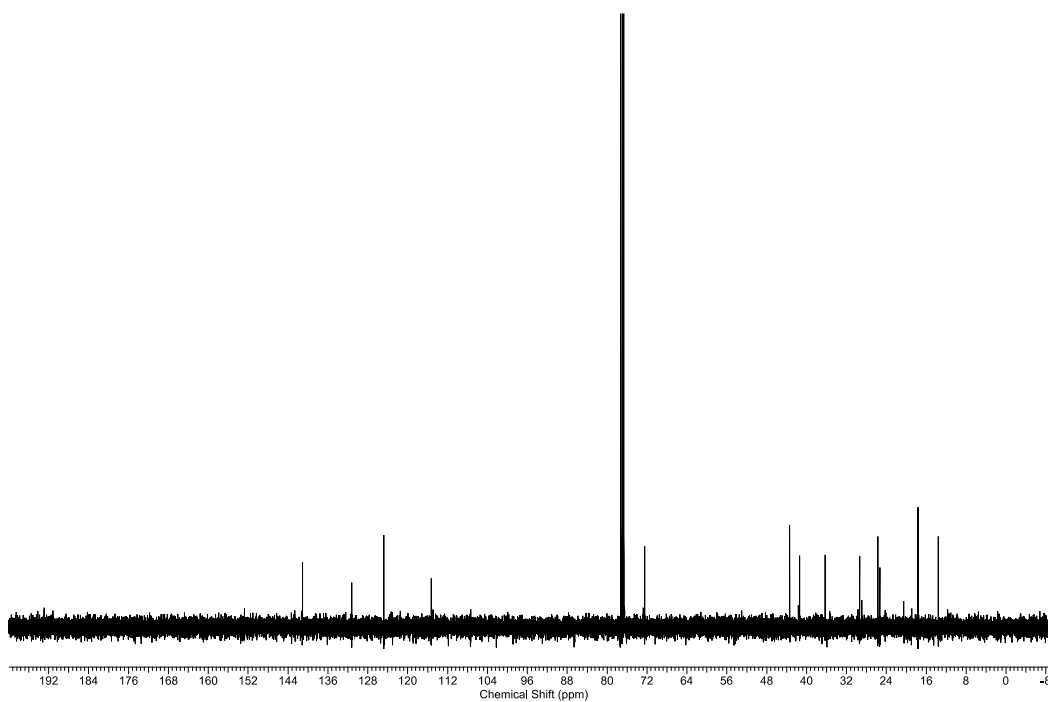
GC (GC Cyclosil-B: Initial temperature: 50 °C (5 min hold); 100 °C (5 min hold), rate: 1 °C/min; 150 °C, rate 0.5 °C/min): *t*_{minor}=89.4 min, *t*_{major}=89.8 min.

[α]_D²⁵ = -38.33 (*c* = 1.0, CHCl₃).

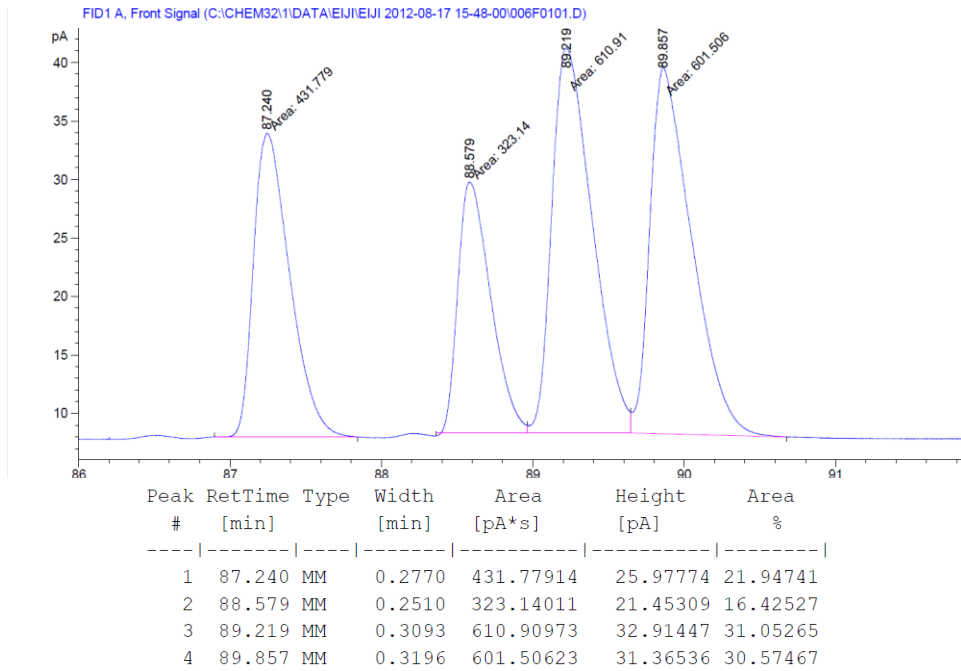
^1H NMR of **3.8e**



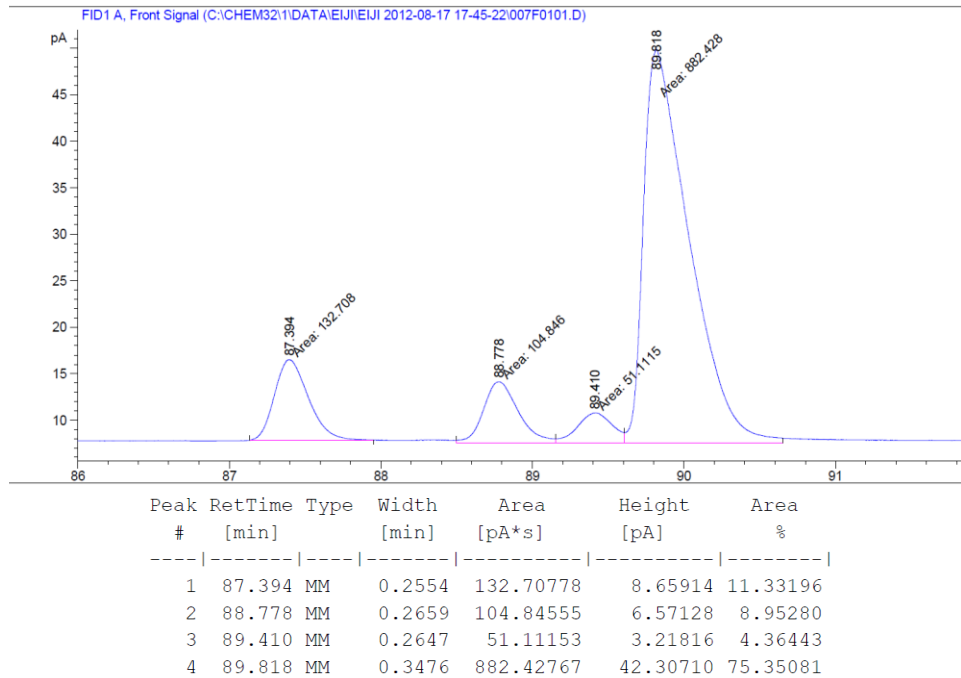
^{13}C NMR of **3.8e**



GC of *rac*-3.8e



GC of 3.8e



(2*R*,3*R*)-3-methyl-1-phenylpent-4-en-2-ol (**3.8f**)

In modification of the general procedure, RuH₂(CO)(PPh₃)₃ (14 mg, 0.015 mmol, 5 mol%), (S)-(-)-5,5'-Bis(diphenylphosphino)-4,4'-bi-1,3-benzodioxole (9.3 mg, 0.015 mmol, 5 mol%), L-TADDOL phosphoric acid (21 mg, 0.03 mmol, 10 mol%) were used. Upon addition of alcohol **3.7f**, butadiene, and acetone and stirring at 95 °C for 72 h, the reaction mixture was concentrated *in vacuo* to afford the crude product (dr = 3.8:1 *syn:anti*, as determined by ¹H NMR spectroscopy). The reaction mixture was then subjected to flash column chromatography (SiO₂: 0-10% EtOAc/hexanes) to furnish **3.8f** (45 mg, 0.26 mmol, 85% yield, 91% ee) as a clear, colorless oil. *The spectroscopic properties of this compound were consistent with the data available in the literature.*¹⁰⁴

TLC (SiO₂): R_f = 0.5 (hexanes:EtOAc = 8:1).

¹H NMR (400 MHz, CDCl₃): δ 7.33-7.30 (m, 2H), 7.25-7.21 (m, 3H), 5.92-5.82 (m, 1H), 5.17-5.09 (m, 2H), 3.74-3.67 (m, 1H), 2.91-2.85 (m, 1H), 2.66-2.58 (m, 1H), 2.34-2.27 (m, 1H), 1.56 (brs, 1H), 1.12 ppm (d, *J* = 6.9 Hz, 3H).

¹³C NMR (100 MHz, CDCl₃): δ 140.9, 129.3, 128.6, 128.5, 126.4, 115.4, 75.7, 43.1, 40.8, 14.5 ppm.

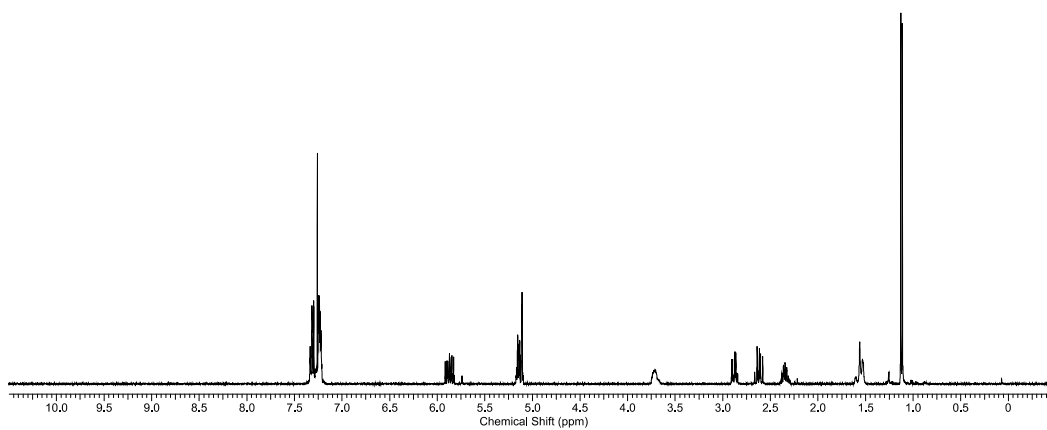
LRMS (CI⁺): *m/z* 177 [M+H]⁺.

FTIR (neat): 3432, 3063, 2964, 1637, 1497, 1453, 1030, 998, 912, 699 cm⁻¹.

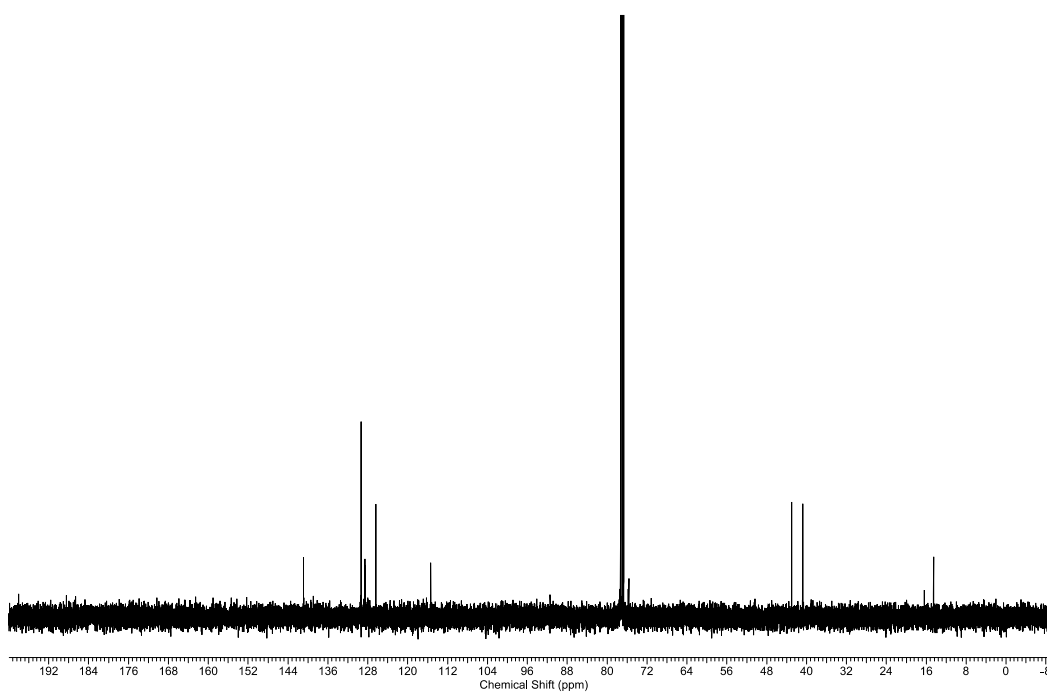
HPLC (Chiralcel OD-H/OD-H/OD-H column, hexanes:PrOH = 98.5:1.5, 0.4 mL/min, 210 nm): t_{minor}=135.3 min, t_{major}=81.3 min.

[α]_D²⁵ = 58.3° (c = 1.0, CHCl₃).

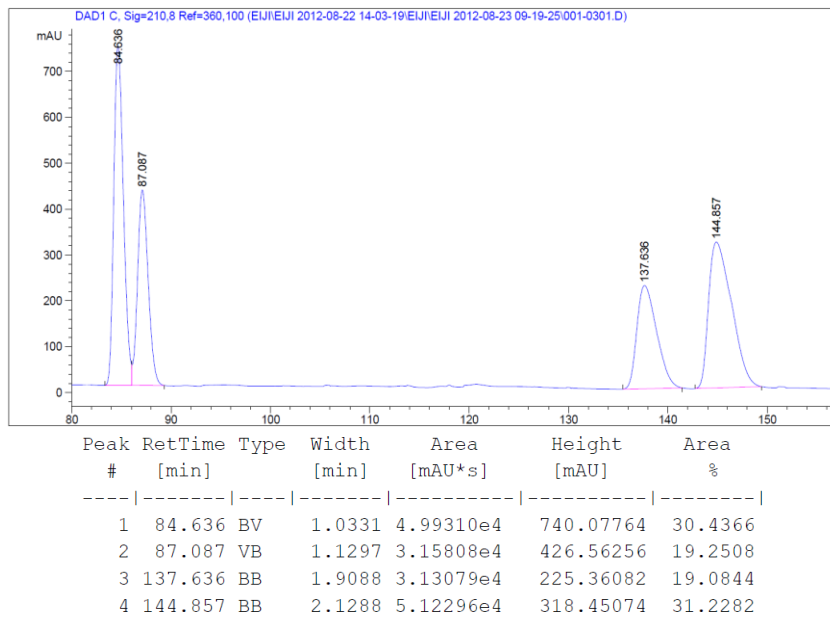
^1H NMR of **3.8f**



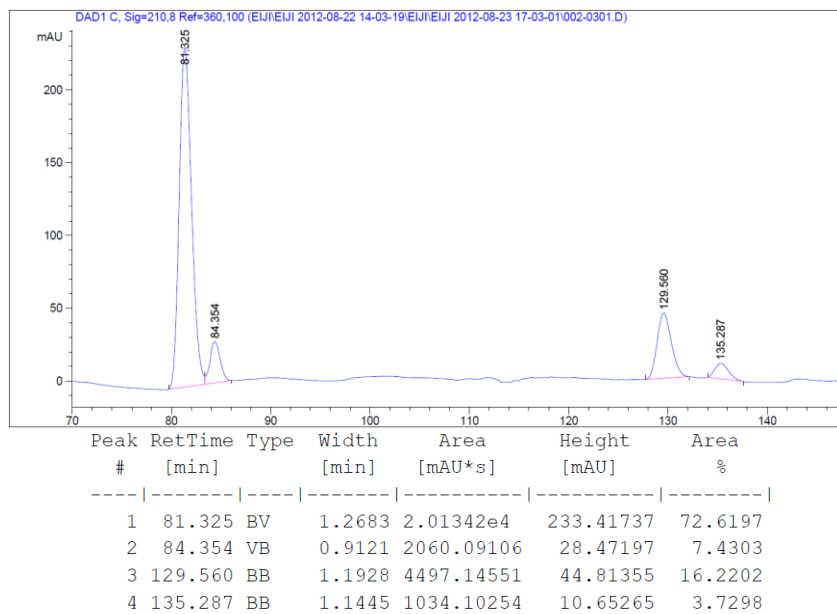
^{13}C NMR of **3.8f**



HPLC of *rac*-3.8f



HPLC of 3.8f



(3*R*,4*R*)-4-methyl-1-phenylhex-5-en-3-ol (**3.8g**)

In modification of the general procedure, RuH₂(CO)(PPh₃)₃ (14 mg, 0.015 mmol, 5 mol%), (S)-(-)-5,5'-Bis(diphenylphosphino)-4,4'-bi-1,3-benzodioxole (9.3 mg, 0.015 mmol, 5 mol%), L-TADDOL phosphoric acid (21 mg, 0.03 mmol, 10 mol%) were added used. Upon addition of alcohol **3.7g**, butadiene, and acetone and stirring at 95 °C for 72, the reaction mixture was concentrated *in vacuo* to afford the crude product (dr = 5.5:1 *syn:anti*, as determined by ¹H NMR spectroscopy). The reaction mixture was then subjected to flash column chromatography (SiO₂: 0-10% EtOAc/hexanes) to furnish **3.8g** (44 mg, 0.23 mmol, 78% yield, 95% ee) as a clear, colorless oil. *The spectroscopic properties of this compound were consistent with the data available in the literature.*^{78d}

TLC (SiO₂): R_f = 0.4 (hexanes:EtOAc = 8:1).

¹H NMR (400 MHz, CDCl₃): δ 7.31-7.27 (m, 2H), 7.22-7.17 (m, 3H), 5.77 (ddd, *J* = 17.4, 9.8, 7.4 Hz, 1H), 5.12-5.07 (m, 2H), 3.53 (ddd, *J* = 9.2, 5.1, 3.1 Hz, 1H), 2.86 (ddd, *J* = 13.7, 10.0, 5.1 Hz, 1H), 2.65 (ddd, *J* = 13.7, 9.8, 6.8 Hz, 1H), 2.34-2.27 (m, 1H), 1.82 (dddd, *J* = 13.9, 10.0, 6.8, 3.1 Hz, 1H), 1.69 (ddd, *J* = 13.9, 9.8, 5.1, Hz, 1H), 1.69 ppm (d, *J* = 6.9 Hz, 1H).

¹³C NMR (100 MHz, CDCl₃): δ 142.3, 140.7, 128.5, 128.4, 125.8, 115.6, 74.0, 43.6, 35.8, 32.5, 14.2 ppm.

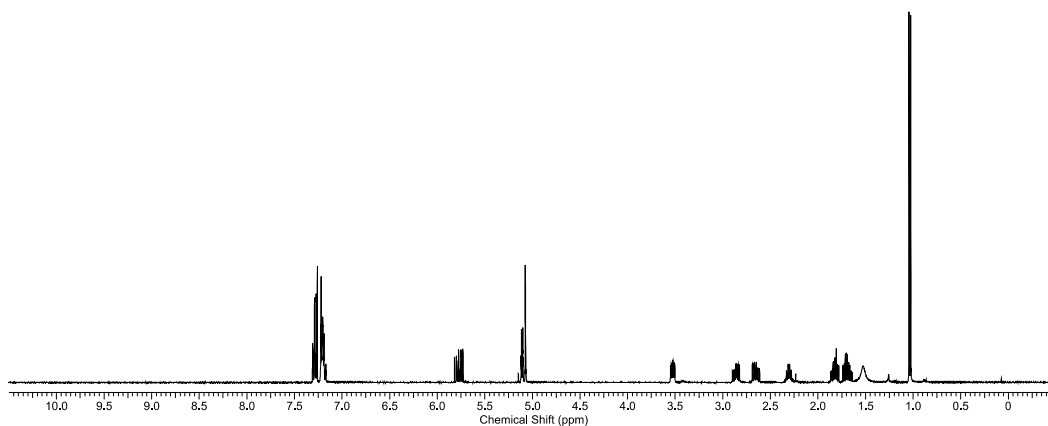
LRMS (Cl⁺): *m/z* 191 [M+H]⁺.

FTIR (neat): 3414, 2928, 2869, 1737, 1454, 1373, 1216, 1032, 938, 699 cm⁻¹.

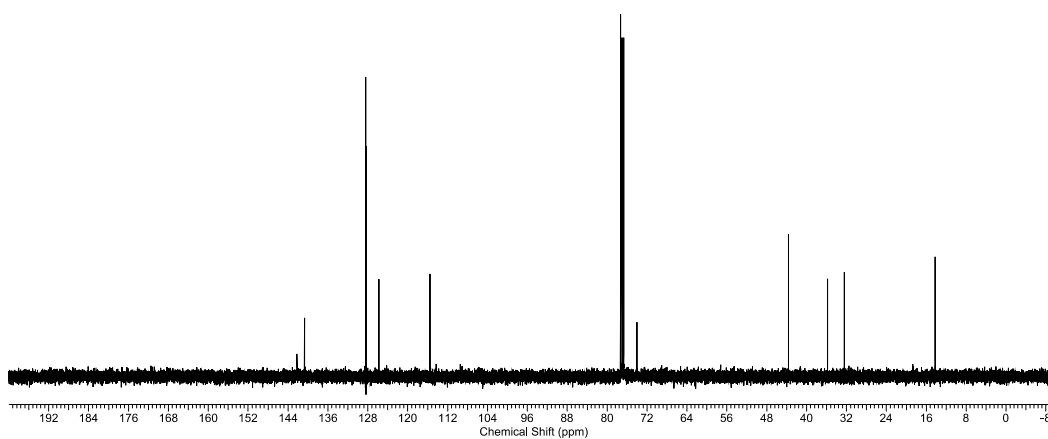
HPLC (Chiralcel OD-H column, hexanes:*i*PrOH = 97:3, 0.7 mL/min, 210 nm): *t*_{minor}=15.5 min, *t*_{major}=27.6 min.

[α]_D²⁵ = 33.0° (c = 1.0, CHCl₃) reported for 96% ee of the (3*S*,4*S*) compound [α]_D²⁵ = -32.5° (c = 0.8, CHCl₃).^{78d}

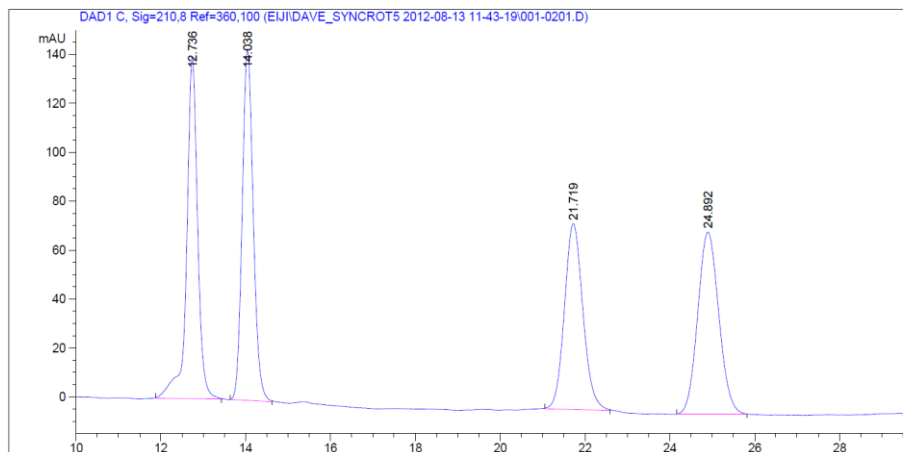
¹H NMR of 3.8g



¹³C NMR of 3.8g

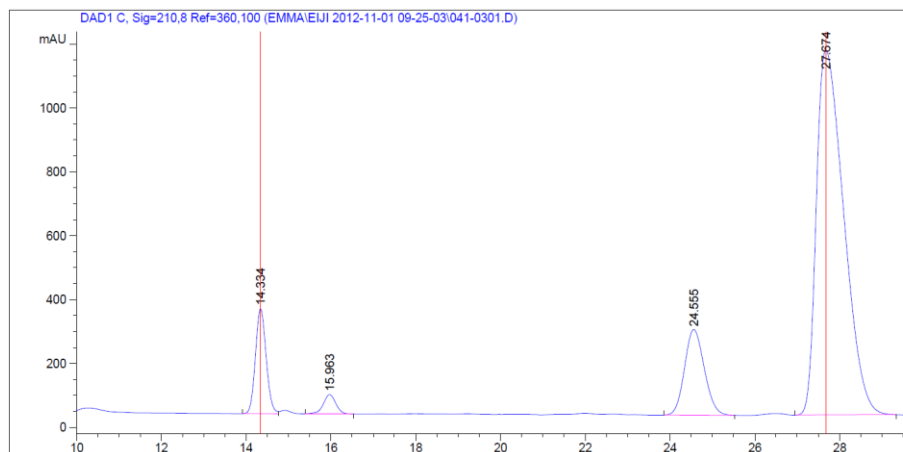


HPLC of *rac*-3.8g



Peak #	RetTime [min]	Type	Width [min]	Area [mAU*s]	Height [mAU]	Area %
1	12.736	BB	0.2711	2524.78613	139.55258	25.2787
2	14.038	BB	0.2783	2585.83911	143.46355	25.8900
3	21.719	BB	0.4677	2304.21509	76.01109	23.0703
4	24.892	BB	0.5410	2572.96533	74.48742	25.7611

HPLC of 3.8g



Peak #	RetTime [min]	Type	Width [min]	Area [mAU*s]	Height [mAU]	Area %
1	14.334	BV	0.2731	5775.56641	328.56348	8.6294
2	15.963	BB	0.3206	1251.60791	60.69165	1.8701
3	24.555	BB	0.5039	8682.60645	268.08081	12.9729
4	27.674	VB	0.7027	5.12189e4	1143.29968	76.5276

(3*R*,4*R*)-4-methyl-1-phenylhex-5-en-3-ol (**3.8h**)

In modification of the general procedure, RuH₂(CO)(PPh₃)₃ (14 mg, 0.015 mmol, 5 mol%), (S)-(-)-5,5'-Bis(diphenylphosphino)-4,4'-bi-1,3-benzodioxole (9.3 mg, 0.015 mmol, 5 mol%), L-TADDOL phosphoric acid (21 mg, 0.03 mmol, 10 mol%) were added used. Upon addition of alcohol **3.7h**, butadiene, and acetone and stirring at 95 °C for 72 h, the reaction mixture was concentrated *in vacuo* to afford the crude product (dr = 4.5:1 *syn:anti*, as determined by ¹H NMR spectroscopy).. The reaction mixture was then subjected to flash column chromatography (SiO₂: 0-10% EtOAc/hexanes) to furnish **3.8h** (36 mg, 0.19 mmol, 62% yield, 95% ee) as a clear, colorless oil.

TLC (SiO₂): R_f = 0.6 (hexanes:EtOAc = 8:1).

¹H NMR (400 MHz, CDCl₃): δ 7.31-7.28 (m, 2H), 7.22-7.17 (m, 3H), 5.80 (ddd, *J* = 17.6, 10.0, 7.4 Hz, 1H), 5.12-5.07 (m, 2H), 3.56-3.51 (m, 1H), 2.71-2.59 (m, 2H), 2.33-2.22 (m, 1H), 1.90-1.70 (m, 1H), 1.72-1.62 (m, 1H), 1.62-1.42 (m, 2H), 1.02 ppm (d, *J* = 6.9 Hz, 3H).

¹³C NMR (100 MHz, CDCl₃): δ 142.4, 140.9, 128.4, 128.3, 125.7, 115.4, 74.5, 43.4, 35.9, 33.6, 27.9, 13.9 ppm.

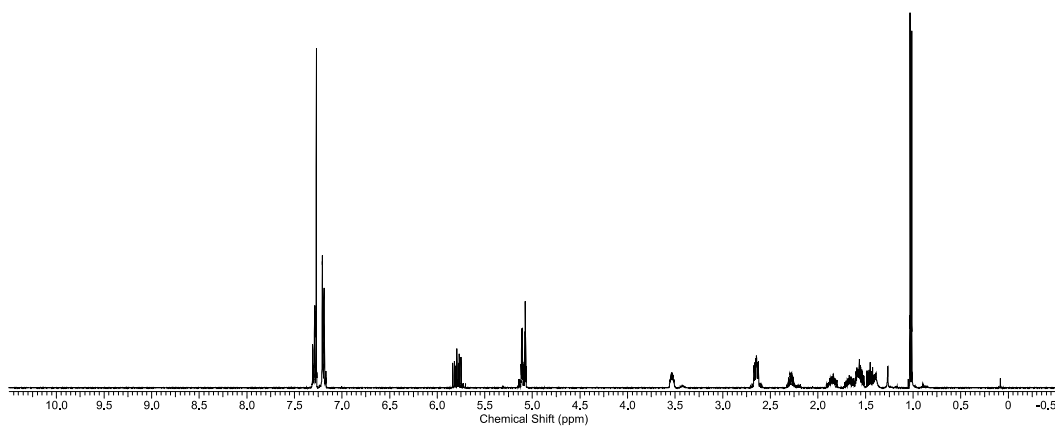
LRMS (CI⁺): *m/z* 205 [M+H]⁺.

FTIR (neat): 3410, 2935, 1712, 1638, 1453, 1374, 1248, 907, 729, 698 cm⁻¹.

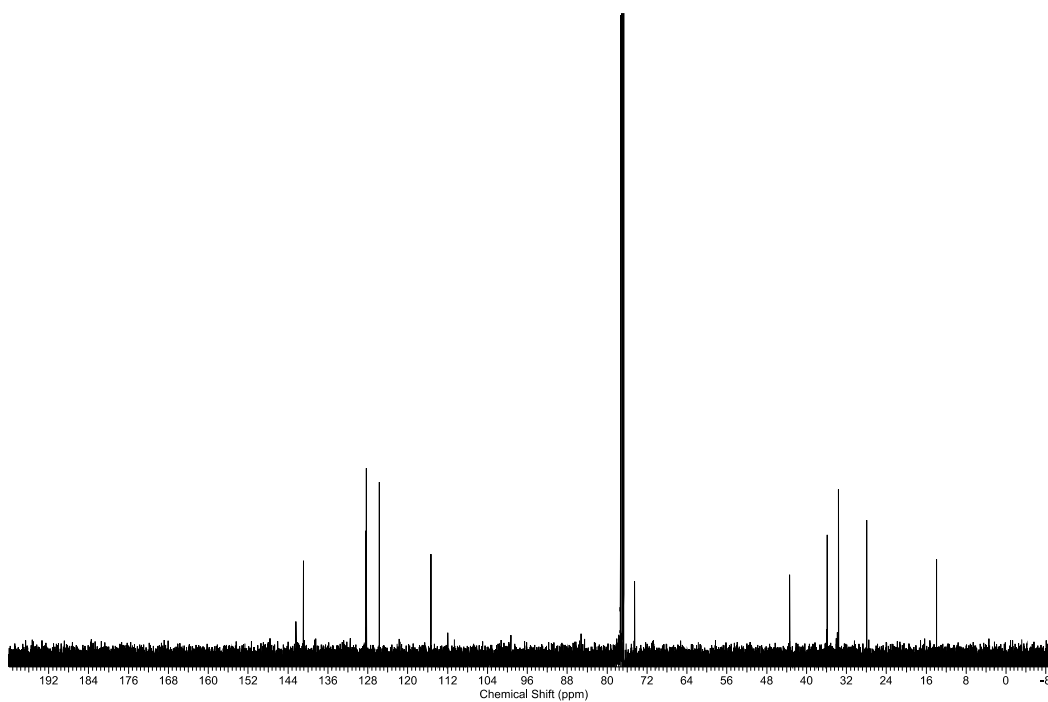
HPLC (Chiralcel OD-H column, hexanes:*i*PrOH = 97:3, 0.7 mL/min, 254 nm): *t*_{major}=15.7 min, *t*_{minor}=19.5 min.

[α]_D²⁵ = 28.5° (c = 0.8, CHCl₃).

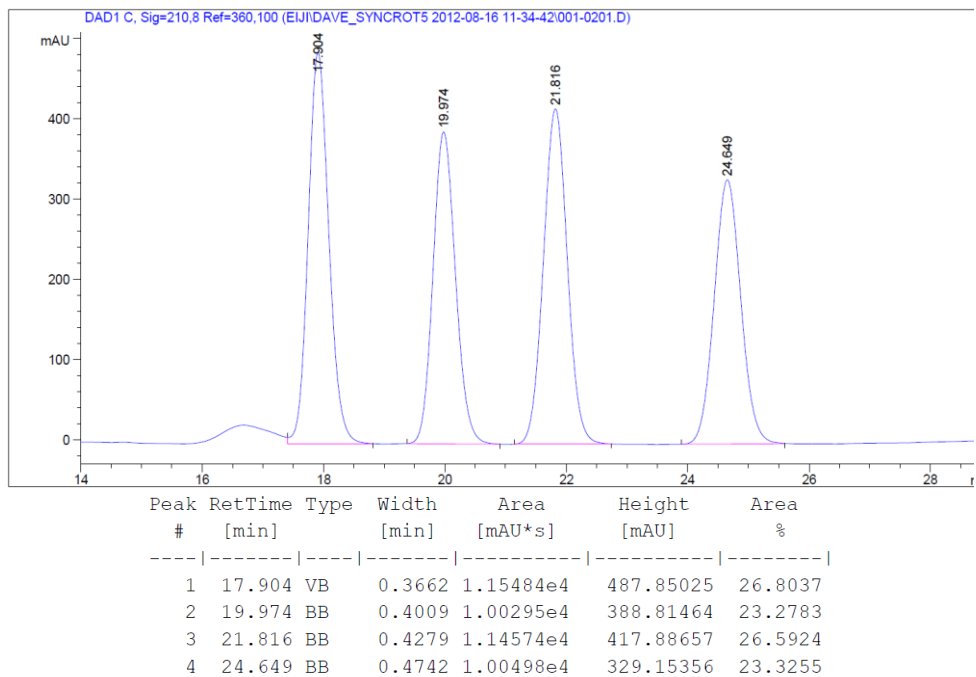
¹H NMR of 3.8h



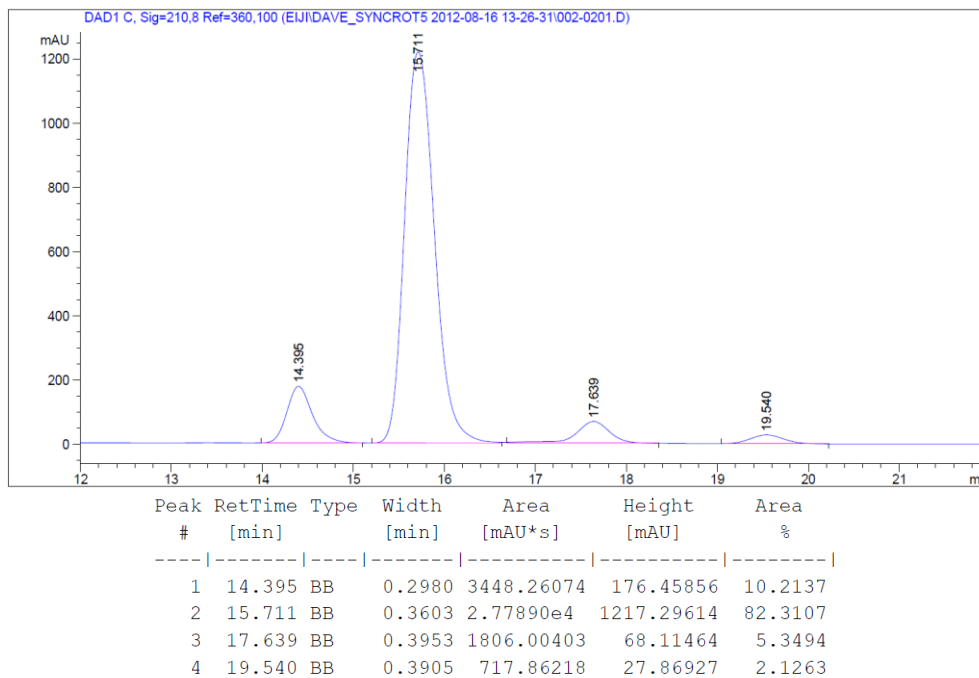
¹³C NMR of 3.8h



HPLC of *rac*-3.8h



HPLC of 3.8h



(3*R*,4*R*)-1-(furan-2-yl)-4-methylhex-5-en-3-ol (**3.8i**)

In accordance with the general procedure using alcohol **3.7i**, upon stirring at 95 °C for 72 h, the reaction mixture was concentrated *in vacuo* to afford the crude product (dr = 4.0:1 *syn:anti*, as determined by ¹H NMR spectroscopy). The reaction mixture was then subjected to flash column chromatography (SiO₂: 0-10% EtOAc/hexanes) to furnish **3.8i** (37 mg, 0.21 mmol, 69% yield, 95% ee) as a clear, colorless oil.

TLC (SiO₂): R_f = 0.35 (hexanes:EtOAc = 10:1).

¹H NMR (400 MHz, CDCl₃): δ 7.31 (d, *J* = 2.1 Hz, 1H), 6.29 (dd, *J* = 3.1, 2.2 Hz, 1H), 6.02 (d, *J* = 3.1 Hz, 1H), 5.83-5.71 (m, 1H), 5.16-5.08 (m, 2H), 3.52 (dd, *J* = 9.6, 5.1, 3.3 Hz, 1H), 2.90-2.82 (m, 1H), 2.77-2.67 (m, 1H), 2.35-2.25 (m, 1H), 1.95-1.84 (m, 1H), 1.73-1.63 (m, 1H), 1.56 (brs, 1H), 1.05 ppm (d, *J* = 6.9 Hz, 3H).

¹³C NMR (100 MHz, CDCl₃): δ 155.9, 140.9, 146.6, 115.6, 110.1, 104.9, 73.9, 43.7, 32.4, 24.7, 14.3 ppm.

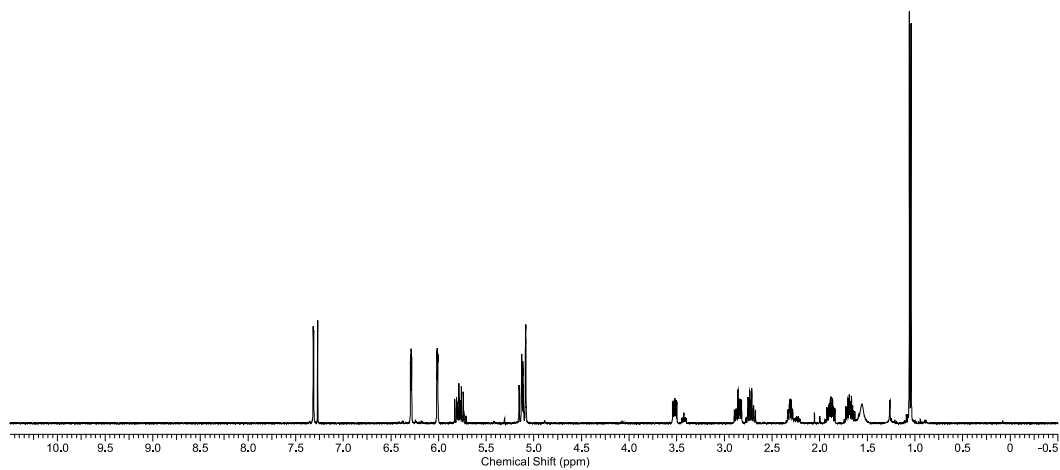
LRMS (CI⁺): *m/z* 181 [M+H]⁺.

FTIR (neat): 3370, 2961, 1639, 1507, 1452, 1145, 1043, 914, 726 cm⁻¹.

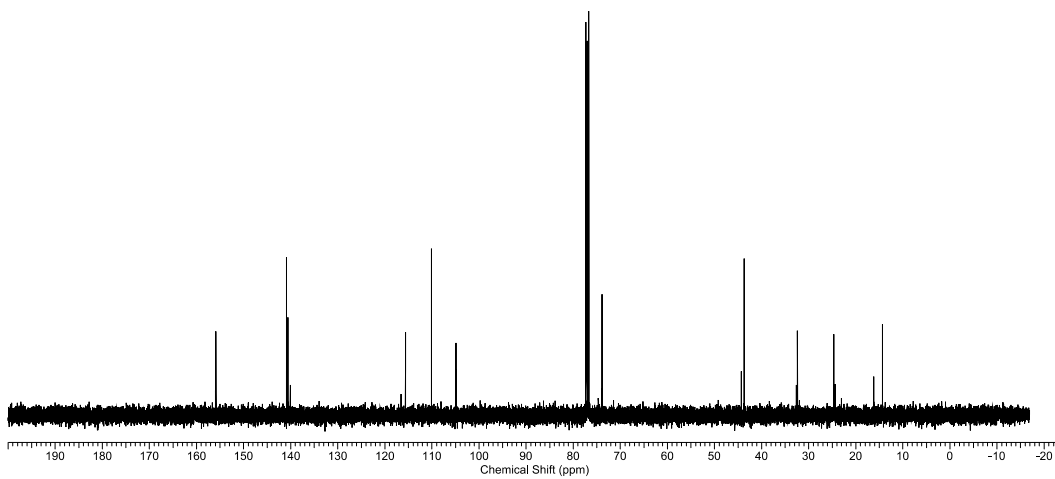
HPLC (Chiralpak AS-H/AS-H column, hexanes:*i*PrOH = 99:1, 0.5 mL/min, 254 nm): *t*_{minor}=29.5 min, *t*_{major}=31.4 min.

[α]_D²⁵ = 49.3° (c = 1.0, CHCl₃).

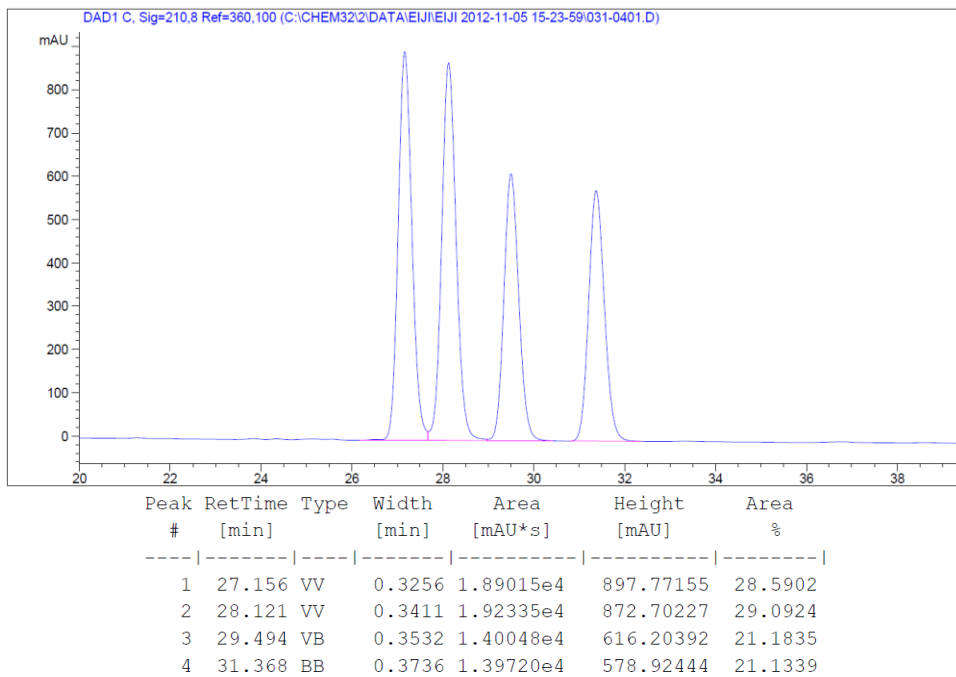
^1H NMR of **3.8i**



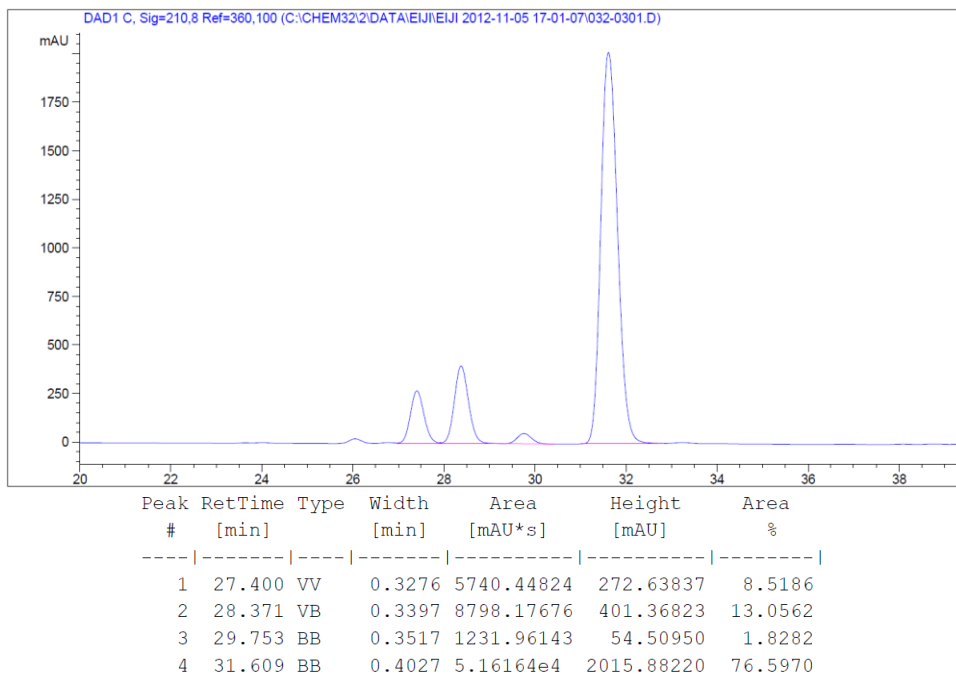
^{13}C NMR of **3.8i**



HPLC of *rac*-3.8i



HPLC of 3.8i



(3*R*,4*R*)-1-(6-bromopyridin-2-yl)-4-methylhex-5-en-3-ol (**3.8j**)

In accordance with the general procedure using alcohol **3.7j**, upon stirring at 95 °C for 72 h, the reaction mixture was concentrated *in vacuo* to afford the crude product (dr = 3.8:1 *syn:anti*, as determined by ¹H NMR spectroscopy). The reaction mixture was then subjected to flash column chromatography (SiO₂: 0-10% EtOAc/hexanes) to furnish **3.8j** (52 mg, 0.19 mmol, 63% yield, 96% ee) as a clear, colorless oil.

TLC (SiO₂): R_f = 0.3 (hexanes:EtOAc = 4:1).

¹H NMR (400 MHz, CDCl₃): δ 7.45 (dd, *J* = 7.8, 7.4 Hz, 1H), 7.32 (*J* = 7.8 Hz, 1H), 7.12 (d, *J* = 7.6 Hz, 1H), 5.82-5.74 (m, 1H), 5.12-5.05 (m, 2H), 3.51 (ddd, *J* = 9.8, 5.4, 2.9 Hz, 1H), 3.01-2.96 (m, 1H), 2.89-2.76 (m, 1H), 2.33-2.28 (m, 1H), 1.98-1.93 (m, 1H), 1.79-1.68 (m, 1H), 1.05 ppm (d, *J* = 6.9 Hz, 1H).

¹³C NMR (100 MHz, CDCl₃): δ 163.6, 141.4, 140.8, 138.8, 125.4, 121.8, 115.4, 74.2, 43.9, 34.6, 33.5, 14.7 ppm.

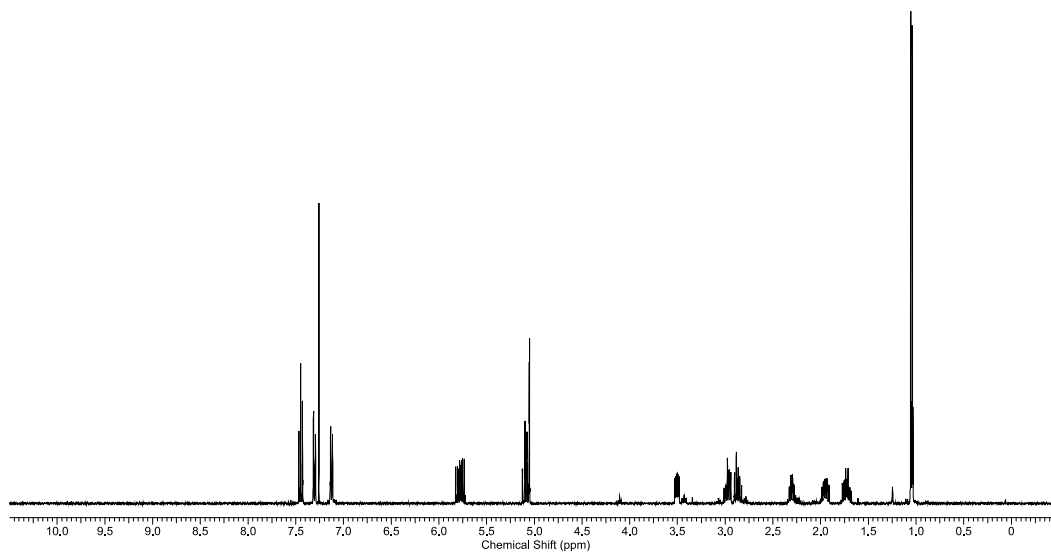
LRMS (Cl⁺): *m/z* 270 [M]⁺.

FTIR (neat): 3376, 2961, 1582, 1552, 1436, 1405, 1121, 985, 909, 789, 730 cm⁻¹.

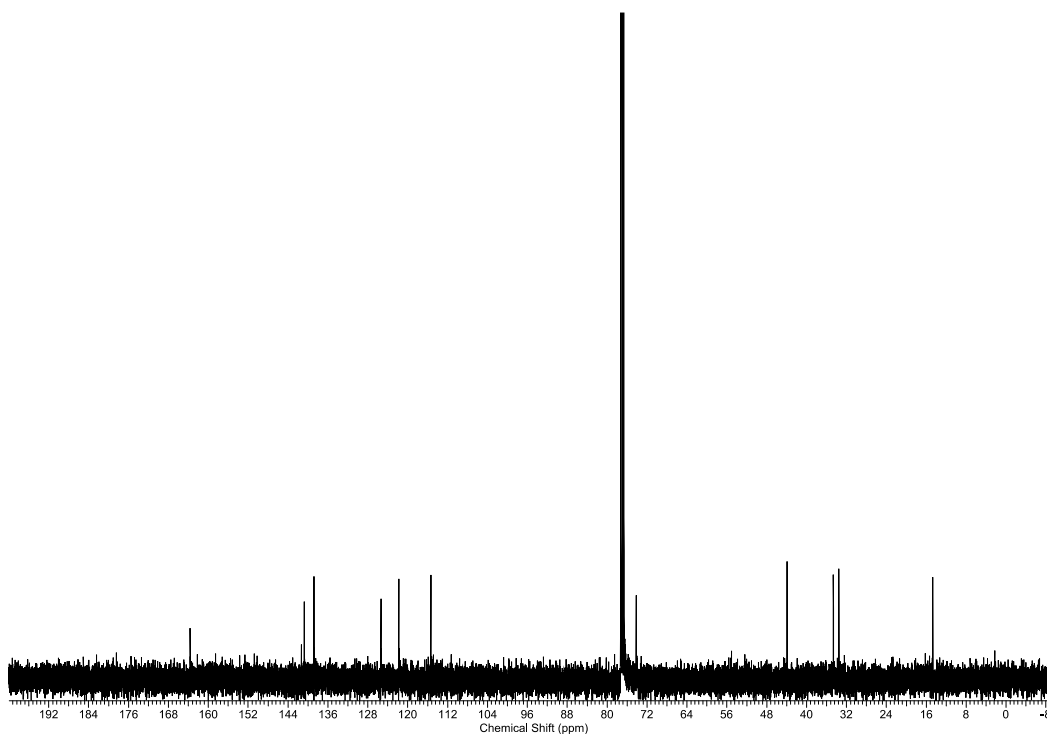
HPLC (Chiralcel OD-H column, hexanes : *i*PrOH = 99:1, 0.4 mL/min, 254 nm): *t*_{minor}=49.0 min, *t*_{major}=62.4 min.

[α]_D²⁵ = -95.6° (c = 1.0, CHCl₃).

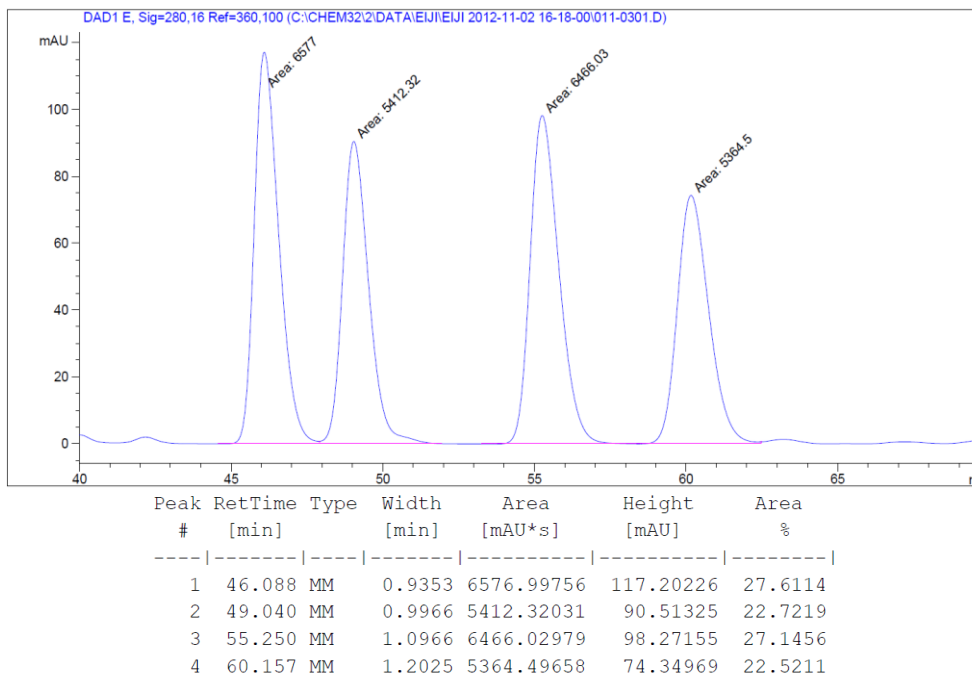
¹H NMR of **3.8j**



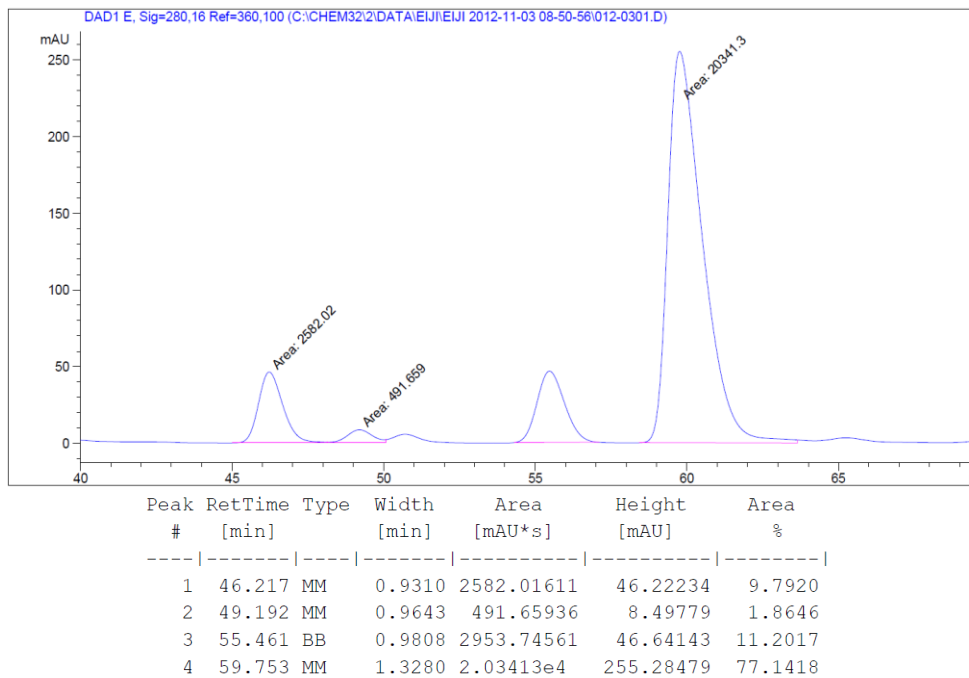
¹³C NMR of **3.8j**



HPLC of *rac*-3.8j



HPLC of 3.8j



3.5.9 Crystal Data and Structure Refinement for 3.10

Empirical formula	C76 H67 O14 P3 Ru	
Formula weight	1398.28	
Temperature	153(2) K	
Wavelength	0.71075 Å	
Crystal system	Monoclinic	
Space group	I2	
Unit cell dimensions	a = 25.919(4) Å	$\alpha = 90^\circ$.
	b = 11.0585(18) Å	$\beta = 115.146(12)^\circ$.
	c = 26.886(4) Å	$\gamma = 90^\circ$.
Volume	6976.1(19) Å ³	
Z	4	
Density (calculated)	1.331 Mg/m ³	
Absorption coefficient	0.358 mm ⁻¹	
F(000)	2896	
Crystal size	0.58 x 0.18 x 0.03 mm	
Theta range for data collection	3.00 to 27.47°.	
Index ranges	-33<=h<=33, -14<=k<=14, -34<=l<=34	
Reflections collected	33971	
Independent reflections	15604 [R(int) = 0.1148]	
Completeness to theta = 27.47°	99.6 %	
Max. and min. transmission	1.00 and 0.525	
Refinement method	Full-matrix least-squares on F ²	
Data / restraints / parameters	15604 / 19 / 837	
Goodness-of-fit on F ²	1.018	
Final R indices [I>2sigma(I)]	R1 = 0.0757, wR2 = 0.1487	
R indices (all data)	R1 = 0.1357, wR2 = 0.1790	
Absolute structure parameter	0.02(3)	
Largest diff. peak and hole	0.968 and -0.632 e.Å ⁻³	

Table 3.4 Atomic coordinates ($\times 10^4$) and equivalent isotropic displacement parameters ($\text{\AA}^2 \times 10^3$) for **3.10**. $U(\text{eq})$ is defined as one third of the trace of the orthogonalized U_{ij} tensor.

	x	y	z	$U(\text{eq})$
Ru1	2832(1)	5822(1)	764(1)	28(1)
P1	2977(1)	7654(2)	445(1)	30(1)
P2	2293(1)	6645(2)	1175(1)	29(1)
P3	1932(1)	4737(2)	-495(1)	26(1)
O1	3932(2)	11328(5)	2216(2)	54(2)
O2	2992(2)	10784(5)	1932(2)	43(1)
O3	1268(2)	11515(5)	384(2)	46(2)
O4	2256(2)	11358(4)	782(2)	42(1)
O5	2109(2)	5430(4)	34(2)	28(1)
O6	2015(2)	3404(4)	-478(2)	33(1)
O7	1272(2)	5130(4)	-797(2)	31(1)
O8	2224(2)	5425(4)	-831(2)	28(1)
O9	733(2)	5122(4)	-2311(2)	38(1)
O10	1549(2)	4205(5)	-2232(2)	39(1)
O11	3269(2)	4618(4)	445(2)	33(1)
O12	2844(2)	3875(4)	945(2)	34(1)
O13	3915(2)	6198(4)	1762(2)	48(2)
C1	3487(3)	7429(7)	144(3)	38(2)
C2	3955(3)	6727(7)	399(4)	49(2)
C3	4319(3)	6466(8)	155(4)	58(2)
C4	4198(4)	6887(10)	-360(5)	70(3)
C5	3721(4)	7587(10)	-636(4)	62(3)
C6	3364(3)	7873(8)	-382(3)	47(2)
C7	2405(3)	8579(6)	-64(3)	30(2)
C8	1846(3)	8153(7)	-357(3)	36(2)
C9	1437(3)	8877(7)	-736(3)	48(2)
C10	1589(4)	10061(7)	-835(3)	50(2)
C11	2142(4)	10467(7)	-537(3)	50(2)
C12	2536(3)	9751(6)	-163(3)	33(2)
C13	3307(3)	8740(6)	1002(3)	31(2)

Table 3.4, continued.

C14	3882(3)	9027(6)	1202(3)	36(2)
C15	4144(3)	9885(6)	1625(3)	39(2)
C16	3798(3)	10426(7)	1824(3)	40(2)
C17	3387(3)	11785(7)	2156(4)	52(2)
C18	3231(3)	10135(6)	1653(3)	30(2)
C19	2952(3)	9276(6)	1238(3)	30(2)
C20	2319(3)	9180(6)	999(3)	30(2)
C21	1976(3)	8159(6)	968(3)	31(2)
C22	1376(3)	8266(6)	734(3)	35(2)
C23	1087(3)	9364(6)	524(3)	39(2)
C24	1422(3)	10346(6)	559(3)	32(2)
C25	1793(3)	12170(6)	517(3)	40(2)
C26	2026(3)	10259(7)	795(3)	35(2)
C27	1680(3)	5705(7)	1099(3)	33(2)
C28	1329(3)	5177(7)	590(3)	47(2)
C29	849(3)	4493(7)	544(4)	57(3)
C30	709(4)	4365(8)	986(4)	52(2)
C31	1043(4)	4914(10)	1476(4)	69(3)
C32	1520(3)	5553(8)	1528(3)	53(2)
C33	2679(3)	6711(6)	1926(3)	35(2)
C34	2680(3)	7719(7)	2231(3)	39(2)
C35	2972(4)	7707(8)	2812(3)	53(2)
C36	3254(3)	6658(9)	3068(3)	52(2)
C37	3250(3)	5619(9)	2768(3)	48(2)
C38	2972(3)	5647(7)	2200(3)	42(2)
C39	839(3)	5122(6)	-1360(3)	26(2)
C40	464(3)	6212(6)	-1367(3)	32(2)
C41	343(3)	6421(6)	-926(3)	39(2)
C42	5(3)	7377(8)	-919(4)	53(2)
C43	-231(3)	8152(7)	-1356(4)	45(2)
C44	-129(3)	7959(7)	-1803(3)	47(2)
C45	226(3)	7009(7)	-1813(3)	43(2)
C46	487(3)	3946(6)	-1473(3)	32(2)
C47	649(3)	2981(7)	-1119(3)	47(2)
C48	313(3)	1941(8)	-1224(4)	62(3)

Table 3.4, continued.

C49	-193(3)	1867(8)	-1691(4)	61(3)
C50	-362(3)	2845(8)	-2056(4)	54(2)
C51	-33(3)	3876(7)	-1950(3)	39(2)
C52	1136(3)	5308(7)	-1748(3)	34(2)
C53	1016(3)	4617(8)	-2616(3)	48(2)
C54	1621(3)	4424(6)	-1683(3)	32(2)
C55	1113(5)	5597(13)	-2960(4)	117(5)
C56	668(4)	3575(10)	-2957(5)	105(5)
C57	2233(3)	4897(7)	-1335(3)	33(2)
C58	2382(3)	5950(8)	-1614(3)	38(2)
C59	2242(3)	7146(7)	-1549(3)	45(2)
C60	2380(4)	8104(8)	-1815(4)	59(3)
C61	2658(4)	7878(10)	-2133(4)	61(3)
C62	2799(4)	6726(11)	-2189(4)	68(3)
C63	2674(3)	5736(10)	-1931(3)	48(2)
C64	2681(3)	3900(7)	-1169(3)	32(2)
C65	3225(3)	4165(8)	-767(3)	50(2)
C66	3663(3)	3298(9)	-622(4)	61(3)
C67	3549(4)	2190(9)	-882(4)	66(3)
C68	3005(4)	1915(8)	-1265(4)	57(2)
C69	2575(3)	2774(7)	-1415(3)	46(2)
C70	3129(3)	3702(7)	649(3)	36(2)
C71	3289(3)	2446(6)	540(4)	48(2)
C72	3486(3)	6084(7)	1379(3)	39(2)
O1A	5002(11)	1789(17)	212(8)	168(4)
C1A	4596(14)	10(20)	386(13)	168(4)
C2A	4905(10)	705(17)	121(9)	168(4)
C3A	5076(18)	20(20)	-245(15)	168(4)
C4A	5328(14)	800(30)	-544(11)	168(4)
O1B	5314(8)	5657(18)	1465(7)	168(4)
C1B	4905(11)	3700(20)	1296(11)	168(4)
C2B	5334(7)	4617(18)	1633(7)	168(4)
C3B	5759(11)	4200(20)	2155(8)	168(4)
C4B	5824(13)	5160(30)	2569(7)	168(4)

Table 3.5 Bond lengths [Å] and angles [°] for **3.10**.

Ru1-C72	1.818(7)	C1-C2	1.354(10)
Ru1-O5	2.106(4)	C1-C6	1.401(11)
Ru1-O11	2.148(5)	C2-C3	1.389(11)
Ru1-O12	2.204(4)	C2-H2	0.95
Ru1-P1	2.292(2)	C3-C4	1.366(13)
Ru1-P2	2.305(2)	C3-H3	0.95
Ru1-C70	2.527(7)	C4-C5	1.378(12)
P1-C13	1.823(7)	C4-H4	0.95
P1-C1	1.836(8)	C5-C6	1.398(11)
P1-C7	1.843(7)	C5-H5	0.95
P2-C33	1.835(7)	C6-H6	0.95
P2-C27	1.835(7)	C7-C12	1.393(9)
P2-C21	1.844(7)	C7-C8	1.405(9)
P3-O6	1.487(5)	C8-C9	1.372(10)
P3-O5	1.505(4)	C8-H8	0.95
P3-O8	1.596(5)	C9-C10	1.424(11)
P3-O7	1.611(4)	C9-H9	0.95
O1-C16	1.384(8)	C10-C11	1.387(11)
O1-C17	1.443(9)	C10-H10	0.95
O2-C18	1.362(8)	C11-C12	1.344(10)
O2-C17	1.453(9)	C11-H11	0.95
O3-C24	1.375(8)	C12-H12	0.95
O3-C25	1.447(8)	C13-C14	1.390(9)
O4-C26	1.361(8)	C13-C19	1.448(9)
O4-C25	1.424(8)	C14-C15	1.413(9)
O7-C39	1.452(7)	C14-H14	0.95
O8-C57	1.485(8)	C15-C16	1.362(10)
O9-C53	1.428(8)	C15-H15	0.95
O9-C52	1.443(7)	C16-C18	1.381(9)
O10-C53	1.403(8)	C17-H17A	0.99
O10-C54	1.428(8)	C17-H17B	0.99
O11-C70	1.275(8)	C18-C19	1.410(9)
O12-C70	1.309(9)	C19-C20	1.488(9)
O13-C72	1.159(7)	C20-C26	1.396(9)

Table 3.5, continued.

C20-C21	1.417(9)	C40-C45	1.403(10)
C21-C22	1.414(9)	C41-C42	1.378(10)
C22-C23	1.413(9)	C41-H41	0.95
C22-H22	0.95	C42-C43	1.371(11)
C23-C24	1.369(9)	C42-H42	0.95
C23-H23	0.95	C43-C44	1.352(11)
C24-C26	1.419(9)	C43-H43	0.95
C25-H25A	0.99	C44-C45	1.405(10)
C25-H25B	0.99	C44-H44	0.95
C27-C32	1.392(9)	C45-H45	0.95
C27-C28	1.409(10)	C46-C47	1.371(10)
C28-C29	1.416(10)	C46-C51	1.413(9)
C28-H28	0.95	C47-C48	1.398(10)
C29-C30	1.389(11)	C47-H47	0.95
C29-H29	0.95	C48-C49	1.379(11)
C30-C31	1.372(12)	C48-H48	0.95
C30-H30	0.95	C49-C50	1.400(12)
C31-C32	1.378(11)	C49-H49	0.95
C31-H31	0.95	C50-C51	1.378(11)
C32-H32	0.95	C50-H50	0.95
C33-C34	1.383(10)	C51-H51	0.95
C33-C38	1.425(10)	C52-C54	1.544(9)
C34-C35	1.418(10)	C52-H52	1.00
C34-H34	0.95	C53-C56	1.509(12)
C35-C36	1.388(12)	C53-C55	1.513(13)
C35-H35	0.95	C54-C57	1.549(9)
C36-C37	1.401(12)	C54-H54	1.00
C36-H36	0.95	C55-H55A	0.98
C37-C38	1.383(9)	C55-H55B	0.98
C37-H37	0.95	C55-H55C	0.98
C38-H38	0.95	C56-H56A	0.98
C39-C40	1.544(9)	C56-H56B	0.98
C39-C46	1.543(9)	C56-H56C	0.98
C39-C52	1.548(9)	C57-C58	1.522(10)
C40-C41	1.368(10)	C57-C64	1.524(9)

Table 3.5, continued.

C58-C63	1.380(9)	C71-H71C	0.98
C58-C59	1.401(12)	O1A-C2A	1.228(9)
C59-C60	1.407(10)	C1A-C2A	1.494(9)
C59-H59	0.95	C1A-H1A1	0.98
C60-C61	1.356(12)	C1A-H1A2	0.98
C60-H60	0.95	C1A-H1A3	0.98
C61-C62	1.351(13)	C2A-C3A	1.453(9)
C61-H61	0.95	C3A-C4A	1.507(10)
C62-C63	1.406(13)	C3A-H3A1	0.99
C62-H62	0.95	C3A-H3A2	0.99
C63-H63	0.95	C4A-H4A1	0.98
C64-C69	1.381(10)	C4A-H4A2	0.98
C64-C65	1.398(9)	C4A-H4A3	0.98
C65-C66	1.407(11)	O1B-C2B	1.229(9)
C65-H65	0.95	C1B-C2B	1.495(9)
C66-C67	1.379(12)	C1B-H1B1	0.98
C66-H66	0.95	C1B-H1B2	0.98
C67-C68	1.381(12)	C1B-H1B3	0.98
C67-H67	0.95	C2B-C3B	1.444(9)
C68-C69	1.387(10)	C3B-C4B	1.493(10)
C68-H68	0.95	C3B-H3B1	0.99
C69-H69	0.95	C3B-H3B2	0.99
C70-C71	1.513(10)	C4B-H4B1	0.98
C71-H71A	0.98	C4B-H4B2	0.98
C71-H71B	0.98	C4B-H4B3	0.98
C72-Ru1-O5	175.9(3)	O12-Ru1-P1	163.02(14)
C72-Ru1-O11	91.0(3)	C72-Ru1-P2	91.2(2)
O5-Ru1-O11	84.95(16)	O5-Ru1-P2	92.66(13)
C72-Ru1-O12	92.0(3)	O11-Ru1-P2	164.95(13)
O5-Ru1-O12	85.85(16)	O12-Ru1-P2	103.58(14)
O11-Ru1-O12	61.45(18)	P1-Ru1-P2	93.39(7)
C72-Ru1-P1	87.8(2)	C72-Ru1-C70	92.6(3)
O5-Ru1-P1	93.21(12)	O5-Ru1-C70	83.76(19)
O11-Ru1-P1	101.57(14)	O11-Ru1-C70	30.3(2)

Table 3.5, continued.

O12-Ru1-C70	31.2(2)	C1-C2-C3	121.5(9)
P1-Ru1-C70	131.86(19)	C1-C2-H2	119.2
P2-Ru1-C70	134.7(2)	C3-C2-H2	119.2
C13-P1-C1	106.1(3)	C4-C3-C2	119.9(8)
C13-P1-C7	101.1(3)	C4-C3-H3	120.0
C1-P1-C7	104.5(3)	C2-C3-H3	120.0
C13-P1-Ru1	111.7(2)	C3-C4-C5	120.2(9)
C1-P1-Ru1	107.9(3)	C3-C4-H4	119.9
C7-P1-Ru1	124.1(2)	C5-C4-H4	119.9
C33-P2-C27	100.7(3)	C4-C5-C6	119.5(9)
C33-P2-C21	105.1(3)	C4-C5-H5	120.2
C27-P2-C21	103.2(3)	C6-C5-H5	120.2
C33-P2-Ru1	112.6(2)	C5-C6-C1	120.0(8)
C27-P2-Ru1	113.3(2)	C5-C6-H6	120.0
C21-P2-Ru1	119.8(2)	C1-C6-H6	120.0
O6-P3-O5	119.5(3)	C12-C7-C8	118.8(6)
O6-P3-O8	113.2(3)	C12-C7-P1	118.3(5)
O5-P3-O8	105.4(2)	C8-C7-P1	122.9(5)
O6-P3-O7	113.0(3)	C9-C8-C7	120.5(7)
O5-P3-O7	99.8(2)	C9-C8-H8	119.8
O8-P3-O7	104.1(2)	C7-C8-H8	119.8
C16-O1-C17	104.5(6)	C8-C9-C10	119.2(7)
C18-O2-C17	102.9(5)	C8-C9-H9	120.4
C24-O3-C25	106.2(5)	C10-C9-H9	120.4
C26-O4-C25	106.9(5)	C11-C10-C9	119.3(7)
P3-O5-Ru1	141.1(3)	C11-C10-H10	120.3
C39-O7-P3	135.1(4)	C9-C10-H10	120.3
C57-O8-P3	121.6(4)	C12-C11-C10	120.7(7)
C53-O9-C52	109.8(5)	C12-C11-H11	119.6
C53-O10-C54	111.3(5)	C10-C11-H11	119.6
C70-O11-Ru1	91.5(4)	C11-C12-C7	121.4(7)
C70-O12-Ru1	88.2(4)	C11-C12-H12	119.3
C2-C1-C6	118.8(8)	C7-C12-H12	119.3
C2-C1-P1	120.8(7)	C14-C13-C19	120.9(6)
C6-C1-P1	120.0(6)	C14-C13-P1	121.3(6)

Table 3.5, continued.

C19-C13-P1	117.8(5)	C23-C24-C26	121.5(7)
C13-C14-C15	122.3(7)	O3-C24-C26	108.9(6)
C13-C14-H14	118.8	O4-C25-O3	108.2(5)
C15-C14-H14	118.8	O4-C25-H25A	110.1
C16-C15-C14	116.1(6)	O3-C25-H25A	110.1
C16-C15-H15	121.9	O4-C25-H25B	110.1
C14-C15-H15	121.9	O3-C25-H25B	110.1
C15-C16-C18	123.5(7)	H25A-C25-H25B	108.4
C15-C16-O1	128.5(7)	O4-C26-C20	126.9(6)
C18-C16-O1	107.9(7)	O4-C26-C24	109.9(6)
O1-C17-O2	105.4(6)	C20-C26-C24	123.2(7)
O1-C17-H17A	110.7	C32-C27-C28	117.2(7)
O2-C17-H17A	110.7	C32-C27-P2	121.7(6)
O1-C17-H17B	110.7	C28-C27-P2	121.0(6)
O2-C17-H17B	110.7	C27-C28-C29	119.2(8)
H17A-C17-H17B	108.8	C27-C28-H28	120.4
O2-C18-C16	111.3(6)	C29-C28-H28	120.4
O2-C18-C19	126.3(6)	C30-C29-C28	121.3(8)
C16-C18-C19	122.4(7)	C30-C29-H29	119.3
C18-C19-C13	114.6(6)	C28-C29-H29	119.3
C18-C19-C20	119.3(6)	C31-C30-C29	119.2(8)
C13-C19-C20	124.8(6)	C31-C30-H30	120.4
C26-C20-C21	115.7(6)	C29-C30-H30	120.4
C26-C20-C19	115.2(6)	C30-C31-C32	119.8(9)
C21-C20-C19	129.1(6)	C30-C31-H31	120.1
C22-C21-C20	120.3(6)	C32-C31-H31	120.1
C22-C21-P2	118.3(5)	C31-C32-C27	123.3(8)
C20-C21-P2	121.2(5)	C31-C32-H32	118.3
C23-C22-C21	123.1(7)	C27-C32-H32	118.3
C23-C22-H22	118.5	C34-C33-C38	119.4(7)
C21-C22-H22	118.5	C34-C33-P2	123.2(6)
C24-C23-C22	116.2(6)	C38-C33-P2	117.3(5)
C24-C23-H23	121.9	C33-C34-C35	120.8(7)
C22-C23-H23	121.9	C33-C34-H34	119.6
C23-C24-O3	129.6(6)	C35-C34-H34	119.6

Table 3.5, continued.

C36-C35-C34	118.4(8)	C44-C45-H45	119.7
C36-C35-H35	120.8	C47-C46-C51	118.6(7)
C34-C35-H35	120.8	C47-C46-C39	122.6(6)
C35-C36-C37	121.8(7)	C51-C46-C39	118.8(6)
C35-C36-H36	119.1	C46-C47-C48	121.3(7)
C37-C36-H36	119.1	C46-C47-H47	119.3
C38-C37-C36	119.3(8)	C48-C47-H47	119.3
C38-C37-H37	120.3	C49-C48-C47	120.1(8)
C36-C37-H37	120.3	C49-C48-H48	119.9
C37-C38-C33	120.2(7)	C47-C48-H48	119.9
C37-C38-H38	119.9	C48-C49-C50	119.1(8)
C33-C38-H38	119.9	C48-C49-H49	120.5
O7-C39-C40	102.2(5)	C50-C49-H49	120.5
O7-C39-C46	109.9(5)	C51-C50-C49	120.8(8)
C40-C39-C46	109.8(5)	C51-C50-H50	119.6
O7-C39-C52	108.4(5)	C49-C50-H50	119.6
C40-C39-C52	112.2(6)	C50-C51-C46	120.1(8)
C46-C39-C52	113.6(5)	C50-C51-H51	120.0
C41-C40-C45	117.0(7)	C46-C51-H51	120.0
C41-C40-C39	119.8(6)	O9-C52-C54	102.7(5)
C45-C40-C39	123.2(7)	O9-C52-C39	110.0(5)
C40-C41-C42	121.6(8)	C54-C52-C39	117.0(6)
C40-C41-H41	119.2	O9-C52-H52	108.9
C42-C41-H41	119.2	C54-C52-H52	108.9
C43-C42-C41	121.4(8)	C39-C52-H52	108.9
C43-C42-H42	119.3	O10-C53-O9	106.8(5)
C41-C42-H42	119.3	O10-C53-C56	110.3(7)
C44-C43-C42	118.7(7)	O9-C53-C56	109.1(7)
C44-C43-H43	120.7	O10-C53-C55	108.3(7)
C42-C43-H43	120.7	O9-C53-C55	109.4(7)
C43-C44-C45	120.7(7)	C56-C53-C55	112.8(9)
C43-C44-H44	119.6	O10-C54-C52	104.3(5)
C45-C44-H44	119.6	O10-C54-C57	109.4(5)
C40-C45-C44	120.6(8)	C52-C54-C57	115.5(6)
C40-C45-H45	119.7	O10-C54-H54	109.1

Table 3.5, continued.

C52-C54-H54	109.1	C58-C63-C62	118.2(10)
C57-C54-H54	109.1	C58-C63-H63	120.9
C53-C55-H55A	109.5	C62-C63-H63	120.9
C53-C55-H55B	109.5	C69-C64-C65	119.3(7)
H55A-C55-H55B	109.5	C69-C64-C57	122.7(6)
C53-C55-H55C	109.5	C65-C64-C57	117.9(7)
H55A-C55-H55C	109.5	C64-C65-C66	120.1(8)
H55B-C55-H55C	109.5	C64-C65-H65	119.9
C53-C56-H56A	109.5	C66-C65-H65	119.9
C53-C56-H56B	109.5	C67-C66-C65	119.4(8)
H56A-C56-H56B	109.5	C67-C66-H66	120.3
C53-C56-H56C	109.5	C65-C66-H66	120.3
H56A-C56-H56C	109.5	C66-C67-C68	120.3(8)
H56B-C56-H56C	109.5	C66-C67-H67	119.8
O8-C57-C58	104.8(6)	C68-C67-H67	119.8
O8-C57-C64	108.8(5)	C67-C68-C69	120.4(8)
C58-C57-C64	112.1(6)	C67-C68-H68	119.8
O8-C57-C54	106.0(5)	C69-C68-H68	119.8
C58-C57-C54	111.7(6)	C64-C69-C68	120.4(7)
C64-C57-C54	112.9(6)	C64-C69-H69	119.8
C63-C58-C59	118.6(8)	C68-C69-H69	119.8
C63-C58-C57	119.6(8)	O11-C70-O12	118.8(6)
C59-C58-C57	121.8(7)	O11-C70-C71	119.7(7)
C58-C59-C60	120.8(8)	O12-C70-C71	121.5(7)
C58-C59-H59	119.6	O11-C70-Ru1	58.2(4)
C60-C59-H59	119.6	O12-C70-Ru1	60.7(3)
C61-C60-C59	120.0(9)	C71-C70-Ru1	176.3(6)
C61-C60-H60	120.0	C70-C71-H71A	109.5
C59-C60-H60	120.0	C70-C71-H71B	109.5
C62-C61-C60	119.1(9)	H71A-C71-H71B	109.5
C62-C61-H61	120.5	C70-C71-H71C	109.5
C60-C61-H61	120.5	H71A-C71-H71C	109.5
C61-C62-C63	123.3(9)	H71B-C71-H71C	109.5
C61-C62-H62	118.4	O13-C72-Ru1	176.2(7)
C63-C62-H62	118.4	C2A-C1A-H1A1	109.5

Table 3.5, continued.

C2A-C1A-H1A2	109.5	C2B-C1B-H1B1	109.5
H1A1-C1A-H1A2	109.5	C2B-C1B-H1B2	109.5
C2A-C1A-H1A3	109.5	H1B1-C1B-H1B2	109.5
H1A1-C1A-H1A3	109.5	C2B-C1B-H1B3	109.5
H1A2-C1A-H1A3	109.5	H1B1-C1B-H1B3	109.5
O1A-C2A-C3A	123.4(9)	H1B2-C1B-H1B3	109.5
O1A-C2A-C1A	121.0(9)	O1B-C2B-C3B	123.5(10)
C3A-C2A-C1A	115.6(8)	O1B-C2B-C1B	120.7(9)
C2A-C3A-C4A	112.7(9)	C3B-C2B-C1B	115.8(8)
C2A-C3A-H3A1	109.0	C2B-C3B-C4B	107.1(10)
C4A-C3A-H3A1	109.0	C2B-C3B-H3B1	110.3
C2A-C3A-H3A2	109.0	C4B-C3B-H3B1	110.3
C4A-C3A-H3A2	109.0	C2B-C3B-H3B2	110.3
H3A1-C3A-H3A2	107.8	C4B-C3B-H3B2	110.3
C3A-C4A-H4A1	109.5	H3B1-C3B-H3B2	108.5
C3A-C4A-H4A2	109.5	C3B-C4B-H4B1	109.5
H4A1-C4A-H4A2	109.5	C3B-C4B-H4B2	109.5
C3A-C4A-H4A3	109.5	H4B1-C4B-H4B2	109.5
H4A1-C4A-H4A3	109.5	C3B-C4B-H4B3	109.5
H4A2-C4A-H4A3	109.5	H4B1-C4B-H4B3	109.5
		H4B2-C4B-H4B3	109.5

Table 3.6 Anisotropic displacement parameters ($\text{\AA}^2 \times 10^3$) for **3.10**. The anisotropic displacement factor exponent takes the form: $-2\pi^2 [h^2 a^{*2} U^{11} + \dots + 2 h k a^* b^* U^{12}]$

	U ¹¹	U ²²	U ³³	U ²³	U ¹³	U ¹²
Ru1	25(1)	23(1)	31(1)	-1(1)	7(1)	-1(1)
P1	27(1)	26(1)	35(1)	-2(1)	12(1)	-3(1)
P2	30(1)	24(1)	31(1)	-1(1)	12(1)	-1(1)
P3	26(1)	23(1)	26(1)	0(1)	8(1)	-1(1)
O1	54(3)	48(4)	47(3)	-16(3)	9(3)	-12(3)
O2	47(3)	39(3)	41(3)	-12(3)	17(2)	-8(3)
O3	40(3)	30(3)	57(4)	11(3)	11(3)	5(2)
O4	35(3)	28(3)	54(4)	8(2)	10(3)	-1(2)
O5	29(2)	28(3)	20(2)	0(2)	5(2)	1(2)
O6	31(3)	26(3)	38(3)	-5(2)	9(2)	-3(2)
O7	26(2)	38(3)	23(3)	-2(2)	6(2)	2(2)
O8	29(2)	31(3)	21(2)	-6(2)	10(2)	-2(2)
O9	37(3)	52(3)	24(3)	-8(2)	12(2)	5(2)
O10	37(3)	54(3)	24(3)	-3(2)	9(2)	10(3)
O11	30(3)	27(3)	36(3)	5(2)	7(2)	1(2)
O12	32(3)	22(3)	38(3)	3(2)	7(2)	2(2)
O13	31(3)	49(4)	49(3)	-9(2)	3(3)	-6(2)
C1	26(4)	32(4)	54(5)	-3(4)	15(4)	-3(3)
C2	46(5)	34(5)	73(6)	-7(4)	30(5)	-8(4)
C3	39(5)	55(6)	77(7)	1(5)	23(5)	4(4)
C4	39(5)	93(8)	89(8)	-17(6)	37(6)	-1(5)
C5	50(5)	88(7)	53(6)	-16(5)	28(5)	-8(5)
C6	33(4)	59(6)	50(5)	-8(4)	17(4)	-7(4)
C7	30(4)	28(4)	32(4)	-1(3)	12(3)	2(3)
C8	34(4)	27(4)	43(5)	8(3)	12(4)	-4(3)
C9	37(4)	44(5)	51(5)	0(4)	8(4)	2(4)
C10	57(5)	42(5)	43(5)	10(4)	14(4)	7(4)
C11	76(6)	33(5)	40(5)	4(3)	24(5)	-6(4)
C12	43(4)	30(4)	23(4)	3(3)	12(3)	-4(3)
C13	35(4)	22(4)	35(4)	-4(3)	14(3)	-5(3)

Table 3.6, continued.

C14	30(4)	34(4)	37(4)	0(3)	8(3)	3(3)
C15	30(4)	31(4)	42(5)	-2(3)	4(4)	-7(3)
C16	45(4)	37(5)	28(4)	-4(3)	4(4)	-11(3)
C17	57(5)	44(5)	54(6)	-17(4)	24(5)	-13(4)
C18	37(4)	28(4)	22(4)	-1(3)	9(3)	-7(3)
C19	31(4)	27(4)	28(4)	-2(3)	8(3)	-5(3)
C20	35(4)	29(4)	21(4)	-1(3)	7(3)	2(3)
C21	39(4)	27(4)	26(4)	3(3)	13(3)	3(3)
C22	27(4)	32(4)	39(4)	4(3)	8(3)	-5(3)
C23	36(4)	35(4)	41(5)	5(3)	10(4)	7(3)
C24	30(4)	24(4)	39(5)	-1(3)	11(3)	2(3)
C25	38(4)	25(4)	58(5)	15(4)	23(4)	1(3)
C26	37(4)	27(4)	37(4)	-2(3)	11(4)	-5(3)
C27	36(3)	19(4)	46(4)	-4(4)	18(3)	3(3)
C28	36(4)	51(5)	59(6)	-14(4)	27(4)	-10(4)
C29	32(4)	49(6)	85(7)	-32(5)	19(5)	-16(4)
C30	47(5)	47(5)	67(6)	13(5)	27(5)	-1(4)
C31	47(5)	98(8)	63(7)	26(6)	24(5)	-12(5)
C32	42(4)	73(7)	35(4)	2(4)	9(4)	-19(4)
C33	45(4)	35(4)	26(4)	-5(3)	16(3)	-8(4)
C34	44(4)	32(4)	44(5)	0(4)	23(4)	4(4)
C35	67(6)	55(6)	34(5)	-13(4)	19(4)	-16(5)
C36	39(4)	79(7)	25(4)	0(4)	3(4)	-13(5)
C37	35(4)	60(7)	41(5)	19(4)	9(4)	1(4)
C38	44(4)	30(5)	43(4)	1(4)	11(3)	0(4)
C39	25(3)	30(4)	21(4)	0(3)	10(3)	-3(3)
C40	27(3)	27(4)	35(4)	-4(3)	8(3)	-2(3)
C41	41(4)	35(4)	55(5)	3(4)	33(4)	9(3)
C42	54(5)	49(5)	68(6)	-9(5)	36(5)	9(4)
C43	38(4)	32(4)	61(6)	0(4)	16(4)	13(4)
C44	43(5)	32(5)	42(5)	4(4)	-4(4)	12(4)
C45	44(4)	44(5)	38(5)	1(4)	16(4)	5(4)
C46	29(4)	35(4)	28(4)	-5(3)	9(3)	7(3)
C47	32(4)	39(5)	61(6)	8(4)	12(4)	4(4)
C48	38(5)	39(5)	97(8)	17(5)	18(5)	8(4)

Table 3.6, continued.

C49	38(5)	33(5)	105(8)	-21(5)	25(5)	-11(4)
C50	33(4)	64(6)	56(6)	-21(5)	10(4)	-11(4)
C51	31(4)	46(5)	35(5)	-11(4)	8(4)	-7(4)
C52	32(4)	43(4)	22(4)	5(3)	6(3)	1(3)
C53	44(4)	66(6)	32(5)	-8(4)	14(4)	7(4)
C54	40(4)	30(4)	25(4)	4(3)	12(3)	0(3)
C55	106(8)	186(14)	93(8)	99(10)	74(7)	91(10)
C56	55(6)	121(10)	119(10)	-81(8)	18(6)	15(6)
C57	23(3)	40(4)	35(4)	-4(3)	12(3)	-3(3)
C58	34(3)	47(5)	27(4)	6(4)	6(3)	-11(4)
C59	38(4)	40(5)	41(5)	10(4)	1(4)	-6(4)
C60	61(6)	56(6)	50(6)	16(5)	14(5)	-13(5)
C61	62(6)	68(7)	56(6)	21(5)	27(5)	-14(5)
C62	53(6)	101(9)	53(6)	9(6)	25(5)	-9(6)
C63	40(4)	72(6)	36(4)	10(5)	21(3)	6(5)
C64	28(4)	47(5)	26(4)	3(3)	16(3)	9(3)
C65	27(4)	63(6)	56(6)	-3(4)	14(4)	10(4)
C66	30(4)	68(7)	71(7)	-14(5)	8(4)	10(4)
C67	56(6)	69(7)	68(7)	6(5)	22(5)	43(5)
C68	54(5)	48(6)	67(6)	2(4)	24(5)	23(4)
C69	39(4)	52(5)	44(5)	-2(4)	15(4)	15(4)
C70	28(4)	28(4)	43(5)	-2(4)	7(4)	2(3)
C71	50(5)	19(4)	73(6)	0(4)	24(5)	1(4)
C72	28(3)	39(5)	45(5)	-7(4)	12(3)	-4(3)

Table 3.7 Hydrogen coordinates ($\times 10^4$) and isotropic displacement parameters ($\text{\AA}^2 \times 10^{-3}$) for **3.10**.

	x	y	z	U(eq)
H2	4035	6407	752	59
H3	4651	5994	347	70
H4	4444	6698	-529	84
H5	3635	7873	-996	74
H6	3039	8367	-567	57
H8	1749	7358	-292	44
H9	1057	8592	-929	57
H10	1314	10567	-1102	60
H11	2244	11260	-598	60
H12	2911	10050	38	39
H14	4107	8634	1049	43
H15	4538	10072	1762	46
H17A	3269	12485	1902	62
H17B	3405	12040	2516	62
H22	1157	7566	717	41
H23	683	9419	368	47
H25A	1803	12493	177	47
H25B	1821	12857	763	47
H28	1413	5278	281	56
H29	618	4114	205	69
H30	385	3903	950	63
H31	945	4855	1778	83
H32	1750	5907	1874	63
H34	2482	8427	2049	46
H35	2974	8400	3022	63
H36	3456	6643	3457	62
H37	3436	4903	2952	58
H38	2977	4955	1993	50
H41	496	5895	-618	47

Table 3.7, continued.

H42	-67	7501	-604	64
H43	-460	8812	-1345	54
H44	-300	8472	-2114	56
H45	305	6904	-2125	51
H47	997	3019	-797	56
H48	432	1284	-973	74
H49	-423	1162	-1764	73
H50	-707	2798	-2381	65
H51	-156	4540	-2197	47
H52	1284	6154	-1705	41
H54	1565	3649	-1520	38
H55A	754	5774	-3278	176
H55B	1397	5321	-3086	176
H55C	1252	6330	-2738	176
H56A	595	2996	-2718	157
H56B	878	3174	-3139	157
H56C	305	3879	-3235	157
H59	2052	7311	-1322	54
H60	2278	8909	-1772	71
H61	2753	8520	-2314	74
H62	2993	6578	-2414	82
H63	2787	4941	-1974	58
H65	3301	4931	-590	60
H66	4033	3475	-348	73
H67	3846	1613	-797	79
H68	2924	1134	-1428	68
H69	2205	2587	-1688	55
H71A	3200	2364	149	72
H71B	3072	1845	641	72
H71C	3697	2315	760	72
H1A1	4704	311	759	252
H1A2	4698	-851	402	252
H1A3	4184	100	171	252
H3A1	4740	-413	-517	202
H3A2	5360	-597	-28	202

Table 3.7, continued.

H4A1	5183	1629	-569	252
H4A2	5219	481	-915	252
H4A3	5744	804	-344	252
H1B1	5015	3370	1016	252
H1B2	4529	4079	1116	252
H1B3	4890	3041	1534	252
H3B1	6126	4061	2133	202
H3B2	5636	3430	2260	202
H4B1	6091	5774	2560	252
H4B2	5970	4796	2936	252
H4B3	5452	5531	2482	252

Table 3.8 Torsion angles [°] for **3.10**.

C72-Ru1-P1-C13	-34.3(3)	O12-Ru1-P2-C21	-161.4(3)
O5-Ru1-P1-C13	149.7(3)	P1-Ru1-P2-C21	18.3(3)
O11-Ru1-P1-C13	-124.8(3)	C70-Ru1-P2-C21	-158.9(3)
O12-Ru1-P1-C13	-124.0(5)	O6-P3-O5-Ru1	60.6(5)
P2-Ru1-P1-C13	56.9(3)	O8-P3-O5-Ru1	-68.1(4)
C70-Ru1-P1-C13	-125.8(3)	O7-P3-O5-Ru1	-175.7(4)
C72-Ru1-P1-C1	82.0(3)	O11-Ru1-O5-P3	-3.5(4)
O5-Ru1-P1-C1	-94.0(3)	O12-Ru1-O5-P3	-65.2(4)
O11-Ru1-P1-C1	-8.5(3)	P1-Ru1-O5-P3	97.8(4)
O12-Ru1-P1-C1	-7.7(5)	P2-Ru1-O5-P3	-168.6(4)
P2-Ru1-P1-C1	173.1(3)	C70-Ru1-O5-P3	-33.9(4)
C70-Ru1-P1-C1	-9.5(4)	O6-P3-O7-C39	-70.8(6)
C72-Ru1-P1-C7	-155.5(3)	O5-P3-O7-C39	161.2(5)
O5-Ru1-P1-C7	28.4(3)	O8-P3-O7-C39	52.5(6)
O11-Ru1-P1-C7	113.9(3)	O6-P3-O8-C57	37.1(5)
O12-Ru1-P1-C7	114.7(5)	O5-P3-O8-C57	169.5(4)
P2-Ru1-P1-C7	-64.4(3)	O7-P3-O8-C57	-86.0(5)
C70-Ru1-P1-C7	112.9(3)	C72-Ru1-O11-C70	93.5(5)
C72-Ru1-P2-C33	-18.1(3)	O5-Ru1-O11-C70	-86.3(4)
O5-Ru1-P2-C33	160.6(3)	O12-Ru1-O11-C70	1.7(4)
O11-Ru1-P2-C33	80.2(6)	P1-Ru1-O11-C70	-178.5(4)
O12-Ru1-P2-C33	74.2(3)	P2-Ru1-O11-C70	-4.9(7)
P1-Ru1-P2-C33	-106.0(3)	C72-Ru1-O12-C70	-91.7(4)
C70-Ru1-P2-C33	76.8(3)	O5-Ru1-O12-C70	84.8(4)
C72-Ru1-P2-C27	-131.6(3)	O11-Ru1-O12-C70	-1.7(4)
O5-Ru1-P2-C27	47.1(3)	P1-Ru1-O12-C70	-2.6(7)
O11-Ru1-P2-C27	-33.3(6)	P2-Ru1-O12-C70	176.5(3)
O12-Ru1-P2-C27	-39.3(3)	C13-P1-C1-C2	77.0(7)
P1-Ru1-P2-C27	140.5(3)	C7-P1-C1-C2	-176.6(6)
C70-Ru1-P2-C27	-36.7(3)	Ru1-P1-C1-C2	-42.8(7)
C72-Ru1-P2-C21	106.2(4)	C13-P1-C1-C6	-110.1(6)
O5-Ru1-P2-C21	-75.1(3)	C7-P1-C1-C6	-3.7(7)
O11-Ru1-P2-C21	-155.5(5)	Ru1-P1-C1-C6	130.1(6)

Table 3.8, continued.

C6-C1-C2-C3	1.6(12)	C16-O1-C17-O2	26.7(8)
P1-C1-C2-C3	174.5(6)	C18-O2-C17-O1	-27.5(8)
C1-C2-C3-C4	-2.1(13)	C17-O2-C18-C16	18.5(8)
C2-C3-C4-C5	1.0(14)	C17-O2-C18-C19	-160.9(7)
C3-C4-C5-C6	0.7(14)	C15-C16-C18-O2	177.9(7)
C4-C5-C6-C1	-1.2(13)	O1-C16-C18-O2	-2.0(8)
C2-C1-C6-C5	0.1(11)	C15-C16-C18-C19	-2.6(12)
P1-C1-C6-C5	-172.9(6)	O1-C16-C18-C19	177.4(6)
C13-P1-C7-C12	44.7(6)	O2-C18-C19-C13	178.6(6)
C1-P1-C7-C12	-65.4(6)	C16-C18-C19-C13	-0.8(10)
Ru1-P1-C7-C12	170.6(4)	O2-C18-C19-C20	11.2(11)
C13-P1-C7-C8	-135.5(6)	C16-C18-C19-C20	-168.2(7)
C1-P1-C7-C8	114.5(6)	C14-C13-C19-C18	3.3(10)
Ru1-P1-C7-C8	-9.5(7)	P1-C13-C19-C18	-178.1(5)
C12-C7-C8-C9	0.4(11)	C14-C13-C19-C20	169.9(7)
P1-C7-C8-C9	-179.4(6)	P1-C13-C19-C20	-11.4(9)
C7-C8-C9-C10	0.9(12)	C18-C19-C20-C26	54.2(9)
C8-C9-C10-C11	-1.6(12)	C13-C19-C20-C26	-111.9(8)
C9-C10-C11-C12	0.9(12)	C18-C19-C20-C21	-123.5(8)
C10-C11-C12-C7	0.4(12)	C13-C19-C20-C21	70.5(10)
C8-C7-C12-C11	-1.1(10)	C26-C20-C21-C22	0.8(10)
P1-C7-C12-C11	178.7(6)	C19-C20-C21-C22	178.5(7)
C1-P1-C13-C14	-13.9(7)	C26-C20-C21-P2	175.7(5)
C7-P1-C13-C14	-122.7(6)	C19-C20-C21-P2	-6.6(10)
Ru1-P1-C13-C14	103.5(6)	C33-P2-C21-C22	-113.9(6)
C1-P1-C13-C19	167.4(5)	C27-P2-C21-C22	-8.8(6)
C7-P1-C13-C19	58.6(6)	Ru1-P2-C21-C22	118.2(5)
Ru1-P1-C13-C19	-75.2(6)	C33-P2-C21-C20	71.1(6)
C19-C13-C14-C15	-2.7(11)	C27-P2-C21-C20	176.2(6)
P1-C13-C14-C15	178.7(5)	Ru1-P2-C21-C20	-56.8(6)
C13-C14-C15-C16	-0.6(11)	C20-C21-C22-C23	-0.2(11)
C14-C15-C16-C18	3.2(11)	P2-C21-C22-C23	-175.2(5)
C14-C15-C16-O1	-176.8(7)	C21-C22-C23-C24	-0.1(11)
C17-O1-C16-C15	164.4(8)	C22-C23-C24-O3	178.8(7)
C17-O1-C16-C18	-15.7(8)	C22-C23-C24-C26	-0.4(11)

Table 3.8, continued.

C25-O3-C24-C23	-179.2(8)	P2-C33-C34-C35	178.1(6)
C25-O3-C24-C26	0.1(8)	C33-C34-C35-C36	-0.3(12)
C26-O4-C25-O3	1.7(8)	C34-C35-C36-C37	-0.9(13)
C24-O3-C25-O4	-1.1(8)	C35-C36-C37-C38	2.0(12)
C25-O4-C26-C20	177.5(7)	C36-C37-C38-C33	-1.9(11)
C25-O4-C26-C24	-1.6(9)	C34-C33-C38-C37	0.7(11)
C21-C20-C26-O4	179.7(7)	P2-C33-C38-C37	-177.1(5)
C19-C20-C26-O4	1.6(11)	P3-O7-C39-C40	-149.8(5)
C21-C20-C26-C24	-1.3(11)	P3-O7-C39-C46	93.7(6)
C19-C20-C26-C24	-179.3(7)	P3-O7-C39-C52	-31.1(8)
C23-C24-C26-O4	-179.7(7)	O7-C39-C40-C41	-40.1(7)
O3-C24-C26-O4	1.0(9)	C46-C39-C40-C41	76.5(8)
C23-C24-C26-C20	1.1(12)	C52-C39-C40-C41	-156.1(6)
O3-C24-C26-C20	-178.2(7)	O7-C39-C40-C45	141.1(6)
C33-P2-C27-C32	19.3(7)	C46-C39-C40-C45	-102.2(7)
C21-P2-C27-C32	-89.2(7)	C52-C39-C40-C45	25.2(9)
Ru1-P2-C27-C32	139.8(6)	C45-C40-C41-C42	-0.5(11)
C33-P2-C27-C28	-165.3(6)	C39-C40-C41-C42	-179.3(6)
C21-P2-C27-C28	86.2(6)	C40-C41-C42-C43	0.8(12)
Ru1-P2-C27-C28	-44.8(7)	C41-C42-C43-C44	0.6(12)
C32-C27-C28-C29	-2.2(11)	C42-C43-C44-C45	-2.2(12)
P2-C27-C28-C29	-177.8(6)	C41-C40-C45-C44	-1.1(11)
C27-C28-C29-C30	2.0(12)	C39-C40-C45-C44	177.7(6)
C28-C29-C30-C31	0.1(13)	C43-C44-C45-C40	2.5(12)
C29-C30-C31-C32	-1.9(14)	O7-C39-C46-C47	-12.0(9)
C30-C31-C32-C27	1.7(14)	C40-C39-C46-C47	-123.6(7)
C28-C27-C32-C31	0.4(13)	C52-C39-C46-C47	109.8(8)
P2-C27-C32-C31	176.0(7)	O7-C39-C46-C51	165.7(6)
C27-P2-C33-C34	-104.3(7)	C40-C39-C46-C51	54.1(8)
C21-P2-C33-C34	2.6(7)	C52-C39-C46-C51	-72.5(8)
Ru1-P2-C33-C34	134.7(6)	C51-C46-C47-C48	0.3(12)
C27-P2-C33-C38	73.4(6)	C39-C46-C47-C48	178.0(7)
C21-P2-C33-C38	-179.6(5)	C46-C47-C48-C49	0.3(14)
Ru1-P2-C33-C38	-47.6(6)	C47-C48-C49-C50	-0.1(14)
C38-C33-C34-C35	0.4(11)	C48-C49-C50-C51	-0.7(14)

Table 3.8, continued.

C49-C50-C51-C46	1.3(12)	O8-C57-C58-C59	-28.2(8)
C47-C46-C51-C50	-1.1(11)	C64-C57-C58-C59	-146.0(7)
C39-C46-C51-C50	-178.8(7)	C54-C57-C58-C59	86.1(8)
C53-O9-C52-C54	-21.9(7)	C63-C58-C59-C60	2.1(10)
C53-O9-C52-C39	-147.2(6)	C57-C58-C59-C60	-179.4(6)
O7-C39-C52-O9	171.3(5)	C58-C59-C60-C61	-1.0(12)
C40-C39-C52-O9	-76.6(7)	C59-C60-C61-C62	0.0(13)
C46-C39-C52-O9	48.8(7)	C60-C61-C62-C63	-0.2(14)
O7-C39-C52-C54	54.7(7)	C59-C58-C63-C62	-2.2(10)
C40-C39-C52-C54	166.8(5)	C57-C58-C63-C62	179.3(7)
C46-C39-C52-C54	-67.9(7)	C61-C62-C63-C58	1.4(13)
C54-O10-C53-O9	0.2(8)	O8-C57-C64-C69	132.7(7)
C54-O10-C53-C56	-118.2(8)	C58-C57-C64-C69	-111.9(8)
C54-O10-C53-C55	117.9(8)	C54-C57-C64-C69	15.4(10)
C52-O9-C53-O10	14.5(8)	O8-C57-C64-C65	-49.9(8)
C52-O9-C53-C56	133.7(7)	C58-C57-C64-C65	65.5(8)
C52-O9-C53-C55	-102.5(8)	C54-C57-C64-C65	-167.3(6)
C53-O10-C54-C52	-13.4(7)	C69-C64-C65-C66	1.2(12)
C53-O10-C54-C57	-137.5(6)	C57-C64-C65-C66	-176.3(8)
O9-C52-C54-O10	21.0(7)	C64-C65-C66-C67	0.2(13)
C39-C52-C54-O10	141.5(6)	C65-C66-C67-C68	-2.5(15)
O9-C52-C54-C57	141.1(6)	C66-C67-C68-C69	3.6(15)
C39-C52-C54-C57	-98.3(7)	C65-C64-C69-C68	-0.2(12)
P3-O8-C57-C58	163.8(4)	C57-C64-C69-C68	177.2(7)
P3-O8-C57-C64	-76.1(6)	C67-C68-C69-C64	-2.2(13)
P3-O8-C57-C54	45.5(7)	Ru1-O11-C70-O12	-3.0(6)
O10-C54-C57-O8	164.3(5)	Ru1-O11-C70-C71	176.5(6)
C52-C54-C57-O8	47.0(7)	Ru1-O12-C70-O11	2.9(6)
O10-C54-C57-C58	50.7(8)	Ru1-O12-C70-C71	-176.6(6)
C52-C54-C57-C58	-66.5(8)	C72-Ru1-C70-O11	-87.5(4)
O10-C54-C57-C64	-76.7(7)	O5-Ru1-C70-O11	90.7(4)
C52-C54-C57-C64	166.0(6)	O12-Ru1-C70-O11	-177.0(6)
O8-C57-C58-C63	150.3(6)	P1-Ru1-C70-O11	1.9(5)
C64-C57-C58-C63	32.5(8)	P2-Ru1-C70-O11	178.2(3)
C54-C57-C58-C63	-95.4(7)	C72-Ru1-C70-O12	89.6(4)

Table 3.8, continued.

O5-Ru1-C70-O12	-92.3(4)	O1A-C2A-C3A-C4A	-6(3)
O11-Ru1-C70-O12	177.0(6)	C1A-C2A-C3A-C4A	174(3)
P1-Ru1-C70-O12	179.0(3)	O1B-C2B-C3B-C4B	43(2)
P2-Ru1-C70-O12	-4.7(5)	C1B-C2B-C3B-C4B	-137(2)

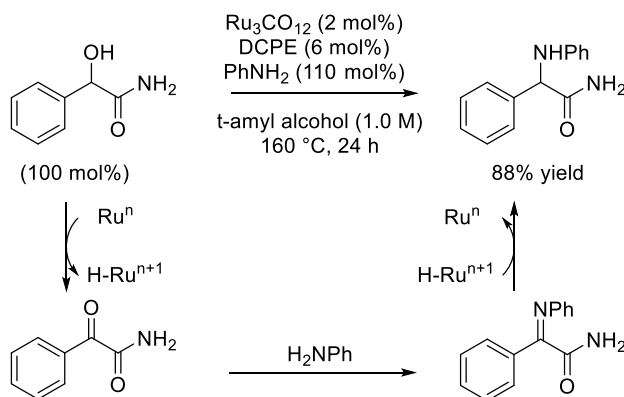
Chapter 4 Reductive Coupling to Ketones

4.1 Introduction

Research in the Krische group has established ruthenium catalyzed hydrogenative methods for allylation, crotylation, vinylation and propargylation via reductive coupling of aldehydes or redox-triggered coupling of the corresponding primary alcohols. Despite progress in understanding the reactivity and selectivity of these processes, reductive coupling to ketones or the redox-triggered coupling to secondary alcohols has remained a significant limitation. One specialized ketone, the cyclic keto-amide of isatin, has proven to be an exception, as it has been shown to participate in ruthenium and iridium catalyzed coupling via transfer hydrogenation.¹⁰⁵

To address this shortcoming, a literature survey of ruthenium catalysts that act on secondary alcohols was undertaken. One complex, $\text{Ru}_3(\text{CO})_{12}$, was found to embody two characteristics that are critical for transfer hydrogenative reductive coupling.^{74, 106} First, the complex had been reported by the Beller group to participate in a transfer hydrogenative amination of α -hydroxy amides (Scheme 4.1).³⁷

Scheme 4.1 Transfer hydrogenative amination of α -hydroxy amide.

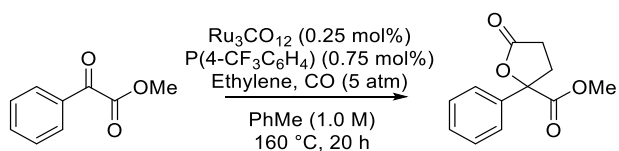


This occurs by a reductive amination pathway, in which ruthenium catalyzed β -hydride elimination forms a keto-amide and ruthenium-hydride. The resulting ketone can condense with

a primary amine to form an imine, which is then subjected to hydrogenation by the ruthenium hydride to produce an α -amino amide and regenerate the Ru^0 catalyst.

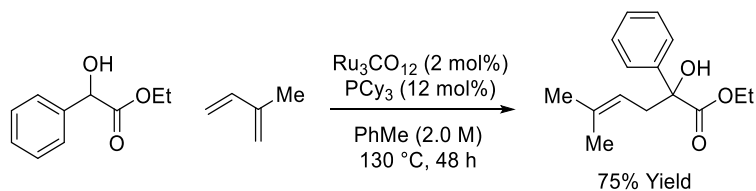
Second, Murai and coworkers reported a $\text{Ru}_3(\text{CO})_{12}$ catalyzed [2+2+1] oxidative coupling reaction of 1,2-dicarbonyl compounds, ethylene and carbon monoxide to furnish spiro lactone products (Scheme 4.2).¹⁰⁷ These reports demonstrate that a Ru^0 complex can perform transfer hydrogenative and oxidative coupling processes, suggesting that similar conditions could be amenable to transfer hydrogenative coupling of unsaturates to α -hydroxy carbonyl compounds.

Scheme 4.2 Oxidative coupling of an α -keto ester with ethylene and CO using $\text{Ru}_3(\text{CO})_{12}$.



This catalytic system was tested using ethyl mandelate as carbonyl precursor and isoprene as unsaturate. After rigorous optimization, it was found that the transfer hydrogenative, reductive coupling was successful (Scheme 4.3). The product exhibited coupling to the C4 position of isoprene, characteristic of an oxidative coupling mechanism and previously unobserved in other reductive coupling of dienes and aldehydes or ketones under ruthenium catalysis.³⁸

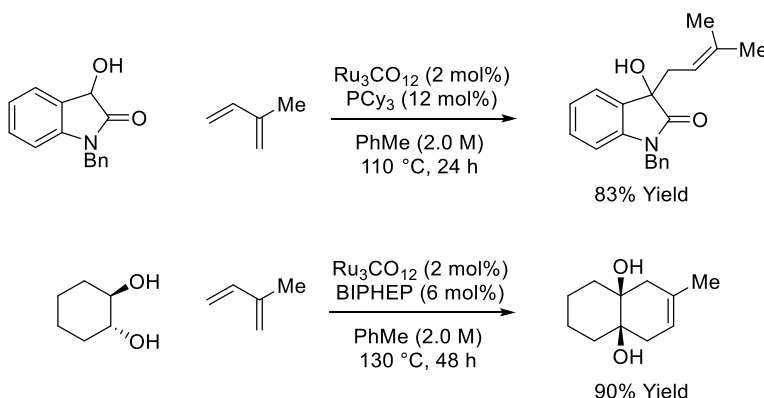
Scheme 4.3 Oxidative coupling of ethyl mandelate and isoprene under transfer hydrogenative conditions.



Slight variation of reaction conditions revealed that this catalyst was also effective for coupling isoprene to 3-hydroxyoxindole (Scheme 4.4, top),³⁹ a cyclic α -hydroxy amide, and to 1,2-diols, which form 1,2-diketones upon dehydrogenation. Interestingly, upon coupling to one ketone,

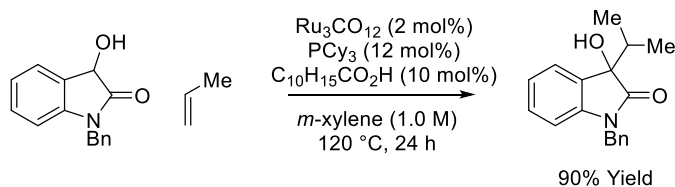
intramolecular addition to the adjacent carbonyl also occurred, furnishing a product of formal [4+2] cycloaddition (Scheme 4.4, bottom).⁴¹

Scheme 4.4 Oxidative coupling of 3-hydroxyoxindole or *trans*-1,2-cyclohexanediol with isoprene under transfer hydrogenative conditions.



The development of oxidative coupling pathways to perform ruthenium catalyzed carbonyl addition to ketones has enabled expansion of the transfer hydrogenative ruthenium catalyzed methodologies, with unique regioselectivity. One important outcome of this line of investigation was the expansion of unsaturate substrates in the direct coupling of α -olefins, a feedstock chemical, with 3-hydroxyoxindoles.¹⁰⁸ Using $\text{Ru}_3(\text{CO})_{12}$ and PCy_3 in combination with 1-adamantanecarboxylic acid ($\text{C}_{10}\text{H}_{15}\text{CO}_2\text{H}$) as an additive, it was found that *N*-benzyl-3-hydroxyoxindole will couple to a wide variety of α -olefin substrates and styrene derivatives (Scheme 4.5).

Scheme 4.5 Oxidative coupling of propene and 3-hydroxyoxindole.



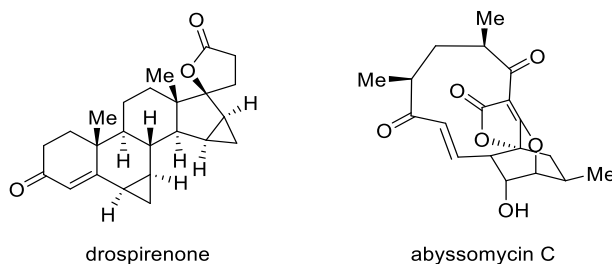
4.2 Oxidative Coupling and Spirolactonization using Acrylates

4.2.1 Introduction

The development of the Ru⁰ catalytic system has enabled expansion of compatible unsaturates that will engage in oxidative coupling. It was proposed that methyl acrylate and other acrylic esters could be used in a similar fashion to furnish spirocyclic γ -butyrolactones after C-C bond formation and spirolactonization.

Spirocyclic lactones are ubiquitous functional groups in natural products with a wide range of biological activity, including pharmaceutically active natural products drospirenone and abyssomicin C. (Figure 4.1)

Figure 4.1 Pharmaceutically active natural products containing spirolactones.

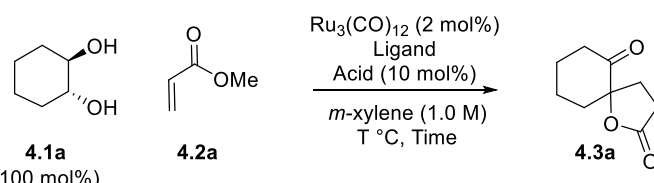


Naturally occurring spirocycles all contain a sterically congested quaternary center, and may contain 2-7 carbon atoms within the ring. While many methods exist for the synthesis of spirocyclic γ -butyrolactones, including oxidative dearomatizations using iodine or cerium ammonium nitrate,¹⁰⁹ Michael additions using α,β -unsaturated esters,¹¹⁰ cationic rearrangements of epoxides and bromonium ions,¹¹¹ *N*-heterocyclic carbene catalyzed Stetter reactions,¹¹² C-H hydroxylation of carboxylic acids,¹¹³ Reformatsky type reactions,¹¹⁴ and Pauson-Khand and other carbonyl insertion reactions,^{107, 115} a transfer hydrogenative variant may provide a complement to these methods, representing a new functional group interconversion that utilizes an inexpensive feedstock chemical, methyl acrylate. Furthermore, only few examples of enantioselective spirolactonization have been disclosed, and this challenge could potentially be addressed using asymmetric catalysis.¹¹⁶

4.2.2 Reaction Development, Optimization and Scope

To probe the reactivity of α,β -unsaturated esters with diols to access spiro lactone products, *trans*-1,2-hexanediol **4.1a** and methyl acrylate **4.2a** were exposed to $\text{Ru}_3(\text{CO})_{12}$ and various ligands (Table 4.1). Although previous work showed that PCy_3 was an effective ligand, no product was obtained when this was used in the reaction (entry 1). Nitrogen based ligands BIPY or Phen were similarly ineffective (entries 2-3). In contrast, bidentate electron rich phosphine ligand DPPP produced the desired spiro lactone in 76% yield (entry 4). While higher loadings of methyl acrylate did improve conversion (entries 5-7), more investigation was made into increasing the reaction efficiency. Variation of reaction temperature was ineffective (entries 8-9) in this regard. In previous work, it was found that carboxylic acid additives can have a drastic effect on reaction yield,¹⁰⁸ possibly due to an accelerated hydrogenolysis of the oxo-metallacycle formed upon oxidative coupling.¹¹⁷ In this reaction, benzoic acid and 1-adamantanecarboxylic acid proved highly effective as acid co-catalysts, with 1-adamantanecarboxylic acid performing best for number of substrates (entries 10-11).

Table 4.1 Optimization of catalytic system for spiro lactonization of **4.1a**.

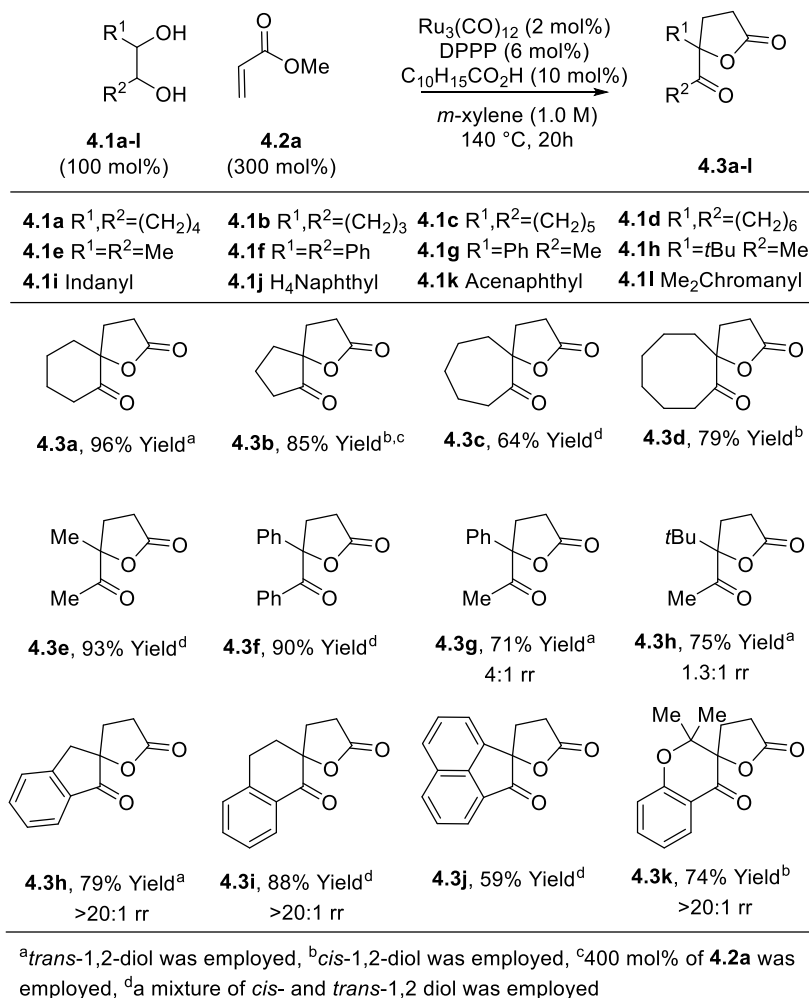


Entry	Ligand (mol%)	Acid	4.2a (mol%)	T (°C)	Time (h)	Yield (%)
1	PCy_3 (12)	-	300	140	20	trace
2	BIPY (6)	-	300	140	20	trace
3	Phen (6)	-	300	140	20	trace
4	DPPP (6)	-	300	140	20	76
5	DPPP (6)	-	200	140	20	56
6	DPPP (6)	-	400	140	20	88
7	DPPP (6)	-	500	140	20	79
8	DPPP (6)	-	300	130	20	33
9	DPPP (6)	-	300	150	20	69
10	DPPP (6)	Benzoic Acid	300	140	20	93
⇒ 11	DPPP (6)	$\text{C}_{10}\text{H}_{15}\text{CO}_2\text{H}$	300	140	20	96

Upon identification of these conditions, the reaction scope was evaluated. Spiro lactones **4.3a-l** were generated in high yield for a variety of cyclic, acyclic, and polycyclic diols (Figure 4.2). For nonsymmetric diols, varying regiocontrol was observed. For acyclic diols **4.1g-h**,

regioselectivity was incomplete, with 4:1 rr for spiro lactone **4.3g** and 1:1 rr for **4.3h**. For cyclic nonsymmetric systems (**4.1i, j, and l**), regiocontrol was complete. Both *cis*- and *trans*- diols were suitable substrates for the reaction.

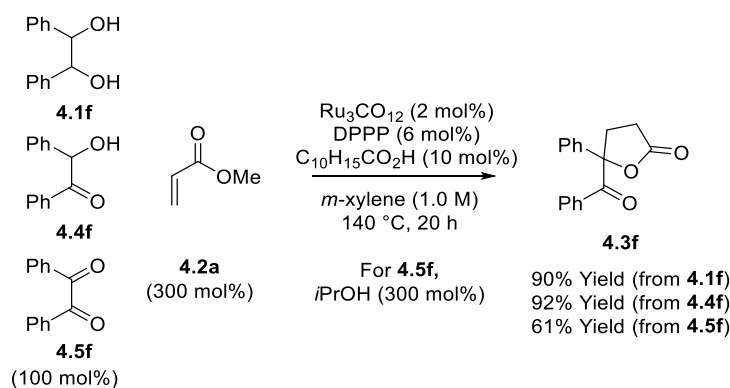
Figure 4.2 Spirolactones **4.3a-l** generated upon coupling diols **4.1a-l** to methyl acrylate **4.2a**.



The postulated mechanism for this transformation (See Figure 4.4) suggests that oxidative coupling occurs from the dione oxidation level, as the 1,2-dicarbonyl moiety is necessary for coupling (simple primary or secondary alcohols did not participate in the reaction). To demonstrate this, the reaction was performed from the diol, α -hydroxy ketone and dione oxidation levels (Scheme 4.6). In this manner, the diol would participate via an oxidative pathway, the α -hydroxy ketone in a redox neutral pathway, and the dione in a reductive pathway with the addition

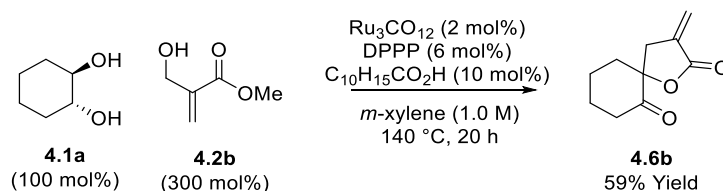
of an exogenous reductant. It was found that all three pathways formed **4.3f**. Diol **4.1f** and α -hydroxy ketone **4.4f** performed similarly in the reaction, producing **4.3f** in excellent yield, but dione **4.5f** exhibited diminished reactivity. This could be due to the competitive reduction of acrylate **4.2a** instead of oxidative coupling upon generation of a ruthenium hydride from the Ru⁰ catalyst and reductant.

Scheme 4.6 Coupling of diol **4.1f**, α -hydroxy ketone **4.4f** or dione **4.5f** with methyl acrylate **4.2a** to generate spiro lactone **4.3f**.



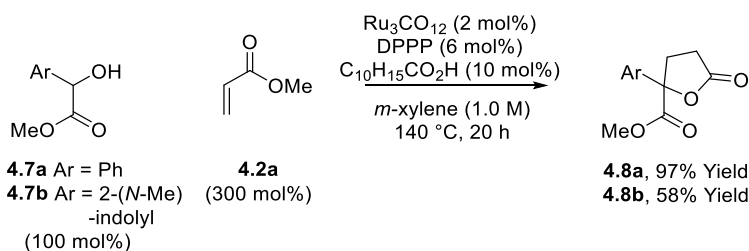
Unfortunately, substituted α,β -unsaturated esters were unsuitable coupling partners in this reaction. It was found that substitution at either α or β position resulted in no product formation. However, 2-hydroxymethyl substituted methyl acrylate **4.2b** did engage in C-C coupling. Interestingly, upon C-C coupling, the adduct underwent dehydration to form α -exocyclic- γ -butyrolactone **4.6b** (Scheme 4.7). One interpretation of the scope of acrylate partners could be that the substituted acrylates do not coordinate ruthenium well due to poor olefin coordination to the metal center. However, 2-hydroxymethyl substituted acrylate **4.2b** may chelate the catalyst and serve as a directing group for olefin coordination and subsequent oxidative coupling.

Scheme 4.7 Coupling of **4.1a** and 2-hydroxymethyl acrylate **4.2b** to access α -exocyclic- γ -butyrolactone **4.6b**.



Other α -hydroxy carbonyl containing compounds had been found to participate in oxidative coupling with $\text{Ru}_3(\text{CO})_{12}$ and dienes, including mandelic esters and 3-hydroxyoxindoles. Mandelic esters **4.7a** and **4.7b** formed **4.8a** and **4.8b** under the optimized conditions in good yield (Scheme 4.8).

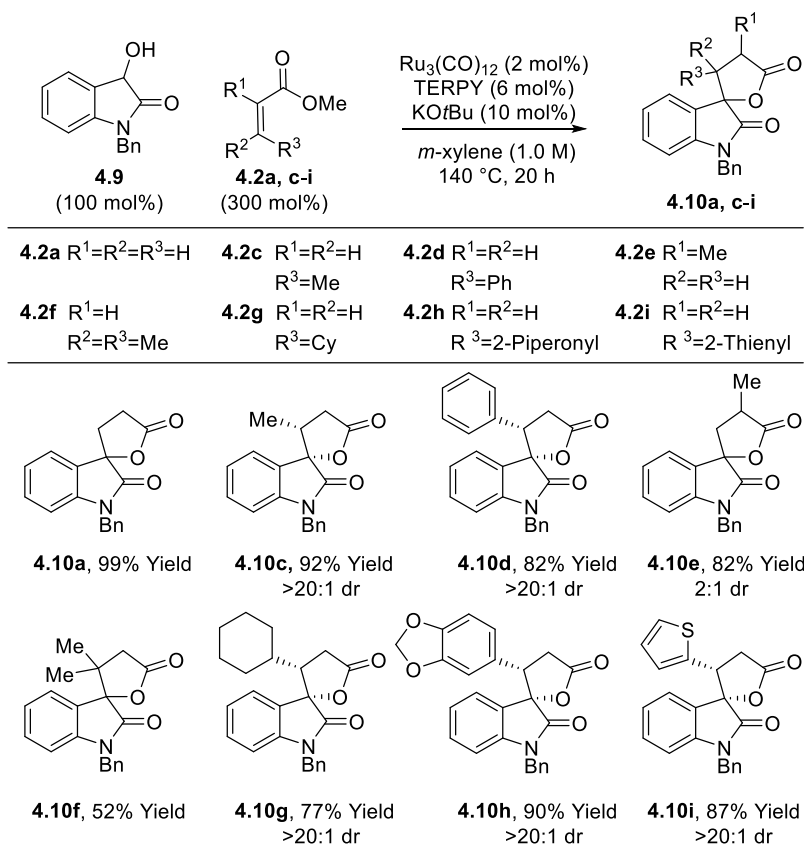
Scheme 4.8 Spirolactonization of α -hydroxy esters **4.7a-b** to access spiro lactones **4.8a-b**.



Interestingly, it was found that 3-hydroxyoxindole **4.9** also would couple to substituted acrylic esters **4.2c-i**. The difference in reactivity of the 3-hydroxyoxindoles and diols may be attributed to the higher energy due to strain of the 5-membered ring present in the isatin (formed after dehydrogenation of 3-hydroxyoxindole), which can compensate for the poor ligand character of substituted acrylic esters.

Under identical conditions to those developed for the spiro lactonization of 1,2-diols, the reaction of 3-hydroxyoxindole **4.9** with methyl crotonate **4.2c** resulted in quantitative conversion to the corresponding spirooxindole as a 1:1 mixture of diastereomers. In an effort to improve selectivity, it was found that the employment of TERPY as ligand and addition of basic additives formed **4.10c** as a single diastereomer in high yield. These reaction conditions were used to generate a variety of substituted spirooxindole products **4.10a, c-i** (Figure 4.3). β -substituted acrylic esters **4.2c-d, g-i** formed products **4.10c-d, g-i** as a single diastereomer. α -substituted methyl methacrylate **4.2e** generated spiro lactone **4.10e** as a mixture of diastereomers, likely due to epimerization of the resulting chiral center under the reaction conditions. Even β,β -disubstituted ester **4.2f** participated in C-C coupling to form spirooxindole **4.10f** containing two adjacent quaternary centers, albeit in diminished yield.

Figure 4.3 Spirooxindole products **4.10a, c-i** generated by coupling 3-hydroxyoxindole **4.9** and substituted acrylic esters **4.2a, c-i**.

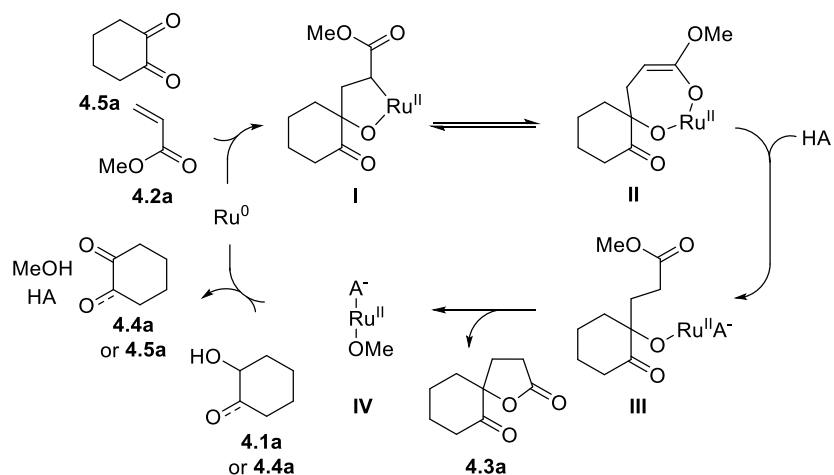


4.2.3 Mechanistic Explanation and Discussion

A plausible mechanism for the oxidative coupling of dione **4.5a**, formed upon oxidation of **4.1a**, and methyl acrylate **4.2a** is shown in Figure 4.4. Oxidative coupling of **4.5a** and **4.2a** by Ru⁰ results in oxaruthenacycle **I**, which can isomerize from C-bound enolate **I** to O-bound enolate **II**. Protonation of the metallacycle by the acid additive results in ruthenium alkoxide **III**. It is postulated that this step is accelerated by the acid additive, leading to significant improvement in yield. Alkoxide **III** can undergo lactonization, releasing spiro lactone product **4.3a** and regenerating Ru^{II} species **IV**. Ligand exchange of methoxide with the alkoxide of diol **4.1a** or α -hydroxy ketone **4.4a** releases methanol. The resulting Ru alkoxide can undergo β -hydride elimination to form **4.4a** or

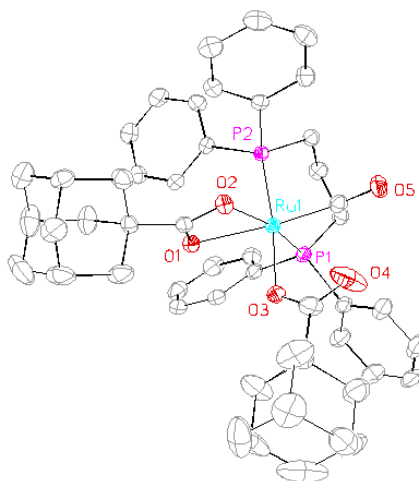
4.5a, and reductive elimination to reform HA and regenerate the Ru^0 complex to close the catalytic cycle.

Figure 4.4 Proposed mechanism for oxidative coupling of dione **4.5a** and methyl acrylate **4.2a** to generate products of spirocyclization **4.3a**.



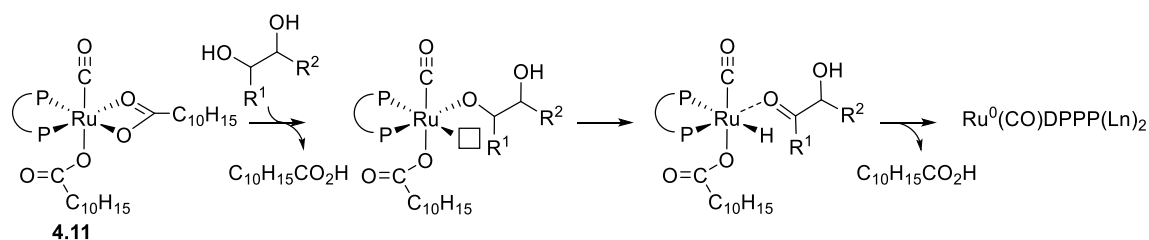
A monomeric ruthenium species is proposed for this transformation, as previous work suggested that $\text{Ru}_3(\text{CO})_{12}$ trimer can be broken into a monomeric form in the presence of phosphine ligands.¹¹⁸ Indeed, upon mixing $\text{Ru}_3(\text{CO})_{12}$, DPPP and 1-adamantane carboxylic acid at reaction temperatures, ruthenium complex **4.11** was obtained (Figure 4.5).

Figure 4.5 ORTEP representation of crystal structure of $\text{Ru}(\text{CO})(\text{DPPP})[(\text{H}_{15}\text{C}_{10}\text{CO}_2^-)_2]$ **4.11**.



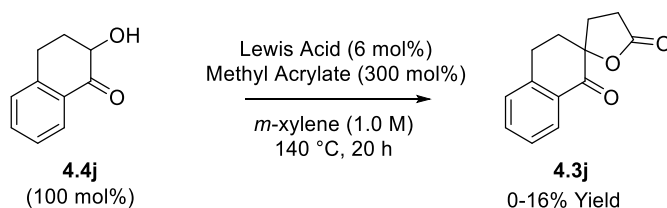
This Ru^{II} complex is active in the catalytic reaction (product **4.3a** was formed under optimized conditions in 86% yield), suggesting protonation by diol, β -hydride elimination and reductive elimination can reform the Ru⁰ complex required for oxidative coupling (Scheme 4.9).

Scheme 4.9 Regeneration of Ru⁰ catalyst from **4.11**.



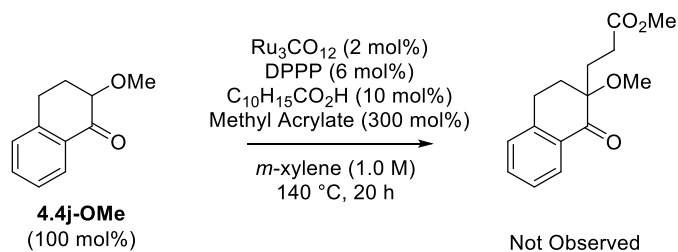
It is plausible that other modes of addition may be occurring, including a Lewis acid catalyzed Michael addition, where the acrylic ester may undergo 1,4-addition by the dienolate of the α -hydroxy ketone that forms from the 1,2-diol. Several control experiments were performed in attempt to probe this mode of reactivity. Hydroxy ketone **4.4j** was synthesized and exposed to methyl acrylate in the presence of various Lewis acids, including Ru₃(CO)₁₂, RuCl₃, B(OMe)₃, MgCl₂, InCl₃ and ZnI₂. Only small quantities of spiro lactone product were isolated (up to 16% yield) (Scheme 4.10). This suggests that while Michael addition may be possible it is not as effective as the reported catalytic system.

Scheme 4.10 Control experiments to probe Lewis acid catalyzed Michael addition.



Another experiment was performed to probe anionic addition. α -Hydroxy ketone **4.4j** was methylated (**4.4j-OMe**) and subjected to the reaction conditions. Using **4.4j-OMe**, enolization and Michael addition could still occur, but an oxidative coupling pathway would not be possible. Only starting material was recovered, suggesting that dione may be required for C-C bond formation.

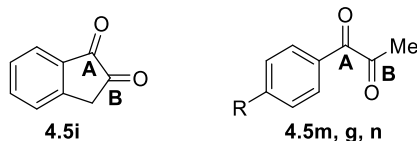
Scheme 4.11 Control experiment to test for Michael addition products.



The observed regioselectivity of products **4.3i**, **4.3j** and **4.3l** compared to acyclic **4.3g** deserved further investigation. To examine two substrates, diol **4.1g** formed spirolactone **4.3g** as a 4:1 ratio of regioisomers, favoring coupling at the benzylic position, whereas diol **4.1i** resulted in single regioisomer **4.3i**, favoring coupling at the carbonyl distal to the aromatic ring. This regioselectivity is consistent with literature reports of oxidative coupling to 1-phenyl-2,3-dione¹¹⁹ and reactions of 1,2-indanedione with nucleophiles or by hydrogenation,¹²⁰ though no clear comparison of the two substrates exists. In studying the oxidative conversion of bis-olefin complexes to metallacyclopentanes, Hoffman proposes that regioselectivity is controlled by interactions of frontier molecular orbitals,¹²¹ suggesting that reactivity should occur at the site that bears the largest LUMO coefficient.

To examine this principle, DFT calculations were carried out to compare the contribution of each ketone to the LUMO energy. Four substrates were evaluated, including 1,2-indanedione **4.5i** (formed from **4.1i**), 1-phenylpropan-1,2-dione **4.5g** (from **4.1g**), and two para-substituted 1-phenylpropan-1,2-dione derivatives, 1-(4-methoxyphenyl)propane-1,2-dione **4.5m** and methyl 4-(2-oxopropanoyl)benzoate **4.5n**. The derivatives **4.5m** and **4.5n** were chosen to further evaluate how the electronics of the system may impact regioselectivity. Table 4.2 describes the experimentally observed regioselectivities when diols **4.1g**, **i**, **m**, **n** were subjected to reaction conditions and the calculated values for the LUMO coefficients.

Table 4.2 Experimentally observed regioselectivities and LUMO coefficients for diones **4.5i**, **g**, **m** and **n**.



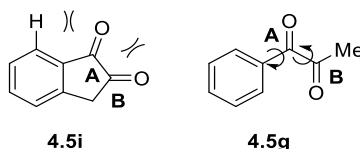
Dione	LUMO Coefficient		$\Delta(A-B)$	Experimental Ratio (A:B)
	A	B		
4.5i	-0.12189	-0.10896	0.013	1:>20
4.5m , R=OMe	-0.13750	-0.11802	0.019	1.3:1
4.5g , R=H	-0.13943	-0.11213	0.027	4:1
4.5n , R=CO ₂ Me	-0.13353	-0.09587	0.038	10:1

For each dione, the carbonyl at the benzylic position (**A**) bore a larger LUMO coefficient than the distal carbonyl (**B**). This supports the experimentally observed regioselectivity for the acyclic diones **4.5g**, **m-n**, but not for 1,2-indanedione **4.5i**. However, by comparing the LUMO coefficient on the two diones, it was found that as the difference increased, so did the regioselectivity for coupling at carbonyl **A**. 1,2-indanedione **4.5i** exhibited the smallest difference between the LUMO coefficient at **A** and **B**, and completely favored coupling at carbonyl **B**. For the acyclic systems, the smallest difference in LUMO coefficients was calculated for **4.5m** (0.019), and the corresponding spiro lactone product was formed as a 1.3:1 mixture of regioisomers. As the aromatic ring became more electron deficient (in dione **4.5n**), a larger gap in LUMO coefficients (0.038) corresponded to a 10:1 mixture of regioisomers isolated from the corresponding spiro lactone product. While this trend is consistent with the observed regioselectivity, this calculation does not fully explain the drastic inversion for cyclic substrate **4.5i**. One important factor to consider is the validity of performing calculations on the ground dione state, which must be coordinated by ruthenium prior to oxidative coupling. Calculations of the energies of the ruthenium-bound diones could reveal more useful information about the reactivity, but would be much more complex and beyond the scope of this work.

Another factor that could impact regioselectivity is the steric environment of carbonyl **A** and **B**. For 1,2-indanedione **4.5i**, most of the atoms are sp² hybridized, resulting in a mostly planar

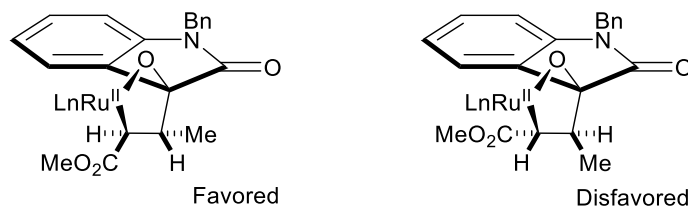
molecule. Based on this geometry, ketone **A** (Figure 4.6) would be coplanar with both an aryl hydrogen and ketone **B**, while ketone **B** is adjacent to carbonyl **A** and a non-eclipsed methylene. This may favor coupling to the more accessible distal carbonyl. For acyclic systems **4.5g**, conformational flexibility by C-C bond rotation alleviates any steric interactions, allowing oxidative coupling to occur at the carbonyl bearing the larger LUMO coefficient (based on DFT calculations).

Figure 4.6 Comparison of conformational flexibility of diones **4.5i** and **4.5g**.



The reaction of α -hydroxy esters **4.7a-b** and 3-hydroxyoxindole **4.9** likely proceed through a similar reaction mechanism to that shown in Scheme 4.8. The high levels of diastereoselectivity attained with spirooxindole formation may be explained by the stereochemical model shown in Figure 4.7. The favored metallacycle orients the ester substituent away from ruthenium, and the ester and methyl substituent are on opposite sides of the ring to avoid eclipsing interactions.

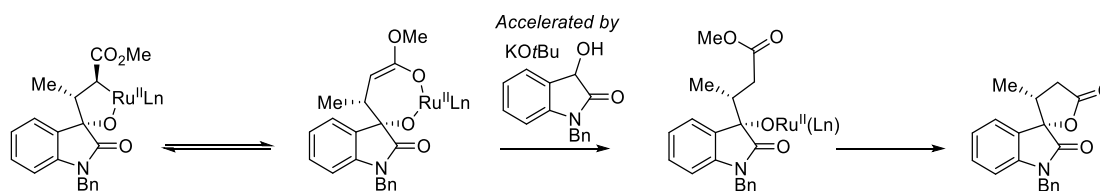
Figure 4.7 Stereochemical model of ruthenacycle generated upon oxidative coupling to explain diastereocontrol in spirooxindole formation.



While this model indicates the favored stereochemistry, it does not provide an explanation for the role of the basic additives in diastereocontrol. If the oxidative coupling process is a concerted event, it would be expected that the favored transition state in Figure 4.7 would form a single diastereomer. However, if protonation of the metallacycle occurs to generate the C-bound

enolate, β -hydride elimination and re-hydrometallation could scramble the stereocenter. Alternatively, after protonation of the metallacycle, retro-Michael addition could release 3-hydroxyoxindole **4.9** and perhaps scramble the olefin geometry of crotonic ester **4.2c**. In other ruthenium catalyzed processes, alkoxide additives have been proposed to accelerate ligand exchange.¹²² By increasing turnover and preventing other modes of reactivity that could scramble the stereoselectivity established at oxidative coupling, high levels of diastereoselectivity would be maintained (Scheme 4.12).

Scheme 4.12 Role of basic additives in diastereoselective spirooxindole formation.



4.2.4 Conclusion

Upon completion of this work, the conversion of 1,2-diols **4.1a-l**, α -hydroxy esters **4.7a-b** and 3-hydroxyoxindole **4.9** to spiro lactone products **4.3a-l**, **4.6b** **4.8a-b** and **4.10a, c-i** was enabled by oxidative coupling to acrylic esters **2a-2i**. This reaction employs inexpensive feedstock chemicals and highly tractable, easily accessed 1,2-diols. While the use of substituted acrylic esters is an attractive way to access highly congested compounds, the reaction was only successful using 3-hydroxyoxindole, which furnished spirooxindole products with complete levels of diastereocontrol. Unfortunately, attempts at asymmetric spiro lactone formation using the ruthenium catalysis described herein were ineffective. Furthermore, the extension of this chemistry to simple, unactivated ketones is an unmet challenge. Improvement in absolute stereocontrol and substrate scope will make a more applicable, useful method.

4.3 Vinylation of Ketones via Alkyne Oxidative Coupling

4.3.1 Introduction

Just as α -olefins, dienes, and acrylates had proven effective π -unsaturates for Ru^0 catalyzed oxidative coupling, alkynes were another substrate to investigate to access vinylation products. $\text{Ru}_3(\text{CO})_{12}$ complexes are known to catalyze [2+2+2] trimerization reactions of alkynes,¹²³ so it was proposed that interception of the alkyne-ruthenium intermediate by an activated ketone could access sterically condensed β,γ -unsaturated α -hydroxy ketones.

4.3.2 Reaction Development and Optimization

Applying conditions developed for other $\text{Ru}_3(\text{CO})_{12}$ catalyzed ketone coupling, the reaction of *trans*-1,2-cyclohexanediol **4.1a** and 1-phenyl-1-propyne **4.11a** successfully underwent oxidative coupling to yield product **4.12a** as a single regioisomer, even in the absence of acid additives (Table 4.3, entries 1-2). After screening a variety of bidentate ligands, including DPPP and DPPF (entries 3-5), little improvement was achieved. However, more electron rich ligand, DCyPF, was more effective in this reaction (entry 6). Based on this observation, electron rich trialkylphosphine ligands were revisited, and it was found that PCy_3 in combination with 1-adamantanecarboxylic acid ($\text{C}_{10}\text{H}_{15}\text{O}_2\text{H}$) resulted in very high isolated yield (entry 7). Notably, the reaction was complete in only 4 h (entries 8-10).

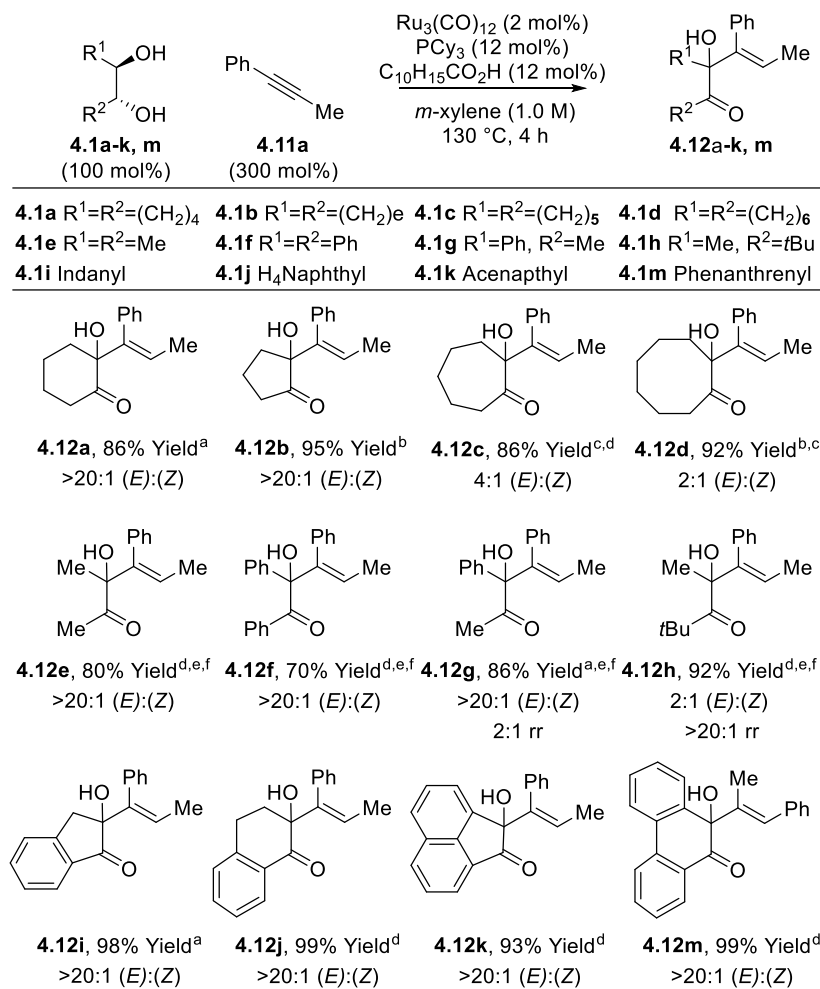
Table 4.3 Optimization of reaction parameters to access α -hydroxy β,γ -unsaturated ketone **4.12a**.

Reaction scheme showing the oxidative coupling of **4.1a** (100 mol%) and **4.11a** (300 mol%) to form **4.12a**. The reaction conditions are $\text{Ru}_3(\text{CO})_{12}$ (2 mol%), Ligand, Acid (12 mol%), *m*-xylene (1.0 M), T °C, Time.

Entry	Ligand (mol%)	Acid	T (°C)	Time (h)	Yield (%)
1	PCy_3 (12)	--	130	20	19
2	DPPP (6)	--	130	20	75
3	DPPP (6)	BzOH	130	20	66
4	DPPP (6)	$\text{C}_{10}\text{H}_{15}\text{CO}_2\text{H}$	130	20	77
5	DPPF (6)	$\text{C}_{10}\text{H}_{15}\text{CO}_2\text{H}$	130	20	77
6	DCyPF (6)	$\text{C}_{10}\text{H}_{15}\text{CO}_2\text{H}$	130	20	87
7	PCy_3 (6)	$\text{C}_{10}\text{H}_{15}\text{CO}_2\text{H}$	130	20	93
⇒ 8	PCy_3 (12)	$\text{C}_{10}\text{H}_{15}\text{CO}_2\text{H}$	130	4	95
9	PCy_3 (12)	$\text{C}_{10}\text{H}_{15}\text{CO}_2\text{H}$	120	4	75
10	PCy_3 (12)	$\text{C}_{10}\text{H}_{15}\text{CO}_2\text{H}$	130	2	84

4.3.3 Reaction Scope and Product Derivatization

Figure 4.8 α -hydroxy, β,γ -unsaturated ketones **4.12a-k, m** generated upon coupling 1,2-diols **4.1a-k, m** and alkyne **4.11a**.

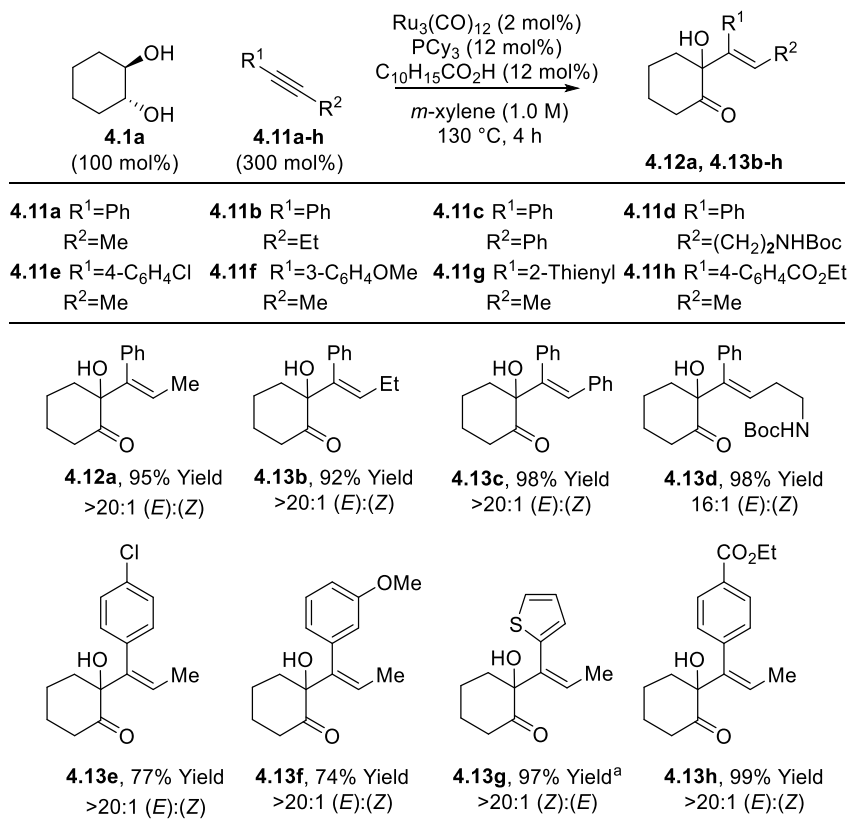


^atrans-1,2-diol was employed, ^bcis-1,2-diol was employed, ^creaction time was shortened to 2 h, ^da mixture of cis- and trans-1,2-diols were employed, ^eDPPF (6 mol%) was used in place of PCy₃ as ligand, ^freaction time was extended to 20 h

Using the optimized conditions above, the scope of the reaction was evaluated using 1-phenyl-1-propyne **4.11a** and different 1,2-diols (Figure 4.9). Cyclic diols **4.1a-d, I-k, m** all delivered coupling products in high yield, as did acyclic diols **4.1e-h**. In all cases but **4.1c** and **4.1d**, complete (E):(Z) olefin geometry selectivity was attained. For acyclic diols **4.12e-h**, PCy₃ generated a mixture of (E) and (Z) olefin isomers. This could be avoided by using DPPF as ligand, however, a longer reaction time (20 h) was required. In non-symmetric systems **4.1g** and **4.1h**, a mixture

of regioisomers was formed, but non-symmetric cyclic diols **4.1i-j** reacted with complete regioselectivity. Interestingly, the regioselectivity of the alkyne coupling partner was identical for all products **4.12a-k**, but inverted for **4.12m**. The stereochemistry of the diol starting material is unimportant for this reaction, as the carbinol stereocenters are destroyed upon oxidation to the dione, and both *cis* and *trans* diols reacted efficiently. The substrate scope was limited to vicinal secondary diols. Terminal vicinal diols resulted in a complex mixture, including mono- and bis-coupled products (detected by LRMS).

Figure 4.9 α -hydroxy, β,γ -unsaturated ketones **4.12a** and **4.13b-h** generated upon coupling diol **4.1a** and alkynes **4.11a-h**.



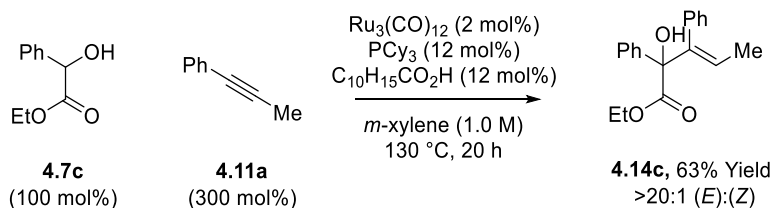
^aReaction time extended to 20 h

Next, a range of different alkynes were examined in the reaction with *trans*-1,2-cyclohexanediol **4.1a** (Figure 4.9). Di-substituted alkynes **4.11a-h** afforded the vinylation product in high yield and very high levels of (*E*):(*Z*) olefin selectivity for nonsymmetric alkynes **4.11a-b, d-**

h. Terminal alkynes and internal alkynes that did not bear an aromatic substituent were unsuitable substrates for this reaction.

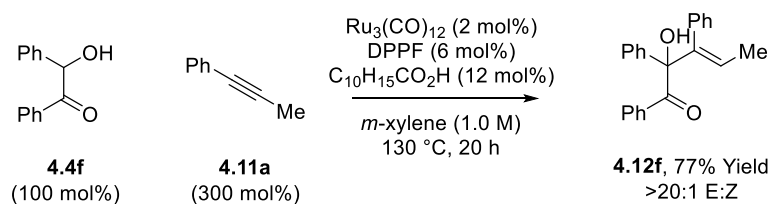
The successful oxidative coupling of alkynes and 1,2-diols suggested that higher oxidized congeners would also be effective in this reaction. α -Hydroxy ester **4.7c** furnished product of vinylation under identical conditions in 63% yield and complete levels of (*E*)-olefin stereoselectivity (Scheme 4.13).

Scheme 4.13 Vinylation of α -hydroxy ester **4.7c**.



α -Hydroxy ketone **4.4f** performed well, however, the corresponding dione (**4.5f**) failed to deliver high yields of product (10% Yield, >20:1 (*E*):(*Z*) ratio when using 200 mol% 1,4-butanediol as reductant) (Scheme 4.14). Using dione **4.5f**, even extension of reaction time and addition of more reductant failed to improve product conversion, as only increased reduction of dione was observed. This could be due to the facile reduction of alkynes in the presence of the ruthenium catalyst and a hydride source, destroying the alkyne needed for C-C coupling.

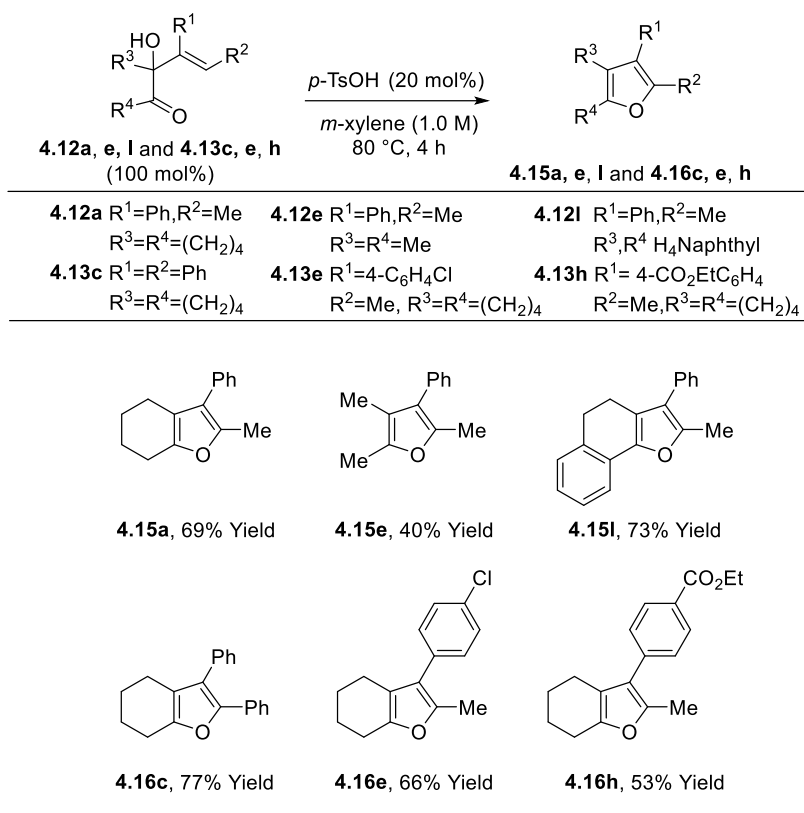
Scheme 4.14 Vinylation of α -hydroxy ketone **4.4f**.



By treating the products of ketone vinylation with catalytic amounts of Brønsted acid, cyclodehydration would result in the formation of tetrasubstituted furans. *p*-Toluenesulfonic acid

was found to be effective at this transformation, converting the vinyl-substituted hydroxy ketones **4.12a, e, I** and **4.13c, e, h** to furans **4.15a, e, I** and **4.16c, e, h** in 4 h at 80 °C.¹²⁴ (Figure 4.10)

Figure 4.10 Cyclodehydration of α -hydroxy β,γ -unsaturated ketones to form tetrasubstituted furans **4.15a, e, I**, and **4.16c, e, h**.



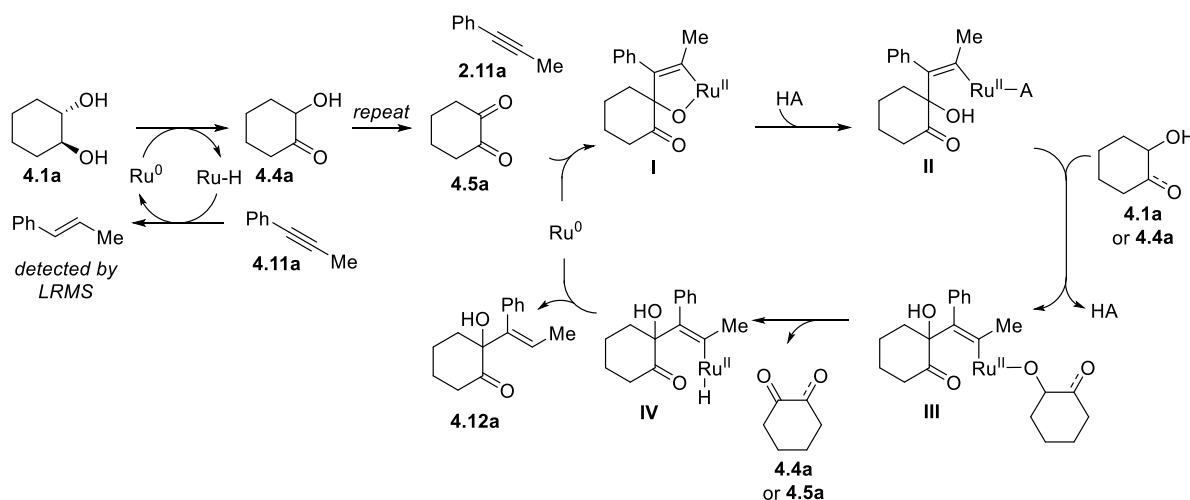
4.3.4 Discussion and Mechanism

Supported by previous work and the resulting olefin geometry in the vinylation products, a mechanism for the oxidative coupling of alkyne **4.11a** and *trans*-1,2-cyclohexanediol **4.1a** is shown in Figure 4.11. Oxidation of diol substrate **4.1a** to dione **4.5a** can occur using excess alkyne **4.11a** as hydrogen acceptor. The product of alkyne reduction was detected by mass spectrometry.

Upon formation of dione **4.5a**, oxidative coupling generates ruthenacycle **I**. Protonation of the metallacycle can occur by the diol **4.1a** (or hydroxyketone **4.4a**) substrate, but is likely

accelerated by the acid additive.¹¹⁷ After protonation of **I** to form **II**, ligand exchange with **4.1a** or **4.4a** provides a ruthenium alkoxide **III** that can undergo β -hydride elimination to generate ruthenium hydride **IV**. Reductive elimination releases the product **4.12a** and regenerates the Ru⁰ catalyst.

Figure 4.11 Proposed mechanism for the generation of dione **4.5a** from diol **4.1a** and subsequent oxidative coupling.

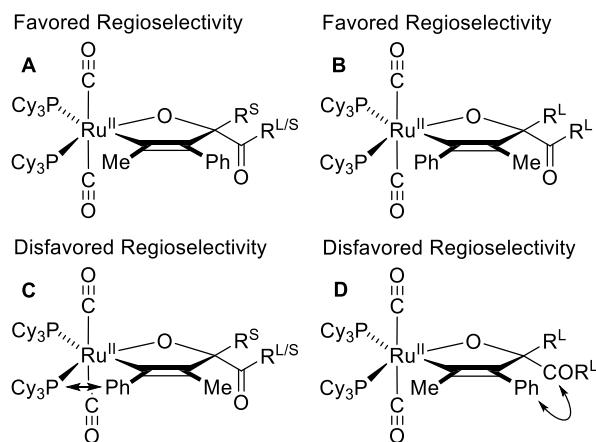


The (*E*)-olefin geometry that is observed in most cases is a hallmark of an oxidative coupling mechanism, where the position of the product olefin substituents are determined by the metallacyclic intermediate formed upon oxidative coupling. In two cases, **4.12c** and **4.12d**, the product contained a mixture of (*E*) and (*Z*) olefins. This is likely due to isomerization that may occur after the reaction has taken place, evidenced by greater isomerization at longer reaction times. By limiting reaction time, higher levels of (*E*):(*Z*) selectivity was obtained.

The regioselectivity observed in products **4.12a-k**, **m** and **4.13b-h** is consistent with the stereochemical models depicted in Figure 4.12, where R^S is a small substituent and R^L is a large substituent. For symmetric diols (R^S=R^S) the alkyne orientation places the larger substituent away from the ruthenium center (models **A** and **C**). For nonsymmetric diols **4.12g**, **h**, **i**, **j** coupling is favored at the carbonyl bearing the smaller substituent (model **A**), and selectivity increases as the size difference increases. As described in section 4.2.3, the enforced planarity of the cyclic

nonsymmetric diols may enhance this steric interaction. The inverted regiochemistry observed for product **4.12m** may be due to the large steric interactions at the dione substituent that are present if the larger alkyne substituent is placed away from the metal center (model **D**). While inverting alkyne orientation will create a steric interaction between the metal center and the alkyne substituent, this must be more energetically favorable (model **B**). The regiochemistry of product **4.12** was confirmed by x-ray crystallography.

Figure 4.12 Stereochemical models of the ruthenacycle intermediate to explain regiochemical outcome of products **4.12a-k, m**.



4.3.5 Conclusion

In this work, β,γ -unsaturated α -hydroxy ketones **4.12a-l, m** and **4.13b-h** have been accessed by coupling internal alkynes to 1,2-diols. This reaction rapidly assembles dense functionality, and adds to the suite of oxidative coupling transformations of unsaturates and activated secondary alcohols in a redox neutral process. Treatment of the products with acid formed tetrasubstituted furans by cyclodehydration.

4.4 Summary and Outlook

The development of Ru^0 catalyzed oxidative coupling pathways for carbon-carbon bond formation has expanded the scope of potential reactive partners. Extension of carbonyl addition chemistry to unactivated ketones would be advantageous. Equally valuable would be deeper

understanding of the reactivity and selectivity of the Ru⁰ complexes with activated ketones in contrast to the catalytic systems that have been developed for primary alcohol or aldehyde coupling. Finally, an enantioselective variant of the oxidative coupling methodologies has not yet been established. As the spirolactonization and vinylation methodologies described herein access highly substituted, functionalized products that traditionally are a challenge in asymmetric synthesis, addressing that problem by enantioselective catalysis would have significance to synthetic chemistry.

4.5 Experimental Details

4.5.1 General Information

All reactions were run under an atmosphere of argon in sealed tubes (13x100 mm²), dried overnight in an oven and cooled under a stream of argon prior to use. Anhydrous solvents were distilled using solvent stills and solvent were transferred by oven-dried syringe. Catalyst Ru₃(CO)₁₂, all ligands and acid additives were used without purification. Diols **4.1c**, **4.1g**, **4.1h** and **4.1i** were prepared from the corresponding alkene using the protocol described by Hayashi et al.¹²⁵ Diol **4.1j** was prepared according to the method described by Rodrigues et al.¹²⁶ Diols **4.1k** and **4.1m** were prepared according to the method described by Dakdouki et al.¹²⁷ Diol **4.1l** was prepared from the corresponding chromene¹²⁸ by osmium catalyzed dihydroxylation. Hydroxyester **4.7b** was prepared by reduction of the corresponding oxoester¹²⁹ by the method described by Hui et al.¹³⁰ 3-Hydroxyoxindole **4.9** was prepared by the method described by Autrey and Tahk.¹³¹ Alkynes were prepared by Sonagashira coupling, in a method analogous to that described by Krische et al.¹³² Thin-layer chromatography (TLC) was carried out using 0.25 mm commercial silica gel plates (Silicycle Siliaplate F-254). Visualization was accomplished with UV light followed by staining. Purification of product was carried out by flash column chromatography using Silicycle silica gel (40-63 μm), according to the method described by Still.⁷⁵

4.5.2 Spectrometry and Spectroscopy

Infrared spectra were recorded on a Thermo Nicolet 380 spectrometer. Low and high resolution mass spectra (LRMS or HRMS) were obtained on a Karatos MS9 and are reported as m/z (relative intensity). Accurate masses are reported for the molecular ion or a suitable fragment ion. Melting points were obtained on a Stuart SMP3 apparatus and are uncorrected. ^1H NMR spectra were recorded on a Varian Gemini (400 MHz) spectrometer at ambient temperature. Chemical shifts are reported in delta (δ) units, parts per million (ppm), relative to the center of the singlet at 7.26 ppm for deuteriochloroform, or other reference solvents as indicated. Data are reported as chemical shift, multiplicity (s=singlet, d=doublet, t=triplet, q=quartet, m=multiplet), integration and coupling constant(s) in Hz. ^{13}C NMR spectra were recorded on a Varian Gemini (100 MHz) spectrometer and were routinely run with broadband decoupling. Chemical shifts are reported in ppm, with the residual solvent resonance employed as the internal standard (CDCl_3 at 77.0 ppm). Regiochemical assignments were made by HMBC or NOESY NMR experiments.

4.5.3 Computational Analysis

All structures were optimized and characterized to determine each atom's contribution to the LUMO orbital. Density functional theory (DFT) calculations were carried out with QChem 4.0 using B3LYP hybrid functional and G-311G(d,p) basis set.

4.5.4 General Procedures for Spirolactonization

General Procedure A: To a re-sealable pressure tube (13 x 100 mm) equipped with magnetic stir bar, diol (or hydroxy ester) (0.3 mmol, 100 mol%), $\text{Ru}_3(\text{CO})_{12}$ (3.8 mg, 0.006 mmol, 2 mol%), 1,3-bis(diphenylphosphino)propane (7.4 mg, 0.018 mmol, 6 mol%), and 1-adamantanecarboxylic acid (5.4 mg, 0.03 mmol, 10 mol%). The tube was sealed with a rubber septum and purged with argon. Methyl acrylate (**2a**) (81 μL , 0.90 mmol, 300 mol%) and *m*-xylene (0.22 mL, 1.0 M overall) were added. The rubber septum was quickly replaced with a screw cap. The mixture was heated at 140 $^\circ\text{C}$ (oil bath temperature) for 20 h, at which point the reaction mixture was allowed to cool to ambient temperature. The reaction mixture was concentrated and

subjected to flash column chromatography to furnish the corresponding product of spirolactonization.

General Procedure B: To a re-sealable pressure tube (13 x 100 mm) equipped with magnetic stir bar, 1-benzyl-3-hydroxyoxindole (**4.9**) (72 mg, 0.30 mmol, 100 mol%), Ru₃(CO)₁₂ (3.8 mg, 0.006 mmol, 2 mol%), 2,2';6,2''-terpyridine (4.2 mg, 0.018 mmol, 6 mol%) and KO^tBu (3.3 mg, 0.03 mmol, 10 mol%) was added. The tube was sealed with a rubber septum and purged with argon. Acrylic ester (0.90 mmol, 300 mol%) and *m*-xylene (1.0 M overall) were added. The rubber septum was quickly replaced with a screw cap. The mixture was heated at 140 °C (oil bath temperature) for 20 h, at which point the reaction mixture was allowed to cool to ambient temperature. The reaction mixture was concentrated and subjected to flash column chromatography to furnish the corresponding product of spirolactonization.

4.5.5 Characterization of 4.3a-l, 4.6b, 4.8a-b, 4.10a, c-i

1-oxaspiro[4.5]decane-2,6-dione (4.3a)

In accordance with general procedure A using *trans*-**4.1a**, upon stirring at 140 °C for 20 h, the reaction mixture was concentrated and subjected to flash column chromatography (SiO₂: 50% EtOAc/hexanes) to furnish **4.3a** (48 mg, 0.29 mmol, 96% yield) as a clear, yellow oil. *The spectroscopic properties of this compound were consistent with the data available in the literature.*^{113b}

TLC (SiO₂): R_f = 0.23 (hexanes:EtOAc = 1:1).

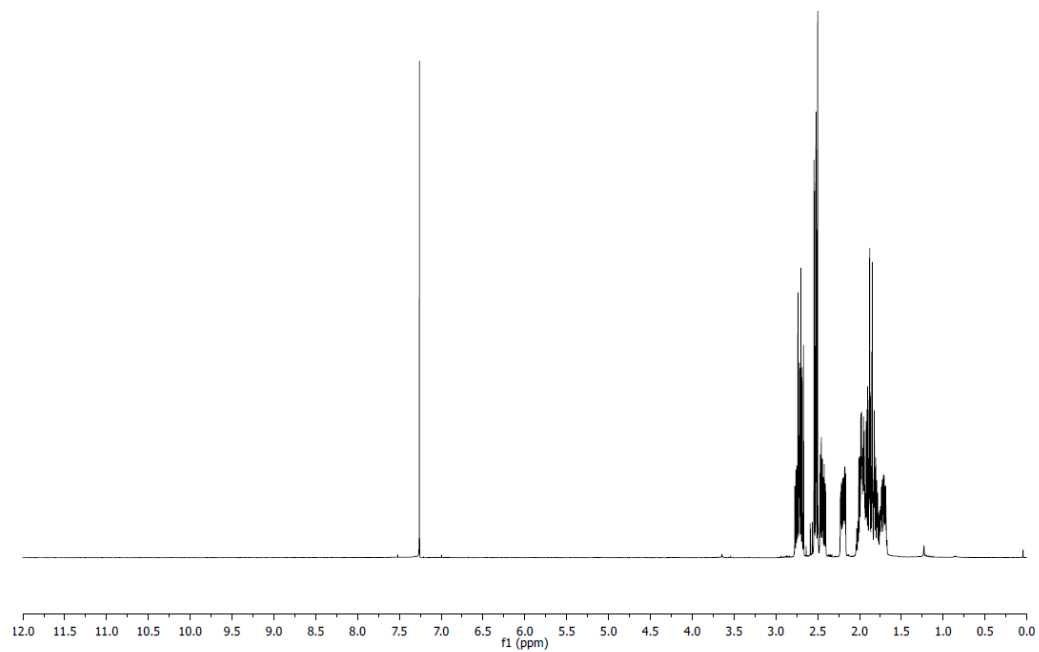
¹H NMR: (400 MHz, CDCl₃): δ 2.77-2.67 (m, 2H) 2.53 (dd, *J* = 9.5, 2.1 Hz, 1H), 2.52-2.50 (m, 1H), 2.47-2.41 (m, 1H), 2.20 (dddd, *J* = 13.2, 6.6, 3.5, 1.8 Hz, 1H), 2.04-1.67 ppm (m, 6H).

¹³C NMR: (100 MHz, CDCl₃): δ 206.0, 175.5, 88.3, 39.2, 38.8, 28.7, 28.2, 26.8, 21.5 ppm.

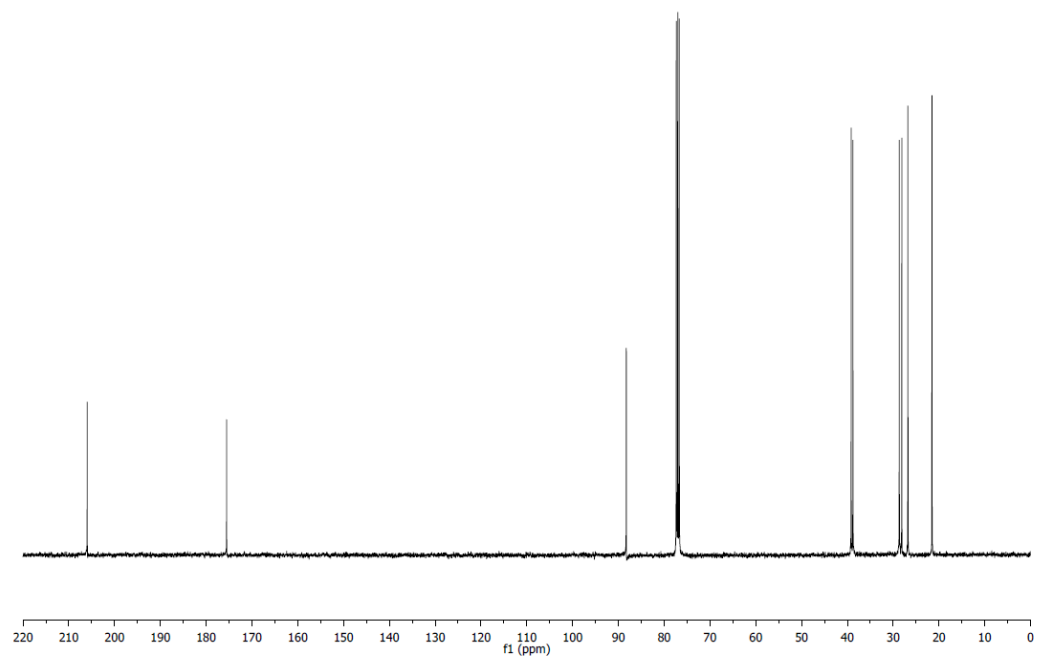
HRMS (ESI): Calculated for C₉H₁₂O₃ [M+Na]⁺: 191.06790, Found: 191.06790.

FTIR (neat): 3538, 2943, 2868, 1776, 1718, 1451, 1421, 1339, 1316, 1253, 1201, 1171, 1145, 1131, 1112, 1094, 1057, 1024 cm^{-1} .

^1H NMR of **4.3a**



^{13}C NMR of **4.3a**



1-oxaspiro[4.4]nonane-2,6-dione (**4.3b**)

In modification of general procedure A using *cis*-**4.1b**, upon addition of Ru₃(CO)₁₂ (3.8 mg, 0.006 mmol, 2 mol%), 1,3-bis(diphenylphosphino)propane (7.4 mg, 0.018 mmol, 6 mol%), and 1-adamantanecarboxylic acid (5.4 mg, 0.03 mmol, 10 mol%), the reaction tube was sealed with a rubber septum and purged with argon. Methyl acrylate (**2a**) (109 μ L, 1.20 mmol, 400 mol%) and *m*-xylene (0.19 mL, 1.0 M overall) were added upon stirring at 140 °C for 20 h, the reaction mixture was concentrated and subjected to flash column chromatography (SiO₂: 30% EtOAc/hexanes) to furnish **4.3b** (39 mg, 0.25 mmol, 85% yield) as a colorless solid. *The spectroscopic properties of this compound were consistent with the data available in the literature.*^{113a}

TLC (SiO₂): R_f = 0.17 (hexanes: EtOAc = 3:1).

¹H NMR: (400 MHz, CDCl₃): δ 2.81 (dt, *J* = 9.7, 9.6 Hz, 1H), 2.57 (ddd, *J* = 17.8, 9.8, 4.0 Hz, 1H), 2.48-2.31 (m, 4H), 2.19-2.01 (m, 3H), 1.98-1.88 ppm (m, 1H).

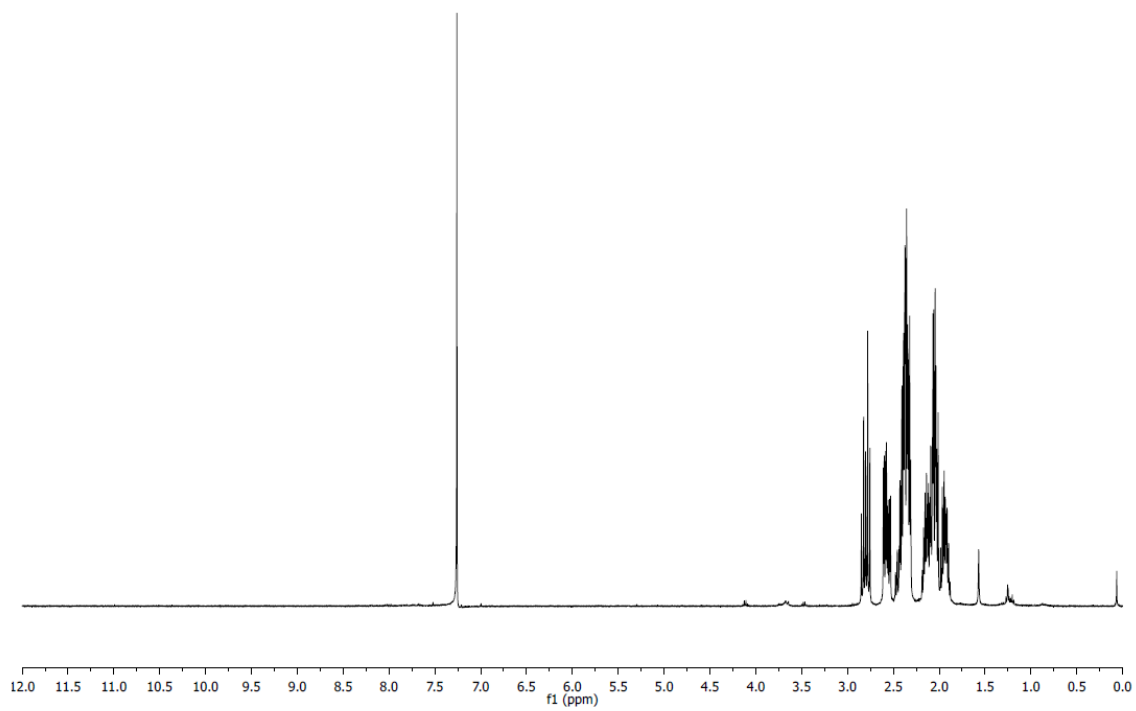
¹³C NMR: (100 MHz, CDCl₃): δ 213.6, 175.8, 86.6, 35.2, 35.0, 28.7, 28.1, 17.8 ppm.

MP: 103 – 104 °C.

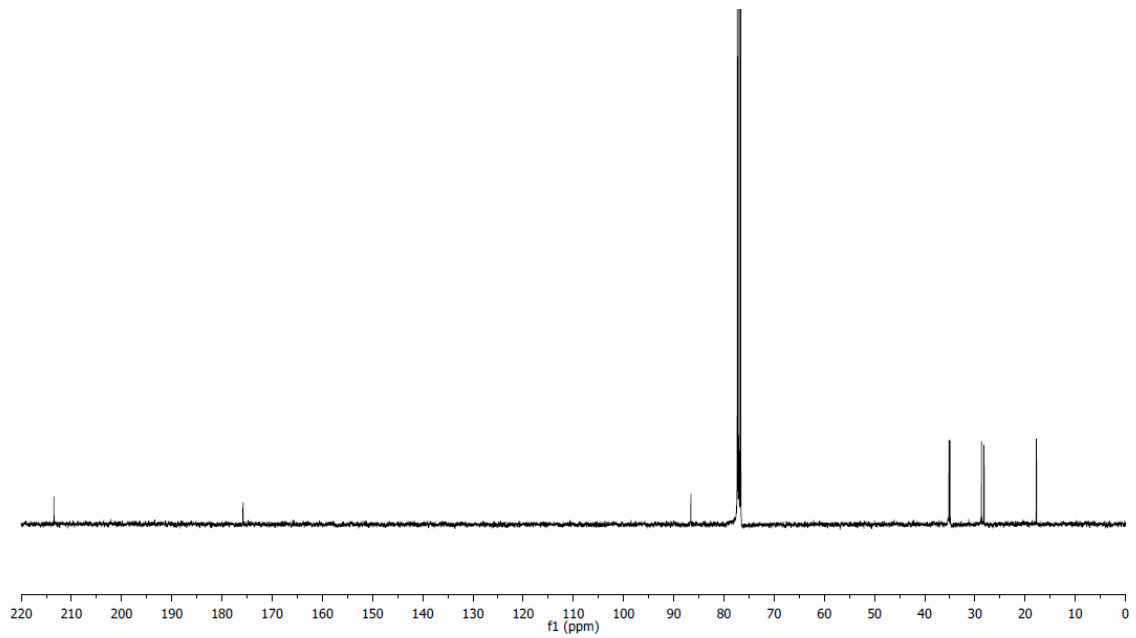
HRMS (ESI): Calculated for C₈H₁₀O₃ [M+Na]⁺: 177.05220, Found: 177.05180.

FTIR (neat): 1981, 1772, 1745, 1454, 1398, 1246, 1222, 1156, 1037 cm⁻¹.

¹H NMR of **4.3b**



¹³C NMR of **4.3b**



1-oxaspiro[4.6]undecane-2,6-dione (**4.3c**)

In accordance with general procedure A using a mixture of *cis*- and *trans*-**4.1c**, upon stirring at 140 °C for 20 h, the reaction mixture was concentrated and subjected to flash column chromatography (SiO₂: 40% EtOAc/hexanes) to furnish **4.3c** (35 mg, 0.19 mmol, 64% yield) as a colorless solid. *The spectroscopic properties of this compound were consistent with the data available in the literature.*^{111a}

TLC (SiO₂): R_f = 0.3 (hexanes:EtOAc = 1:1).

¹H NMR: (400 MHz, CDCl₃): δ 2.68 (m, 1H), 2.63 – 2.49 (m, 3H), 2.42 (ddd, *J* = 13.0, 8.8, 4.1 Hz, 1H), 2.13 (ddd, *J* = 15.0, 7.1, 1.8 Hz, 1H), 1.99 (m, 1H), 1.94 – 1.56 (m, 6H), 1.41 ppm (m, 1H).

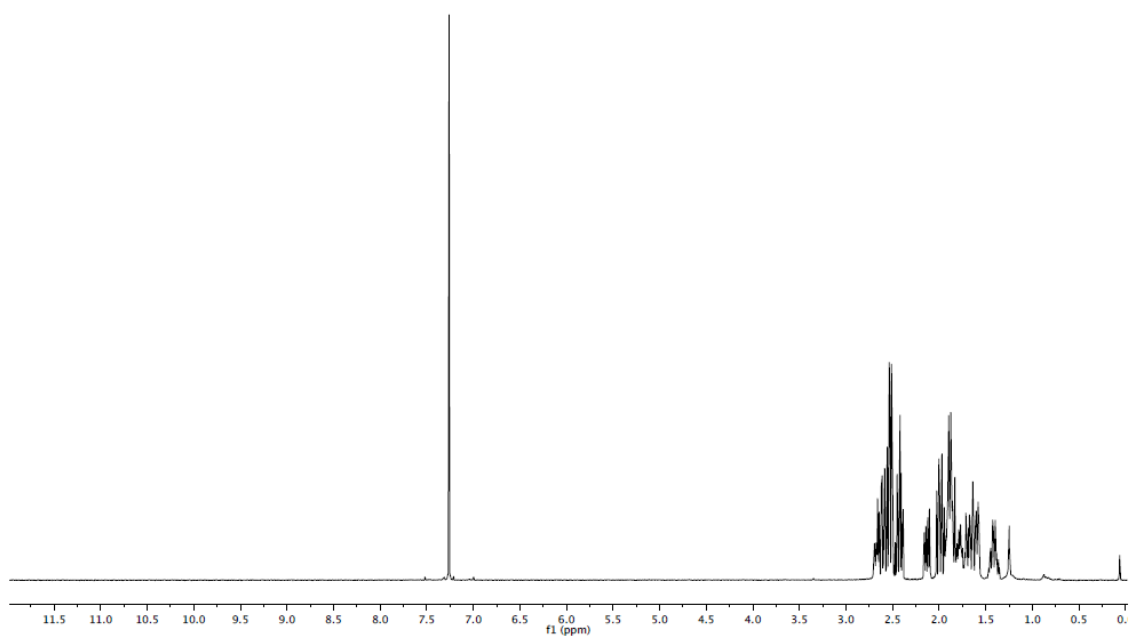
¹³C NMR: (100 MHz, CDCl₃): δ 209.2, 176.0, 90.7, 40.1, 37.1, 31.3, 29.0, 27.9, 25.2, 24.7 ppm.

MP: 64 - 65 °C.

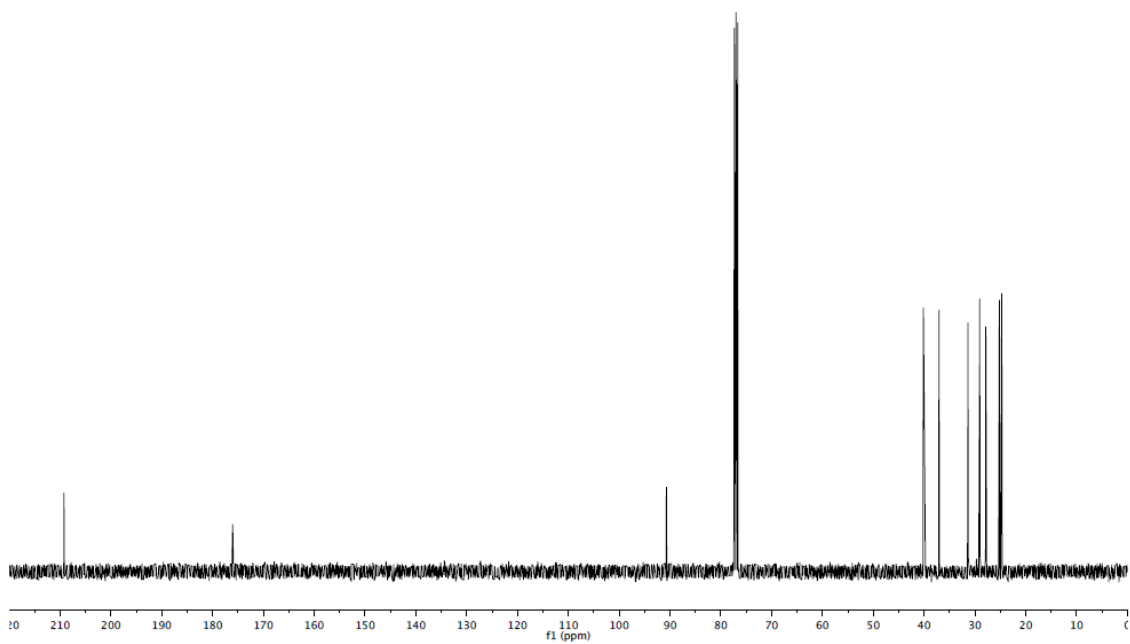
HRMS (ESI): Calculated for C₁₀H₁₄O₃ [M+Na]⁺: 205.08350, Found: 205.08390.

FTIR (neat): 2930, 2860, 1773, 1713, 1455, 1227, 1150, 943, 694 cm⁻¹.

^1H NMR of **4.3c**



^{13}C NMR of **4.3c**



1-oxaspiro[4.7]dodecane-2,6-dione (**4.3d**)

In accordance with general procedure A using *cis*-**4.1d**, upon stirring at 140 °C for 20 h, the reaction mixture was concentrated and subjected to flash column chromatography (SiO₂: 40% EtOAc/hexanes) to furnish **4.3d** (46 mg, 0.24 mmol, 79% yield) as a clear yellow oil.

TLC (SiO₂): R_f = 0.27 (hexanes:EtOAc = 3:2).

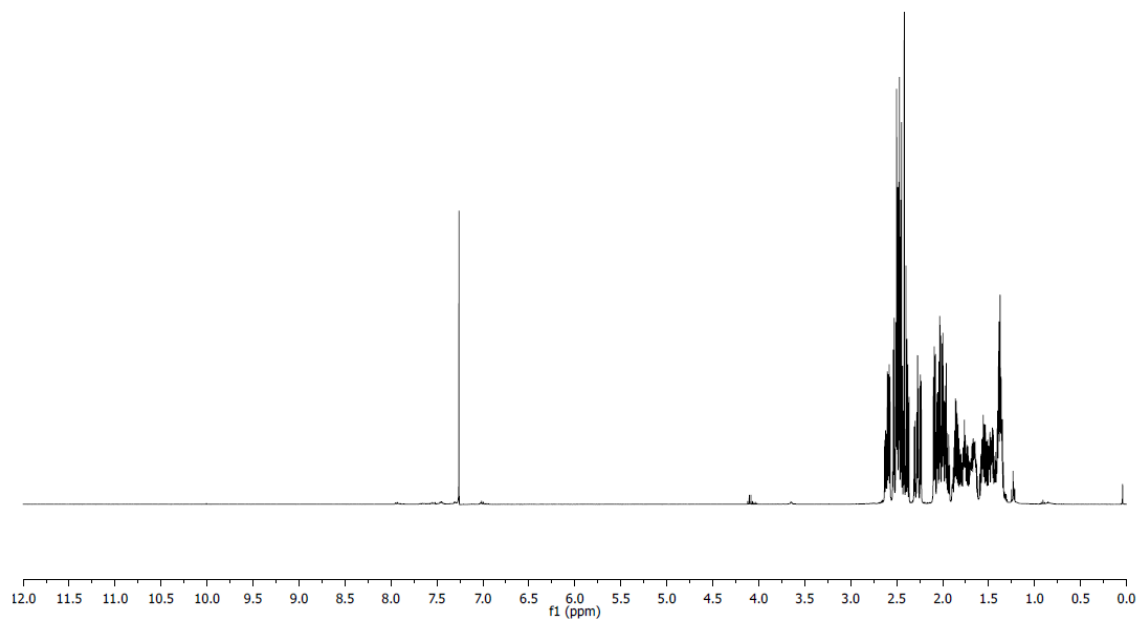
¹H NMR: (400 MHz, CDCl₃): δ 2.60 (ddd, *J* = 12.2, 7.1, 4.0 Hz, 1H), 2.54-2.37 (m, 4H), 2.27 (ddd, *J* = 14.9, 11.7, 4.0 Hz, 1H), 2.10-1.92 (m, 3H), 1.90-1.62 (m, 3H), 1.60-1.34 ppm (m, 4H).

¹³C NMR: (100 MHz, CDCl₃): δ 212.6, 176.0, 90.3, 38.1, 36.4, 31.0, 28.1, 27.7, 26.3, 24.4, 22.8 ppm.

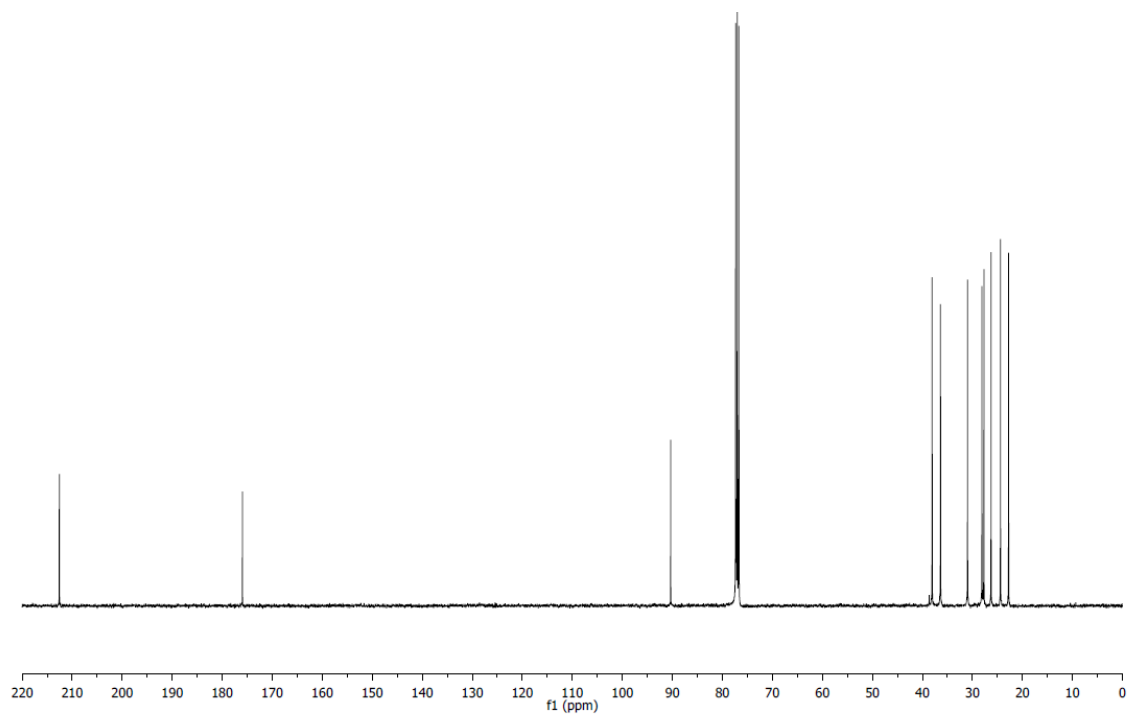
HRMS (ESI): Calculated for C₁₁H₁₆O₃ [M+Na]⁺: 219.09920, Found 219.09890.

FTIR (neat): 2923, 2854, 1708, 1438, 1408, 1205, 1170, 1032 cm⁻¹.

^1H NMR of **4.3d**



^{13}C NMR of **4.3d**



5-acetyl-5-methyldihydrofuran-2(3H)-one (**4.3e**)

In accordance with general procedure A using a mixture of *cis*- and *trans*-**4.1e**, upon stirring at 140 °C for 20 h, the reaction mixture was concentrated and subjected to flash column chromatography (SiO₂: 40% EtOAc/hexanes) to furnish **4.3e** (40 mg, 0.28 mmol, 93% yield) as a colorless solid. *The spectroscopic properties of this compound were consistent with the data available in the literature.*^{107b}

TLC (SiO₂): R_f = 0.3 (hexanes:EtOAc = 2:1).

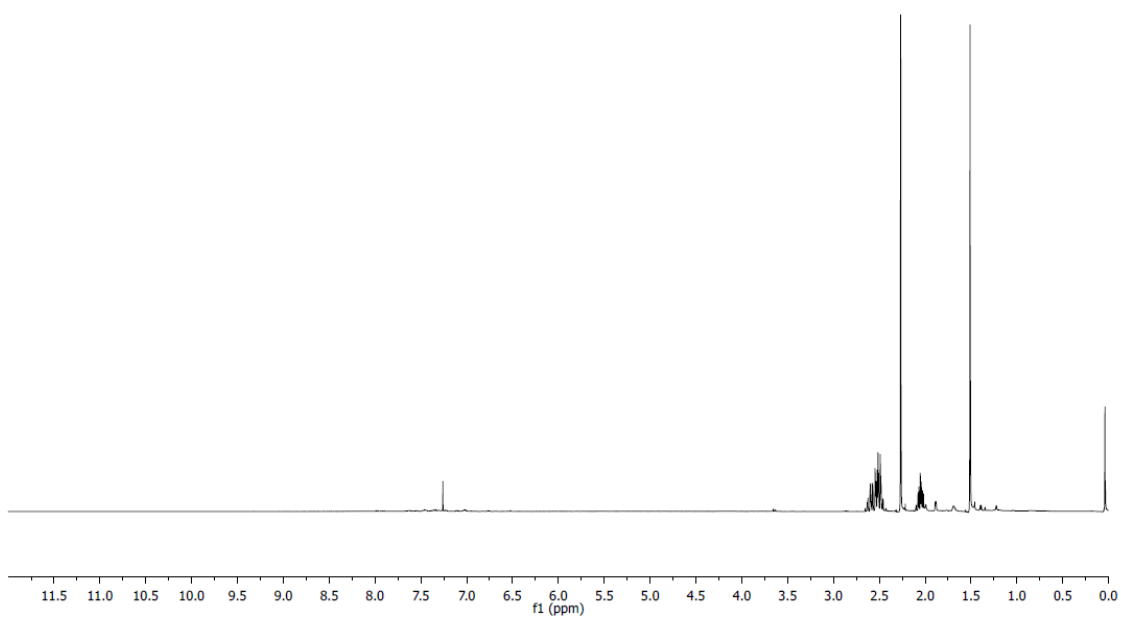
¹H NMR: (400 MHz, CDCl₃): δ 2.63-2.46 (m, 3H), 2.27 (s, 3H), 2.08-2.02 (m, 1H), 1.51 ppm (s, 3H).

¹³C NMR: (100 MHz, CDCl₃): δ 207.1, 174.6, 88.2, 39.8, 27.3, 24.3, 22.4 ppm.

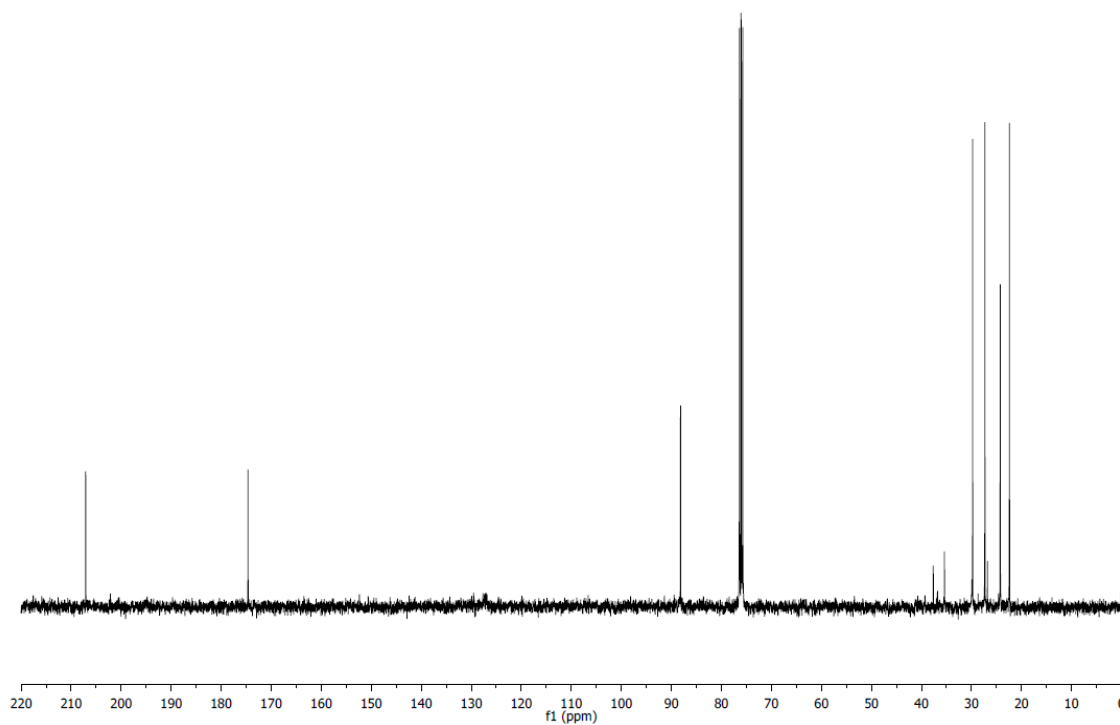
HRMS (ESI): Calculated for C₇H₁₀O₃ [M+Na]⁺:165.05220, Found: 165.05200.

FTIR: (neat): 1774, 1718, 1361, 1234, 1209, 1166, 1139, 1092, 10003, 947, 903, 667 cm⁻¹.

^1H NMR of **4.3e**



^{13}C NMR of **4.3e**



5-benzoyl-5-phenyldihydrofuran-2(3H)-one (**4.3f**)

In accordance with general procedure A using a mixture of *cis*- and *trans*-**4.1f**, upon stirring at 140 °C for 20 h, the reaction mixture was concentrated and subjected to flash column chromatography (SiO₂: 40% EtOAc/hexanes) to furnish **4.3f** (72 mg, 0.27 mmol, 90% yield) as a colorless oil. *The spectroscopic properties of this compound were consistent with the data available in the literature.*^{107b}

TLC (SiO₂): R_f = 0.14 (hexanes:EtOAc = 9:1).

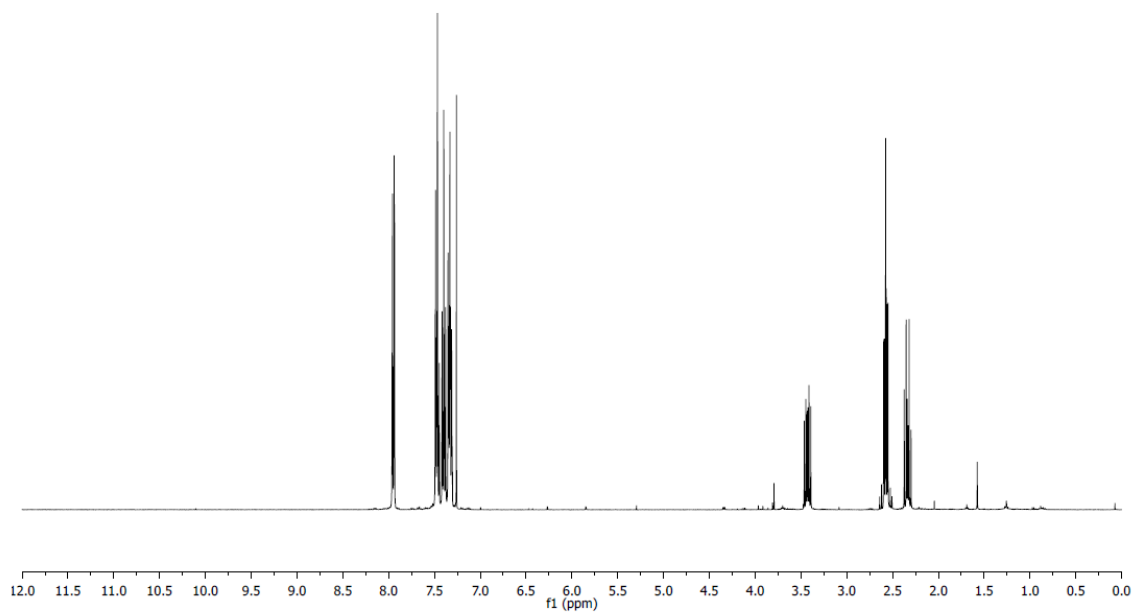
¹H NMR: (400 MHz, CDCl₃): δ 7.96-7.94 (m, 2H), 7.49-7.44 (m, 3H), 7.42-7.37 (m, 2H), 7.36-7.30 (m, 3H), 3.43 (ddd, *J* = 13.0, 8.3, 7.1 Hz, 1H), 2.60-2.55 (m, 2H), 2.34 ppm (dt, *J* = 13.0, 8.3 Hz, 1H).

¹³C NMR: (100 MHz, CDCl₃): δ 195.2, 175.6, 139.3, 133.5, 133.4, 13.7, 129.3, 128.5, 128.3, 123.7, 92.1, 34.3, 28.0 ppm.

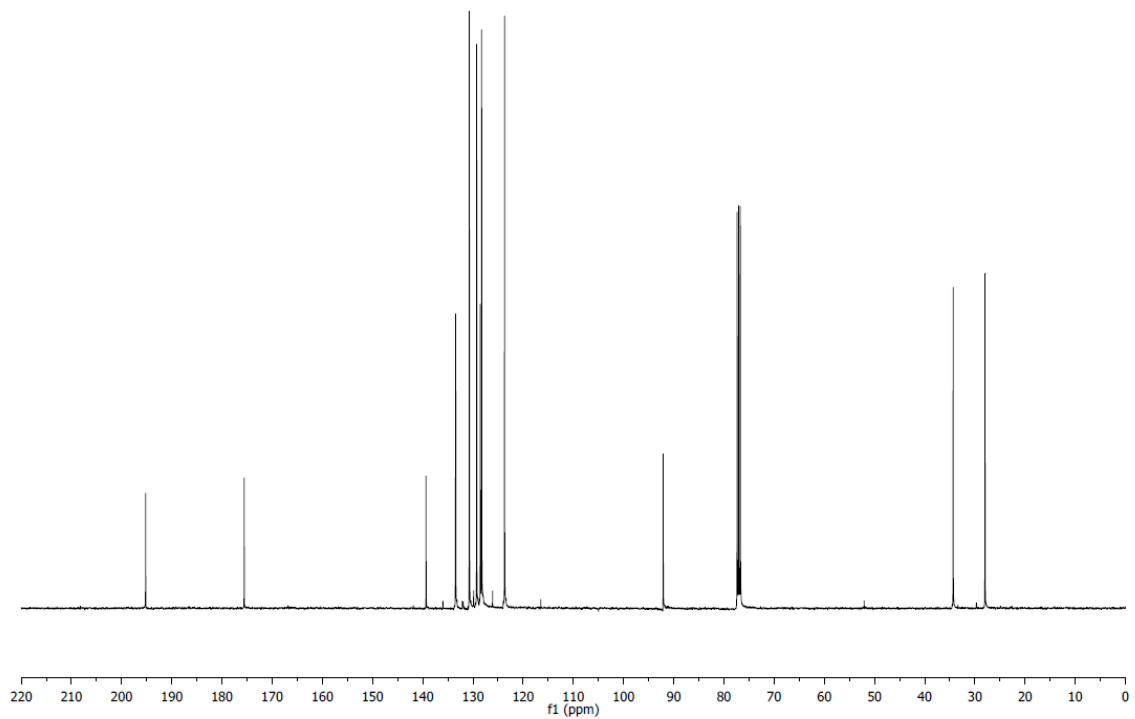
HRMS (ESI): Calculated for C₁₇H₁₄O₃ [M+Na]⁺:289.08350, Found: 289.08430.

FTIR (neat): 3062, 1784, 1580, 1597, 1448, 1268, 1159, 1086, 1056, 899, 758, 701, 687 cm⁻¹.

^1H NMR of **4.3f**



^{13}C NMR of **4.3f**



5-acetyl-5-phenyldihydrofuran-2(3H)-one (**4.3g**)

In accordance with general procedure A using *trans*-**4.1g**, upon stirring at 140 °C for 20 h, the reaction mixture was concentrated to afford the crude spirolactones (rr = 4:1, as determined by ¹H NMR spectroscopy). The crude reaction mixture was subjected to flash column chromatography (SiO₂: 30% EtOAc/hexanes) to furnish **4.3g** (36 mg, 0.18 mmol, 74% yield) as a colorless oil. *The spectroscopic properties of this compound were consistent with the data available in the literature.*^{107b}

TLC (SiO₂): R_f = 0.57 (hexanes:EtOAc = 1:1).

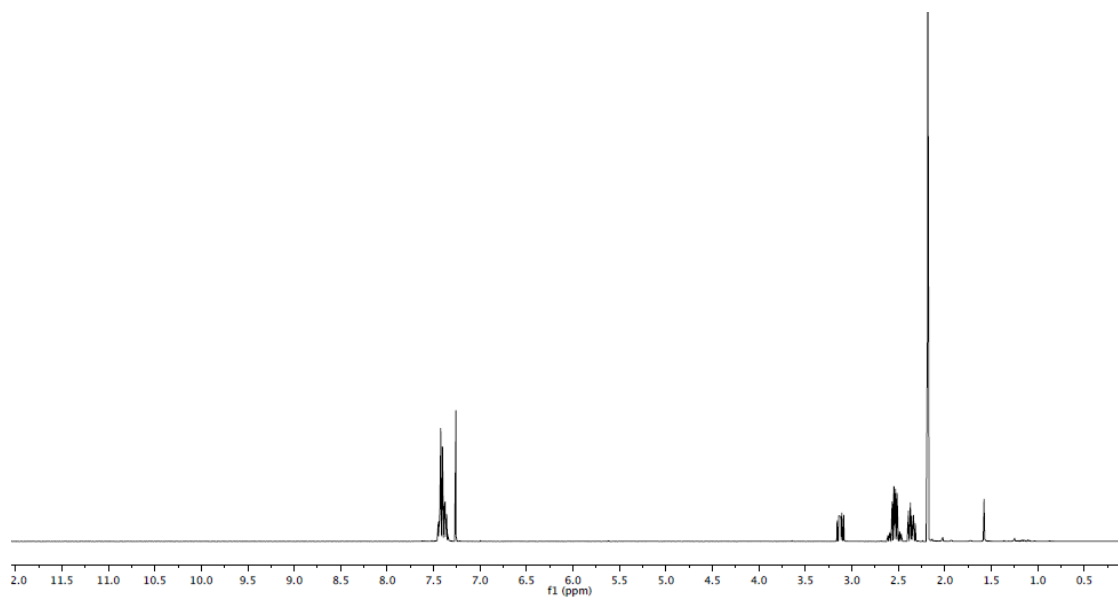
¹H NMR: (400 MHz, CDCl₃): δ 7.46 – 7.33 (m, 5H), 3.12 (ddd, *J* = 12.9, 8.7, 7.0 Hz, 1H), 2.64 – 2.45 (m, 2H), 2.35 (m, 1H), 2.19 ppm (s, 3H).

¹³C NMR: (100 MHz, CDCl₃): δ 204.7, 175.2, 137.7, 129.0, 128.8, 124.4, 92.1, 31.6, 28.2, 25.1 ppm.

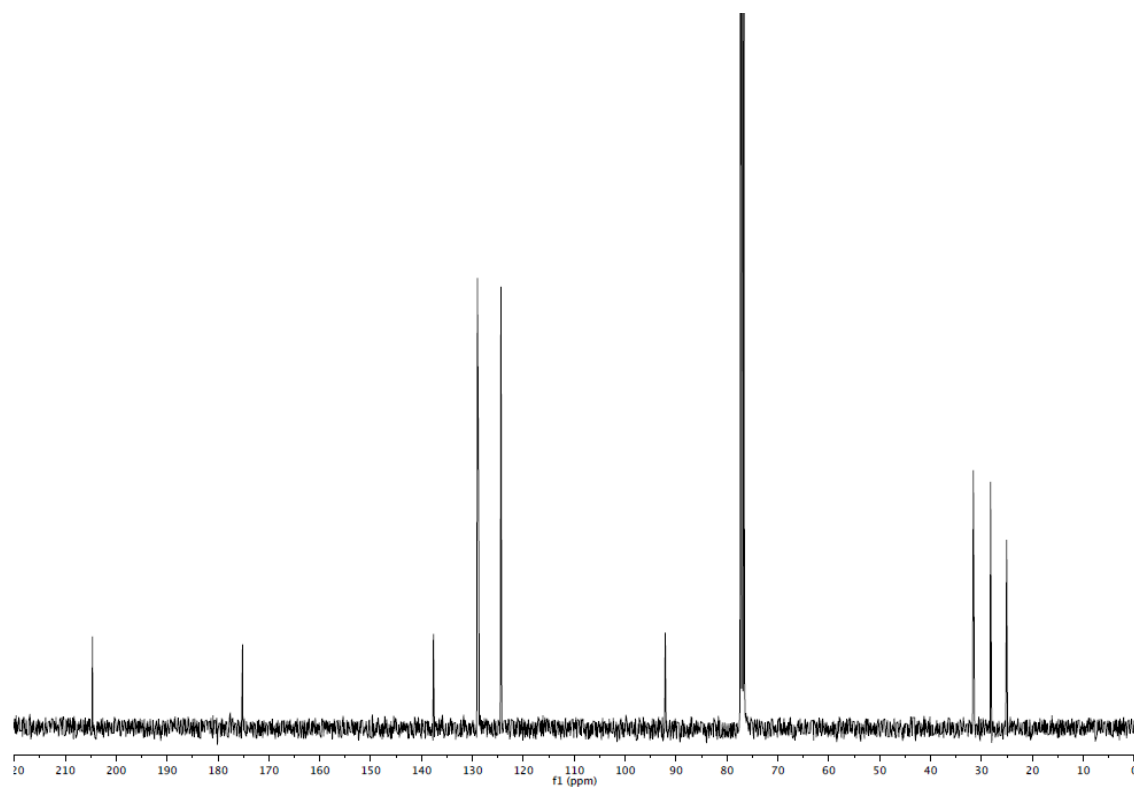
HRMS (ESI): Calculated for C₁₂H₁₂O₃ [M+Na]⁺: 227.06790, Found: 227.06790.

FTIR (neat): 3062, 2922, 2852, 1783, 1719, 1682, 1449, 1235, 1153, 1091, 700 cm⁻¹.

¹H NMR of 4.3g



¹³C NMR of 4.3g



5-acetyl-5-(*tert*-butyl)dihydrofuran-2(3H)-one (**4.3h**)

In accordance with general procedure A using *trans*-**4.1h**, upon stirring at 140 °C for 20 h, the reaction mixture was concentrated to afford the crude spiro lactones (rr = 1.3:1, as determined by ¹H NMR spectroscopy). The crude reaction mixture was subjected to flash column chromatography (SiO₂: 20% EtOAc/hexanes) to furnish **4.3h** (42 mg, 0.25 mmol, 75% yield) as a colorless oil.

TLC (SiO₂): R_f = 0.50 (hexanes:EtOAc = 2:1).

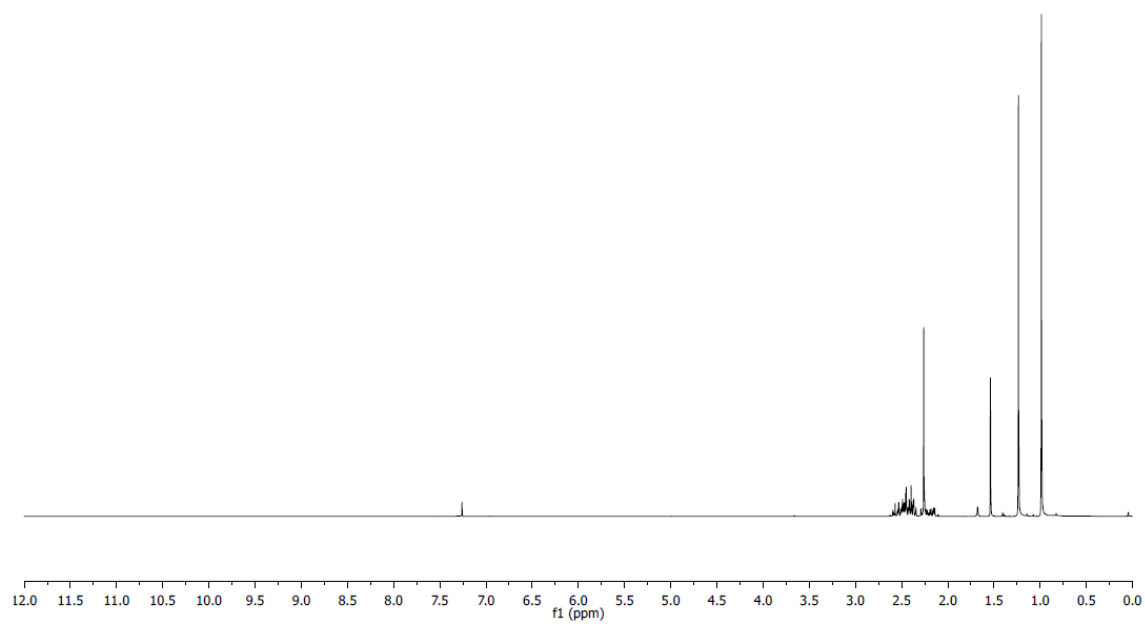
¹H NMR: (400 MHz, CDCl₃): δ 2.59-2.10 (m, 7.4H), 2.26 (s, 3H, *major*), 1.54 (s, 2.3H, *minor*), 1.24 (s, 7.4H, *minor*), 0.99 ppm (s, 9H, *major*).

¹³C NMR: (100 MHz, CDCl₃): δ 214.9, 211.1, 175.9, 175.9, 96.8, 90.8, 44.9, 37.1, 33.4, 29.6, 28.8, 27.8, 26.9, 26.3, 26.3, 24.8 ppm.

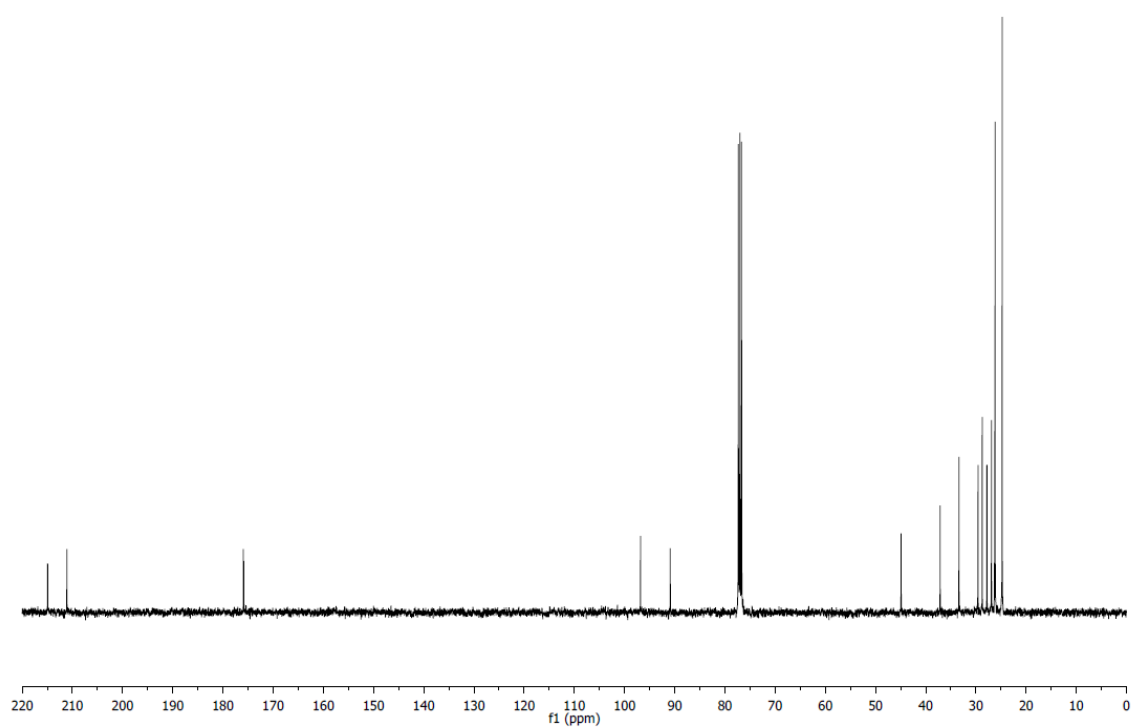
HRMS (ESI): Calculated for C₁₀H₁₆O₃ [M+Na]⁺: 207.09920, Found: 207.09910.

FTIR (neat): 2971, 1778, 1714, 1699, 1370, 1251, 1153, 1128, 1053, 1008, 904, 675 cm⁻¹.

^1H NMR of **4.3h**



^{13}C NMR of **4.3h**



1,3-dihydrospiro[indene-2,2'-oxolane]-1,5'-dione (**4.3i**)

In accordance with general procedure A using *trans*-**4.1i**, upon stirring at 140 °C for 20 h, the reaction mixture was concentrated to afford the crude spiro lactones (rr = >20:1, as determined by ¹H NMR spectroscopy). The crude reaction mixture was subjected to flash column chromatography (SiO₂: 50% EtOAc/hexanes) to furnish **4.3i** (54 mg, 0.27 mmol, 89% yield) as a colorless solid.

TLC (SiO₂): R_f = 0.35 (hexanes:EtOAc = 1:1).

¹H NMR: (400 MHz, CDCl₃): δ 7.80 (d, *J* = 7.7 Hz, 1H), 7.68 (td, *J* = 7.6, 1.2 Hz, 1H), 7.46 (m, 2H), 3.61 (d, *J* = 17.4 Hz, 1H), 3.33 (d, *J* = 17.4 Hz, 1H), 3.02 (dt, *J* = 17.7, 9.6 Hz, 1H), 2.67 (ddd, *J* = 17.7, 9.5, 4.0 Hz, 1H), 2.51 (ddd, *J* = 13.6, 9.7, 4.0 Hz, 1H), 2.27 ppm (dt, *J* = 13.1, 9.6 Hz, 1H).

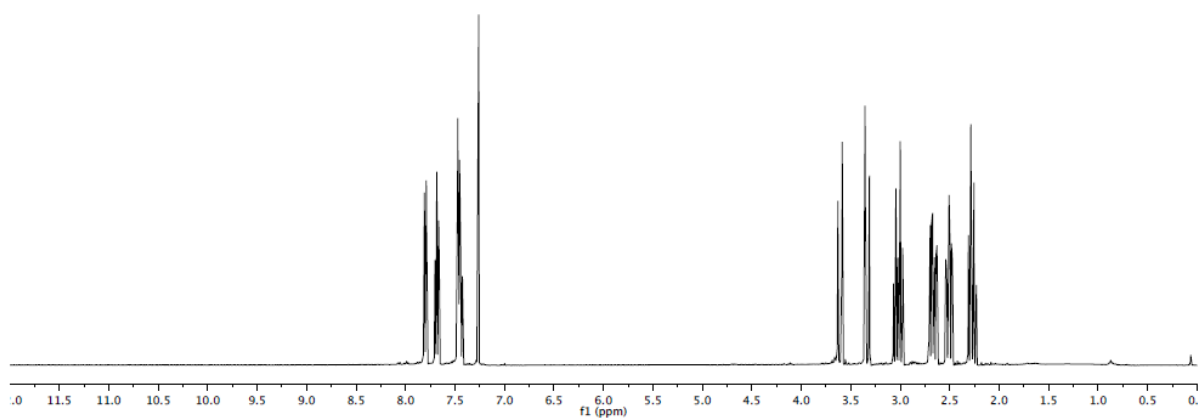
¹³C NMR: (100 MHz, CDCl₃): δ 201.5, 176.2, 150.1, 136.5, 133.1, 128.5, 126.6, 125.2, 86.4, 39.7, 31.2, 28.6 ppm.

MP: 68 - 70 °C.

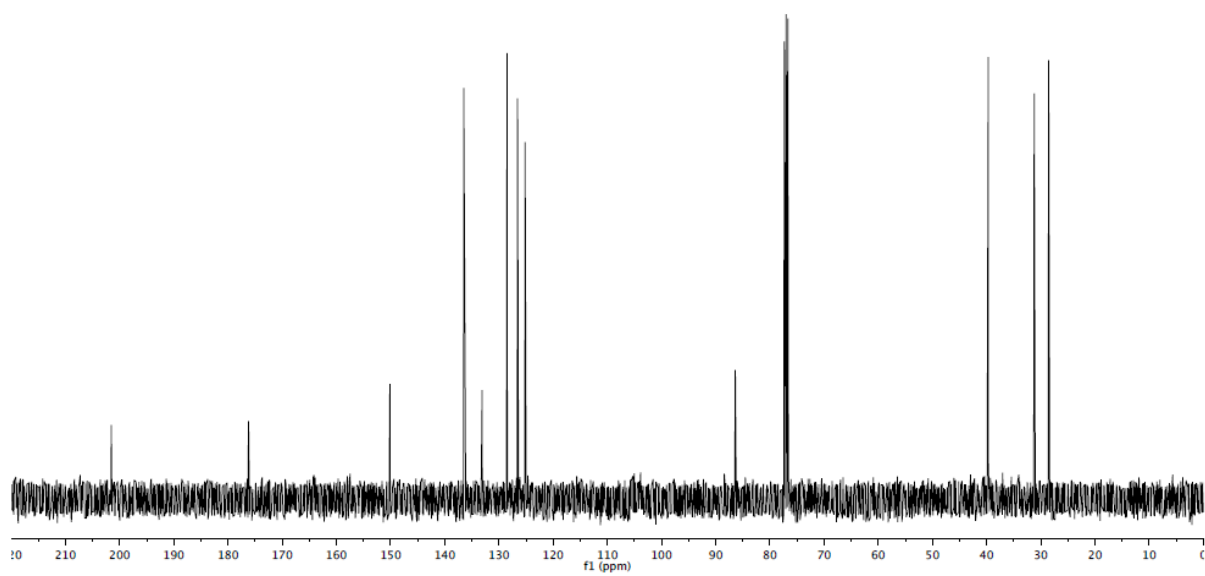
HRMS (ESI): Calculated for C₁₂H₁₀O₃ [M+Na]⁺: 225.05220, Found: 225.05190.

FTIR (neat): 2942, 1776, 1713, 1603, 1462, 1227, 1167, 1061, 940, 759 cm⁻¹.

¹H NMR of **4.3i**



¹³C NMR of **4.3i**



3,4-dihydro-1H-spiro[naphthalene-2,2'-oxolane]-1,5'-dione (**4.3j**)

In accordance with general procedure A using a mixture of *cis*- and *trans*-**4.1j**, upon stirring at 140 °C for 20 h, the reaction mixture was concentrated to afford the crude spiro lactones (rr = >20:1, as determined by ¹H NMR spectroscopy). The crude reaction mixture was subjected to flash column chromatography (SiO₂: 30% EtOAc/hexanes) to furnish **4.3j** (57 mg, 0.26 mmol, 88% yield) as a colorless solid. *The spectroscopic properties of this compound were consistent with the data available in the literature.*^{113b}

TLC (SiO₂): R_f = 0.38 (hexanes:EtOAc = 1:1).

¹H NMR: (400 MHz, CDCl₃): δ 8.07 (dd, *J* = 7.9, 1.3 Hz, 1H), 7.54 (td, *J* = 7.5, 1.4 Hz, 1H), 7.37 (dd, *J* = 7.8, 7.4 Hz, 1H), 7.28 (d, *J* = 7.8 Hz, 1H), 3.20 (dt, *J* = 17.2, 5.3 Hz, 1H), 3.09 (ddd, *J* = 17.2, 9.9, 4.7 Hz, 1H), 2.80 (ddd, *J* = 17.9, 10.8, 9.8 Hz, 1H), 2.59 (m, 3H), 2.31 (ddd, *J* = 13.5, 5.5, 5.0 Hz, 1H), 2.15 ppm (ddd, *J* = 13.0, 10.8, 9.7 Hz, 1H).

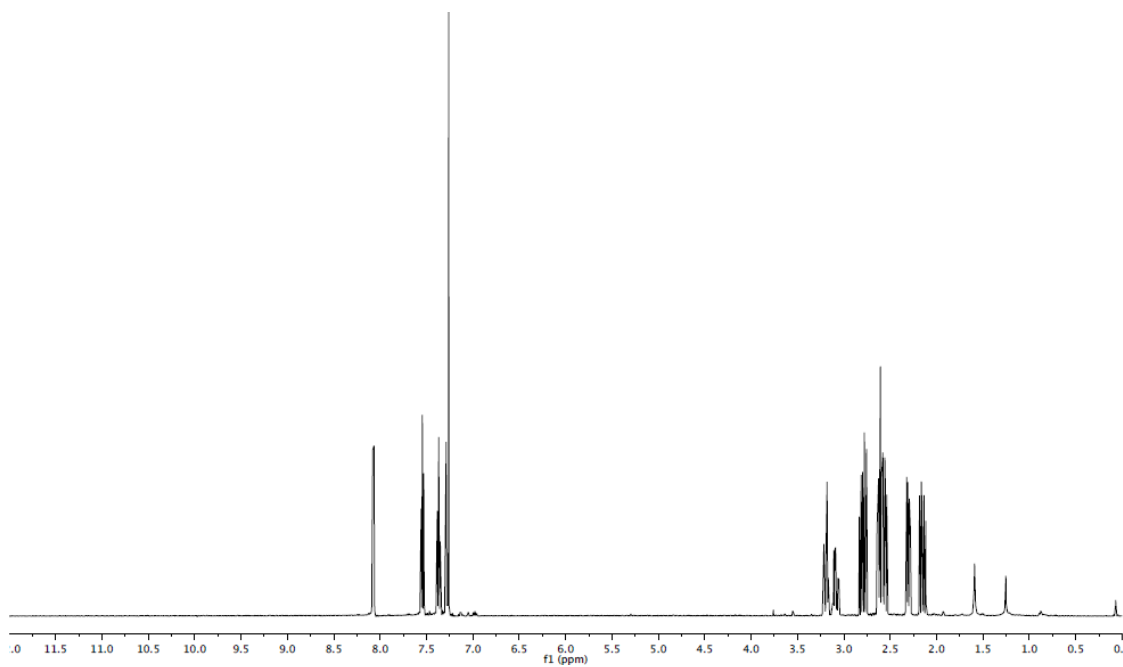
¹³C NMR: (100 MHz, CDCl₃): δ 193.5, 176.1, 143.0, 134.4, 130.0, 128.7, 128.5, 127.3, 85.0, 34.5, 29.6, 27.9, 25.7 ppm.

MP: 94 - 95 °C.

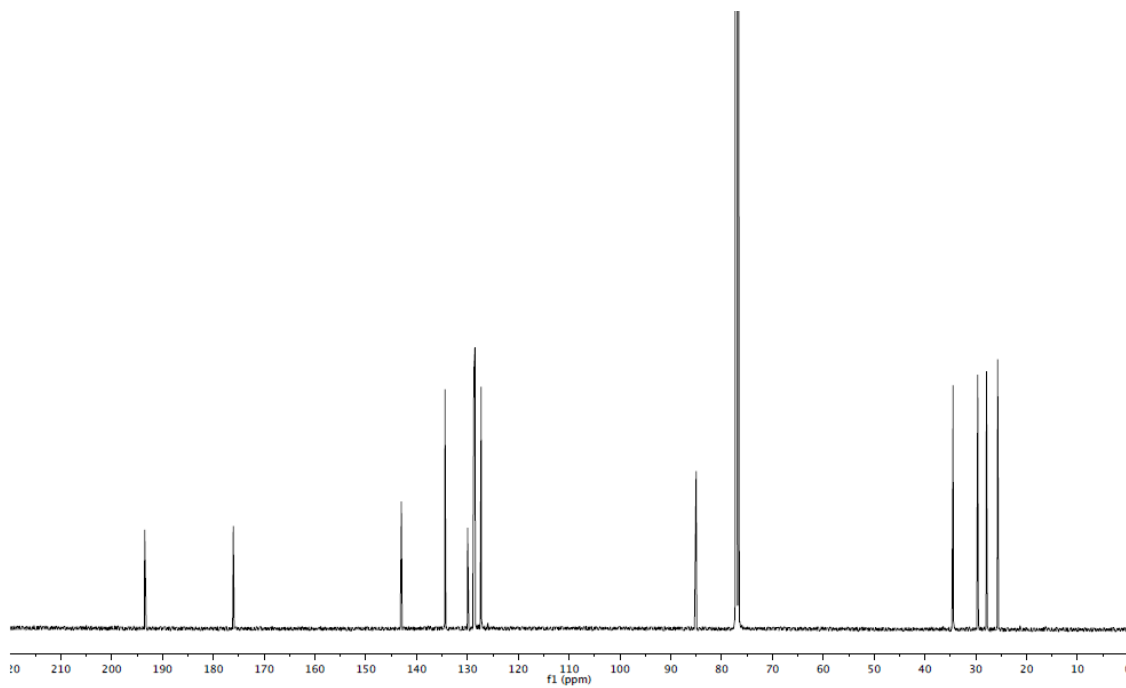
HRMS (ESI). Calculated for C₁₃H₁₂O₃ [M+Na]⁺: 239.06790, Found: 239.08610.

FTIR (neat): 2951, 2937, 1772, 1687, 1602, 1454, 1217, 1067, 949, 743 cm⁻¹.

¹H NMR of **4.3j**



¹³C NMR of **4.3j**



2H,3'H-spiro[acenaphthylene-1,2'-furan]-2,5'(4'H)-dione (**4.3k**)

In accordance with general procedure A using a mixture of *cis*- and *trans*-**4.1k**, upon stirring at 140 °C for 20 h, the reaction mixture was concentrated and subjected to flash column chromatography (SiO₂: 20% EtOAc/hexanes) to furnish **4.3k** (42 mg, 0.18 mmol, 59% yield) as a tan solid.

TLC (SiO₂): R_f = 0.28 (hexanes:EtOAc = 3:1).

¹H NMR: (400 MHz, CDCl₃): δ 8.19 (dd, *J* = 8.3, 0.6 Hz, 1H), 8.03 (dd, *J* = 7.1, 0.7 Hz, 1H), 7.98 (dd, *J* = 8.3, 0.7 Hz, 1H), 7.80 (dd, *J* = 8.3, 7.1 Hz, 1H), 7.74 (dd, *J* = 8.3, 7.1 Hz, 1H), 7.66 (dd, *J* = 7.1, 0.7 Hz, 1H), 3.25 (ddd, *J* = 17.7, 9.7, 10.4 Hz, 1H), 2.87 (ddd, *J* = 17.7, 9.0, 3.9 Hz, 1H), 2.68-2.55 ppm (m, 2H).

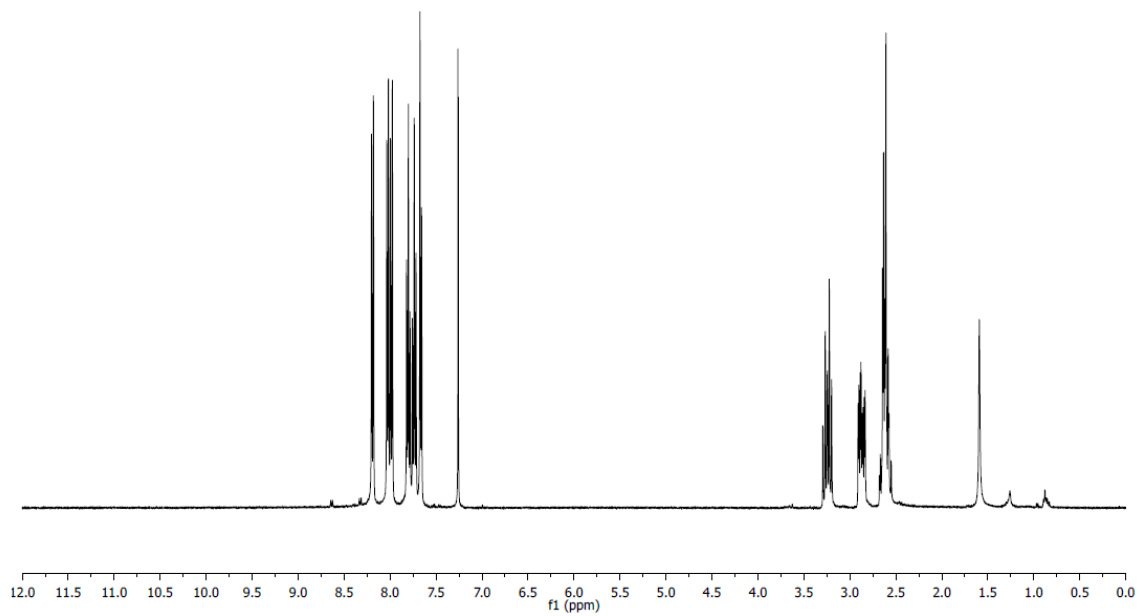
¹³C NMR: (100 MHz, CDCl₃): δ 200.2, 176.3, 142.1, 136.1, 132.4, 130.6, 129.6, 128.9, 128.8, 126.6, 123.0, 120.8, 86.0, 31.3, 28.6 ppm.

MP: 131 - 132 °C.

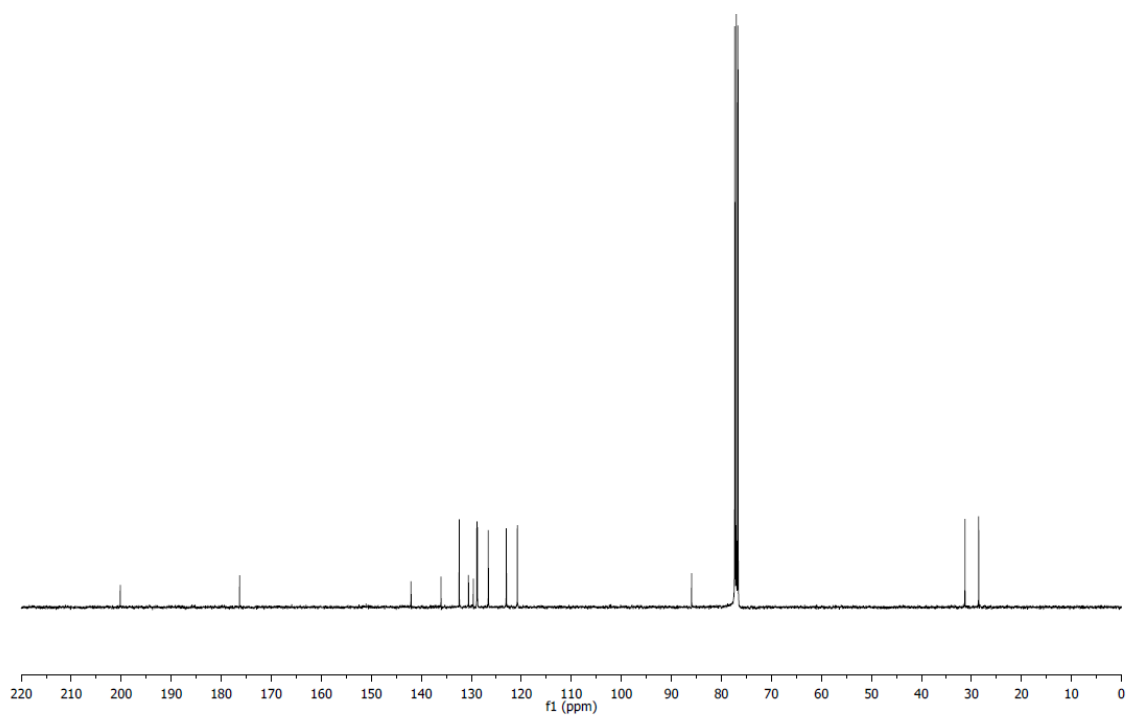
HRMS (ESI): Calculated for C₁₅H₁₀O₃ [M+Na]⁺:261.05220, Found: 261.05230.

FTIR (neat): 1778, 1719, 1493, 1452, 1203, 1179, 1160, 1135, 1029, 919, 876, 782 cm⁻¹.

¹H NMR of **4.3k**



¹³C NMR of **4.3k**



3,4-dihydro-1H-spiro[naphthalene-2,2'-oxolane]-1,5'-dione (**4.3I**)

In accordance with general procedure A using *cis*-**4.1I**, upon stirring at 140 °C for 20 h, the reaction mixture was concentrated to afford the crude spiro lactones (*rr* = >20:1, as determined by ¹H NMR spectroscopy). The crude reaction mixture was subjected to flash column chromatography (SiO₂: 20% EtOAc/hexanes) to furnish **4.3I** (55 mg, 0.22 mmol, 74% yield) as a colorless solid.

TLC (SiO₂): R_f = 0.54 (hexanes:EtOAc = 1:1)

¹H NMR: (400 MHz, CDCl₃): δ 7.88 (dd, *J* = 7.9, 1.6 Hz, 1H), 7.53 (td, *J* = 8.5, 1.8 Hz, 1H), 7.05 (dt, *J* = 7.9, 0.9 Hz, 1H), 6.94 (dd, *J* = 8.4, 0.5 Hz, 1H), 2.74 (dt, *J* = 18.1, 10.0 Hz, 1H), 2.61 (ddd, *J* = 18.0, 9.4, 4.2 Hz, 1H), 2.36 (m, 2H), 1.49 (s, 3H), 1.46 ppm (s, 3H).

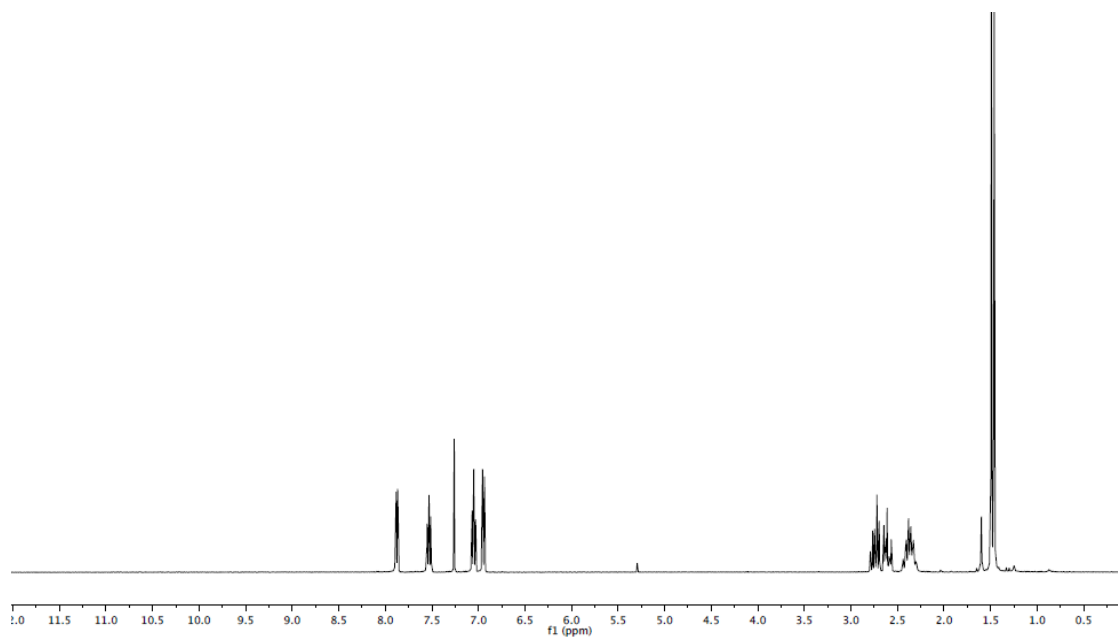
¹³C NMR: (100 MHz, CDCl₃): δ 189.6, 175.4, 158.6, 137.0, 127.6, 121.7, 118.4, 118.2, 86.5, 81.8, 28.0, 24.6, 21.3, 21.2 ppm.

MP: 145 - 147 °C.

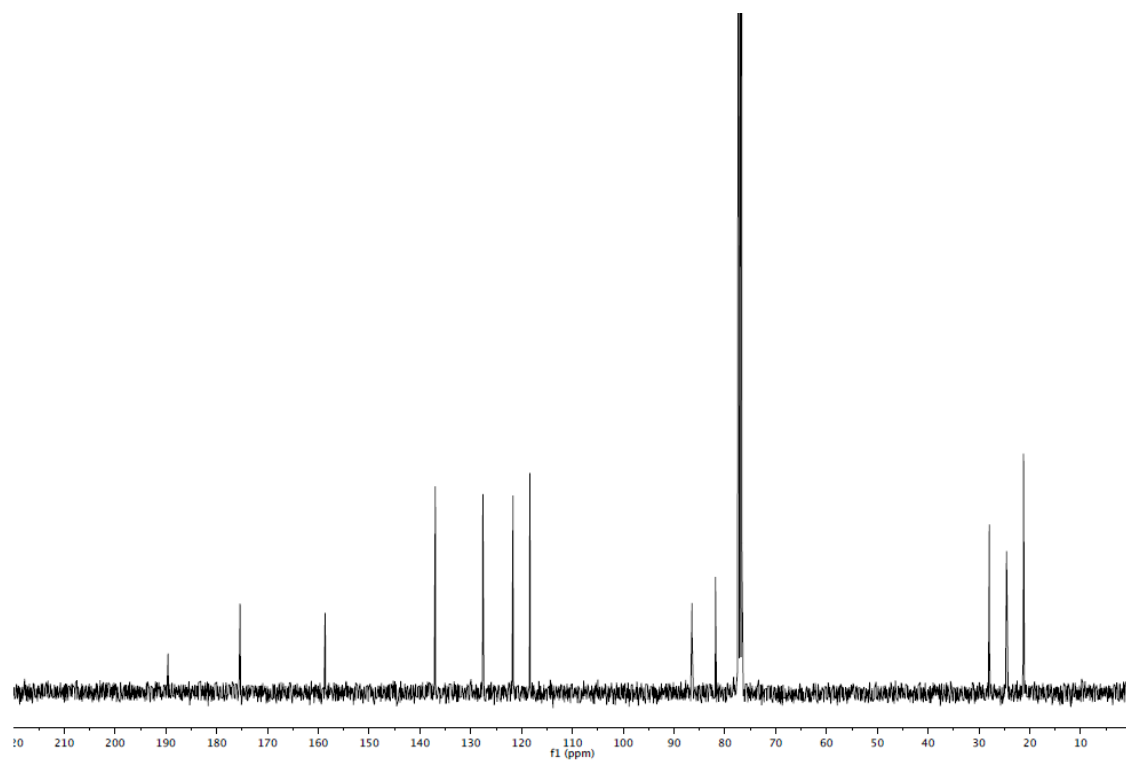
HRMS (ESI): Calculated for C₁₄H₁₄O₄ [M+Na]⁺: 269.07840, Found: 269.07820.

FTIR (neat): 2982, 2921, 1776, 1703, 1610, 1462, 1424, 1327, 1307, 1165, 1138, 1065, 922, 749. cm⁻¹.

¹H NMR of **4.3I**



¹³C NMR of **4.3I**



3-methylene-1-oxaspiro[4.5]decane-2,6-dione (**4.6b**)

In modification of general procedure A, upon addition *trans*-**4.1a** (0.3 mmol, 100 mol%), Ru₃(CO)₁₂ (3.8 mg, 0.006 mmol, 2 mol%), 1,3-bis(diphenylphosphino)propane (7.4 mg, 0.018 mmol, 6 mol%), and 1-adamantanecarboxylic acid (5.4 mg, 0.03 mmol, 10 mol%), the tube was sealed with a rubber septum and purged with argon. Acrylate **4.2b** (104 mg, 0.90 mmol, 300 mol%) and *m*-xylenes (0.22 mL, 1.0 M overall) The reaction mixture was concentrated and subjected to flash column chromatography (SiO₂: 30% EtOAc/hexanes) to furnish **4.6b** (32 mg, 0.18 mmol, 59% yield) as a clear, colorless oil.

TLC (SiO₂): R_f = 0.23 (hexanes:EtOAc = 2:1).

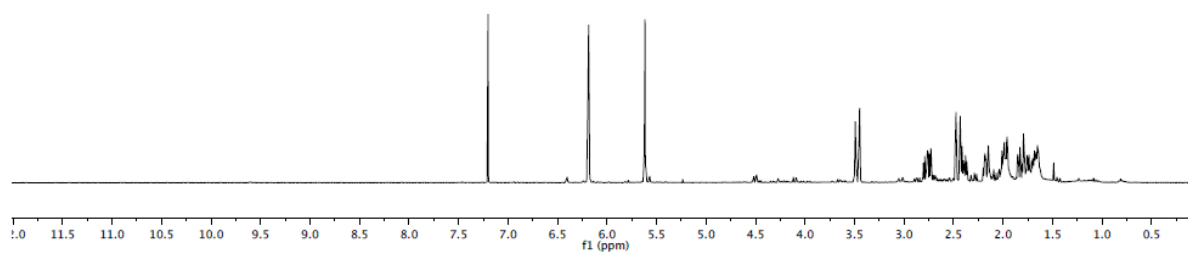
¹H NMR: (400 MHz, CDCl₃): δ 6.24 (t, *J* = 2.9 Hz, 1H), 5.67 (t, *J* = 2.5 Hz, 1H), 3.53 (dt, *J* = 17.3, 2.6 Hz, 1H), 2.83 (ddd, *J* = 13.9, 10.9, 6.0 Hz, 1H), 2.51 (d, *J* = 17.3, 2.9 Hz, 1H), 2.45 (m, 1H), 2.22 (m, 1H), 2.09 – 2.00 (m, 2H), 1.92 – 1.67 ppm (m, 3H).

¹³C NMR: (100 MHz, CDCl₃): δ 205.1, 168.5, 133.4, 123.5, 85.3, 39.9, 38.8, 33.6, 27.1, 21.3 ppm.

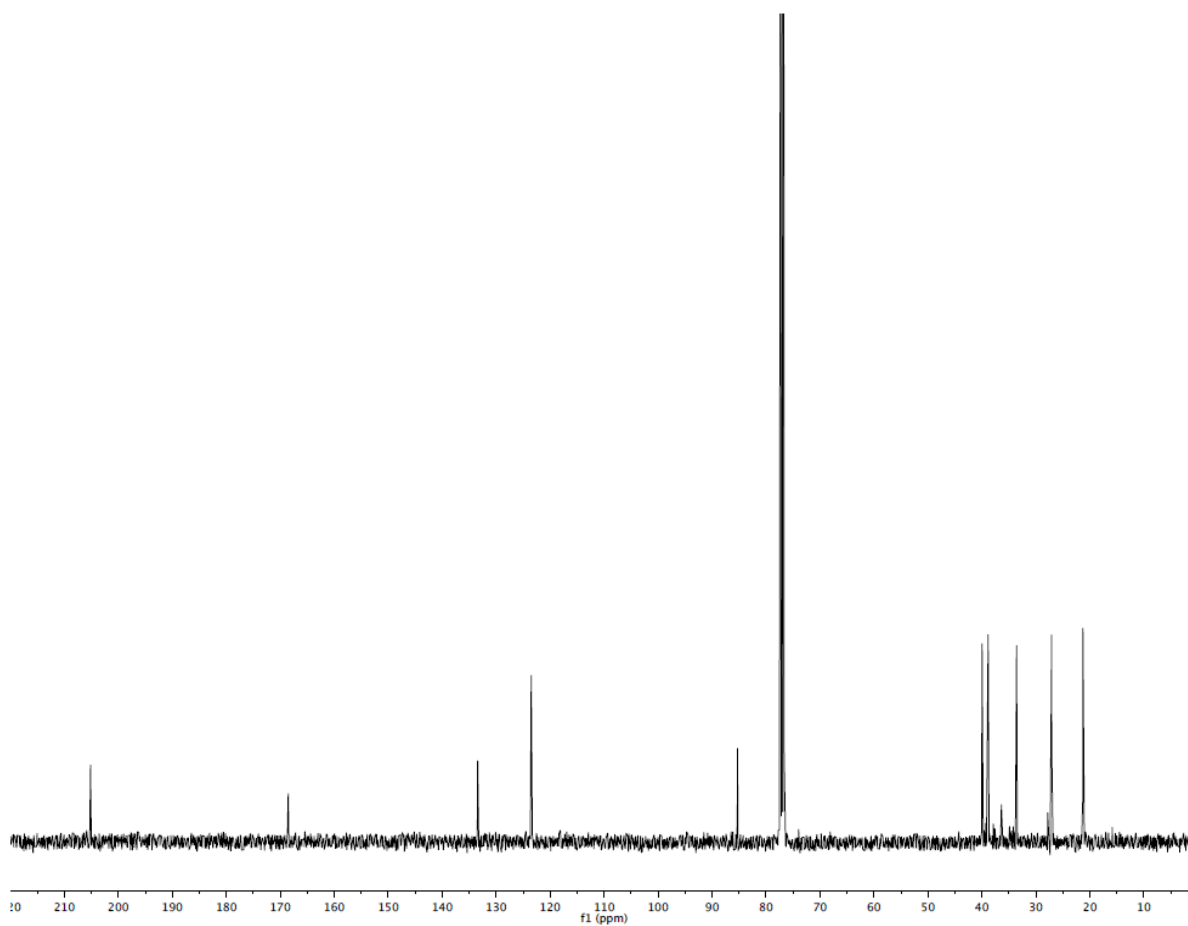
HRMS (ESI): Calculated for C₁₀H₁₂O₃ [M+Na]⁺: 203.06790, Found: 203.06750.

FTIR (neat): 2941, 2868, 1767, 1724, 1665, 1452, 1265, 1083, 957 cm⁻¹.

¹H NMR of 4.6b



¹³C NMR of 4.6b



2H,3'H-spiro[acenaphthylene-1,2'-furan]-2,5'(4'H)-dione (**4.8a**)

In accordance with general procedure A using α -hydroxy ester **4.7a**, upon stirring at 140 °C for 20 h, the reaction mixture was concentrated and subjected to flash column chromatography (SiO₂: 30% EtOAc/hexanes) to furnish **4.8a** (64 mg, 0.29 mmol, 97% yield) as a colorless solid. *The spectroscopic properties of this compound were consistent with the data available in the literature.*^{107a}

TLC (SiO₂): R_f = 0.31 (hexanes:EtOAc = 3:1).

¹H NMR: (400 MHz, CDCl₃): δ 7.52-7.50 (m, 2H), 7.42-7.34 (m, 3H), 3.75 (s, 3H), 3.10 (ddd, J = 10.5, 8.6, 3.1 Hz), 2.72-2.51 ppm (m, 3H).

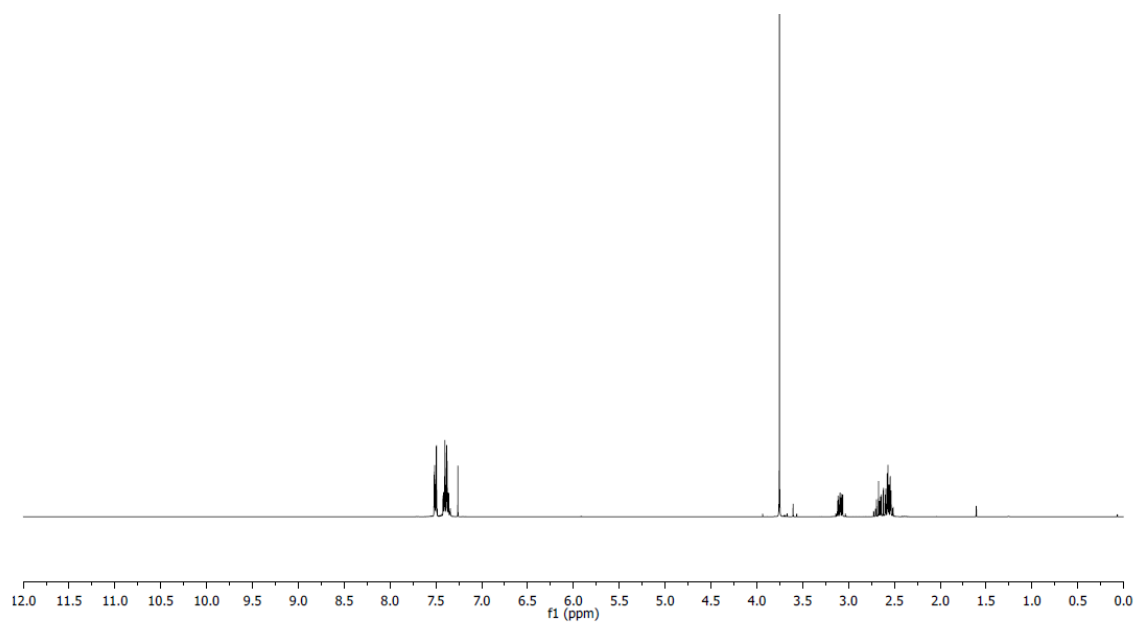
¹³C NMR: (100 MHz, CDCl₃): δ 174.9, 170.8, 138.0, 128.8, 128.7, 125.0, 53.4, 33.4, 28.1 ppm.

MP: 48 °C.

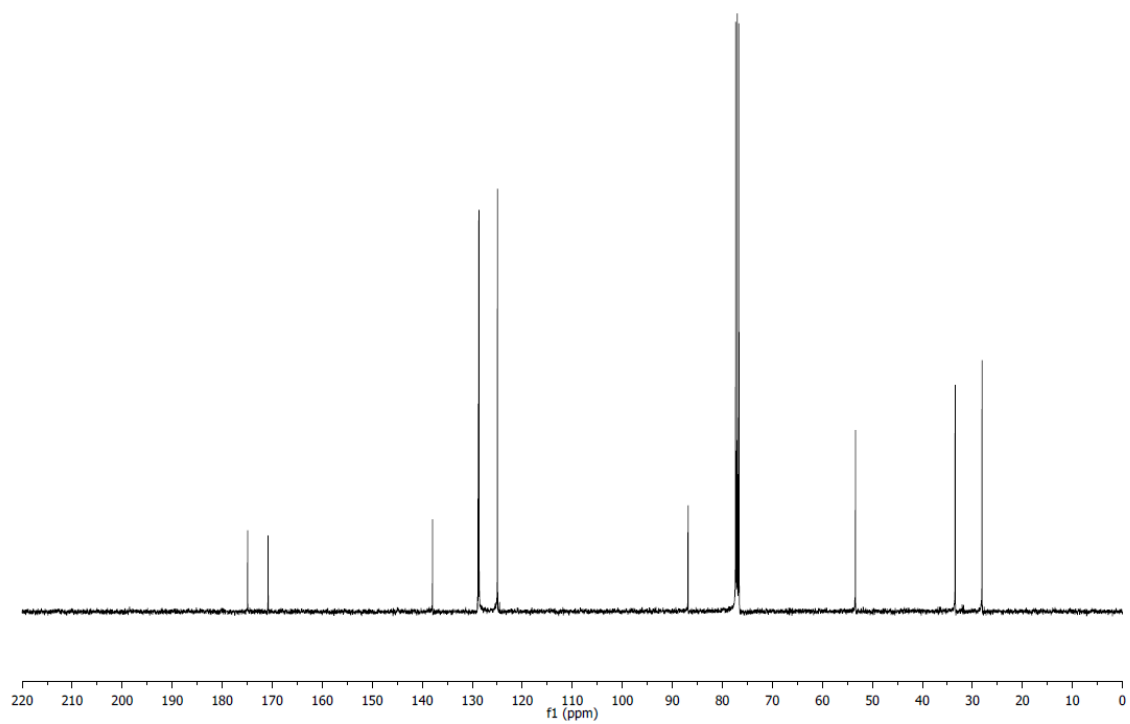
HRMS (ESI): Calculated for C₁₂H₁₂O₄ [M+Na]⁺: 243.06280, Found: 243.06260.

FTIR (neat): 2957, 1783, 1737, 1450, 1262, 1228, 1190, 1156, 1091, 1058, 1005, 905, 742, 700 cm⁻¹.

¹H NMR of **4.8a**



¹³C NMR of **4.8a**



methyl 2-(1-methyl-1*H*-indol-2-yl)-5-oxotetrahydrofuran-2-carboxylate (**4.8b**)

In accordance with general procedure A using α -hydroxy ester **4.7b**, upon stirring at 140 °C for 20 h, the reaction mixture was concentrated and subjected to flash column chromatography (SiO₂: 30% EtOAc/hexanes) to furnish **4.8b** (48 mg, 0.18 mmol, 58% yield) as a yellow solid.

TLC (SiO₂): R_f = 0.29 (hexanes:EtOAc = 2:1).

¹H NMR: (400 MHz, CDCl₃): δ 7.63 (dt, J = 8.0, 0.9 Hz, 1H), 7.36 – 7.27 (m, 2H), 7.14 (ddd, J = 8.0, 6.7, 1.2 Hz, 1H), 6.66 (d, J = 0.5 Hz, 1H), 3.79 (s, 3H), 3.75 (s, 3H), 3.06 (ddd, J = 12.1, 9.5, 8.2 Hz, 1H), 2.89 – 2.79 (m, 1H), 2.78 – 2.65 ppm (m, 2H).

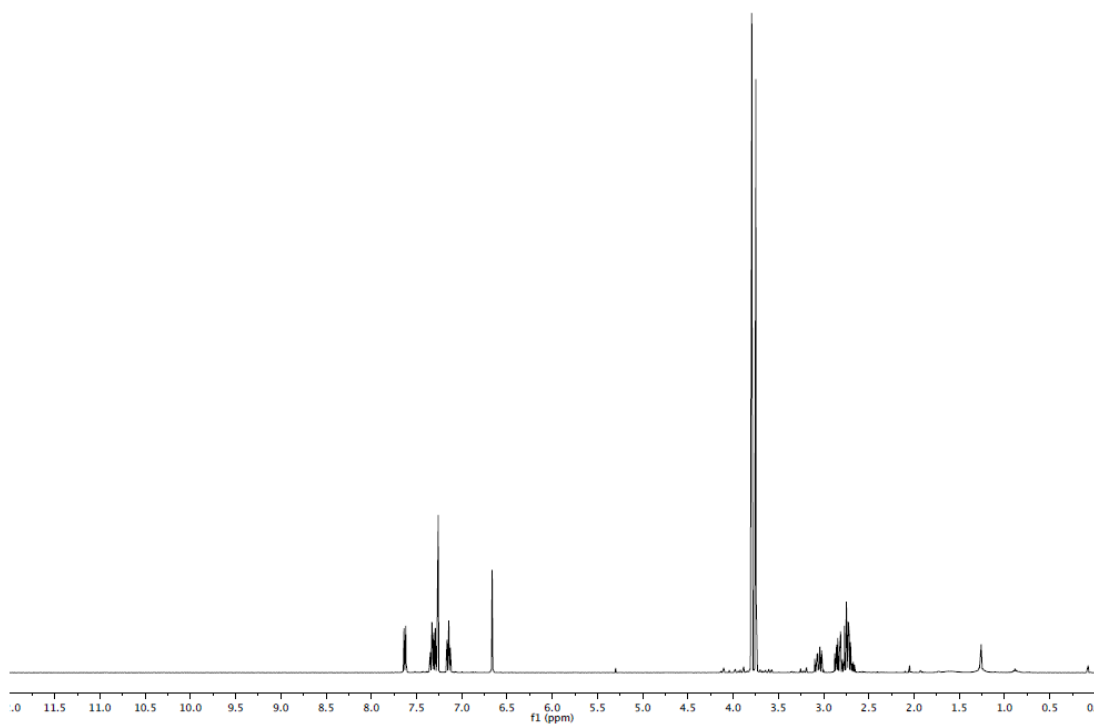
¹³C NMR: (100 MHz, CDCl₃): δ 174.9, 170.6, 138.8, 134.4, 126.3, 123.1, 121.2, 120.1, 109.5, 102.2, 82.5, 53.6, 31.5, 31.1, 27.8 ppm.

MP: 109 - 110 °C.

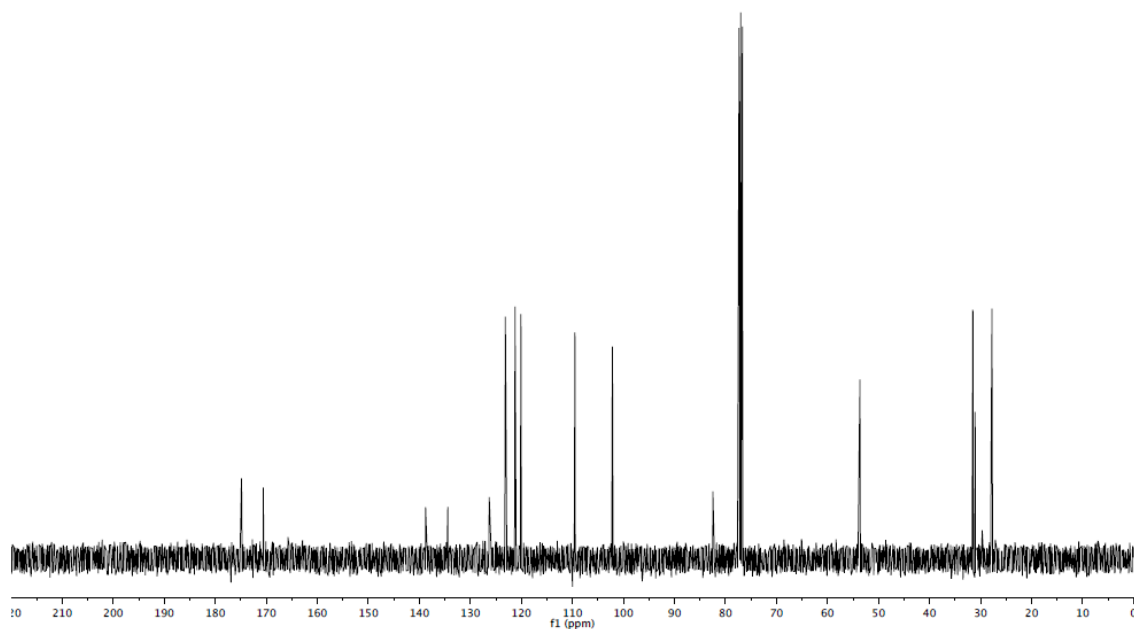
HRMS (ESI): Calculated for C₁₅H₁₅NO₄ [M+Na]⁺: 296.08930, Found: 296.08980.

FTIR (neat): 2958, 2920, 1771, 1745, 1614, 1460, 1262, 1199, 1170, 1047, 800 cm⁻¹.

^1H NMR of **4.8b**



^{13}C NMR of **4.8b**



1'-benzyl-3H-spiro[furan-2,3'-indoline]-2',5(4H)-dione (**4.10a**)

In accordance with general procedure B using acrylic ester **4.2a**, upon stirring at 140 °C for 20 h, the reaction mixture was concentrated and subjected to flash column chromatography (SiO₂: 25% EtOAc/hexanes) to furnish **4.10a** (88 mg, 0.30 mmol, 99% yield) as a colorless solid.

TLC (SiO₂): R_f = 0.44 (hexanes:EtOAc = 5:2).

¹H NMR: (400 MHz, CDCl₃): δ 7.76-7.37 (m, 7H), 7.10 (td, *J* = 7.7, 0.9 Hz, 1H), 6.75 (d, *J* = 7.7 Hz, 1H), 4.88 (s, 2H), 3.26 (ddd, *J* = 17.6, 10.8, 9.7 Hz, 1H), 2.80 (ddd, *J* = 17.6, 9.6, 3.0 Hz, 1H), 2.64 (ddd, *J* = 13.4, 9.7, 3.0 Hz, 1H), 2.50 ppm (ddd, *J* = 13.4, 10.8, 9.6 Hz, 1H).

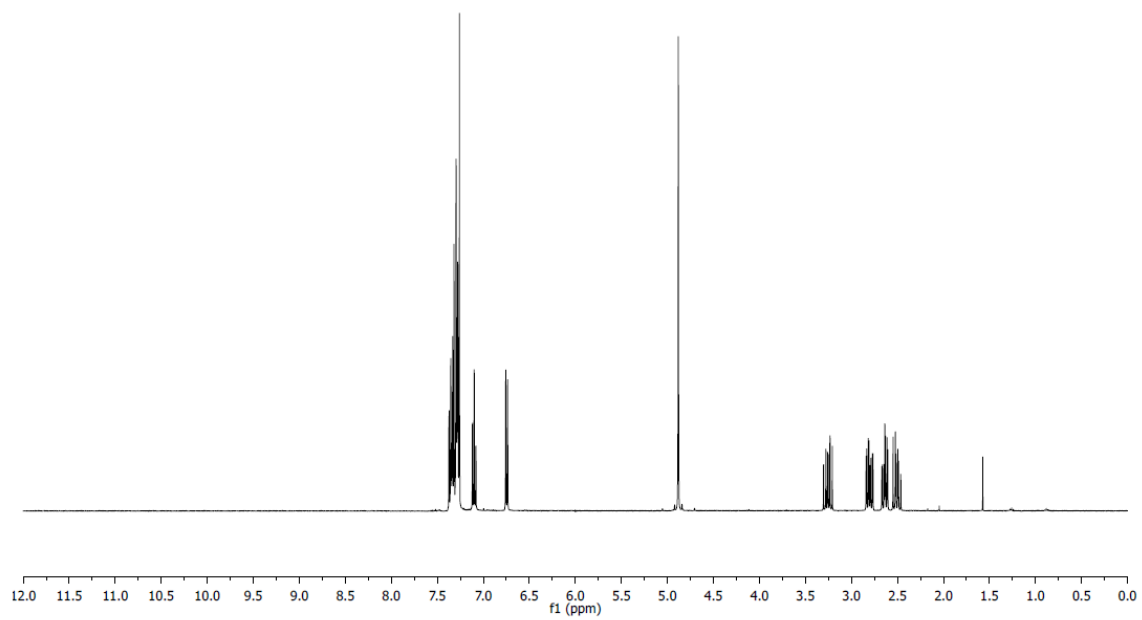
¹³C NMR: (100 MHz, CDCl₃): δ 176.0, 174.4, 143.0, 134.9, 131.1, 128.9, 127.9, 127.2, 126.3, 124.3, 123.6, 109.9, 82.3, 43.9, 31.4, 28.3 ppm.

MP: 118 – 119 °C.

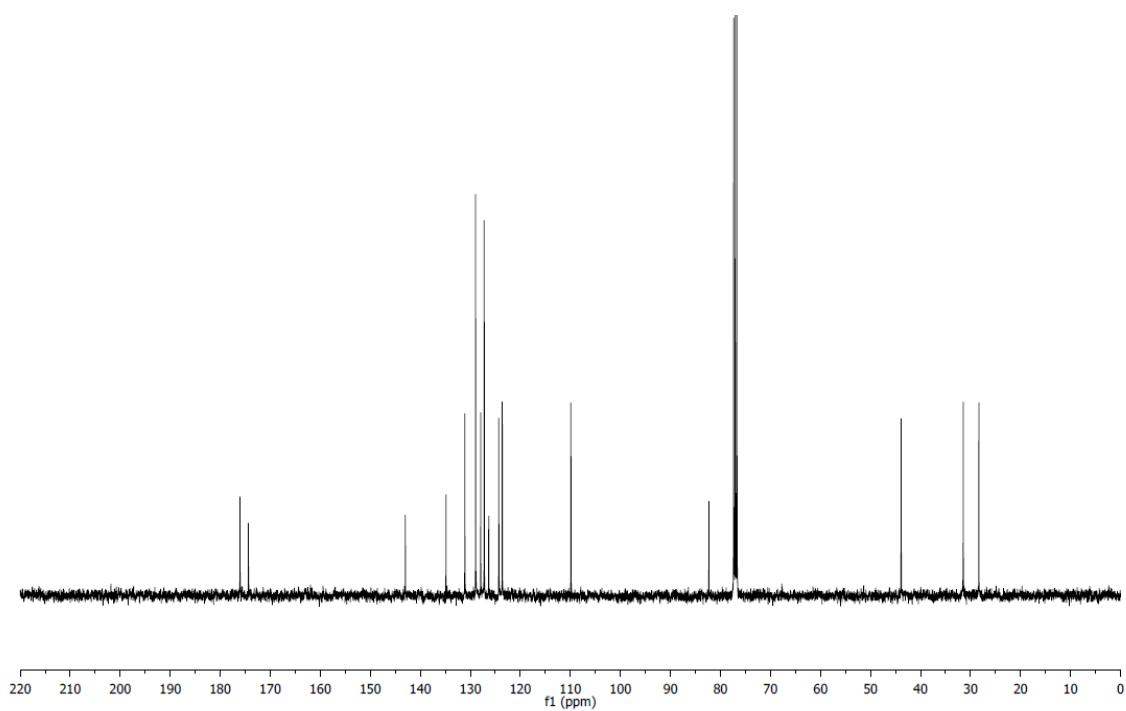
HRMS (ESI): Calculated for C₁₈H₁₅NO₃ [M+Na]⁺: 316.09440, Found: 316.09430.

FTIR (neat): 1782, 1720, 1615, 1468, 1367, 1175, 1054, 983, 753, 723, 697, 680 cm⁻¹.

¹H NMR of **4.10a**



¹³C NMR of **4.10a**



1'-benzyl-3-methyl-3H-spiro[furan-2,3'-indoline]-2',5(4H)-dione (**4.10c**)

In accordance with general procedure B using acrylic ester **4.2c**, upon stirring at 140 °C for 20 h, the reaction mixture was concentrated to afford the crude spiro lactone (dr = >20:1, as determined by ¹H NMR spectroscopy). The crude reaction mixture was subjected to flash column chromatography (SiO₂: 25% EtOAc/hexanes) to furnish **4.10c** (85 mg, 0.28 mmol, 92% yield) as a colorless solid.

TLC (SiO₂): R_f = 0.50 (hexanes:EtOAc = 5:2).

¹H NMR: (400 MHz, CDCl₃): δ 7.35-7.26 (m, 7H), 7.07 (td, J = 7.7, 1.0 Hz, 1H), 6.77 (d, J = 7.8 Hz, 1H), 4.90 (dd, J = 62.3, 15.7 Hz, 2H), 3.28 (dd, J = 17.4, 8.4, 1H), 3.08-2.99 (m, 1H), 2.53 (dd, J = 17.4, 7.5 Hz, 1H), 1.04 ppm (d, J = 7.0 Hz, 1H).

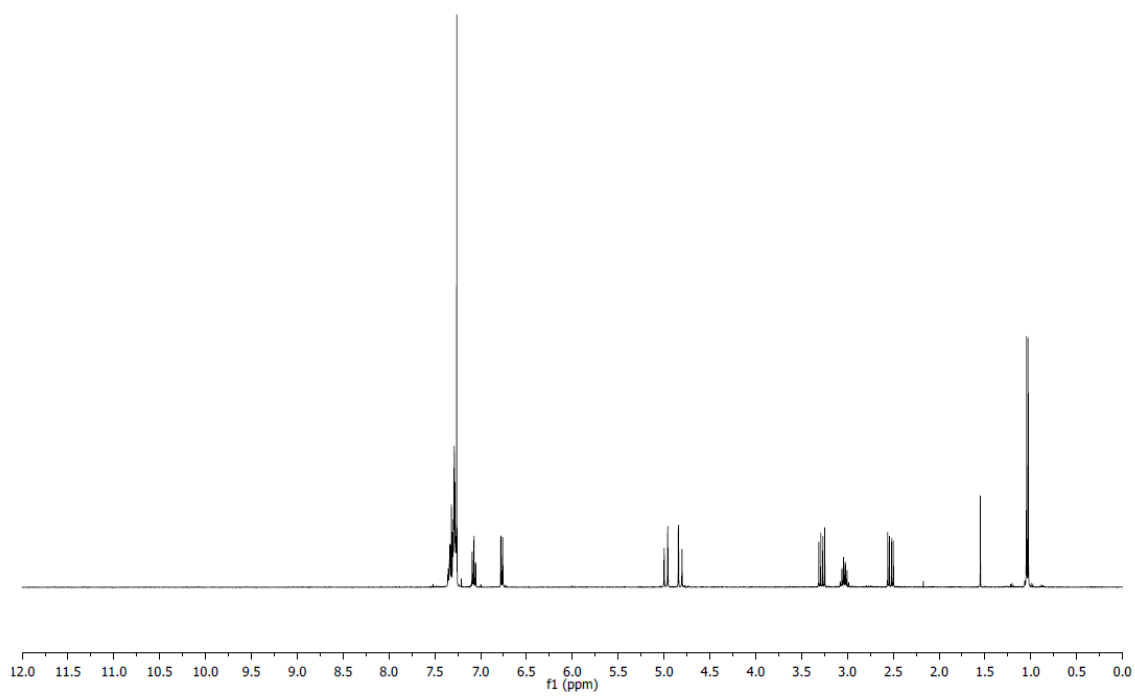
¹³C NMR: (100 MHz, CDCl₃): δ 175.4, 174.2, 143.0, 135.0, 130.9, 129.0, 127.9, 127.2, 137.2, 124.0, 123.0, 110.1, 85.8, 44.1, 37.3, 35.9, 16.2 ppm.

MP: 146 – 147 °C.

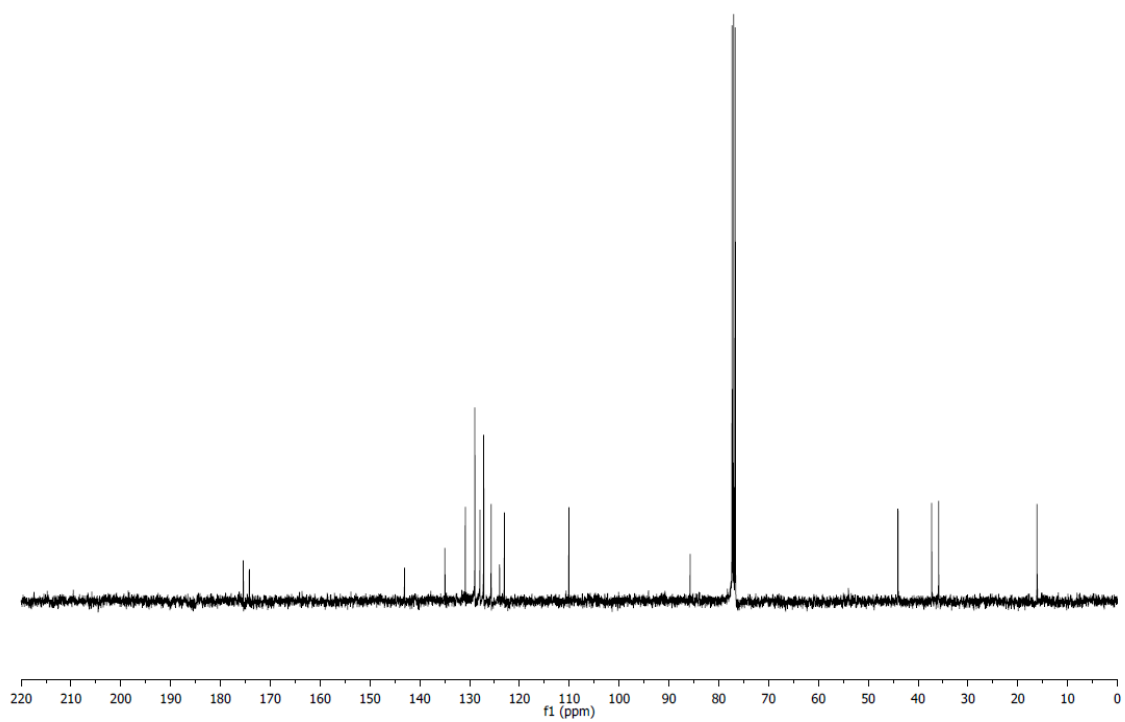
HRMS (ESI): Calculated for C₁₉H₁₇NO₃ [M+H]⁺: 308.12810, Found: 308.12830.

FTIR (neat): 1783, 1727, 1612, 1490, 1471, 1373, 1212, 1164, 1004, 969, 767, 757, 734, 693, 673 cm⁻¹.

¹H NMR of **4.10c**



¹³C NMR of **4.10c**



1'-benzyl-3-phenyl-3H-spiro[furan-2,3'-indoline]-2',5(4H)-dione (**4.10d**)

In accordance with general procedure B using acrylic ester **4.2d**, upon stirring at 140 °C for 20 h, the reaction mixture was concentrated to afford the crude spiro lactone (dr = >20:1, as determined by ¹H NMR spectroscopy). The crude reaction mixture was subjected to flash column chromatography (SiO₂: 25% EtOAc/hexanes) to furnish **4.10d** (91 mg, 0.25 mmol, 82% yield) as a colorless solid. *The spectroscopic properties of this compound were consistent with the data available in the literature.*¹³¹

TLC (SiO₂): R_f = 0.62 (hexanes:EtOAc = 5:2).

¹H NMR: (400 MHz, CDCl₃): δ 7.35-7.19 (m, 7H), 7.10 (td, *J* = 7.8, 1.2 Hz, 1H), 7.02-6.99 (m, 2H), 6.73 (td, *J* = 7.6, 1.0 Hz, 1H), 6.62 (d, *J* = 7.8, 1H), 6.42 (dq, *J* = 7.6, 0.6 Hz, 1H), 4.98 (d, *J* = 15.8 Hz, 1H), 4.81 (d, *J* = 15.8 Hz, 1H), 4.08 (dd, *J* = 8.6, 5.8 Hz, 1H), 3.67 (dd, *J* = 17.4, 8.6 Hz, 1H) 3.15 ppm (3d, *J* = 17.4, 5.8 Hz, 1H).

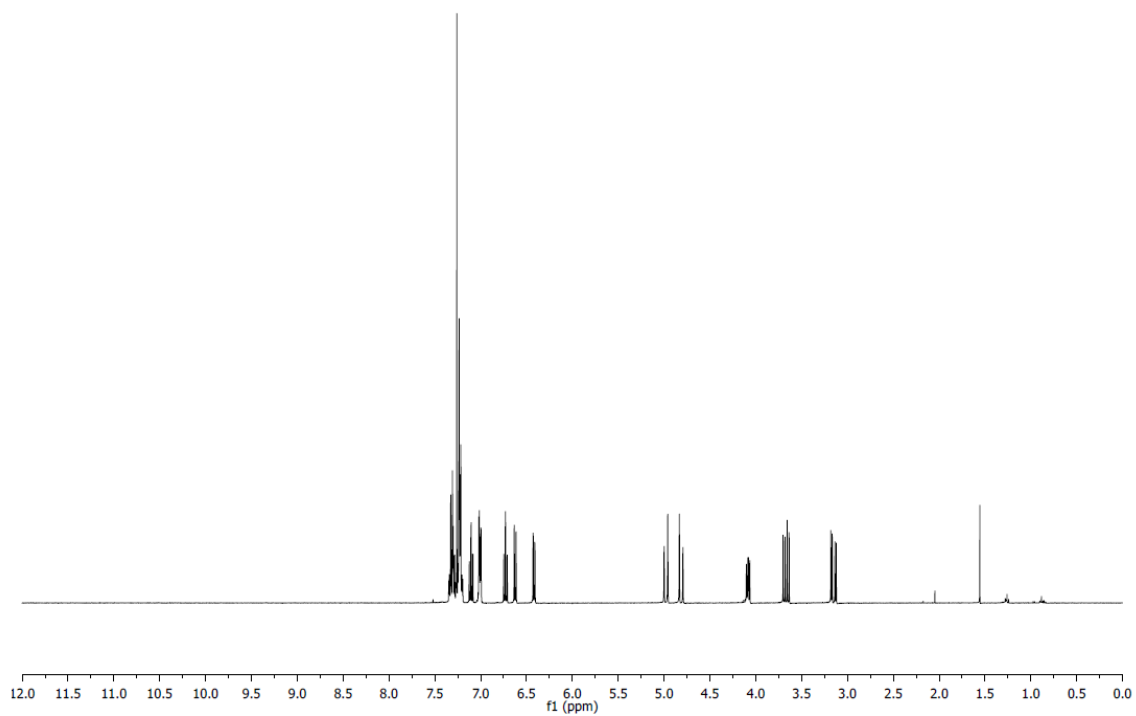
¹³C NMR: (100 MHz, CDCl₃): δ 175.7, 174.2, 142.9, 136.3, 134.8, 130.7, 128.9, 128.7, 128.2, 128.0, 127.9, 127.2, 126.0, 123.4, 122.7, 109.6, 86.0, 48.3, 44.0, 34.0 ppm.

MP: 176 – 177 °C.

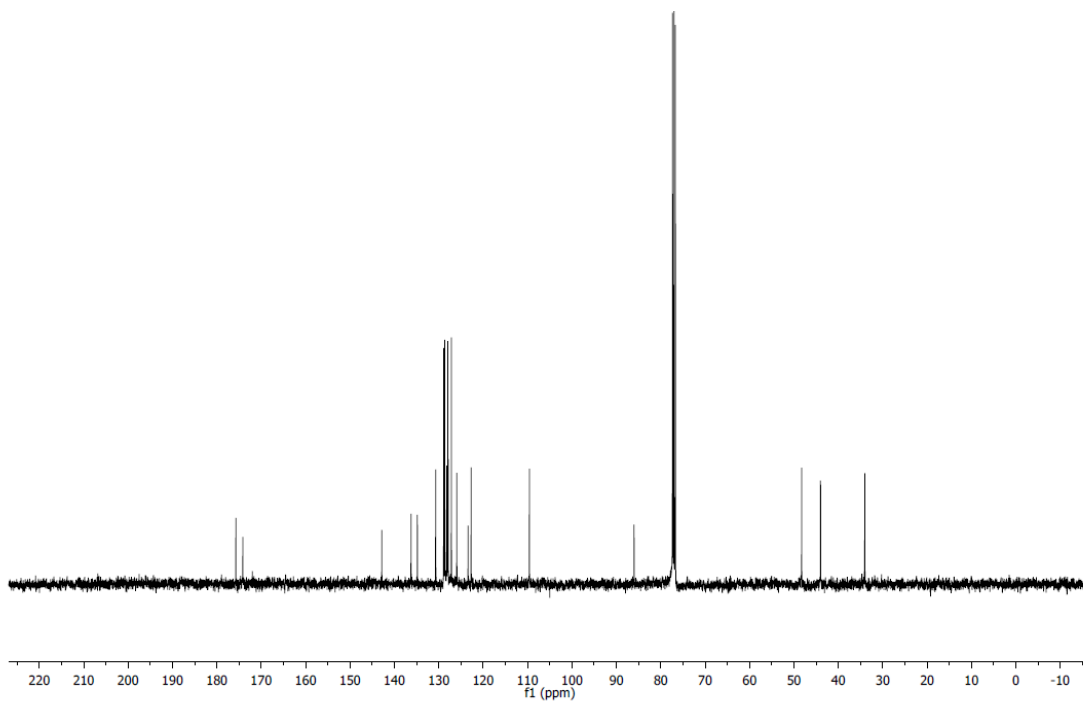
HRMS (ESI): Calculated for C₂₄H₁₀NO₃ [M+Na]⁺: 392.12570, Found: 392.12580.

FTIR (neat): 1793, 1723, 1614, 1468, 1365, 1182, 1153, 1029, 1001, 752, 699 cm⁻¹.

¹H NMR of **4.10d**



¹³C NMR of **4.10d**



1'-benzyl-4-methyl-3H-spiro[furan-2,3'-indoline]-2',5(4H)-dione (**4.10e**)

In accordance with general procedure B using acrylic ester **4.2e**, upon stirring at 140 °C for 20 h, the reaction mixture was concentrated to afford the crude spiro lactone (dr = 2:1, as determined by ¹H NMR spectroscopy). The crude reaction mixture was subjected to flash column chromatography (SiO₂: 25% EtOAc/hexanes) to furnish **4.10e** (92 mg, 0.30 mmol, 99% yield) as a colorless solid.

TLC (SiO₂): R_f (minor) = 0.62, R_f (major) = 0.47 (hexanes:EtOAc = 5:2).

Spectral Data for Major Isomer:

¹H NMR (400 MHz, CDCl₃): δ 7.35-7.23 (m, 7H), 7.06 (t, *J* = 7.6 Hz, 1H), 6.74 (d, *J* = 7.9 Hz, 1H), 4.94 (d, *J* = 15.6 Hz, 1H), 4.87 (d, *J* = 15.6 Hz, 1H), 3.20-3.10 (m, 1H), 2.62 (dd, *J* = 13.1, 9.5 Hz, 1H), 2.46 (dd, *J* = 13.1, 9.5 Hz, 1H), 1.54 ppm (d, *J* = 7.2 Hz, 3H).

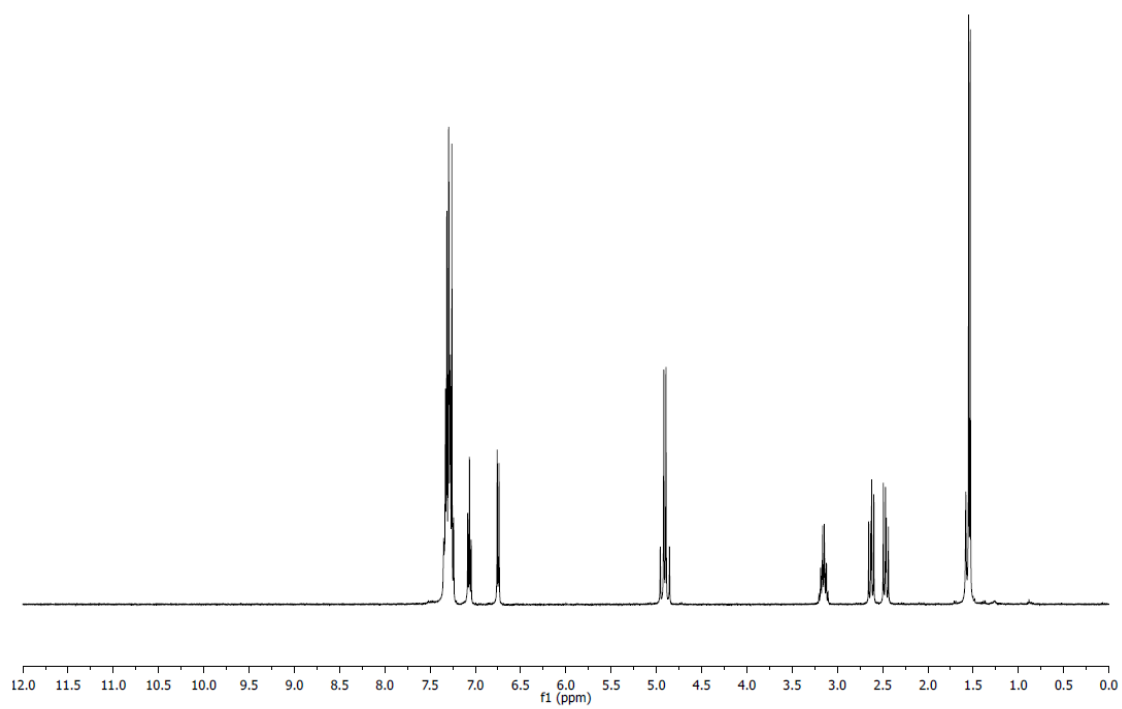
¹³C NMR (100 MHz, CDCl₃): δ 178.5, 173.8, 142.6, 134.9, 130.9, 128.9, 127.9, 127.8, 127.2, 123.7, 123.5, 110.0, 80.6, 44.1, 38.4, 34.7, 16.5 ppm.

MP: 122 – 123 °C.

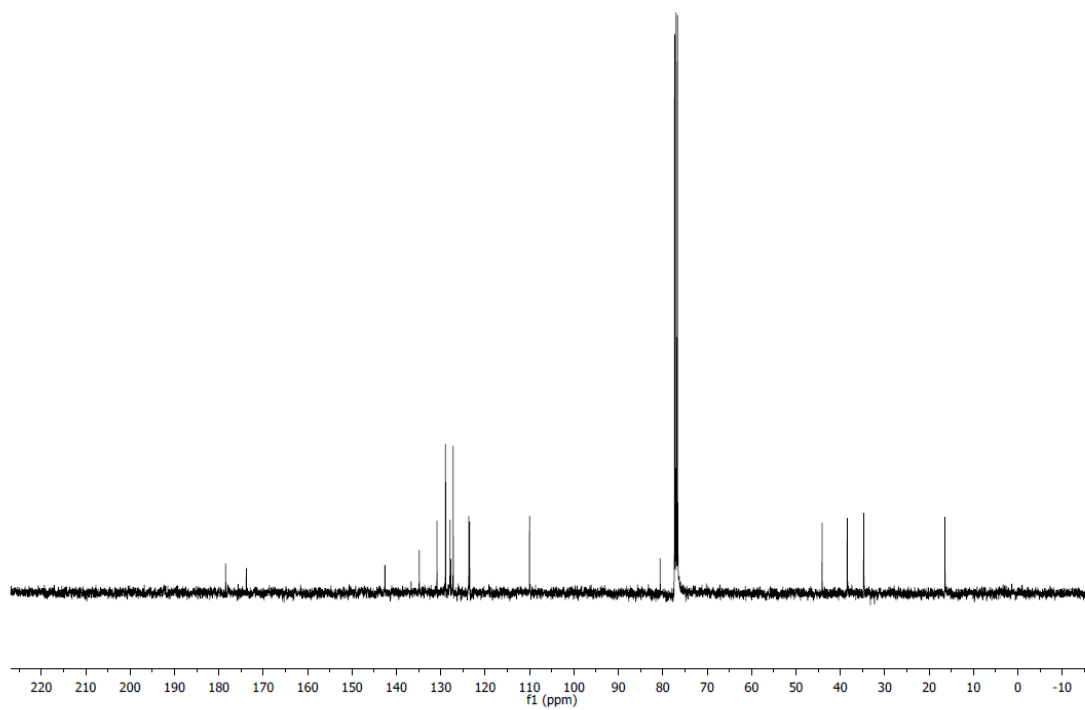
HRMS (ESI): Calculated for C₁₉H₁₇NO₃ [M+Na]⁺: 330.11010, Found: 330.11050.

FTIR (neat): 1783, 1727, 1615, 1489, 1469, 1369, 1178, 1024, 984, 752, 697 cm⁻¹.

^1H NMR of **4.10e**



^{13}C NMR of **4.10e**



1'-benzyl-3,3-dimethyl-3H-spiro[furan-2,3'-indoline]-2',5(4H)-dione (**4.10f**)

In accordance with general procedure B using acrylic ester **4.2f**, upon stirring at 140 °C for 20 h, the reaction mixture was concentrated and subjected to flash column chromatography (SiO₂: 25% EtOAc/hexanes) to furnish **4.10f** (50 mg, 0.16 mmol, 52% yield) as a colorless solid.

TLC (SiO₂): R_f = 0.59 (hexanes:EtOAc = 5:2).

¹H NMR (400 MHz, CDCl₃): δ 7.30-7.27 (m, 7H), 7.07 (td, *J* = 7.6, 0.8 Hz, 1H), 6.76 (d, *J* = 7.6 Hz, 1H), 5.08 (d, *J* = 15.6 Hz, 1H), 4.66 (d, *J* = 15.6 Hz, 1H), 3.46 (d, *J* = 16.6 Hz, 1H), 2.41 (d, *J* = 16.6 Hz, 1H), 1.32 (s, 3H), 1.10 ppm (2, 3H).

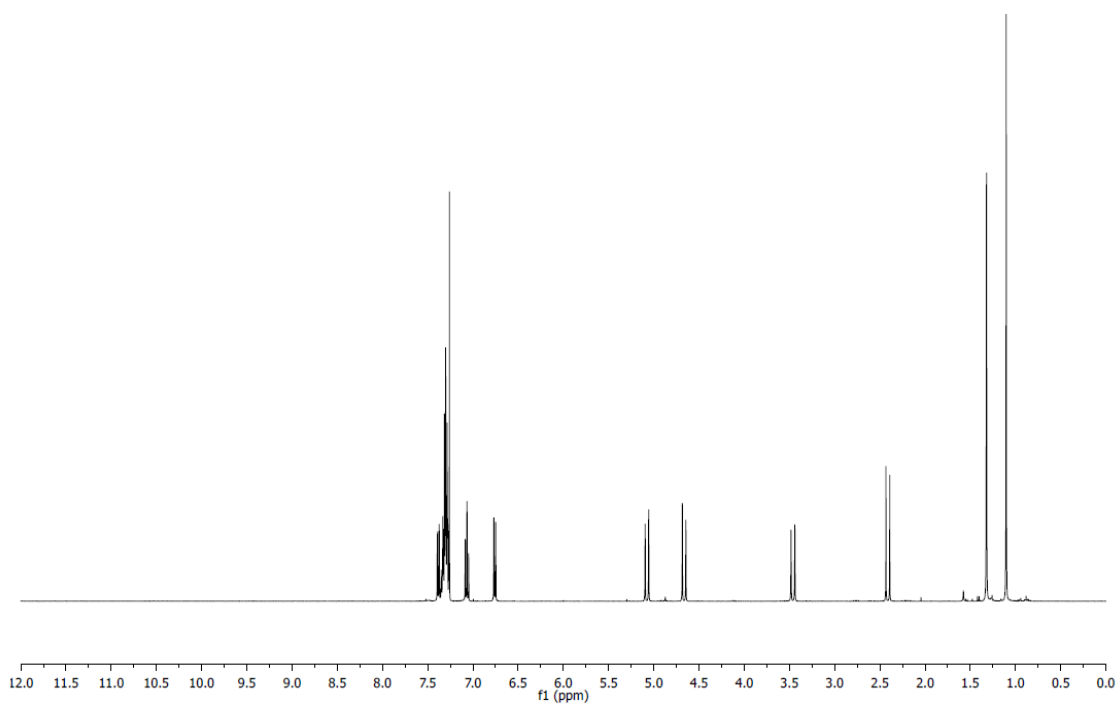
¹³C NMR (100 MHz, CDCl₃): δ 175.7, 174.9, 144.1, 135.1, 130.9, 128.9, 127.9, 127.3, 127.1, 122.7, 122.2, 109.8, 88.4, 44.0, 43.4, 41.7, 26.0, 21.7 ppm.

MP: 142 – 143 °C.

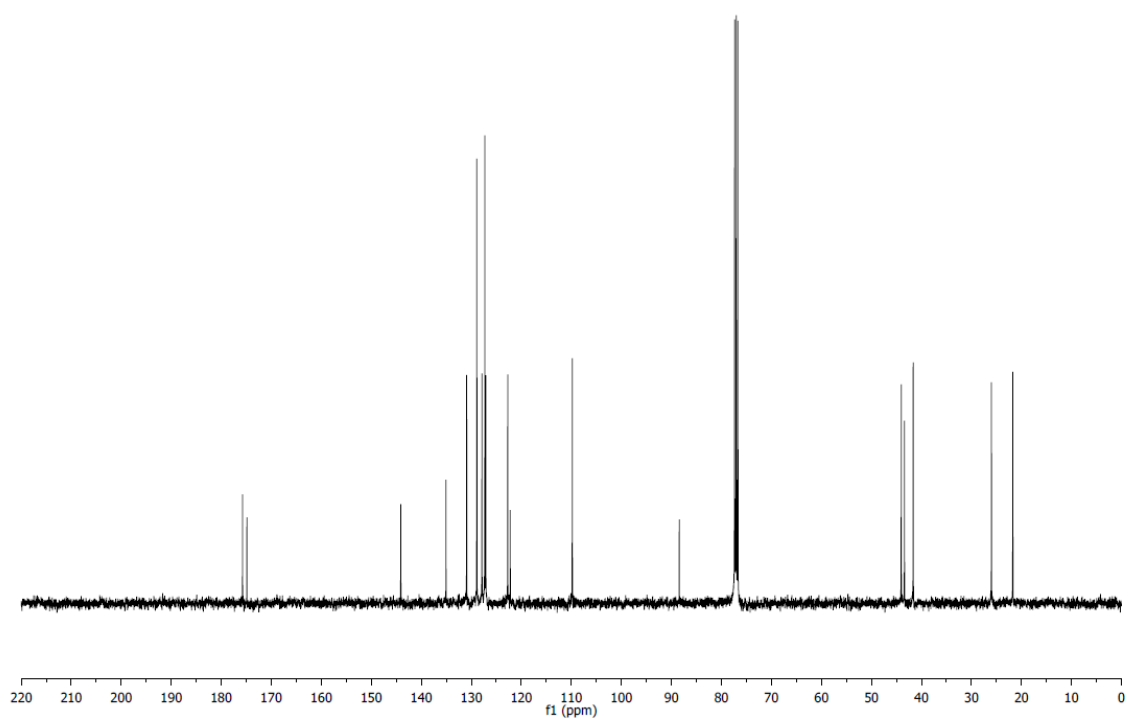
HRMS (ESI): Calculated for C₂₀H₁₉NO₃ [M+Na]⁺: 344.12570, Found: 344.12580.

FTIR (neat): 1793, 1723, 1614, 1467, 1368, 1224, 1185, 1017, 755 cm⁻¹.

¹H NMR of **4.10f**



¹³C NMR of **4.10f**



1'-benzyl-3- cyclohexyl-3H-spiro[furan-2,3'-indoline]-2',5(4H)-dione (**4.10g**)

In accordance with general procedure B using acrylic ester **4.2g**, upon stirring at 140 °C for 20 h, the reaction mixture was concentrated to afford the crude spiro lactone (dr = >20:1, as determined by ¹H NMR spectroscopy). The crude reaction mixture was subjected to flash column chromatography (SiO₂: 25% EtOAc/hexanes) to furnish **4.10g** (86 mg, 0.23 mmol, 77% yield) as a tan solid.

TLC (SiO₂): R_f = 0.34 (hexanes:EtOAc = 7:3).

¹H NMR: (400 MHz, CDCl₃): δ 7.34-7.23 (m, 7H), 7.07 (td, *J* = 7.6, 0.9 Hz, 1H), 6.82 (d, *J* = 7.8 Hz, 1H), 4.98 (d, *J* = 15.4 Hz, 1H), 4.83 (d, *J* = 15.5 Hz, 1H), 3.00-2.86 (m, 2H), 2.74-2.60 (m, 1H), 1.73-1.62 (m, 2H), 1.53-1.46 (m, 1H), 1.36-1.21 (m, 2H), 1.17-0.98 (m, 3H), 0.93-0.84 (m, 1H), 0.77-0.67 ppm (m, 2H).

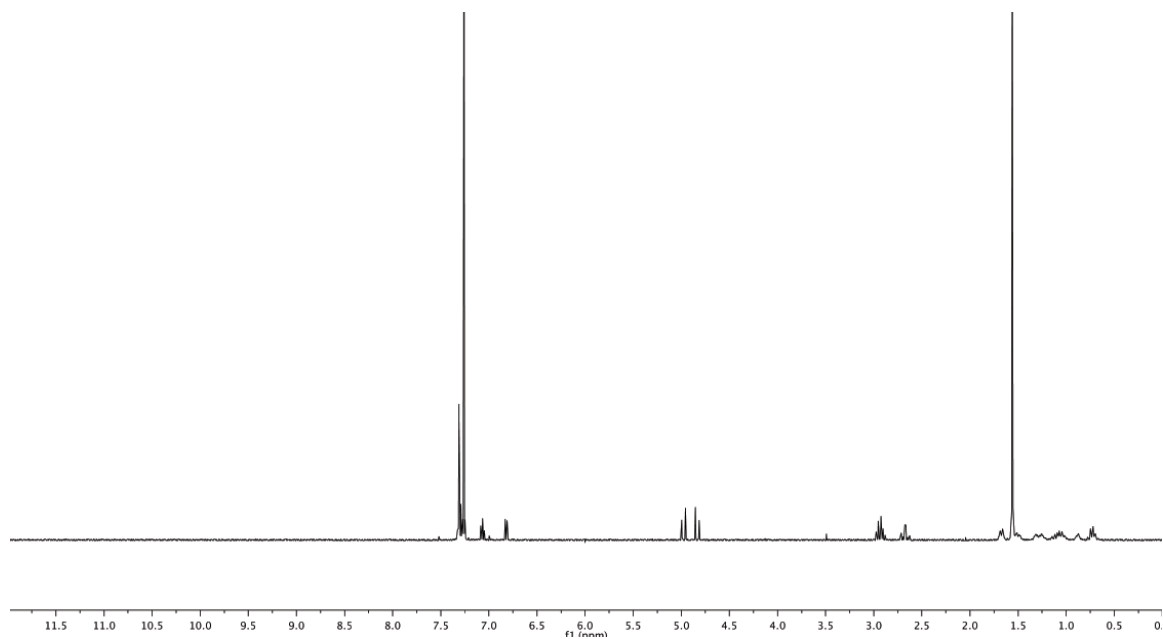
¹³C NMR: (100 MHz, CDCl₃): δ 174.8, 173.2, 143.3, 134.9, 131.1, 128.9, 128.1, 127.8, 125.2, 124.7, 123.3, 110.3, 85.2, 47.9, 44.5, 38.8, 33.8, 31.8, 30.5, 25.8, 25.6, 25.2 ppm.

MP: 161 – 163 °C.

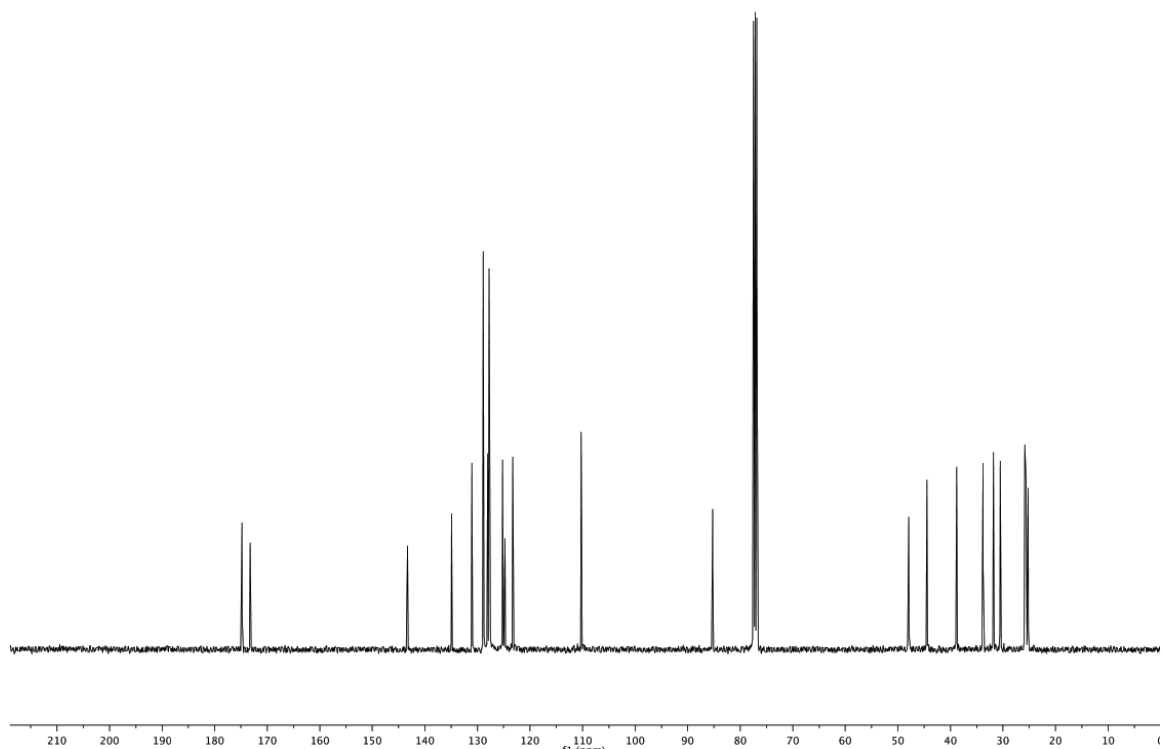
HRMS (ESI): Calculated for C₂₄H₂₅NO₃ [M+Na]⁺: 398.17270, Found: 398.17290.

FTIR (neat): 2934, 1788, 1731, 1614, 1487, 1350, 1206, 1184, 1159, 976, 770, 753, 708 cm⁻¹.

^1H NMR of 4.10g



^{13}C NMR of 4.10g



(3-(benzo[d][1,3]dioxol-5-yl)-1'-benzyl-3H-spiro[furan-2,3'-indoline]-2',5(4H)-dione (**4.10h**))

In accordance with general procedure B using acrylic ester **4.2h**, upon stirring at 140 °C for 20 h, the reaction mixture was concentrated to afford the crude spiro lactone (dr = >20:1, as determined by ¹H NMR spectroscopy). The crude reaction mixture was subjected to flash column chromatography (SiO₂: 25% EtOAc/hexanes) to furnish **4.10h** (112 mg, 0.27 mmol, 90% yield) as a pale pink solid.

TLC (SiO₂): R_f = 0.28 (hexanes:EtOAc = 7:3).

¹H NMR: (400 MHz, CDCl₃): δ 7.34-7.22 (m, 5H), 7.14 (td, *J* = 7.8, 1.2 Hz, 1H), 6.82 (td, *J* = 7.6, 0.9 Hz, 1H), 6.66-6.61 (m, 3H), 6.50-6.48 (m, 2H), 5.92 (d, *J* = 1.4 Hz, 1H), 5.91 (d, *J* = 1.4 Hz, 1H), 4.99 (d, *J* = 15.8 Hz, 1H), 4.80 (d, *J* = 15.8, 1H), 4.03 (dd, *J* = 8.6, 6.4 Hz, 1H), 3.60 (dd, *J* = 17.5, 8.6 Hz, 1H), 3.08 ppm (dd, *J* = 17.5, 6.4 Hz, 1H).

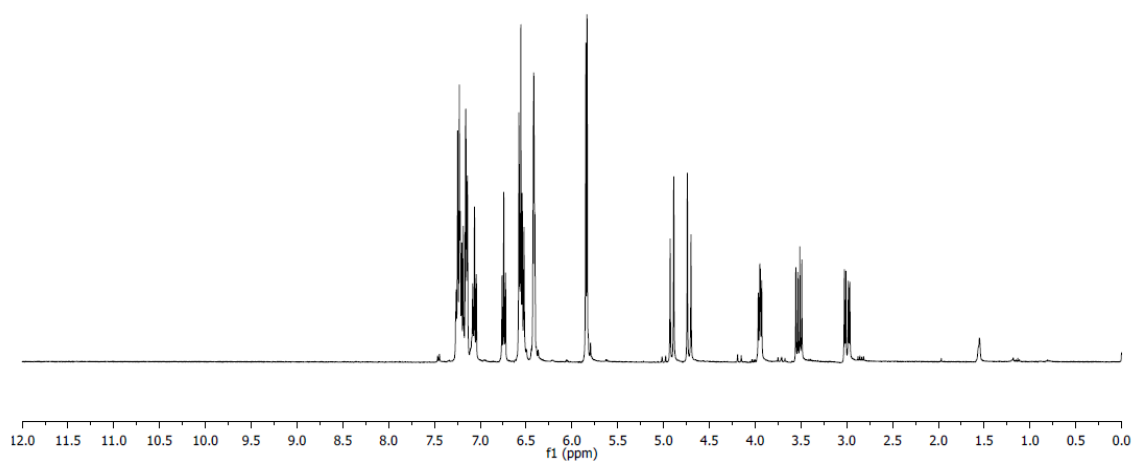
¹³C NMR: (100 MHz, CDCl₃): δ 175.5, 174.0, 147.9, 147.4, 142.9, 134.8, 130.8, 129.8, 128.9, 127.9, 127.1, 125.9, 123.5, 122.9, 121.3, 109.7, 108.3, 101.3, 86.1, 48.1, 44.0, 34.3, 14.2 ppm.

MP: 177 – 178 °C.

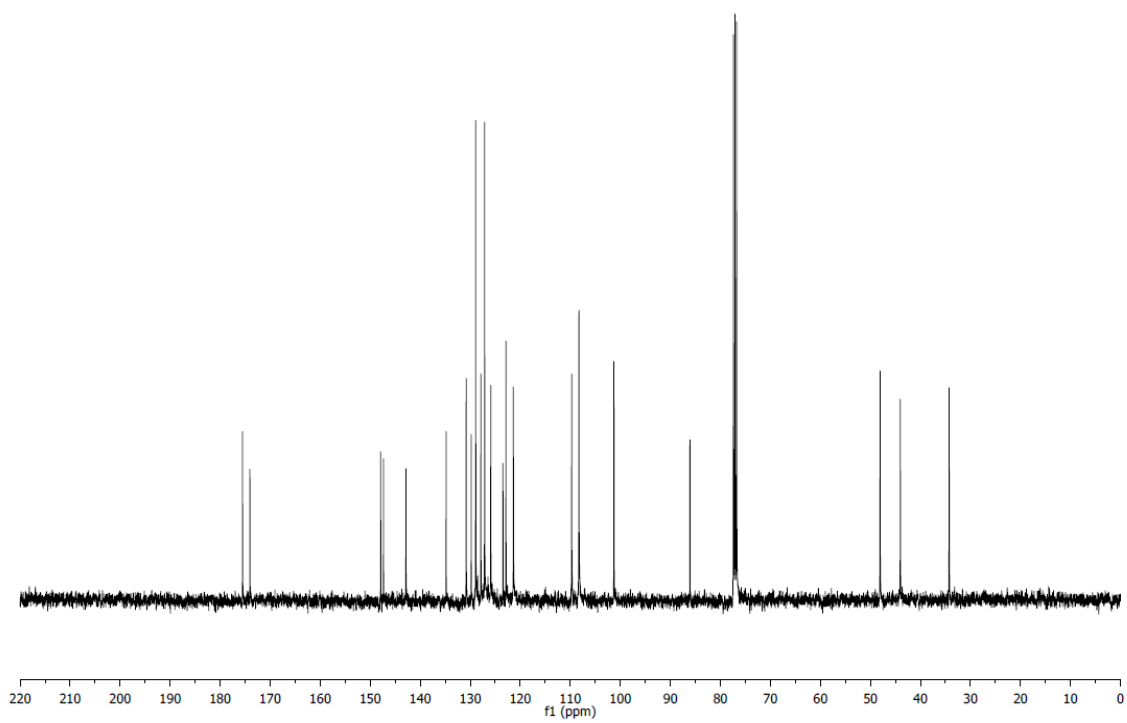
HRMS (ESI): Calculated for C₂₅H₁₉NO₅ [M+Na]⁺: 436.11550, Found: 436.11510.

FTIR (neat): 1791, 1730, 1489, 1468, 1368, 1234, 1184, 1155, 1035, 1000, 760, cm⁻¹

¹H NMR of **4.10h**



¹³C NMR of **4.10h**



1'-benzyl-3-(thiophen-2-yl)-3H-spiro[furan-2,3'-indoline]-2',5(4H)-dione (**4.10i**)

In accordance with general procedure B using acrylic ester **4.2i**, upon stirring at 140 °C for 20 h, the reaction mixture was concentrated to afford the crude spiro lactone (dr = >20:1, as determined by ¹H NMR spectroscopy). The crude reaction mixture was subjected to flash column chromatography (SiO₂: 25% EtOAc/hexanes) to furnish **4.10i** (98 mg, 0.26 mmol, 87% yield) as a white solid.

TLC (SiO₂): R_f = 0.49 (hexanes:EtOAc = 2:1).

¹H NMR: (400 MHz, CDCl₃): δ 7.33-7.26 (m, 3H), 7.22-7.19 (m, 2H), 7.16 (dd, *J* = 7.8, 1.2 Hz, 2H), 7.13 (dd, *J* = 5.1, 1.2 Hz, 1H), 6.89 (dd, *J* = 5.1, 3.6 Hz, 1H), 6.85 (dd, *J* = 7.6, 0.9 Hz, 1H), 6.79 (ddd, *J* = 3.6, 1.1, 0.6 Hz, 1H), 6.72 (ddd, *J* = 7.6, 1.2, 0.6 Hz, 1H), 6.66 (d, *J* = 7.8 Hz, 1H), 4.96 (d, *J* = 15.8 Hz, 1H), 4.85 (d, *J* = 15.8 Hz, 1H), 4.38 (m, 1H), 3.65 (dd, *J* = 17.5, 8.7 Hz, 1H), 3.15 ppm (dd, *J* = 17.5, 7.2 Hz, 1H).

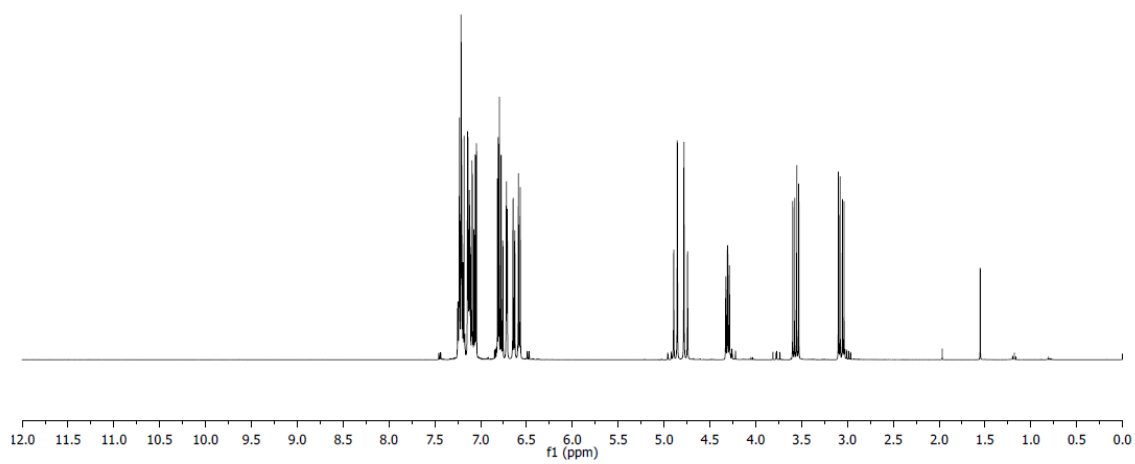
¹³C NMR: (100 MHz, C₆D₆): δ 173.5, 173.3, 143.0, 138.7, 135.1, 130.5, 128.6, 126.9, 126.6, 126.2, 125.4, 124.7, 123.8, 122.5, 109.5, 85.2, 44.1, 43.4, 35.4 ppm.

MP: 158 – 159 °C.

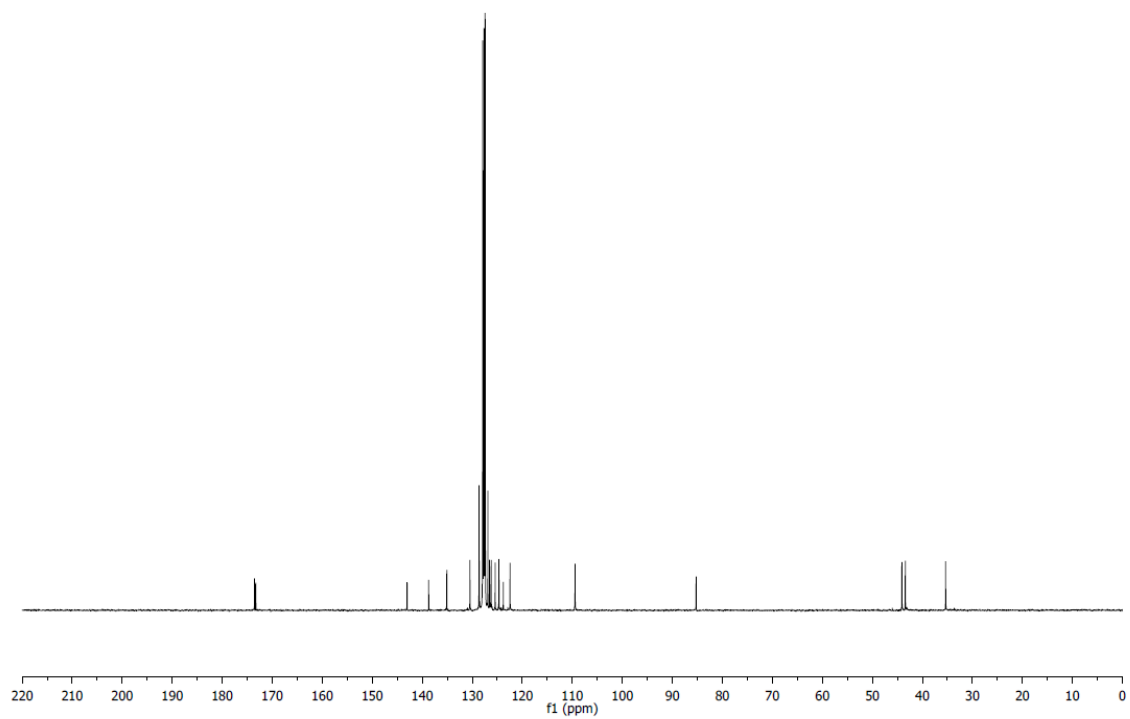
HRMS (ESI): Calculated for C₂₂H₁₇NO₃S [M+Na]⁺:398.08210, Found: 398.08200.

FTIR (neat): 1790, 1722, 1614, 1467, 1379, 1368, 1194, 1183, 1155, 999, 768, 757, 732, 709, 694, 676 cm⁻¹.

¹H NMR of **4.10i**



¹³C NMR of **4.10i**



4.5.6 Crystal Data and Structure Refinement for 4.11

Empirical formula	C ₅₂ H ₆₀ Cl ₄ O ₅ P ₂ Ru	
Formula weight	1069.81	
Temperature	153(2) K	
Wavelength	0.71073 Å	
Crystal system	Triclinic	
Space group	P-1	
Unit cell dimensions	a = 11.3017(3) Å	α = 71.0490(10)°.
	b = 14.8706(4) Å	β = 86.7940(10)°.
	c = 15.7363(4) Å	γ = 81.2220(10)°.
Volume	2471.99(11) Å ³	
Z	2	
Density (calculated)	1.437 Mg/m ³	
Absorption coefficient	0.645 mm ⁻¹	
F(000)	1108	
Crystal size	0.30 x 0.20 x 0.08 mm	
Theta range for data collection	1.46 to 27.50°.	
Index ranges	-14 ≤ h ≤ 14, -19 ≤ k ≤ 19, -20 ≤ l ≤ 20	
Reflections collected	57107	
Independent reflections	11369 [R(int) = 0.0478]	
Completeness to theta = 27.50°	99.9 %	
Absorption correction	Semi-empirical from equivalents	
Max. and min. transmission	1.00 and 0.855	
Refinement method	Full-matrix least-squares on F ²	
Data / restraints / parameters	11369 / 0 / 577	
Goodness-of-fit on F ²	1.206	
Final R indices [I > 2σ(I)]	R1 = 0.0419, wR2 = 0.0977	
R indices (all data)	R1 = 0.0529, wR2 = 0.1036	
Largest diff. peak and hole	2.563 and -1.677 e.Å ⁻³	

Table 4.3 Atomic coordinates ($\times 10^4$) and equivalent isotropic displacement parameters ($\text{\AA}^2 \times 10^3$) for **4.11**. $U(\text{eq})$ is defined as one third of the trace of the orthogonalized U_{ij} tensor.

	x	y	z	U(eq)
C(1)	6057(3)	8955(2)	2956(2)	25(1)
C(2)	5030(3)	9625(2)	2787(2)	35(1)
C(3)	4799(3)	10278(2)	3262(3)	43(1)
C(4)	5581(4)	10260(2)	3902(2)	45(1)
C(5)	6596(4)	9595(3)	4081(3)	51(1)
C(6)	6844(3)	8935(2)	3607(2)	41(1)
C(7)	7551(2)	7226(2)	2889(2)	24(1)
C(8)	7186(3)	6477(2)	3600(2)	27(1)
C(9)	8022(3)	5702(2)	4046(2)	34(1)
C(10)	9208(3)	5670(2)	3780(2)	37(1)
C(11)	9576(3)	6403(2)	3083(2)	36(1)
C(12)	8759(3)	7192(2)	2640(2)	30(1)
C(13)	7172(2)	8926(2)	1318(2)	24(1)
C(14)	7647(2)	8488(2)	583(2)	27(1)
C(15)	6684(2)	8292(2)	55(2)	24(1)
C(16)	7020(2)	6250(2)	836(2)	19(1)
C(17)	7548(2)	6056(2)	80(2)	25(1)
C(18)	8431(2)	5271(2)	175(2)	29(1)
C(19)	8805(2)	4680(2)	1026(2)	29(1)
C(20)	8299(2)	4874(2)	1775(2)	26(1)
C(21)	7401(2)	5654(2)	1685(2)	22(1)
C(22)	4884(2)	7246(2)	-157(2)	20(1)
C(23)	4527(2)	6376(2)	-109(2)	24(1)
C(24)	3727(3)	6328(2)	-722(2)	32(1)
C(25)	3268(3)	7152(2)	-1392(2)	35(1)
C(26)	3616(3)	8023(2)	-1455(2)	34(1)
C(27)	4416(3)	8069(2)	-839(2)	29(1)
C(28)	4162(2)	5878(2)	2422(2)	20(1)
C(29)	3726(2)	4909(2)	2720(2)	21(1)
C(30)	4796(3)	4106(2)	2894(3)	38(1)

Table 4.3, continued.

C(31)	4341(3)	3118(2)	3208(3)	49(1)
C(32)	3567(3)	3056(2)	2475(3)	41(1)
C(33)	2485(3)	3830(2)	2318(2)	29(1)
C(34)	2923(3)	4821(2)	1998(2)	31(1)
C(35)	1767(3)	3743(2)	3169(2)	39(1)
C(36)	2542(4)	3804(3)	3900(2)	47(1)
C(37)	3624(4)	3031(3)	4062(3)	63(1)
C(38)	2989(3)	4799(2)	3585(2)	39(1)
C(39)	2985(3)	8161(2)	3106(2)	32(1)
C(40)	2335(2)	8028(2)	4011(2)	25(1)
C(41)	2205(4)	8953(3)	4260(3)	54(1)
C(42)	1462(4)	8838(3)	5135(3)	62(1)
C(43)	2119(4)	8017(5)	5881(3)	87(2)
C(44)	2236(4)	7106(4)	5652(3)	82(2)
C(45)	2970(3)	7213(3)	4776(2)	58(1)
C(46)	1083(3)	7822(3)	3908(3)	55(1)
C(47)	364(3)	7704(3)	4791(3)	59(1)
C(48)	1006(4)	6894(3)	5515(4)	85(2)
C(49)	246(3)	8611(3)	5009(3)	58(1)
C(50)	4255(2)	8706(2)	1188(2)	23(1)
C(51)	1597(3)	7832(3)	619(4)	82(2)
O(1)	5128(2)	5994(1)	2722(1)	21(1)
O(2)	3571(2)	6602(1)	1858(1)	23(1)
O(3)	3932(2)	7568(1)	3112(1)	24(1)
O(4)	2574(2)	8809(2)	2436(2)	69(1)
O(5)	3896(2)	9425(1)	668(1)	34(1)
P(1)	6400(1)	8163(1)	2270(1)	20(1)
P(2)	5880(1)	7302(1)	693(1)	17(1)
Ru(1)	4859(1)	7516(1)	1934(1)	17(1)
CI(1)	896(1)	8981(1)	379(2)	114(1)
CI(2)	643(1)	7042(1)	500(1)	88(1)
C(52)	641(3)	10702(3)	1848(3)	51(1)
CI(3)	-719(1)	10414(1)	2407(1)	77(1)
CI(4)	1166(1)	11612(1)	2139(1)	92(1)

Table 4.4 Bond lengths [Å] and angles [°] for **4.11**.

C(1)-C(6)	1.383(4)	C(15)-H(15B)	0.99
C(1)-C(2)	1.386(4)	C(16)-C(21)	1.391(4)
C(1)-P(1)	1.828(3)	C(16)-C(17)	1.396(4)
C(2)-C(3)	1.393(4)	C(16)-P(2)	1.829(2)
C(2)-H(2)	0.95	C(17)-C(18)	1.389(4)
C(3)-C(4)	1.368(5)	C(17)-H(17)	0.95
C(3)-H(3)	0.95	C(18)-C(19)	1.389(4)
C(4)-C(5)	1.372(5)	C(18)-H(18)	0.95
C(4)-H(4)	0.95	C(19)-C(20)	1.376(4)
C(5)-C(6)	1.403(4)	C(19)-H(19)	0.95
C(5)-H(5)	0.95	C(20)-C(21)	1.395(4)
C(6)-H(6)	0.95	C(20)-H(20)	0.95
C(7)-C(8)	1.394(4)	C(21)-H(21)	0.95
C(7)-C(12)	1.397(4)	C(22)-C(23)	1.392(4)
C(7)-P(1)	1.814(3)	C(22)-C(27)	1.393(4)
C(8)-C(9)	1.389(4)	C(22)-P(2)	1.826(3)
C(8)-H(8)	0.95	C(23)-C(24)	1.383(4)
C(9)-C(10)	1.381(5)	C(23)-H(23)	0.95
C(9)-H(9)	0.95	C(24)-C(25)	1.383(4)
C(10)-C(11)	1.369(5)	C(24)-H(24)	0.95
C(10)-H(10)	0.95	C(25)-C(26)	1.381(4)
C(11)-C(12)	1.387(4)	C(25)-H(25)	0.95
C(11)-H(11)	0.95	C(26)-C(27)	1.387(4)
C(12)-H(12)	0.95	C(26)-H(26)	0.95
C(13)-C(14)	1.538(4)	C(27)-H(27)	0.95
C(13)-P(1)	1.828(3)	C(28)-O(1)	1.270(3)
C(13)-H(13A)	0.99	C(28)-O(2)	1.272(3)
C(13)-H(13B)	0.99	C(28)-C(29)	1.514(3)
C(14)-C(15)	1.522(4)	C(28)-Ru(1)	2.538(2)
C(14)-H(14A)	0.99	C(29)-C(38)	1.530(4)
C(14)-H(14B)	0.99	C(29)-C(30)	1.532(4)
C(15)-P(2)	1.829(3)	C(29)-C(34)	1.543(4)
C(15)-H(15A)	0.99	C(30)-C(31)	1.548(4)

Table 4.4, continued.

C(30)-H(30A)	0.99	C(42)-H(42)	1.00
C(30)-H(30B)	0.99	C(43)-C(44)	1.497(8)
C(31)-C(37)	1.510(6)	C(43)-H(43A)	0.99
C(31)-C(32)	1.520(5)	C(43)-H(43B)	0.99
C(31)-H(31)	1.00	C(44)-C(48)	1.513(8)
C(32)-C(33)	1.516(4)	C(44)-C(45)	1.544(5)
C(32)-H(32A)	0.99	C(44)-H(44)	1.00
C(32)-H(32B)	0.99	C(45)-H(45A)	0.99
C(33)-C(35)	1.506(4)	C(45)-H(45B)	0.99
C(33)-C(34)	1.545(4)	C(46)-C(47)	1.543(6)
C(33)-H(33)	1.00	C(46)-H(46A)	0.99
C(34)-H(34A)	0.99	C(46)-H(46B)	0.99
C(34)-H(34B)	0.99	C(47)-C(49)	1.482(6)
C(35)-C(36)	1.516(5)	C(47)-C(48)	1.487(6)
C(35)-H(35A)	0.99	C(47)-H(47)	1.00
C(35)-H(35B)	0.99	C(48)-H(48A)	0.99
C(36)-C(37)	1.515(6)	C(48)-H(48B)	0.99
C(36)-C(38)	1.554(4)	C(49)-H(49A)	0.99
C(36)-H(36)	1.00	C(49)-H(49B)	0.99
C(37)-H(37A)	0.99	C(50)-O(5)	1.146(3)
C(37)-H(37B)	0.99	C(50)-Ru(1)	1.829(3)
C(38)-H(38A)	0.99	C(51)-Cl(1)	1.700(5)
C(38)-H(38B)	0.99	C(51)-Cl(2)	1.769(5)
C(39)-O(4)	1.231(4)	C(51)-H(51A)	0.99
C(39)-O(3)	1.277(3)	C(51)-H(51B)	0.99
C(39)-C(40)	1.534(4)	O(1)-Ru(1)	2.1816(17)
C(40)-C(46)	1.521(4)	O(2)-Ru(1)	2.1708(18)
C(40)-C(45)	1.522(4)	O(3)-Ru(1)	2.0964(18)
C(40)-C(41)	1.532(4)	P(1)-Ru(1)	2.2776(7)
C(41)-C(42)	1.546(5)	P(2)-Ru(1)	2.2985(7)
C(41)-H(41A)	0.99	C(52)-Cl(4)	1.752(4)
C(41)-H(41B)	0.99	C(52)-Cl(3)	1.768(4)
C(42)-C(49)	1.503(6)	C(52)-H(52A)	0.99
C(42)-C(43)	1.520(7)	C(52)-H(52B)	0.99

Table 4.4, continued.

C(6)-C(1)-C(2)	119.3(3)	C(7)-C(12)-H(12)	120.1
C(6)-C(1)-P(1)	120.9(2)	C(14)-C(13)-P(1)	116.54(18)
C(2)-C(1)-P(1)	119.6(2)	C(14)-C(13)-H(13A)	108.2
C(1)-C(2)-C(3)	120.3(3)	P(1)-C(13)-H(13A)	108.2
C(1)-C(2)-H(2)	119.9	C(14)-C(13)-H(13B)	108.2
C(3)-C(2)-H(2)	119.9	P(1)-C(13)-H(13B)	108.2
C(4)-C(3)-C(2)	120.3(3)	H(13A)-C(13)-H(13B)	107.3
C(4)-C(3)-H(3)	119.8	C(15)-C(14)-C(13)	114.8(2)
C(2)-C(3)-H(3)	119.8	C(15)-C(14)-H(14A)	108.6
C(3)-C(4)-C(5)	120.0(3)	C(13)-C(14)-H(14A)	108.6
C(3)-C(4)-H(4)	120.0	C(15)-C(14)-H(14B)	108.6
C(5)-C(4)-H(4)	120.0	C(13)-C(14)-H(14B)	108.6
C(4)-C(5)-C(6)	120.4(3)	H(14A)-C(14)-H(14B)	107.6
C(4)-C(5)-H(5)	119.8	C(14)-C(15)-P(2)	114.45(19)
C(6)-C(5)-H(5)	119.8	C(14)-C(15)-H(15A)	108.6
C(1)-C(6)-C(5)	119.7(3)	P(2)-C(15)-H(15A)	108.6
C(1)-C(6)-H(6)	120.2	C(14)-C(15)-H(15B)	108.6
C(5)-C(6)-H(6)	120.2	P(2)-C(15)-H(15B)	108.6
C(8)-C(7)-C(12)	119.4(3)	H(15A)-C(15)-H(15B)	107.6
C(8)-C(7)-P(1)	117.7(2)	C(21)-C(16)-C(17)	119.1(2)
C(12)-C(7)-P(1)	122.7(2)	C(21)-C(16)-P(2)	121.37(19)
C(9)-C(8)-C(7)	119.8(3)	C(17)-C(16)-P(2)	119.5(2)
C(9)-C(8)-H(8)	120.1	C(18)-C(17)-C(16)	120.4(3)
C(7)-C(8)-H(8)	120.1	C(18)-C(17)-H(17)	119.8
C(10)-C(9)-C(8)	120.1(3)	C(16)-C(17)-H(17)	119.8
C(10)-C(9)-H(9)	120.0	C(19)-C(18)-C(17)	120.1(3)
C(8)-C(9)-H(9)	120.0	C(19)-C(18)-H(18)	120.0
C(11)-C(10)-C(9)	120.6(3)	C(17)-C(18)-H(18)	120.0
C(11)-C(10)-H(10)	119.7	C(20)-C(19)-C(18)	119.9(2)
C(9)-C(10)-H(10)	119.7	C(20)-C(19)-H(19)	120.0
C(10)-C(11)-C(12)	120.2(3)	C(18)-C(19)-H(19)	120.0
C(10)-C(11)-H(11)	119.9	C(19)-C(20)-C(21)	120.3(3)
C(12)-C(11)-H(11)	119.9	C(19)-C(20)-H(20)	119.8
C(11)-C(12)-C(7)	119.9(3)	C(21)-C(20)-H(20)	119.8
C(11)-C(12)-H(12)	120.1	C(16)-C(21)-C(20)	120.2(2)

Table 4.4, continued.

C(16)-C(21)-H(21)	119.9	C(29)-C(30)-H(30B)	109.8
C(20)-C(21)-H(21)	119.9	C(31)-C(30)-H(30B)	109.8
C(23)-C(22)-C(27)	118.3(2)	H(30A)-C(30)-H(30B)	108.2
C(23)-C(22)-P(2)	120.1(2)	C(37)-C(31)-C(32)	110.6(3)
C(27)-C(22)-P(2)	121.5(2)	C(37)-C(31)-C(30)	108.4(3)
C(24)-C(23)-C(22)	120.9(3)	C(32)-C(31)-C(30)	108.9(3)
C(24)-C(23)-H(23)	119.6	C(37)-C(31)-H(31)	109.7
C(22)-C(23)-H(23)	119.6	C(32)-C(31)-H(31)	109.7
C(25)-C(24)-C(23)	120.0(3)	C(30)-C(31)-H(31)	109.7
C(25)-C(24)-H(24)	120.0	C(33)-C(32)-C(31)	109.9(3)
C(23)-C(24)-H(24)	120.0	C(33)-C(32)-H(32A)	109.7
C(26)-C(25)-C(24)	120.1(3)	C(31)-C(32)-H(32A)	109.7
C(26)-C(25)-H(25)	120.0	C(33)-C(32)-H(32B)	109.7
C(24)-C(25)-H(25)	120.0	C(31)-C(32)-H(32B)	109.7
C(25)-C(26)-C(27)	119.8(3)	H(32A)-C(32)-H(32B)	108.2
C(25)-C(26)-H(26)	120.1	C(35)-C(33)-C(32)	111.1(3)
C(27)-C(26)-H(26)	120.1	C(35)-C(33)-C(34)	108.4(2)
C(26)-C(27)-C(22)	120.9(3)	C(32)-C(33)-C(34)	108.6(2)
C(26)-C(27)-H(27)	119.5	C(35)-C(33)-H(33)	109.6
C(22)-C(27)-H(27)	119.5	C(32)-C(33)-H(33)	109.6
O(1)-C(28)-O(2)	118.0(2)	C(34)-C(33)-H(33)	109.6
O(1)-C(28)-C(29)	121.3(2)	C(29)-C(34)-C(33)	109.9(2)
O(2)-C(28)-C(29)	120.7(2)	C(29)-C(34)-H(34A)	109.7
O(1)-C(28)-Ru(1)	59.25(12)	C(33)-C(34)-H(34A)	109.7
O(2)-C(28)-Ru(1)	58.77(12)	C(29)-C(34)-H(34B)	109.7
C(29)-C(28)-Ru(1)	178.97(18)	C(33)-C(34)-H(34B)	109.7
C(28)-C(29)-C(38)	109.1(2)	H(34A)-C(34)-H(34B)	108.2
C(28)-C(29)-C(30)	110.0(2)	C(33)-C(35)-C(36)	110.4(3)
C(38)-C(29)-C(30)	109.4(3)	C(33)-C(35)-H(35A)	109.6
C(28)-C(29)-C(34)	110.9(2)	C(36)-C(35)-H(35A)	109.6
C(38)-C(29)-C(34)	108.4(2)	C(33)-C(35)-H(35B)	109.6
C(30)-C(29)-C(34)	109.1(2)	C(36)-C(35)-H(35B)	109.6
C(29)-C(30)-C(31)	109.6(2)	H(35A)-C(35)-H(35B)	108.1
C(29)-C(30)-H(30A)	109.8	C(37)-C(36)-C(35)	110.2(3)
C(31)-C(30)-H(30A)	109.8	C(37)-C(36)-C(38)	108.3(3)

Table 4.4, continued.

C(35)-C(36)-C(38)	108.7(3)	C(43)-C(42)-H(42)	109.8
C(37)-C(36)-H(36)	109.9	C(41)-C(42)-H(42)	109.8
C(35)-C(36)-H(36)	109.9	C(44)-C(43)-C(42)	109.8(4)
C(38)-C(36)-H(36)	109.9	C(44)-C(43)-H(43A)	109.7
C(31)-C(37)-C(36)	110.8(3)	C(42)-C(43)-H(43A)	109.7
C(31)-C(37)-H(37A)	109.5	C(44)-C(43)-H(43B)	109.7
C(36)-C(37)-H(37A)	109.5	C(42)-C(43)-H(43B)	109.7
C(31)-C(37)-H(37B)	109.5	H(43A)-C(43)-H(43B)	108.2
C(36)-C(37)-H(37B)	109.5	C(43)-C(44)-C(48)	109.6(3)
H(37A)-C(37)-H(37B)	108.1	C(43)-C(44)-C(45)	109.9(4)
C(29)-C(38)-C(36)	109.6(2)	C(48)-C(44)-C(45)	108.8(4)
C(29)-C(38)-H(38A)	109.8	C(43)-C(44)-H(44)	109.5
C(36)-C(38)-H(38A)	109.8	C(48)-C(44)-H(44)	109.5
C(29)-C(38)-H(38B)	109.8	C(45)-C(44)-H(44)	109.5
C(36)-C(38)-H(38B)	109.8	C(40)-C(45)-C(44)	109.6(3)
H(38A)-C(38)-H(38B)	108.2	C(40)-C(45)-H(45A)	109.8
O(4)-C(39)-O(3)	124.7(3)	C(44)-C(45)-H(45A)	109.8
O(4)-C(39)-C(40)	119.4(3)	C(40)-C(45)-H(45B)	109.8
O(3)-C(39)-C(40)	115.9(2)	C(44)-C(45)-H(45B)	109.8
C(46)-C(40)-C(45)	109.3(3)	H(45A)-C(45)-H(45B)	108.2
C(46)-C(40)-C(41)	107.7(3)	C(40)-C(46)-C(47)	110.5(3)
C(45)-C(40)-C(41)	108.4(3)	C(40)-C(46)-H(46A)	109.5
C(46)-C(40)-C(39)	107.6(3)	C(47)-C(46)-H(46A)	109.5
C(45)-C(40)-C(39)	112.9(2)	C(40)-C(46)-H(46B)	109.5
C(41)-C(40)-C(39)	110.6(2)	C(47)-C(46)-H(46B)	109.5
C(40)-C(41)-C(42)	110.2(3)	H(46A)-C(46)-H(46B)	108.1
C(40)-C(41)-H(41A)	109.6	C(49)-C(47)-C(48)	110.9(4)
C(42)-C(41)-H(41A)	109.6	C(49)-C(47)-C(46)	109.1(3)
C(40)-C(41)-H(41B)	109.6	C(48)-C(47)-C(46)	108.6(3)
C(42)-C(41)-H(41B)	109.6	C(49)-C(47)-H(47)	109.4
H(41A)-C(41)-H(41B)	108.1	C(48)-C(47)-H(47)	109.4
C(49)-C(42)-C(43)	109.7(4)	C(46)-C(47)-H(47)	109.4
C(49)-C(42)-C(41)	109.7(4)	C(47)-C(48)-C(44)	110.4(3)
C(43)-C(42)-C(41)	108.1(4)	C(47)-C(48)-H(48A)	109.6
C(49)-C(42)-H(42)	109.8	C(44)-C(48)-H(48A)	109.6

Table 4.4, continued.

C(47)-C(48)-H(48B)	109.6	C(15)-P(2)-Ru(1)	114.78(9)
C(44)-C(48)-H(48B)	109.6	C(16)-P(2)-Ru(1)	119.17(9)
H(48A)-C(48)-H(48B)	108.1	C(50)-Ru(1)-O(3)	98.70(9)
C(47)-C(49)-C(42)	110.1(3)	C(50)-Ru(1)-O(2)	104.20(10)
C(47)-C(49)-H(49A)	109.6	O(3)-Ru(1)-O(2)	84.58(7)
C(42)-C(49)-H(49A)	109.6	C(50)-Ru(1)-O(1)	164.26(9)
C(47)-C(49)-H(49B)	109.6	O(3)-Ru(1)-O(1)	79.94(7)
C(42)-C(49)-H(49B)	109.6	O(2)-Ru(1)-O(1)	60.08(6)
H(49A)-C(49)-H(49B)	108.1	C(50)-Ru(1)-P(1)	89.08(8)
O(5)-C(50)-Ru(1)	174.9(2)	O(3)-Ru(1)-P(1)	91.91(5)
Cl(1)-C(51)-Cl(2)	112.5(2)	O(2)-Ru(1)-P(1)	166.62(5)
Cl(1)-C(51)-H(51A)	109.1	O(1)-Ru(1)-P(1)	106.61(5)
Cl(2)-C(51)-H(51A)	109.1	C(50)-Ru(1)-P(2)	86.14(8)
Cl(1)-C(51)-H(51B)	109.1	O(3)-Ru(1)-P(2)	174.55(5)
Cl(2)-C(51)-H(51B)	109.1	O(2)-Ru(1)-P(2)	91.83(5)
H(51A)-C(51)-H(51B)	107.8	O(1)-Ru(1)-P(2)	94.72(5)
C(28)-O(1)-Ru(1)	90.74(14)	P(1)-Ru(1)-P(2)	90.67(2)
C(28)-O(2)-Ru(1)	91.15(15)	C(50)-Ru(1)-C(28)	134.26(10)
C(39)-O(3)-Ru(1)	122.49(18)	O(3)-Ru(1)-C(28)	80.64(7)
C(7)-P(1)-C(13)	105.61(13)	O(2)-Ru(1)-C(28)	30.08(7)
C(7)-P(1)-C(1)	104.60(13)	O(1)-Ru(1)-C(28)	30.01(7)
C(13)-P(1)-C(1)	100.67(12)	P(1)-Ru(1)-C(28)	136.58(6)
C(7)-P(1)-Ru(1)	110.66(9)	P(2)-Ru(1)-C(28)	94.20(6)
C(13)-P(1)-Ru(1)	116.50(9)	Cl(4)-C(52)-Cl(3)	111.4(2)
C(1)-P(1)-Ru(1)	117.41(9)	Cl(4)-C(52)-H(52A)	109.3
C(22)-P(2)-C(15)	101.82(12)	Cl(3)-C(52)-H(52A)	109.3
C(22)-P(2)-C(16)	103.93(11)	Cl(4)-C(52)-H(52B)	109.3
C(15)-P(2)-C(16)	102.62(12)	Cl(3)-C(52)-H(52B)	109.3
C(22)-P(2)-Ru(1)	112.48(8)	H(52A)-C(52)-H(52B)	108.0

Table 4.5 Anisotropic displacement parameters ($\text{\AA}^2 \times 10^3$) for **4.11**. The anisotropic displacement factor exponent takes the form: $-2\pi^2 [h^2 a^{*2} U^{11} + \dots + 2 h k a^* b^* U^{12}]$

	U ¹¹	U ²²	U ³³	U ²³	U ¹³	U ¹²
C(1)	34(2)	20(1)	25(1)	-10(1)	6(1)	-8(1)
C(2)	36(2)	28(1)	43(2)	-17(1)	5(1)	-3(1)
C(3)	51(2)	27(2)	55(2)	-20(2)	18(2)	-6(1)
C(4)	76(3)	30(2)	39(2)	-21(1)	19(2)	-16(2)
C(5)	80(3)	42(2)	40(2)	-24(2)	-6(2)	-12(2)
C(6)	55(2)	33(2)	38(2)	-19(1)	-10(2)	0(1)
C(7)	28(1)	20(1)	25(1)	-11(1)	-4(1)	-2(1)
C(8)	35(2)	27(1)	23(1)	-12(1)	-3(1)	-2(1)
C(9)	54(2)	26(1)	22(1)	-8(1)	-5(1)	-2(1)
C(10)	41(2)	34(2)	38(2)	-18(1)	-14(1)	9(1)
C(11)	28(2)	40(2)	41(2)	-18(1)	-9(1)	2(1)
C(12)	30(2)	28(1)	32(2)	-9(1)	-6(1)	-3(1)
C(13)	25(1)	21(1)	28(1)	-8(1)	2(1)	-8(1)
C(14)	24(1)	28(1)	29(2)	-10(1)	7(1)	-10(1)
C(15)	28(1)	20(1)	23(1)	-6(1)	6(1)	-8(1)
C(16)	16(1)	18(1)	25(1)	-8(1)	3(1)	-4(1)
C(17)	22(1)	27(1)	23(1)	-7(1)	4(1)	-2(1)
C(18)	22(1)	33(1)	35(2)	-16(1)	8(1)	-2(1)
C(19)	18(1)	27(1)	41(2)	-12(1)	2(1)	1(1)
C(20)	22(1)	25(1)	30(2)	-7(1)	-3(1)	0(1)
C(21)	22(1)	22(1)	24(1)	-10(1)	1(1)	-3(1)
C(22)	17(1)	24(1)	20(1)	-8(1)	2(1)	-1(1)
C(23)	21(1)	25(1)	25(1)	-6(1)	0(1)	-4(1)
C(24)	25(1)	39(2)	37(2)	-15(1)	0(1)	-11(1)
C(25)	24(1)	52(2)	32(2)	-15(1)	-5(1)	-6(1)
C(26)	28(2)	38(2)	30(2)	-3(1)	-9(1)	2(1)
C(27)	28(1)	25(1)	32(2)	-7(1)	-2(1)	0(1)
C(28)	19(1)	20(1)	21(1)	-7(1)	4(1)	-2(1)
C(29)	20(1)	20(1)	22(1)	-4(1)	4(1)	-4(1)
C(30)	27(2)	25(1)	60(2)	-10(1)	-4(1)	-3(1)

Table 4.6, continued.

C(31)	40(2)	25(2)	76(3)	-9(2)	-19(2)	1(1)
C(32)	38(2)	32(2)	57(2)	-20(2)	10(2)	-8(1)
C(33)	29(1)	34(2)	30(2)	-16(1)	2(1)	-9(1)
C(34)	33(2)	30(1)	28(2)	-7(1)	0(1)	-10(1)
C(35)	35(2)	44(2)	43(2)	-19(2)	15(1)	-18(1)
C(36)	64(2)	60(2)	28(2)	-18(2)	18(2)	-36(2)
C(37)	91(3)	49(2)	40(2)	15(2)	-26(2)	-38(2)
C(38)	48(2)	48(2)	32(2)	-21(1)	17(1)	-25(2)
C(39)	24(1)	40(2)	28(2)	-11(1)	2(1)	4(1)
C(40)	20(1)	25(1)	28(1)	-8(1)	4(1)	0(1)
C(41)	72(3)	42(2)	54(2)	-22(2)	26(2)	-22(2)
C(42)	88(3)	51(2)	59(3)	-37(2)	33(2)	-22(2)
C(43)	54(3)	170(6)	42(3)	-44(3)	6(2)	-9(3)
C(44)	58(3)	92(3)	42(2)	25(2)	22(2)	43(2)
C(45)	38(2)	69(3)	39(2)	6(2)	14(2)	23(2)
C(46)	30(2)	80(3)	72(3)	-46(2)	10(2)	-16(2)
C(47)	28(2)	68(3)	85(3)	-28(2)	19(2)	-17(2)
C(48)	76(3)	36(2)	117(4)	0(2)	62(3)	0(2)
C(49)	49(2)	53(2)	49(2)	-4(2)	17(2)	24(2)
C(50)	22(1)	22(1)	26(1)	-10(1)	4(1)	-3(1)
C(51)	30(2)	74(3)	99(4)	24(3)	9(2)	7(2)
O(1)	18(1)	20(1)	23(1)	-6(1)	1(1)	-3(1)
O(2)	21(1)	20(1)	26(1)	-5(1)	-1(1)	-3(1)
O(3)	24(1)	23(1)	23(1)	-9(1)	4(1)	0(1)
O(4)	49(2)	94(2)	30(1)	2(1)	6(1)	41(2)
O(5)	40(1)	21(1)	33(1)	-2(1)	-1(1)	4(1)
P(1)	22(1)	17(1)	22(1)	-8(1)	1(1)	-2(1)
P(2)	18(1)	16(1)	18(1)	-5(1)	2(1)	-2(1)
Ru(1)	17(1)	15(1)	19(1)	-5(1)	2(1)	-1(1)
CI(1)	68(1)	102(1)	201(2)	-83(1)	-55(1)	3(1)
CI(2)	65(1)	54(1)	127(1)	-21(1)	31(1)	15(1)
C(52)	42(2)	59(2)	48(2)	-14(2)	-4(2)	-1(2)
CI(3)	36(1)	83(1)	98(1)	-13(1)	1(1)	0(1)
CI(4)	104(1)	95(1)	90(1)	-38(1)	6(1)	-44(1)

Table 4.7 Hydrogen coordinates ($\times 10^4$) and isotropic displacement parameters ($\text{\AA}^2 \times 10^3$) for 4.11.

	x	y	z	U(eq)
H(2)	4481	9640	2345	42
H(3)	4095	10737	3141	52
H(4)	5420	10708	4222	54
H(5)	7135	9582	4529	61
H(6)	7548	8476	3732	49
H(8)	6368	6496	3779	33
H(9)	7777	5193	4534	41
H(10)	9775	5136	4084	44
H(11)	10393	6370	2901	43
H(12)	9021	7708	2169	36
H(13A)	6614	9520	1036	29
H(13B)	7855	9116	1554	29
H(14A)	8144	8930	157	32
H(14B)	8174	7877	866	32
H(15A)	7060	8147	-477	29
H(15B)	6098	8883	-163	29
H(17)	7302	6463	-504	30
H(18)	8780	5138	-343	35
H(19)	9408	4143	1090	34
H(20)	8564	4474	2356	31
H(21)	7049	5778	2205	27
H(23)	4837	5807	351	29
H(24)	3494	5728	-682	39
H(25)	2713	7120	-1809	42
H(26)	3308	8589	-1920	41
H(27)	4649	8670	-882	35
H(30A)	5314	4151	3361	46
H(30B)	5277	4175	2337	46
H(31)	5039	2593	3325	58

Table 4.7, continued.

H(32A)	4039	3140	1912	49
H(32B)	3301	2416	2656	49
H(33)	1968	3776	1846	35
H(34A)	3380	4899	1429	37
H(34B)	2226	5335	1883	37
H(35A)	1450	3122	3371	47
H(35B)	1080	4265	3053	47
H(36)	2065	3726	4468	57
H(37A)	4135	3091	4526	76
H(37B)	3357	2391	4288	76
H(38A)	2296	5316	3476	47
H(38B)	3488	4853	4059	47
H(41A)	1804	9495	3766	65
H(41B)	3007	9100	4345	65
H(42)	1377	9446	5291	74
H(43A)	2923	8164	5959	105
H(43B)	1671	7940	6454	105
H(44)	2649	6565	6152	99
H(45A)	3779	7350	4855	70
H(45B)	3058	6606	4631	70
H(46A)	1139	7227	3746	66
H(46B)	663	8356	3418	66
H(47)	-450	7556	4715	71
H(48A)	1085	6298	5353	102
H(48B)	540	6793	6082	102
H(49A)	-234	8548	5566	69
H(49B)	-176	9142	4516	69
H(51A)	1895	7605	1244	99
H(51B)	2297	7818	214	99
H(52A)	1250	10121	2006	61
H(52B)	517	10915	1190	61

Table 4.8 Torsion angles [°] for **4.11**.

C(6)-C(1)-C(2)-C(3)	0.6(5)	P(2)-C(22)-C(27)-C(26)	-177.0(2)
P(1)-C(1)-C(2)-C(3)	-175.5(2)	O(1)-C(28)-C(29)-C(38)	86.4(3)
C(1)-C(2)-C(3)-C(4)	-0.3(5)	O(2)-C(28)-C(29)-C(38)	-94.0(3)
C(2)-C(3)-C(4)-C(5)	-0.2(5)	O(1)-C(28)-C(29)-C(30)	-33.7(3)
C(3)-C(4)-C(5)-C(6)	0.4(6)	O(2)-C(28)-C(29)-C(30)	146.0(3)
C(2)-C(1)-C(6)-C(5)	-0.4(5)	O(1)-C(28)-C(29)-C(34)	-154.4(2)
P(1)-C(1)-C(6)-C(5)	175.7(3)	O(2)-C(28)-C(29)-C(34)	25.3(3)
C(4)-C(5)-C(6)-C(1)	-0.1(6)	C(28)-C(29)-C(30)-C(31)	179.4(3)
C(12)-C(7)-C(8)-C(9)	-0.7(4)	C(38)-C(29)-C(30)-C(31)	59.5(3)
P(1)-C(7)-C(8)-C(9)	174.6(2)	C(34)-C(29)-C(30)-C(31)	-58.8(3)
C(7)-C(8)-C(9)-C(10)	-0.5(4)	C(29)-C(30)-C(31)-C(37)	-60.0(4)
C(8)-C(9)-C(10)-C(11)	0.6(5)	C(29)-C(30)-C(31)-C(32)	60.3(4)
C(9)-C(10)-C(11)-C(12)	0.7(5)	C(37)-C(31)-C(32)-C(33)	57.0(4)
C(10)-C(11)-C(12)-C(7)	-2.0(4)	C(30)-C(31)-C(32)-C(33)	-62.0(4)
C(8)-C(7)-C(12)-C(11)	2.0(4)	C(31)-C(32)-C(33)-C(35)	-57.4(3)
P(1)-C(7)-C(12)-C(11)	-173.1(2)	C(31)-C(32)-C(33)-C(34)	61.7(3)
P(1)-C(13)-C(14)-C(15)	66.6(3)	C(28)-C(29)-C(34)-C(33)	-179.8(2)
C(13)-C(14)-C(15)-P(2)	-70.4(3)	C(38)-C(29)-C(34)-C(33)	-60.1(3)
C(21)-C(16)-C(17)-C(18)	0.8(4)	C(30)-C(29)-C(34)-C(33)	59.0(3)
P(2)-C(16)-C(17)-C(18)	178.8(2)	C(35)-C(33)-C(34)-C(29)	60.7(3)
C(16)-C(17)-C(18)-C(19)	-0.8(4)	C(32)-C(33)-C(34)-C(29)	-60.1(3)
C(17)-C(18)-C(19)-C(20)	0.0(4)	C(32)-C(33)-C(35)-C(36)	57.7(3)
C(18)-C(19)-C(20)-C(21)	0.9(4)	C(34)-C(33)-C(35)-C(36)	-61.6(3)
C(17)-C(16)-C(21)-C(20)	0.0(4)	C(33)-C(35)-C(36)-C(37)	-57.2(4)
P(2)-C(16)-C(21)-C(20)	-177.9(2)	C(33)-C(35)-C(36)-C(38)	61.4(4)
C(19)-C(20)-C(21)-C(16)	-0.8(4)	C(32)-C(31)-C(37)-C(36)	-57.6(4)
C(27)-C(22)-C(23)-C(24)	-0.1(4)	C(30)-C(31)-C(37)-C(36)	61.7(4)
P(2)-C(22)-C(23)-C(24)	176.9(2)	C(35)-C(36)-C(37)-C(31)	57.4(4)
C(22)-C(23)-C(24)-C(25)	-0.2(4)	C(38)-C(36)-C(37)-C(31)	-61.5(4)
C(23)-C(24)-C(25)-C(26)	0.6(5)	C(28)-C(29)-C(38)-C(36)	-179.7(3)
C(24)-C(25)-C(26)-C(27)	-0.8(5)	C(30)-C(29)-C(38)-C(36)	-59.4(3)
C(25)-C(26)-C(27)-C(22)	0.5(5)	C(34)-C(29)-C(38)-C(36)	59.5(3)
C(23)-C(22)-C(27)-C(26)	-0.1(4)	C(37)-C(36)-C(38)-C(29)	59.6(4)

Table 4.8, continued.

C(35)-C(36)-C(38)-C(29)	-60.2(4)	C(29)-C(28)-O(1)-Ru(1)	-179.0(2)
O(4)-C(39)-C(40)-C(46)	60.5(4)	O(1)-C(28)-O(2)-Ru(1)	-1.4(2)
O(3)-C(39)-C(40)-C(46)	-119.2(3)	C(29)-C(28)-O(2)-Ru(1)	178.9(2)
O(4)-C(39)-C(40)-C(45)	-178.7(4)	O(4)-C(39)-O(3)-Ru(1)	-6.6(5)
O(3)-C(39)-C(40)-C(45)	1.6(4)	C(40)-C(39)-O(3)-Ru(1)	173.13(18)
O(4)-C(39)-C(40)-C(41)	-57.0(4)	C(8)-C(7)-P(1)-C(13)	-173.1(2)
O(3)-C(39)-C(40)-C(41)	123.3(3)	C(12)-C(7)-P(1)-C(13)	2.1(3)
C(46)-C(40)-C(41)-C(42)	58.1(4)	C(8)-C(7)-P(1)-C(1)	81.2(2)
C(45)-C(40)-C(41)-C(42)	-60.1(4)	C(12)-C(7)-P(1)-C(1)	-103.7(2)
C(39)-C(40)-C(41)-C(42)	175.5(3)	C(8)-C(7)-P(1)-Ru(1)	-46.2(2)
C(40)-C(41)-C(42)-C(49)	-59.0(4)	C(12)-C(7)-P(1)-Ru(1)	129.0(2)
C(40)-C(41)-C(42)-C(43)	60.6(5)	C(14)-C(13)-P(1)-C(7)	69.7(2)
C(49)-C(42)-C(43)-C(44)	58.7(4)	C(14)-C(13)-P(1)-C(1)	178.3(2)
C(41)-C(42)-C(43)-C(44)	-60.8(5)	C(14)-C(13)-P(1)-Ru(1)	-53.6(2)
C(42)-C(43)-C(44)-C(48)	-58.3(5)	C(6)-C(1)-P(1)-C(7)	18.5(3)
C(42)-C(43)-C(44)-C(45)	61.2(5)	C(2)-C(1)-P(1)-C(7)	-165.4(2)
C(46)-C(40)-C(45)-C(44)	-58.2(5)	C(6)-C(1)-P(1)-C(13)	-90.9(3)
C(41)-C(40)-C(45)-C(44)	59.0(5)	C(2)-C(1)-P(1)-C(13)	85.2(2)
C(39)-C(40)-C(45)-C(44)	-178.0(4)	C(6)-C(1)-P(1)-Ru(1)	141.6(2)
C(43)-C(44)-C(45)-C(40)	-60.3(5)	C(2)-C(1)-P(1)-Ru(1)	-42.4(3)
C(48)-C(44)-C(45)-C(40)	59.6(5)	C(23)-C(22)-P(2)-C(15)	150.3(2)
C(45)-C(40)-C(46)-C(47)	58.3(4)	C(27)-C(22)-P(2)-C(15)	-32.9(2)
C(41)-C(40)-C(46)-C(47)	-59.3(4)	C(23)-C(22)-P(2)-C(16)	43.9(2)
C(39)-C(40)-C(46)-C(47)	-178.6(3)	C(27)-C(22)-P(2)-C(16)	-139.3(2)
C(40)-C(46)-C(47)-C(49)	61.3(4)	C(23)-C(22)-P(2)-Ru(1)	-86.4(2)
C(40)-C(46)-C(47)-C(48)	-59.6(5)	C(27)-C(22)-P(2)-Ru(1)	90.5(2)
C(49)-C(47)-C(48)-C(44)	-58.4(5)	C(14)-C(15)-P(2)-C(22)	-177.17(19)
C(46)-C(47)-C(48)-C(44)	61.3(5)	C(14)-C(15)-P(2)-C(16)	-69.8(2)
C(43)-C(44)-C(48)-C(47)	58.2(5)	C(14)-C(15)-P(2)-Ru(1)	61.0(2)
C(45)-C(44)-C(48)-C(47)	-61.9(5)	C(21)-C(16)-P(2)-C(22)	-135.5(2)
C(48)-C(47)-C(49)-C(42)	58.6(4)	C(17)-C(16)-P(2)-C(22)	46.7(2)
C(46)-C(47)-C(49)-C(42)	-60.9(4)	C(21)-C(16)-P(2)-C(15)	118.8(2)
C(43)-C(42)-C(49)-C(47)	-58.4(4)	C(17)-C(16)-P(2)-C(15)	-59.1(2)
C(41)-C(42)-C(49)-C(47)	60.2(4)	C(21)-C(16)-P(2)-Ru(1)	-9.3(2)
O(2)-C(28)-O(1)-Ru(1)	1.4(2)	C(17)-C(16)-P(2)-Ru(1)	172.80(17)

Table 4.8, continued.

C(39)-O(3)-Ru(1)-C(50)	19.1(2)	C(1)-P(1)-Ru(1)-P(2)	156.75(10)
C(39)-O(3)-Ru(1)-O(2)	-84.4(2)	C(7)-P(1)-Ru(1)-C(28)	13.51(13)
C(39)-O(3)-Ru(1)-O(1)	-145.0(2)	C(13)-P(1)-Ru(1)-C(28)	134.13(12)
C(39)-O(3)-Ru(1)-P(1)	108.5(2)	C(1)-P(1)-Ru(1)-C(28)	-106.42(13)
C(39)-O(3)-Ru(1)-C(28)	-114.5(2)	C(22)-P(2)-Ru(1)-C(50)	-67.12(12)
C(28)-O(2)-Ru(1)-C(50)	-178.30(16)	C(15)-P(2)-Ru(1)-C(50)	48.67(13)
C(28)-O(2)-Ru(1)-O(3)	-80.67(15)	C(16)-P(2)-Ru(1)-C(50)	170.91(12)
C(28)-O(2)-Ru(1)-O(1)	0.83(14)	C(22)-P(2)-Ru(1)-O(2)	36.99(10)
C(28)-O(2)-Ru(1)-P(1)	-5.4(3)	C(15)-P(2)-Ru(1)-O(2)	152.78(11)
C(28)-O(2)-Ru(1)-P(2)	95.23(14)	C(16)-P(2)-Ru(1)-O(2)	-84.98(10)
C(28)-O(1)-Ru(1)-C(50)	2.3(4)	C(22)-P(2)-Ru(1)-O(1)	97.12(10)
C(28)-O(1)-Ru(1)-O(3)	88.67(15)	C(15)-P(2)-Ru(1)-O(1)	-147.09(11)
C(28)-O(1)-Ru(1)-O(2)	-0.83(14)	C(16)-P(2)-Ru(1)-O(1)	-24.86(10)
C(28)-O(1)-Ru(1)-P(1)	177.67(13)	C(22)-P(2)-Ru(1)-P(1)	-156.16(9)
C(28)-O(1)-Ru(1)-P(2)	-90.22(14)	C(15)-P(2)-Ru(1)-P(1)	-40.36(10)
C(7)-P(1)-Ru(1)-C(50)	-169.44(13)	C(16)-P(2)-Ru(1)-P(1)	81.87(9)
C(13)-P(1)-Ru(1)-C(50)	-48.82(13)	C(22)-P(2)-Ru(1)-C(28)	67.02(11)
C(1)-P(1)-Ru(1)-C(50)	70.63(13)	C(15)-P(2)-Ru(1)-C(28)	-177.19(11)
C(7)-P(1)-Ru(1)-O(3)	91.88(11)	C(16)-P(2)-Ru(1)-C(28)	-54.95(11)
C(13)-P(1)-Ru(1)-O(3)	-147.50(11)	O(1)-C(28)-Ru(1)-C(50)	-179.13(15)
C(1)-P(1)-Ru(1)-O(3)	-28.05(11)	O(2)-C(28)-Ru(1)-C(50)	2.3(2)
C(7)-P(1)-Ru(1)-O(2)	17.4(3)	O(1)-C(28)-Ru(1)-O(3)	-86.07(14)
C(13)-P(1)-Ru(1)-O(2)	138.1(2)	O(2)-C(28)-Ru(1)-O(3)	95.37(15)
C(1)-P(1)-Ru(1)-O(2)	-102.5(2)	O(1)-C(28)-Ru(1)-O(2)	178.6(2)
C(7)-P(1)-Ru(1)-O(1)	11.82(11)	O(2)-C(28)-Ru(1)-O(1)	-178.6(2)
C(13)-P(1)-Ru(1)-O(1)	132.43(11)	O(1)-C(28)-Ru(1)-P(1)	-3.25(18)
C(1)-P(1)-Ru(1)-O(1)	-108.12(11)	O(2)-C(28)-Ru(1)-P(1)	178.19(11)
C(7)-P(1)-Ru(1)-P(2)	-83.31(10)	O(1)-C(28)-Ru(1)-P(2)	92.18(13)
C(13)-P(1)-Ru(1)-P(2)	37.31(10)	O(2)-C(28)-Ru(1)-P(2)	-86.39(14)

4.5.7 General Procedures for Vinylation of Ketones and Furan Formation

General Procedure A: To a re-sealable pressure tube (13 x 100 mm) equipped with magnetic stir bar, diol (or hydroxy ester) (0.3 mmol, 100 mol%), $\text{Ru}_3(\text{CO})_{12}$ (3.8 mg, 0.006 mmol, 2 mol%), tricyclohexylphosphine (10 mg, 0.036 mmol, 12 mol%), and 1-adamantanecarboxylic acid (6.5 mg, 0.036 mmol, 12 mol%). The tube was sealed with a rubber septum and purged with argon. Alkyne (0.90 mmol, 300 mol%) and *m*-xylenes (1.0 M overall) were added. The rubber septum was quickly replaced with a screw cap. The mixture was heated at 130 °C (oil bath temperature) for 4 h, at which point the reaction mixture was allowed to cool to ambient temperature and concentrated to afford the crude product. The reaction mixture was subjected to flash column chromatography to furnish the corresponding product of vinylation.

General Procedure B: To a re-sealable pressure tube (13 x 100 mm) equipped with magnetic stir bar, diol (0.3 mmol, 100 mol%), $\text{Ru}_3(\text{CO})_{12}$ (3.8 mg, 0.006 mmol, 2 mol%), 1,1'-Bis(diphenylphosphino)ferrocene (10 mg, 0.036 mmol, 6 mol%), and 1-adamantanecarboxylic acid (6.5 mg, 0.036 mmol, 12 mol%). The tube was sealed with a rubber septum and purged with argon. Alkyne (0.90 mmol, 300 mol%) and *m*-xylenes (1.0 M overall) were added. The rubber septum was quickly replaced with a screw cap. The mixture was heated at 130 °C (oil bath temperature) for 20 h, at which point the reaction mixture was allowed to cool to ambient temperature and concentrated to afford the crude product. The reaction mixture was subjected to flash column chromatography to furnish the corresponding product of vinylation.

General Procedure C: To a re-sealable pressure tube (13 x 100 mm) equipped with magnetic stir bar, ketone (100 mol%) and *p*-toluenesulfonic acid (20 mol%) were

added. The tube was sealed with a rubber septum and purged with argon, and *m*-xylenes (1.0 M) was added. The rubber septum was quickly replaced with a screw cap. The mixture was heated at 80 °C (oil bath temperature) for 4 h, at which point the reaction mixture was allowed to cool to ambient temperature. The reaction mixture was concentrated and subjected to flash column chromatography to furnish the corresponding furan.

4.5.8 Characterization of 4.12a-k, 4.12m, 4.13b-h, 4.14c, 4.15a, 4.15e, 4.15l, 4.16c, 4.16e, 4.16h.

(*E*)-2-hydroxy-2-(1-phenylprop-1-en-1-yl)cyclohexan-1-one (**4.12a**)

In accordance with the general procedure using *trans*-**4.1a** and alkyne **4.11a**, upon stirring at 130 °C for 4 h, the reaction mixture was concentrated to afford the crude product (*E*:*Z* = >20:1, as determined by ¹H NMR spectroscopy). The reaction mixture was subjected to flash column chromatography (SiO₂: 10% EtOAc/hexanes) to furnish **4.12a** (66 mg, 0.29 mmol, 95% yield) as a colorless oil.

TLC (SiO₂): R_f = 0.32 (hexanes: EtOAc = 9:1).

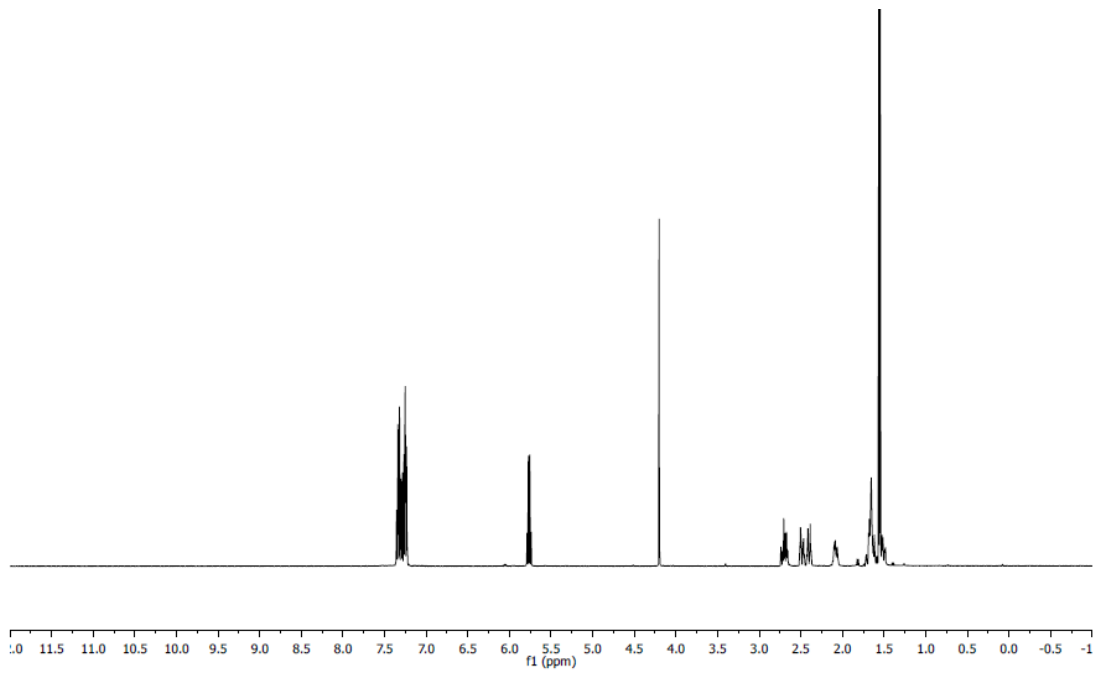
¹H NMR: (400 MHz, CDCl₃): δ 7.36-7.23 (m, 5H), 5.76 (q, *J* = 6.8 Hz, 1H), 4.20 (s, 1H), 2.74-2.66 (m, 1H), 2.51-2.47 (m, 1H), 2.42-2.37 (m, 1H), 2.11-2.06 (m, 1H), 1.71-1.48 (m, 4H), 1.55 ppm (d, *J* = 6.8 Hz, 3H)

¹³C NMR: (100 MHz, CDCl₃): δ 213.3, 142.1, 136.9, 129.6, 128.0, 127.2, 126.9, 81.8, 39.5, 38.8, 28.2, 22.7, 15.1 ppm.

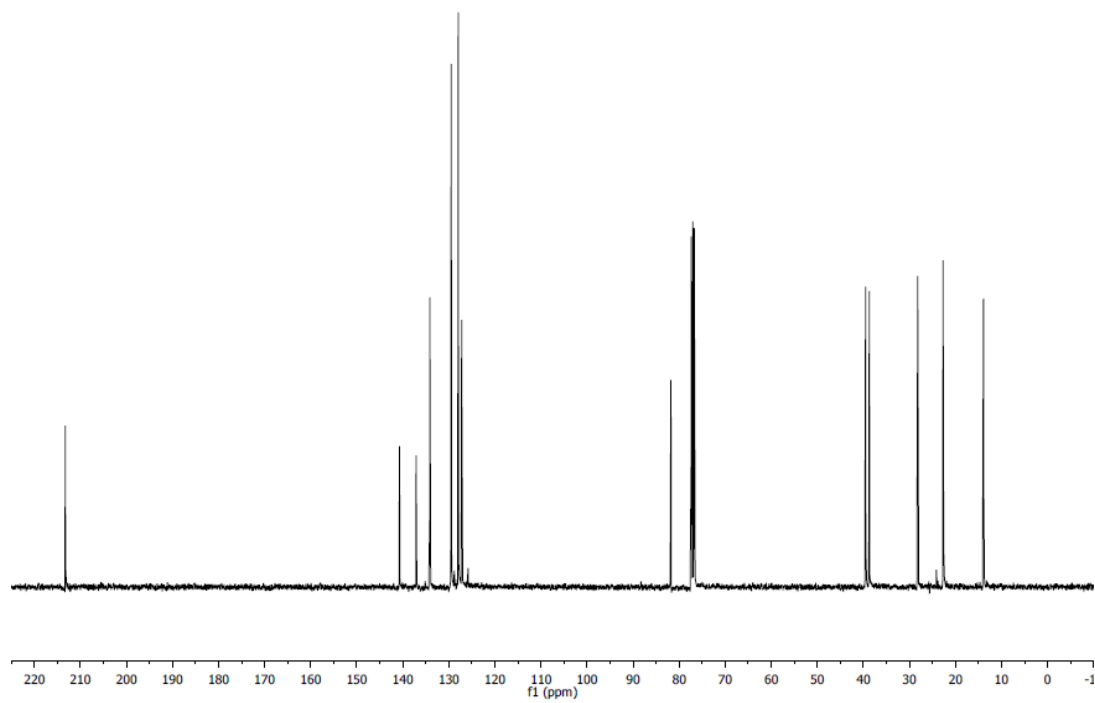
HRMS (ESI): *m/z* 239 [M+Na]⁺

FTIR (neat): 3448, 2969, 1739, 1492, 1441, 1158, 1073, 1048, 1028, 844 756, 705 1037 cm⁻¹.

¹H NMR of **4.12a**



¹³C NMR of **4.12a**



(E)-2-hydroxy-2-(1-phenylprop-1-en-1-yl)cyclopentan-1-one (4.12b)

In accordance with general procedure A using *cis*-**4.1b** and alkyne **4.11a**, upon stirring at 130 °C for 4 h, the reaction mixture was concentrated to afford the crude product (E:Z = >20:1, as determined by ¹H NMR spectroscopy). The reaction mixture was subjected to flash column chromatography (SiO₂: 10% EtOAc/hexanes) to furnish **4.12b** (56 mg, 0.26 mmol, 86% yield) as a colorless oil.

TLC (SiO₂): R_f = 0.29 (hexanes: EtOAc = 9:1).

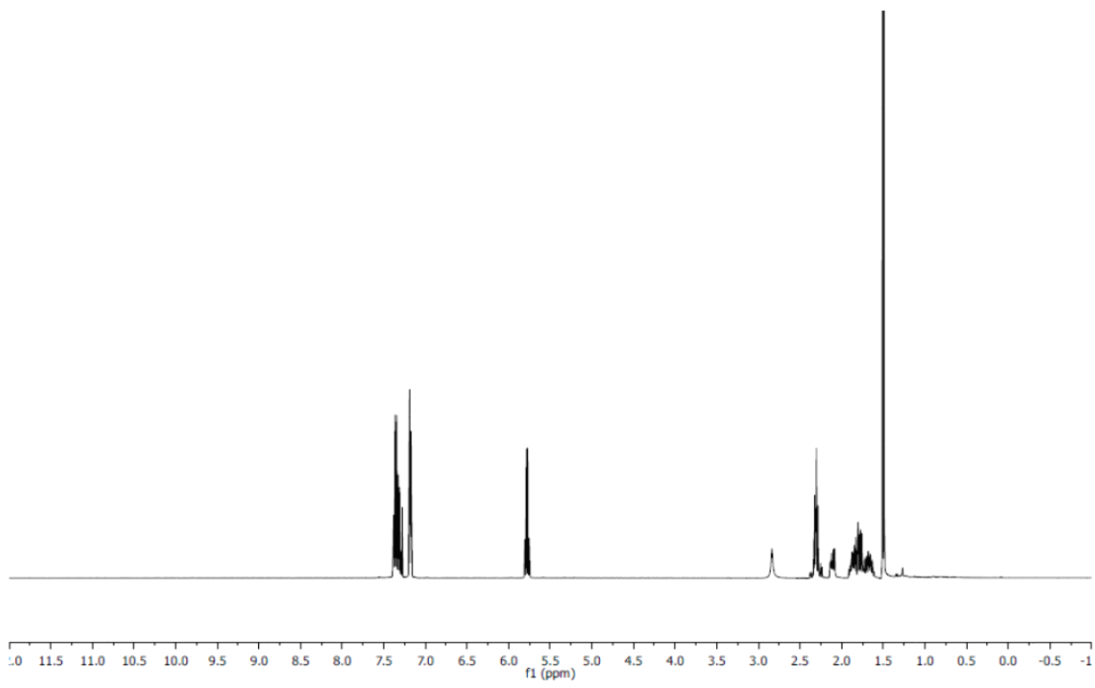
¹H NMR: (400 MHz, CDCl₃): δ 7.38-7.28 (m, 3H), 7.19-7.17 (m, 2H), 5.74 (q, *J* = 6.8 Hz, 1H), 2.84 (br s, 1H), 2.34-2.23 (m, 2H), 2.14-2.08 (m, 1H), 1.90-1.75 (m, 2H), 1.72-1.63 (m, 1H), 1.50 ppm (d, *J* = 6.8 Hz, 3H).

¹³C NMR: (100 MHz, CDCl₃): δ 218.9, 140.8, 136.8, 129.7, 128.2, 127.3, 125.6, 82.4, 35.2, 34.8, 16.8, 14.9 ppm.

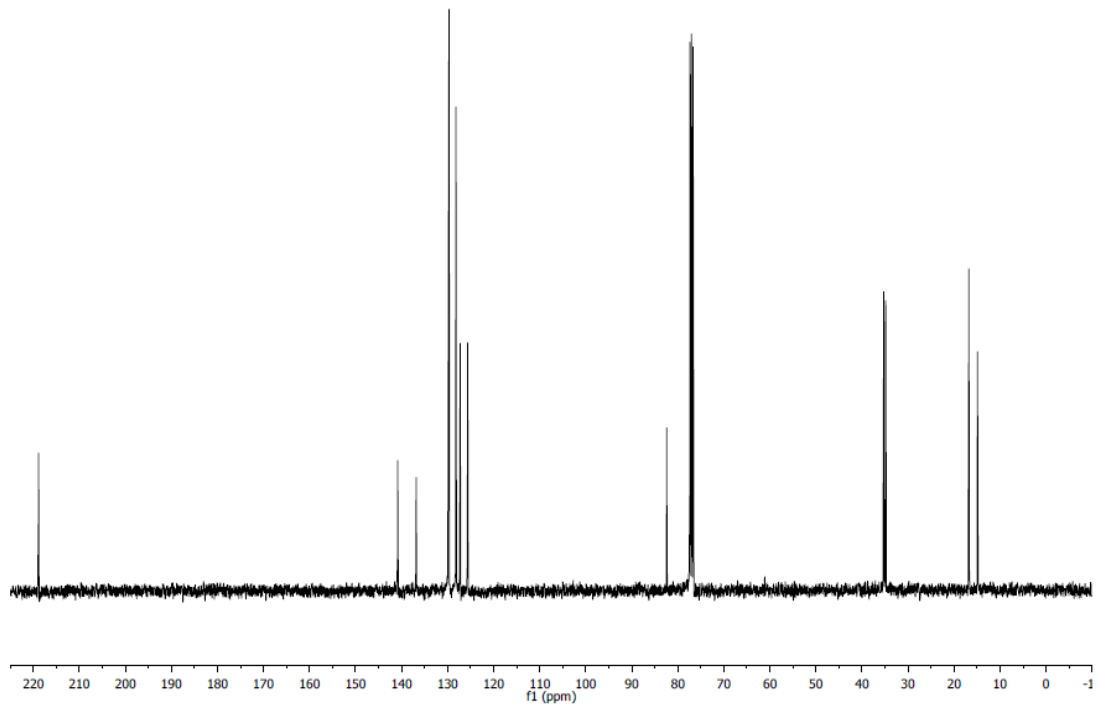
MS (ESI): *m/z* = 230 [M+Na]⁺

FTIR (neat): 3448, 2969, 1739, 1492, 1401, 1363, 1310, 1158, 1073, 1048, 1028, 936, 884, 815, 766, 705 cm⁻¹.

¹H NMR of **4.12b**



¹³C NMR of **4.12b**



(*E*)-2-hydroxy-2-(1-phenylprop-1-en-1-yl)cycloheptan-1-one (**4.12c**)

In modification of general procedure A using a mixture of *cis*- and *trans*-**4.1c** and alkyne **4.11a**, upon stirring at 130 °C for 2 h, the reaction mixture was concentrated to afford the crude product (E:Z = 4:1, as determined by ¹H NMR spectroscopy). The reaction mixture was subjected to flash column chromatography (SiO₂: 10% EtOAc/hexanes) to furnish **4.12c** (63 mg, 0.26 mmol, 86% yield) as a colorless oil.

TLC (SiO₂): R_f = 0.36 (hexanes: EtOAc = 9:1).

¹H NMR of Major Isomer: (400 MHz, CDCl₃): δ 7.39-7.26 (m, 3H), 7.20-7.15 (m, 2H), 6.54 (q, *J* = 7.2 Hz, 1H, Major Isomer), 3.30 (s, 1H, Major Isomer), 1.73 (d, *J* = 7.2 Hz, 3H, Major Isomer), 1.69-1.38 (m, 9H), 1.14-1.04 ppm (m, 1H).

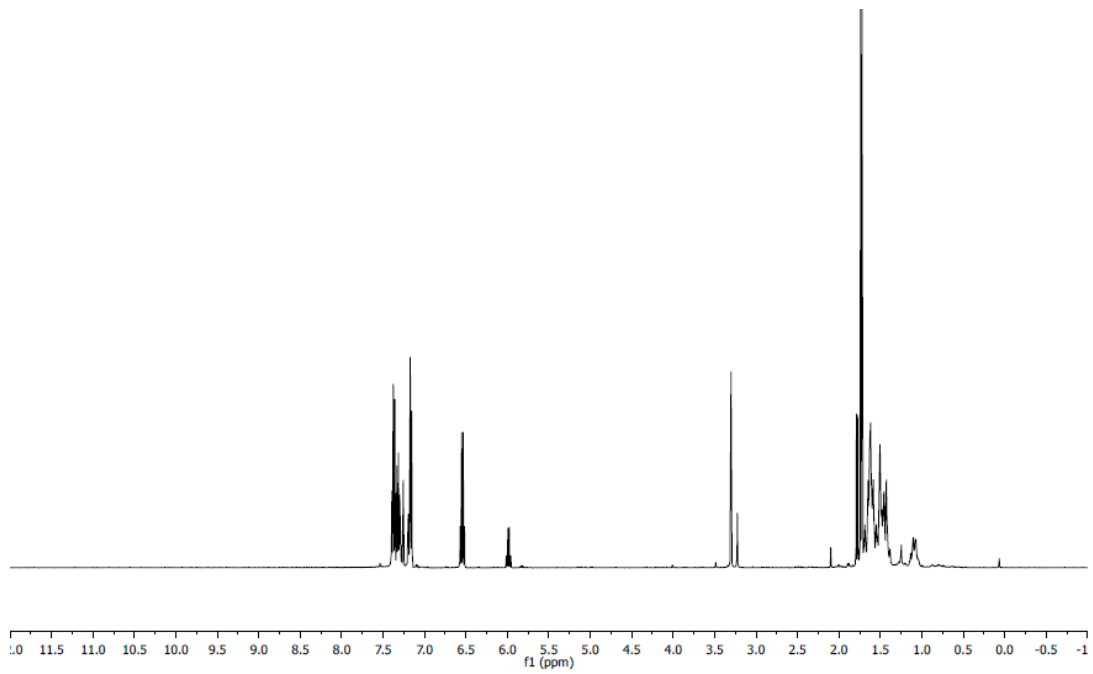
Characteristic ¹H NMR of Minor Isomer: 5.99 (q, *J* = 7.2 Hz, 0.27H), 3.22 (s, 0.27H), 1.78 ppm (d, *J* = 7.2 Hz, 0.81H)

¹³C NMR of Mixture of Isomers: (100 MHz, CDCl₃): δ 212.5, 208.1, 142.1, 141.8, 137.1, 135.3, 134.9, 129.4, 128.8, 128.4, 127.8, 127.8, 126.0, 79.6, 79.1, 54.3, 35.7, 35.2, 34.8, 25.1, 25.1, 21.5, 21.2, 21.0, 16.1, 15.0 ppm.

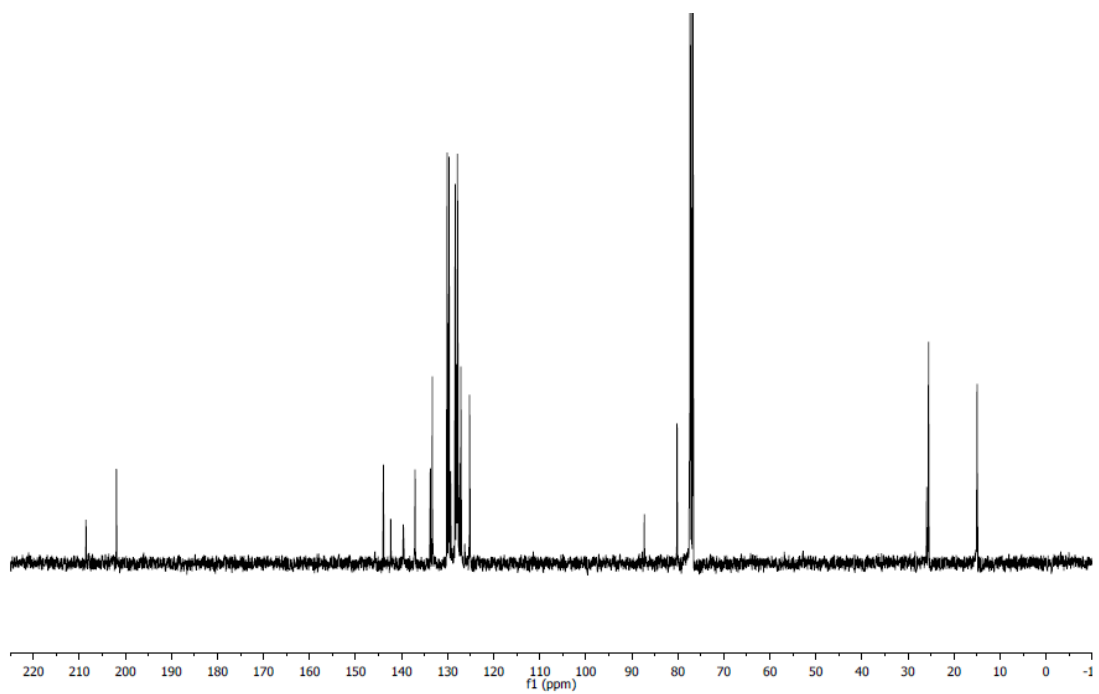
MS (ESI): *m/z* 267 [M+Na]⁺

FTIR (neat): 2933, 1677, 1442, 1233, 1127, 1098, 1036, 988, 909, 760, 730, 701, 666 cm⁻¹.

¹H NMR of **4.12c**



¹³C NMR of **4.12c**



(E)-2-hydroxy-2-(1-phenylprop-1-en-1-yl)cyclooctan-1-one (4.12d)

In modification of general procedure A using *cis*-**4.1d** and alkyne **4.11a**, upon stirring at 130 °C for 2 h, the reaction mixture was concentrated to afford the crude product (E:Z = 2:1, as determined by ¹H NMR spectroscopy). The reaction mixture was subjected to flash column chromatography (SiO₂: 10% EtOAc/hexanes) to furnish **4.12d** (71 mg, 0.27 mmol, 92% yield) as a colorless oil.

TLC (SiO₂): R_f = 0.33 (hexanes: EtOAc = 9:1).

¹H NMR of Major Isomer: (400 MHz, CDCl₃): δ 7.41-7.27 (m, 3H), 7.17-7.14 (m, 2H), 6.66 (q, *J* = 7.2 Hz, 1H), 3.50 (s, 1H), 1.88 (ddd, *J* = 16.0 Hz, 10.4 Hz, 2.0 Hz, 1H), 1.73 (d, *J* = 7.2 Hz, 3H), 1.79-1.39 (m, 11H) ppm.

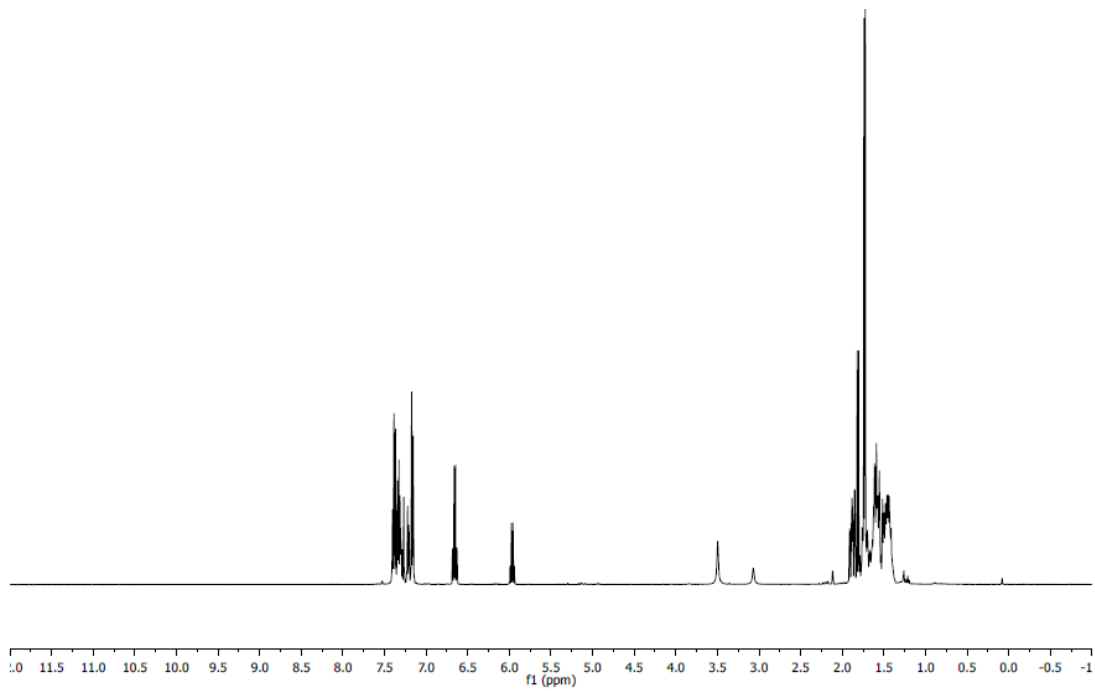
Characteristic ¹H NMR of Minor Isomer: 7.22-7.19 (m, 0.92H), 5.96 (q, *J* = 7.2 Hz, 0.46H), 3.07 (s, 0.46H), 1.80 ppm (d, *J* = 7.2 Hz, 1.38H)

¹³C NMR of Mixture of Isomers: (100 MHz, CDCl₃): δ 212.7, 207.8, 142.5, 141.5, 137.5, 136.3, 135.5, 129.5, 128.8, 128.8, 128.4, 127.8, 127.7, 126.2, 82.5, 81.5, 39.1, 38.6, 29.1, 28.6, 22.9, 22.3, 16.1, 15.2 ppm.

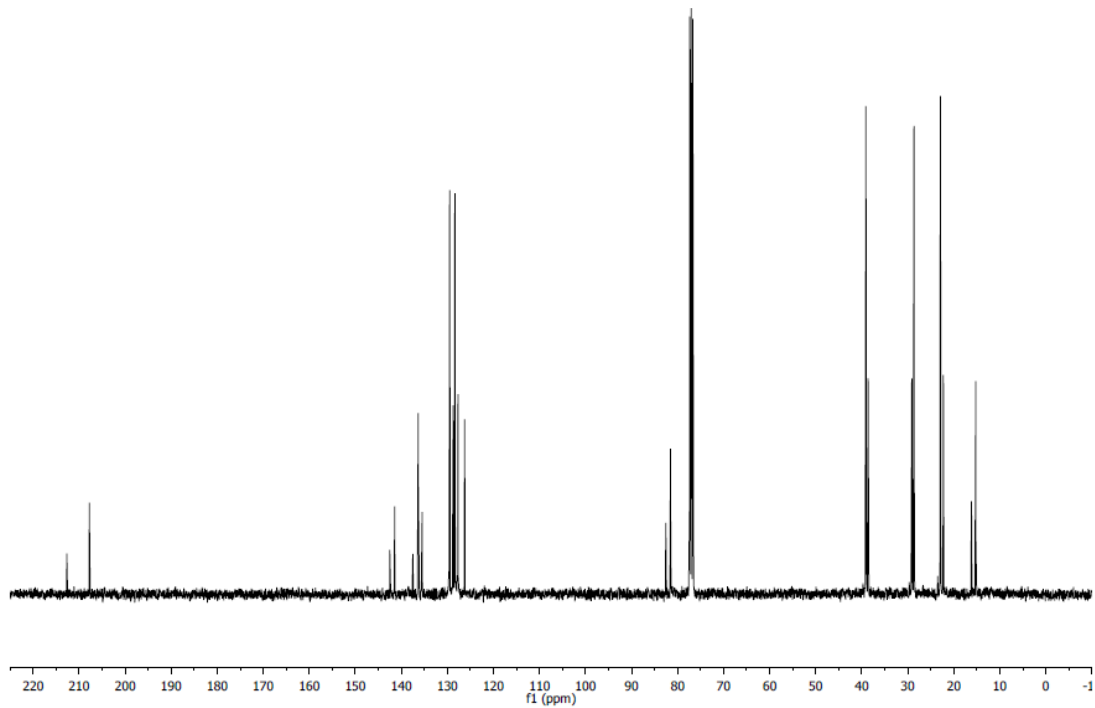
MS (ESI): *m/z* 247 [M+H]⁺.

FTIR (neat): 3473, 2922, 2856, 1678, 1458, 1442, 1239, 1137, 1051, 760, 701 cm⁻¹.

¹H NMR of **4.12d**



¹³C NMR of **4.12d**



(E)-3-hydroxy-3-methyl-4-phenylhex-4-en-2-one (4.12e)

In accordance with general procedure B using a mixture of *cis*- and *trans*-**4.1e** and alkyne **4.11a**, upon stirring at 130 °C for 20 h, the reaction mixture was concentrated to afford the crude product (E:Z = >20:1, as determined by ¹H NMR spectroscopy). The reaction mixture was subjected to flash column chromatography (SiO₂: 10% EtOAc/hexanes) to furnish **4.12e** (50 mg, 0.24 mmol, 80% yield) as a colorless oil.

TLC (SiO₂): R_f = 0.25 (hexanes: EtOAc = 9:1).

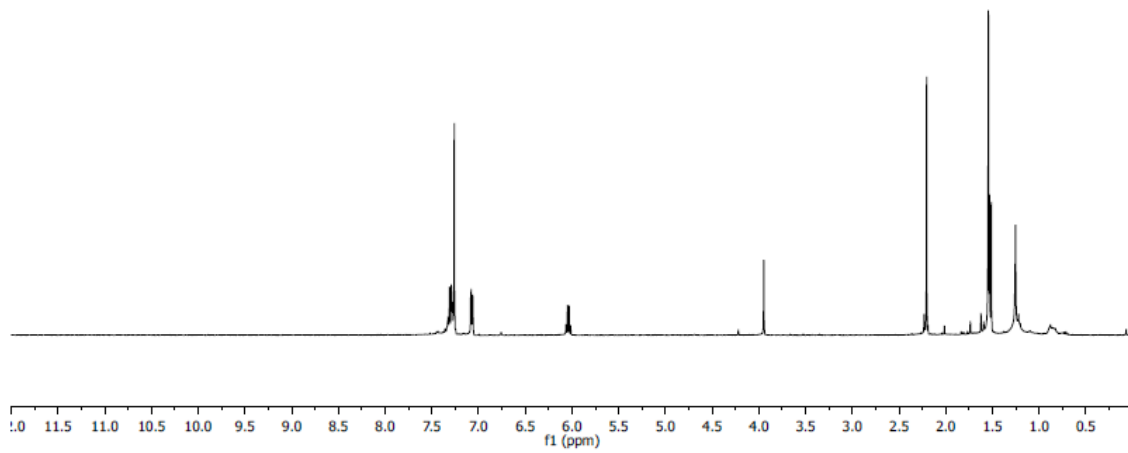
¹H NMR: (400 MHz, CDCl₃): δ 7.33-7.24 (m, 3H), 7.08-7.05 (m, 2H), 6.04 (q, *J* = 6.8 Hz, 1H), 3.95 (s, 1H), 2.20 (s, 3H), 1.54 (s, 3H), 1.51 ppm (d, *J* = 6.8 Hz, 3H).

¹³C NMR: (100 MHz, CDCl₃): δ 210.2, 142.5, 137.0, 129.5, 128.0, 127.2, 125.5, 81.3, 23.9, 23.3, 15.0 ppm.

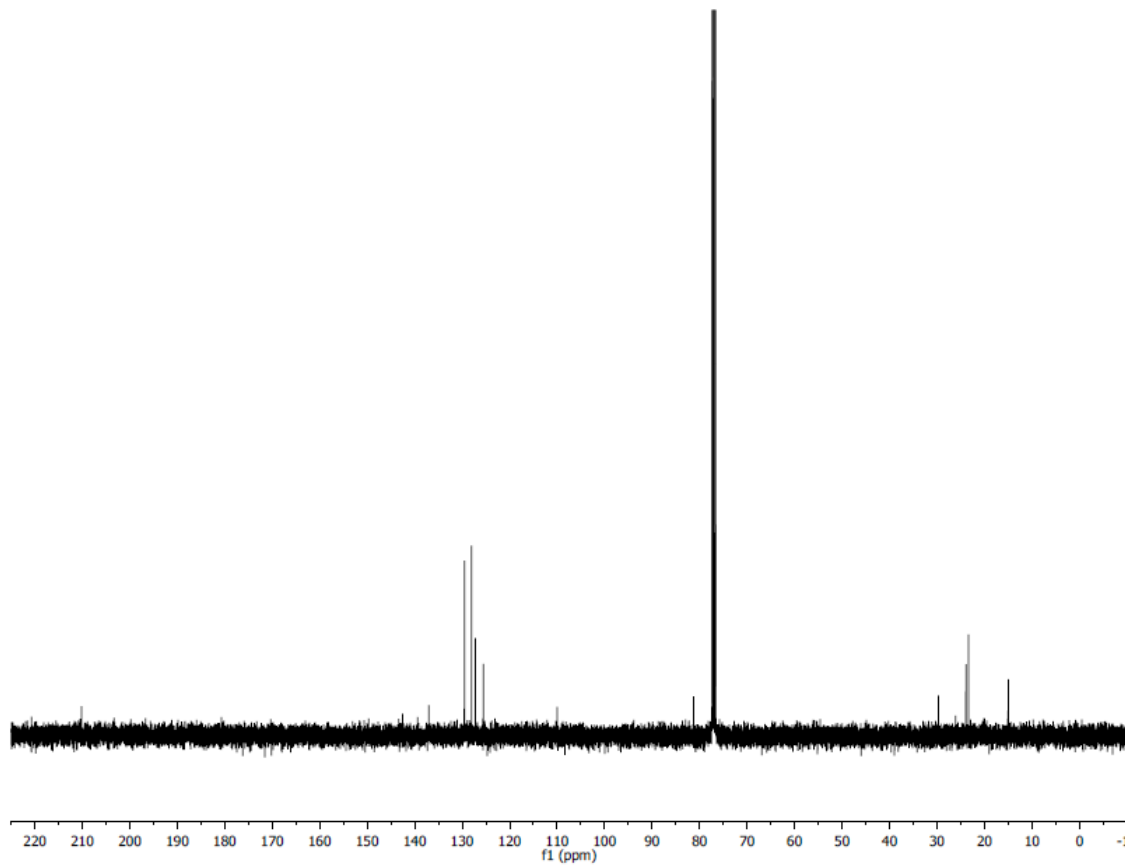
MS (ESI): *m/z* = 227 [M+Na]⁺

FTIR (neat): 3391, 1738, 1713, 1442, 1354, 1217, 1228, 1132, 76, 704, 667 cm⁻¹.

¹H NMR of **4.12e**



¹³C NMR of **4.12e**



(*E*)-2-hydroxy-1,2,3-triphenylpent-3-en-1-one (**4.12f**)

In accordance with general procedure B using a mixture of *cis*- and *trans*-**4.1f** and alkyne **4.11a**, upon stirring at 130 °C for 20 h, the reaction mixture was concentrated to afford the crude product (E:Z = >20:1, as determined by ¹H NMR spectroscopy). The reaction mixture was subjected to flash column chromatography (SiO₂: 10% EtOAc/hexanes) to furnish **4.12f** (69 mg, 0.21 mmol, 70% yield) as a colorless oil.

TLC (SiO₂): R_f = 0.39 (hexanes: EtOAc = 9:1).

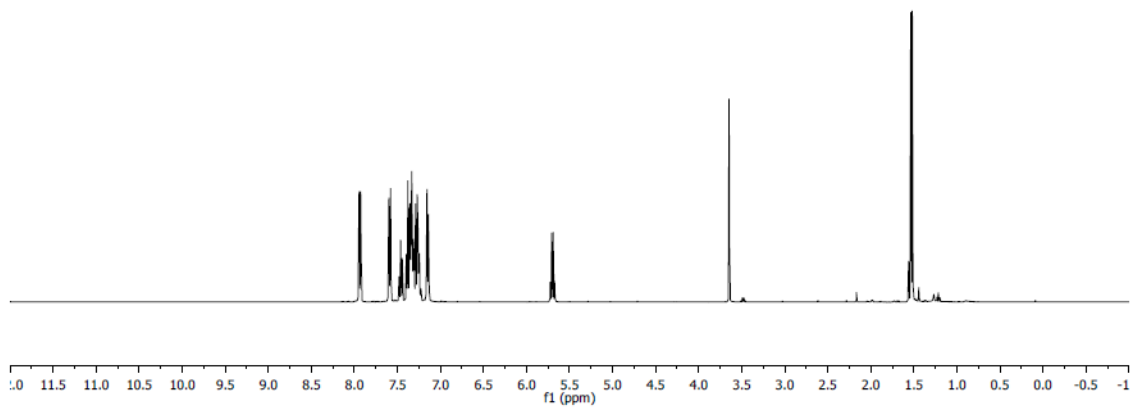
¹H NMR: (400 MHz, CDCl₃): δ 7.95-7.92 (m, 2H), 7.60-7.58 (m, 2H), 7.4807.44 (m, 1H), 7.40-7.24 (m, 8H), 7.16-7.14 (m, 2H), 5.70 (q, *J* = 6.8 Hz, 1H), 3.65 (s, 1H), 1.52 ppm (d, *J* = 6.8 Hz, 3H).

¹³C NMR: (100 MHz, CDCl₃): δ 201.0, 143.1, 140.9, 136.7, 135.6, 132.6, 130.7, 130.4, 128.9, 128.3, 128.1, 127.9, 127.9, 127.8, 127.5, 86.7, 15.1 ppm.

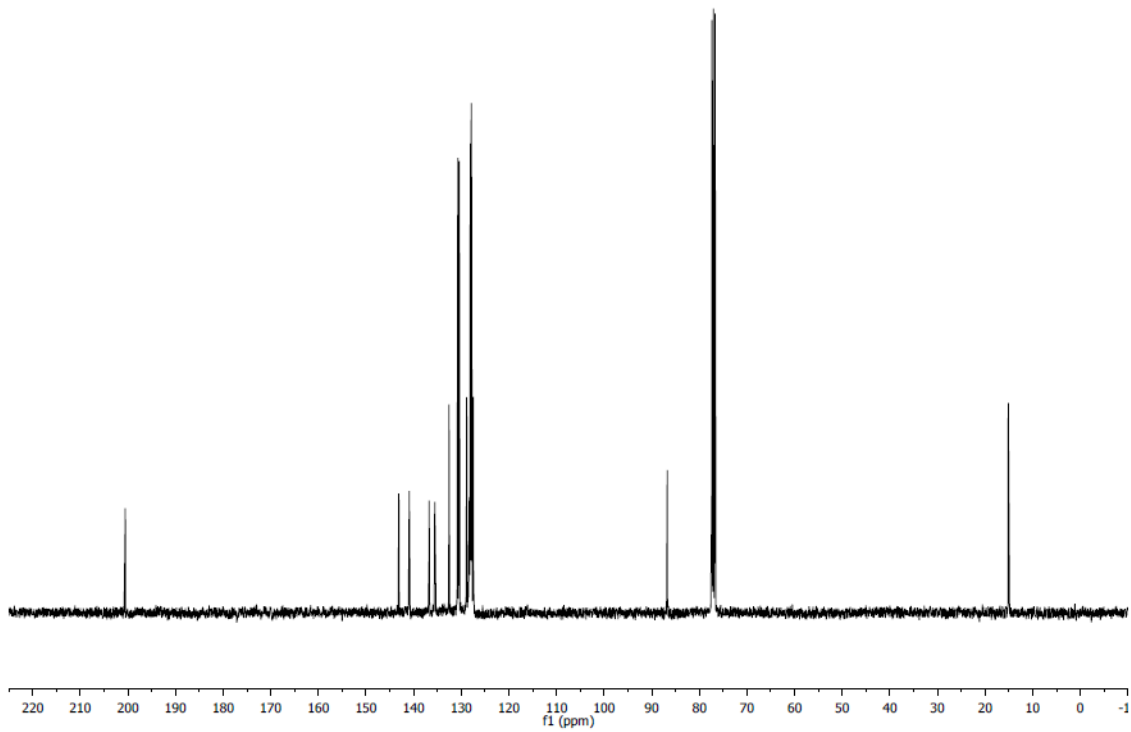
MS (ESI): *m/z* 351 [M+Na]⁺.

FTIR (neat): 3026, 2361, 1738, 1365, 1229, 1217, 701 cm⁻¹.

¹H NMR of **4.12f**



¹³C NMR of **4.12f**



(E)-2-hydroxy-2-methyl-1,3-diphenylpent-3-en-1-one (4.12g)

In accordance with general procedure B using *trans*-**4.1g 1f** and alkyne **4.11a**, upon stirring at 130 °C for 20 h, the reaction mixture was concentrated to afford the crude product ((*E*):(*Z*) = >20:1, rr = 2:1 as determined by ¹H NMR spectroscopy). The reaction mixture was subjected to flash column chromatography (SiO₂: 10% EtOAc/hexanes) to furnish **4.12g** (59 mg, 0.22 mmol, 74% yield) as a colorless oil.

TLC (SiO₂): R_f = 0.45 (hexanes:EtOAc = 9:1).

¹H NMR of Major Isomer: (400 MHz, CDCl₃): δ 8.12 (d, *J* = 8.0 Hz, 1H), 7.61-7.06, m, 10H), 6.16 (q, *J* = 6.8 Hz, 1H), 4.58 (s, 1H), 1.70 (s, 3H), 1.57 ppm (d, *J* = 6.8 Hz, 3H).

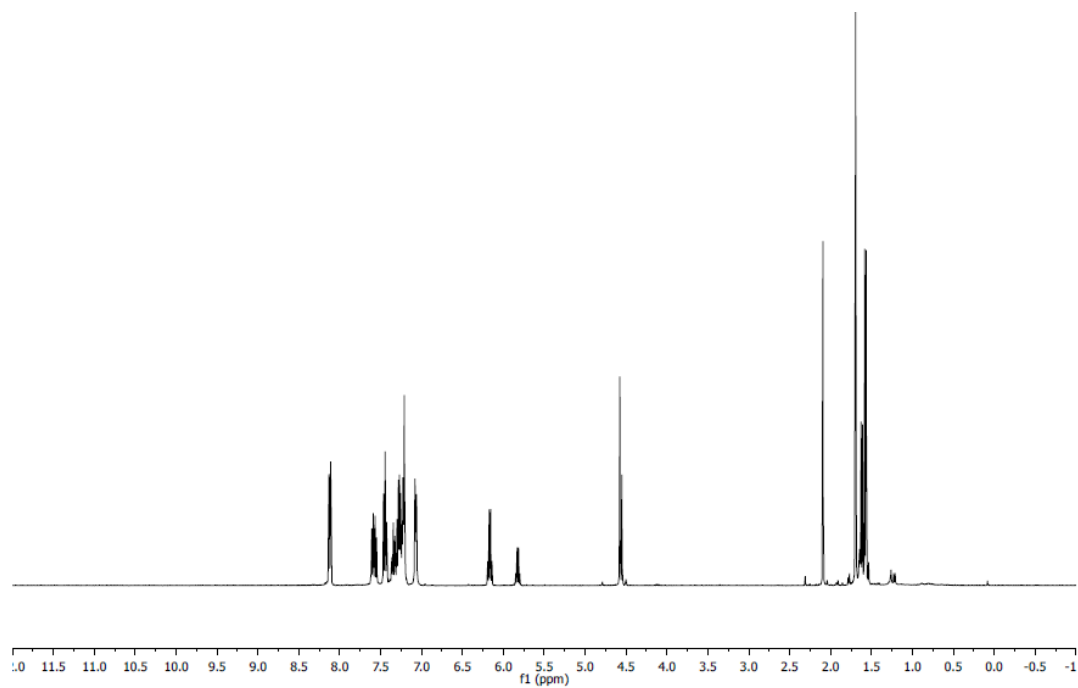
Characteristic ¹H NMR of Minor Isomer: δ 5.84 (q, *J* = 6.8 Hz, 1H), 4.55 (s, 1H), 2.09 (s, 3H), 1.62 ppm (d, *J* = 6.8 Hz, 3H).

¹³C NMR of Mixture of Major and Minor Isomers: (100 MHz, CDCl₃): δ 208.5, 201.9, 143.9, 142.4, 139.6, 137.2, 137.1, 133.7, 133.3, 130.1, 129.9, 129.7, 129.3, 128.3, 128.1, 128.0, 128.0, 127.9, 127.8, 127.3, 127.1, 125.2, 87.3, 80.2, 25.9, 25.5, 15.2, 15.0 ppm.

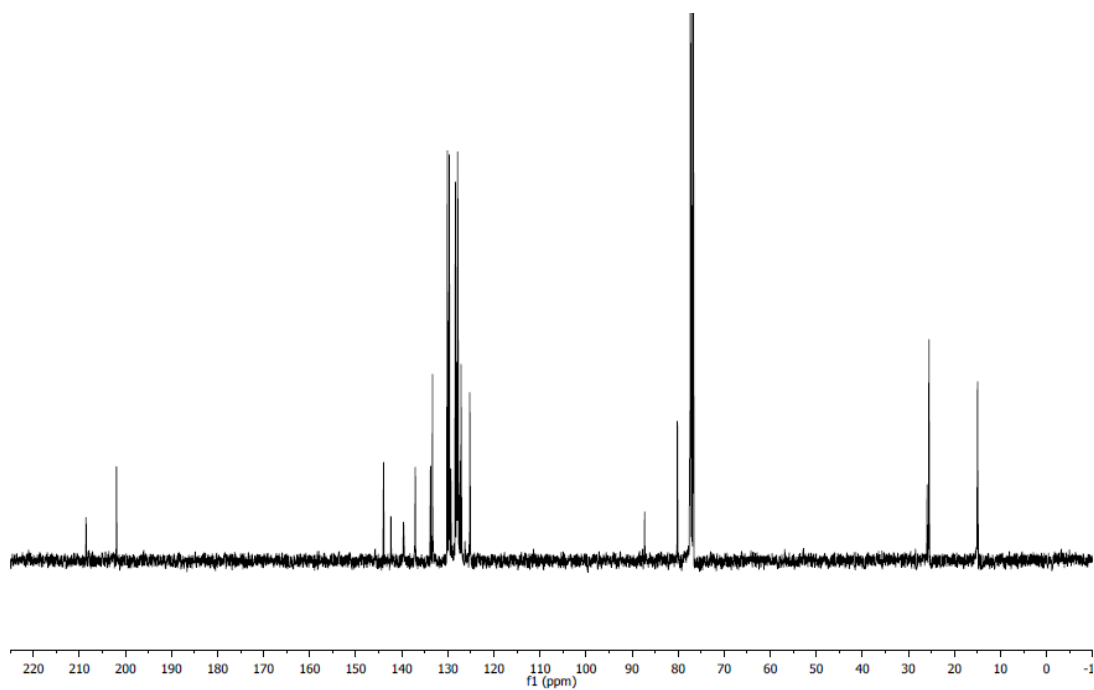
HRMS (ESI): *m/z* = 300 [M+Na]⁺.

FTIR (neat): 3441, 1707, 1672, 1597, 1446, 1354, 1245, 1153, 1128, 964, 943, 767, 751, 704, 669 cm⁻¹.

¹H NMR of 4.12g



¹³C NMR of 4.12g



(*E*)-4-hydroxy-2,2,4-trimethyl-5-phenylhept-5-en-3-one (**4.12h**)

In accordance with general procedure B using *trans*-**4.1h** and alkyne **4.11a**, upon stirring at 130 °C for 20 h, the reaction mixture was concentrated to afford the crude product ((*E*):(*Z*) = >20:1, *rr* = >20:1 as determined by ¹H NMR spectroscopy). The reaction mixture was subjected to flash column chromatography (SiO₂: 10% EtOAc/hexanes) to furnish **4.12h** (56 mg, 0.30 mmol, 99% yield) as a colorless oil.

TLC (SiO₂): R_f = 0.34 (hexanes: EtOAc = 9:1).

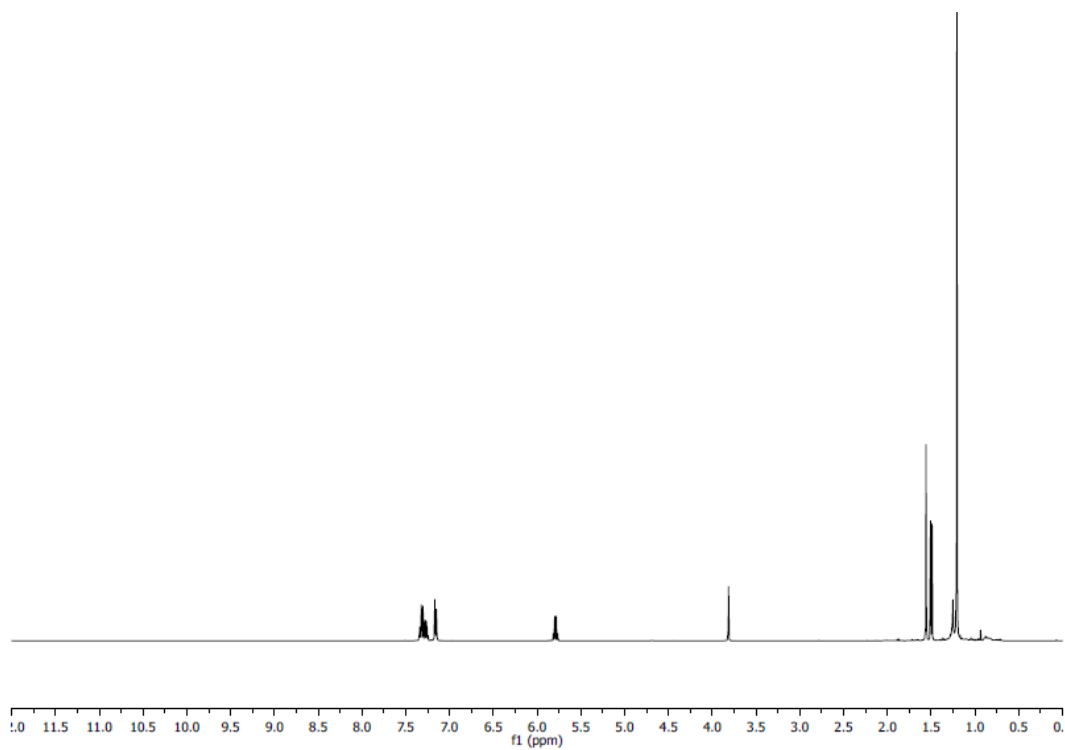
¹H NMR: (400 MHz, CDCl₃): δ 7.34-7.25 (m, 3H), 7.17-7.15 (m, 2H), 5.79 (q, *J* = 7.0 Hz, 1H), 3.81 (s, 1H), 1.56 (s, 3H), 1.50 (d, *J* = 7.0 Hz, 3H), 1.21 ppm (s, 9H).

¹³C NMR: (100 MHz, CDCl₃): δ 216.9, 142.9, 137.0, 129.9, 128.0, 127.2, 124.6, 82.4, 44.3, 28.4, 25.3, 15.0 ppm.

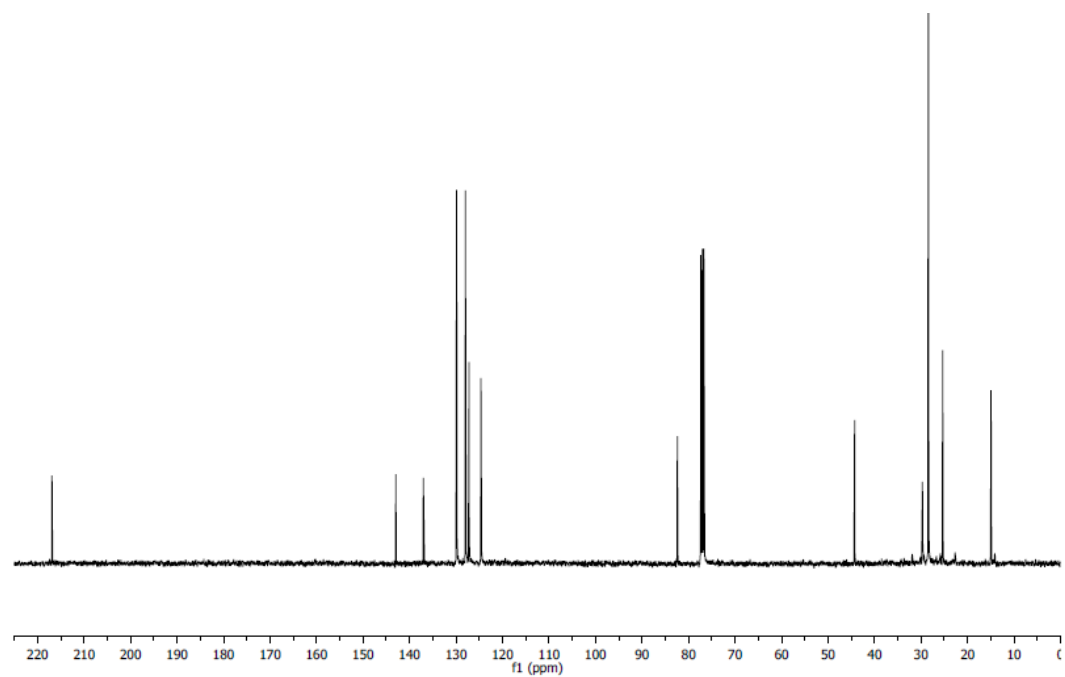
MS (CI): *m/z* 247 [M+H]⁺

FTIR (neat): 2970, 2360, 1739, 1442, 1365, 1229, 1217, 701 cm⁻¹.

¹H NMR of 4.12h



¹³C NMR of 4.12h



(*E*)-2-hydroxy-2-(1-phenylprop-1-en-1-yl)-2,3-dihydro-1H-inden-1-one (**4.12i**)

In accordance with general procedure A using *trans*-**4.1i** and alkyne **4.11a**, upon stirring at 130 °C for 4 h, the reaction mixture was concentrated to afford the crude product (*E*:*Z* = >20:1, *rr* = >20:1 as determined by ¹H NMR spectroscopy). The reaction mixture was subjected to flash column chromatography (SiO₂: 10% EtOAc/hexanes) to furnish **4.12i** (81 mg, 0.30 mmol, 98% yield) as a colorless oil.

TLC (SiO₂): R_f = 0.20 (hexanes: EtOAc = 9:1).

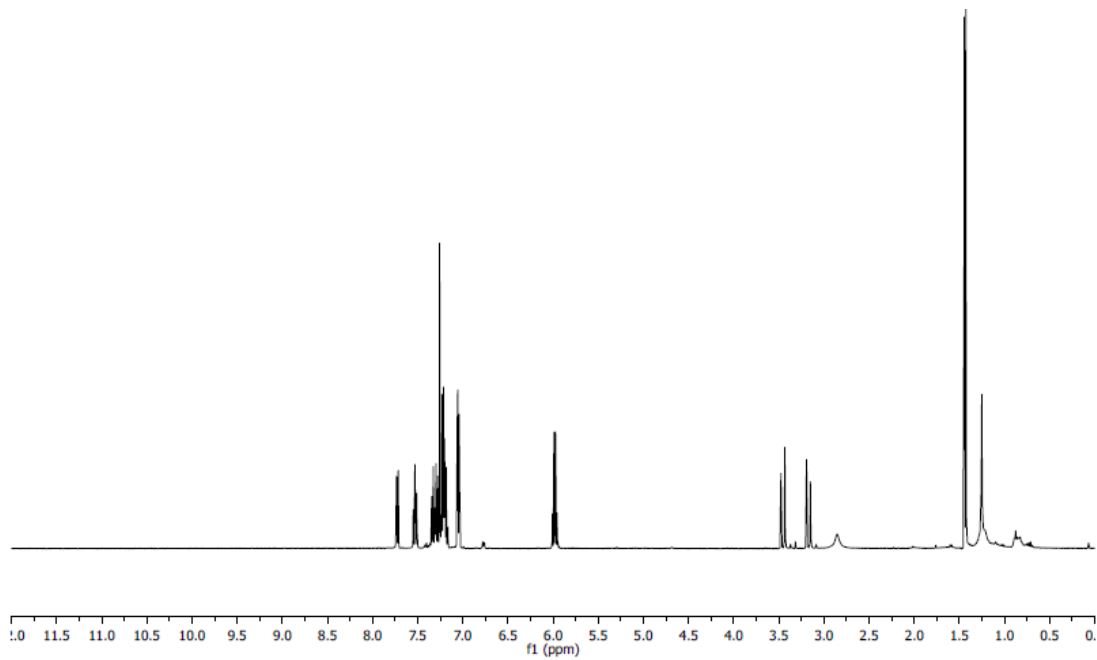
¹H NMR: (400 MHz, CDCl₃): δ 7.74 (d, *J* = 8.0 Hz, 1H), 7.53 (t, *J* = 7.6 Hz, 1H), 7.35-7.17 (m, 5H), 7.08-7.06 (m, 2H), 6.02 (q, *J* = 6.8 Hz, 1H), 3.47 (d, *J* = 17.2 Hz, 1H), 3.19 (d, *J* = 17.2 Hz, 1H), 3.14 (s, 1H), 1.45 ppm (d, *J* = 6.8 Hz, 3H).

¹³C NMR: (100 MHz, CDCl₃): δ 206.6, 151.6, 141.7, 136.9, 135.6, 134.7, 129.8, 128.0, 127.7, 127.1, 126.2, 124.6, 124.1, 82.3, 41.0, 14.7 ppm.

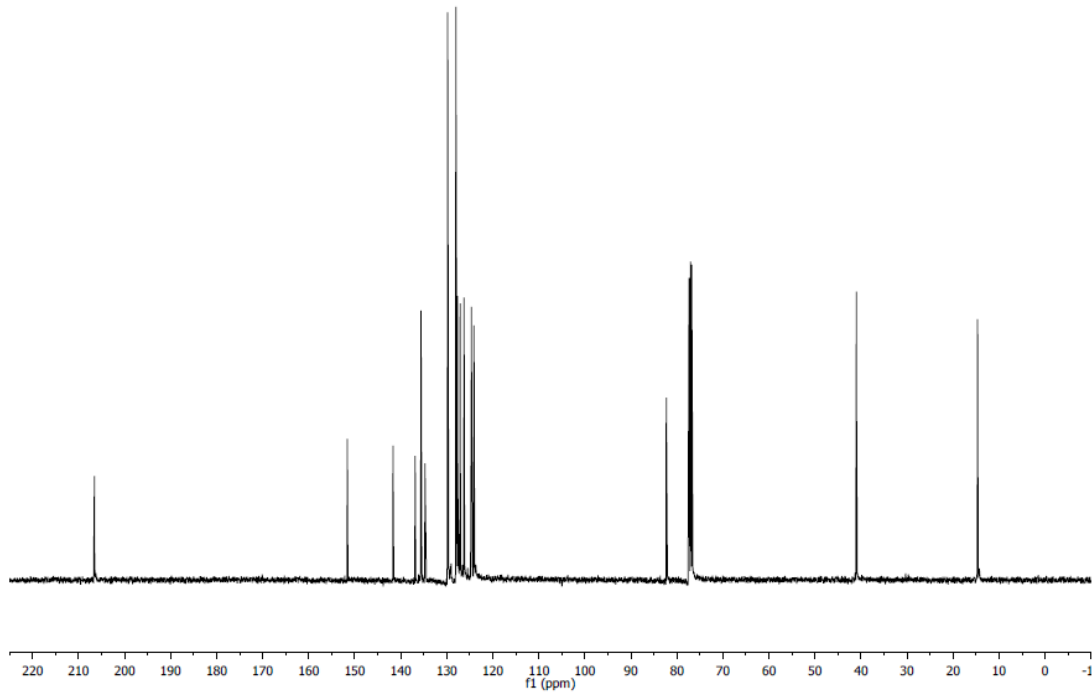
MS (CI): *m/z* 264 [M+Na]⁺.

FTIR (neat): 3454, 1737, 1716, 1608, 1365, 1229, 1209, 926, 738, 702 cm⁻¹.

¹H NMR of **4.12i**



¹³C NMR of **4.12i**



(*E*)-2-hydroxy-2-(1-phenylprop-1-en-1-yl)-3,4-dihydronaphthalen-1(2H)-one (**4.12j**)

In accordance with general procedure A using a mixture of *cis*- and *trans*-**4.1j** and alkyne **4.11a**, upon stirring at 130 °C for 4 h, the reaction mixture was concentrated to afford the crude product (*E*:*Z* = >20:1, *rr* = >20:1 as determined by ¹H NMR spectroscopy). The reaction mixture was subjected to flash column chromatography (SiO₂: 10% EtOAc/hexanes) to furnish **4.12j** (74 mg, 0.27 mmol, 89% yield) as a colorless oil.

TLC (SiO₂): R_f = 0.47 (hexanes: EtOAc = 9:1).

¹H NMR: (400 MHz, CDCl₃): δ 8.09 (dd, *J* = 7.6, 1.2 Hz, 1H), 7.51 (td, *J* = 7.6, 1.6 Hz, 1H), 7.37-7.25 (m, 6H), 7.22 (d, *J* = 7.6 Hz, 1H), 5.46 (q, *J* = 6.8 Hz, 1H), 4.15 (s, 1H), 3.02 (ddd, *J* = 17.2, 13.0, 4.4 Hz, 1H), 2.78 (ddd, *J* = 17.2, 4.4, 2.4 Hz, 1H), 2.21 (ddd, *J* = 13.2, 4.4, 2.4 Hz, 1H), 2.06 (td, *J* = 13.2, 4.8 Hz, 1H), 1.41 ppm (d, *J* = 6.8 Hz, 3H).

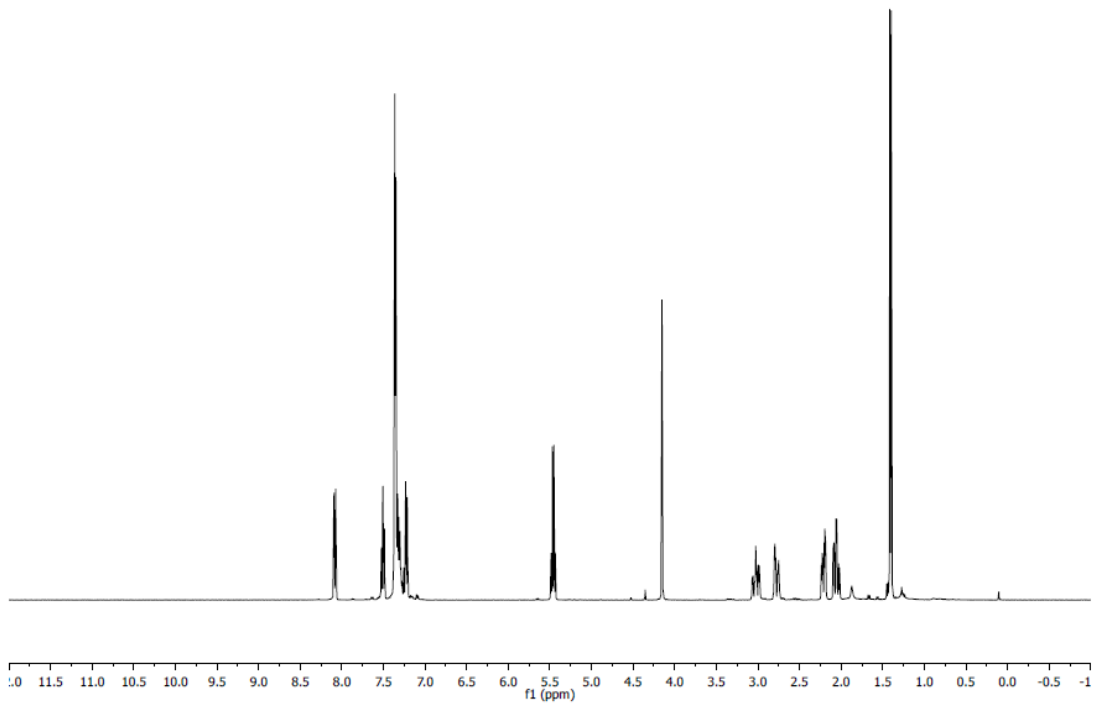
¹³C NMR: (100 MHz, CDCl₃): δ 201.3, 144.1, 141.7, 136.9, 134.0, 131.4, 130.0, 128.9, 127.9, 127.5, 127.3, 127.1, 126.8, 79.3, 33.9, 26.3, 15.2 ppm.

MS (ESI): *m/z* = 301 [M+Na]⁺

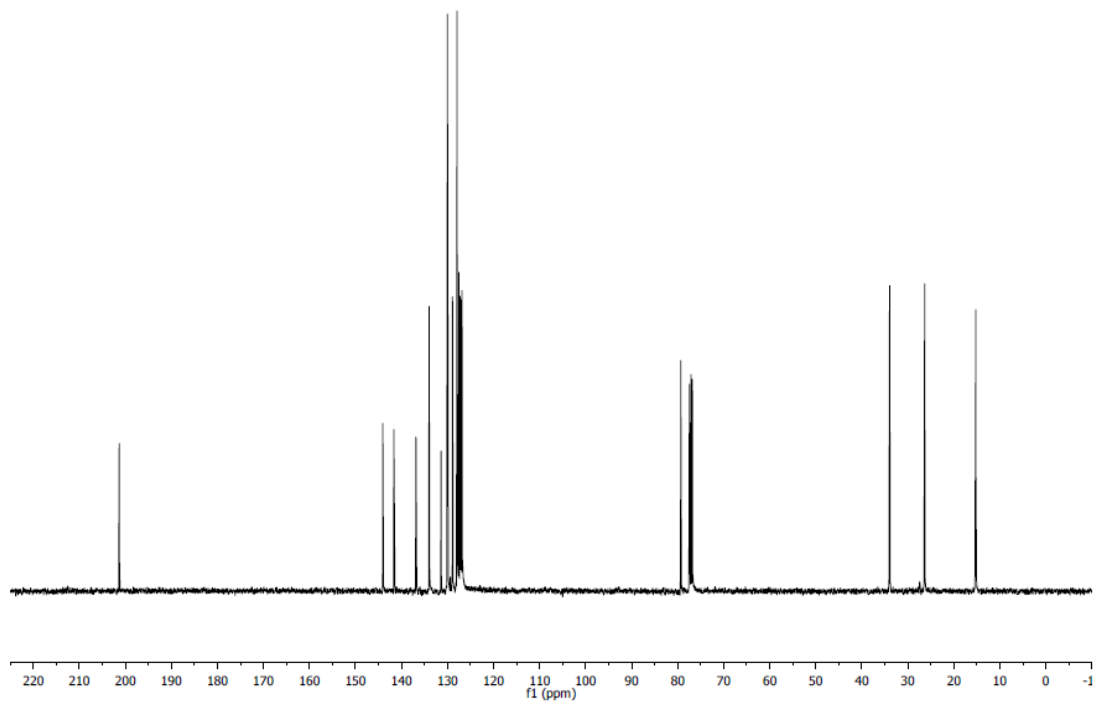
FTIR (neat): 3481, 2931, 1681, 1601, 1288, 1229, 1076, 963, 995, 936, 772, 734, 704 cm⁻¹.

1.

¹H NMR of 4.12j



¹³C NMR of 4.12j



(*E*)-2-hydroxy-2-(1-phenylprop-1-en-1-yl)acenaphthylen-1(2H)-one (**4.12k**)

In accordance with general procedure A using a mixture of *cis*- and *trans*-**4.1k** and alkyne **4.11a**, upon stirring at 130 °C for 4 h, the reaction mixture was concentrated to afford the crude product (*E*:*Z* = >20:1, *rr* = >20:1 as determined by ¹H NMR spectroscopy). The reaction mixture was subjected to flash column chromatography (SiO₂: 10% EtOAc/hexanes) to furnish **4.12k** (84 mg, 0.28 mmol, 93% yield) as a colorless solid.

TLC (SiO₂): R_f = 0.17 (hexanes: EtOAc = 9:1).

¹H NMR: (400 MHz, CDCl₃): δ 8.00 (d, *J* = 8.0 Hz, 1H), 7.82 (t, *J* = 8.4 Hz, 2H), 7.67-7.59 (m, 2H), 7.54 (d, *J* = 6.8 Hz, 1H), 7.05-7.02 (m, 3H), 6.81-6.77 (m, 2H), 6.21 (q, *J* = 6.8 Hz, 1H), 3.24 (s, 1H, broad), 1.47 ppm (d, *J* = 6.8 Hz, 3H)

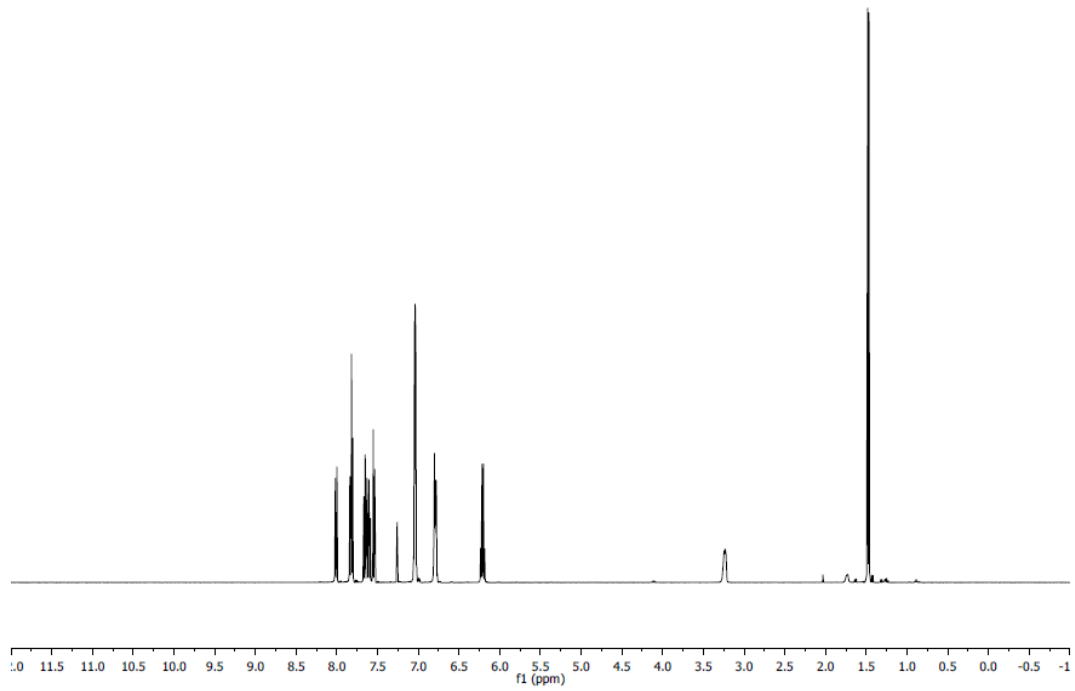
¹³C NMR: (100 MHz, CDCl₃): δ 204.5, 142.0, 141.0, 139.2, 126.2, 131.71, 131.2, 130.4, 129.9, 128.6, 128.1, 127.7, 127.0, 125.3, 124.2, 122.0, 121.3, 83.1, 14.4 ppm.

MP: 148-150 °C.

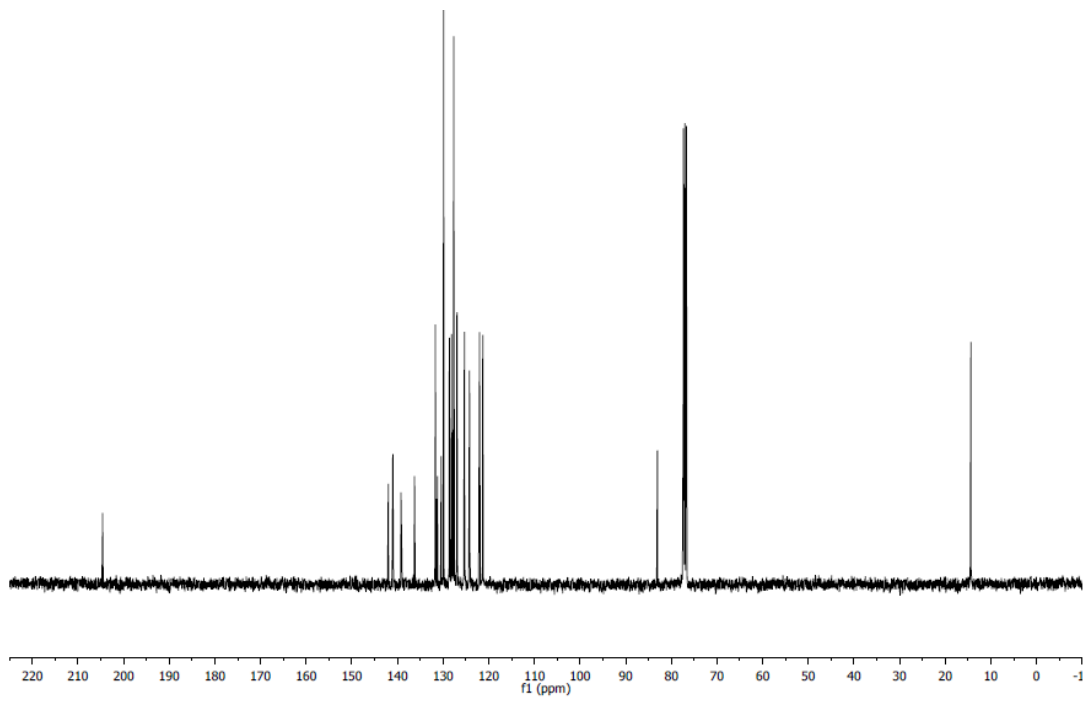
MS (ESI): *m/z* = 323.1 [M+Na]⁺.

FTIR (neat): 3396, 1717, 1604, 1492, 1435, 1367, 1348, 1260, 1217, 1182, 1910, 996, 908, 893, 835, 782, 764 730, 701, 668 cm⁻¹.

¹H NMR of 4.12k



¹³C NMR of 4.12k



(E)-10-hydroxy-10-(1-phenylprop-1-en-1-yl)phenanthren-9(10H)-one (4.12m)

In accordance with general procedure A using a mixture of *cis*- and *trans*- **4.1m** and alkyne **4.11a**, upon stirring at 130 °C for 4 h, the reaction mixture was concentrated to afford the crude product (*E:Z* = >20:1 as determined by ¹H NMR spectroscopy). The reaction mixture was subjected to flash column chromatography (SiO₂: 10% EtOAc/hexanes) to furnish **4.12m** (98 mg, 0.30 mmol, 99% yield) as a colorless solid.

TLC (SiO₂): R_f = 0.40 (hexanes: EtOAc = 9:1).

¹H NMR: (400 MHz, CDCl₃): δ 7.94-7.92 (m, 2H), 7.90-7.87 (m, 1H), 7.84-7.82 (m, 1H), 7.68 (td, *J* = 5.0, 1.2 Hz, 1H), 7.49-7.46 (m, 2H), 7.42 (td, *J* = 7.6, 1.2, Hz, 1H), 7.27-7.21 (m, 2H), 7.17-7.13 (m, 1H), 7.01 (d, *J* = 7.2 Hz, 2H), 6.29 (s, 1H), 4.52 (s, 1H), 1.77 ppm (d, *J* = 1.2 Hz, 3H).

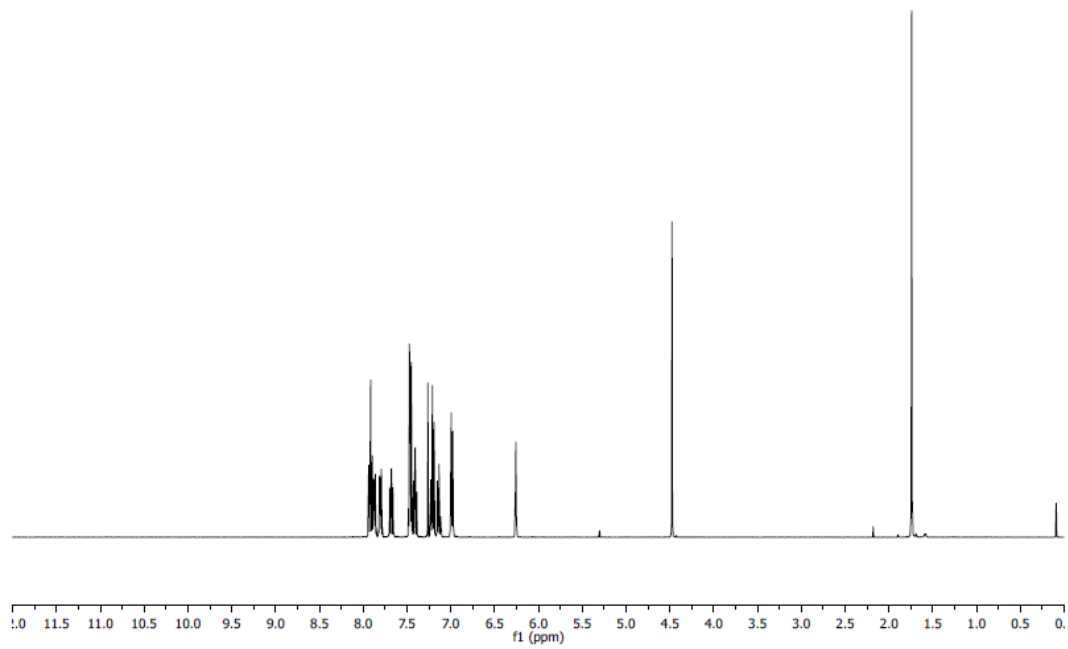
¹³C NMR: (100 MHz, C₆D₆): δ 201.5, 139.4, 139.1, 137.7., 137.2, 134.4, 130.8, 129.1, 128.9, 128.2, 128.2, 128.2, 128.1, 127.8, 127.5, 127.1, 126.4, 123.5, 122.8, 82.6, 13.0 ppm.

MP: 149 – 150 °C.

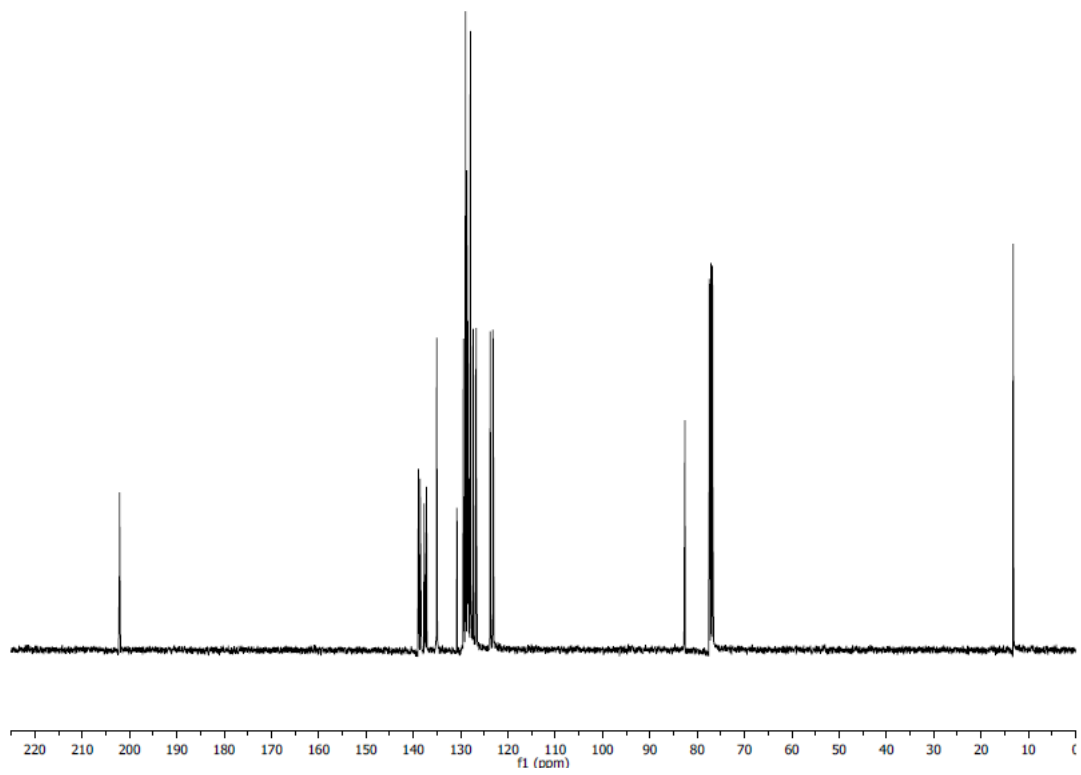
MS (CI): *m/z* 327 [M+H]⁺.

FTIR (neat): 3482, 1686, 1599, 1450, 1268, 1000, 777, 761, 732, 708, 697, 666 cm⁻¹.

¹H NMR of 4.12m



¹³C NMR of 4.12m



(E)-2-hydroxy-2-(1-phenylbut-1-en-1-yl)cyclohexan-1-one (**4.13b**)

In accordance with general procedure A using *trans*- **4.1a** and alkyne **4.11b**, upon stirring at 130 °C for 4 h, the reaction mixture was concentrated to afford the crude product (*E:Z* = >20:1 as determined by ¹H NMR spectroscopy). The reaction mixture was subjected to flash column chromatography (SiO₂: 10% EtOAc/hexanes) to furnish **4.13b** (67 mg, 0.28 mmol, 92% yield) as a colorless oil.

TLC (SiO₂): R_f = 0.36 (hexanes: EtOAc = 9:1).

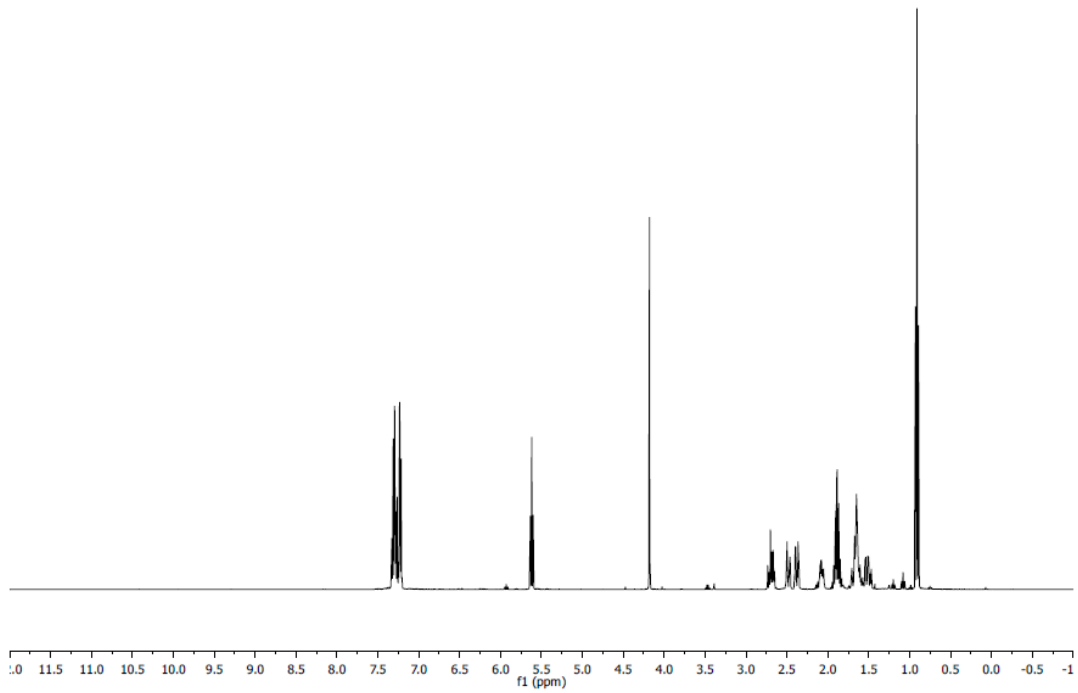
¹H NMR: (400 MHz, CDCl₃): δ 7.27 (m, 5H), 5.62 (t, *J* = 7.4 Hz, 1H), 4.18 (s, 1H), 2.73-2.65 (m, 1H), 2.51-2.46 (m, 1H), 2.38 (dq, *J* = 13.2, 2.8 Hz, 1H), 2.14-2.05 (m, 1H), 1.95-1.83 (m, 2H), 1.71-1.57 (m, 3H), 1.55-1.47 (m, 1H), 0.91 ppm (t, *J* = 7.4 Hz, 3H).

¹³C NMR: (100 MHz, CDCl₃): δ 213.3, 140.7, 137.1, 134.1, 129.5, 128.0, 127.2, 81.8, 39.5, 38.7, 28.2, 22.7, 22.6, 13.9 ppm.

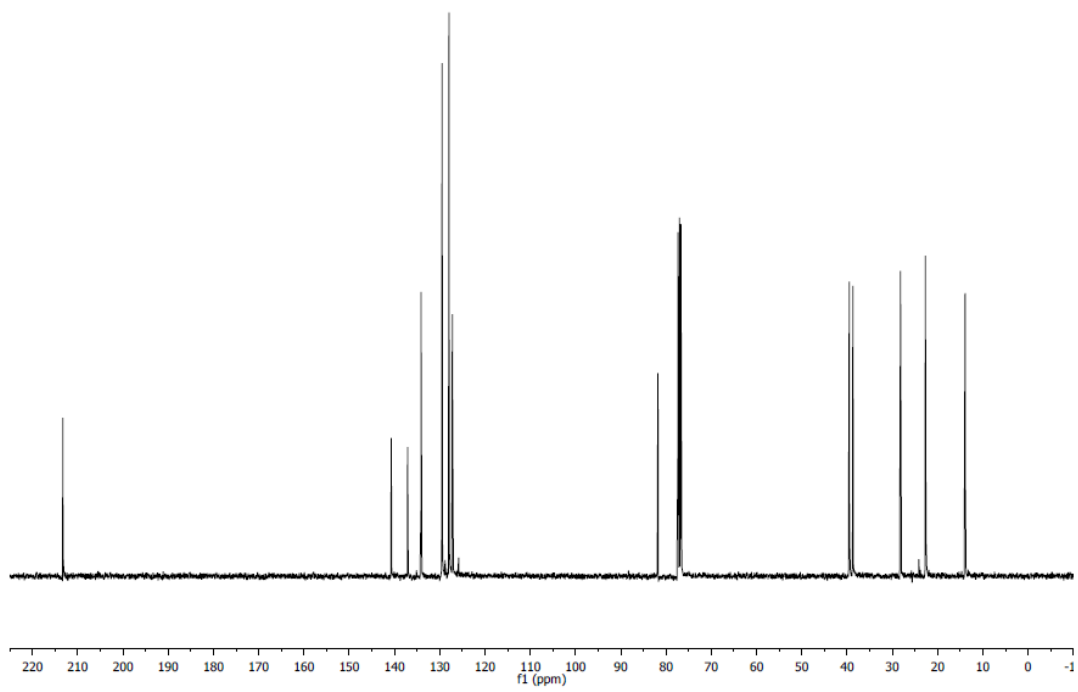
MS (ESI): *m/z* 267 [M+Na]⁺.

FTIR (neat): 2941, 2868, 1708, 1446, 1252, 1088, 1067, 1052, 760, 705 cm⁻¹.

¹H NMR of **4.13b**



¹³C NMR of **4.13b**



(E)-2-(1,2-diphenylvinyl)-2-hydroxycyclohexan-1-one (4.13c)

In accordance with general procedure A using *trans*- **4.1a** and alkyne **4.11c**, upon stirring at 130 °C for 4 h, the reaction mixture was concentrated to afford the crude product (*E:Z* = >20:1 as determined by ¹H NMR spectroscopy). The reaction mixture was subjected to flash column chromatography (SiO₂: 10% EtOAc/hexanes) to furnish **4.13c** (105 mg, 0.29 mmol, 98% yield) as a colorless solid.

TLC (SiO₂): R_f = 0.30 (hexanes: EtOAc = 9:1).

¹H NMR: (400 MHz, CDCl₃): δ 7.33-7.23 (m, 5H), 7.10-7.08 (m, 3H), 6.88-6.86 (m, 2H), 6.56 (s, 1H), 4.36 (s, 1H), 2.79 (td, *J* = 13.2, 6.8 Hz, 1H), 2.56 (t, *J* = 13.2 Hz, 2H), 2.14-2.07 (s, 1H, broad), 1.84-1.58 ppm (m, 4H).

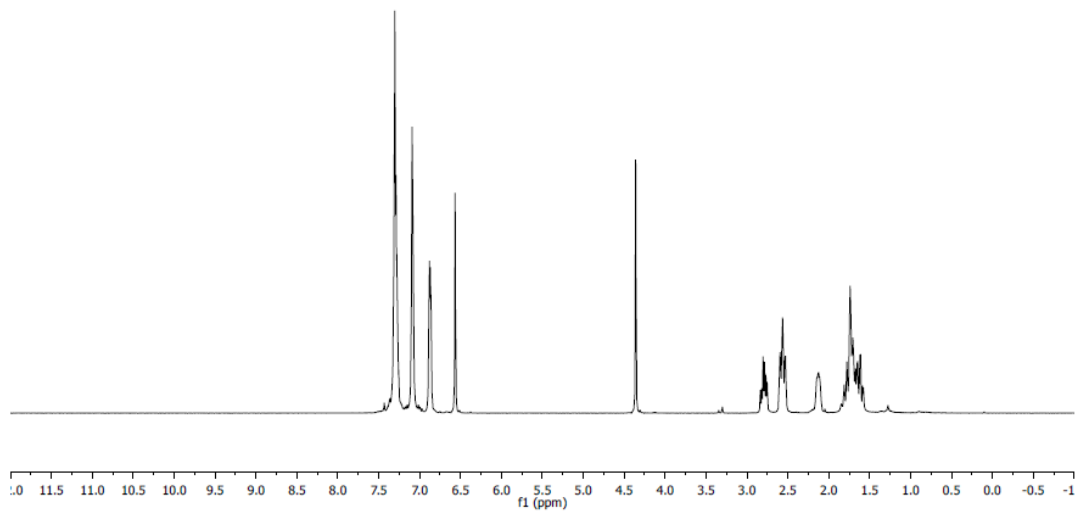
¹³C NMR: (100 MHz, CDCl₃): δ 213.0, 141.8, 137.2, 135.9, 130.5, 129.7, 129.6, 128.6, 127.9, 127.7, 127.3, 82.4, 39.7, 28.7, 28.3, 22.7 ppm.

MP: 96 – 98 °C.

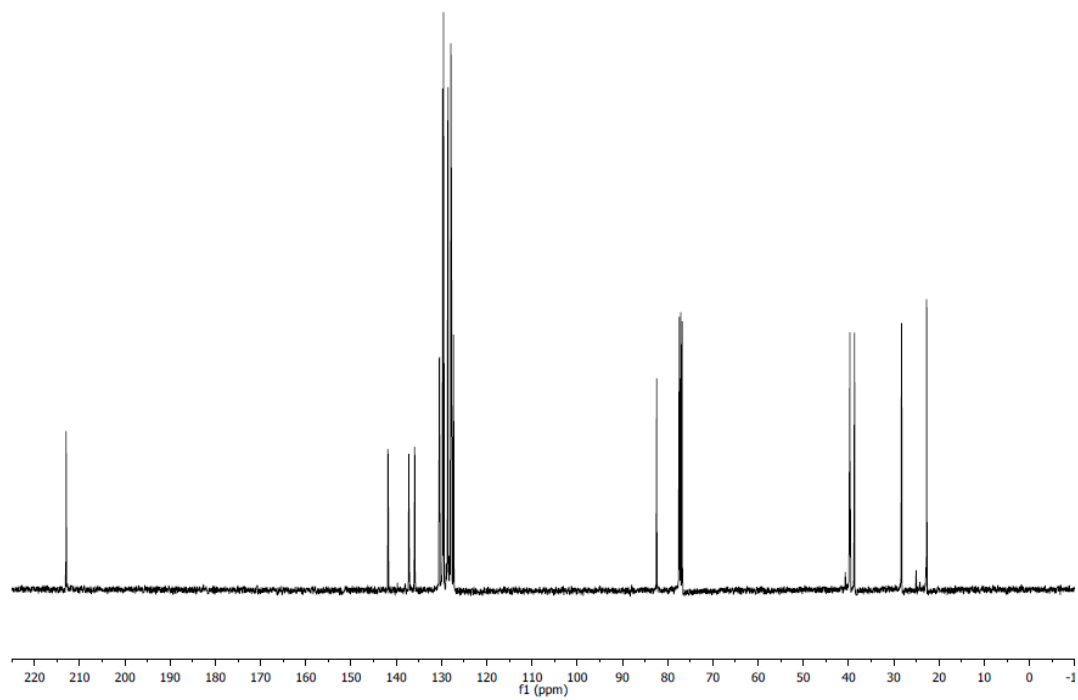
MS (ESI): *m/z* 315 [M+Na]⁺.

FTIR (neat): 3462, 1698, 1408, 1365, 1352, 1228, 1217, 1191, 1975, 1050, 962, 931, 915, 902, 702, 694 cm⁻¹.

¹H NMR of **4.13c**



¹³C NMR of **4.13c**



tert-Butyl-(*E*)-(4-(1-hydroxy-2-oxocyclohexyl)-4-phenylbut-3-en-1-yl)carbamate (**4.13d**)

In accordance with general procedure A using *trans*- **4.1a** and alkyne **4.11d**, upon stirring at 130 °C for 4 h, the reaction mixture was concentrated to afford the crude product (*E*:*Z* = 16:1 as determined by ¹H NMR spectroscopy). The reaction mixture was subjected to flash column chromatography (SiO₂: 10% EtOAc/hexanes) to furnish **4.13d** (105 mg, 0.29 mmol, 98% yield) as a colorless solid.

TLC (SiO₂): R_f = 0.24 (hexanes: EtOAc = 4:1).

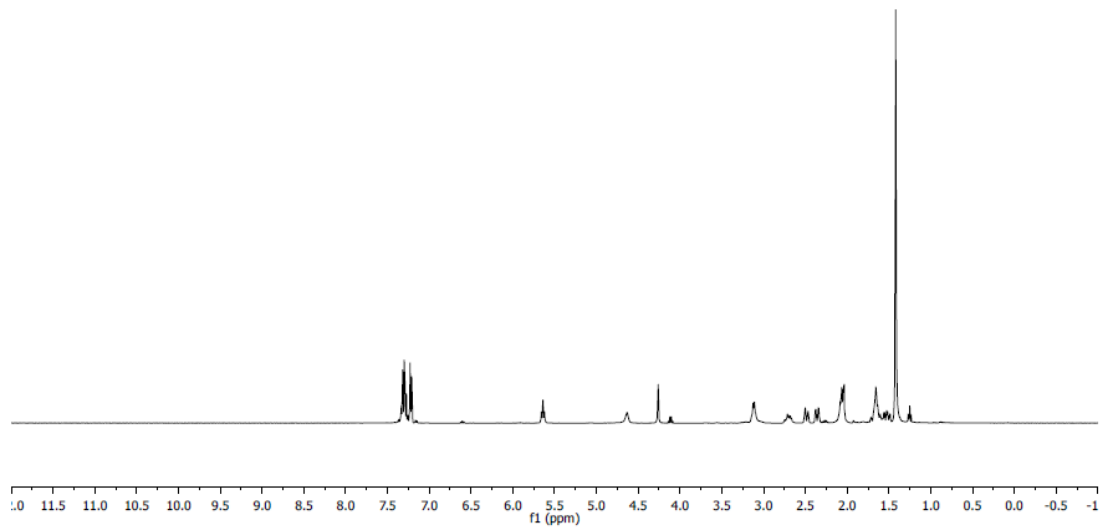
¹H NMR: (400 MHz, CDCl₃): δ 7.38-7.15 (m, 5H), 5.64 (t, *J* = 7.2 Hz, 1H), 4.63 (s, 1H, broad), 4.26 (s, 1H), 3.13-3.10 (m, 2H), 2.76-2.67 (m, 1H), 2.48 (d, *J* = 13.6 Hz, 1H), 2.38-2.34 (m, 1H), 2.08-2.04 (m, 3H), 1.68-1.49 (m, 4H), 1.42 ppm (s, 9H).

¹³C NMR: (100 MHz, CDCl₃): δ 213.0, 155.8, 143.6, 136.7, 129.4, 128.9, 128.1, 127.4, 81.7, 79.1, 39.8, 39.5, 38.6, 30.1, 28.4, 28.1, 22.6 ppm.

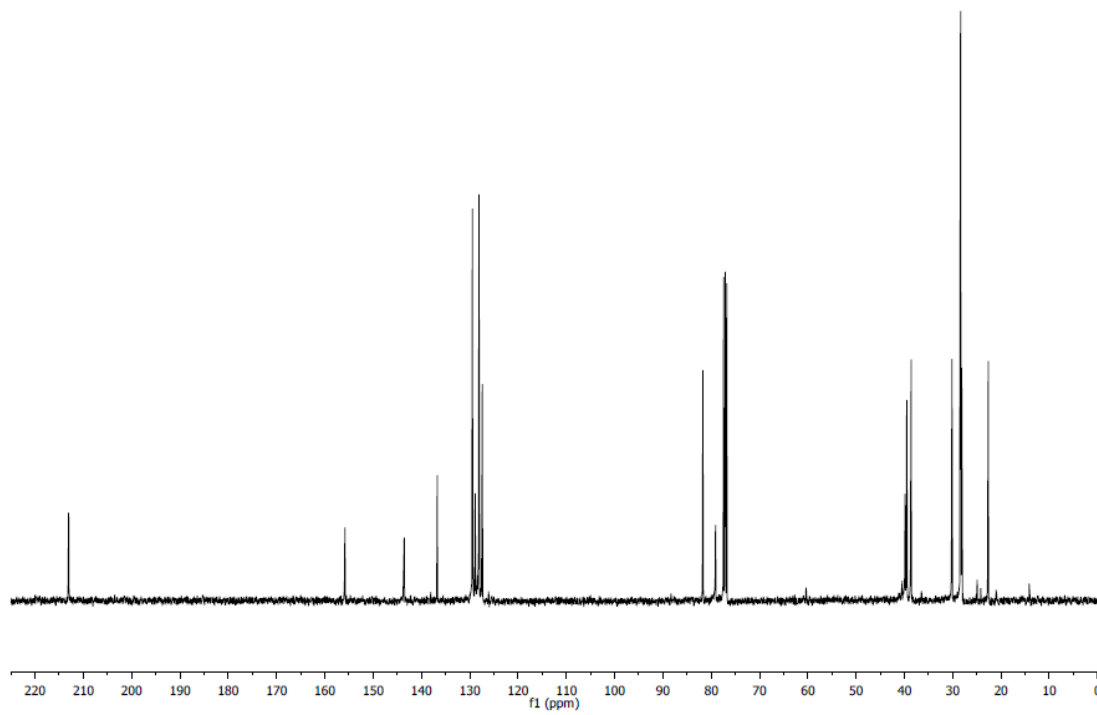
MS (ESI): *m/z* 382 [M+Na]⁺

FTIR (neat): 2970, 2943, 1738, 1712, 1515, 1447, 1365, 1249, 1230, 1217, 1167, 1102, 1087 908, 731, 706 cm⁻¹.

¹H NMR of **4.13d**



¹³C NMR of **4.13d**



(E)-2-(1-(4-chlorophenyl)prop-1-en-1-yl)-2-hydroxycyclohexan-1-one (4.13e)

In accordance with general procedure A using *trans*- **4.1a** and alkyne **4.11e**, upon stirring at 130 °C for 4 h, the reaction mixture was concentrated to afford the crude product (*E:Z* = >20:1 as determined by ¹H NMR spectroscopy). The reaction mixture was subjected to flash column chromatography (SiO₂: 10% EtOAc/hexanes) to furnish **4.13e** (61 mg, 0.23 mmol, 77% yield) as a colorless oil.

TLC (SiO₂): R_f = 0.34 (hexanes: EtOAc = 9:1).

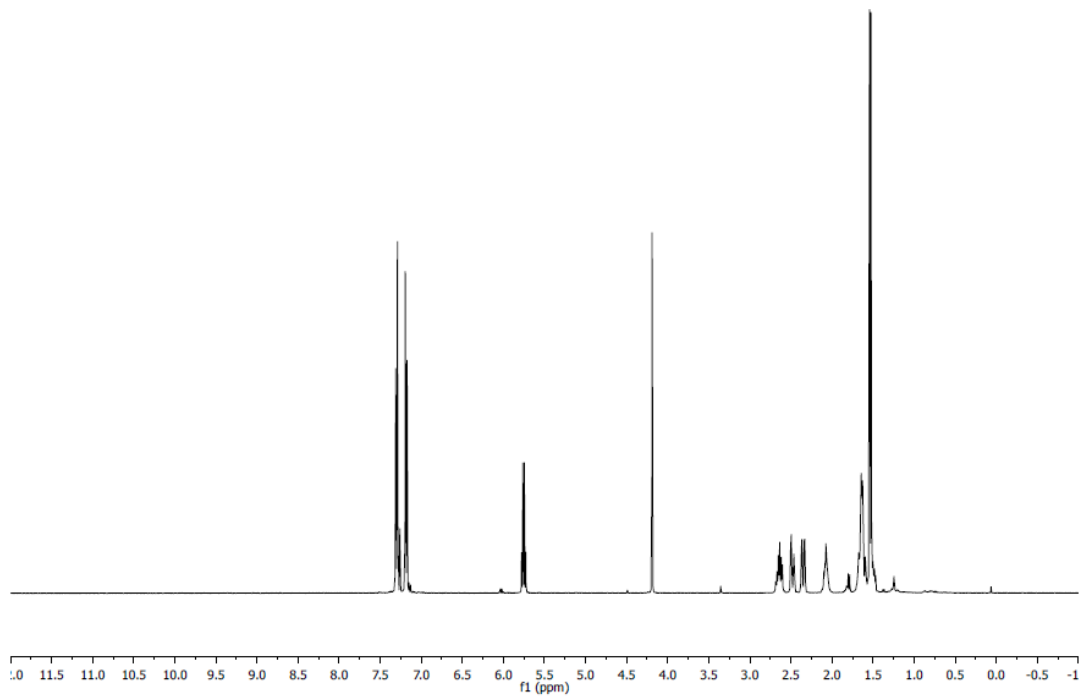
¹H NMR: (400 MHz, CDCl₃): δ 7.30 (dt, *J* = 8.8, 2.4 Hz, 2H), 7.18 (dt, *J* = 8.8, 2.4 Hz, 2H), 5.57 (q, *J* = 6.8 Hz, 1H), 4.19 (s, 1H), 2.68-2.60 (m, 1H), 2.50-2.45 (m, 1H), 2.37-2.31 (m, 1H), 2.12-2.00 (m, 1H), 1.71-1.58 (m, 4H), 1.53 ppm (d, *J* = 6.8 Hz, 3H).

¹³C NMR: (100 MHz, CDCl₃): δ 213.0, 141.0, 135.3, 133.2, 131.0, 128.3, 127.5, 81.7, 39.4, 38.7, 28.2, 22.6, 15.1 ppm.

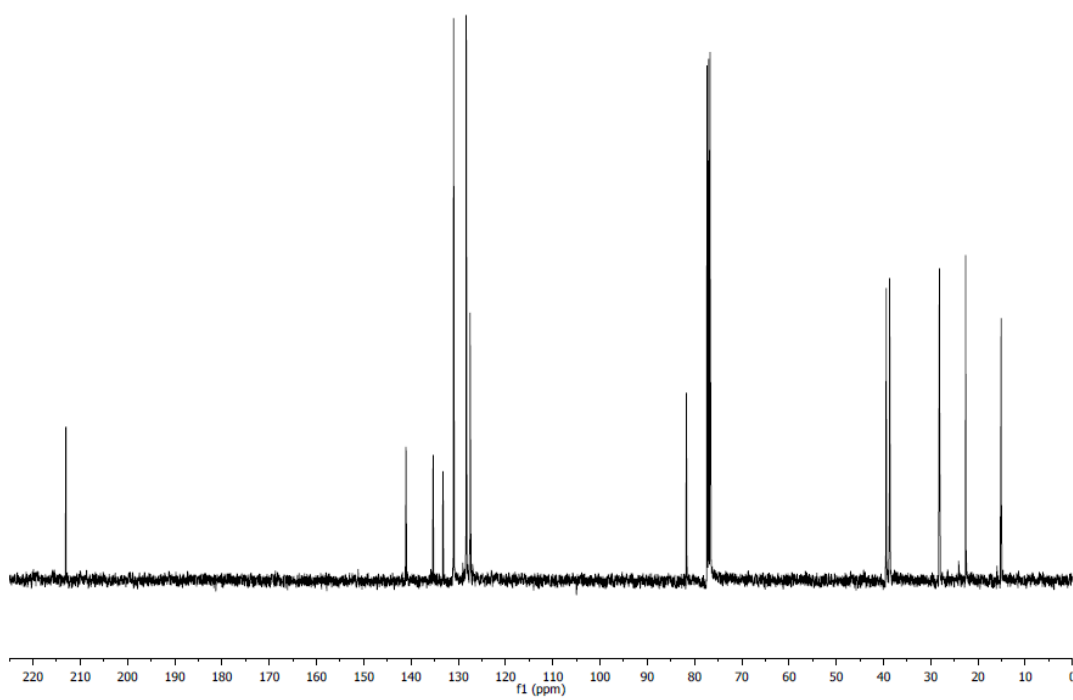
MS (CI): *m/z* 264 [M]⁺

FTIR (neat): 2942, 1738, 1711, 1447, 1366, 1229, 1217, 1087, 1015, 825 cm⁻¹.

¹H NMR of **4.13e**



¹³C NMR of **4.13e**



(E)-2-hydroxy-2-(1-(3-methoxyphenyl)prop-1-en-1-yl)cyclohexan-1-one (**4.13f**)

In accordance with general procedure A using *trans*- **4.1a** and alkyne **4.11f**, upon stirring at 130 °C for 4 h, the reaction mixture was concentrated to afford the crude product (*E:Z* = >20:1 as determined by ¹H NMR spectroscopy). The reaction mixture was subjected to flash column chromatography (SiO₂: 10% EtOAc/hexanes) to furnish **4.13f** (58 mg, 0.22 mmol, 74% yield) as a colorless oil.

TLC (SiO₂): R_f = 0.22 (hexanes: EtOAc = 9:1).

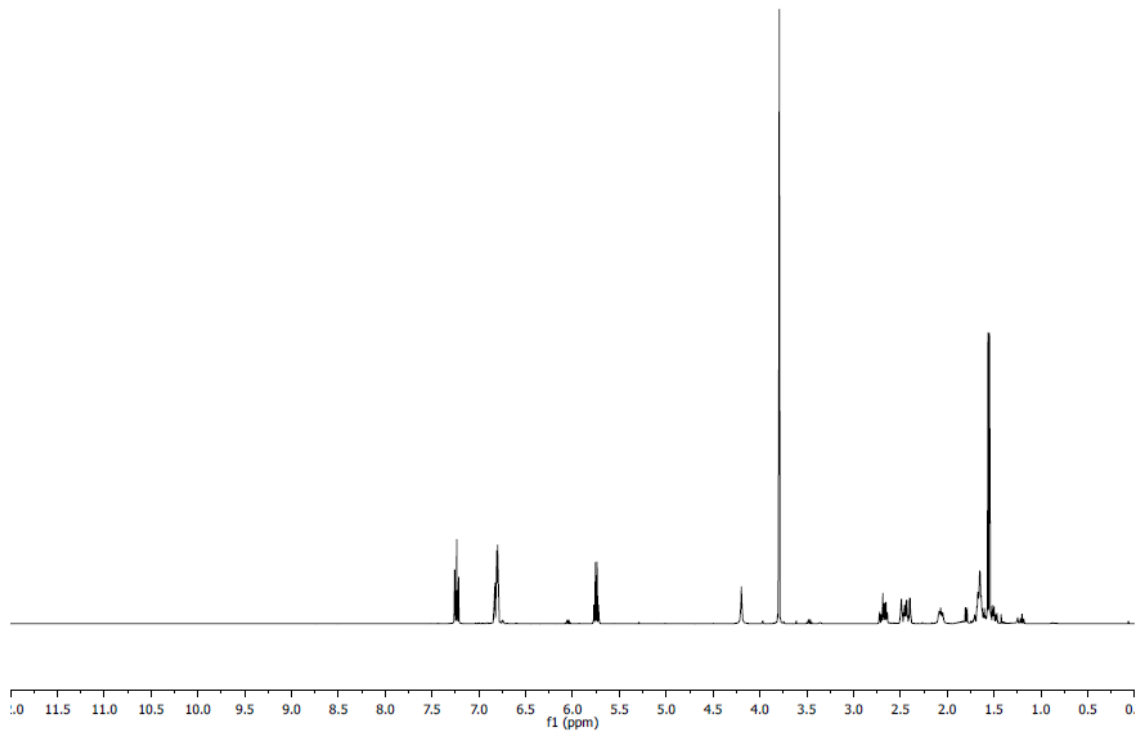
¹H NMR: (400 MHz, CDCl₃): δ 7.24 (t, *J* = 8.0 Hz, 1H), 6.84-6.79 (m, 3H), 5.75 (q, *J* = 6.8 Hz, 1H), 4.20 (s, 1H), 3.79 (s, 3H), 2.72-2.64 (m, 1H), 2.50-2.44 (m, 1H), 2.42 (ddd, *J* = 13.6, 5.6, 2.8 Hz, 1H), 2.09-2.04 (m, 1H), 1.70-1.60 (m, 4H), 1.56 ppm (d, *J* = 6.8 Hz, 3H).

¹³C NMR: (100 MHz, CDCl₃): δ 213.2, 159.2, 141.9, 13.8.3, 129.0, 126.9, 122.0, 115.4, 112.6, 81.8, 55.2, 39.4, 38.8, 28.2, 22.7, 15.1 ppm.

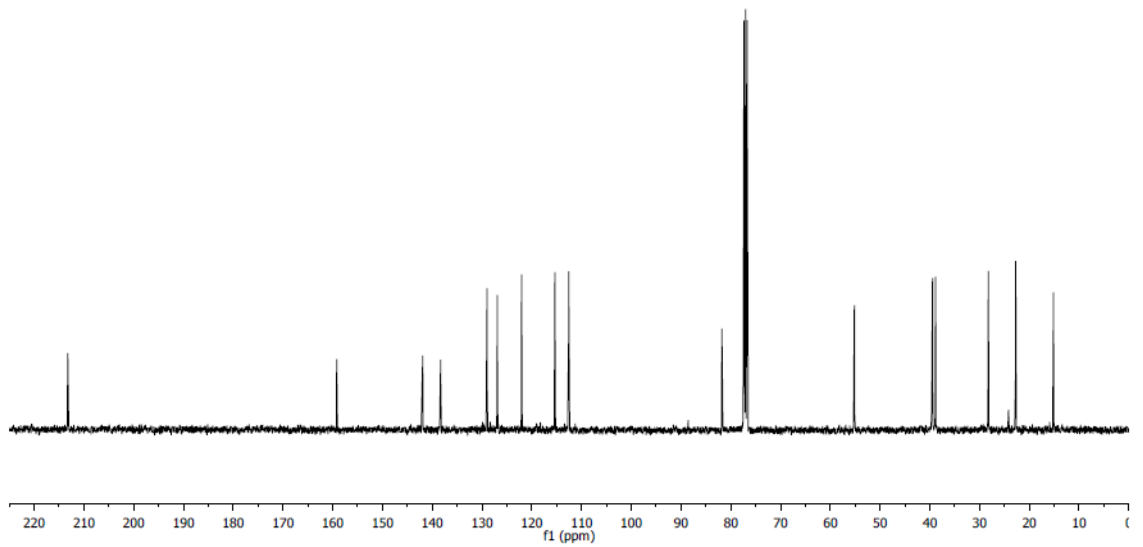
MS (ESI): *m/z* 281 [M+Na]⁺.

FTIR (neat): 1738, 1575, 1448, 1427, 1366, 1285, 1256, 1228, 1217, 1203, 1086, 1048, 903, 787, 710 cm⁻¹.

¹H NMR of **4.13f**



¹³C NMR of **4.13f**



(Z)-2-hydroxy-2-(1-(thiophen-2-yl)prop-1-en-1-yl)cyclohexan-1-(4.13g)

In accordance with general procedure A using *trans*- **4.1a** and alkyne **4.11g**, upon stirring at 130 °C for 20 h, the reaction mixture was concentrated to afford the crude product (*Z:E* = >20:1 as determined by ¹H NMR spectroscopy). The reaction mixture was subjected to flash column chromatography (SiO₂: 10% EtOAc/hexanes) to furnish **4.13g** (69 mg, 0.29 mmol, 97% yield) as a colorless oil.

TLC (SiO₂): R_f = 0.25 (hexanes: EtOAc = 9:1).

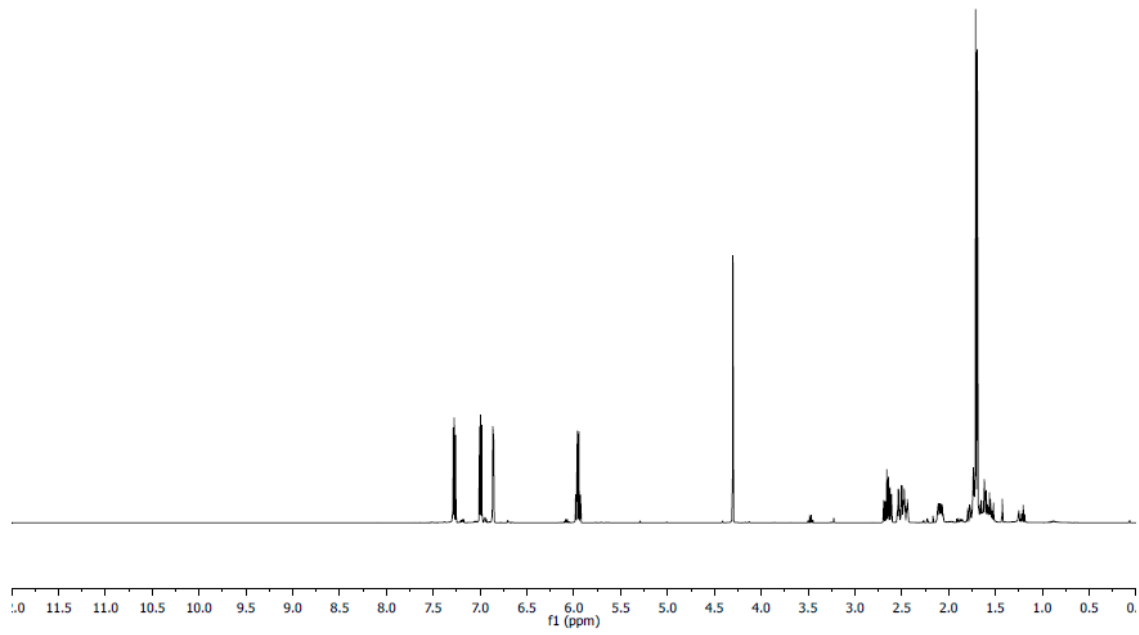
¹H NMR: (400 MHz, CDCl₃): δ 7.28 (dd, *J* = 5.2, 1.2 Hz, 1H), 6.99 (dd, *J* = 5.2, 3.6 Hz, 1H), 6.86 (dd, *J* = 3.6, 1.2 Hz, 1H), 5.95 (q, *J* = 6.8 Hz, 1H), 4.30 (s, 1H), 2.69-2.61 (m, 1H), 2.52 (ddd, *J* = 13.6, 6.0, 2.8 Hz, 1H), 2.48-2.43 (m, 1H), 2.12-2.06 (m, 1H), 1.79-1.52 (m, 4H), 1.70 ppm (d, *J* = 6.8 Hz, 3H).

¹³C NMR: (100 MHz, CDCl₃): δ 212.8, 136.5, 134.9, 129.8, 127.6, 126.4, 125.8, 81.5, 39.2, 38.6, 28.4, 23.0, 15.4 ppm.

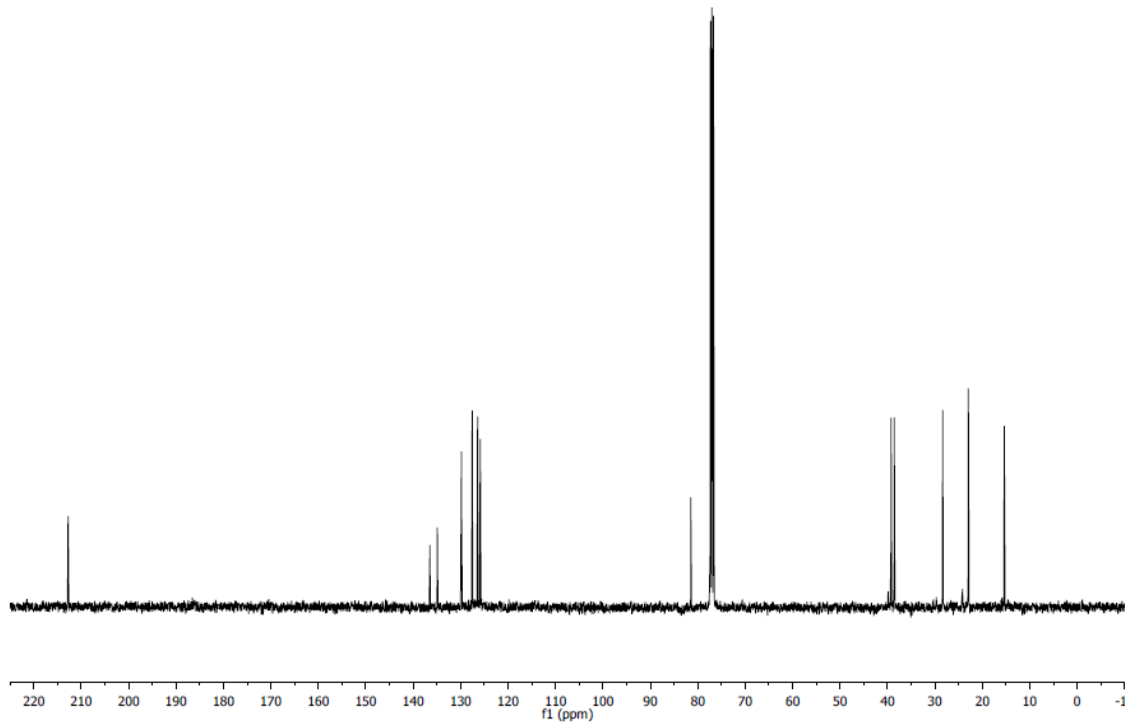
MS (CI): *m/z* 236 [M]⁺.

FTIR (neat): 2942, 1738, 1713, 1365, 1227, 1217, 1100, 1086, 699 cm⁻¹.

¹H NMR of 4.13g



¹³C NMR of 4.13g



Ethyl (*E*)-4-(1-(1-hydroxy-2-oxocyclohexyl)prop-1-en-1-yl)benzoate (**4.13h**)

In accordance with general procedure A using *trans*- **4.1a** and alkyne **4.11h**, upon stirring at 130 °C for 4 h, the reaction mixture was concentrated to afford the crude product (*E:Z* = >20:1 as determined by ¹H NMR spectroscopy). The reaction mixture was subjected to flash column chromatography (SiO₂: 10% EtOAc/hexanes) to furnish **4.13h** (69 mg, 0.29 mmol, 97% yield) as a colorless oil.

TLC (SiO₂): R_f = 0.21 (hexanes: EtOAc = 9:1).

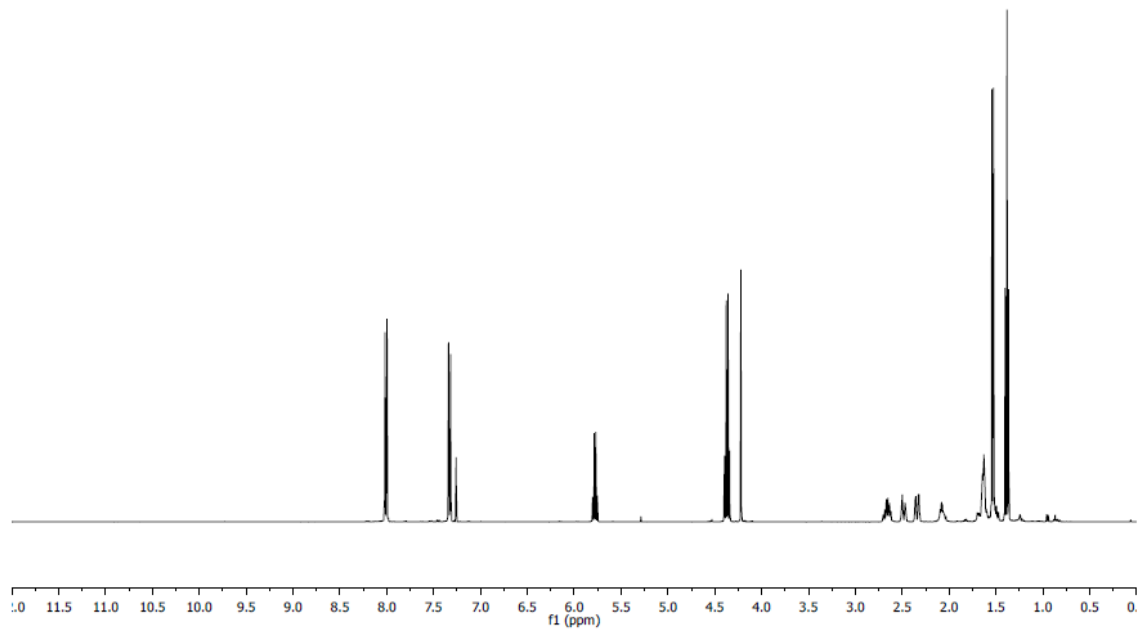
¹H NMR: (400 MHz, CDCl₃): δ 8.01 (d, *J* = 8.8 Hz, 2H), 7.33 (d, *J* = 8.8 Hz, 2H), 5.78 (q, *J* = 6.8 Hz, 1H), 4.37 (q, *J* = 7.2 Hz, 2H), 4.22 (s, 1H), 2.70-2.62 (m, 1H) 2.51-2.46 (m, 1H), 2.36-2.31 (m, 1H), 2.10-2.03 (m, 1H), 1.70-1.56 (m, 4H), 1.53 (d, *J* = 6.8 Hz, 3H), 1.38 ppm (t, *J* = 7.2 Hz, 3H).

¹³C NMR: (100 MHz, CDCl₃): δ 212.9, 166.4, 141.9, 141.5, 129.7, 129.4, 129.3, 127.6, 81.6, 60.9, 39.4, 38.8, 28.2, 22.6, 15.1, 14.3 ppm.

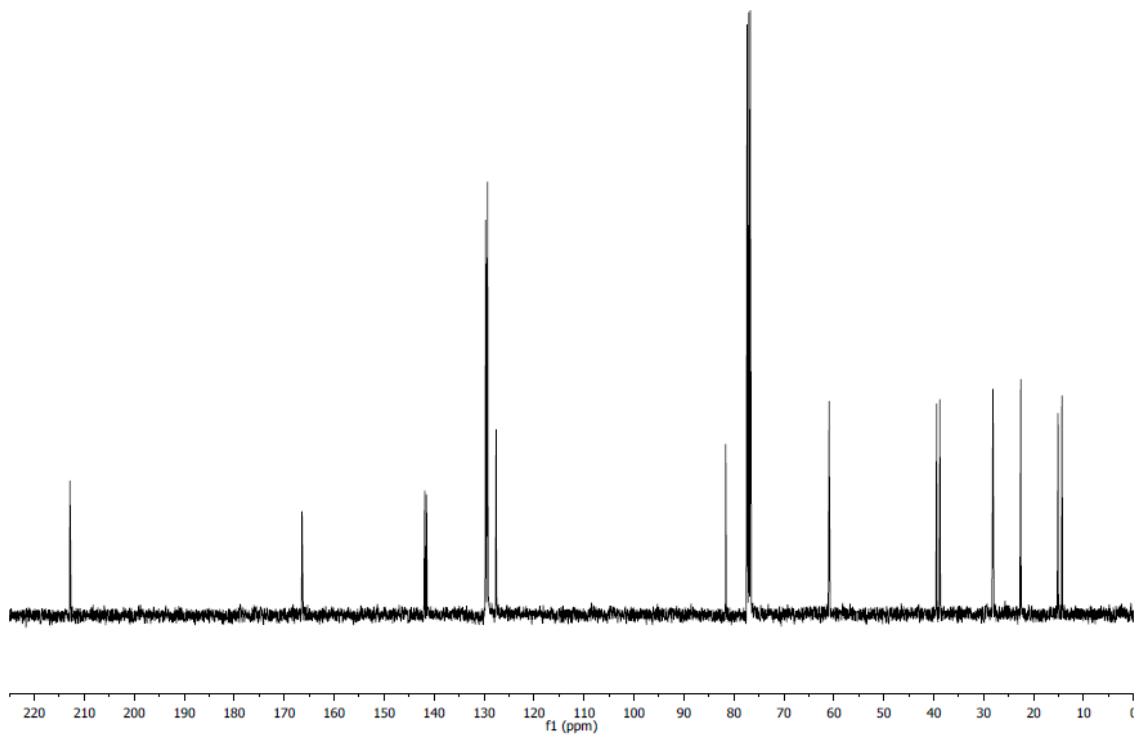
MS (CI): *m/z* 303 [M+H]⁺.

FTIR (neat): 2938, 1709, 1608, 1271, 1177, 1100, 1022, 904, 869, 832, 778, 720 cm⁻¹.

¹H NMR of 4.13h



¹³C NMR of 4.13h



Ethyl (*E*)-2-hydroxy-2,3-diphenylpent-3-enoate (**4.14c**)

In accordance with general procedure A using α -hydroxy ester **4.7c** and alkyne **4.11a**, upon stirring at 130 °C for 20 h, the reaction mixture was concentrated to afford the crude product (E:Z = >20:1 as determined by ¹H NMR spectroscopy). The reaction mixture was subjected to flash column chromatography (SiO₂: 10% EtOAc/hexanes) to furnish **4.14c** (56 mg, 0.19 mmol, 63% yield) as a yellow oil.

TLC (SiO₂): R_f = 0.37 (hexanes:EtOAc = 9:1).

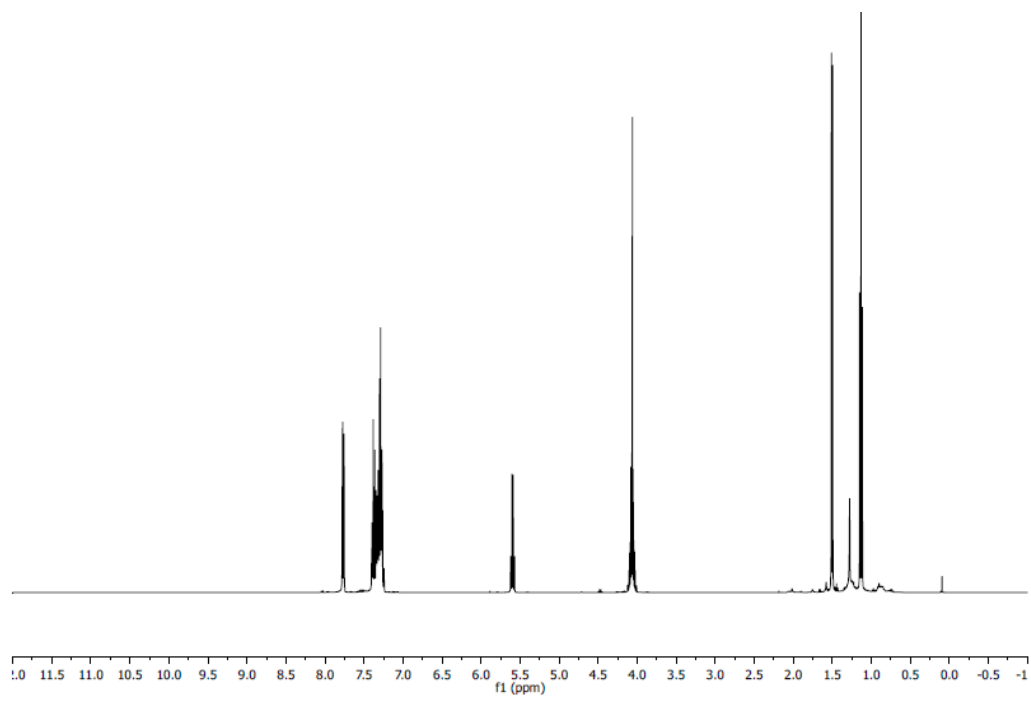
¹H NMR: (400 MHz, CDCl₃): δ 7.78-7.75 (m, 2H), 7.40-7.24 (m, 8H), 5.60 (q, *J* = 6.8 Hz, 1H), 4.12-4.10 (m, 2H), 4.06 (s, 1H), 3.26 (d, *J* = 6.8 Hz, 3H), 1.13 ppm (t, *J* = 7.2 Hz, 3H).

¹³C NMR: (100 MHz, CDCl₃): δ 174.2, 143.3, 139.8, 137.9, 130.0, 128.4, 127.8, 127.7, 127.7, 127.6, 127.0, 82.2, 62.6, 14.9, 13.8 ppm.

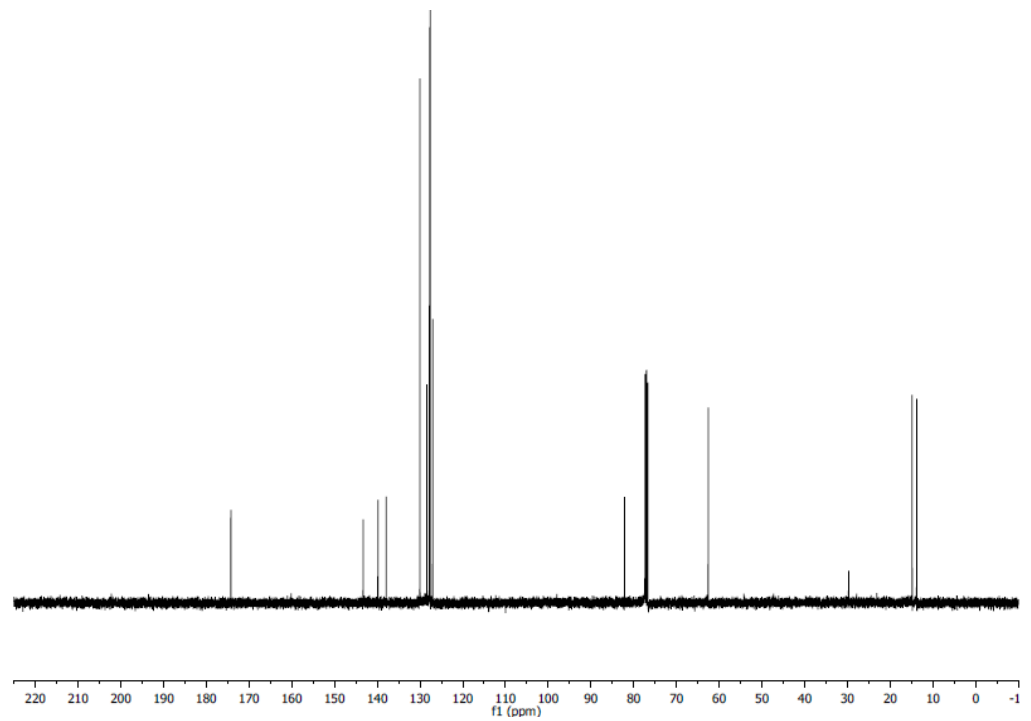
MS (ESI): *m/z* 319 [M+Na]⁺

FTIR (neat): 3489, 2921, 1722, 1492, 1446, 1241, 1176, 1116, 1098, 1069, 1053, 1014, 921, 860, 766, 740, 700 cm⁻¹.

¹H NMR of **4.14c**



¹³C NMR of **4.14c**



Ethyl (*E*)-2-hydroxy-2,3-diphenylpent-3-enoate (**4.15a**)

In accordance with general procedure C using ketone **4.12a** (39 mg, 0.17 mmol, 100 mol%) and para-toluene sulfonic acid (5.9 mg, 0.034 mmol, 20 mol%), upon stirring at 80 °C for 4 h, the reaction mixture was concentrated and subjected to flash column chromatography (SiO₂: hexanes) to furnish **4.15a** (26 mg, 0.12 mmol, 69% yield) as a yellow oil. *The spectroscopic properties of this compound were consistent with the data available in the literature.*¹³³

TLC (SiO₂): R_f = 0.51 (hexanes).

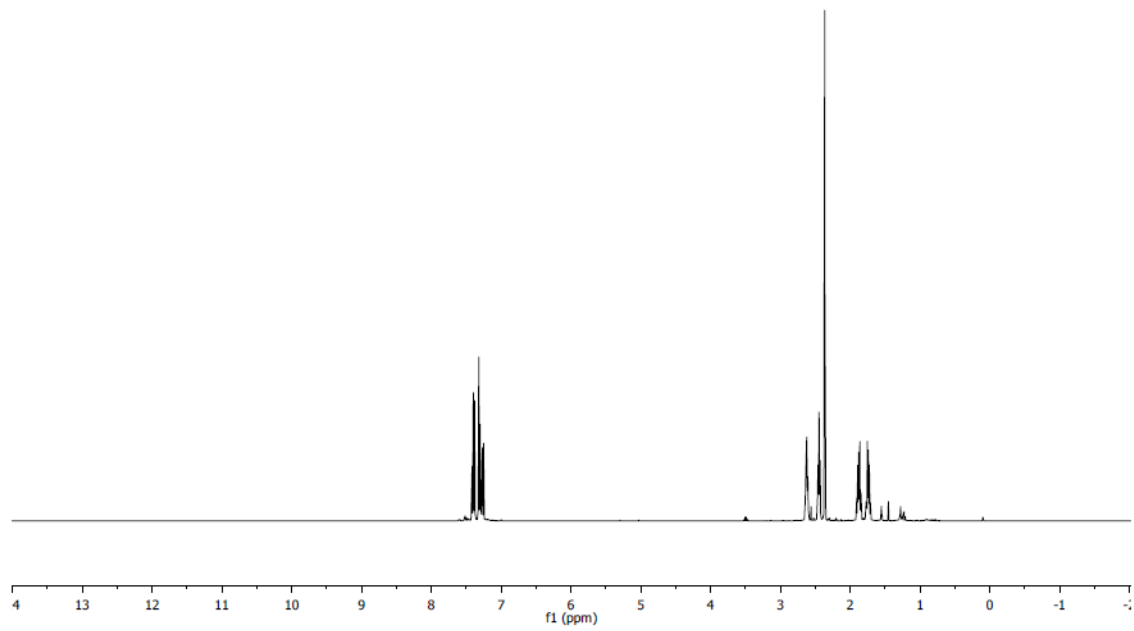
¹H NMR: (400 MHz, CDCl₃): δ 7.42-7.38 (m, 2H), 7.32-7.25 (m, 3H), 2.62 (t, *J* = 6.0 Hz, 2H), 2.44 (tt, *J* 6.0 Hz, 2.0 Hz, 2H), 2.36 (s, 3H), 1.90-1.84 (m, 2H), 1.77-1.71 ppm (m, 2H).

¹³C NMR: (100 MHz, CDCl₃): δ 148.6, 145.7, 134.1, 128.6, 128.3, 126.1, 120.9, 117.0, 23.3, 23.2, 23.0, 21.9, 12.5 ppm.

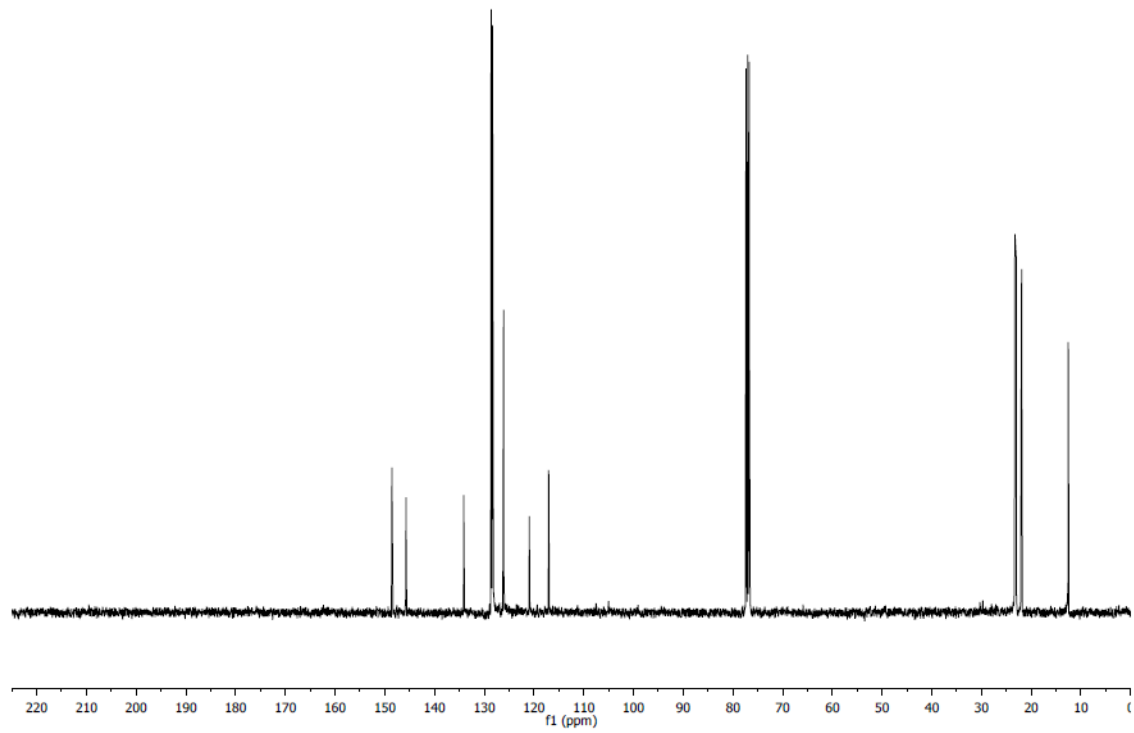
MS (CI): *m/z* 213 [M+H]⁺.

FTIR (neat): 2929, 2846, 1606, 1496, 1443, 1251, 1198, 1015, 971, 758, 699, 682 cm⁻¹.

¹H NMR of **4.15a**



¹³C NMR of **4.15a**



2,3-diphenyl-4,5,6,7-tetrahydrobenzofuran (**4.15e**)

In accordance with general procedure C using ketone **4.12e** (97 mg, 0.46 mmol, 100 mol%) and para-toluene sulfonic acid (16 mg, 0.09 mmol, 20 mol%), upon stirring at 80 °C for 4 h, the reaction mixture was concentrated and subjected to flash column chromatography (SiO₂: hexanes) to furnish **4.15e** (34 mg, 0.18 mmol, 40% yield) as a yellow oil. *The spectroscopic properties of this compound were consistent with the data available in the literature.*¹³⁴

TLC (SiO₂): R_f = 0.74 (20:1 hexanes:EtOAc).

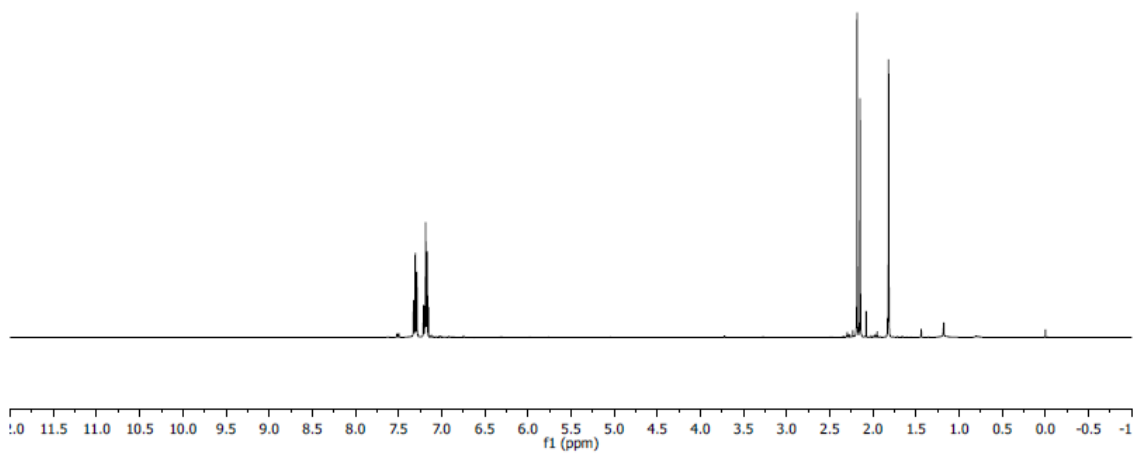
¹H NMR: (400 MHz, CDCl₃): δ 7.32-7.28 (m, 2H), 7.21-7.15 (m, 3H), 2.18 (s, 3H), 2.15 (s, 3H), 1.82 ppm (s, 3H).

¹³C NMR: (100 MHz, CDCl₃): δ 145.4, 145.1, 134.3, 129.2, 128.3, 126.3, 122.6, 113.0, 12.3, 11.4, 9.2 ppm.

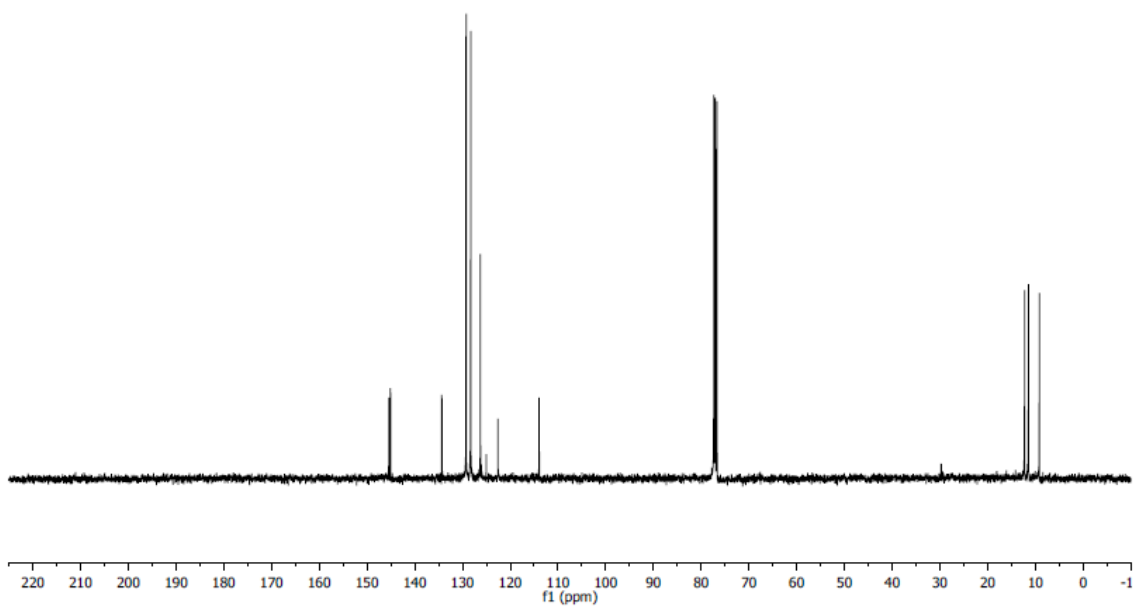
MS (CI): m/z 187 [M+H]⁺.

FTIR (neat): 2902, 1607, 1495, 1442, 1387, 1297, 1196, 1133, 1074, 994, 912, 825, 759, 697 cm⁻¹.

¹H NMR of **4.15e**



¹³C NMR of **4.15e**



2-methyl-3-phenyl-4,5-dihydronaphtho[1,2-b]furan (**4.15I**)

In accordance with general procedure C using ketone **4.12I** (43 mg, 0.15 mmol, 100 mol%) and para-toluene sulfonic acid (5.5 mg, 0.032 mmol, 20 mol%), upon stirring at 80 °C for 4 h, the reaction mixture was concentrated and subjected to flash column chromatography (SiO₂: hexanes) to furnish **4.15I** (30 mg, 0.12 mmol, 73% yield) as a white solid.

TLC (SiO₂): R_f = 0.44 (19:1 EtOAc:hexanes).

¹H NMR: (400 MHz, CDCl₃): δ 7.49-7.47 (d, *J* = 7.6 Hz, 1H), 7.46-7.41 (m, 2H), 7.34-7.29 (m, 3H), 7.24-7.18 (m, 2H), 7.11 (td, *J* = 7.2, 1.2 Hz, 1H), 2.97 (t, *J* = 7.6 Hz, 2H), 2.76 (t, *J* = 7.6 Hz, 2H), 2.47 (s, 3H) ppm.

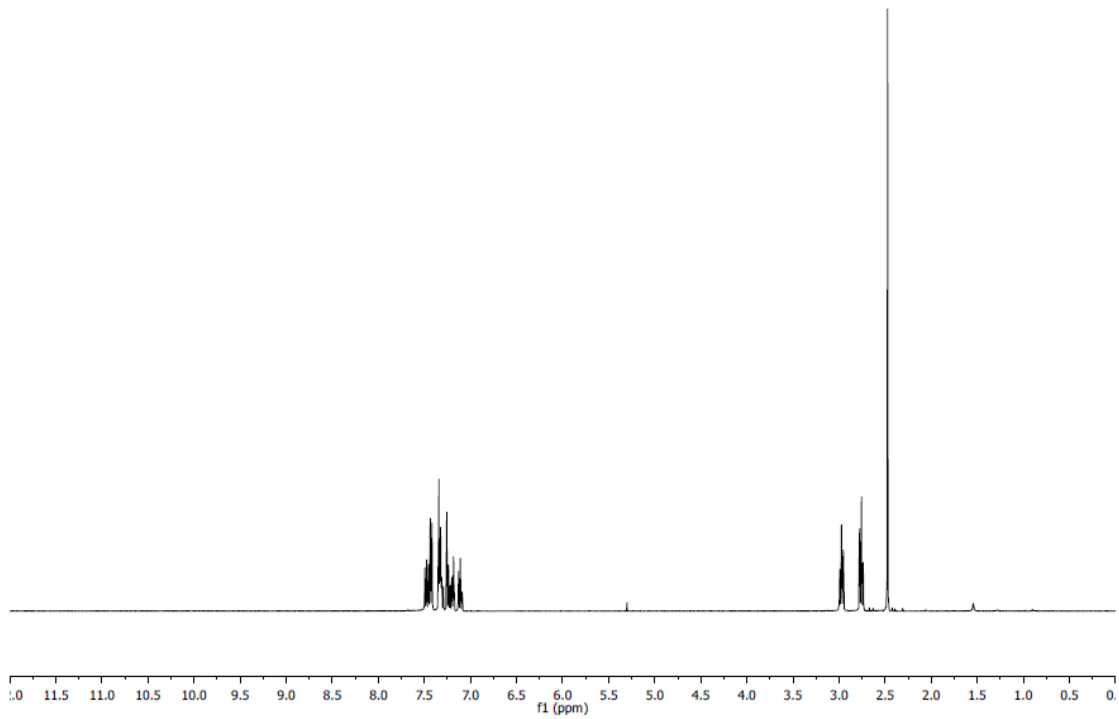
¹³C NMR: (100 MHz, CDCl₃): δ 148.1, 147.9, 134.3, 133.5, 128.7, 128.5, 128.2, 127.8, 126.7, 126.5, 125.9, 121.7, 119.6, 118.8, 29.2, 20.4, 12.9 ppm.

MP: 106 – 107 °C.

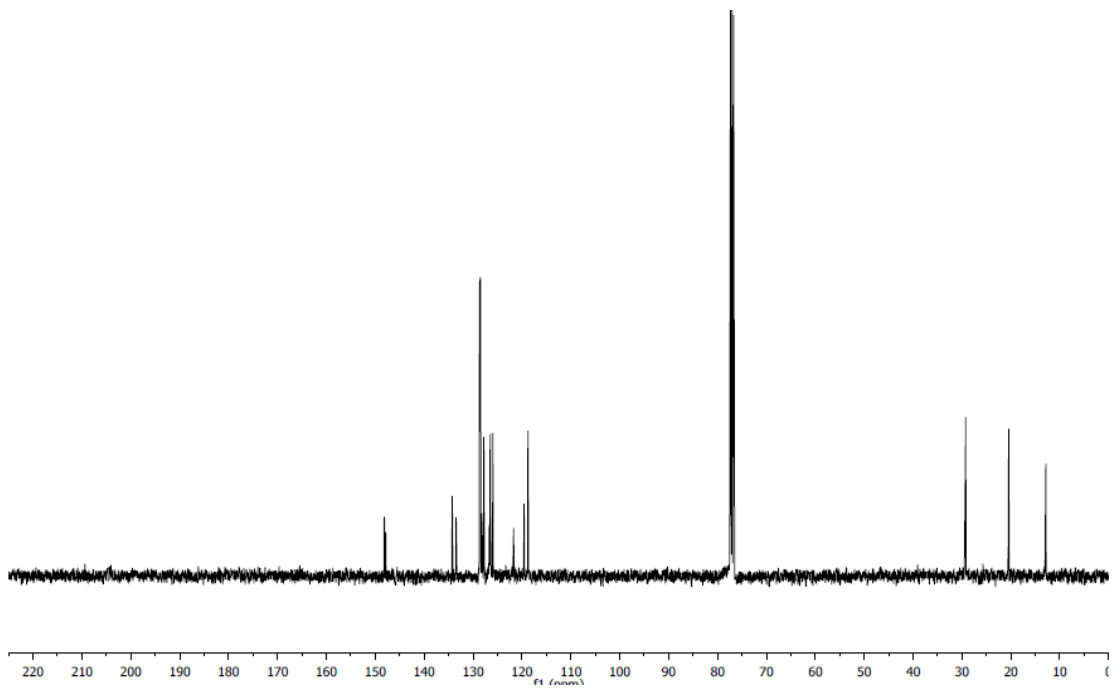
MS (CI): *m/z* 261 [M+H]⁺.

FTIR (neat): 1497, 1437, 956, 766, 757, 712, 700, 690 cm⁻¹.

¹H NMR of **4.15I**



¹³C NMR of **4.15I**



2,3-diphenyl-4,5,6,7-tetrahydrobenzofuran (**4.16c**)

In accordance with general procedure C using ketone **4.13c** (57 mg, 0.20 mmol, 100 mol%) and para-toluenesulfonic acid (7.0 mg, 0.04 mmol, 20 mol%), upon stirring at 80 °C for 4 h, the reaction mixture was concentrated and subjected to flash column chromatography (SiO₂: hexanes) to furnish **4.16c** (42 mg, 0.15 mmol, 77% yield) as a white solid.

TLC (SiO₂): R_f = 0.55 (hexanes).

¹H NMR: (400 MHz, CDCl₃): δ 7.47-7.44 (m, 2H), 7.40-7.30 (m, 5H), 7.25-7.14 (m, 3H), 2.72 (t, *J* = 6.4 Hz, 2H), 2.36 (t, *J* = 6.0 Hz, 2H), 1.94-1.88 (m, 2H), 1.79-1.73 ppm (m, 2H).

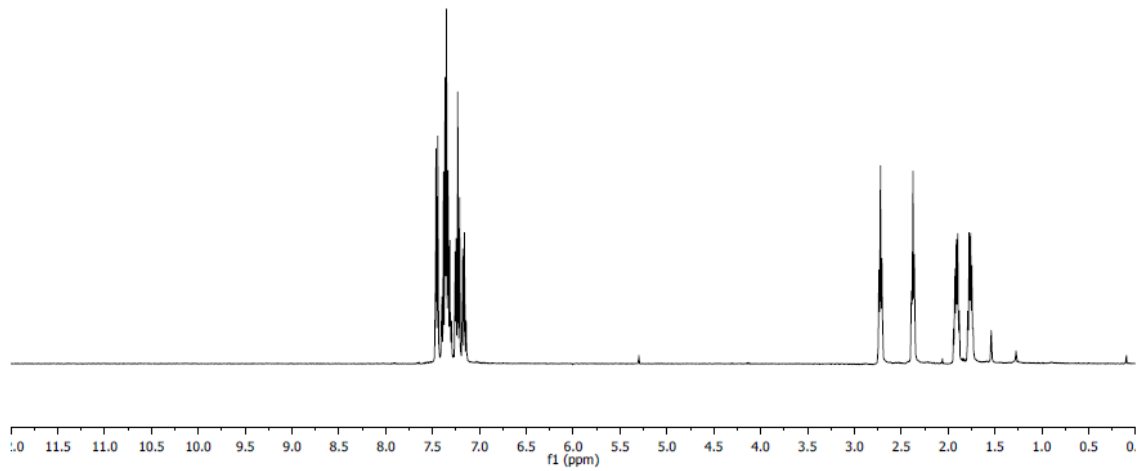
¹³C NMR: (100 MHz, CDCl₃): δ 150.2, 146.6, 134.1, 131.6, 129.4, 128.6, 128.2, 126.9, 126.6, 125.6, 123.4, 119.5, 23.3, 23.1, 23.0, 21.4 ppm.

MP: 120 – 122 °C.

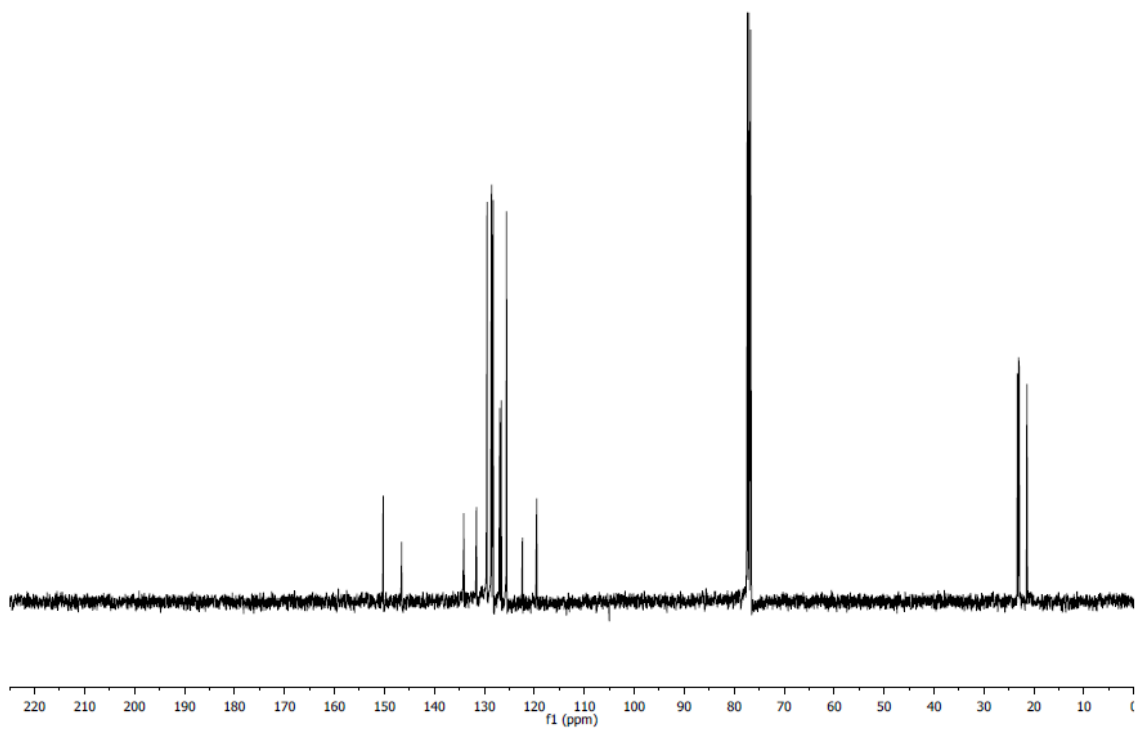
MS (CI): *m/z* 275 [M+H]⁺.

FTIR (neat): 1437, 1065, 966, 930, 909, 784, 752, 711, 692, 667, 652 cm⁻¹

¹H NMR of **4.16c**



¹³C NMR of **4.16c**



3-(4-chlorophenyl)-2-methyl-4,5,6,7-tetrahydrobenzofuran (**4.16e**)

In accordance with general procedure C using ketone **4.13e** (59 mg, 0.22 mmol, 100 mol%) and para-toluenesulfonic acid (7.7 mg, 0.045 mmol, 20 mol%), upon stirring at 80 °C for 4 h, the reaction mixture was concentrated and subjected to flash column chromatography (SiO₂: hexanes) to furnish **4.16e** (37 mg, 0.15 mmol, 66% yield) as a pale yellow solid. *The spectroscopic properties of this compound were consistent with the data available in the literature.*¹³⁴

TLC (SiO₂): R_f = 0.32 (hexanes).

¹H NMR: (400 MHz, CDCl₃): δ 7.35 (d, *J* = 8.8 Hz, 2H), 7.22 (d, *J* = 8.8 Hz, 2H), 2.60 (t, *J* = 6.0 Hz, 2H), 2.42-2.36 (m, 2H), 2.33 (s, 3H), 1.90-1.82 (m, 2H), 1.76-1.68 ppm (m, 2H).

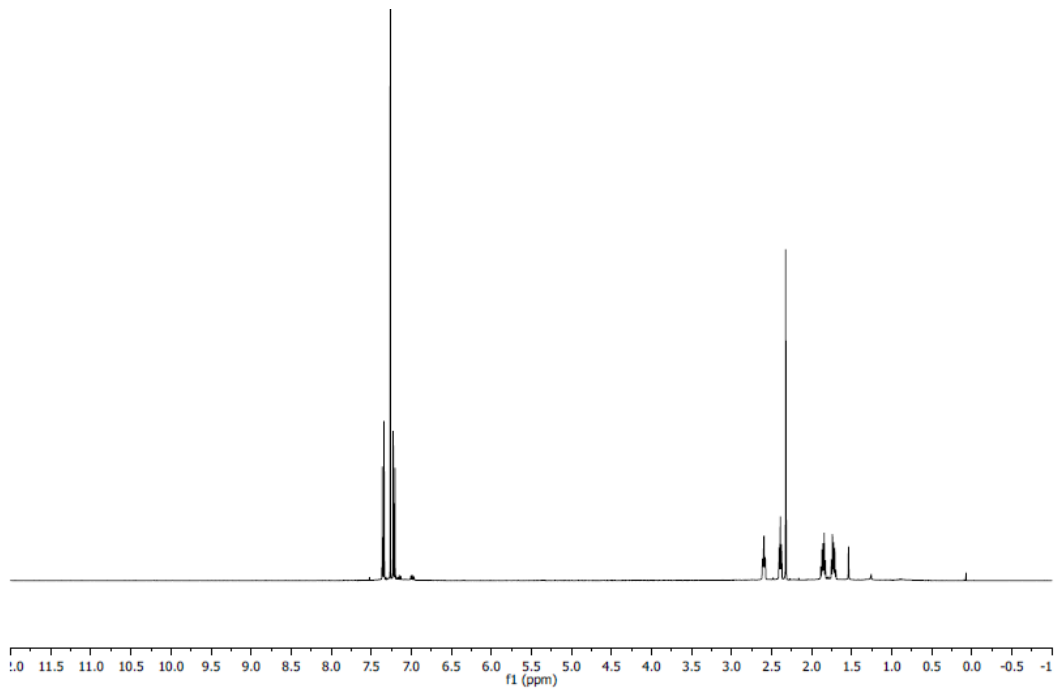
¹³C NMR: (100 MHz, CDCl₃): δ 148.8 145.9, 132.6, 131.9, 129.8, 128.5, 119.9, 116.8, 23.2, 23.1, 22.9, 21.8, 12.5 ppm.

MP: 67 – 68 °C.

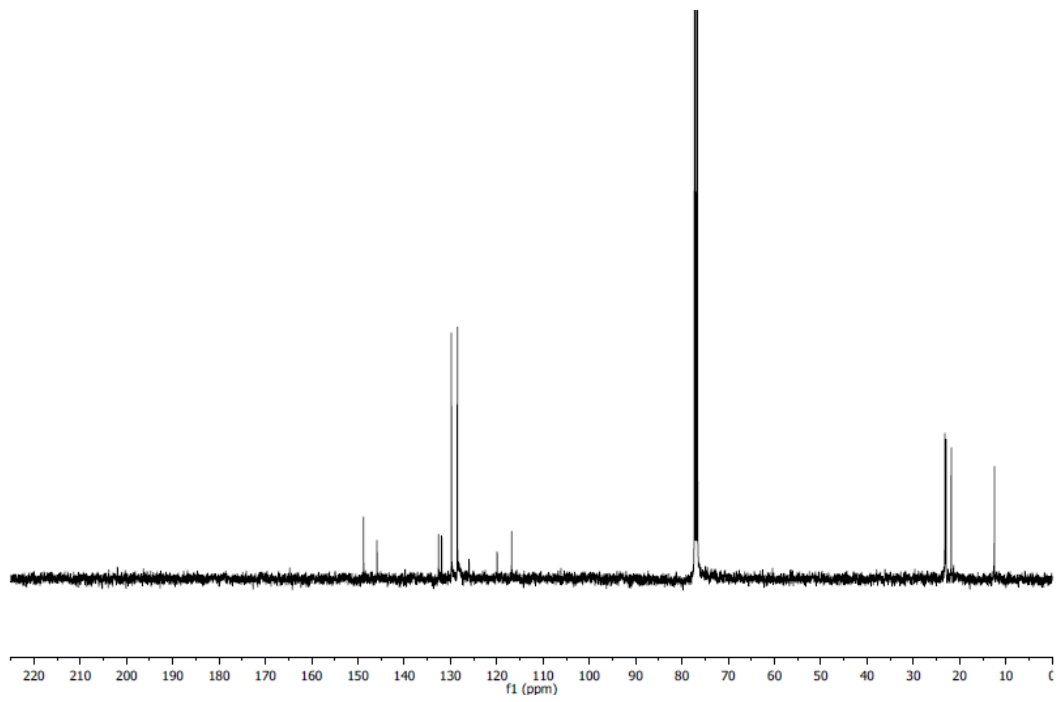
MS (CI): *m/z* 247 [M+H]⁺.

FTIR (neat): 2928, 2849, 1582, 1490, 1444, 1251, 1198, 1091, 1012, 972, 834, 805 cm⁻¹.

¹H NMR of **4.16e**



¹³C NMR of **4.16e**



Ethyl 4-(2-methyl-4,5,6,7-tetrahydrobenzofuran-3-yl)benzoate (**4.16h**)

In accordance with general procedure C using ketone **4.13h** (40 mg, 0.13 mmol, 100 mol%) and para-toluenesulfonic acid (4.6 mg, 0.026 mmol, 20 mol%), upon stirring at 80 °C for 4 h, the reaction mixture was concentrated and subjected to flash column chromatography (SiO₂: hexanes) to furnish **4.16h** (20 mg, 0.070 mmol, 53% yield) as a clear, colorless oil.

TLC (SiO₂): R_f = 0.39 (hexanes).

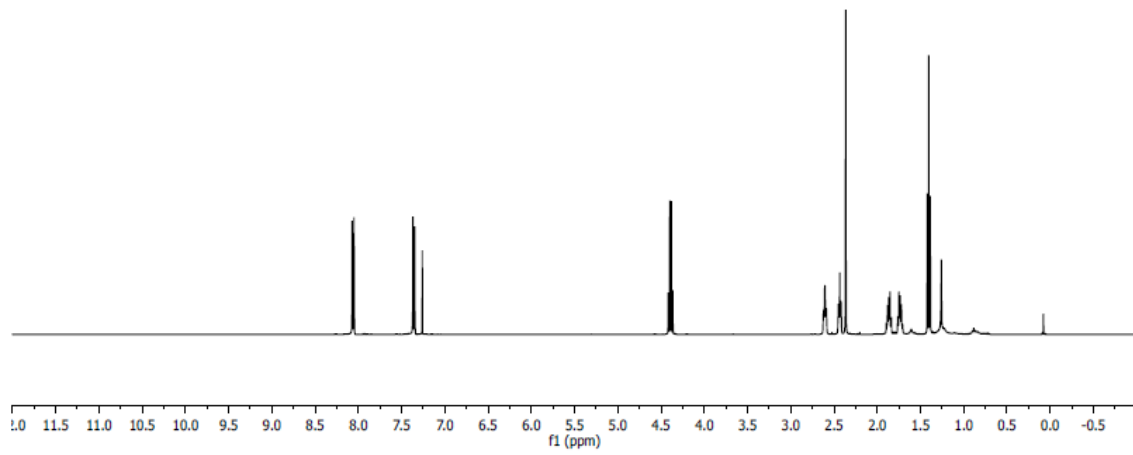
¹H NMR: (400 MHz, CDCl₃): δ 8.06 (d, *J* = 8.4 Hz, 2H), 7.35 (d, *J* = 8.4 Hz, 2H), 4.39 (q, *J* = 7.2 Hz, 2H), 2.62 (br t, *J* = 6.0 Hz, 2H), 2.43 (tt, *J* = 6.0, 1.6 Hz, 2H), 2.36 (s, 3H), 1.90-1.84 (m, 2H), 1.76-1.71 (m, 2H), 1.40 ppm (t, *J* = 7.2 Hz, 3H).

¹³C NMR: (100 MHz, CDCl₃): δ 166.6, 149.0, 146.6, 139.0, 129.6, 128.3, 128.0, 120.3, 116.7, 60.8, 23.2, 23.1, 22.9, 22.0, 14.3, 12.7 ppm.

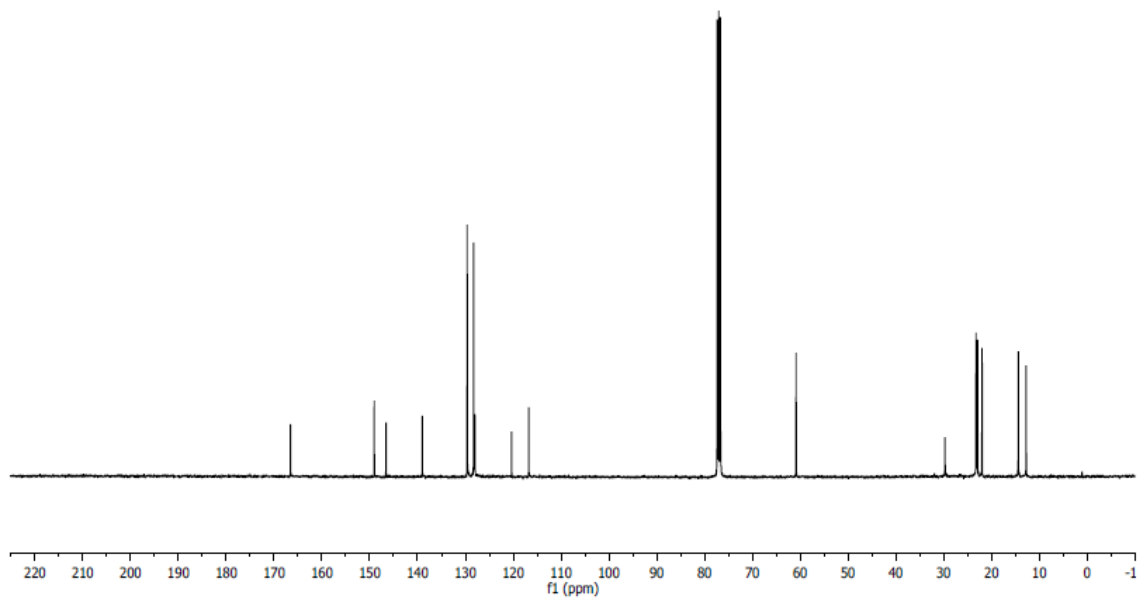
MS (ESI): *m/z* 285 [M+H]⁺.

FTIR (neat): 2927, 2850, 1715, 1610, 1270, 1252, 1177, 1102, 1015, 973, 866 771 cm⁻¹.

¹H NMR of 4.16h



¹³C NMR of 4.16h



Appendix

List of Abbreviations and Acronyms

acac	Acetoacetyl
BINOL	1,1'-Bi-2-naphthol
BIPHEP	2,2'-Bis(diphenylphosphino)-1,1'-biheptyl
BIPY	2,2'-Bipyridine
cod	1,5-Cyclooctadiene
cot	Cyclooctatetraene
Cy	Cyclohexyl
DBU	1,8-Diazabicycloundec-7-ene
DCE	Dichloroethane
DCM	Dichloromethane
DCyPF	1,1'-Bis(dicyclohexylphosphino)ferrocene
DFT	Density functional theory
D <i>i</i> PPF	1,1'-Bis(di- <i>i</i> -propylphosphino)ferrocene
DMB	Dimethoxybenzyl
DM-Segphos	(<i>S</i>)-(-)-5,5'-Bis(diphenylphosphino)-4,4'-bi-1,3-benzodioxole
DMSO	Dimethylsulfoxide
DPPB	1,4-Bis(diphenylphosphino)butane
DPPF	1,1'-Bis(diphenylphosphino)ferrocene
DPPP	1,3-Bis(diphenylphosphino)propane
HMBC	Heteronuclear Multiple Bond Correlation
Ipc	Isopinocampheol
LUMO	Lowest Unoccupied Molecular Orbital
Mes	Mesityl
MOM	Methoxymethyl
NHC	<i>N</i> -Heterocyclic Carbene
NOESY	Nuclear Overhauser Enhancement Spectroscopy

ORTEP	Oak Ridge Thermal Ellipsoid Plot
Phen	Phenanthroline
Pin	Pinacol
DMB	Dimethoxybenzyl
PMHS	Polymethylhydrosiloxane
BINAP	2,2'-Bis(diphenylphosphino)-1,1'-binaphthyl
<i>p</i> TSOH	<i>para</i> -Toluenesulfonic Acid
Segphos	5,5'-Bis(diphenylphosphino)-4,4'-bi-1,3-benzodioxole
TADDOL	$\alpha, \alpha, \alpha, \alpha$ -tetraaryl-1,3-dioxalane-4,5-dimethanol
TBAF	Tetrabutylammonium fluoride
TBAI	Tetrabutylammonium iodide
TBS	<i>Tert</i> -Butyldimethylsilyl
TERPY	2,2':6',2''-Terpyridine
TFA	Trifluoroacetic acid
THF	Tetrahydrofuran
TRIP	Triisopropylbenzene
WALPHOS	(1 <i>S</i>)-1-[(1 <i>R</i>)-1-[Bis[3,5-bis(trifluoromethyl)phenyl]phosphino]ethyl]-2-[2-(diphenylphosphino)phenyl]ferrocene
XANTPHOS	9,9-Dimethyl-4,5-bis(diphenylphosphino)xanthene

References

1. Masanari Kimura, Y. T., Metal Catalyzed Reductive C-C Bond Formation. In *Topics in Current Chemistry*, Krische, M. J., Ed. Springer Berlin Heidelberg: Berlin, 2007; pp 173-207.
2. Akutagawa, S., *Bull. Chem. Soc. Jpn.* **1976**, *49* (12), 3646-3648.
3. Baker, R.; Crimmin, M. J., *J. Chem. Soc., Perkin Trans. 1* **1979**, (0), 1264-1267.
4. Kimura, M.; Ezoe, A.; Shibata, K.; Tamaru, Y., *J. Am. Chem. Soc.* **1998**, *120* (16), 4033-4034.
5. Kimura, M.; Fujimatsu, H.; Ezoe, A.; Shibata, K.; Shimizu, M.; Matsumoto, S.; Tamaru, Y., *Angew. Chem., Int. Ed.* **1999**, *38* (3), 397-400.
6. Ogoshi, S.; Tonomori, K.-i.; Oka, M.-a.; Kurosawa, H., *J. Am. Chem. Soc.* **2006**, *128* (21), 7077-7086.
7. Kimura, M.; Matsuo, S.; Shibata, K.; Tamaru, Y., *Angew. Chem., Int. Ed.* **1999**, *38* (22), 3386-3388.
8. Kimura, M.; Shibata, K.; Koudahashi, Y.; Tamaru, Y., *Tetrahedron Lett.* **2000**, *41* (35), 6789-6793.
9. Shibata, K.; Kimura, M.; Kojima, K.; Tanaka, S.; Tamaru, Y., *J. Organomet. Chem.* **2001**, *624* (1-2), 348-353.
10. Kimura, M.; Ezoe, A.; Tanaka, S.; Tamaru, Y., *Angew. Chem., Int. Ed.* **2001**, *40* (19), 3600-3602.
11. Oblinger, E.; Montgomery, J., *J. Am. Chem. Soc.* **1997**, *119* (38), 9065-9066.
12. Kimura, M.; Ezoe, A.; Mori, M.; Tamaru, Y., *J. Am. Chem. Soc.* **2004**, *127* (1), 201-209.
13. Kimura, M.; Ezoe, A.; Mori, M.; Iwata, K.; Tamaru, Y., *J. Am. Chem. Soc.* **2006**, *128* (26), 8559-8568.
14. Takimoto, M.; Hiraga, Y.; Sato, Y.; Mori, M., *Tetrahedron Lett.* **1998**, *39* (25), 4543-4546.
15. Sato, Y.; Sawaki, R.; Mori, M., *Organometallics* **2001**, *20* (26), 5510-5512.
16. Sawaki, R.; Sato, Y.; Mori, M., *Org. Lett.* **2004**, *6* (7), 1131-1133.
17. Sato, Y.; Hinata, Y.; Seki, R.; Oonishi, Y.; Saito, N., *Org. Lett.* **2007**, *9* (26), 5597-5599.
18. Yang, Y.; Zhu, S.-F.; Duan, H.-F.; Zhou, C.-Y.; Wang, L.-X.; Zhou, Q.-L., *J. Am. Chem. Soc.* **2007**, *129* (8), 2248-2249.
19. Saito, N.; Kobayashi, A.; Sato, Y., *Angew. Chem., Int. Ed.* **2012**, *51* (5), 1228-1231.
20. Loh, T.-P.; Hu, Q.-Y.; Ma, L.-T., *J. Am. Chem. Soc.* **2001**, *123* (10), 2450-2451.
21. Cho, H. Y.; Morken, J. P., *J. Am. Chem. Soc.* **2008**, *130* (48), 16140-16141.
22. Cho, H. Y.; Morken, J. P., *J. Am. Chem. Soc.* **2010**, *132* (22), 7576-7577.
23. Cho, H. Y.; Yu, Z.; Morken, J. P., *Org. Lett.* **2011**, *13* (19), 5267-5269.
24. Kopfer, A.; Sam, B.; Breit, B.; Krische, M. J., *Chem. Sci.* **2013**, *4* (4), 1876-1880.
25. Jang, H.-Y.; Krische, M. J., *Acc. Chem. Res.* **2004**, *37* (9), 653-661.
26. Jang, H.-Y.; Huddleston, R. R.; Krische, M. J., *Angew. Chem., Int. Ed.* **2003**, *42* (34), 4074-4077.

27. Kimura, M.; Nojiri, D.; Fukushima, M.; Oi, S.; Sonoda, Y.; Inoue, Y., *Org. Lett.* **2009**, *11* (17), 3794-3797.
28. Zbieg, J. R.; Fukuzumi, T.; Krische, M. J., *Adv. Synth. Catal.* **2010**, *352* (14-15), 2416-2420.
29. Omura, S.; Fukuyama, T.; Horiguchi, J.; Murakami, Y.; Ryu, I., *J. Am. Chem. Soc.* **2008**, *130* (43), 14094-14095.
30. Shibahara, F.; Bower, J. F.; Krische, M. J., *J. Am. Chem. Soc.* **2008**, *130* (20), 6338-6339.
31. Shibahara, F.; Bower, J. F.; Krische, M. J., *J. Am. Chem. Soc.* **2008**, *130* (43), 14120-14122.
32. Smejkal, T.; Han, H.; Breit, B.; Krische, M. J., *J. Am. Chem. Soc.* **2009**, *131* (30), 10366-10367.
33. Han, H.; Krische, M. J., *Org. Lett.* **2010**, *12* (12), 2844-2846.
34. Zbieg, J. R.; Moran, J.; Krische, M. J., *J. Am. Chem. Soc.* **2011**, *133* (27), 10582-10586.
35. Zbieg, J. R.; Yamaguchi, E.; McInturff, E. L.; Krische, M. J., *Science* **2012**, *336* (6079), 324-327.
36. McInturff, E. L.; Yamaguchi, E.; Krische, M. J., *J. Am. Chem. Soc.* **2012**, *134* (51), 20628-20631.
37. Zhang, M.; Imm, S.; Bähn, S.; Neumann, H.; Beller, M., *Angew. Chem., Int. Ed.* **2011**, *50* (47), 11197-11201.
38. Leung, J. C.; Geary, L. M.; Chen, T.-Y.; Zbieg, J. R.; Krische, M. J., *J. Am. Chem. Soc.* **2012**, *134* (38), 15700-15703.
39. Chen, T.-Y.; Krische, M. J., *Org. Lett.* **2013**, *15* (12), 2994-2997.
40. Park, B. Y.; Montgomery, T. P.; Garza, V. J.; Krische, M. J., *J. Am. Chem. Soc.* **2013**, *135* (44), 16320-16323.
41. Geary, L. M.; Glasspoole, B. W.; Kim, M. M.; Krische, M. J., *J. Am. Chem. Soc.* **2013**, *135* (10), 3796-3799.
42. Suginome, M.; Nakamura, H.; Ito, Y., *Chem. Commun.* **1996**, (24), 2777-2778.
43. Suginome, M.; Nakamura, H.; Matsuda, T.; Ito, Y., *J. Am. Chem. Soc.* **1998**, *120* (17), 4248-4249.
44. Takahashi, S.; Shibano, T.; Hagihara, N., *Tetrahedron Lett.* **1967**, *8* (26), 2451-2453.
45. Haynes, P., *Tetrahedron Lett.* **1970**, *11* (42), 3687-3690.
46. Manyik, R. M.; Walker, W. E.; Atkins, K. E.; Hammack, E. S., *Tetrahedron Lett.* **1970**, *11* (43), 3813-3816.
47. (a) Ohno, K.; Mitsuyasu, T.; Tsuji, J., *Tetrahedron* **1972**, *28* (14), 3705-3720; (b) Ohno, K.; Mitsuyasu, T.; Tsuji, J., *Tetrahedron Lett.* **1971**, *12* (1), 67-70.
48. Fukushima, M.; Takushima, D.; Kimura, M., *J. Am. Chem. Soc.* **2010**, *132* (46), 16346-16348.
49. (a) Hoveyda, A. H.; Morken, J. P., *Angew. Chem., Int. Ed.* **1996**, *35* (12), 1262-1284; (b) Yasuda, H.; Tatsumi, K.; Nakamura, A., *Acc. Chem. Res.* **1985**, *18* (4), 120-126.
50. Bareille, L.; Le Gendre, P.; Moise, C., *Chem. Commun.* **2005**, (6), 775-777.
51. Berk, S. C.; Kreutzer, K. A.; Buchwald, S. L., *J. Am. Chem. Soc.* **1991**, *113* (13), 5093-5095.

52. (a) Kennedy, J. W. J.; Hall, D. G., *Angew. Chem., Int. Ed.* **2003**, *42* (39), 4732-4739; (b) Keck, G. E.; Tarbet, K. H.; Geraci, L. S., *J. Am. Chem. Soc.* **1993**, *115* (18), 8467-8468; (c) Costa, A. L.; Piazza, M. G.; Tagliavini, E.; Trombini, C.; Umani-Ronchi, A., *J. Am. Chem. Soc.* **1993**, *115* (15), 7001-7002; (d) Denmark, S. E.; Coe, D. M.; Pratt, N. E.; Griedel, B. D., *J. Org. Chem.* **1994**, *59* (21), 6161-6163; (e) Denmark, S. E.; Fu, J., *J. Am. Chem. Soc.* **2001**, *123* (38), 9488-9489; (f) Kim, I. S.; Ngai, M.-Y.; Krische, M. J., *J. Am. Chem. Soc.* **2008**, *130* (20), 6340-6341.
53. (a) Hassan, A.; Krische, M. J., *Org. Process Res. Dev.* **2011**, *15* (6), 1236-1242; (b) Bower, J. F.; Kim, I. S.; Patman, R. L.; Krische, M. J., *Angew. Chem., Int. Ed.* **2009**, *48* (1), 34-46; (c) Shibahara, F.; Krische, M. J., *Chem. Lett.* **2008**, *37* (11), 1102-1107.
54. Bergmeier, S. C., *Tetrahedron* **2000**, *56* (17), 2561-2576.
55. Ito, H.; Taguchi, T.; Hanzawa, Y., *Tetrahedron Lett.* **1992**, *33* (31), 4469-4472.
56. Murakami, M.; Ito, H.; Ito, Y., *J. Org. Chem.* **1993**, *58* (24), 6766-6770.
57. Yamada, K.-i.; Nakano, M.; Maekawa, M.; Akindede, T.; Tomioka, K., *Org. Lett.* **2008**, *10* (17), 3805-3808.
58. Ona Burgos, P.; Fernandez, I.; Iglesias, M. J.; Garcia-Granda, S.; Lopez Ortiz, F., *Org. Lett.* **2008**, *10* (4), 537-540.
59. (a) Barrett, A. G. M.; Seefeld, M. A., *J. Chem. Soc., Chem. Commun.* **1993**, (4), 339-341; (b) Barrett, A. G. M.; Seefeld, M. A.; White, A. J. P.; Williams, D. J., *J. Org. Chem.* **1996**, *61* (8), 2677-2685; (c) Barrett, A. G. M.; Seefeld, M. A., *Tetrahedron* **1993**, *49* (36), 7857-7870; (d) Barrett, A. G. M.; Seefeld, M. A.; Williams, D. J., *J. Chem. Soc., Chem. Commun.* **1994**, (9), 1053-1054.
60. Zhong, Y.-W.; Dong, Y.-Z.; Fang, K.; Izumi, K.; Xu, M.-H.; Lin, G.-Q., *J. Am. Chem. Soc.* **2005**, *127* (34), 11956-11957.
61. (a) Karimi, B.; Enders, D.; Jafari, E., *Synthesis* **2013**, *45* (EFirst), 2769-2812; (b) List, B.; Pojarliev, P.; Biller, W. T.; Martin, H. J., *J. Am. Chem. Soc.* **2002**, *124* (5), 827-833; (c) Matsunaga, S.; Yoshida, T.; Morimoto, H.; Kumagai, N.; Shibasaki, M., *J. Am. Chem. Soc.* **2004**, *126* (28), 8777-8785; (d) Trost, B. M.; Terrell, L. R., *J. Am. Chem. Soc.* **2002**, *125* (2), 338-339.
62. Skucas, E.; Zbieg, J. R.; Krische, M. J., *J. Am. Chem. Soc.* **2009**, *131* (14), 5054-5055.
63. Patman, R. L.; Williams, V. M.; Bower, J. F.; Krische, M. J., *Angew. Chem., Int. Ed.* **2008**, *47* (28), 5220-5223.
64. Zbieg, J. R.; McInturff, E. L.; Krische, M. J., *Org. Lett.* **2010**, *12* (11), 2514-2516.
65. (a) Bai, T.; Zhu, J.; Xue, P.; Sung, H. H.-Y.; Williams, I. D.; Ma, S.; Lin, Z.; Jia, G., *Organometallics* **2007**, *26* (23), 5581-5589; (b) F. Hill, A.; T. Ho, C.; D. E. T. Wilton-Ely, J., *Chem. Commun.* **1997**, (22), 2207-2208; (c) Hiraki, K.; Sasada, Y.; Kitamura, T., *Chem. Lett.* **1980**, *9* (4), 449-452; (d) Nakanishi, S.; Sasabe, H.; Takata, T., *Chem. Lett.* **2000**, *29* (9), 1058-1059; (e) Sasabe, H.; Kihara, N.; Mizuno, K.; Ogawa, A.; Takata, T., *Chem. Lett.* **2006**, *35* (2), 212-213; (f) Sasabe, H.; Nakanishi, S.; Takata, T., *Inorg. Chem. Commun.* **2002**, *5* (3), 177-180; (g) Sasabe, H.; Nakanishi, S.; Takata, T., *Inorg. Chem. Commun.* **2003**, *6* (8), 1140-1143; (h) Xue, P.; Bi, S.; Sung, H. H. Y.; Williams, I. D.; Lin, Z.; Jia, G., *Organometallics* **2004**, *23* (20), 4735-4743.

66. Åberg, J. B.; Nyhlén, J.; Martín-Matute, B. n.; Privalov, T.; Bäckvall, J.-E., *J. Am. Chem. Soc.* **2009**, *131* (27), 9500-9501.
67. (a) Bella, M.; Gasperi, T., *Synthesis* **2009**, 2009 (EFirst), 1583-1614; (b) Christoffers, J.; Baro, A., *Adv. Synth. Catal.* **2005**, *347* (11-13), 1473-1482; (c) Christoffers, J.; Mann, A., *Angew. Chem., Int. Ed.* **2001**, *40* (24), 4591-4597; (d) Corey, E. J.; Guzman-Perez, A., *Angew. Chem., Int. Ed.* **1998**, *37* (4), 388-401; (e) Das, J. P.; Marek, I., *Chem. Commun.* **2011**, *47* (16), 4593-4623; (f) Douglas, C. J.; Overman, L. E., *Proc. Natl. Acad. Sci. U. S. A.* **2004**, *101* (15), 5363-5367; (g) Fuji, K., *Chem. Rev.* **1993**, *93* (6), 2037-2066; (h) Martin, S. F., *Tetrahedron* **1980**, *36* (4), 419-460; (i) Trost, B. M.; Jiang, C., *Synthesis* **2006**, 2006, 369-396.
68. Ngai, M.-Y.; Skucas, E.; Krische, M. J., *Org. Lett.* **2008**, *10* (13), 2705-2708.
69. (a) Moore, W. R.; Ward, H. R., *J. Org. Chem.* **1962**, *27* (12), 4179-4181; (b) von E. Doering, W.; LaFlamme, P. M., *Tetrahedron* **1958**, *2* (1-2), 75-79.
70. (a) Denmark, S. E.; Fu, J., *Org. Lett.* **2002**, *4* (11), 1951-1953; (b) Denmark, S. E.; Fu, J.; Lawler, M. J., *J. Org. Chem.* **2006**, *71* (4), 1523-1536.
71. Jia, G.; Morris, R. H., *J. Am. Chem. Soc.* **1991**, *113* (3), 875-883.
72. Zbieg, J. R.; McInturff, E. L.; Leung, J. C.; Krische, M. J., *J. Am. Chem. Soc.* **2010**, *133* (4), 1141-1144.
73. Joseph, T.; Deshpande, S. S.; Halligudi, S. B.; Vinu, A.; Ernst, S.; Hartmann, M., *J. Mol. Catal. A: Chem.* **2003**, *206* (1-2), 13-21.
74. Johnson, T. C.; Totty, W. G.; Wills, M., *Org. Lett.* **2012**, *14* (20), 5230-5233.
75. Still, W. C.; Kahn, M.; Mitra, A., *J. Org. Chem.* **1978**, *43* (14), 2923-2925.
76. (a) Khosla, C.; Kapur, S.; Cane, D. E., *Curr. Opin. Chem. Biol.* **2009**, *13* (2), 135-143; (b) Wong, F. T.; Khosla, C., *Curr. Opin. Chem. Biol.* **2012**, *16* (1-2), 117-123.
77. (a) Denmark, S. E.; Fu, J., *Chem. Rev.* **2003**, *103* (8), 2763-2794; (b) Hall, D. G., *Synlett* **2007**, 2007 (11), 1644-1655.
78. (a) Hoffmann, R. W.; Zeiss, H.-J., *Angew. Chem., Int. Ed.* **1979**, *18* (4), 306-307; (b) Hoffmann, R. W.; Zeiss, H. J., *J. Org. Chem.* **1981**, *46* (7), 1309-1314; (c) Herold, T.; Hoffmann, R. W., *Angew. Chem., Int. Ed.* **1978**, *17* (10), 768-769; (d) Lachance, H.; Lu, X.; Gravel, M.; Hall, D. G., *J. Am. Chem. Soc.* **2003**, *125* (34), 10160-10161; (e) Hoffmann, R. W.; Ditrich, K.; Köster, G.; Stürmer, R., *Chem. Ber.* **1989**, *122* (9), 1783-1789; (f) Roush, W. R.; Ando, K.; Powers, D. B.; Palkowitz, A. D.; Halterman, R. L., *J. Am. Chem. Soc.* **1990**, *112* (17), 6339-6348; (g) Roush, W. R.; Palkowitz, A. D.; Ando, K., *J. Am. Chem. Soc.* **1990**, *112* (17), 6348-6359; (h) Roush, W. R.; Palkowitz, A. D.; Palmer, M. J., *J. Org. Chem.* **1987**, *52* (2), 316-318; (i) Roush, W. R.; Halterman, R. L., *J. Am. Chem. Soc.* **1986**, *108* (2), 294-296; (j) Roush, W. R.; Walts, A. E.; Hoong, L. K., *J. Am. Chem. Soc.* **1985**, *107* (26), 8186-8190; (k) Garcia, J.; Kim, B. M.; Masamune, S., *J. Org. Chem.* **1987**, *52* (21), 4831-4832; (l) Corey, E. J.; Yu, C. M.; Kim, S. S., *J. Am. Chem. Soc.* **1989**, *111* (14), 5495-5496; (m) Burgos, C. H.; Canales, E.; Matos, K.; Soderquist, J. A., *J. Am. Chem. Soc.* **2005**, *127* (22), 8044-8049.
79. (a) Rudolf O. Duthaler, A. H., Martin Riediker, *Pure Appl. Chem.* **1990**, *62* (4), 631-642; (b) Hafner, A.; Duthaler, R. O.; Marti, R.; Rihs, G.; Rothe-Streit, P.; Schwarzenbach, F., *J. Am. Chem. Soc.* **1992**, *114* (7), 2321-2336; (c) Duthaler, R. O.; Hafner, A., *Chem. Rev. (Washington, DC, U. S.)* **1992**, *92* (5), 807-832; (d)

- Hackman, B. M.; Lombardi, P. J.; Leighton, J. L., *Org. Lett.* **2004**, *6* (23), 4375-4377; **(e)** Wang, X.; Meng, Q.; Nation, A. J.; Leighton, J. L., *J. Am. Chem. Soc.* **2002**, *124* (36), 10672-10673; **(f)** Spletstoser, J. T.; Zacuto, M. J.; Leighton, J. L., *Org. Lett.* **2008**, *10* (24), 5593-5596.
- 80.** **(a)** Furuta, K.; Mouri, M.; Yamamoto, H., *Synlett* **1991**, *1991* (08), 561-562; **(b)** Yanagisawa, A.; Kageyama, H.; Nakatsuka, Y.; Asakawa, K.; Matsumoto, Y.; Yamamoto, H., *Angew. Chem., Int. Ed.* **1999**, *38* (24), 3701-3703; **(c)** Aoki, S.; Mikami, K.; Terada, M.; Nakai, T., *Tetrahedron* **1993**, *49* (9), 1783-1792; **(d)** Motoyama, Y.; Okano, M.; Narusawa, H.; Makihara, N.; Aoki, K.; Nishiyama, H., *Organometallics* **2001**, *20* (8), 1580-1591; **(e)** Evans, D. A.; Aye, Y.; Wu, J., *Org. Lett.* **2006**, *8* (10), 2071-2073.
- 81.** **(a)** Iseki, K.; Kuroki, Y.; Takahashi, M.; Kishimoto, S.; Kobayashi, Y., *Tetrahedron* **1997**, *53* (10), 3513-3526; **(b)** Nakajima, M.; Saito, M.; Shiro, M.; Hashimoto, S.-i., *J. Am. Chem. Soc.* **1998**, *120* (25), 6419-6420; **(c)** Lou, S.; Moquist, P. N.; Schaus, S. E., *J. Am. Chem. Soc.* **2006**, *128* (39), 12660-12661; **(d)** Malkov, A. V.; Dufková, L.; Farrugia, L.; Kočovský, P., *Angew. Chem., Int. Ed.* **2003**, *42* (31), 3674-3677; **(e)** Denmark, S. E.; Fu, J., *Chem. Commun.* **2003**, (2), 167-170.
- 82.** **(a)** Bandini, M.; Cozzi, P. G.; Umani-Ronchi, A., *Chem. Commun.* **2002**, (9), 919-927; **(b)** Bandini, M.; Cozzi, P. G.; Umani-Ronchi, A., *Angew. Chem., Int. Ed.* **2000**, *39* (13), 2327-2330.
- 83.** **(a)** Gao, X.; Han, H.; Krische, M. J., *J. Am. Chem. Soc.* **2011**, *133* (32), 12795-12800; **(b)** Kim, I. S.; Han, S. B.; Krische, M. J., *J. Am. Chem. Soc.* **2009**, *131* (7), 2514-2520.
- 84.** Li, J.; Menche, D., *Synthesis* **2009**, *2009* (EFirst), 2293-2315.
- 85.** **(a)** Brown, H. C.; Bhat, K. S., *J. Am. Chem. Soc.* **1986**, *108* (2), 293-294; **(b)** Brown, H. C.; Bhat, K. S., *J. Am. Chem. Soc.* **1986**, *108* (19), 5919-5923; **(c)** Brown, H. C.; Veeraraghavan Ramachandran, P., *J. Organomet. Chem.* **1995**, *500* (1-2), 1-19; **(d)** Herbert C. Brown, P. V. R., *Pure Appl. Chem.* **1994**, *66* (2), 201-212.
- 86.** **(a)** Ojima, I.; Wiley online, I., *Catalytic asymmetric synthesis*. Wiley-VCH: New York, 2000; p xiv, 864 p; **(b)** Mayer, S.; List, B., *Angew. Chem., Int. Ed.* **2006**, *45* (25), 4193-4195; **(c)** Lacour, J.; Hebbe-Viton, V., *Chem. Soc. Rev.* **2003**, *32* (6), 373-382; **(d)** Akiyama, T.; Itoh, J.; Fuchibe, K., *Adv. Synth. Catal.* **2006**, *348* (9), 999-1010; **(e)** Brak, K.; Jacobsen, E. N., *Angew. Chem., Int. Ed.* **2013**, *52* (2), 534-561; **(f)** Phipps, R. J.; Hamilton, G. L.; Toste, F. D., *Nat Chem* **2012**, *4* (8), 603-614; **(g)** Allen, A. E.; MacMillan, D. W. C., *Chem. Sci.* **2012**, *3* (3), 633-658.
- 87.** **(a)** Alper, H.; Hamel, N., *J. Am. Chem. Soc.* **1990**, *112* (7), 2803-2804; **(b)** Komanduri, V.; Krische, M. J., *J. Am. Chem. Soc.* **2006**, *128* (51), 16448-16449; **(c)** Gregory L. Hamilton, E. J. K., Miriam Mba, F. Dean Toste, *Science* **2007**, *27*, 496-499; **(d)** Rueping, M.; Antonchick, A. P.; Brinkmann, C., *Angew. Chem., Int. Ed.* **2007**, *46* (36), 6903-6906; **(e)** Mukherjee, S.; List, B., *J. Am. Chem. Soc.* **2007**, *129* (37), 11336-11337; **(f)** Lv, J.; Luo, S., *Chem. Commun.* **2013**, *49* (9), 847-858; **(g)** Liao, S.; List, B., *Angew. Chem., Int. Ed.* **2010**, *49* (3), 628-631; **(h)** Cai, Y.; Shi, Y., *Dalton Trans.* **2013**, *42* (15), 5232-5236; **(i)** Patil, N. T.; Shinde, V. S.; Gajula, B., *Org. Biomol. Chem.* **2012**, *10* (2), 211-224; **(j)** Mahlau, M.; List,

- B., *Isr. J. Chem.* **2012**, *52* (7), 630-638; **(k)** Guo, B.; Schwarzwalder, G.; Njardarson, J. T., *Angew. Chem.* **2012**, *124* (23), 5773-5776.
88. Jiang, G.; List, B., *Chem. Commun.* **2011**, *47* (36), 10022-10024.
89. **(a)** Uraguchi, D.; Terada, M., *J. Am. Chem. Soc.* **2004**, *126* (17), 5356-5357; **(b)** Akiyama, T.; Itoh, J.; Yokota, K.; Fuchibe, K., *Angew. Chem., Int. Ed.* **2004**, *43* (12), 1566-1568.
90. Zhang, F.-Y.; Kwok, W. H.; Chan, A. S. C., *Tetrahedron: Asymmetry* **2001**, *12* (16), 2337-2342.
91. **(a)** Klussmann, M.; Ratjen, L.; Hoffmann, S.; Wakchaure, V.; Goddard, R.; List, B., *Synlett* **2010**, *2010* (14), 2189-2192; **(b)** Hatano, M.; Moriyama, K.; Maki, T.; Ishihara, K., *Angew. Chem., Int. Ed.* **2010**, *49* (22), 3823-3826.
92. Murakami, M.; Itami, K.; Ito, Y., *Organometallics* **1999**, *18* (7), 1326-1336.
93. Maytum, H. C.; Francos, J.; Whatrup, D. J.; Williams, J. M. J., *Chemistry – An Asian Journal* **2010**, *5* (3), 538-542.
94. Seebach, D.; Beck, A. K.; Heckel, A., *Angew. Chem., Int. Ed.* **2001**, *40* (1), 92-138.
95. **(a)** Lam, H. W., *Synthesis* **2011**, *2011* (13), 2011-2043; **(b)** Pellissier, H., *Tetrahedron* **2008**, *64* (45), 10279-10317; **(c)** Akiyama, T.; Saitoh, Y.; Morita, H.; Fuchibe, K., *Adv. Synth. Catal.* **2005**, *347* (11-13), 1523-1526.
96. Yamanaka, M.; Itoh, J.; Fuchibe, K.; Akiyama, T., *J. Am. Chem. Soc.* **2007**, *129* (21), 6756-6764.
97. Albert K. Bek, P. G., Luigi La Vecchia, Dieter Seebach, *Org. Synth.* **1999**, *76*, 12.
98. Takizawa, S.; Horii, A.; Sasai, H., *Tetrahedron: Asymmetry* **2010**, *21* (8), 891-894.
99. Gao, X.; Townsend, I. A.; Krische, M. J., *J. Org. Chem.* **2011**, *76* (7), 2350-2354.
100. Kim, J. D.; Kim, I. S.; Jin, C. H.; Zee, O. P.; Jung, Y. H., *Org. Lett.* **2005**, *7* (18), 4025-4028.
101. **(a)** Jozak, T.; Sun, Y.; Thiel, W. R., *New J. Chem.* **2011**, *35* (10), 2114-2121; **(b)** Lu, X.; Byun, H.-S.; Bittman, R., *J. Org. Chem.* **2004**, *69* (16), 5433-5438.
102. Marshall, J. A.; Palovich, M. R., *J. Org. Chem.* **1998**, *63* (13), 4381-4384.
103. Millán, A.; Campaña, A. G.; Bazdi, B.; Miguel, D.; Álvarez de Cienfuegos, L.; Echavarren, A. M.; Cuerva, J. M., *Chem. Eur. J.* **2011**, *17* (14), 3985-3994.
104. Canterbury, D. P.; Micalizio, G. C., *J. Am. Chem. Soc.* **2010**, *132* (22), 7602-7604.
105. **(a)** Itoh, J.; Han, S. B.; Krische, M. J., *Angew. Chem., Int. Ed.* **2009**, *48* (34), 6313-6316; **(b)** Grant, C. D.; Krische, M. J., *Org. Lett.* **2009**, *11* (20), 4485-4487.
106. **(a)** Pinggen, D.; Müller, C.; Vogt, D., *Angew. Chem., Int. Ed.* **2010**, *49* (44), 8130-8133; **(b)** Bähn, S.; Tillack, A.; Imm, S.; Mevius, K.; Michalik, D.; Hollmann, D.; Neubert, L.; Beller, M., *ChemSusChem* **2009**, *2* (6), 551-557.
107. **(a)** Chatani, N.; Tobisu, M.; Asaumi, T.; Fukumoto, Y.; Murai, S., *J. Am. Chem. Soc.* **1999**, *121* (30), 7160-7161; **(b)** Tobisu, M.; Chatani, N.; Asaumi, T.; Amako, K.; Ie, Y.; Fukumoto, Y.; Murai, S., *J. Am. Chem. Soc.* **2000**, *122* (51), 12663-12674.
108. Yamaguchi, E.; Mowat, J.; Luong, T.; Krische, M. J., *Angew. Chem., Int. Ed.* **2013**, *52* (32), 8428-8431.

109. (a) Dohi, T.; Takenaga, N.; Nakae, T.; Toyoda, Y.; Yamasaki, M.; Shiro, M.; Fujioka, H.; Maruyama, A.; Kita, Y., *J. Am. Chem. Soc.* **2013**, *135* (11), 4558-4566; (b) Uyanik, M.; Yasui, T.; Ishihara, K., *Tetrahedron* **2010**, *66* (31), 5841-5851; (c) Cox, C.; Danishefsky, S. J., *Org. Lett.* **2000**, *2* (22), 3493-3496; (d) Tamura, Y.; Yakura, T.; Haruta, J.; Kita, Y., *J. Org. Chem.* **1987**, *52* (17), 3927-3930.
110. (a) Curran, D. P.; Chen, M. H.; Spletzer, E.; Seong, C. M.; Chang, C. T., *J. Am. Chem. Soc.* **1989**, *111* (24), 8872-8878; (b) Zhang, W.; Pugh, G., *Tetrahedron Lett.* **2001**, *42* (33), 5617-5620; (c) Zhang, W., *Tetrahedron Lett.* **2000**, *41* (15), 2523-2527; (d) Merlic, C. A.; Walsh, J. C., *J. Org. Chem.* **2001**, *66* (7), 2265-2274; (e) Otsubo, K.; Inanaga, J.; Yamaguchi, M., *Tetrahedron Lett.* **1986**, *27* (47), 5763-5764; (f) Fukuzawa, S.-i.; Nakanishi, A.; Fujinami, T.; Sakai, S., *J. Chem. Soc., Chem. Commun.* **1986**, (8), 624-625; (g) Streuff, J., *Synthesis* **2013**, *45*, 281-307.
111. (a) Mandal, A. K.; Jawalkar, D. G., *J. Org. Chem.* **1989**, *54* (10), 2364-2369; (b) Fujioka, H.; Matsuda, S.; Horai, M.; Fujii, E.; Morishita, M.; Nishiguchi, N.; Hata, K.; Kita, Y., *Chem. Eur. J.* **2007**, *13* (18), 5238-5248; (c) Faraj, H.; Claire, M.; Rondot, A.; Aumelas, A.; Auzou, G., *J. Chem. Soc., Perkin Trans. 1* **1990**, (11), 3045-3048; (d) Eipert, M.; Maichle-Mössmer, C.; Maier, M. E., *Tetrahedron* **2003**, *59* (40), 7949-7960; (e) Mandal, A. K.; Jawalkar, D. G., *Tetrahedron Lett.* **1986**, *27* (1), 99-100.
112. (a) Ye, W.; Cai, G.; Zhuang, Z.; Jia, X.; Zhai, H., *Org. Lett.* **2005**, *7* (17), 3769-3771; (b) Burstein, C.; Glorius, F., *Angew. Chem., Int. Ed.* **2004**, *43* (45), 6205-6208.
113. (a) Bigi, M. A.; Reed, S. A.; White, M. C., *Nat Chem* **2011**, *3* (3), 216-222; (b) Uyanik, M.; Suzuki, D.; Yasui, T.; Ishihara, K., *Angew. Chem., Int. Ed.* **2011**, *50* (23), 5331-5334.
114. (a) Choudhury, P. K.; Foubelo, F.; Yus, M., *Tetrahedron Lett.* **1998**, *39* (21), 3581-3584; (b) Csuk, R.; Glänzer, B. I.; Hu, Z.; Boese, R., *Tetrahedron* **1994**, *50* (4), 1111-1124; (c) Fouquet, E.; Gabriel, A.; Maillard, B.; Pereyre, M., *Tetrahedron Lett.* **1993**, *34* (48), 7749-7752; (d) RenČsuk; Hua, Z.; Abdou, M.; Kratky, C., *Tetrahedron* **1991**, *47* (34), 7037-7044; (e) Machrouhi, F.; Namy, J.-L., *Tetrahedron* **1998**, *54* (37), 11111-11122; (f) Yves Michellys, P.; Pellissier, H.; Santelli, M., *Tetrahedron Lett.* **1993**, *34* (12), 1931-1934.
115. Xiong, H.; Rieke, R. D., *J. Org. Chem.* **1992**, *57* (26), 7007-7008.
116. Bartoli, A.; Rodier, F.; Commeiras, L.; Parrain, J.-L.; Chouraqui, G., *Nat. Prod. Rep.* **2011**, *28* (4), 763-782.
117. (a) Musashi, Y.; Sakaki, S., *J. Am. Chem. Soc.* **2002**, *124* (25), 7588-7603; (b) Ngai, M.-Y.; Barchuk, A.; Krische, M. J., *J. Am. Chem. Soc.* **2006**, *129* (2), 280-281.
118. Sanchez-Delgado, R. A.; Bradley, J. S.; Wilkinson, G., *J. Chem. Soc., Dalton Trans.* **1976**, (5), 399-404.
119. (a) Nishigaichi, Y.; Orimi, T.; Takuwa, A., *J. Organomet. Chem.* **2009**, *694* (24), 3837-3839; (b) Kang, S.-K.; Baik, T.-G.; Jiao, X.-H., *Synth. Commun.* **2002**, *32* (1), 75-78; (c) Gewald, R.; Kira, M.; Sakurai, H., *Synthesis* **1996**, *1996* (01), 111-115; (d) Ramachandran, P. V.; Rudd, M. T.; Burghardt, T. E.; Ram Reddy, M. V.,

- J. Org. Chem.* **2003**, *68* (24), 9310-9316; **(e)** Dhondi, P. K.; Carberry, P.; Choi, L. B.; Chisholm, J. D., *J. Org. Chem.* **2007**, *72* (25), 9590-9596; **(f)** Inaba, S.-i.; Rieke, R. D., *Synthesis* **1984**, *1984* (10), 844-845.
- 120.** **(a)** Petrovskaia, O.; Taylor, B. M.; Hauze, D. B.; Carroll, P. J.; Joullié, M. M., *J. Org. Chem.* **2001**, *66* (23), 7666-7675; **(b)** Vanden Eynden, M. J.; Kunchithapatham, K.; Stambuli, J. P., *J. Org. Chem.* **2010**, *75* (24), 8542-8549; **(c)** Fatiadi, A. J., *Synthesis* **1978**, *1978* (03), 165-204; **(d)** Nieminen, V.; Taskinen, A.; Hotokka, M.; Murzin, D. Y., *J. Catal.* **2007**, *245* (1), 228-236; **(e)** Busygin, I.; Rosenholm, M.; Toukoniitty, E.; Murzin, D.; Leino, R., *Catal. Lett.* **2007**, *117* (3-4), 91-98.
- 121.** Stockis, A.; Hoffmann, R., *J. Am. Chem. Soc.* **1980**, *102* (9), 2952-2962.
- 122.** Nyhlén, J.; Privalov, T.; Bäckvall, J.-E., *Chem. Eur. J.* **2009**, *15* (21), 5220-5229.
- 123.** Kawatsura, M.; Yamamoto, M.; Namioka, J.; Kajita, K.; Hirakawa, T.; Itoh, T., *Org. Lett.* **2011**, *13* (5), 1001-1003.
- 124.** McInturff, E. L.; Nguyen, K. D.; Krische, M. J. *Angew. Chem., Int. Ed.* **2014**, ASAP.
- 125.** Hayashi, M.; Terashima, S.; Koga, K., *Tetrahedron* **1981**, *37* (16), 2797-2803.
- 126.** Lunardi, I.; Cazetta, T.; Conceição, G. J. A.; Moran, P. J. S.; Rodrigues, J. A. R., *Adv. Synth. Catal.* **2007**, *349* (6), 925-932.
- 127.** Dakdouki, S. C.; Villemin, D.; Bar, N., *Eur. J. Org. Chem.* **2012**, *2012* (4), 780-784.
- 128.** de Boer, J. W.; Browne, W. R.; Harutyunyan, S. R.; Bini, L.; Tiemersma-Wegman, T. D.; Alsters, P. L.; Hage, R.; Feringa, B. L., *Chem. Commun.* **2008**, (32), 3747-3749.
- 129.** Hlasta, D. J.; Luttinger, D.; Perrone, M. H.; Silbernagel, M. J.; Ward, S. J.; Haubrich, D. R., *J. Med. Chem.* **1987**, *30* (9), 1555-1562.
- 130.** Chiba, S.; Zhang, L.; Ang, G. Y.; Hui, B. W.-Q., *Org. Lett.* **2010**, *12* (9), 2052-2055.
- 131.** Autrey, R. L.; Tahk, F. C., *Tetrahedron* **1967**, *23* (2), 901-917.
- 132.** Leung, J. C.; Patman, R. L.; Sam, B.; Krische, M. J., *Chem. Eur. J.* **2011**, *17* (44), 12437-12443.
- 133.** York, M., *Tetrahedron Lett.* **2011**, *52* (47), 6267-6270.
- 134.** Nishibayashi, Y.; Yoshikawa, M.; Inada, Y.; Milton, M. D.; Hidai, M.; Uemura, S., *Angew. Chem., Int. Ed.* **2003**, *42* (23), 2681-2684.

Vita

Emma McInturff attended Century High School in Pocatello, Idaho. Upon graduating, she attended Boise State University, Boise, Idaho, where she was an active member of the Honors College and conducted organic chemistry research under the supervision of Dr. Don L. Warner. In the summer of 2007, Emma studied at the Universidad de Málaga, Málaga, Spain, and in the summer of 2008, Emma participated in a National Science Foundation Research Experience for Undergraduates at Syracuse University, Syracuse, New York, under the supervision of Dr. Nancy I. Totah. After receiving the degree of Bachelor of Science in Biochemistry from Boise State University in 2009, Emma entered the graduate program at the University of Texas at Austin to study transition metal catalyzed reaction development in the laboratory of Professor Michael J. Krische.

Permanent address (or email): elmcinturff@gmail.com

This dissertation was typed by the author.